

Bridge Deck Design Criteria and Testing Procedures

FINAL REPORT

Prepared for
NCHRP
Transportation Research Board
of
The National Academies

TRANSPORTATION RESEARCH BOARD
OF THE NATIONAL ACADEMIES
PRIVILEGED DOCUMENT

This report, not released for publication, is furnished only for review to members of or participants in the work of the CRP. This report is to be regarded as fully privileged, and dissemination of the information included herein must be approved by the CRP.

Prepared By:
Robert J. Connor, Judy Liu, Christopher Higgins

Purdue University
West Lafayette, Indiana
JULY 2012

ACKNOWLEDGMENT OF SPONSORSHIP

This work was sponsored by the following:

- American Association of State Highway and Transportation Officials, in cooperation with the Federal Highway Administration, and was conducted in the **National Cooperative Highway Research Program**,

which is administered by the Transportation Research Board of the National Academies

DISCLAIMER

This is an uncorrected draft as submitted by the research agency. The opinions and conclusions expressed or implied in the report are those of the research agency. They are not necessarily those of the Transportation Research Board, the National Academies, or the program sponsors.

TABLE OF CONTENTS	I
LIST OF FIGURES	VI
LIST OF TABLES	X
 EXECUTIVE SUMMARY	 XII
 CHAPTER 1 BACKGROUND	 1
1.1 Problem Statement	1
1.2 Research Objectives	2
1.3 Literature Review	2
1.4 Existing Standard Testing Protocols	2
1.5 Performance Factors Experimentally Studied	3
1.6 Development of Standard Testing Methods	4
1.7 Analytical Studies	4
 CHAPTER 2 RESEARCH APPROACH	 5
2.1 Research Approach	5
2.1.1 Experimental Approach	5
2.1.2 Analytical Approach	5
2.2 TMC Test	5
2.2.1 Selection of Materials	6
2.2.2 Test Procedure	8
2.2.3 Mechanical Test Setup	9
2.2.4 Instrumentation	11
2.2.5 Chemical Deicers	12
2.2.6 Temperature Range	12
2.2.7 Failure Criteria	13
2.3 Sliding Abrasion Tests	15
2.3.1 Test Procedure	15
2.3.2 Selection of Materials	16
2.4 Impact Test	17

2.4.1	Motivation for Test	17
2.4.2	Test Introduction	17
2.4.3	Materials Used	18
2.4.4	Impact Test Frame	19
2.4.5	Impact Head Assembly	21
2.4.6	Test Procedure	22
2.5	Large-Scale Specimen	22
2.5.1	Experimental Design	22
2.5.2	Specimen Configuration and Materials	22
2.5.3	Investigated Details and Instrumentation	24
2.6	Large-Scale Specimen Experimental Procedures	24
2.6.1	Introduction	24
2.6.2	Truck Roll Tests	24
2.6.3	Longitudinal Splice Test	25
2.6.4	Transverse Splice Tests	27
2.7	Subassembly Stiffness Tests	29
2.7.1	Experimental Design	30
2.7.2	Specimen Configuration and Materials	30
2.7.3	Stiffness Test Experimental Setup	32
2.7.4	Stiffness Test Experimental Procedure	34
2.8	Subassembly Longitudinal Splice Test	36
2.8.1	Experimental Design	36
2.8.2	Specimen Configuration and Materials	36
2.8.3	Strength Verification Test	37
2.8.4	Cyclic Load Test	38
2.9	Subassembly Deck-to-Superstructure Connection Test	39
2.9.1	Experimental Design	39
2.9.2	Specimen Configuration and Materials	40
2.9.3	Cyclic Load Test	41
2.9.4	Strength Load Test	42
2.10	Subassembly Transverse Splice Test	43
2.10.1	Experimental Design	43
2.10.2	Specimen Configuration and Materials	43
2.10.3	Strength Verification Test	44
2.10.4	Cyclic Load Test	45

2.11	Summary	45
CHAPTER 3	FINDINGS AND APPLICATIONS	47
3.1	TMC Tests	47
3.1.1	Failure Modes Observed	47
3.1.2	Pull-off Results and Quantification	49
3.1.3	Application Summary	54
3.2	Sliding Abrasion Tests	54
3.2.1	Concrete Calibration	54
3.2.2	Steel Orthotropic and FRP Results	55
3.2.3	Rating System and Calculations	56
3.2.4	Failure Modes Observed	57
3.2.5	Application Summary	60
3.3	Impact Test	60
3.3.1	83B83B Reinforced Concrete Calibration	60
3.3.2	Evaluation System	61
3.3.3	Results	62
3.3.4	Impact Test Summary	67
3.3.5	Introduction	67
3.3.6	Composite Action of the Deck	67
3.3.7	General Roll Test Findings	70
3.3.8	Roll Test Positions #1 and #4: Critical Findings	75
3.3.9	Roll Test Position #2: Critical Findings	76
3.3.10	Roll Test Position #3: Critical Findings	77
3.3.11	Roll Test Positions #5 and #6: Critical Findings	78
3.3.12	Application Summary - Truck Roll Tests	78
3.3.13	Longitudinal Splice Cyclic Load Test	79
3.3.14	Transverse Splice Cyclic Load Test #1	86
3.3.15	Transverse Splice Cyclic Load Test #2	90
3.3.16	Application Summary - Transverse Splice Tests	95
3.4	Subassembly Stiffness Tests	95
3.4.1	Strong Axis Stiffness	96
3.4.2	Weak Axis Stiffness	98
3.4.3	Torsion Stiffness	99
3.4.4	Overall Stiffness Properties	101
3.4.5	Standard Test Methods	102
3.4.6	Application Summary	103

3.5 Subassembly Longitudinal Splice Test	103
3.5.1 Strength Verification Test Performance	103
3.5.2 Cyclic Load Test Performance	107
3.5.3 Comparison to Large-Scale Specimen	110
3.5.4 Standard Test Method	112
3.5.5 Application Summary	113
3.6 Subassembly Deck-to-Superstructure Connection Test Performance	113
3.6.1 Cyclic Load Test	114
3.6.2 Strength Load Test	119
3.6.3 Standard Test Method	120
3.6.4 Application	120
3.7 Subassembly Transverse Splice Test Performance	121
3.7.1 Strength Verification Test	121
3.7.2 Cyclic Load Test	122
3.7.3 Comparison to Large-Scale Specimen	126
3.7.4 Standard Test Methods	129
3.7.5 Application Summary	129
3.8 Proposed Changes to AASHTO-LRFD	130
3.8.1 Current Items	130
3.8.2 Proposed New Items	131
CHAPTER 4 CONCLUSIONS AND SUGGESTED RESEARCH	134
4.1 Small-Scale Wearing Surface Tests	135
4.1.1 TMC Test	135
4.1.2 Sliding Abrasion Test	135
4.1.3 Direct Impact Test	136
4.2 Large-Scale Specimen Tests	137
4.3 Subassembly Stiffness Tests	137
4.4 Subassembly Cyclic Tests	138
4.5 Proposed Changes to AASHTO-LRFD	138
4.6 Recommended Future Work	140
4.6.1 TMC Test	140
4.6.2 Sliding Abrasion Test	140
4.6.3 Direct Impact Test	141

4.6.4 Large-Scale and Subassembly Specimen Tests	141
REFERENCES	142
ATTACHMENTS	145
ATTACHMENT A - Proposed Test Method and Commentary for TMC Resistance of Bridge Deck Wearing Surfaces	
ATTACHMENT B - Proposed Test Method and Commentary for Sliding Abrasion Wear Resistance of Bridge Deck Wearing Surfaces	
ATTACHMENT C - Proposed Test Method and Commentary for Qualitative Comparison of Various Deck Types Subjected to Direct Impact	
ATTACHMENT D - Proposed Recommended Method for Verifying Strength of Bridge Decks	
ATTACHMENT E - Proposed Test Method and Commentary for Determining Strong Axis Flexural Stiffness (D_x) of Bridge Decks	
ATTACHMENT F - Proposed Test Method and Commentary for Determining Weak Axis Flexural Stiffness (D_y) of Bridge Decks	
ATTACHMENT G - Proposed Test Method and Commentary for Determining Torsional Stiffness (D_{xy}) of Bridge Decks	
ATTACHMENT H - Proposed Test Method and Commentary for Subassembly Cyclic Load Testing of Longitudinal Splices in Prefabricated Bridge Deck Panels	
ATTACHMENT I - Proposed Test Method and Commentary for Subassembly Cyclic Load Testing of Deck-to-Superstructure Connections for Prefabricated Bridge Decks	
ATTACHMENT J - Proposed Test Method and Commentary for Subassembly Cyclic Load Testing of Transverse Splices in Prefabricated Bridge Deck Panels	
ATTACHMENT K - Proposed Revisions to AASHTO LRFD Bridge Design Specifications	
APPENDIX A – Specimen Details and Instrumentation Plans	
APPENDIX B – Calculations and Supplemental Data	
APPENDIX C – Results of Deck Specimen Coring	

LIST OF FIGURES

Figure 2-1: ZellComp deck cross section (Zhao et al. 2006).....	6
Figure 2-2: FRP specimen before testing.....	7
Figure 2-3: Mechanical test frame	9
Figure 2-4: TMC loading device.....	10
Figure 2-5: Hydraulic control and feedback system	11
Figure 2-6: Strain gage location.....	11
Figure 2-7: One final TMC cycle pattern	13
Figure 2-8: Pull-off test failure modes (ASTM C 1583, 2007)	14
Figure 2-9: Sliding abrasion test setup.....	15
Figure 2-10: Concrete calibration slab reinforcement plan view.....	16
Figure 2-11: ZellComp 5” deck cross section.....	18
Figure 2-12: Steel orthotropic deck panel cross section	18
Figure 2-13: Impact test frame picture and elevation view	20
Figure 2-14: Impact head with tip bolted to weight carriage.....	21
Figure 2-15: Final installation of grid deck before concrete placement	23
Figure 2-16: Center lines of roll test positions.....	24
Figure 2-17: Truck load simulator	25
Figure 2-18: Cyclic test load frame	26
Figure 2-19: Transverse splice load test positions.....	29
Figure 2-20: Open grid deck specimen #1	31
Figure 2-21: Grid deck specimen prior to concrete placement.....	31
Figure 2-22: Partially filled grid deck specimen.....	32
Figure 2-23: Line load on deck specimen for strong axis direction stiffness test.....	33
Figure 2-24: Edge of deck on rigid support.....	33
Figure 2-25: Torsion test (left) setup; (right) inverted point support before installation.....	34
Figure 2-26: “Slice” of large-scale deck represented by subassembly longitudinal splice test....	36
Figure 2-27: Subassembly longitudinal splice specimen (left) on stringers; (right) bolted connection to stringers	37

Figure 2-28: Longitudinal splice strength verification test (left) flexible supports; (right) rigid supports	38
Figure 2-29: Subassembly longitudinal splice cyclic load test (left) setup; (right) application of load.....	39
Figure 2-30: “Slice” of a large-scale bridge deck represented by subassembly deck-to-superstructure connection test.....	40
Figure 2-31: Deck-to-superstructure connection detail	41
Figure 2-32: Subassembly deck-to-superstructure connection test (left) setup; (right) clamping system	41
Figure 2-33: “Slice” of large-scale bridge deck represented by subassembly transverse splice test	43
Figure 2-34: Transverse splice (left) details; (right) specimen after concrete placement.....	44
Figure 2-35: Transverse splice strength verification and cyclic load test.....	45
Figure 3-1: Delamination of T-48 wear surface on FRP specimen	48
Figure 3-2: FRP/T-48 specimen #5 after pull-off tests	48
Figure 3-3: Steel/T-48 specimen #3 after pull-off tests	49
Figure 3-4: Sliding test concrete calibration	55
Figure 3-5: FRP sliding abrasion test results	56
Figure 3-6: Steel orthotropic sliding abrasion test results	56
Figure 3-7: Concrete groove at completion of testing	58
Figure 3-8: Side view of wear groove after 35,000 cycles, specimen #1	58
Figure 3-9: ZellComp FRP deck w/ Flexolith wear surface after 35,000 cycles.....	59
Figure 3-10: ZellComp FRP deck from lower angle	60
Figure 3-11: Concrete calibration data	61
Figure 3-12: 4000 ft-lb impact on 1/2" steel plate deck	63
Figure 3-13: Bottom view of typical steel impact site.....	63
Figure 3-14: FRP damage level 1; damage to bottom of top plate	64
Figure 3-15: FRP deck with grouted stud connection (Zhao et al. 2006) (left) elevation; (right) cross section	65
Figure 3-16: FRP damage level 2, permitting water leakage.....	65
Figure 3-17: FRP damage level 3, punch through	66
Figure 3-18: Effective flange widths	68

Figure 3-19: Middle girder stresses	71
Figure 3-20: Cross bar global and local responses	72
Figure 3-21: Main bar local bending	73
Figure 3-22: Reinforcing steel and cross bar local stresses	74
Figure 3-23: Longitudinal splice reinforcing steel stresses	75
Figure 3-24: Cross bar local bending.....	76
Figure 3-25: Main bar under negative moment	77
Figure 3-26: 58.2 kip static test results – longitudinal splice reinforcing steel	80
Figure 3-27: 30 kip static test results – longitudinal splice reinforcing steel	81
Figure 3-28: Main bar stresses one foot from LS splice	82
Figure 3-29: Main bar stresses two feet from LS splice	83
Figure 3-30: Initial cracking near load patches (prior to any load cycles) (left) north side; (right) south side	84
Figure 3-31: Cracking after strength test (after 100 cycles at the strength load) (left) north side; (right) south side	84
Figure 3-32: Concrete cracking at completion of longitudinal splice cyclic test (after 4.3 million cycles)	85
Figure 3-33: Transverse splice #1 north cross bar stresses.....	87
Figure 3-34: Transverse splice #1 south cross bars stresses	87
Figure 3-35: Transverse splice #1 main bar stresses	88
Figure 3-36: Transverse splice #1 reinforcing steel stresses	89
Figure 3-37: (Left) bottom of transverse splice; (right) transverse splice load patch (note steel plate is still in place)	90
Figure 3-38: Transverse splice #2 cross bar stresses	92
Figure 3-39: Transverse splice test #2 main bar stresses.....	93
Figure 3-40: Transverse splice test #2 reinforcing steel stresses.....	94
Figure 3-41: Diagonal crack transverse splice test #2 (left) bottom; (right) top	95
Figure 3-42: Linear deflection underneath line load.....	97
Figure 3-43: Torsion stiffness test set-up for open grid deck specimen #1	100
Figure 3-44: Torsion stiffness test set-up for partially filled grid deck specimen	101
Figure 3-45: Cracks on subassembly longitudinal splice deck specimen.....	104
Figure 3-46: Displacements for strength verification load test with flexible stringers.....	105

Figure 3-47: Displacements for strength verification load test with rigid stringers	106
Figure 3-48: Largest crack found in concrete at termination of subassembly longitudinal splice cyclic load test.....	107
Figure 3-49: Displacements at fatigue load throughout cyclic load test.....	108
Figure 3-50: Reinforcing steel stresses at fatigue load throughout cyclic load test.....	109
Figure 3-51: Stresses in main bars near patches leveling off after 2-3 million load cycles	109
Figure 3-52: Main bar stresses near interior stringer	110
Figure 3-53: Fatigue cracking in central main bar near stringer (Left) Early crack growth; (Right) Crack growth at end of cyclic load test.....	114
Figure 3-54: Stress range for top gages on main bars near interior stringer.....	115
Figure 3-55: Fatigue cracks in other main bars (Left) East (second) main bar damaged; (Right) West (third) main bar damaged.....	116
Figure 3-56: Stress range for bottom gages on main bars near interior stringer.....	117
Figure 3-57: Main bar fatigue cracking near patch load.....	117
Figure 3-58: Fatigue cracking in cross bars	118
Figure 3-59: Measured displacement range at fatigue load range throughout testing.....	119
Figure 3-60: Displacements for strength verification load test.....	120
Figure 3-61: Displacements for strength verification load test.....	122
Figure 3-62: Cracking on underside of subassembly transverse splice deck specimen	122
Figure 3-63: Fatigue cracking in form pans (Left) Typical crack observed; (Right) Other crack observed	123
Figure 3-64: Displacements measured throughout testing at 29.1 kip load.....	124
Figure 3-65: Reinforcing steel stresses measured throughout testing at 29.1 kip load.....	125
Figure 3-66: Transverse splice configurations (top) subassembly specimen; (bottom) large-scale specimen	128

LIST OF TABLES

Table 1-1: Tests and performance factors addressed in experimental program	3
Table 2-1: TMC specimen matrix.....	8
Table 2-2: Sliding test specimen matrix	17
Table 2-3: Impact test matrix	19
Table 2-4: Concrete strength.....	23
Table 2-5: Subassembly Stiffness Test Matrix	30
Table 2-6: Measured concrete compressive strength.....	32
Table 2-7: Summary of loads applied for strong axis stiffness tests	34
Table 2-8: Summary of loads applied for weak axis stiffness tests.....	35
Table 2-9: Summary of loads applied for torsion stiffness tests.....	35
Table 2-10: Measured concrete compressive strength.....	37
Table 3-1: Pull-off results from 1st TMC procedure	52
Table 3-2: Pull-off results from 2nd procedure	53
Table 3-3: TMC results summary	54
Table 3-4: Sliding abrasion test results.....	57
Table 3-5: Sliding abrasion test average results	57
Table 3-6: FRP impact behavior	66
Table 3-7: Longitudinal splice test girder moments	69
Table 3-8: Transverse splice tests girder moments.....	69
Table 3-9: Longitudinal splice reinforcing steel comparison	80
Table 3-10: Transverse splice cyclic test #1 roll test comparison	86
Table 3-11: Transverse splice cyclic test #2 roll test comparison	90
Table 3-12: Comparison of transverse splice cyclic tests	91
Table 3-13: Comparison of measured and theoretical stiffness in strong axis direction (D_x)	98
Table 3-14: Comparison of measured and theoretical stiffness in weak axis direction (D_y).....	99
Table 3-15: Measured torsion stiffness.....	101
Table 3-16: Comparison of measured and theoretical orthotropic ratios (D).....	102
Table 3-17: Comparison of measured and theoretical twisting stiffness parameters (α).....	102
Table 3-18: Comparison of strength verification load computed	102
Table 3-19: Comparison of stress & displacement with flexible & rigid stringers	106

Table 3-20: Comparison of displacements of subassembly test to large-scale test	111
Table 3-21: Comparison of stresses at 25 kips	112
Table 3-22: Initial and final stresses for transverse splice at 29.1 kip load	126
Table 3-23: Comparison of displacements of subassembly test to large-scale test	127
Table 3-24: Comparison of transverse splice configuration	127

EXECUTIVE SUMMARY

This research was sponsored by the National Cooperative Highway Research Program (NCHRP) as Project 10-72 “Bridge Deck Design Criteria and Testing Procedures”. The research program was directed toward developing realistic and practical design and testing protocols for the most common types of deck elements. The analytical results were calibrated with the experimental findings to develop reasonable estimates of limit state performance and permit development of appropriate resistance models. Given the large numbers of deck types, the variation in component proportions, the wide array of superstructure connection types, the proprietary nature of many systems, the work focused on developing general purpose testing protocols that can be broadly used to evaluate and validate the performance of modular deck systems. Specific issues, based on previously noted in-service performance concerns that must be addressed for certain deck systems were included in this study. However, coverage of all possible issues was not possible. A similar approach was taken to develop design criteria to provide more consistent designs and in-service durability while still addressing specific performance factors unique to a given material or deck system.

Laboratory and analytical studies led to the development of testing protocols for the qualification and acceptance of various deck systems.

A total of ten (10) unique performance-based test methods were proposed to evaluate performance factors associated with various pre-fabricated deck systems. These tests are intended to provide increased confidence and reliability of deck panel systems. In particular, the test methods cover wearing surface durability, deck panel strength and fatigue of connections and attachments to the superstructure. In addition, recommended changes to the AASHTO LRFD Bridge Design Specifications were proposed. Specifically, changes to the equations used to estimate the moments used for the design of deck elements for fatigue and strength loading. The results of the research will be useful to practitioners and researchers alike and will enable uniform levels of reliability among different deck systems.

CHAPTER 1 Background

1.1 Problem Statement

Although not often recognized for their significance by the motoring public, deck elements of highway bridges are important components for an efficient highway system. Robust performance of these components over the long-term is critical for smooth daily traffic operations as well as adequate bridge system performance during extreme events. Failure of bridge deck systems results in direct economic costs associated with maintenance, repair, and replacement. There are further costs associated with maintenance and repair or premature replacement due to poor performance. These costs include traffic delays to the motoring public, environmental impacts of energy consumption, generation of construction and demolition waste.

Causes of deck system failures range from load induced fatigue due to primary stresses to degradation of the deck materials or components in an unreasonably short service life. A key issue associated with decks, in comparison to other superstructure components, is the direct application of wheel loads to the elements. This has the effect of producing millions of strain cycles. Poorly designed and detailed deck components can accumulate damage very quickly. For this same reason, demands on the deck, in terms of durability, can vary dramatically from site-to-site, based on the local traffic conditions.

Presently, there are no recognized uniform national specifications for the design, performance, or construction installation of deck systems. As has been previously demonstrated with many other bridge components, in the absence of specifications, the low bid process often results in less durable products because manufacturers design, fabricate, and install components to achieve the lowest initial cost. This can be especially true for proprietary systems where open source information is lacking and fair comparisons cannot be made with alternatives. Unfortunately, outcomes from the current approach have sometimes resulted in poor performance and unreasonably short service lives.

The research program was directed toward developing realistic and practical design and testing protocols for the most common types of deck elements. The analytical results were calibrated with the experimental findings to develop reasonable estimates of limit state performance and permit development of appropriate resistance models. Given the large numbers of deck types, the variation in component proportions, the wide array of superstructure connection types, the proprietary nature of many systems, and the project budget, the research could not explicitly include all deck types and associated connections. Therefore, the work focused on developing general purpose testing protocols that can be broadly used to evaluate and validate the performance of modular deck systems. Specific issues, based on previously noted in-service performance concerns that must be addressed for certain deck systems were included in this study. However, coverage of all possible issues was not possible. A similar approach was taken to develop design criteria to provide more consistent designs and in-service durability while still addressing specific performance factors unique to a given material or deck system.

Laboratory and analytical studies led to the development of testing protocols for the qualification and acceptance of various deck systems. In addition, rational design criteria were developed, which will enable uniform levels of reliability among different deck systems.

1.2 Research Objectives

The primary objectives of this research were to:

- Determine critical performance factors that affect the durability, strength, and design of deck systems;
- Develop testing protocols that can be used to objectively evaluate critical performance factors for deck systems;
- Develop rational evaluation criteria, based on the testing protocols, for various deck systems to address durability, strength, fatigue, deflection, and other performance factors;
- Prepare recommended revisions to the existing AASHTO LRFD Bridge Design Specifications for Highway Bridges based on the results of the research.

1.3 Literature Review

A review of the technical literature revealed the following:

- Virtually no full-scale experimental programs have been conducted on entire bridge decks or integrated deck-superstructure systems (with the exception of orthotropic decks) that accurately represented in-situ boundary conditions.
- Experiments taken to fatigue failure or that explicitly considered performance factors affecting long-term durability, such as temperature, deicing chemicals, impact, abrasion, system behavior, etc. were lacking.
- Only limited studies on small-sized bridge deck specimens or sub-assemblies have been performed that considered long-term durability parameters, such as temperature, deicing chemicals, impact, abrasion, etc.

1.4 Existing Standard Testing Protocols

At the time this report was written, no AASHTO or ASTM standard tests are available that can be broadly applied to the wide array of different bridge deck types, such as fiber reinforced polymer (FRP), open grid, exodermic decks, orthotropic decks, etc. The most closely related standard test specification would have been ASTM D6275-98, “*Standard Practice for Laboratory Testing of Bridge Decks*,” which has now been withdrawn. While no longer in force, ASTM D6275 did provide some useful information for developing the proposed test protocols. For example, ASTM D6275 emphasized the importance of realistically representing boundary conditions in the laboratory.

While no specific deck testing standards are available, several other ASTM standard tests have been considered, adapted or modified, and incorporated into experimental test programs by other researchers (Wattanadechachan, et al, 2006; Gopalaratnam, et al 1989; Xi et al., 2004). Unfortunately in those studies, little justification was provided for the modifications that were employed. Directly adopting these previous techniques for the current research was not considered appropriate without supporting rationale. However, in many cases, the suggested modifications appeared reasonable and the previously adapted testing protocols were able to reveal certain performance issues for the test specimens. For example, the work performed by Wattanadechachan (2006), began by studying the influence temperature changes on the bond between the wearing surface and Glass Fiber Reinforced Polymer (GFRP) bridge deck using ASTM C884 – “*Standard Test Method for Thermal Compatibility between Concrete and an*

Epoxy-Resin Overlay”. However, the research found that the temperature range cited in C884 was too narrow for deck overlay applications and that it did not reveal bond problems that were observed when the temperature range was extended to those more representative of in-service conditions.

It is noted that standard material tests, such as those for strength, strength vs. temperature, ductility, were not reviewed. Many of the ASTM tests are well established for such general material evaluation and were utilized and/or referenced in the research when appropriate.

1.5 Performance Factors Experimentally Studied

Several performance factors were identified as of principal importance, both from the perspective of owners and based on observed and reported problems for various deck systems. Those found to be most critical and which could be addressed experimentally, were included in the experimental program. The performance factors and in-service issues addressed through testing are listed in the first two columns of Table 1-1, without regard to order of importance. The last two columns of Table 1-1 list the testing protocols employed and the objective of the test.

The performance factors included in Table 1-1 were identified through the literature review, survey of transportation agencies, and through informal discussions with owners and engineers.

Table 1-1: Tests and performance factors addressed in experimental program

Performance Factor	In-Service Issue	Proposed Test	Test Objective
Impact Resistance, Durability, Compatibility of Wearing Surface	Vertical impact of locally concentrated force such as an object falling off a vehicle	Direct Impact Resistance	Evaluate short-term performance of deck to vertical localized impact
Durability, Compatibility of Wearing Surface, Skid Resistance	Horizontal impact and abrasion such as from snowplow blade sliding across deck surface	Sliding Abrasion	Evaluate long-term performance of deck surface to horizontal impact and abrasion
Durability, Compatibility of Wearing Surface, Fatigue of Wearing Surface	Debonding, cracking, peeling, general failure of the wearing surface	Cyclic Temperature, Mechanical Strain, & Deicing Chemicals	Evaluate long-term performance of wearing surface installed on deck
Durability, Fatigue of connections and components	Fatigue failures of the deck components, failures in field splices, and failures of connections to supporting superstructure	System Fatigue and Durability	Evaluate the long-term fatigue and durability of the deck system under repeated loads. The test examines the deck, splices, and connections to the supporting structure.
Strength, Stiffness, Deflection	General lack of understanding of behavior of deck and superstructure interactions and shortcomings of current analytical models and design methods	Overall System Behavior	Evaluate strength and service limit states of deck systems. Obtain behaviors of deck systems for development and calibration of analytical and design methods

1.6 Development of Standard Testing Methods

The completed research consists of proposed standard testing methods for evaluating the following:

- Effects of change in temperature, cyclic mechanical strains, and exposure to chemicals on bridge decks;
- Impact loading;
- Sliding abrasion;
- Stiffness properties of bridge decks (e.g., orthotropic properties);
- Resistance of critical details in bridge decks to cyclic loading; and
- Strength verification of bridge decks.

The main goal of this research was to develop tests and evaluation criteria that were applicable to any type of bridge deck. This research was, therefore, focused on the development of these test methods rather than the evaluation of specific types of bridge decks and wearing surfaces.

1.7 Analytical Studies

At the direction of NCHRP, the analytical portion of the research was limited. However, valuable information was still obtained regarding recommended procedures for the simplified analysis of various orthotropic deck types. It is noted that orthotropic does not refer only to traditional steel decks, but rather any deck with different stiffness properties in orthogonal directions (i.e., D_x , D_y , D_{xy}).

CHAPTER 2 Research Approach

2.1 Research Approach

2.1.1 Experimental Approach

One of the primary objectives of the research was to develop test methods that can be used to evaluate various deck systems and establish uniform performance levels regardless of the material or deck type. Hence, a comprehensive laboratory experimental program was developed. The laboratory research was divided into three specific portions.

1. Small-scale wearing surface tests
2. A single large-scale test
3. Multiple subassembly tests

All details associated with the specimens and instrumentation plans are included in Appendix A. Appendix B contains all various calculations and details associated with the loads used for the fatigue testing.

2.1.2 Analytical Approach

During the development of the test methods, consideration was given to ensuring the resulting tests could be reasonably performed in most testing laboratories. A basic assumption was that a single tire patch load placed at midspan on a finite width deck was considered practical for most laboratory settings. The span length is specified by the manufacturer and/or specific application and the sample width is selected to be representative of in-situ deck elements shipped to the field.

2.2 TMC Test

One of the protocols developed was the Cyclic Temperature, Mechanical and Chemical (TMC) Test, which addresses delamination of thin epoxy concrete wearing surfaces applied to bridge deck top plates subjected to combined temperature cycles, exposure to deicing chemicals, and mechanical strains. This procedure was designed to test the resistance of thin (less than 1 inch) wear surfaces to long term attack by environmental and mechanical factors equivalent to those present in field installations. The TMC Test was designed with consideration that a wear surface on a bridge deck would not be subject to mechanical cycling, chemical cycling, or temperature cycling alone, but rather a combination of the three. Failure of a wearing surface in service is caused by a complex synergy of all three factors; therefore, considering any one damage factor in isolation could lead to an overestimate of the performance. It was decided that the best way to test a wear surface for compatibility with a deck system is to include all three factors in a single test procedure.

In order to make the test practical, the temperature, chemical, and mechanical loadings were not run simultaneously, but rather broken into blocks of loading which were repeated in cycles to achieve the combined effects. Each specimen was subjected to chemical exposure, temperature cycling, and then one group of mechanical cycles. A set of all three exposures was considered to be one TMC cycle. After a TMC cycle was completed, the entire process was repeated.

After completing a defined number of TMC cycles, the samples were visually inspected for delaminations and any visible areas of damage were recorded. The samples were then tested for remaining bond strength between the wear surface and the substrate using ASTM C 1583 (2004) “Standard Test Method for Tensile Strength of Concrete Surfaces and the Bond Strength or Tensile Strength of Concrete Repair and Overlay Materials by Direct Tension.” The remaining bond was tested at four locations near the center of the specimen, and the bond strength was recorded.

2.2.1 Selection of Materials

This section describes the samples used for TMC testing and the wearing surfaces applied to them.

Sample Section and Size. The samples used for this test were 6”x20” plates with wearing surface applied to the top. This size was selected because it is small enough to be easily handled by an individual technician, and six samples can fit in a five cubic foot temperature chamber. The ½” thick FRP plates were Pultex Fiber Reinforced Polymer Flat Sheets, 1525 Series, produced by Creative Pultrusions. This is the same material used for the top plates on the ZellComp deck system. In the ZellComp deck system, the reinforcing fibers in the flat plate are oriented transverse to traffic flow, so as to span between the T sections of the bottom deck segment. This assembly procedure is illustrated by the cross section view in Figure 2-1 (and Figure 2-11 in Section 2.4.2).

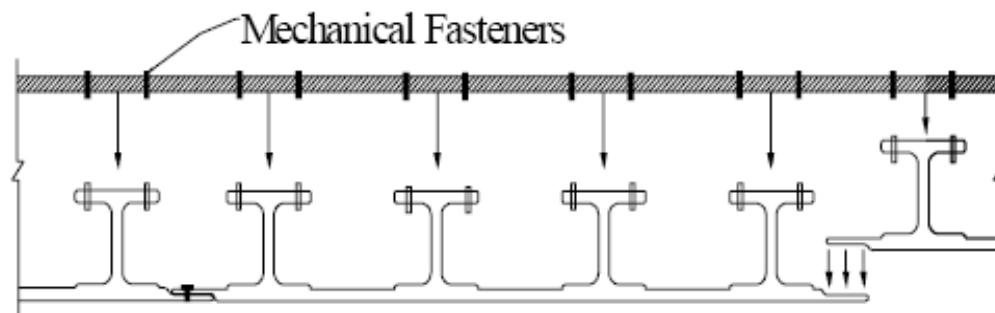


Figure 2-1: ZellComp deck cross section (Zhao et al. 2006)

The reinforcing fibers in the test specimens were oriented the same direction, along the span, parallel with the 20 inch direction. Figure 2-2 shows the FRP samples before testing. Epoxy pads added to the ends of the sample after the wear surface had cured allow even contact with the angles on the loading device. The steel specimens were also made from 6”x20” plates, but were ¼” thick instead of ½” thick.



Figure 2-2: FRP specimen before testing

Wearing Surfaces. For each specimen, the wear surface was applied to the top surface, which had been prepared by sanding and cleaning per the wearing surface manufacturer instructions. Tape was used to create a dam-like boundary along the edges to prevent the surface from thinning out as it approached the edge of the sample. After the wearing surface had cured, any spills were ground from the edges to bring the specimen back to the desired size.

During testing, there were two wearing surfaces which were evaluated on both the steel and FRP specimens. The first set of specimens had Flexolith Low Modulus Epoxy Binder and Broadcast Overlay System, produced by Euclid Chemical Company. This surface consisted of a two component flexible epoxy resin that was mixed by hand and then spread onto the prepared surface. The 3M Indag basalt aggregate, provided by the wearing surface manufacturers, was then broadcast into the resin until refusal, meaning the point at which the epoxy could hold no more aggregate. The second set of specimens used T-48 (Transpo Industries, Inc.) wear surface, which was applied by single coat slurry with the same 3M aggregate broadcast until refusal.

Specimen Matrix. Four groups of six TMC specimens were run during laboratory testing, as shown in Table 2-1. The first steel and FRP groups were fabricated with the Flexolith wear surface and run through the first procedure (discussed in detail in Section 2.2.6) concurrently. The second steel and FRP groups were fabricated with T-48 and run together with the second procedure, also discussed in Section 2.2.6. Three different deicing chemicals were used for each group, as described later in Section 2.2.6.

Table 2-1: TMC specimen matrix

Substrate	Wear Surface	Deicer	# of Specimens	TMC Run #
Steel	Flexolith	NaCl	2	1
Steel	Flexolith	CaCl ₂	2	1
Steel	Flexolith	MgCl ₂	2	1
FRP	Flexolith	NaCl	2	1
FRP	Flexolith	CaCl ₂	2	1
FRP	Flexolith	MgCl ₂	2	1
Steel	T-48	NaCl	2	2
Steel	T-48	CaCl ₂	2	2
Steel	T-48	MgCl ₂	2	2
FRP	T-48	NaCl	2	2
FRP	T-48	CaCl ₂	2	2
FRP	T-48	MgCl ₂	2	2

2.2.2 Test Procedure

The test procedure described herein constitutes one TMC cycle. As described above, all specimens were subjected to multiple TMC cycles before the pull-off tests (ASTM C 1583-04) were performed.

Mechanical Strain Range. The goal for mechanical cycling of the TMC samples was to reproduce the comparable fatigue strain ranges to which a bridge deck would be subjected in the field. To achieve this, the TMC samples were mechanically cycled at a strain range representative of that in the deck plate at the most severe location in the deck.

The challenge presented by this procedure was to accurately represent the strain range created by the AASHTO Fatigue Truck (AASHTO LRFD 3.6.1.4 2007) in the real bridge deck, which includes local strain field effects which are unique to each bridge deck system. The proposed bridge deck under consideration must be analyzed and the most severe strain range determined. The determination of the maximum strain range in a particular deck can be done by one of two methods, both of which were used during laboratory testing, and are presented in the following section.

AASHTO Standard Fatigue Category (Steel Deck Plates Only). The first and simplest method for determining the strain range for testing steel deck plates is to use the standard fatigue categories provided in Table 6.6.1.2.3-1 “Detail Categories for Load Induced Fatigue of the AASHTO LRFD Specification” (AASHTO 2007). The deck samples would be cycled at a strain range corresponding to the threshold stress (i.e., the fatigue limit) for infinite life of the controlling detail in the deck plate.

The first set of steel samples used in laboratory testing was mechanically cycled at a strain range corresponding to 10 ksi, consistent with a category C detail.

Finite Element Modeling Method (Non-Steel Decks). The alternate method for determining the stress range for mechanical testing is to use finite element modeling of the specific deck. This method involves significantly more work on the part of the testing engineer, because it requires the development of an accurate finite element model, including validation of results. This method will be required for wearing surfaces which are to be qualified for all non-steel decks, as these are not covered in the AASHTO fatigue categories.

2.2.3 Mechanical Test Setup

The mechanical portion of the TMC test was developed with the object of testing six samples in three point bending simultaneously. The test frame, shown in Figure 2-3, uses twin columns, which were post tensioned to the laboratory strong floor with welded base plates. A fatigue rated, hydraulic actuator with a capacity of 11,000 lbs was hung from a cross beam at the top of the frame to supply the loading to the specimens. The actuator applied tension cycles, which resulted in bending moment in the specimens and tensile stress in the wearing surface.



Figure 2-3: Mechanical test frame

The loading device, shown in Figure 2-4, consists of a pair of vertical channels which support six evenly spaced 1" steel bars. The entire loading device was attached to the actuator by a clevis which is capable of pivoting about all three axes.



Figure 2-4: TMC loading device

Each of the specimens was fixed to the frame by 2" x 2" angles and standard "C-clamps." Adjustability of the specimens was provided by 1.5" slotted holes cut into the vertical legs of the angles where they were connected to the columns. This allowed the strain range applied to each specimen to be fine tuned by loosening the bolts and moving the angles a small distance up or down, and by adding or removing $\frac{1}{8}$ " rubber spacers.

Hydraulic Control System. Cyclic strains were applied using a closed-loop, servo-controlled MTS actuator and MTS 458.20 controller with a micro profiler. The 458 controller had feedback inputs from a Linear Variable Differential Transducer (LVDT) mounted inside the actuator, as well as a load cell mounted between the actuator and loading device, both shown in Figure 2-5. The actuator was operated in displacement control mode for this testing, with safety limits set on the maximum force allowable from the actuator.

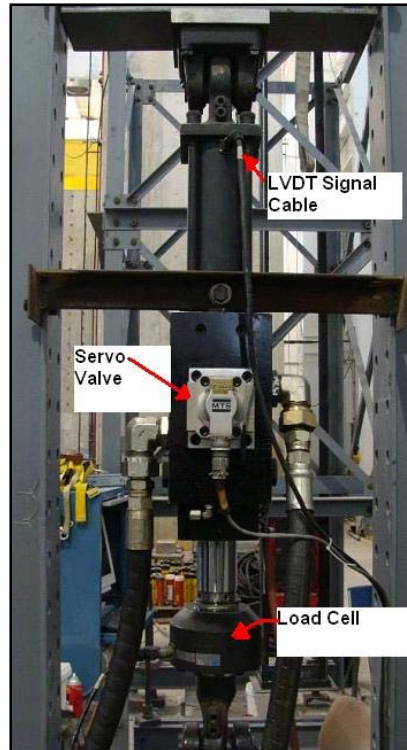


Figure 2-5: Hydraulic control and feedback system

2.2.4 Instrumentation

During mechanical testing, the strain range in each sample was measured to allow the load to be tuned precisely to bring each sample within an acceptable strain range of the target value.

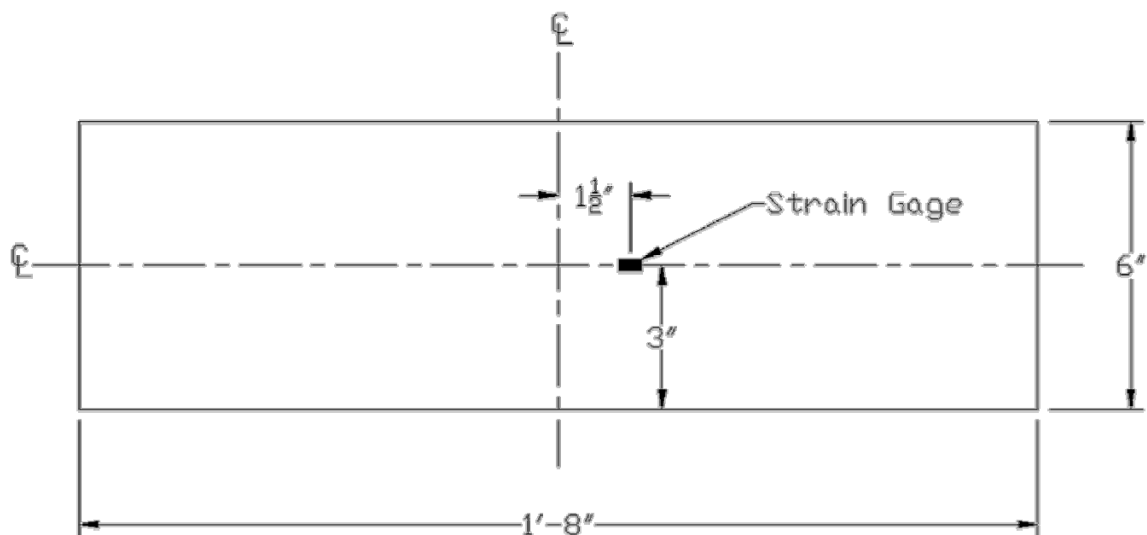


Figure 2-6: Strain gage location

2.2.5 Chemical Deicers

After reviewing the research by Xi (2004) and the available ASTM tests, it was concluded that there are two factors which must be considered in the TMC test. The first is direct chemical attack by the deicing chemical, as was considered in Xi's 2004 study. In this mode, the epoxy wearing surface or the substrate could sustain damage, corrosion in the case of steel, or reduced tensile strength in the case of FRP. In service, the chemical damage would accumulate over time as demonstrated by Xi (2004) and would likely contribute to the failure.

The second factor which must be considered is freeze/thaw expansion of the water in the deicing solutions. ASTM C 672 (2003) and C 666 (2003) are intended to target this behavior directly. This freeze/thaw behavior, which could occur many times per winter in even moderate climates, is well known to have damaging effects on any road surface that has become permeable to water. In the case of the TMC test, small cracks developed from the mechanical cycling could later expand by freeze/thaw prying action.

In order to account for both factors, it was necessary to ensure that the cold part of the temperature cycle was cold enough to freeze the deicing solution. In order to account for the possibility of different deck materials, especially new formulations of FRP, responding differently to each of the three deicers, it was deemed necessary to use all three solutions. It was therefore decided that since there were six specimens in each run, two should be treated consistently in each solution to ensure that any possible reactions with each type of deicer were accounted for in the testing.

2.2.6 Temperature Range

It was decided that a temperature range of -10 to 140° F (-20 to 60 °C) was reasonable (a total temperature range of 150° F). This temperature range incorporates the high recommended by Wattanadechachan et al. (2006), while ensuring a sufficiently low temperature to freeze the NaCl, MgCl₂, and CaCl₂ solutions. The temperature chamber is controlled by a programmable ramping thermostat, which automatically engages the refrigerator or heater as needed to follow the program.

Load/Temperature Cycle Pattern. The goal of the TMC test is to recreate the failure of thin wearing surfaces used on plate type bridge deck components in the laboratory. However, as mentioned before, the failure of these surfaces is almost always the result of multiple factors. It is therefore critical that the test consider the damage from chemical attack, temperature cycles, and mechanical cycles is related to the combination of these factors rather than only considering them individually. The loading pattern used for the TMC test is shown in Figure 2-7.

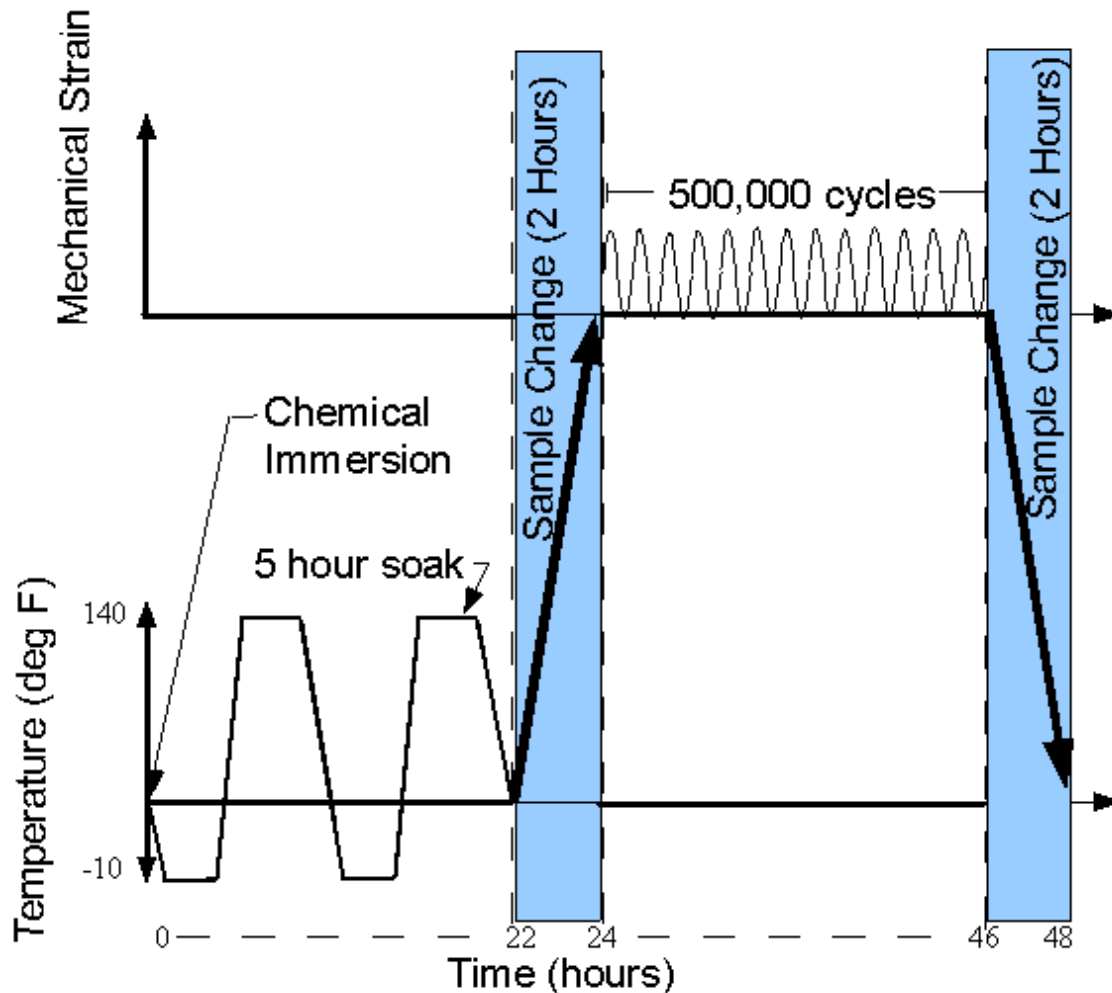


Figure 2-7: One final TMC cycle pattern

2.2.7 Failure Criteria

The goal of the TMC test was to qualify a wearing surface for use on a given substrate (either steel or FRP) up to the strain range tested. The State of Indiana is producing a draft specification for thin epoxy concrete wearing surfaces applied to reinforced concrete bridge decks, which requires that the surface have a minimum bond strength of 250 psi using ASTM 1583 (ASTM 2004) after 24 hours (Indiana Department of Transportation 2009). The 250 psi minimum bond strength provided in the Indiana Department of Transportation (INDOT) and manufacturer specifications are often limited by the tensile strength of the concrete substrate (Stenko and Chawalwala 2001). At the completion of the TMC cycles, pull-off tests using ASTM 1583 are performed. It was decided to use 250 psi as the target bond strength because that value agrees with state specifications, an apparent industry standard, and the limit of effective adhesion on a traditional reinforced concrete deck.

A cross-section view of the pull-off test and four possible failure modes is shown in Figure 2-8. A pull-off test was inconclusive if failure of the bond to the steel disk, Mode (d) in the figure, occurred below the 250 psi target. To account for the possibility that an individual pull could fail to yield usable results, the specification for the TMC test was written such that a

minimum of nine pull-off tests be used to calculate the average bond strength, and that an individual result be discarded if it fails in Mode (d) below 250 psi. Therefore, in order to “pass” the TMC test, the deck must have at least nine successful pull-off tests, and the average of all successful tests must show a strength of at least 250 psi, with not more than one test failing below 50 psi in Modes (a), (b), or (c). The 50 psi minimum requirement recognizes that a wear surface could fail and still have some bond remaining. If a deck has several locations failing to meet at least 50 psi, then the wear surface has failed, and would be unsuitable in the field.

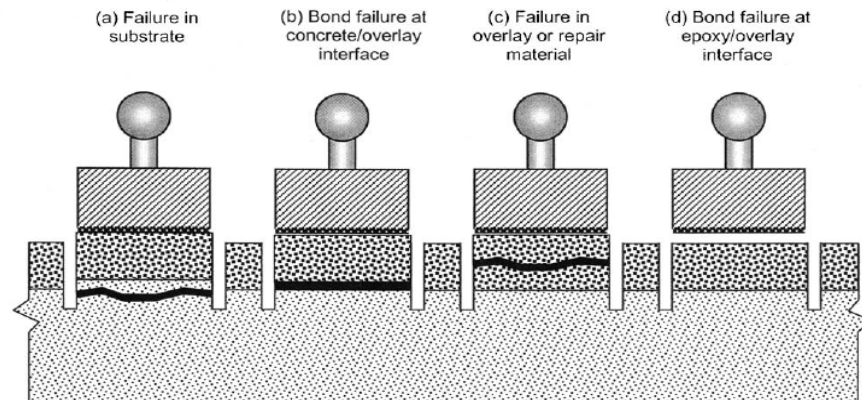


Figure 2-8: Pull-off test failure modes (ASTM C 1583, 2007)

2.3 Sliding Abrasion Tests

In many states, road surfaces are subject to general wear from vehicular traffic and abrasion from snow plows. For example, the carbide wear points and metal blades of snow plows can cause damage to the wearing surface on bridge decks. Hence, the following test was developed so that relative comparisons between traditional reinforced concrete decks and other thin wearing surface systems could be made.

2.3.1 Test Procedure

This test uses a small 3'x5' sample of bridge deck for testing and a skid with a snow plow wear plate mounted at the front to simulate in-situ conditions. This skid, which is loaded with weight, is moved forward and back on the bridge deck by an electric long-stroke actuator continuously over a period of several days. As the deck wears, the skid drops vertically. The amount of vertical drop, which equals the wear in the deck, is measured by laser displacement sensors mounted on the skid. The test was run to establish a stable wear pattern for each deck surface, which typically took 35,000 cycles. At the conclusion of testing, the wear depth for each type of deck was plotted against the cycle count and compared to concrete calibration specimens.

Load Application Skid. The skid was fabricated from a 40" section of W24x55 laid on its weak axis as shown in Figure 2-9. The laser sensors are mounted on the front just forward of the snow plow wear point. Two 500 lb blocks were strapped to the top of the skid using ratchet straps. The 500 lb load was selected to represent the load on a given plow shoe for a typical state plow. Vibration of the blocks against the skid is prevented by elastomeric bearing pads placed below each block. The total load over the wear point was measured at 630 lbs.

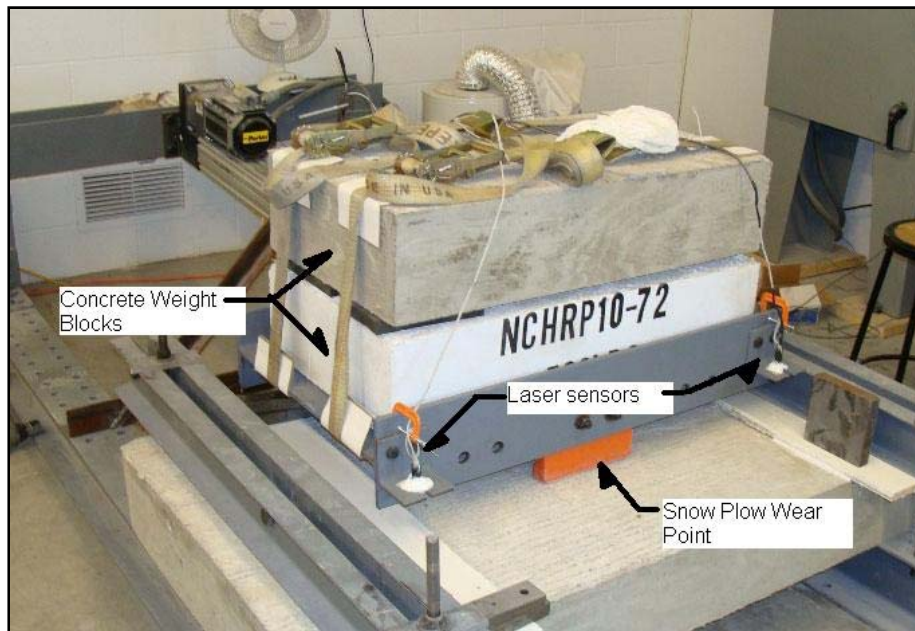


Figure 2-9: Sliding abrasion test setup

2.3.2 Selection of Materials

This section describes the specimens which were tested during the development of the Sliding Abrasion Test. All of the specimens must be five feet wide, and at least 30" long in order to fit in the test frame and be wide enough for the wear path.

Concrete Calibration Slabs. The initial calibration runs on the Sliding Abrasion test were performed on standard 8" thick reinforced concrete samples. The calibration samples had top and bottom rebar running in both directions, and were based on Indiana Department of Transportation plans for a slab on girder bridge for I-65 over State Road 25. The calibration slabs were fabricated with 2 ½" of top cover and one inch of bottom cover. The longitudinal (five foot direction) reinforcement consisted of #4 bars at 14" on center on the top and #5 bars at 14" on center on the bottom. The transverse reinforcement consisted of #5 bars at 8" on center on the top and bottom. A plan view showing the arrangement of the rebar in the slab is shown below in Figure 2-10.

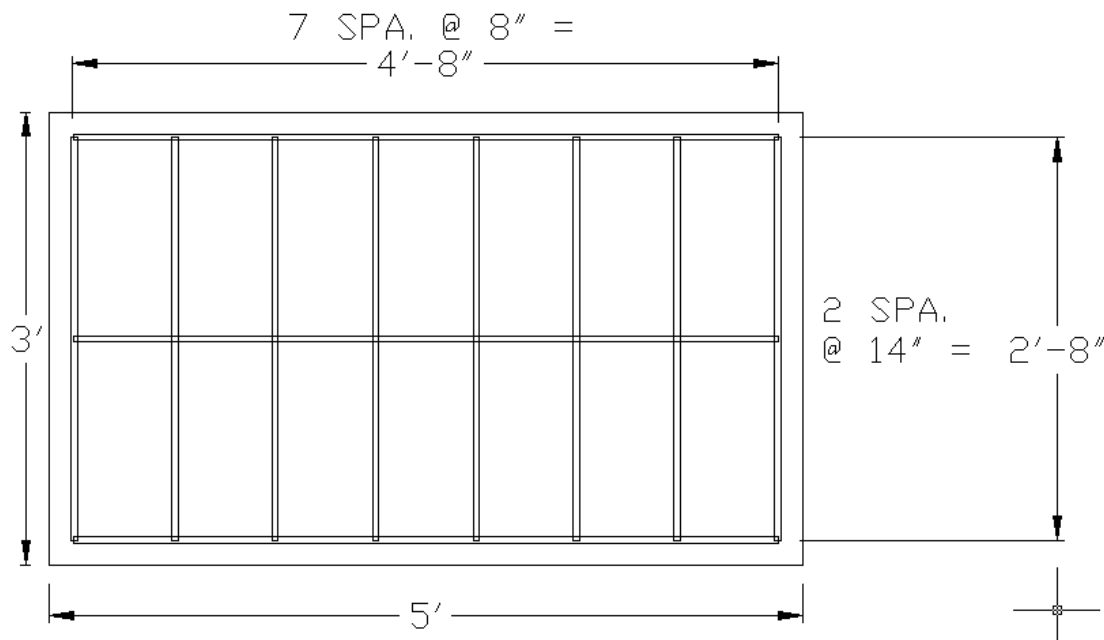


Figure 2-10: Concrete calibration slab reinforcement plan view

Wear Surfaces and Deck Types. The same two wearing surfaces described in Section 2.2.1 were used for this procedure. Both surfaces were thin epoxy and aggregate wear surfaces. The first surface was T-48, applied by the Slurry Method as described in the manufacturer's literature. Euclid Chemical's Flexolith wear surface, applied by two coat broadcast, was also tested. Table 2-2 shows all of the specimens tested. There were also two steel plate specimens tested, one with Flexolith, and the other with T-48.

Table 2-2: Sliding test specimen matrix

Specimen Type	Number	Wear Surface
Concrete	3	None
5" ZellComp FRP	2	Flexolith
5" ZellComp FRP	2	T-48
Steel Orthotropic	1	Flexolith
Steel Orthotropic	1	T-48

2.4 Impact Test

2.4.1 Motivation for Test

During the lifespan of a bridge, it is likely that a deck would be subjected to direct impacts of varying intensity at some time. Examples of this type of loading include vehicle collisions, freight falling off truck beds, and trailer hitches coming loose. The test described below subjects a sample piece of the bridge deck under consideration to direct impacts of variable intensity and rates its performance using an indexing system relative to a traditional reinforced concrete deck.

2.4.2 Test Introduction

Due to the random nature of impact loading that a deck may see over its lifetime, it would be impractical to attempt to replicate every type of possible impact and to evaluate each individually. It was therefore decided to use a single impact tip, which is described in Section 2.4.5, and vary the impact energy in order to determine the behavior of a deck. Reinforced concrete decks were the first tested in order to establish a “calibration” baseline for damage. Following the calibration testing, FRP and Steel Orthotropic decks were tested and rated using the indexing scale developed for comparison.

Direct impact on any deck with a non-uniform cross section presents a unique challenge for this test and assessment of damage because the amount of damage varies depending on the relative location of the impact. For example, in the ZellComp FRP deck, shown in Figure 2-11, an impact over the clear spans between the T sections produced more severe damage to the top plate than if the impact were over the webs or flanges of the T sections.

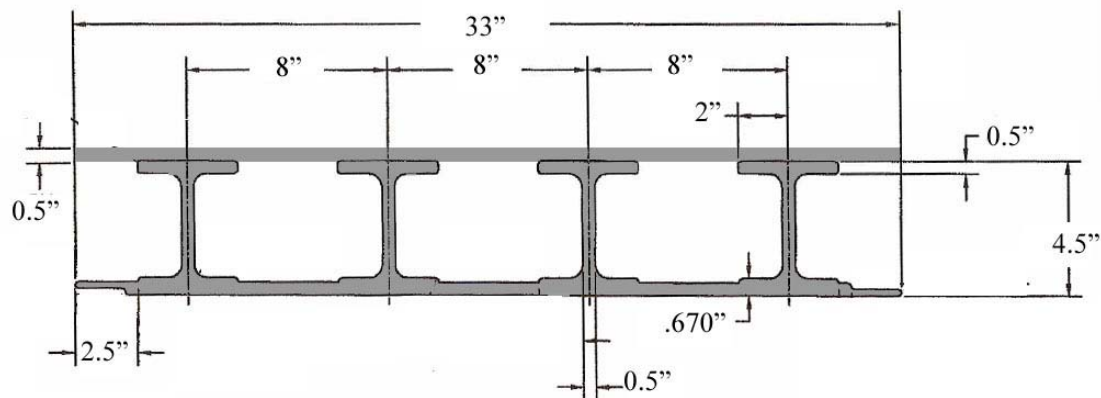


Figure 2-11: ZellComp 5" deck cross section

Another example of a non-uniform type of cross section is a Steel Orthotropic deck. This deck would have a different behavior depending on whether an impact struck the deck directly over a rib, where there would be greater local stiffness, or on the plate between ribs. The concept of variable damage by location is applicable to all deck types which have a non-homogeneous cross section. The variable damage will be accounted for using the indices described in Section 3.4.

2.4.3 Materials Used

The reinforced concrete specimens used for this testing were identical to those used for the Sliding Abrasion Test described in Section 2.3.2. The FRP decks were 5 inch ZellComp decks with epoxy concrete wearing surfaces applied in the laboratory, also identical to those used for the Sliding Abrasion Test described in Section 2.3.2. The two 3'x5' orthotropic steel plate decks were fabricated in the lab using L4x4x $\frac{3}{8}$ " angles welded at 14 inches on center along the five foot direction to $\frac{5}{8}$ inch or $\frac{1}{2}$ inch plates as shown in Figure 2-12. These specimens were intended to replicate the local stiffness at the rib to plate intersections of typical orthotropic bridge deck. As shown in **Error! Reference source not found.**, this was achieved by providing angles with the same vertical leg thickness of typical ribs welded at the same spacing. This approximation of local stiffness was performed to avoid fabricating the exact deck, which would have been cost prohibitive.

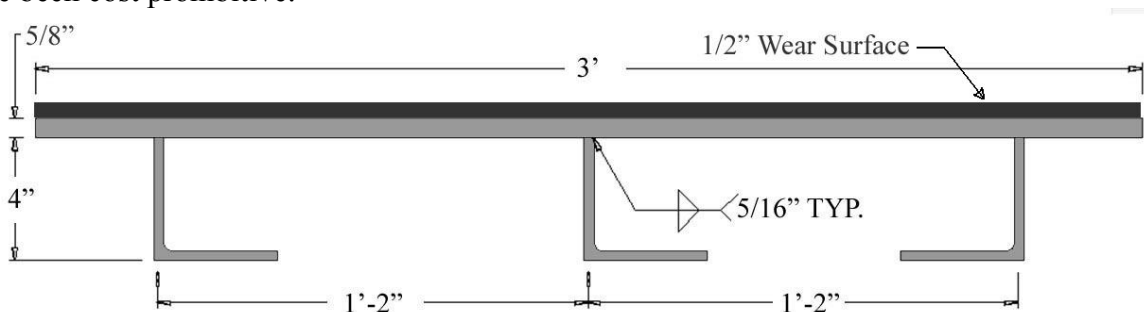


Figure 2-12: Steel orthotropic deck panel cross section

The specimen matrix for the Direct Impact Test is shown in Table 2-3. The three identical concrete specimens were tested first, followed by two FRP decks, one with a Flexolith

wear surface and the other with a PolyCarb surface. The two steel specimens were tested last, one with T-48 wear surface and the other with Flexolith.

Table 2-3: Impact test matrix

Material	# of Specimens	# of Drops	Wear Surface
Concrete	3	41	N/A
FRP	1	17	PolyCarb
FRP	1	10	Flexolith
Steel Orthotropic	1	10	Flexolith
Steel Orthotropic	1	10	T-48

2.4.4 Impact Test Frame

Figure 2-13 shows the impact frame in elevation view along with a picture of the installed frame. The frame is a 15 foot tall square with four columns at the corners made of 4 inch angles. There are three vertical bays, with X bracing in the top two, and rigid base plates on each column. The entire frame was post tensioned to the laboratory strong floor using DWYIDAG rods. The Impact Head assembly, shown in the bottom of the figure, travels along a set of guide tracks running through the center of the frame. The guide tracks are supported by 4 inch angles at 5 feet and 15 feet above the laboratory floor.

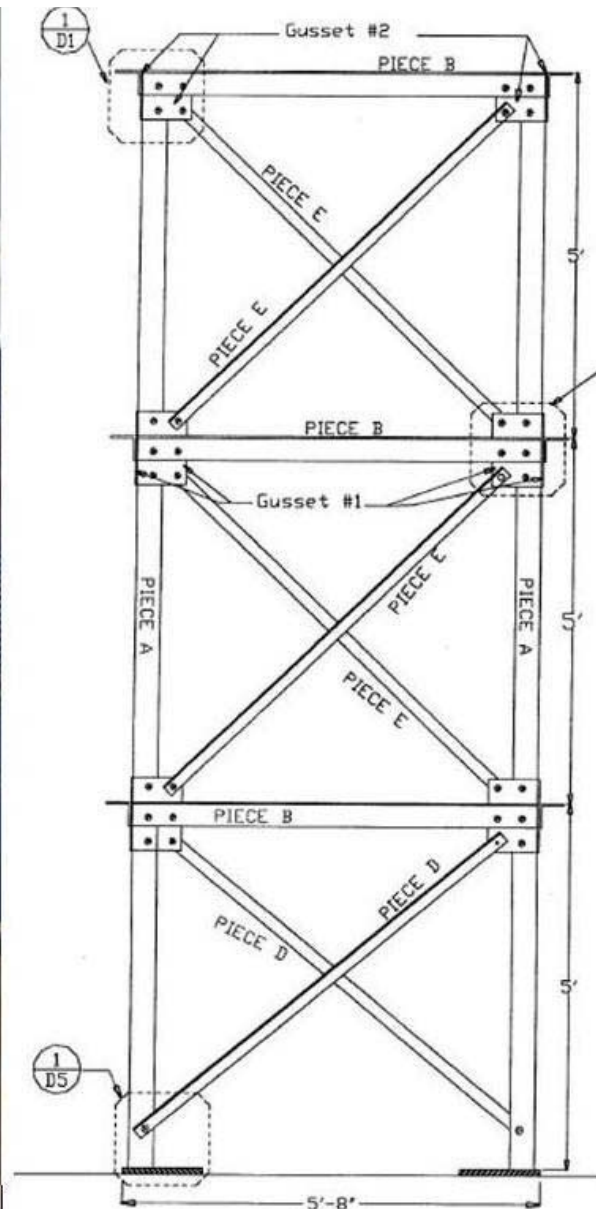
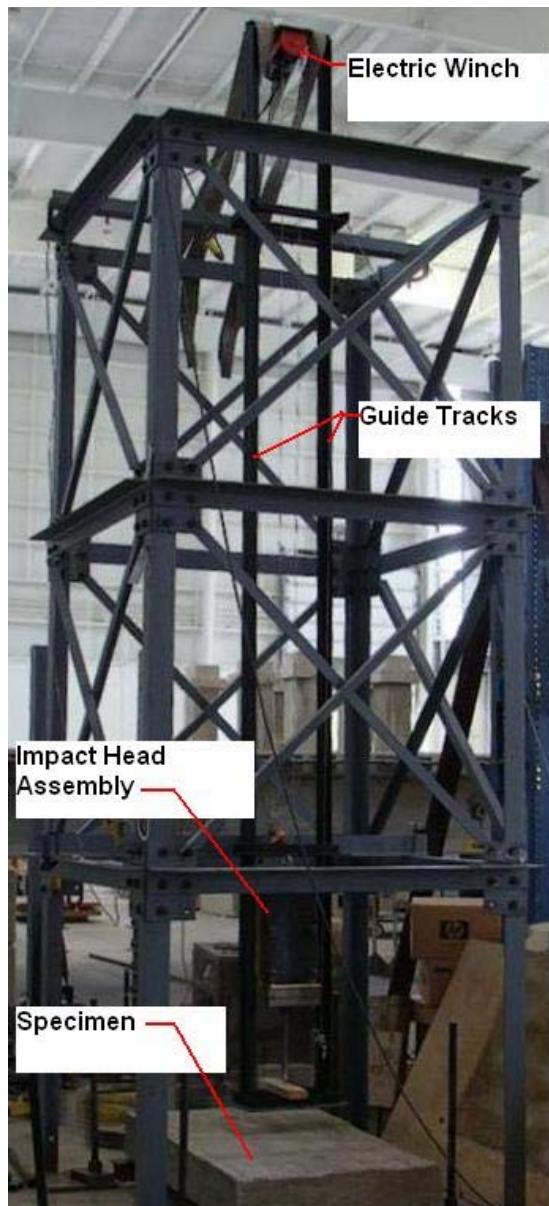


Figure 2-13: Impact test frame picture and elevation view

2.4.5 Impact Head Assembly

The Impact Head was fabricated to use commercial jackhammer bits as the striking piece in place of pipe because they were designed for impact loading against concrete. The head, shown in Figure 2-14, used two 1 inch plates welded together, with a 2 inch pipe welded into a center-hole to support the impact tip. A set screw tapped into the 2 inch pipe allowed the jackhammer bit to be fastened in place without welding and easily changed when it became worn. Several bits were tested on concrete for maximum effect in this apparatus, and a 1½ inch spade bit was determined to be the best because it produced deep, regularly shaped divots and did not become stuck in the concrete. This head with spade bit was used for all subsequent calibration and testing.

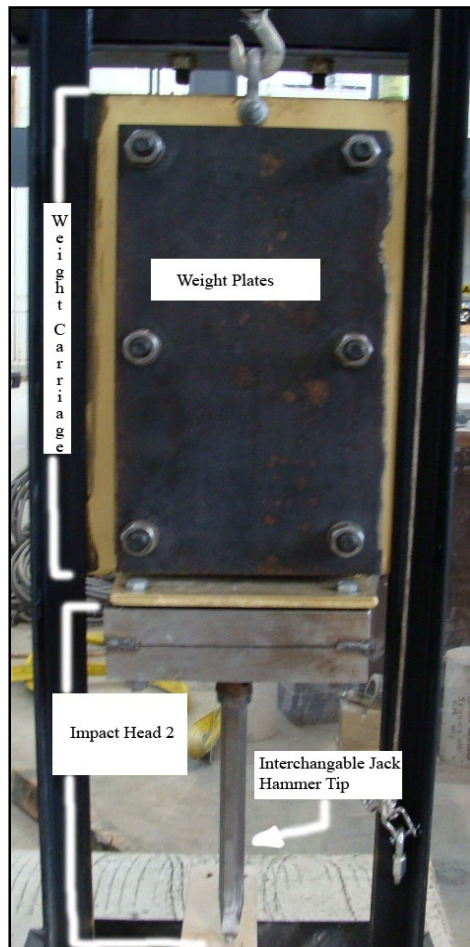


Figure 2-14: Impact head with tip bolted to weight carriage

2.4.6 Test Procedure

Impact testing began at low energy levels and progressed to higher levels until a serviceability issue had been created. The energy for the drops was measured using foot-pounds as shown in Equation 2-9. For this calculation, the height was measured as the total distance of the drop, from the top of the specimen to the bottom of the impact tip. The weight is the measurement of the entire Impact Head assembly. For each drop the desired amount of weight plates were bolted to the Impact Head and the bolts were pre-tensioned to prevent the weight plates from slipping. The drop assembly was positioned over an undamaged portion of the deck specimen using the overhead crane and secured to the frame. Before the head was raised, the tip was inspected for damage and if its point was fractured, the tip was replaced. An electric winch, mounted at the top of the frame, was used to raise the impact head to the desired height. A quick release mechanism, mounted between the impact head and the lift cable, was then triggered to drop the head onto the specimen.

$$\text{Energy(ft * lbs)} = H \text{ (ft)} * W(\text{lbs}) \quad (2-9)$$

Each drop site was inspected visually and depth, length, and width of the damage area were recorded in the log book.

2.5 Large-Scale Specimen

2.5.1 Experimental Design

A large-scale specimen was designed and subjected to various loading conditions to better understand the behavior of bridge decks subjected to truck traffic. The specimen included both longitudinal and transverse deck splines, which were the focus of the testing. This specimen was constructed and tested prior to the subassembly tests so that data could be used to aid in the development of the subassembly tests. A partially-filled grid deck was selected since it is a unique type of deck that could have durability issues with its many critical details (e.g. welds and joints). It was also found that an FRP deck of the size required for the testing was cost prohibitive and could not be incorporated into the available project budget.

2.5.2 Specimen Configuration and Materials

Specimen Overview. The large-scale partially filled grid deck specimen was designed as a single-span, three girder bridge. The bridge had a 40 foot span length and a 20 foot wide deck. The bridge deck was supported by three W30x124 rolled beams spaced at 8 feet. Pin and roller supports were used to simulate the simple span condition. These supports were placed on concrete blocks which were post-tensioned to the strong floor in the laboratory.

Diaphragm bracing was used to brace the girders at the centerline of each bearing and at the mid-span of the bridge during construction. The diaphragm bracing system consisted of channels connected to the girders by bolted angles.

Deck Panel Overview. Steel grid deck panels were obtained for use as the bridge deck for the large-scale specimen. This deck type was constructed of:

- 5 3/16" rolled beams for the main bars spaced at 10"
- 1/4" x 2" rolled beams for the crossbars spaced at 4"

- 5/16" x 1" rolled beams for the supplemental bars spaced at 3.33"

The bridge deck consisted of three 8' by 20' panels and four 8' by 10' panels. The three 20 foot panels spanned the entire width of the bridge while the four 10 foot panels spanned from the outside girders to the middle girder and were connected by a longitudinal splice across the middle girder. This configuration allowed for four transverse splices and a longitudinal splice for testing. This also permitted evaluation and comparison of local behavior of the deck in regions with and without longitudinal splices.

A galvanized form pan was located just below the grid of crossbars and supplemental bars which left the lower half of the main bars exposed out of the concrete. Final installation of the partially filled grid deck before the concrete was placed can be seen in Figure 2-15.



Figure 2-15: Final installation of grid deck before concrete placement

Deck-to-Superstructure Connection. The deck-to-girder connection was made with shear studs encased in a full depth haunch as per the manufacturer specification. Shear studs were installed along the length of each girder to create composite action of the deck with the girders. The size of shear studs that were used was 3/4" diameter by 7" long with a 13" spacing to achieve a fully composite connection based on AASHTO LRFD design requirements.

Deck Concrete. The concrete mix used in the partially filled grid deck for the large-scale specimen was a standard INDOT Class C mix with a #12 sieve aggregate size. This mix met the manufacturer's requirements of a minimum concrete compressive strength of 4000 psi and a maximum aggregate size of 3/8". Two full truck loads of concrete were required for placement of concrete of the bridge deck due to its size. Table 2-4 below shows the concrete strengths for each truck after cylinder tests.

Table 2-4: Concrete strength

Strength (psi)		
	7 Days	28 Days

Truck 1	5400	7060
Truck 2	5300	6730

2.5.3 Investigated Details and Instrumentation

A total of 178 strain gages were installed on the steel grid of the specimen to investigate the stresses at critical locations discussed in the following sections. Including the 21 strain gages installed on the girders, 199 strain gages were installed on the large-scale specimen. Detailed instrumentation plans are included in the Research report for this project.

2.6 Large-Scale Specimen Experimental Procedures

2.6.1 Introduction

The experimental procedures for the large-scale specimen include truck roll tests, a longitudinal splice cyclic test, and two transverse splice cyclic tests. The truck roll tests were used to determine the behavior of the partially filled steel grid deck under rolling live load. Cyclic load testing procedures were developed to evaluate the relative durability of critical deck details under millions of cycles of simulated truck tire loading.

2.6.2 Truck Roll Tests

Roll Test Positions. The simulated truck was rolled in six transverse positions on the deck. The positions, which correspond to the centerline of the “truck”, are shown in Figure 2-16. All positions were selected to either represent a normal traffic position and/or produce maximum stresses at critical locations within the deck (e.g. longitudinal splice). Originally, only Positions 1-5 were going to be tested, but to better characterize the response and behavior of the deck to rolling loads, Position 6 was added to the test.

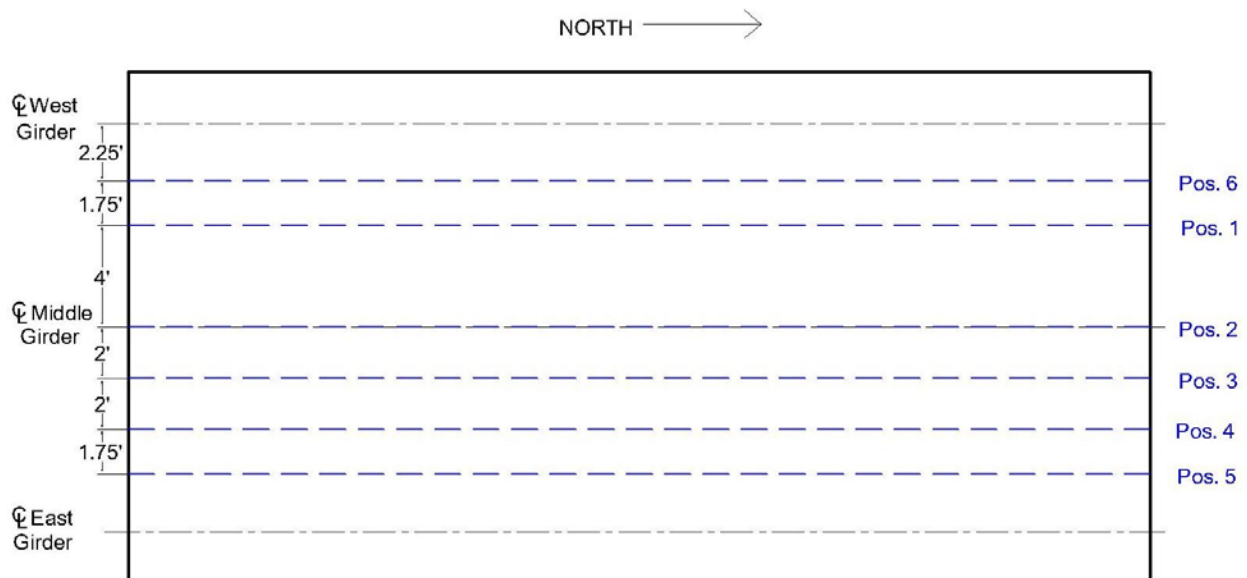


Figure 2-16: Center lines of roll test positions

Truck Load Simulator. The truck load simulator used for the roll tests is shown in Figure 2-17. The truck load simulator consists of a frame, loaded with steel blocks, connected to tandem axles. The truck load simulator provides an accurate representation of the interaction of the deck elements to two axles at a spacing of four feet. The steel blocks used for the load on the truck load simulator weighed 39.2 kips. Each set of tires on the axles was weighed independently to determine the distribution of load from the truck to the deck. The load was equally distributed by all of the tires with a total truck load of 42.1 kips.



Figure 2-17: Truck load simulator

2.6.3 Longitudinal Splice Test

Longitudinal Splice Test Position. The longitudinal splice is a detail which is thought to be vulnerable to damage by fatigue due to bending across the splice. Through analysis of the stresses in this splice during the truck roll test, it was found that Position 2, where the truck was centered over the splice, would produce the highest stresses. In this position, the truck tires caused a negative moment in the splice. Thus, due to these stresses, two load patches were used to load the bridge representing tire loading in this transverse position. The longitudinal position chosen for the load patches was 12 feet from the north end of the bridge. In this position, the load patches were located midway between transverse splices, and there were strain gages on the main bars and the reinforcing steel crossing the splice at this position.

Longitudinal Splice Test Setup. A 220 kip actuator was used to apply the load during the cyclic load test. The actuator along with the load frame is shown in Figure 2-18.



Figure 2-18: Cyclic test load frame

The load patches, which simulate the loading produced by a track axle, were 20 inches wide by 10 inches long, and were spaced at 6 feet center to center. This size and spacing represents the AASHTO LRFD design tire contact area and spacing. The steel plates were attached to the deck with Hydrostone in order to allow for uniform contact to the bridge deck without much compressibility.

Longitudinal Splice Test Procedure. Static tests were conducted to compare the stresses in the deck induced by the load patches to the stresses caused by the truck roll test. These static tests were done at loads of 21 kips and 25 kips. Data were also collected for a load of 30 kips to compare the stresses measured in later static tests. The area around the load patches was inspected and marked for cracks in the concrete after the initial static testing was completed. Since there was previous cracking of the entire structure due to shrinkage and the truck roll test, these marks were used as a baseline for cracking at the beginning of the cyclic test.

After completion of the static tests, the AASHTO design strength load for one axle, 58.2 kips, was used to load the bridge. This load was computed by taking one-half of the AASHTO design tandem, (i.e., 50 kips / 2 = 25 kips), and multiplying by the AASHTO impact factor, 1.33, and the AASHTO Strength I load factor, 1.75. This calculation is shown below:

$$25 \text{ kips} \times 1.33 \times 1.75 = 58.2 \text{ kips}$$

This magnitude of loading promoted the initiation of cracking in the concrete bridge deck that could further propagate during the cyclic loading. The magnitude of the cyclic loading alone may not have been able to generate the same cyclic damage a structure in service, subjected to overloads, could produce in the absence of this applied design strength load. To introduce

cracking, 100 load cycles of 58.2 kips were applied to the bridge. Following this loading, the bridge was marked for crack growth. A 30 kip static test was carried out to check for any noticeable structural damage from this loading which would result in an increase in stresses.

The cyclic load range used during cyclic testing was calculated from the AASHTO HS-20 axle by dividing the tandem, 32 kips, into two axles and multiplying by the AASHTO Fatigue II load factor, 0.75, and the AASHTO impact factor, 1.15. This calculation is shown below:

$$32 \text{ kips} \times 0.5 \times 0.75 \times 1.15 = 13.8 \text{ kips}$$

This load was then doubled in order to accelerate the testing procedure giving a total load range of 27.6 kips. It is noted that doubling the cyclic load is actually equivalent to the AASHTO Fatigue I load combination and hence, not unreasonably high. The number of cycles for the test was calculated by multiplying the assumed number of axles per truck by the ADTT and the desired life. This calculation is shown below:

$$4.5 \text{ cycles} \times 1500 \text{ ADTT} \times 20 \text{ yrs} \times 365 \frac{\text{days}}{\text{yr}} = 49.3 \text{ million cycles}$$

Since the load was doubled to accelerate the testing procedure, AASHTO LRFD 5th Edition equation 6.6.1.2.5-2, seen below, was consulted to determine that doubling the stress range would decrease the cycles by a factor of 8 (2^3) in order to cause the same cumulative fatigue damage. This calculation can also be seen below:

$$(\Delta F)_n = \left(\frac{A}{N} \right)^{\frac{1}{3}} \quad \text{LRFD Eq. 6.6.1.2.5-2}$$

A = constant

N = number of cycles

$(\Delta F)_n$ = the nominal stress range

$$\frac{49.3 \text{ million cycles}}{2^3} = 6.2 \text{ million cycles}$$

Therefore, a load range of 27.6 kips was applied for 6.2 million cycles for the cyclic load test. It is recognized that the above presumes Miner's rule can be applied to the deck system.

A small preload was used to keep all of the plates in contact during testing. Every 500,000 cycles, the deck was inspected for crack growth and static tests were completed to check stresses. A high frequency pneumatic vibrator was used to simulate the vibrations caused by trucks passing over a bridge. The vibrator was installed on the bridge deck at 1 million cycles and run for 1 minute at half million cycle intervals.

Initially, the static tests were run up to a load of 30 kips to compare to the data collected prior to the cyclic test. The 30 kip static tests were carried out at 193,500 and 526,000 cycles. Later, it was decided to increase the maximum load of the static tests to 58.2 kips in order to simulate the interspersed heavier trucks which would likely add to the fatigue damage of the deck. This load was used for all remaining static tests.

As will be discussed in further detail in Section 3.5.9, it was decided to terminate the longitudinal splice test after 4.3 million cycles instead of running it to 6.2 million cycles due to a lack of significant damage.

2.6.4 Transverse Splice Tests

Transverse Splice Test Positions. The transverse splice in the bridge deck is a detail which is thought to be vulnerable to fatigue damage due to bending across the splice. In many cases, the transverse splice in steel grid type decks is located over a stringer or floorbeam. Hence, negative moments are produced. In the large-scale specimen for this testing program, no stringers or floorbeams were utilized. Therefore positive moments are produced in the transverse splice detail.

To evaluate this detail, loading was applied on one side of the splice to cause bending stresses across the splice. If the load patch was centered on the splice, it was thought that the load from the patch would directly load the crossbars on either side of the splice and produce less local bending across the splice. The shear would also be considerably less. Two transverse splice tests were completed on separate locations of the large-scale specimen to check the repeatability of the results.

The transverse splice test for each position only used one load patch. If both load patches would have been used and at the same 6 foot spacing as the longitudinal splice test, the other tire patch would have been very close to a girder. The girder would have stiffened the transverse splice at that location and carried most of the load directly across the splice. This added stiffness would not have allowed for a thorough investigation of the possible damage of the splice.

To produce the largest demands on the splice, the transverse position of the single load patch for the transverse splice tests was located halfway between the middle and edge girders. The longitudinal position of the load patch was centered 7 inches south of the centerline of the transverse splice. In this position, the north edge of the load patch was 2 inches south of the centerline of the transverse splice. Also, the load patch was located very close to the centerline of the splice but in a position so it did not cross the centerline of the splice to ensure there was no “bridging” across the splice. The location of the load patch during the first transverse splice test can be seen in Figure 2-19.

In addition to the initial transverse splice cyclic load test, another transverse splice location was tested to determine if similar behavior and performance would result. The same transverse splice was tested midway between the middle girder and the other exterior girder. Since this position was similar to the previous transverse splice position, a good comparison could be made to the results of the first transverse splice cyclic test. The position for the second transverse splice cyclic load test is shown in Figure 2-19.

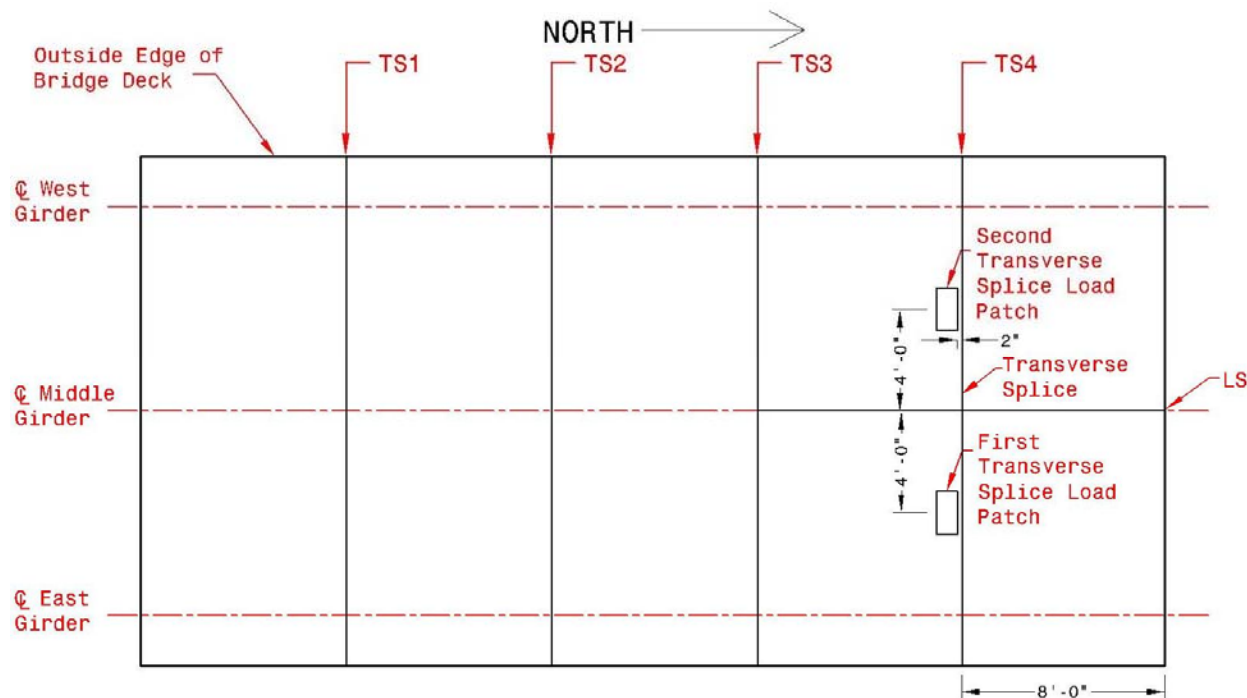


Figure 2-19: Transverse splice load test positions

Due to the close proximity of these load patch areas to the position where the longitudinal splice test was previously tested, the load patch areas were closely inspected for cracking and compared to similar transverse splice areas on the other side of the bridge. It was found that the cracking caused by the longitudinal splice test was localized and did not cause a significant increase in damage at the chosen transverse splice locations. Hence, the earlier testing would not affect the results or performance of the transverse splice test.

Transverse Splice Test Procedure. A similar testing procedure was used for the transverse splice tests as was used during the longitudinal splice test. One major difference was that by only using one load patch, the load needed for the test could be reduced by half. Thus, the cyclic load range used for the transverse splice test was 13.8 kips and the load for the static tests was 29.1 kips. Static tests were conducted at the commencement of the transverse splice test and at 500,000 cycle intervals. These static tests allowed for changes in the stresses during the test to be monitored. The transverse splice was inspected for damage on the top and bottom of the deck after each set of the static tests was completed. The first transverse splice test was terminated after approximately 6.5 million load cycles. The second transverse splice test was terminated after approximately 10 million cycles. This test was extended to see if any additional damage would occur beyond the 6.5 million cycles originally planned.

2.7 Subassembly Stiffness Tests

Two subassembly steel grid deck specimens were obtained for stiffness testing. The first specimen was an open grid deck, and the second was an open grid deck with a form pan such that the specimen could be partially filled with concrete. Therefore, a total of three specimens

were tested to determine stiffness properties and validate the test methods developed. The three subassembly stiffness specimens tested were:

- Open Grid Deck Specimen #1 – the first specimen obtained;
- Open Grid Deck Specimen #2 – the second specimen obtained prior to being partially filled with concrete; and
- Partially Filled Grid Deck Specimen – the second specimen obtained after partially filled with concrete and cured for 28 days.

These orthotropic specimens were each subjected to the three stiffness tests to isolate and obtain the following properties:

- Strong Axis Direction Stiffness (D_x);
- Weak Axis Direction Stiffness (D_y); and
- Torsion Stiffness (D_{xy}).

Table 2-5 shows a test matrix for the subassembly stiffness specimens. The stiffness properties determined from these tests could then be used to compute the minimum load required for the strength verification tests of subassembly longitudinal splice, transverse splice, and deck-to-superstructure connection specimens.

Table 2-5: Subassembly Stiffness Test Matrix

Specimen	Strong Axis Stiffness Test	Weak Axis Stiffness Test	Torsion Stiffness Test
Open Grid Deck #1	X	X	X
Open Grid Deck #2	X	X	X
Partially Filled Grid Deck	X	X	X

Note: “X” indicates test completed.

2.7.1 Experimental Design

These tests were used to develop methods to establish the various stiffness parameters associated with a given deck type. Specifically, standard tests were developed to obtain strong and weak direction bending stiffness (D_x and D_y) as well as torsion stiffness (D_{xy}) of a given deck type. The stiffness parameters determined from these tests could then be used to determine the appropriate load to be applied for the strength verification tests discussed later in this report.

2.7.2 Specimen Configuration and Materials

Open Grid Deck Specimen #1. Subassembly open steel grid deck panels were obtained for stiffness testing. The selected specimen, shown in Figure 2-20, had dimensions of 6’-3” long by 6’-3” wide (i.e., a square) and consisted of:

- 5-3/16” deep main bars spaced at 7-1/2”
- 1” deep, 1/4” thick supplemental bars spaced at 7-1/2” alternating with main bars
- 2” deep, 1/4” thick cross bars, spaced at 3-3/4”, running transverse to the main and supplemental bars; and
- 1” deep, 1/4” thick diagonal bars.



Figure 2-20: Open grid deck specimen #1

Open Grid Deck Specimen #2. A second grid deck specimen was obtained to determine the stiffness properties both with and without concrete. The configuration of the steel in the deck panel was identical to that used in the large-scale specimen. This specimen, shown in Figure 2-21, had total dimensions of 6'-8" long by 6'-8" wide. The configuration of steel was different than that of open grid deck specimen #1. The main bars were spaced at 10 inches center to center with two supplemental bars equally spaced in between. The cross bars were spaced at 4 inches center to center. Additionally, a 20 gauge thick form pan was tack welded to the main bars for the placement of concrete. However, no diagonal bars were included for this specimen. Both open grid deck specimens tested were considered typical types of steel grid decks used in practice.

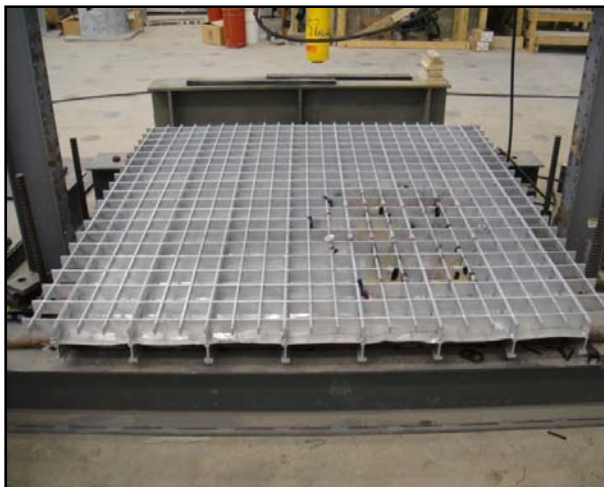


Figure 2-21: Grid deck specimen prior to concrete placement

Partially Filled Grid Deck Specimen. The steel open grid deck specimen discussed in the previous section was then partially filled with concrete, as shown in Figure 2-22. A concrete

overfill of 2 inches was used, giving a total concrete depth of 4.5 inches. This made the deck specimen a representative sample deck panel of the large-scale specimen previously discussed.



Figure 2-22: Partially filled grid deck specimen

The concrete mix that was used was an INDOT Class C mix with a #12 sieve aggregate size (*i.e., the same as was used for the large-scale specimen*). This mix met the manufacturer requirements of a concrete compressive strength of 4000 psi and a maximum aggregate size of 3/8". The concrete compressive strengths, shown in Table 2-6, were measured by breaking two cylinders weekly up to 28 days when the stiffness tests were to commence.

Table 2-6: Measured concrete compressive strength

Test Day	Test #1 Strength (psi)	Test #2 Strength (psi)	Average Strength (psi)
7	4204	4280	4242
14	4513	4429	4471
21	4779	5145	4962
28	5294	5601	5448

2.7.3 Stiffness Test Experimental Setup

Strong Axis Direction. The strong axis direction stiffness, for each specimen, was tested by applying a line load transverse to the main bars as shown in Figure 2-23. The line load was constructed from a 2" wide steel plate placed on top of a 3/4" wide bearing/rubber material to distribute the load evenly to the deck specimen. Both the steel and bearing material were 1" thick.



Figure 2-23: Line load on deck specimen for strong axis direction stiffness test

The line load was applied at the mid span of the deck specimens which were supported near the edges on rigid supports as shown in Figure 2-24. The main bars were shimmed to ensure that they were all in contact with the supports.

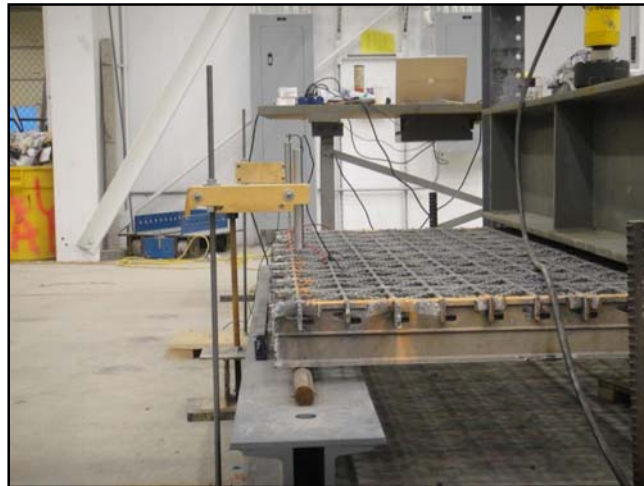


Figure 2-24: Edge of deck on rigid support

Weak Axis Direction. After completion of the strong axis direction stiffness test, the deck specimens were rotated 90°. The same materials and test set-up were used for the application of the line load as were used for the strong axis direction. Again, the main bars were shimmed as required to ensure that they were fully in contact with the supports.

Torsion. The torsion stiffness test set-up is different than those of the strong and weak axis direction stiffness tests. The bridge deck panel was arranged such that three corners were placed on supports while the fourth corner, where load was to be applied, was free (i.e., no restraint). Two corners sat on point supports while the corner opposite to the loading was restrained from vertical movement. This restraint was created by placing a point support below the corner of the specimen and placing an inverted point support above it as shown in Figure 2-25.

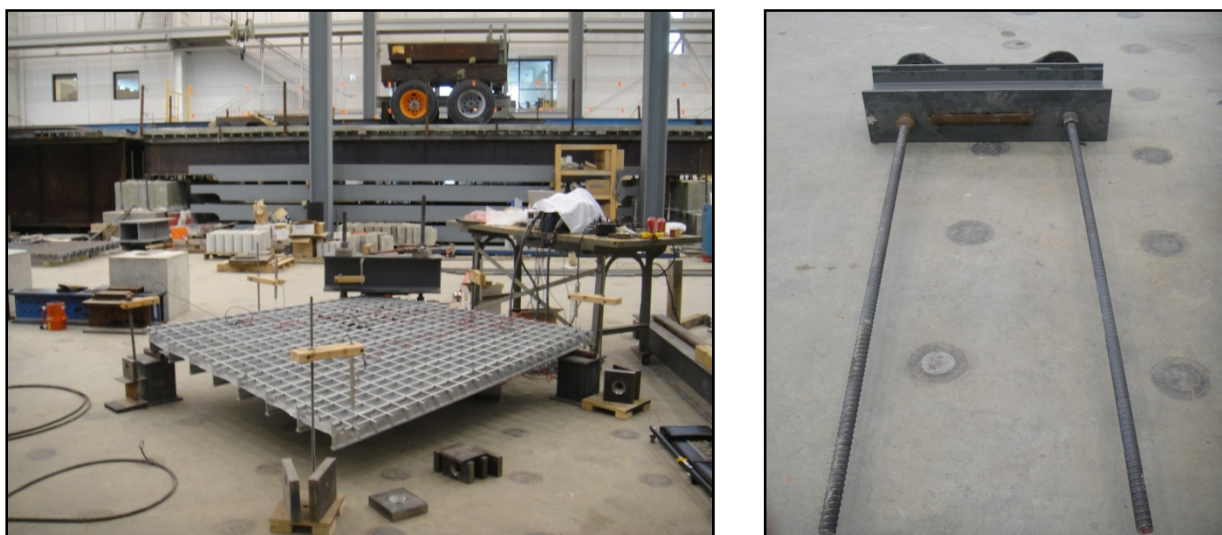


Figure 2-25: Torsion test (left) setup; (right) inverted point support before installation

2.7.4 Stiffness Test Experimental Procedure

Strong Axis Direction. Before beginning testing of each specimen, the deck was loaded and unloaded to a previously established load level three times. The preload was then reapplied to bring all bearings into contact and to “shake down” the specimen in the fixture. As shown in Table 2-7, the partially filled grid deck required a larger preload to seat the specimen since it was stiffer. After the application of the preload, all instrumentation was zeroed. Data were then collected at five approximately equal force intervals up to a pre-determined maximum load. At each load increment, the load was maintained for a minimum of ten seconds to collect data. The summary of the loads applied are shown in Table 2-7.

Table 2-7: Summary of loads applied for strong axis stiffness tests

Specimen	Open Grid Deck #1	Open Grid Deck #2	Partially Filled Gird Deck
Preload (kips)	5	5	6
Force Increment (kips)	1	1	1.2
Maximum Load (kips) [preload taken as zero]	5	5	6

This procedure was repeated three times for each specimen to collect an adequate amount of data and ensure that the results were repeatable and consistent. Once all tests were completed, the data were used to determine stiffness properties of the deck for this direction.

Weak Axis Direction. Similar to the strong axis direction stiffness test, the deck was loaded and unloaded to a pre-determined preload three times. The preload was then reapplied to bring everything into contact. After the application of the preload, a digital zero was applied to the instrumentation. Data were then collected at five approximately equal force intervals up to a pre-determined maximum load. At each load increment, the load was maintained for a minimum of ten seconds to collect data. The summary of the loads applied are shown in Table 2-8.

Table 2-8: Summary of loads applied for weak axis stiffness tests

Specimen	Open Grid Deck #1	Open Grid Deck #2	Partially Filled Gird Deck
Preload (kips)	1	1	6
Force Increment (kips)	0.5	0.5	1.2
Maximum Load (kips) [preload taken as zero]	2.5	2.5	6

Torsion. Since the deck was very flexible in torsion, it was found that it was not necessary to apply a preload to fully seat and shake down the specimen. Furthermore, calibrated steel plates were deemed to be appropriate for applying load. Before any load was placed on the free corner, a digital zero was applied to all instrumentation. Load was then placed on a 6" x 6" patch at the free corner of the deck in five approximately equal load increments as shown in Table 2-9.

Table 2-9: Summary of loads applied for torsion stiffness tests

Specimen	Open Grid Deck #1	Open Grid Deck #2	Partially Filled Gird Deck
Preload (lbs)	0	0	0
Force Increment (lbs)	7	7	50
Maximum Load (lbs) [preload taken as zero]	38	38	250

This test was repeated after the specimen was rotated 90°, to measure the stresses in a different region of the deck under the same loading. Finally, the deck was again rotated 90° to ensure data were collected in multiple positions. These rotations also ensured the repeatability of the displacements measured during the test. Once again, this procedure was repeated a minimum of three times to collect an adequate amount of data and ensure that the results were reasonable and consistent. Once all runs of this test were completed, the data were organized and used to determine torsion stiffness properties of the deck.

2.8 Subassembly Longitudinal Splice Test

2.8.1 Experimental Design

Prior to the development of the subassembly longitudinal splice test, data from the large-scale specimen were collected and analyzed to understand the critical loading scenario. Furthermore, the large-scale testing was used to understand the behavior and stresses experienced by this detail of the bridge deck. Using the data obtained, a longitudinal splice test method for subassembly specimens was developed and verified. The standard test method was developed so that a “slice” of a large-scale bridge deck, as shown in Figure 2-26, could be tested to reveal and identify any deficiencies of the longitudinal splice or deck that would occur in service.

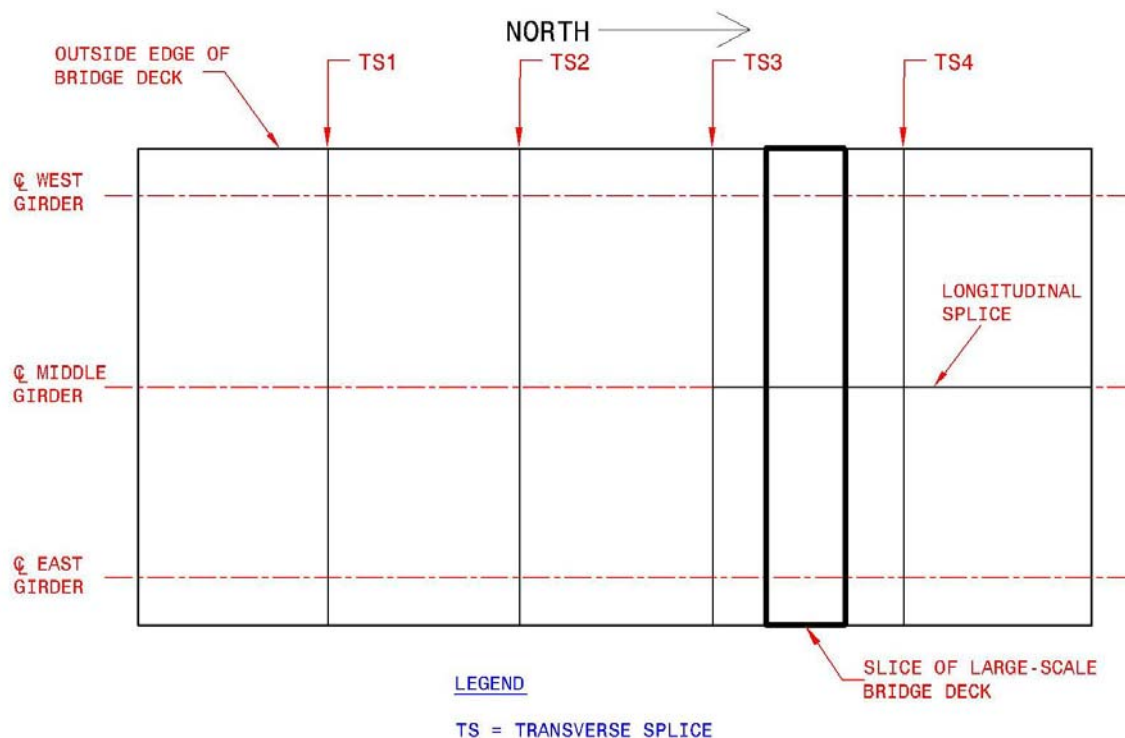


Figure 2-26: “Slice” of large-scale deck represented by subassembly longitudinal splice test

2.8.2 Specimen Configuration and Materials

Steel grid deck specimens and reinforcing steel were obtained for the subassembly longitudinal splice tests. Two steel grid decks were placed on stringers set at 6 feet center to center spacing as shown in Figure 2-27(left). The decks bolted to the stringers as shown in the details in Figure 2-27(right). The configuration of structural steel in the deck panels was similar to that of the open grid deck specimen #2 (i.e., same spacing and size of bars). These two decks specimens were connected through a longitudinal splice using 5' long #4 reinforcing steel spaced at 3-5/16". The steel grid deck specimen was then partially filled with concrete, as shown in Figure 2-27(left). This was done to ensure it was representative of the large-scale specimen and similar to the partially filled grid deck specimen used for the subassembly stiffness tests previously discussed.



Figure 2-27: Subassembly longitudinal splice specimen (left) on stringers; (right) bolted connection to stringers

An INDOT Class C concrete mix with a #12 sieve aggregate size (i.e., the same as was used for the large-scale specimen and subassembly stiffness tests) was used. Concrete was not cast over the exterior bolt down plates to allow access if required to make adjustments to the deck to stringer connection prior to or during testing. The compressive strength of the concrete was tested at 7, 14, 21 and 28-days and compared to those of the subassembly stiffness tests. As shown in Table 2-10, the concrete compressive strengths at 28 days were within 3% of each other. Therefore, the stiffness of the subassembly longitudinal splice deck specimen did not need to be re-evaluated.

Table 2-10: Measured concrete compressive strength

Test Day	Stiffness Test Average Strength (psi)	Longitudinal Splice Test Average Strength (psi)	Ratio of Long. Splice to Stiffness Test Conc. Strength
7	4242	4898	1.15
14	4471	5362	1.20
21	4962	5514	1.11
28	5448	5638	1.03

2.8.3 Strength Verification Test

This static test was intended to verify that the longitudinal splice in the deck meets a minimum strength requirement. The “Proposed Recommended Method for Verifying Strength of Bridge Decks,” included in Appendix D of this report, was developed for simple spans. Therefore, this test was conducted following the “Proposed Recommended Method for Verifying Strength of Bridge Decks” and making adjustments to the load to account for a two-span system.

For a simple span deck, the load would be applied through a patch load at mid span of the deck (i.e., the positive moment region). However, the longitudinal splice, which was the critical detail, was located in the negative moment region (i.e., over the interior stringer) of the two-span system. Therefore, the minimum requirement of the load for the strength verification test was adjusted to account for the following factors:

- Application of load through two patches rather than a single load patch;
- Locations of the load patches;
- Two-span deck system rather than a simple span; and
- Critical detail located in negative moment region rather than positive moment region.

This test was conducted prior to the cyclic loading test to evaluate the strength of the deck and to introduce cracks in the concrete before cyclic load testing would commence. The test was conducted both with flexible supports and rigid supports as shown in Figure 2-28. The use of concrete blocks on top of steel plates at the location of the deck specimen gives the effect of having rigid girders. Therefore, the strength of the longitudinal splice could be tested independent of the rest of the structural system, which is preferred for this test. A hydraulic jack was used for the longitudinal splice strength verification test because the required load, 59 kips, was greater than could be applied by the 55-kip actuator that was being used for the cyclic load tests. The load was distributed through two 20" x 10" patches equally spaced at 2 feet from centerline of the interior stringer (i.e., 4 feet center to center spacing of patches) using a spreader beam. The patch loads were oriented such that they represented the direction of traffic. Hydro-stone was placed between the plates and the deck to ensure they were level and that the load was applied properly.

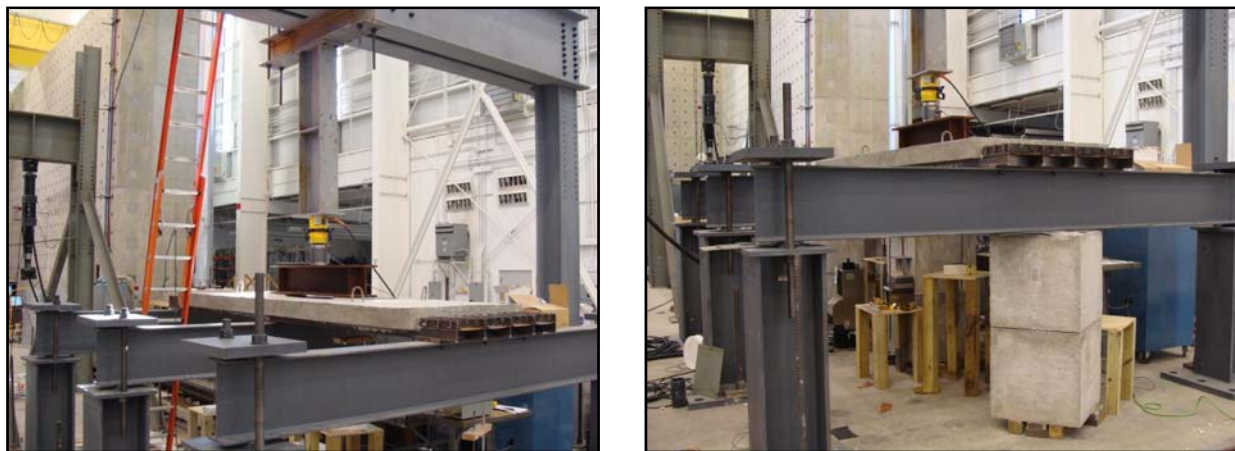


Figure 2-28: Longitudinal splice strength verification test (left) flexible supports; (right) rigid supports

2.8.4 Cyclic Load Test

A cyclic load test of the longitudinal splice was also conducted. It was desirable to test the longitudinal splice as a part of the entire structural system rather than independent of the flexible superstructure (i.e., stringers). Therefore, flexible girders simulating those expected to be used in service (e.g. the large-scale specimen) were used rather than rigid girders.

An applied load range of 27.6 kips with a small preload was applied (i.e., as was done for the large-scale longitudinal splice cyclic loading test) by a 55-kip actuator. The load was distributed equally through two 20" x 10" patches as was done for the strength verification test described in the previous section. Angles, shown in the Figure 2-29, were installed on either side of the spreader beam along its length as a safety precaution to prevent lateral movement of the spreader beam. The test was terminated after approximately 6.75 million load cycles.



Figure 2-29: Subassembly longitudinal splice cyclic load test (left) setup; (right) application of load

A high frequency pneumatic vibrator was installed on the interior stringer adjacent to the deck. At half million cycle intervals, the pneumatic vibrator was excited for a minimum of one minute to simulate the vibrations caused by trucks passing over a bridge. Fatigue load static tests were conducted after the pneumatic vibrator was excited and data were collected.

2.9 Subassembly Deck-to-Superstructure Connection Test

2.9.1 Experimental Design

Prior to development of the subassembly deck-to-superstructure connection test, literature regarding deck-to-superstructure connections was reviewed. The literature review was primarily used to determine common deck-to-superstructure connection failures and associated causes. The information found in the literature, as well as data and observations from testing the large-scale specimen, was used in development of the subassembly deck-to-superstructure connection test. The standard test method was developed so that a “slice” of a large-scale deck, as shown in Figure 2-30, could be tested to reveal and identify any deficiencies of the deck-to-superstructure connection or deck that would occur in service. It is noted that a different type of bridge deck was tested for the subassembly deck-to-superstructure connection test than was tested for the large-scale specimen as will be discussed in the following section. However, Figure 2-30 shows a “slice” of the large-scale specimen tested for illustrative purposes.

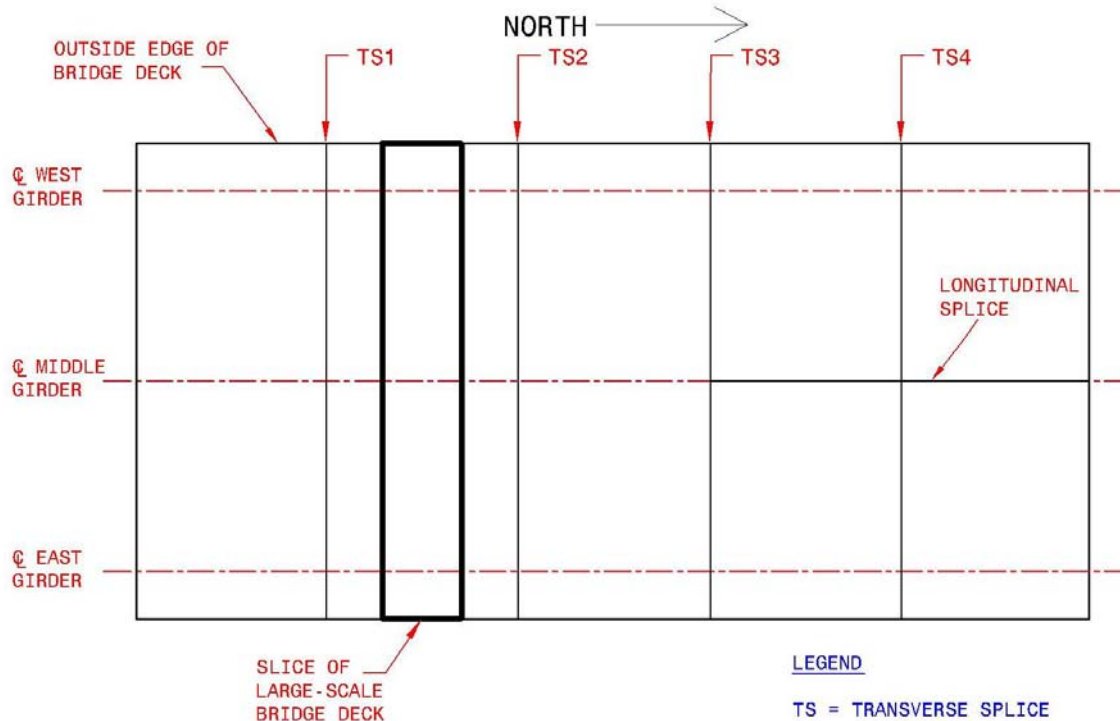


Figure 2-30: “Slice” of a large-scale bridge deck represented by subassembly deck-to-superstructure connection test

2.9.2 Specimen Configuration and Materials

An open grid deck was used rather than a partially filled grid deck because the deck-to-superstructure connections are typically of more concern for open grid specimens since they often consist of welds rather than shear studs. In this case, the main bars of the grid deck were welded to bolt down plates, which were in turn bolted to the stringers, as shown in Figure 2-31. The deck configuration of the structural steel in the deck specimen was similar to that open grid deck specimen #2 used for the subassembly stiffness tests.



Figure 2-31: Deck-to-superstructure connection detail

2.9.3 Cyclic Load Test

As shown in Figure 2-32(left), the test set-up was very similar to that of the subassembly longitudinal splice cyclic load test. The load was distributed using a spreader beam through two 20" x 10" patches equally spaced from centerline of the interior stringer at 3 feet (i.e., 6 feet center to center spacing between patches). The patches were placed such that the long edges ran parallel to the main bars so that their orientation represented the direction of traffic. Unlike for the longitudinal splice test, the spreader beam was clamped to the underside of the deck at the location of the patches, shown in Figure 2-32(right), so that the force could be applied by both pushing down and pulling up. This would create both compression and tension, respectively, in the welds connecting the main bars to the bolt down plates.

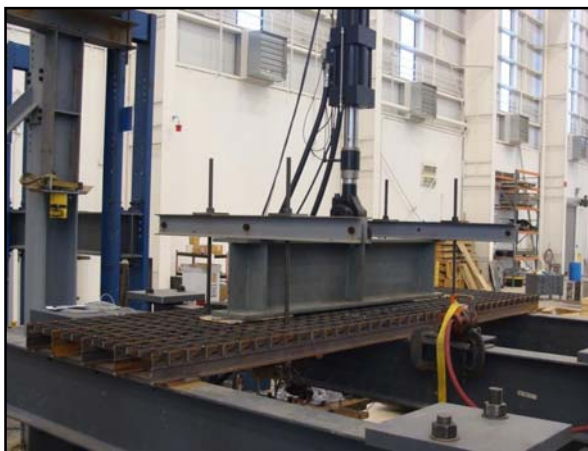


Figure 2-32: Subassembly deck-to-superstructure connection test (left) setup; (right) clamping system

The same 55-kip actuator used for the subassembly longitudinal splice test was used to push with a total load of 27.6 kips (i.e., 13.8 kips at each patch) and pull up with 9.2 kips (i.e.,

one-third of 27.6 kips). Therefore, a total cyclic load range of 36.8 kips was applied. Although pulling up is not the actual in-service loading, the tension produced in the deck-to-superstructure connection (i.e., the welds) simulates the effect of trucks travelling on adjacent deck spans. The cyclic load test was terminated after approximately 750,000 cycles due to extensive damage as will be discussed later in this report.

2.9.4 Strength Load Test

After termination of the cyclic load test, a load of 50 kips was applied to test the strength of the deck after substantial damage had been sustained. The load was distributed through two patch loads as described for the cyclic load test in the previous section. The girders remained flexible as was done for the cyclic load test. Although the applied load was not that of the strength verification test, this load applied was sufficient in determining whether the application of a heavy truck axle load would cause a failure of the deck after substantial damage had already been sustained.

2.10 Subassembly Transverse Splice Test

2.10.1 Experimental Design

Prior to the development of the subassembly transverse splice test, data from the large-scale specimen were collected and analyzed to understand the critical loading scenario. Furthermore, the large-scale testing was used to understand the behavior and stresses experienced by this detail of the bridge deck. Based on the results of this testing, a subassembly transverse splice test was developed and verified. The standard test method was developed so that a “slice” of a large-scale deck, as shown in Figure 2-33, could be tested to reveal and identify any deficiencies of the longitudinal splice or deck that would occur in service.

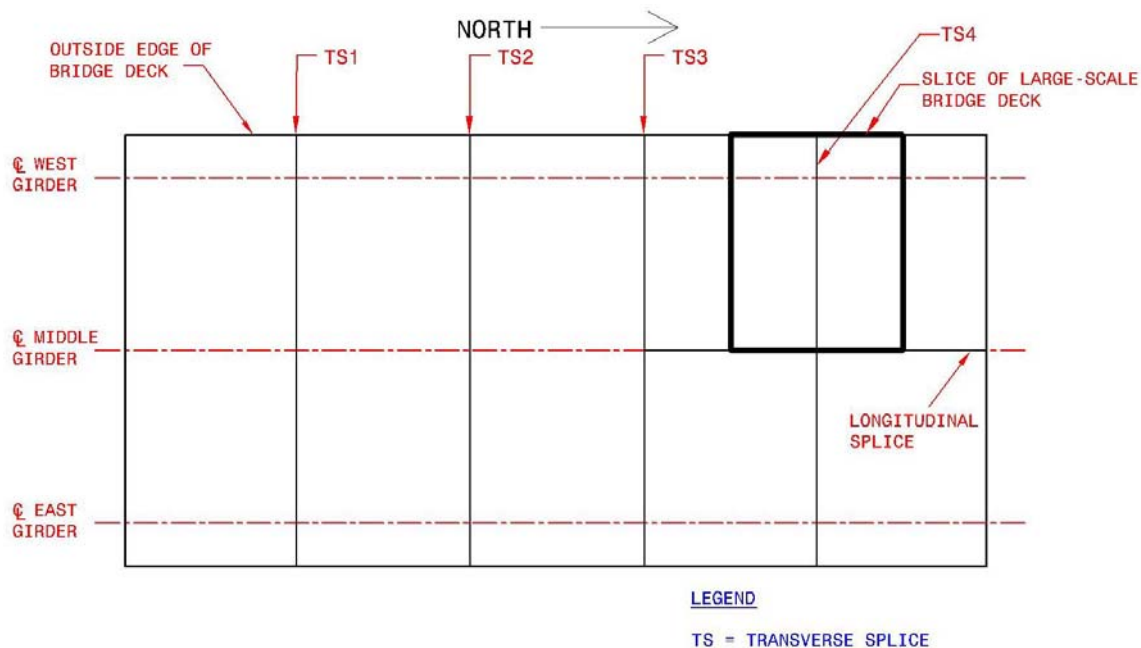


Figure 2-33: “Slice” of large-scale bridge deck represented by subassembly transverse splice test

2.10.2 Specimen Configuration and Materials

Two steel grid deck panels with bolt down plates and reinforcing steel were obtained. The configuration of structural steel in the deck panels was similar to that of open grid deck specimen #2 (i.e., same spacing and size of bars). These two deck specimens were connected through a transverse splice consisting of 3'-4" long #4 reinforcing steel spaced at 8 inches. The steel grid deck specimen was then partially filled with concrete, as shown in Figure 2-34, to make it representative of the large-scale specimen and similar to the partially filled grid deck specimen used for the subassembly stiffness test previously discussed. The concrete mix (INDOT Class C mix with a #12 sieve aggregate size) was placed from the same batch as the subassembly longitudinal splice specimen.

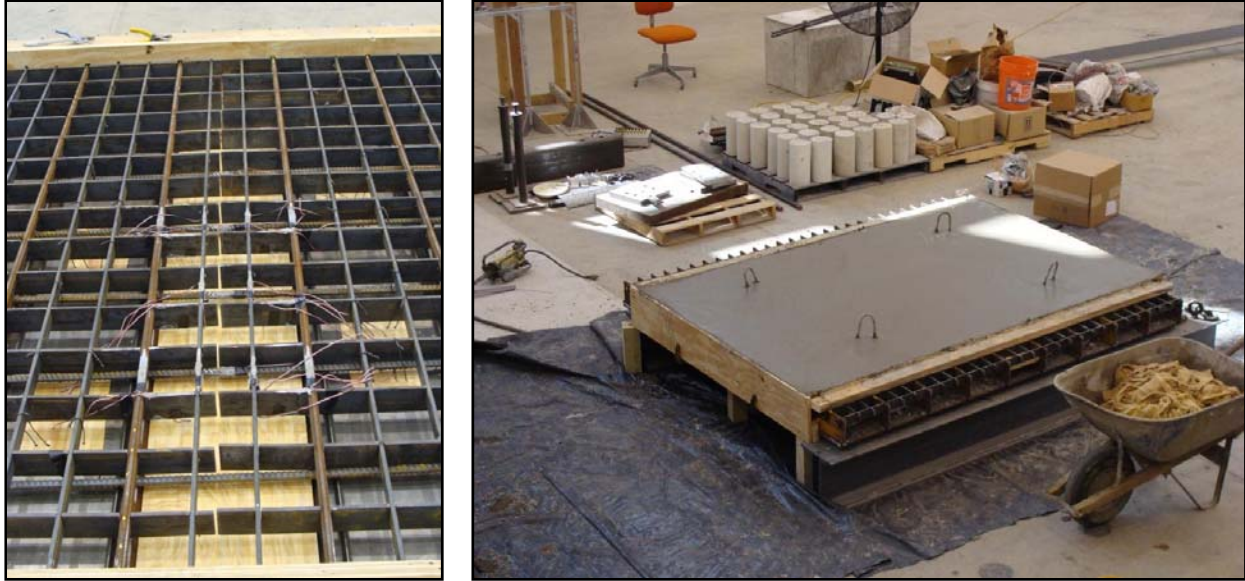


Figure 2-34: Transverse splice (left) details; (right) specimen after concrete placement

2.10.3 Strength Verification Test

This static test was intended to verify that the transverse splice in the deck meets a minimum strength requirement. The “Proposed Recommended Method for Verifying Strength of Bridge Decks” included in Appendix D of this report is intended for simple spans. Therefore, since this test implemented a single span, it could simply be conducted by following the “Proposed Recommended Method for Verifying Strength of Bridge Decks,” whereas adjustments were made to account for a two-span system for the longitudinal splice strength verification test as discussed in Section 2.8.3.

The transverse splice strength verification test was conducted prior to the cyclic loading test. This test evaluated the strength of the deck and introduced cracks into the concrete before commencement of cyclic load testing. The test was conducted with flexible supports only, as shown in Figure 2-35, because the rigid body movement of the deck could be easily accounted for since it was a single span. It was computed that the minimum load to be applied was 38.7 kips. Hence, the 55-kip actuator could be used for this test in which it was chosen to apply a 40-kip load. The load was applied through one 20” x 10” patch placed such that the edge nearest the splice was 2 inches from the centerline of the splice. The patch was placed such that the long edges ran parallel to the main bars so that it represented the direction of traffic. Hydro-stone was placed between the plate and the deck to ensure it was level and that the load was applied properly.



Figure 2-35: Transverse splice strength verification and cyclic load test

2.10.4 Cyclic Load Test

A cyclic load test of the transverse splice was also completed. An applied load range of 13.8 kips (i.e., half of the 27.6 kips used for the longitudinal splice) with a small preload was applied by the same 55-kip actuator used for the other subassembly cyclic load tests. The load was applied through one 20" x 10" patch at the same location that was used for the strength verification test described in the previous section.

As was done for the other cyclic load tests, a high frequency pneumatic vibrator was installed on one of the stringers adjacent to the deck to simulate the high frequency impact effects of passing wheels and other vibrations. At half million cycle intervals, the pneumatic vibrator was excited for a minimum of 1 minute to simulate the vibrations caused by trucks passing over a bridge.

Static tests were also conducted every half million cycles after the high frequency pneumatic vibrator was excited. For these tests, the maximum load was taken as the load applied for the strength verification test to simulate the effect of heavier trucks mixed in with design truck traffic. The subassembly transverse splice cyclic load test was terminated after over 10.5 million load cycles were applied. Initially, approximately 6.5 million load cycles were planned to be applied. However, it was desirable to observe whether additional load cycles would cause more extensive damage to the transverse splice and deck, and hence, the test was extended an additional 4 million cycles.

2.11 Summary

Small-scale steel and FRP specimens were fabricated with Flexolith and T-48 wearing surfaces. These specimens were tested to determine the resistance of a thin wearing surface to the effects of combined temperature cycles, mechanical strains, and deicing chemicals.

Further small-scale tests were developed and validated in the laboratory to rate the resistance of thin wearing surfaces to sliding abrasion (e.g., the effect of a snow plow). This was done by testing a concrete slab, as well as steel and FRP decks fabricated with Flexolith and T-48 wearing surfaces (i.e., the same as was done for the TMC test). The resistance of the thin

wearing surfaces (i.e., Flexolith and T-48) to sliding abrasion could then be rated by comparing them to the concrete slab (i.e., the calibration slab).

Another small-scale concrete slab, steel specimens fabricated with Flexolith and T-48 wearing surfaces, and FRP specimens fabricated with Flexolith and PolyCarb wearing surfaces were tested to determine their resistance to impact loading (e.g., freight falling off a truck bed). The impact loading started at low levels and gradually increased until damage causing a serviceability issue was found through inspections.

A large-scale partially filled grid deck specimen was constructed and tested to determine the general behavior of a large-scale partially filled grid deck under service loading conditions in a controlled environment, verify critical performance factors found from review of the literature and determine any additional critical performance factors, and evaluate the validity of load application to be used for developing standard test protocols. Tests were carried out by rolling a truck representing a set of tandem axles across the bridge and collecting stress data. Cyclic loading tests of the longitudinal and transverse splices were then carried out to help develop subassembly cyclic loading tests.

Three deck panels (two steel open grid decks and one partially filled steel grid deck) were tested to experimentally determine the stiffness properties of each type of bridge deck in the strong (D_x) and weak (D_y) directions, as well as in torsion (D_{xy}). The stiffness tests relied on monitoring the load applied, displacements at the supports and location of maximum displacement (i.e., underneath the load), as well as limited strain gaging to monitor the stresses and understand the behavior of the deck at critical locations.

Subassembly tests were carried out to evaluate the resistance of critical details (longitudinal and transverse splice and deck-to-superstructure connection) to cyclic loading. Tests were also carried out to experimentally verify the minimum strength required for the longitudinal and transverse splices. A strength load test was carried out for the deck-to-superstructure connection specimen to determine if a heavy axle would cause failure of the deck after substantial damage had already been sustained. Instrumentation was used to monitor the displacements and stresses at the critical details throughout testing. These subassembly tests were used to evaluate a representative “slice” of a large-scale bridge deck such that any deficiencies expected for an in service bridge could be revealed and identified.

CHAPTER 3 Findings and Applications

After completion of the tests discussed in Chapter 2, physical observations and the corresponding data from the small-scale tests were analyzed in order to:

- Evaluate the resistance of the thin wearing surfaces tested to combined temperature cycles, mechanical strain cycles, and deicing chemicals;
- Evaluate and rank the resistance of thin wearing surfaces to sliding abrasion; and
- Determine the resistance of decks and their wearing surfaces to impact loads.

Upon completion of truck roll and cyclic loading tests of the large-scale partially filled grid deck specimen, physical observations and data were used to:

- Determine the general behavior of a large-scale partially filled grid deck under service loading conditions in a controlled environment;
- Verify critical performance factors found from review of the literature and determine any additional critical performance factors; and
- Evaluate the validity of load application to be used for developing standard test protocols.

Physical observations and data from the subassembly tests were analyzed to:

- Determine the stiffness properties of the subassembly bridge deck panels;
- Compare the experimentally measured and theoretically computed stiffness properties of the subassembly bridge deck panels;
- Evaluate the cyclic loading resistance of the critical details;
- Evaluate and understand the behavior of the deck and critical details throughout testing; and
- Ensure the behavior and results of the subassembly tests were representative of the large-scale specimen tested.

This chapter discusses the findings and applications of the small-scale, large-scale and subassembly tests. Furthermore, as will be discussed, the findings of these tests were incorporated into the appropriate standard test methods developed. Throughout chapter 3 reference is made to concrete cores that were taken after cyclic testing was completed. Details and discussion of the results associates with these cores are contained in Appendix C.

3.1 TMC Tests

This section will first describe the modes of failure observed in the specimens during testing, and then present the results of all of the specimens tested.

3.1.1 Failure Modes Observed

During testing of the TMC specimens, delamination was observed on several of the FRP specimens. The delamination ran horizontally between the wear surface and the FRP substrate. Figure 3-1 shows a typical delamination in an FRP specimen with a T-48 wear surface which was subjected to the second test procedure. The cracks were first noted after the 6th cycle, and the photograph was taken after the 10th. The delamination shown in the figure compromised the

bond across the entire specimen, causing the pull-off tests in the center to have zero bond strength.



Figure 3-1: Delamination of T-48 wear surface on FRP specimen

Some of the specimens showed evidence of salt water intrusion below the wearing surface. Figure 3-2 shows a FRP specimen with a T-48 wear surface after the completion of loading and pull-off tests. The specimen had two successful pull-off tests, both of which failed in Mode (b). On this specimen, there were salt deposits found under the wear surface resulting from the drying of salt water from the deicing solutions. This indicates that the delaminations extended across the specimen. Pull-off location #1 (lower middle) in the figure, which showed the largest amount of salt deposits, retained only 17 psi of bond strength. Location #2 had sufficient areas still bonded to achieve 100 psi.



Figure 3-2: FRP/T-48 specimen #5 after pull-off tests

Most of the pull-off tests on the steel specimens failed in Mode (d), with the bond between the steel disk and the epoxy adhesive failing first. Figure 3-3 shows two pull-off locations on a steel specimen with a T-48 wear surface. The pull-off test labeled with a “1” failed in Mode (d) at 560 psi. This result does not provide the bond strength between the wear surface because the epoxy adhesive failed below that level. The second pull-off on the specimen failed in Mode (c) at 1050 psi; the failure surface passed through the top layer of aggregates. This indicates that the bond of the wearing surface to the steel is stronger than the surface itself.

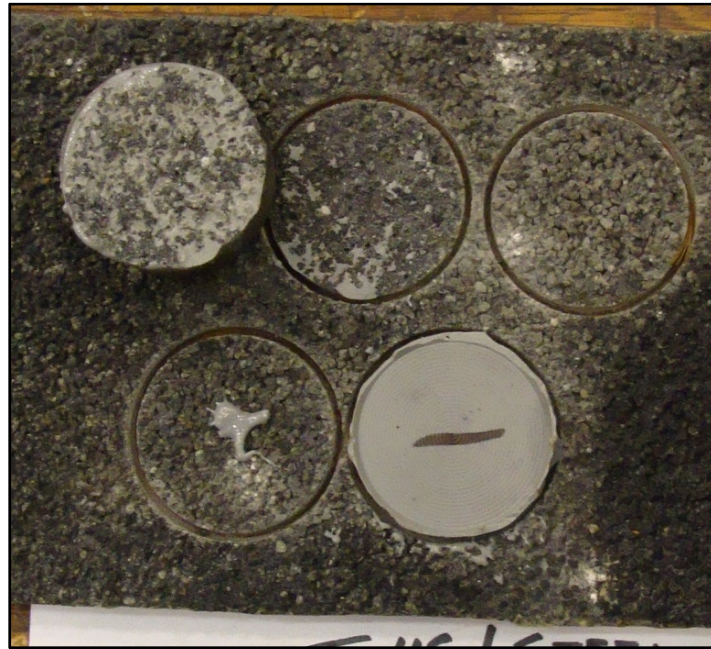


Figure 3-3: Steel/T-48 specimen #3 after pull-off tests

3.1.2 Pull-off Results and Quantification

The results of the pull-off tests performed on specimens from the first procedure are shown in

Table 3-1. The pull-off tests on steel specimens with Flexolith wear surface all showed excellent adhesion and failed primarily in Mode (d). This failure mode indicates that the bond between the wear surface and the steel substrate was at least as strong as the values shown in the table. There were no visible delamination cracks in any of the steel specimens. In order to determine the true bond strength of the steel specimens, it would be necessary to find a stronger adhesive than the ASTM C 881 epoxy that was specified in the ASTM C 1583 pull-off test specification. Due to the failure mode of the pull-off tests on the steel specimens, it is not possible to draw any conclusions about differences between the deicing solutions.

The results of the pull-off tests on the FRP specimens with Flexolith are also shown in

Table 3-1. These pull-off tests all failed in Mode (b), therefore indicating the amount of bond remaining between wear surface and FRP substrate. Sample #1 had delamination large enough to cause the surface to lose bond entirely under one of the pulls. However, all of the other pull locations retained at least some bond. There was a notable increase in remaining bond strength in the samples which were exposed to CaCl_2 compared with the other two deicing solutions. The FRP specimens as a group showed much lower bond strength than the steel specimens.

Table 3-1: Pull-off results from 1st TMC procedure

Substrate	W/S	Specimen #	Pull off #	Electrolyte	Failure Mode	Strength (lbs)	Strength (psi)
Steel	Flexolith	1	1	NaCl	d	1150	390
			2	NaCl	d	700	237
		2	1	NaCl	d	1050	356
			2	NaCl	d	1450	492
		3	1	CaCl ₂	d	1350	458
			2	CaCl ₂	d	700	237
		4	1	CaCl ₂	d	1300	441
			2	CaCl ₂	d	1100	373
		5	1	MgCl ₂	d	1700	577
			2	MgCl ₂	d	1300	441
		6	1	MgCl ₂	d	1300	441
			2	MgCl ₂	d	1250	424
FRP	Flexolith	1	1	NaCl	b	0	0
			2	NaCl	b	300	102
		2	1	NaCl	b	200	68
			2	NaCl	b	0	0
		3	2	CaCl ₂	b	200	68
			3	CaCl ₂	b	550	187
		4	1	CaCl ₂	b	900	305
			2	CaCl ₂	b	1400	475
		5	1	MgCl ₂	b	500	170
			2	MgCl ₂	b	350	119
		6	1	MgCl ₂	b	850	288
			2	MgCl ₂	b	600	204

The results of the pull-off tests performed on steel and FRP specimens subjected to the modified loading procedure are shown in Table 3-2. All of these specimens had the T-48 wearing surface installed. The steel specimens showed excellent bond, with every pull-off test failing in Mode (d) and no visible delamination cracks. There were only eight pull-off tests which yielded acceptable results because four of the tests failed in Mode (d) below 250 psi. These tests illustrate the extreme care which must be taken when preparing for the pull-off test. It is, however, still possible to draw conclusions about the qualification of the T-48 wear surface, because two of the pull-off tests, on specimens 4 and 6, failed just 13 psi below the 250 limit. It is not possible to draw any conclusion about the effect of the different deicing solutions because of the mode of failure.

Table 3-2 also shows the pull-off tests on FRP specimens with T-48 wear surface which had very poor remaining bond strength. Eight of the test locations showed zero remaining bond,

including all four of the pull locations on specimens 1 and 2, which were exposed to NaCl. There were four pull locations which still had some bond strength between specimens 4, 5 and 6. There were visible salt deposits below the wear surface on several of the pull locations, indicating that the deicing solution had penetrated completely under the wear surface. There were large delaminations observed on specimens 1, 2, 3, and 6, small cracks on specimen 4, and no significant cracks observed on specimen 5.

Table 3-2: Pull-off results from 2nd procedure

Substrate	W/S	Specimen #	Pull off #	Electrolyte	Failure Mode	Strength (lbs)	Strength (psi)
Steel	T-48	1	1	NaCl	d	1000	339
			2	NaCl	d	1000	339
		2	1	NaCl	d	750	254
			2	NaCl	d	1800	611
		3	1	CaCl ₂	d	1650	560
			2	CaCl ₂	c	3200	1085
		4	1	CaCl ₂	d	600	204
			2	CaCl ₂	d	700	237
		5	1	MgCl ₂	d	950	322
			2	MgCl ₂	c	1800	611
		6	1	MgCl ₂	d	200	68
			2	MgCl ₂	d	700	237
FRP	T-48	1	1	NaCl	b	0	0
			2	NaCl	b	0	0
		2	1	NaCl	b	0	0
			2	NaCl	b	0	0
		3	2	CaCl ₂	b	0	0
			3	CaCl ₂	b	0	0
		4	1	CaCl ₂	b	0	0
			2	CaCl ₂	b	375	127
		5	1	MgCl ₂	b	50	17
			2	MgCl ₂	b	300	102
		6	1	MgCl ₂	b	0	0
			2	MgCl ₂	b	350	119

A summary of results of the TMC tests is shown in Table 3-3. The average bond from the successful pull-off tests on each set of specimens is also shown in the table. Both of the wear surfaces tested on steel specimens qualified for use at 345 microstrain (10 ksi) because they retained excellent bond well above the 250 psi minimum and had no areas delaminate and leave zero bond strength. The Flexolith wear surface failed the test because it showed an average

remaining bond of 165 psi on the FRP specimens, which was short of the minimum. The T-48 wear also failed because the surface retained very little bond with an average strength of 30 psi, and there were too many locations with zero bond strength. It is likely there would be better bond for both wear surfaces if more aggressive surface preparation methods were used on the FRP plates such as sand blasting, or sanding with 75 grit paper. The Flexolith wear surface used on an FRP deck may pass without modification of the installation procedure at a lower stress range, perhaps for use on a stiffer deck system.

Table 3-3: TMC results summary

Deck Material, Wearing Surface, Strain Range	Average Bond (psi)	Pass/Fail
Steel, Flexolith, 345 $\mu\epsilon$	439	Pass
Steel, T-48, 345 $\mu\epsilon$	515	Pass
FRP, Flexolith, 900 $\mu\epsilon$	165	Fail
FRP, T-48, 900 $\mu\epsilon$	30	Fail

The pass or fail results in Table 3-3 are specific to the tested wearing surface, substrate, application method, and stress range tested. In order to determine if these surfaces qualify in a different situation, such as a different stress range or different application methods, they must be retested.

3.1.3 Application Summary

The TMC test has been demonstrated to be an effective way of evaluating the complex interaction of thermal strain, freeze/thaw, chemical attack, and mechanical strain on a thin epoxy concrete wear surface. The test provides a simple procedure for evaluating the overall durability of a wear surface and gives pass or fail acceptance criteria. The primary drawback to this test is that it requires expensive hydraulic equipment for producing the fatigue loading portion of the procedure, and that the procedure takes at least 30 days to complete. A complete technical specification has been included in Appendix A.

3.2 Sliding Abrasion Tests

This section will present the results of the Sliding Abrasion tests performed on concrete, Steel Orthotropic, and FRP specimens. A rating system is also presented, and the relative wear rate for each wear surface is calculated.

3.2.1 Concrete Calibration

As expected, the groove depth varied depending on the type of wear surface. All of the concrete calibration specimens produced a fairly predictable wear groove that grew deeper at a linear rate. Figure 3-4 shows the combined results for all of the concrete calibration specimens plotted together. All of these results fit neatly within a damage envelope between 43,000 and 63,000 cycles per inch of wear. Other wear surfaces would be compared to the average concrete wear rate of 54,000 cycles per inch.

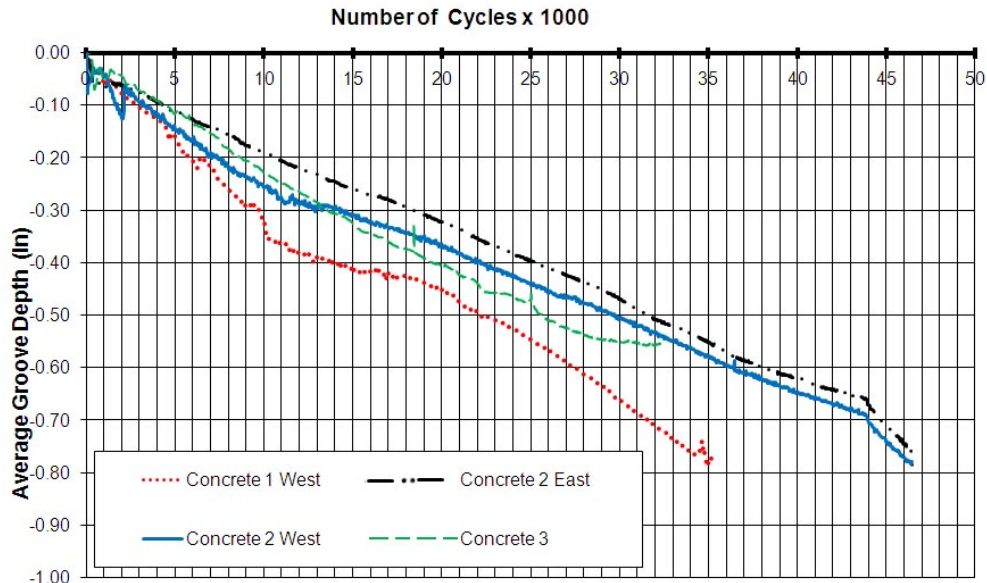


Figure 3-4: Sliding test concrete calibration

3.2.2 Steel Orthotropic and FRP Results

Both the Flexolith and T-48 epoxy wear surfaces produced a behavior different from the concrete calibration specimens characterized by an initial jump in depth of approximately $\frac{1}{20}$ th of an inch, which happened rather quickly, but was followed by very little wear. It is important to note that both the Flexolith and T-48 wearing surfaces tested used a chipped basalt aggregate produced by 3M under the trade name Indag.

Figure 3-5 shows the results of the sliding test on the FRP decks with both Flexolith and T-48 wearing surfaces. There were four identical ZellComp 5" Decks tested, two with the Flexolith and two with the T-48 wear surfaces. The data is plotted on the same scales as Figure 3-4 for comparison. The initial wear followed by minimal damage is clearly visible in all of the wearing surface test records. There was no difference in the performance of the T-48 and Flexolith wear surfaces.

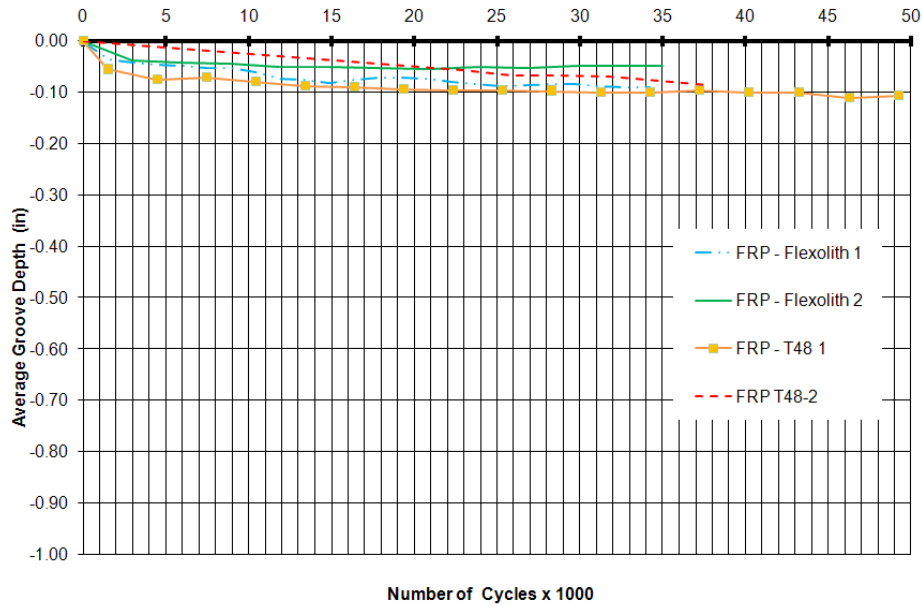


Figure 3-5: FRP sliding abrasion test results

The results of the Steel Orthotropic specimens are shown in Figure 3-6. There were two tests performed on identical decks, one with T-48 and one with Flexolith. Both of these test records show a wear rate of approximately 500,000 cycles per inch. There was no significant difference in performance between the two wearing surfaces used on the steel specimens. The Steel Orthotropic specimens performed in the same manner, with the same wear rate as the FRP deck specimens.

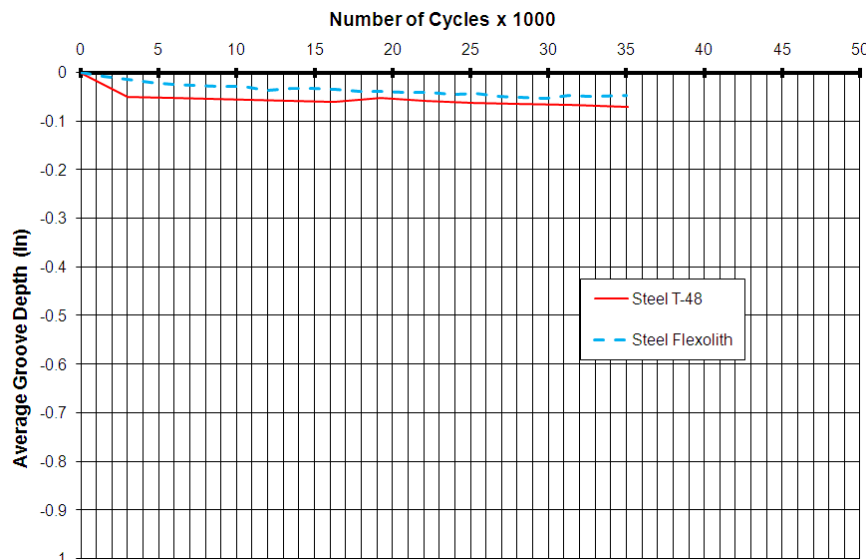


Figure 3-6: Steel orthotropic sliding abrasion test results

3.2.3 Rating System and Calculations

The rating system for the Sliding Abrasion Test compares the average wear resistance of a deck surface (W_r) to the rate observed in the concrete calibration decks by a ratio shown in Equation 3-1. The wear rate of a surface (W) was measured in cycles per inch from the results of

each wear surface. The wear rate was divided by 54,000 cycles per inch to find the W_r ratio. A W_r of 1.0 indicates that a surface has the same wear resistance as concrete. A W_r of 0.5 indicates that a surface has half the wear resistance of concrete, and a W_r of 2 indicates twice the resistance of concrete.

$$W_r = \frac{W}{54,000 \text{ cycles/inch}} \quad \text{Wear Ratio Calculation} \quad (3-1)$$

The results of the wear surface calculation for each specimen are shown in Table 3-4. There was some scatter in the data for the epoxy concrete wear surfaces because the wear tracks were too shallow to measure accurately by hand or with the laser sensors. The epoxy concrete wear surfaces performed surprisingly well with every specimen showing at least seven times the wear resistance of concrete.

Table 3-4: Sliding abrasion test results

Specimen	Wear Rate (cycle/in)	W_r
Concrete 1	45,000	0.84
Concrete 2	60,000	1.11
Concrete 3	57,000	1.06
FRP Flexolith #1	390,000	7.25
FRP Flexolith #2	700,000	12.96
Steel Flexolith	780,000	14.40
FRP T-48 #1	440,000	8.15
FRP T-48 #2	470,000	8.68
Steel T-48	500,000	9.29

The average results of the wear resistance ratios are shown in Table 3-5. There was no significant difference between the performance of the Flexolith and T-48 wear surfaces. This is attributed to the fact that both wear surfaces used identical aggregates, and similar epoxy resin binders. There was also no significant difference between the average wear resistances of the FRP or Steel Orthotropic deck systems. Close inspection of Table 3-4 revealed that there was also no significant difference between the Flexolith wear surfaces installed on FRP specimens and those installed on the Steel Orthotropic specimens. The same was true for the data from the T-48 specimens. This evidence led to the conclusion that the results of the Sliding Abrasion Test are dependent on the wear surface, not the type of deck on which it is installed, provided that it is installed properly to prevent bond failures.

Table 3-5: Sliding abrasion test average results

Average	W_r
Concrete	1.00
FRP	9.26
Steel Orthotropic	11.84
Flexolith	11.53
T-48	8.71

3.2.4 Failure Modes Observed

There were two types of wear observed in the Sliding Abrasion test samples. Figure 3-7 shows a typical concrete groove photographed from above at the end of testing. In the

photograph, the deck has been cleaned to make the worn aggregates visible. As the testing progressed, the grooves in the surfaces of all the concrete calibration specimens grew steadily deeper at a predictable rate as shown in Figure 3-4. During testing, the deck was worn down slowly, with the aggregates and mortar being shaved down a little more after each pass. The figure shows the resulting exposed cross sections of the aggregates in the concrete.



Figure 3-7: Concrete groove at completion of testing

Figure 3-8 shows a typical wear groove in a concrete calibration specimen as photographed from the side. The groove in Figure 3-7 has an average depth of 0.8", and was photographed after 35,000 cycles of testing, which was the typical duration for the concrete specimens tested. This wear groove was accompanied by large amounts of dust created by the abrasion of the surface. The figure also shows that the aggregates were not chipped out of the surface, but rather ground down smoothly.



Figure 3-8: Side view of wear groove after 35,000 cycles, specimen #1

The wear pattern on the FRP and Steel Orthotropic decks with epoxy concrete wear surfaces was much slower than that observed in the concrete calibration specimens. Figure 3-9

shows a top view of the wear groove created on a ZellComp FRP deck with a Flexolith wear surface. The groove is barely visible in the picture as it was very shallow. Close inspection revealed that only the top layer of aggregates had been broken off, or worn down, and the skid did not wear into the surface as expected. The Sliding Abrasion Test produced identical wear paths on the Steel Orthotropic specimens.



Figure 3-9: ZellComp FRP deck w/ Flexolith wear surface after 35,000 cycles

Figure 3-10 shows the same FRP specimen from a lower angle, which clearly shows the shallow depth of the groove. The specimen has also retained a significant portion of its skid resistance because the aggregates did not wear beyond the level of the epoxy. The Steel Orthotropic specimens with both T-48 and Flexolith behaved in the same manner, showing minimal groove depth after 35,000 cycles and a wear rate of approximately 500,000 cycles/inch, which is 10 times the resistance of the concrete specimens.

The large increase in wear resistance was likely due to the use of basalt aggregates in both of the epoxy wear surfaces. Upon close examination of the specimen at the end of testing, it was discovered that the portion of the top layer of aggregates which stuck above the epoxy binder was broken off by the snow plow wear point. This depth corresponds with the 0.05" initial drop measured by the laser sensors. The pile of debris from the specimen contained the chips of broken aggregates and minimal dust indicating that there had been very little wear after the initial drop. This suggests a surface with softer aggregates would possess a reduced wear resistance, perhaps closer to that of the concrete specimens tested.



Figure 3-10: ZellComp FRP deck from lower angle

3.2.5 Application Summary

The Sliding Abrasion Test provides a simple method for comparing the abrasion wear resistance of different wearing surfaces. This test could be used to avoid surfaces being placed which have insufficient durability to abrasion wear. During the test development, the thin epoxy concrete wear surfaces were shown to have surprisingly good wear resistance, with a wear resistance ratio (W_r) of 10, meaning they showed 10 times the wear resistance of the concrete specimens. The excellent wear resistance of these specimens is attributed to the extremely hard basalt aggregates which were used in both epoxy concrete surfaces.

There were two FRP specimens, and one Steel specimen with Flexolith wear surface, and two FRP specimens and one Steel specimen with T-48 wear surface which were tested using the Sliding Abrasion Test. There was no significant difference in the results of the Flexolith or T-48 wear surfaces observed during the test. This is attributed to the fact that both surfaces used the same aggregate and similar epoxy binder systems.

There was no difference in the Sliding Abrasion Test results between the Steel and FRP Specimens. There were no areas of debonding observed in any of the tests on the epoxy concrete wear surfaces, on either Steel or FRP. It is therefore concluded that the results of the Sliding Abrasion Test are dependant only on the wear surface, and not on the substrate, provided that the surface is installed properly such that there is sufficient bond to prevent debonding. A complete technical test specification has been included in Appendix B.

3.3 Impact Test

This section will present the results of the Impact Tests performed on concrete, Steel Orthotropic, and FRP specimens. The physical results and standard method for evaluating the resistance to impact loading is described herein.

3.3.1 Reinforced Concrete Calibration

The Direct Impact Test results for all bridge decks were based on the relative durability compared to reinforced concrete bridge decks. The goal of the calibration of the reinforced

concrete was to establish the maximum amount of energy that would produce zero damage in the deck and the minimum amount of energy that would produce damage that required a timely repair to prevent further degradation of the deck. The energies required to produce these two damage levels were then used as the basis for an index for rating of other decks. The zero damage level for concrete was determined to be the energy level where the mean plus two standard deviations, or 97.5% in a normal distribution, of impacts produce a divot less than two inches deep. The serviceability index is the amount of energy required that the mean minus two standard deviations of impacts produce a divot of at least two inches deep. Two inches was chosen as the target depth because the minimum cover over rebar per AASHTO LRFD 2007 Bridge Code is 2.5 inches and if an impact penetrated a full 2 inches, there would likely be cracks extending at least ½ inch deeper. If the reinforcing steel was exposed to water by these cracks, the resulting corrosion would cause deck deterioration. Figure 3-11 shows the individual impacts used for the test calibration along with the upper and lower bounds created by the mean plus or minus two standard deviations. The zero damage index was calibrated to 2,400 ft-lbs, because that is where the 2 inch depth line and the mean plus two standard deviations line intersect. The serviceability index will be calibrated to 3,600 ft-lbs, because that is where the 2 inch depth line and the mean minus two standard deviations line cross.

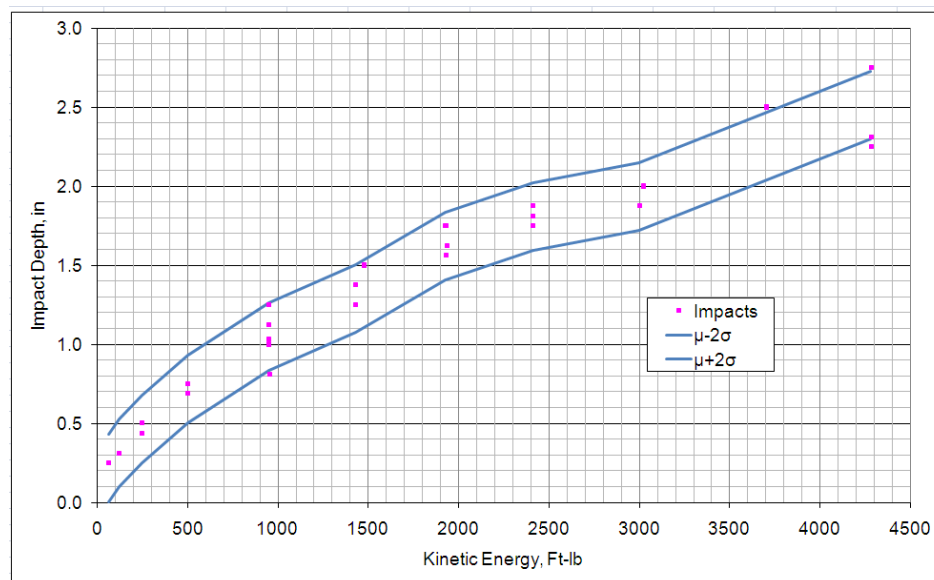


Figure 3-11: Concrete calibration data

3.3.2 Evaluation System

All of the decks tested by this procedure were rated by their durability relative to reinforced concrete using the zero damage and the serviceability indices. This rating allows deck owners to consider the relative durability compared to a familiar material. What constitutes negligible damage, and what damage constitutes a serviceability problem must be determined for each deck. Testing must then establish the energy levels at which zero damage and damage requiring repair is created in all cases. The testing plan for each deck should consider all variations in cross section (for example, perform impacts directly over ribs and between them). Equation 3-2 and Equation 3-3 show the procedure for calculating the damage indices. When calculating the damage indices, the energy should be calculated to the nearest 50 ft-lbs, and the

index rounded to the closest multiple of five. Greater accuracy would be misleading because the specification requires the height to be measured within ½ inch, and with a 200 lb impact head assembly, ½ inch is 50 ft-lbs, or a value of four on the zero damage scale. For both Equation 3-2 and Equation 3-3, the test energy should be calculated using Equation 2-9 in Section 2.4.6.

$$I_0 = \frac{\text{Energy}}{2400 \text{ ft} * \text{lb}} * 100 \quad \text{Zero Damage Index Formula} \quad (3-2)$$

$$I_s = \frac{\text{Energy}}{3600 \text{ ft} * \text{lb}} * 100 \quad \text{Serviceability Index Formula} \quad (3-3)$$

The Zero Damage Index is intended to calculate the ratio of the test energy that always produced no damage as described in Section 2.4.6. An I_0 value of 100 indicates that the deck can withstand the same impact energy as a reinforced concrete deck without sustaining any significant damage. An I_0 value of less than 100 means that the deck was damaged more easily than a concrete deck.

The Serviceability Index is intended to calculate the ratio of test energy that always produced damage requiring repair as described in Section 2.4.6. An I_s value of 100 indicates that a deck will require repair every time at the same impact energy as a concrete deck. An I_s value of greater than 100 indicates that a deck can withstand a greater impact energy than a concrete deck without needing repairs every time.

3.3.3 Results

The results have been separated by deck type. The following sections describe the specific behaviors observed in the steel orthotropic and FRP specimens, along with their ratings using the damage indices.

Steel Orthotropic Performance. The steel specimens tested showed excellent impact resistance compared to the concrete decks. Figure 3-12 shows a top view of a 4,000 ft-lb impact performed on the ½ inch plate steel specimen. This was the maximum energy the impact setup was capable of producing. Impacts ranging from 1,000 ft-lbs to 4,000 ft-lbs were performed on both steel over the angle-plate connection and over the span of the deck. The deepest dents were produced in the ½ inch plate over the span. All impacts resulted in small areas of chipped off wearing surface as shown in the figure.



Figure 3-12: 4000 ft-lb impact on 1/2" steel plate deck

Figure 3-13 shows a typical bottom view of an impact on the steel plate decks. The local yielding in the figure was produced by a 2,000 ft-lb impact over the angle leg in the 1/2 inch plate specimen. The impact sites were checked for water leaks and all were found to be watertight. None of the impacts produced any conditions which would seriously affect the serviceability of a bridge deck in the field. The impact sites would produce, at worst, a minor bump in the road surface. None of the wear surface debonding areas were larger than 4 inches in any direction and would not constitute a safety concern.

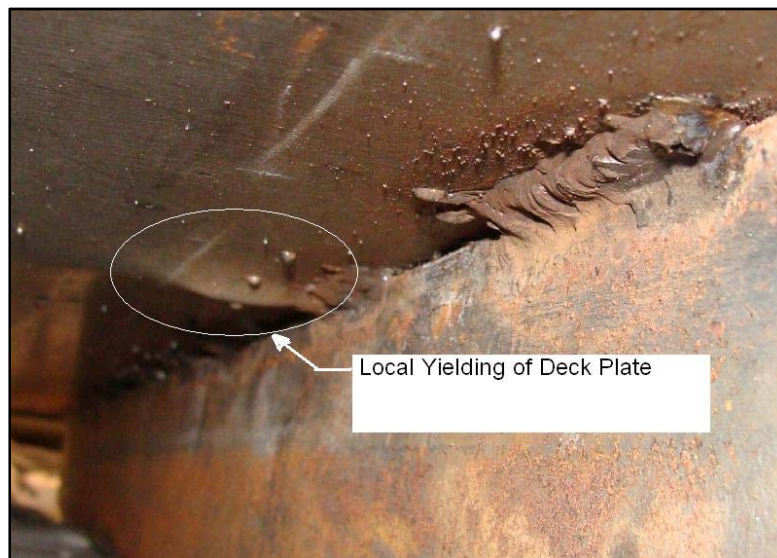


Figure 3-13: Bottom view of typical steel impact site

Because the test was not capable of producing damage which must be repaired in a steel deck, it is not possible to calculate the indices accurately. The Zero Damage Index is based on the maximum damage a deck can sustain without requiring repair after any impact, which is something greater than 4,000 ft-lbs in the case of the steel decks,. Therefore, the Zero Damage Index for these decks would be greater than 167 as shown in Equation 3-4.

$$I_0 > \frac{4000 \text{ ft} * \text{lb}}{2400 \text{ ft} * \text{lb}} * 100 > 167 \quad \text{Steel Zero Damage Calculation} \quad (3-4)$$

The Serviceability Index could not be calculated because no damage requiring repair was ever produced in the steel decks. The highest energy tested was 4000 ft-lbs and the decks did not show significant damage, therefore they performed better than concrete. The Serviceability Index is greater than 111, as shown in Equation 3-5, and could be calculated accurately if the Direct Impact tester were modified to achieve a greater energy.

$$I_s > \frac{4000 \text{ ft} * \text{lb}}{3600 \text{ ft} * \text{lb}} * 100 > 111 \quad \text{Steel } I_s \text{ Calculation} \quad (3-5)$$

FRP Performance. The measurement of the damage created by the impact test to the ZellComp FRP decks was not as simple as the concrete calibration samples. The deck had a tendency to lose its wearing surface very easily and in an unpredictable pattern, with different amounts of surface area flaking off around the impact site, making measurement of impact depth meaningless. As a result, three damage levels were defined after initial testing; these levels corresponded to the damage indices and allowed the varying levels of damage to be described by simple criteria. The damage levels are in the order of increasing severity, and were all accompanied by varying amounts of damage to the epoxy wear surface. The first structural damage level that was observed was cracking on the bottom of the top plate, as seen in Figure 3-14. This damage was considered negligible provided that the damaged area remained watertight because it was localized and would likely go unnoticed in the field.



Figure 3-14: FRP damage level 1; damage to bottom of top plate

The second damage level was defined as damage to the top plate severe enough to permit water leakage when the deck was wetted for 20 minutes. This condition could create a serviceability issue that must be repaired depending on drainage of the deck cavity and type of connection to stringers. For example, a simple deck on girder bridge with the bottom sections running transverse to traffic, as shown in Figure 2-5 in Section 2.2.1 (and Figure 2-35 in Section 2.4.2), which has grouted stud connections, as shown in Figure 3-15, would have cavities between interior stringers which could not drain.

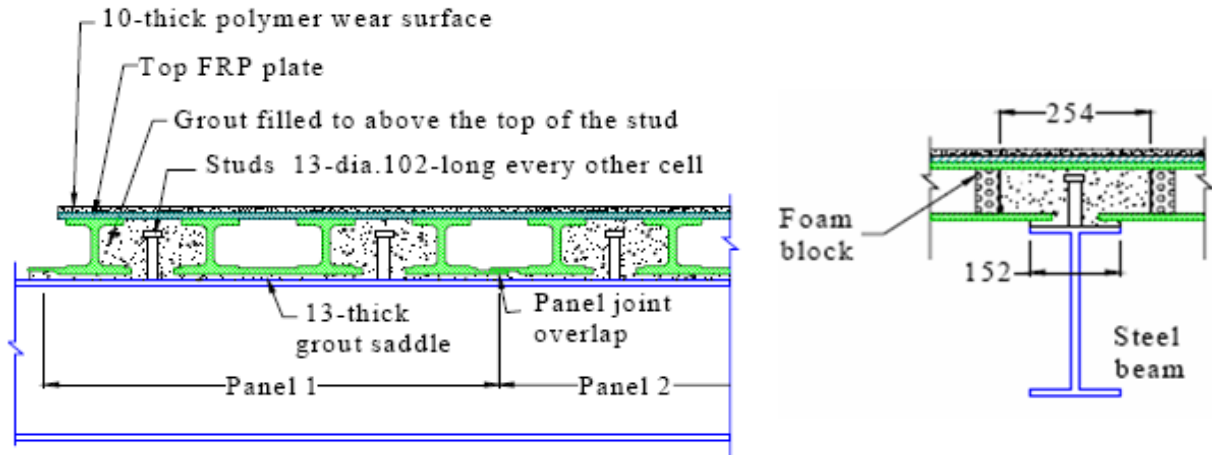


Figure 3-15: FRP deck with grouted stud connection (Zhao et al. 2006) (left) elevation; (right) cross section

If the deck developed a leak over one of these pockets, it would fill with water and create serviceability problems during the first winter freeze. An example of a leaky top plate is shown in Figure 3-16.



Figure 3-16: FRP damage level 2, permitting water leakage

The most severe damage level in the FRP decks was a complete punch through of the deck, such that the tip of the impact head was visible from below, as seen in Figure 3-17. This condition created rapid water leakage, and was accompanied by large wear surface delaminations which would reduce ride quality and traction.



Figure 3-17: FRP damage level 3, punch through

Once the damage levels were defined, impacts were performed over the clear spans between the T sections, on the T flanges, and over the T webs of the ZellComp Deck to completely describe the behavior of the deck. Drops were repeated several times at each location to establish the amount of energy required to consistently produce each damage condition at each location. The results of the testing on the FRP specimens are shown below in Table 3-6. The energy values given in the table are the minimum energy required to create the damage level every time in the FRP deck.

Table 3-6: FRP impact behavior

Damage Criteria	Energy Required (ft-lb) Location on Deck		
	Web	Flange	Span
Level 1	1000	800	300
Level 2	1250	1250	500
Level 3	3500	1750	1000

After the behavior of the ZellComp deck had been satisfactorily described, the damage indices were calculated. For the purpose of this calculation, it was assumed that the deck will be used on a bridge where not all of the interior cavities will be drained. This means that for the purposes of the serviceability index, water leakage (damage level 2) constitutes damage that must be repaired.

Equation 3-6 shows the calculation of the Zero Damage Index for the FRP decks. The impact testing produced no water leakage on any drop of 450 ft-lbs or less, but there was water leakage consistently at 500 ft-lbs over the clear span. Therefore, 450 ft-lbs meets the criteria for the Zero Damage Index requirement of “zero damage created in all cases.” To calculate the Zero Damage Index for FRP, the 450 ft-lbs is then divided by 2,400 ft-lbs, multiplied by 100, and rounded to 20. This indicates that it takes 20% of the energy to produce damage in some areas (the clear spans between bottom section T’s) of the ZellComp FRP decks than it does to produce damage in a concrete deck.

$$I_0 = \frac{450 \text{ ft} * \text{lb}}{2400 \text{ ft} * \text{lb}} * 100 = 18.8 \xrightarrow[\text{nearest 5}]{\text{round to}} 20 \quad \text{FRP } I_0 \text{ Calculation} \quad (3-6)$$

The Serviceability Index for the FRP decks is calculated in Equation 3-7. In this case, 1,250 ft-lbs was used because that was the energy level required to create level 2 damage in all relative locations: over the span, web, and flange of the bottom T sections with every drop. When the index is calculated using Equation 3-3 it yields an index value of 35. This means that it only takes 35% as much energy to produce damage which must be repaired in an FRP deck as it does in a concrete deck.

$$I_s = \frac{1250 \text{ ft} * \text{lb}}{3600 \text{ ft} * \text{lb}} * 100 = 34.7 \xrightarrow[\text{nearest 5}]{\text{round to}} 35 \quad \text{FRP } I_s \text{ Calculation} \quad (3-7)$$

3.3.4 Impact Test Summary

The impact test has been shown to be an effective means of evaluating the durability of unfamiliar types of bridge decks which may be subjected to impact loading. The Zero Damage Index and Serviceability Index provide an objective means of comparing a new deck to reinforced concrete. The weakness of the test is that the criteria of what constitutes damage that must be repaired is subjective, and varies with the specific deck system. This weakness could lead to a deck receiving different index scores from different researchers who disagree about what damage must be repaired, and what could be tolerated. Despite its weakness, the impact test fills a gap in current testing procedures and would be useful for a bridge owner considering the use of an unfamiliar deck type. A complete technical test specification has been included in Appendix C.

Large-Scale Specimen Performance

3.3.5 Introduction

This section describes the findings from the truck roll tests and the longitudinal and transverse splice cyclic tests. The general behavior of the bridge deck is described, including the composite action of the deck and girders. The unique behavior of critical elements in the bridge deck during each roll test position is also further discussed. The stresses produced by the cyclic loading are compared to those produced by the truck load simulator, and the final results of the cyclic tests are described, including the evaluation of the deck steel stress changes and concrete cracking throughout the tests. Finally, the applications of the findings of the experimental testing procedures are summarized.

3.3.6 Composite Action of the Deck

The measured composite action between the deck and girders of the large-scale specimen was analyzed and compared to that which would be estimated using calculations. Specifically, experimental moments measured during the initial static tests using the hydraulic actuator for the longitudinal and transverse splice tests were compared to the theoretical moments caused by the same loading. The experimental moments were computed by multiplying the theoretical section modulus of the transformed section for each girder by the experimental stresses at the bottom flange of the girders.

The theoretical section modulus for each girder was calculated considering that the deck was fully composite with the girders and using the AASHTO LRFD requirements for the effective width of composite partially filled steel grid decks. Using the AASHTO method, the total effective flange width used for the middle girder was eight feet, which was the distance to the centerline of the adjacent girders on either side. The effective flange width used for the exterior girders was six feet because of the two foot overhang on one side of these girders. The longitudinal cross bars were included in the calculation for the moment of inertia of the composite section since strain gages on these bars displayed compressive stresses due to global composite behavior. The haunch was included in the composite section for all girders. The effective widths used for the middle and outside girders are shown in Figure 3-18.

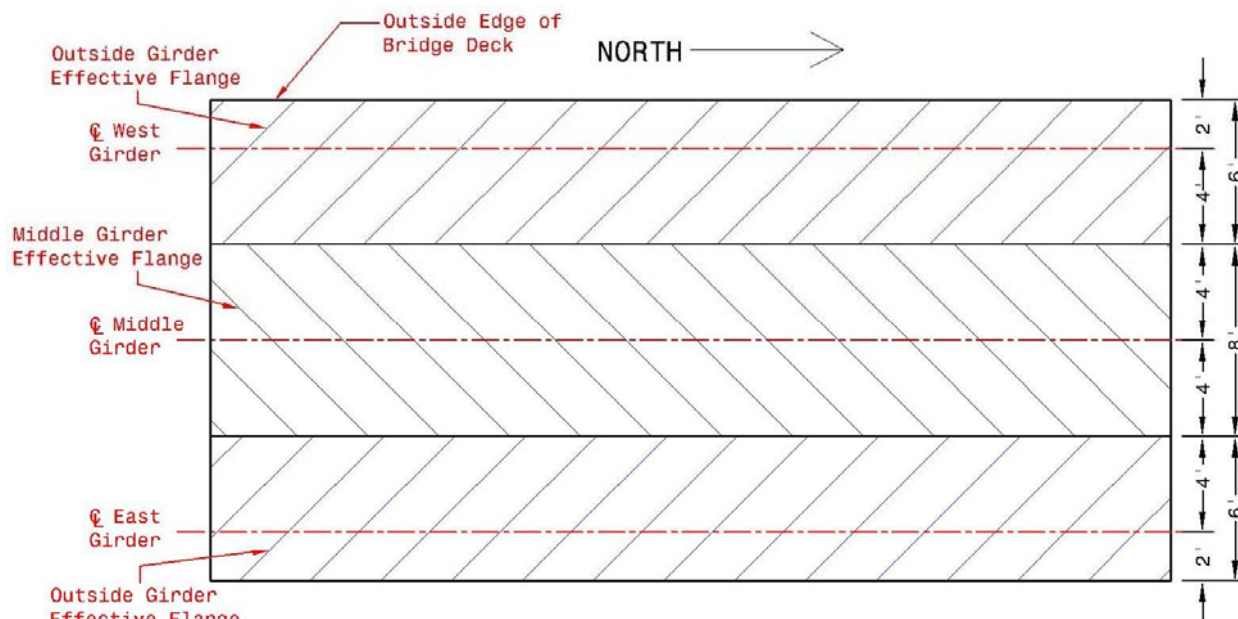


Figure 3-18: Effective flange widths

The Lever Rule was used to calculate the distribution factor for the exterior girders. Since the bridge had three girders, the distribution factor for the middle girder was calculated as follows:

$$DF_{Interior} = 1 - \Sigma(DF_{Exterior}) \quad (3-8)$$

By using Equation 3-8 for the middle girder distribution factor, the summation of the distributed moments of the girders was equal to the total longitudinal moment in the bridge.

Table 3-7 displays the theoretical and experimental girder moments at midspan from both 30 kip and 58 kip initial static tests during the longitudinal splice cyclic test. For this test, the load was located 8 feet from midspan.

Table 3-7: Longitudinal splice test girder moments

Moment at Midspan (k-ft)						
	30 kip Static Test			58 kip Static Test		
Girder	Theoretical	Experimental	Percent Error	Theoretical	Experimental	Percent Error
West	33.8	42.0	24%	65.3	80.6	24%
Middle	112.5	85.6	-24%	217.5	166.8	-23%
East	33.8	41.7	24%	65.3	80.6	24%
Total	180.0	169.3	-6%	348.0	328.1	-6%

Table 3-8 displays the theoretical and experimental girder moments at midspan from the 29.1 kip initial static tests during the transverse splice cyclic tests. For this test, the load was located 12 feet from midspan.

Table 3-8: Transverse splice tests girder moments

Moment at Midspan (k-ft)						
	TS Test 1			TS Test 2		
Girder	Theoretical	Experimental	Percent Error	Theoretical	Experimental	Percent Error
West	NA*	7.2		62.4	59.2	-5%
Middle	62.4	51.4	-18%	62.4	50.9	-18%
East	62.4	58.1	-7%	NA*	6.7	
Total	124.9	116.7	-7%	124.9	116.8	-6%

*Lever Rule not valid since the load patch is located on the other side of middle girder

From Table 3-7 and Table 3-8, reasonably good agreement was found for the comparison of the total experimental and theoretical moments considering the very simple load distribution model used. The total experimental moments were found to be slightly lower than the total theoretical moments during the longitudinal and transverse splice tests. This difference is attributed to plate action and two-way bending which occurs in the deck resulting in a much more complex load distribution. In reality, behavior of the deck, and hence the moment carried by a given girder much more resembles that explained by orthotropic plate theory. This is evidenced by the fact that the total measured and estimated moments are in very good agreement.

Tests by Gangarao et al. (1993) on subassembly composite fully filled steel grid deck specimens found that the experimental moments were lower than the theoretical moments. The results for the theoretical moments calculated by the orthotropic plate theory were found to be in good correlation (Gangarao et al., 1993). Higgins has also shown that an orthotropic plate model best characterizes the behavior of these types of decks (Turan and Higgins, 2011; Higgins et al., 2011).

As noted, a larger difference in the experimental and theoretical moments was found for the individual girders than for the total of all the girders. This is due to the use of the simplified assumptions associated with the lever rule for the distribution of the moments. Although this model is able to roughly estimate the distribution, it also makes many assumptions such that the load can be represented by point loads and that the load will only be carried by adjacent girders. As shown in Table 3-8, some of the moment applied to the bridge by the load patch will be transferred to the exterior girder on the opposite side of the bridge.

The experimental moments were also compared to the theoretical moments at the strain gages located on the girders 8 feet from the north side of the bridge. Similar results were found for these strain gages for the longitudinal and transverse splice tests as the midspan girder gages. The experimental and theoretical moments were also evaluated for the truck roll tests for the midspan girder gages and the girder gages located 8' from the north end of the bridge. A reasonably good comparison using the transformed composite section properties was found for these moments with the difference between the total theoretical and experimental moments in the girders within 15% for the midspan strain gages and 8% for the strain gages 8 feet from the north side of the bridge.

The AASHTO LRFD specification distribution factor for an interior girder with a partially filled grid deck with one lane loaded was compared to the results computed with Equation 3-8 for Position 2. This position was chosen for comparison since the truck was centered over the middle girder which yielded the greatest stress in this member. According to AASHTO LRFD Table 4.6.2.2.2b-1, when the number of girders for a beam-slab bridge with steel girders and a partially filled grid deck is equal to 3, the lesser of the values obtained from the One Design Lane Loaded equation with $N_b = 3$ or the lever rule is to be used. It was found that the Lever Rule of the actual location of the truck tires with a spacing of 6.4' was lower than predicted by the AASHTO one lane loaded equation. If the AASHTO Design Truck would have been used with tire spacing of 6' (instead of the actual truck), the lever rule would have been larger and the AASHTO one lane loaded equation would have controlled. It was found that the theoretical moment from the Lever Rule was within 3% of the experimental moment in this girder from the truck roll test in Position 2, but it was slightly unconservative.

If the AASHTO distribution factor for one lane loaded would have controlled due to the difference in the Lever Rule calculation, the theoretical moment would have been within 1% of the experimental moment in this girder. The AASHTO distribution factor should be conservative due to the fact that they are suitable for limited skews and all possible design loading conditions. Another influence in the AASHTO one lane loaded distribution factor for partially filled grid decks is that the deck thickness of the specimen, 4.5", is the lower bound of the range of applicability for this equation. Nevertheless, there is good agreement between the measured and calculated distributions.

Application Summary - Composite Action of the Deck. The findings and applications of the composite action of the deck are summarized as follows:

- The partially filled grid deck was fully composite with the girders.
- The longitudinal deck steel and concrete haunch should be included in composite section.
- Effective widths from AASHTO LRFD specification were a reasonable model for the composite behavior of the deck.
- The AASHTO live load distribution factor for an interior beam was reasonable to determine the maximum load in the middle girder during the truck roll tests.

Therefore, no changes to the effective widths or distribution factors for partially filled steel grid decks in the AASHTO LRFD specification are required.

3.3.7 General Roll Test Findings

Composite Action of the Deck. The stresses in the middle girder at midspan during a roll test at Position 2 are shown in Figure 3-19. Channel 86 (CH_86) is a strain gage on the top

flange of the girder. CH_87 is a strain gage on the web of the girder halfway between the top and bottom flange. CH_88 is a strain gage on the bottom flange of the girder. Due to the much lower stresses at the top flange than the bottom flange of the girder, this figure illustrates that significant composite action was found to occur between the girder and the deck. It was found that the neutral axis of the middle girder section was located slightly below the top flange. The neutral axis of the exterior girders was located a few inches lower than in the middle girder due to the smaller effective flange width.

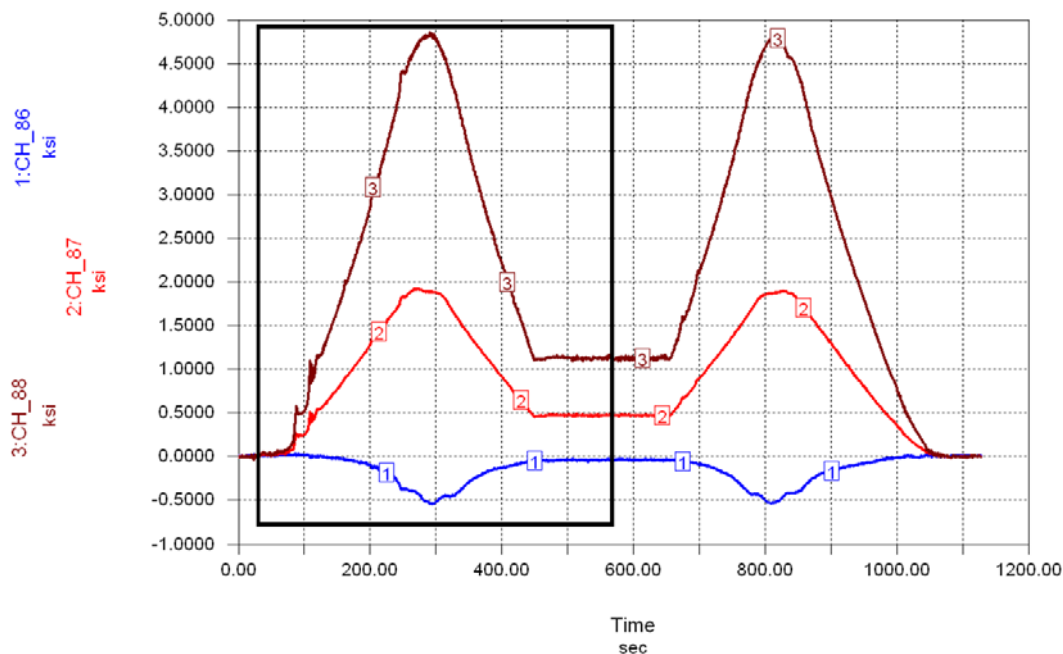


Figure 3-19: Middle girder stresses

As was stated in Section 2.6.2, the roll test procedure involved rolling the truck on the bridge, across the bridge, and back off of the bridge. This procedure is evident in the mirrored data shown in Figure 3-19 since the truck crossed the same point twice in each roll test. For all of the following roll test data, only the data from the first half of each truck roll when the truck was rolled to the south will be displayed. It is noted that all of the gage readings returned to zero stress when the truck was rolled back off of the bridge. The portion of the data which will be displayed is represented by the black box in Figure 3-19.

Observed Cross Bar Response. Strain gages on the cross bars, which run longitudinally in the bridge deck, also showed that the bridge was acting compositely with the girders. These strain gages display both a global response and a local response when the truck rolls over the bridge in varying positions. The global response of the cross bars occurred when the truck was rolled in a transverse position on the bridge deck away from the cross bar in question. The global response of the cross bars was axial compression due to composite action with the girders. The local response of the cross bars occurred when the truck was rolled near the cross bar in question. The local response caused large bending stresses due to direct loading of each truck axle.

Figure 3-20 shows both the global and local response of a cross bar. The response of CH_47, which is a strain gage located along the top of a cross bar between the middle and west

girder near mid span, was chosen for comparison of these responses. The line labeled as "1" displays the local response when the truck was rolled in Position 2 with the tires rolling directly over this cross bar. The line labeled as "2" shows the global response when the truck was rolled in Position 4 in which the tires were located in a transverse location of the bridge away from this cross bar.

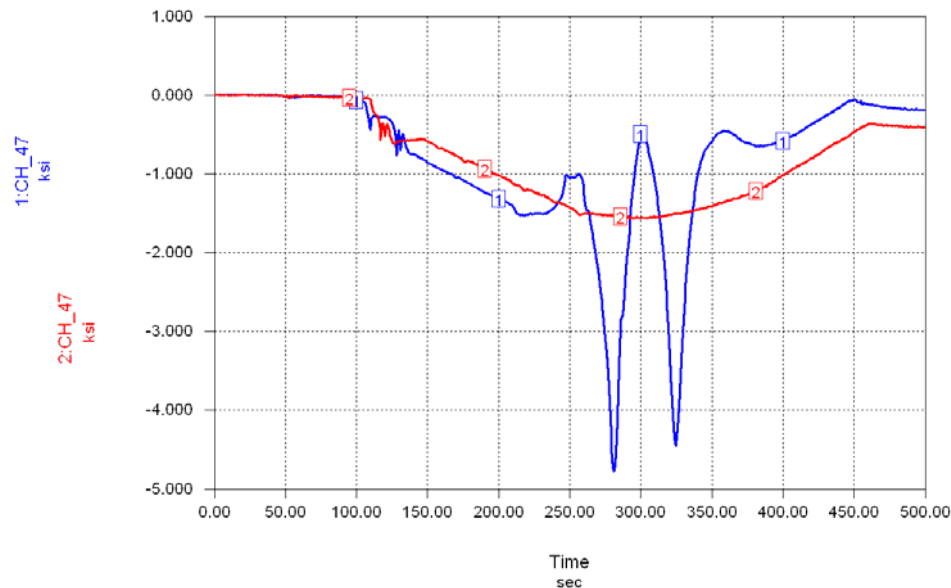


Figure 3-20: Cross bar global and local responses

Due to the local response of the cross bars, significant tensile stress spikes could occur in the bottom of the cross bars when each axle rolls over them. This local effect strongly depends on the location of the tires with respect to the cross bar. For example, it was found that the local tensile effect on the bottom of a cross bar was only large enough to counteract the compression caused by composite action when the truck was rolled in a transverse position centered over the cross bar. At this location, the edge of the inside truck tires was 2 feet away from this cross bar. When the truck was rolled in a transverse position with the truck tires rolling directly over the cross bar in question, the tensile local effect on the bottom of the cross bar from the tires overcame the compression caused by the composite action and resulted in a tensile stress of 6 ksi at this location.

Observed Response of Main Bars. The main bars, which run in the transverse direction, display both positive and negative moment behavior depending on the distance from the girders along the length of the bar and the truck position, as expected. When the deck is loaded with the tires on both sides of a girder, the main bar changed from positive moment under the tires to negative moment over the support (girder). The positive moment (shown as stress) from the truck axles carried by the main bars was quite significant as shown in Figure 3-21. This figure shows the stresses in a main bar midway between the west and middle girders from a truck roll test in Position 2 where the truck tires rolled directly over this location. CH_9 was located on the top of the main bar and experiences compression from the positive moment while CH_10 was located directly below CH_9 on the main bar and experienced tension. The larger stress in the bottom of the main bar compared to the top was due to a shift in the neutral axis of the main

bars. This upward shift of the neutral axis was due to the concrete only being placed along the top half of the deck.

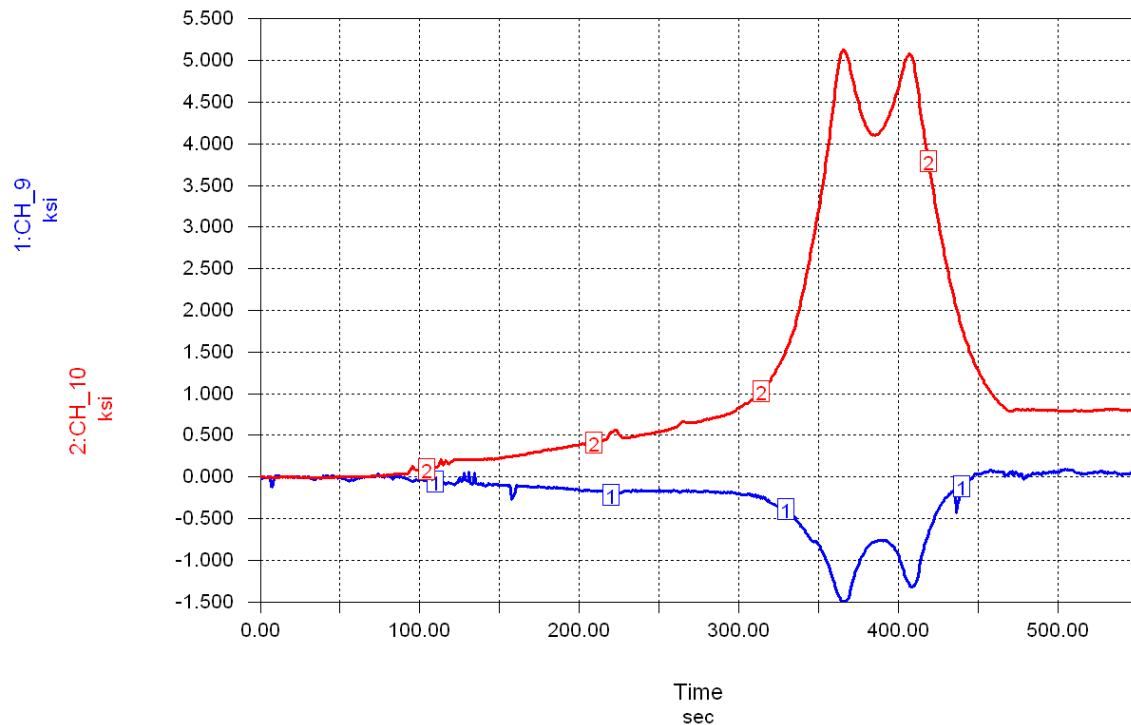


Figure 3-21: Main bar local bending

The local effect of the truck axles caused negative moment to be primarily found over the middle girder since the main bar was acting like a continuous beam supported at the three girders. The restraint at these girders is provided by the composite haunch. Some of the main bars underwent a change from positive moment to negative moment during a single loading cycle due to the interaction of global and local effects at this connection to the girders. An example of this unique behavior will be further discussed in the following sections.

Observed Response of the Transverse Splices. The longitudinal reinforcing steel crossing the transverse splices experienced a compressive stress due to global composite action with the girders similar to the response of the cross bars. The reinforcing steel across these splices also experienced tensile stress caused by local effects when each tire passed directly over the splice near the reinforcing steel. This local effect is dependent on the relative position of the tires to the reinforcing steel. It was found that the local bending effects which cause the tensile stresses are much lower in the reinforcing steel crossing the transverse splice than the cross bars in the same location. Figure 3-22 shows reinforcing steel and cross bar stresses near the transverse splice located midway between the east and middle girder during a roll test at Position 2.

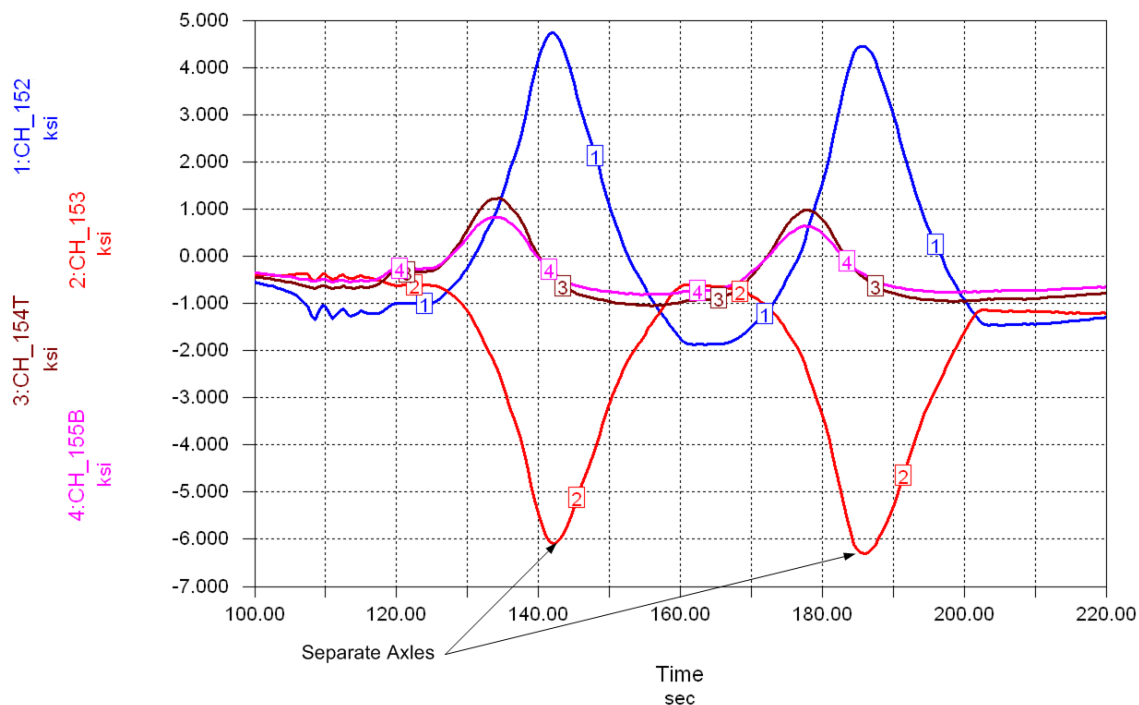


Figure 3-22: Reinforcing steel and cross bar local stresses

CH_152 is a strain gage on the bottom of a cross bar near the transverse splice while CH_153 is on the top of this cross bar at the same location as CH_153. CH_154T and CH_155B are located on the top and bottom (12 o'clock and the 6 o'clock position), respectively, of a reinforcing steel bar crossing the transverse splice. This reinforcing steel bar is located at the same transverse location as the cross bar containing CH_152 and CH_153. It can be seen that the local tensile stress spike for the same truck roll was much lower for the reinforcing steel gages than the cross bar gages.

Figure 3-22 also illustrates that the reinforcing steel did not undergo significant bending since both reinforcing steel strain gages had similar stresses. Thus, the transverse splice reinforcing steel was usually loaded by axial compression due to global effects (i.e., primary bending) or axial tension due to local effects (i.e., local wheel loads). In this case, the average of the reinforcing steel stresses was axial tension. Since the reinforcing steel was located toward the bottom of the transverse splice, similar to the bottom of the cross bars, the reinforcing steel stresses would be expected to display similar behavior as strain gages on the bottom of the cross bars. This can be seen because CH_152, located on the bottom of a cross bar, also underwent tension.

Observed Response of the Longitudinal Splice. The reinforcing steel in the longitudinal splice was subjected to both a local and a global effect, similar to the response of the main bars over the middle girder. The local effect was caused when each axle of the truck passed over the reinforcing steel in the splice while the global effect was caused by the girder displacements when the truck rolled across the bridge. Figure 3-23 shows the stresses in a reinforcing steel bar crossing the longitudinal splice during a roll test in Position 2. CH_120T was a strain gage on the top of a reinforcing steel bar located at the middle of the splice while

CH_121B was a strain gage on the bottom of the reinforcing steel bar at the same location. The local effect from the truck axles loading the splice in negative moment caused tensile stress in the reinforcing steel since it is located toward the top of the splice. Since the splice was located closer to the north edge of the bridge, the local effect occurred before the global effect which placed the reinforcing steel in compression. This compressive stress in the reinforcing steel was caused by positive moment in the splice since the middle girder will deflect more than the outside girders.

Since the splice was mainly loaded in negative moment by the truck tires located on each side of the middle girder, the top of the section was expected to experience tensile stresses. Although the stresses in both the top and bottom of the longitudinal splice reinforcing steel were found to be in tension due to this loading, the top of the reinforcing steel was found to experience lower stresses than the bottom of the reinforcing steel. This is a contradiction of the expected stresses since the top of the reinforcing steel should experience more tension than the bottom. Through analysis of main bar stresses, which were located one foot away from both sides of the longitudinal splice, it was found that these members experienced negative moment. Thus, it should be noted that although the sign of the longitudinal splice reinforcing steel stresses seem to be correct, local effects, though not fully characterized, likely caused the difference compared to the expected magnitude of these stresses.

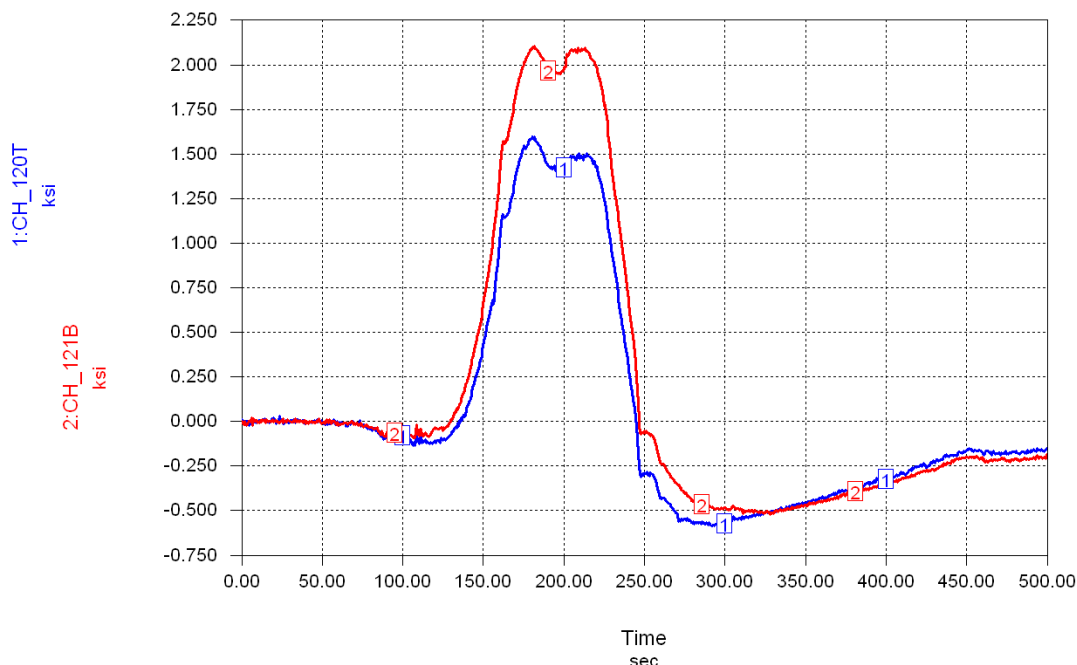


Figure 3-23: Longitudinal splice reinforcing steel stresses

3.3.8 Roll Test Positions #1 and #4: Critical Findings

Roll test Positions 1 and 4 were very similar since they were mirrored about the middle girder. In roll test Position 1, the centerline of the truck was rolled halfway between the west and middle girder while in roll test Position 4, the centerline of the truck is rolled halfway between the east and middle girder. It was chosen to roll the truck in both of these positions to verify that the response of the bridge deck was consistent and repeatable.

In these roll test positions, the centerline of the truck was located halfway between the middle and outside girder, which places the outside of the truck tires over the girders. This positioning produces compression in the strain gages on the cross bars and transverse splice reinforcing steel due to the composite action with the girders. Since the truck was centered over the cross bar and transverse splice strain gages, there were not significant local stresses in these bars.

The longitudinal splice experienced both local and global effects at this location. Local tensile stresses occurred in these strain gages since the longitudinal splice was only loaded on one side. Since the truck only loaded one of the panels connecting to the splice directly, it deflected much more than the panel on the other side of the splice, placing the splice in tension. The global effect was caused by positive bending in the reinforcing steel due to the greater displacement of the middle girder compared to the outside girders. This effect placed the longitudinal splice reinforcing steel in compression.

3.3.9 Roll Test Position #2: Critical Findings

In roll test position 2, the centerline of the truck was located over the middle girder, which placed the truck tires between the middle and outside girders. As shown in Figure 3-20 in Section 3.3.7, the cross bars underwent significant local stresses when the truck was rolled in this position. This local bending is also illustrated in Figure 3-24 which displays the response of cross bar gages between the east and middle girders. CH_140 was located on the bottom of a cross bar midway between the east and middle girders while CH_141 was located on the top of the cross bar at the same location. Significant local bending in the cross bars from each truck axle rolling over the point of instrumentation is displayed in Figure 3-24.

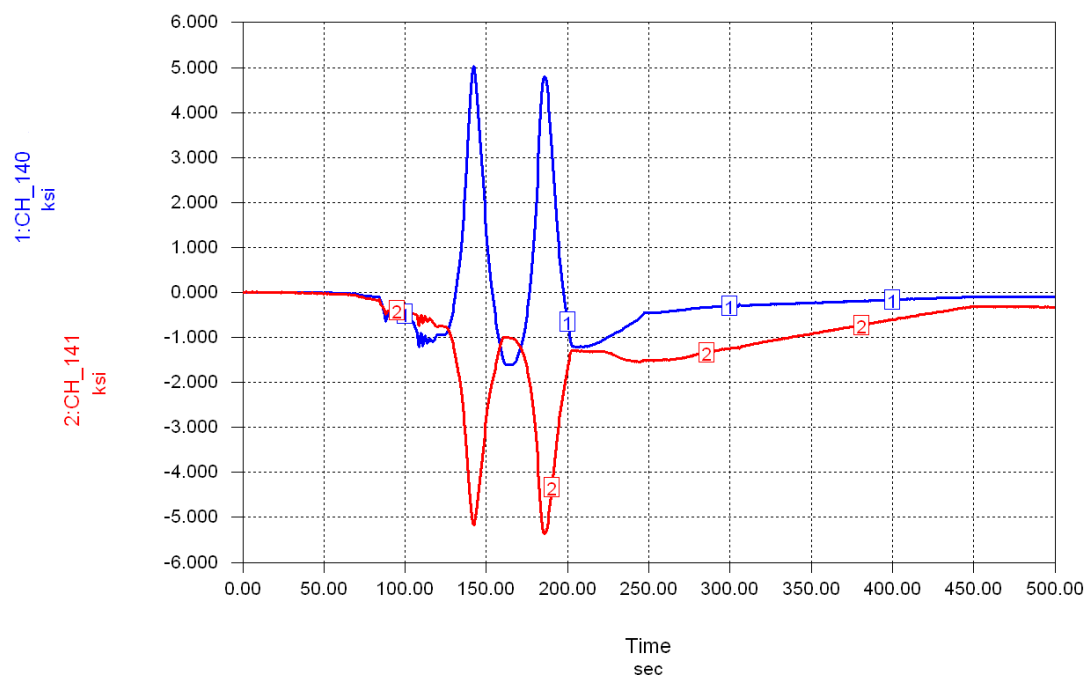


Figure 3-24: Cross bar local bending

Unique main bar behavior where the main bar underwent both positive and negative moment during a single loading cycle was previously discussed in Section 3.3.7. Figure 3-25 illustrates this type of response of a main bar over the middle girder during a truck roll test in Position 2. CH_3 in Figure 3-25 was a strain gage located on the top of the main bar over the middle girder. CH_4 in Figure 3-25 was located on the bottom of the main bar directly below CH_3. The global effect of the truck roll occurred before the local effect of the individual axles crossing the bar because the truck was rolled on the bridge from the opposite side as the location of these strain gages.

Since the truck was centered over the middle girder for this truck roll test, the middle girder carried more of the load than the exterior girders. This caused the middle girder to vertically displace more than the exterior girders. This deflection caused the main bar, which is attached to the girder, to be "pulled down" over the middle girder inducing a positive moment global effect in these bars. (The response is analogous to the positive moment produced at a settling support.) Later in the roll test, there was a local effect that induced a negative moment in the main bar at the same location due to the tires of the truck loading the main bar on both sides of the middle girder. Therefore, at the deck to girders connections, both the top and bottom of the main bar experienced tension during a loaded cycle at certain transverse truck positions.

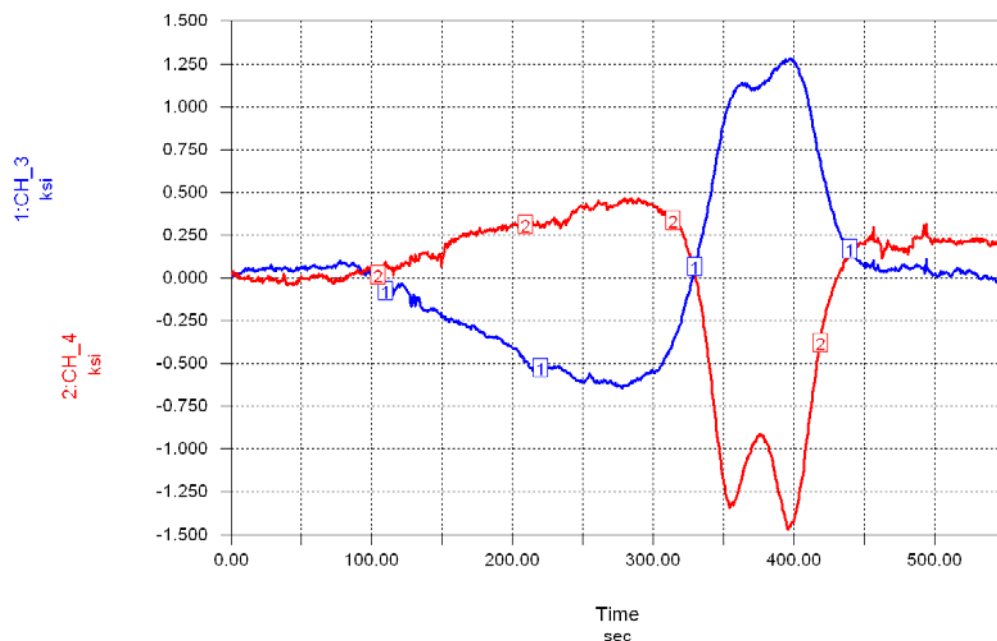


Figure 3-25: Main bar under negative moment

3.3.10 Roll Test Position #3: Critical Findings

In this roll test position, the centerline of the truck was located 2' east of the middle girder. This truck position placed the west truck tires near the middle girder and the edge of the east truck tires halfway between the middle and east girder. The truck was rolled in this position since it is halfway between Position 2 and Position 4, which helped to determine critical stresses in the deck.

Because, in this position, the edge of the truck tires rolled over the easternmost cross bar and transverse splice strain gages, significant local effects were found in these strain gages. The

response of these strain gages is comparable to the response and magnitude of similar gages during the truck roll test in Position 2 shown in Figure 3-22 and Figure 3-24.

The main bar and longitudinal splice stresses were also found to be very similar to those of the roll test in Position 2. In the positive moment region, the main bar stresses were approximately the same magnitude as those found in Position 2 since the tires in both of these roll positions were located close to the midpoint between the middle and outside girders. The response of the negative moment region main bars and longitudinal splice reinforcing steel were found to be very similar to the roll test in Position 2, but the stresses in these strain gages were found to be slightly lower in magnitude in Position 3 than in Position 2. In Position 3, the edge of the west tires rolled over the edge of the middle girder. The deck is stiffened at this location since the load will be directly transferred to the haunch and the girder. Therefore, the main bars did not experience as high a value of stresses as they had in Position 2 when the tires loaded the main bars at an equal distance on both sides of the middle girder.

3.3.11 Roll Test Positions #5 and #6: Critical Findings

Roll test Positions 5 and 6 are similar since they are mirrored about the middle girder. In roll test Position 5, the truck is rolled along the east side of the bridge while in roll test Position 6 the truck is along the west side of the bridge. It was chosen to roll the truck in both of these positions to verify that the response of the bridge deck was consistent and repeatable.

In these positions, the tires of the truck between the middle and exterior girders were rolled in a similar position as the tires in Position 2. Therefore, significant local stresses were found in the cross bars and transverse splice reinforcing steel strain gages for Positions 5 and 6. The stresses measured during the roll tests were similar in magnitude to the stresses measured from Position 2.

A difference in the compressive stress in the cross bars due to composite action was investigated in Position 6. In this position, the truck was rolled along the west edge of the bridge causing the west and middle girders to primarily carry the load. Three adjacent cross bars, between the middle and east girders exhibited decreasing compressive stresses with decreasing distance to the east girder. This behavior was expected since the east girder was carrying negligible load. Therefore, the cross bars near this girder should not have sustained much stress due to composite action.

One of the critical reasons for roll test Position 5 was to measure the stresses in the main bars over the outside girder when the truck was rolled along the edge of the deck. Since the axles were on both sides of the outside girder, it was found that negative moment would be induced in the main bars over the girder. Although the main bar was cantilevered, the stresses found in the main bar over the outside girder were lower than the stresses in the main bar over the middle girder in Position 2. The reason for this difference is that the cantilever was not very long so one of the tires was very close to the girder in Position 5 whereas the tires in Position 2 loaded the main bar approximately 3' from both sides of the girder.

3.3.12 Application Summary - Truck Roll Tests

The truck roll tests were used to characterize the local and global behavior of the bridge deck subjected to rolling wheel loads. Cross bars, main bars, and longitudinal and transverse splice reinforcing steel were instrumented and analyzed for all truck roll test positions. The location of the truck tires in relation to the loading of each instrumented element was considered

and used to determine the location of the longitudinal and transverse cyclic tests. The findings and applications are summarized as follows:

- The bridge deck experienced localized behavior beneath wheel loads during the truck roll tests.
- The response of the bridge deck elements depended greatly on the location of the truck tires and the type of bridge deck element (i.e., main bar, cross bar, etc.).
- Stress reversals occurred in the main bars depending on the longitudinal and transverse position of the truck.
- The stresses in the main bars were found to be small in the negative moment region (i.e., over the girders) with the stresses below 1.5 ksi for all roll tests. These stresses are below the AASHTO Constant-Amplitude Fatigue Threshold (CAFT) for the poorest fatigue category (i.e., Category E') of 2.6 ksi. Therefore, negative moment fatigue checks are not recommended for the steel grid located within the concrete.
- The local tire loads caused the cross bars and the main bars to primarily undergo bending stresses
- The local tire loads caused the longitudinal and transverse splice reinforcing steel to primarily undergo axial stresses.

3.3.13 Longitudinal Splice Cyclic Load Test

Comparison to Roll Test Data. A comparison between the stresses in the reinforcing steel crossing the longitudinal splice was made between the longitudinal splice cyclic test and the truck roll tests as shown in Table 3-9. This comparison was used to assess how well the load patches and spreader beam represent the tire loading.

The estimated stresses in Table 3-9 were calculated using data obtained from the truck roll test Position 2 because it resembled the position of loading for the longitudinal splice cyclic load test. Using data from the laser displacement sensor, the stresses in the longitudinal splice reinforcing steel gages were evaluated when the front and back axle of the truck was located at the same longitudinal location as the actuator location (i.e. 12 feet from the north end of the bridge). Due to the interaction of both axles of the truck inducing load into the splice during the truck roll tests, the smaller of the front and back axle stresses was used for the estimated stresses. The use of the smaller axle stress reduces the effect of the additional load from the leading or trailing axle on the stress measured. Since this effect cannot be fully eliminated, a greater load was needed to induce similar stresses in the splice when loaded with a single axle during the static test compared to the two-axle truck. As illustrated in Table 3-9, the stresses in the longitudinal splice produced during a 25 kip static test were comparable to those produced during the truck roll test with 21 kip axle loads.

Table 3-9: Longitudinal splice reinforcing steel comparison

Gage	Estimated Stress (ksi)	Experimental Stress (ksi)	
		25 kip	21 kip
94	0.42	0.19	0.17
95	1.20	1.11	0.89
107	0.99	0.91	0.72
120	1.43	1.53	1.23
121	1.98	1.82	1.46

Strain Gage Data. Strain gage data were collected for 30 kip and 58.2 kip static loads to check against stresses in later static tests. The 58.2 kip static load was originally only going to be used at the beginning of the test to initiate cracking of the concrete while 30 kip static tests were going to be used for comparison to following static tests during the cyclic test. At 1 million load cycles, it was decided that the 58.2 kip static test would be used for all the static tests since this would simulate heavy truck loadings which would likely add to the fatigue damage of the deck and more accurately simulate the spectrum of truck traffic of a bridge.

The strain gages on the reinforcing steel crossing the longitudinal splice were monitored for any changes throughout the cyclic test. Of the six strain gages that were installed on the reinforcing steel, only three strain gages were working by the end of the cyclic test. These strain gages underwent a slight change of stresses during the first 2 million cycles before leveling off and sustaining the same stress for the remainder of the test. Figure 3-26 displays these strain gages for the 58.2 kip static tests which were run at the beginning of the test and repeatedly at half million cycle increments from 1 million cycles until the end of the test.

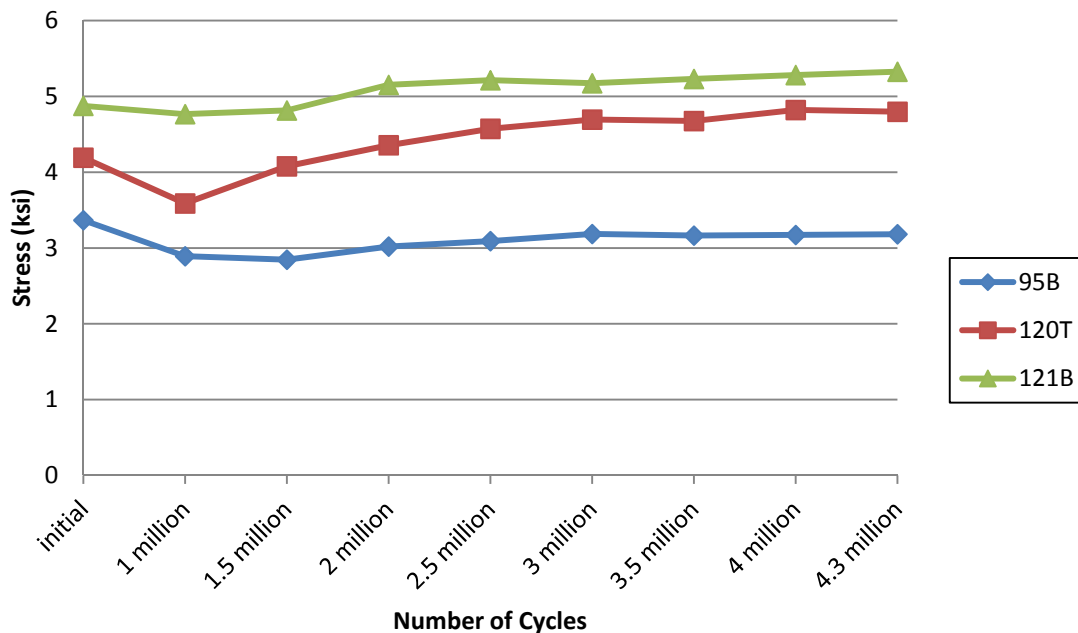


Figure 3-26: 58.2 kip static test results – longitudinal splice reinforcing steel

The results from the 30 kip static tests for the longitudinal splice reinforcing steel are given in Figure 3-27. As seen in this figure, the strain gages followed the same trend as in the 58.2 kip static tests with the strain gages changing stresses during the first 2 million cycles before leveling off. The strain gages also seem to follow a slightly upward trend from the beginning of the test as was seen in Figure 3-26.

The slight increase in stresses which was observed in Figure 3-26 and Figure 3-27 could be due to some cracking and slight damage occurring in the longitudinal splice. Since the splice is mainly loaded in negative moment due to the load patches on both sides of the middle girder, tensile stresses will develop on the top of the splice. These tensile stresses could crack the concrete at the top of the deck. Since the reinforcing steel is located near the top of the splice, it carries all the tension across the splice which could cause an increase in stress if more damage occurred in the splice. It seems that if any cracking and damage occurred in the splice, it only caused a very minor increase in the stress in the reinforcing steel and happened during the first 2 million cycles before stopping altogether. This behavior could also be described as an initial "shake down" period where the deck was settling into place.

It should be noted that, as discussed in Section 3.3.7, even though the longitudinal splice reinforcing steel strain gages overall demonstrated behavior consistent with the expected behavior, these gages seemed to be slightly inconsistent in the magnitude of the stresses. For example, the top of the reinforcing steel displayed less tensile stress than the bottom of the reinforcing steel although the splice region was found to be loaded primarily in negative moment. Even with these inconsistencies, the response of the longitudinal splice reinforcing steel was repeatable and exhibited the correct behavior (i.e. tension) throughout the test. The same behavior was observed for the longitudinal splice reinforcing steel during both the longitudinal splice cyclic test and the truck roll tests.

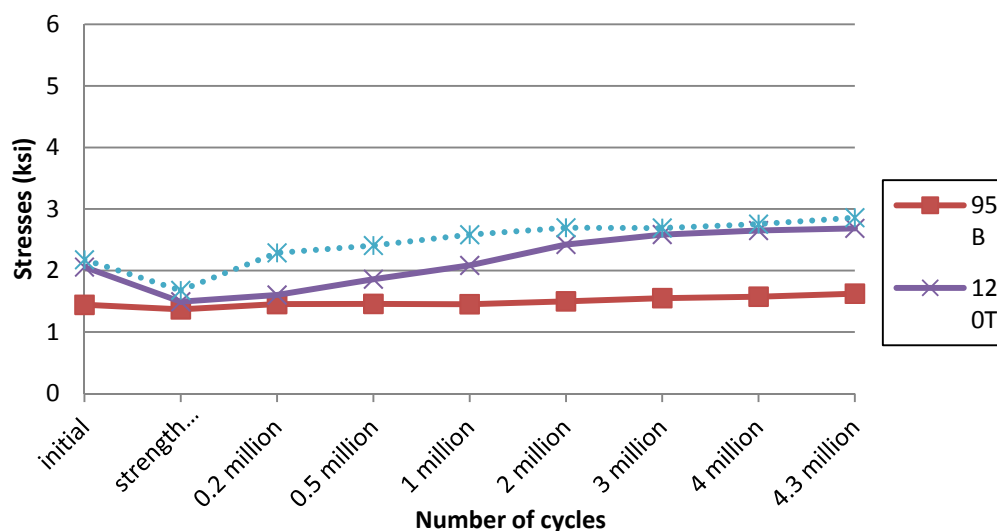


Figure 3-27: 30 kip static test results – longitudinal splice reinforcing steel

It was found that the 30 kip and 58.2 kip static tests produced similar trends of stress, but different magnitudes. Therefore, the remaining stresses shown in this section will be shown for the 58.2 kip static loads.

The results from the 58.2 kip static tests for the main bar strain gages located one foot away from either side of the longitudinal splice are shown in Figure 3-28. Since these strain

gages were located on the main bars near the longitudinal splice, any damage in the longitudinal splice may have induced a change in the stresses in the main bars at this location. The stresses at Channel 104 and Channel 109, located on the bottom of the main bars, did not exhibit any large stress changes throughout the test. These stresses seemed to decrease slightly before leveling off and staying constant after approximately 2 million load cycles.

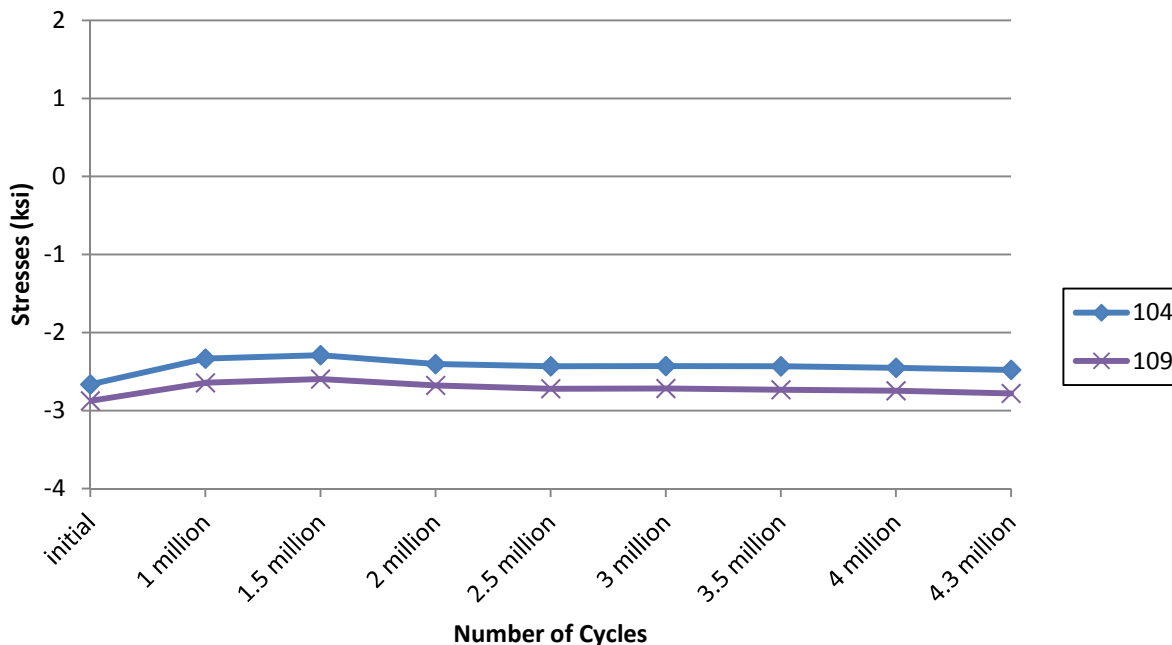


Figure 3-28: Main bar stresses one foot from LS splice

The results from the 58.2 kip static tests for the main bar strain gages located two feet away from either side of the longitudinal splice are shown in Figure 3-29. These strain gages were evaluated to determine if any significant changes in stresses occurred throughout the cyclic load test. Since these strain gages were located between the load patches and the longitudinal splice, the stresses at this location would be expected to change if the deck underwent cracking in the longitudinal splice or near the load patches. As illustrated in Figure 3-29, some of these strain gages experienced a slight decrease in stress the first one million cycles before having a constant stress for the remainder of the test. Therefore, it seems that no significant damage occurred in this region throughout the test. Visual inspection of the deck confirmed that only minimal cracking occurred throughout the test. These findings will be discussed in further detail in the following section.

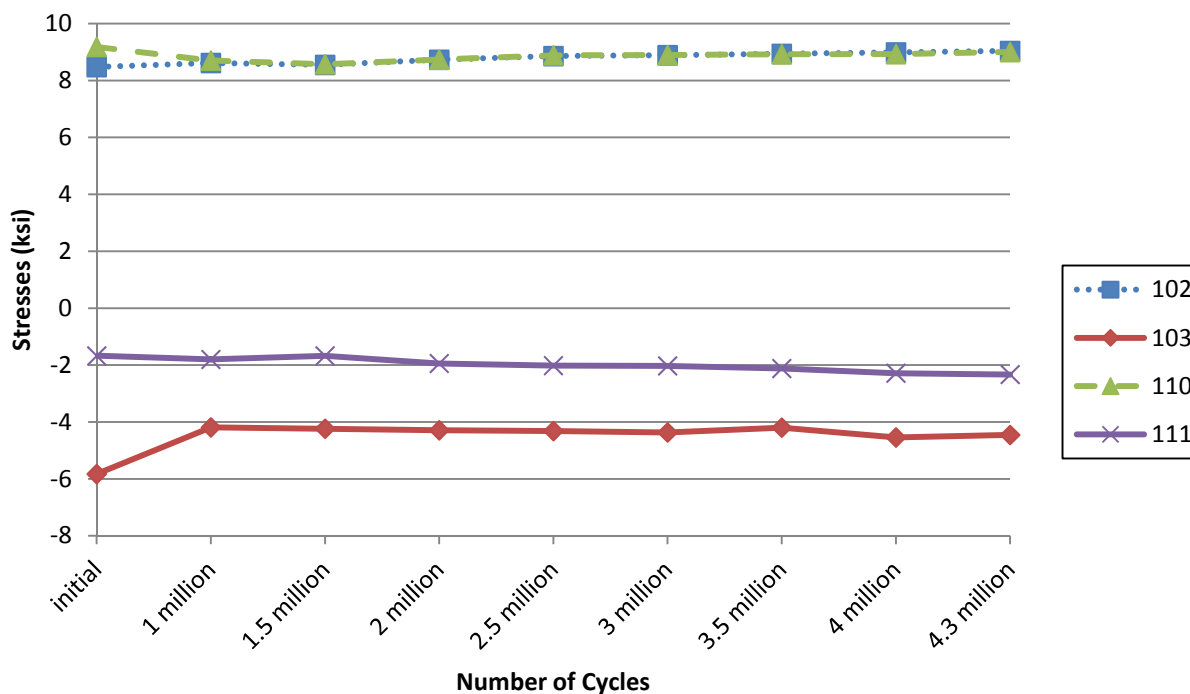


Figure 3-29: Main bar stresses two feet from LS splice

The stresses in the main bars midway between the middle and outside girders during the cyclic test were found to stay constant throughout testing. This seems to indicate that not much damage occurred in the bridge deck near these strain gages. If the concrete degraded and did not act compositely with the main bars, it would be expected that these stresses would increase.

The stresses in the bottom flange of the girders at mid span and near the longitudinal splice test location were also monitored throughout testing. It was found that these stresses also stayed constant throughout testing. This was to be expected since the loading stayed constant and no damage was expected at this location.

Strain gage data from the initial static tests when the actuator applied a total load of 30 kips to the spreader beam. The tables only give the stresses for the strain gages in critical locations in the bridge which were hooked up to the data logger and functioning properly during the longitudinal splice static tests.

Concrete Cracking. The concrete near the load patches was inspected and marked for cracking after the initial static testing was completed. Figure 3-30(left) illustrates the cracking found on the north side of the loading patches while Figure 3-30(right) illustrates the cracking on the south side of the loading patches. Since there was previous cracking due to shrinkage and the truck roll test, these marks were used as a baseline for cracking at the beginning of the cyclic load test.



Figure 3-30: Initial cracking near load patches (prior to any load cycles) (left) north side; (right) south side

After 100 load cycles of the 58.2 kip strength load were applied, the deck was inspected again for any increase in concrete cracking. Figure 3-31(left) illustrates the cracking on the north side of the load patches after this loading. Figure 3-31(right) illustrates the cracking on the south side of the load patches. It should be noted that an increase in cracking was found when comparing this figure to Figure 3-30.



Figure 3-31: Cracking after strength test (after 100 cycles at the strength load) (left) north side; (right) south side

The concrete cracking at the conclusion of the longitudinal splice cyclic test is shown in Figure 3-32. As can be seen in this figure, the cracking that occurred was concentrated over the longitudinal splice between the load patches. Most of the cracks that occurred were very small and could only be found if the deck was sprayed with water. It was found that some of the early cracks caused by shrinkage of the concrete did grow slightly during the initial portion of the cyclic test and were the largest cracks in this location after testing. It was observed that these larger cracks would “pump” open and closed during the cyclic testing when water was sprayed on the deck.



Figure 3-32: Concrete cracking at completion of longitudinal splice cyclic test (after 4.3 million cycles)

Test Termination. According to the calculations shown in Section 2.6.3, the longitudinal splice test was planned to run for 6.2 million load cycles. As previously discussed, the test was terminated at approximately 4.3 million load cycles. It was decided to terminate the test early for the following reasons:

- No changes in strain gage measurements or crack extension occurred from approximately 2-4 million load cycles. Hence, it was determined that additional cycling would not result in more damage.
- No significant damage had been observed, even at the strength load application and with the severe vibration induced by the air-driven vibrator.
- No observed changes in composite behavior between the deck and the main girders.
- The number of load cycles was selected somewhat arbitrarily (i.e., the ADTT of 1,500 was arbitrarily selected).

Application Summary – Longitudinal Splice Test. The longitudinal splice cyclic test was used to develop the subassembly longitudinal splice cyclic tests. The findings and applications of this test are summarized as follows:

- The stresses in the longitudinal splice reinforcing steel during the test compared well to the roll tests. Therefore this test represented similar damage as repeated tire loading.
- Small amounts of initial concrete cracking along with small stress changes in critical members (i.e., main bars and reinforcing steel) occurred throughout testing. These changes reinforce that this test should be able to distinguish poor splice details which would sustain more damage during the test.
- The concrete cracking in the longitudinal splice was able to be compared to control cracks away from the test region through the use of fluorescent epoxy and concrete cores. These cores gave a good indication of the depth of the concrete cracks and the possibility of infiltration of deicing salts into the deck which could cause durability issues and corrosion of the steel bars.

- The cracks in the longitudinal splice region were found to be of similar size to the control cracks on large shrinkage cracks outside of the tested region. Therefore, although this test is able to evaluate the damage caused to the splice through repeated loading, the amplitude of the cyclic loading was not so high that unrealistic damage was created.

3.3.14 Transverse Splice Cyclic Load Test #1

Because of the close proximity of the transverse splice load patch areas to the longitudinal splice location, the transverse splice load patch areas were checked for cracking and compared to similar transverse splice areas on the other side of the bridge. The cracking caused by the longitudinal splice test was found to be localized and did not cause a significant increase in concrete cracking at the transverse splice locations which were chosen.

Comparison to Roll Test Data. To determine the ability of the loading apparatus for the transverse splice cyclic test to simulate the truck loading, data for the initial transverse splice static tests were compared to the roll test data. This comparison was made to see if the load patch induced similar stresses in the splice as the truck tires. Since the cross bar and reinforcing steel stresses were driven mainly by local effects, the load induced through each axle caused the maximum stresses. Since the truck axles weighed approximately 21 kips, which was split between two tires, stresses at a 10 kip load during the initial static tests were compared to the maximum from the truck roll tests. Table 3-10 shows this comparison for the reinforcing steel stresses crossing the transverse splice near where the transverse splice cyclic test position. The stresses for these strain gages were found to correspond well to the maximum roll test stresses. Thus, the single load patch used in the transverse splice load test reasonably represents the maximum stresses caused by the truck roll tests.

Table 3-10: Transverse splice cyclic test #1 roll test comparison

Gage	Maximum Stress from Truck Roll Tests (ksi)	Stress from 10 Kip Static Load (ksi)
142T	0.93	1.27
143B	1.08	1.23
154T	1.17	1.05
155B	0.79	0.71
166T	1.22	0.83
167B	0.93	0.79

Strain Gage Data. The stress measurements of the critical strain gages near the transverse splice were monitored and static test data were collected at the beginning of the test, after the 100 strength load cycles, and at half million cycle intervals as discussed in Section 2.6.4. The cross bar and main bar stresses near the transverse splice test location were found to stay constant during the testing procedure. The stresses found at these locations throughout testing are shown in the following figures.

The cross bar stresses on the north side of the transverse splice (i.e., opposite side of loading) are shown in Figure 3-33 while the cross bar stresses on the south side of the transverse splice (i.e., loaded side) are shown in Figure 3-34. These figures display the stresses on both the top (odd numbered gages) and the bottom (even numbered gages) of the cross bars.

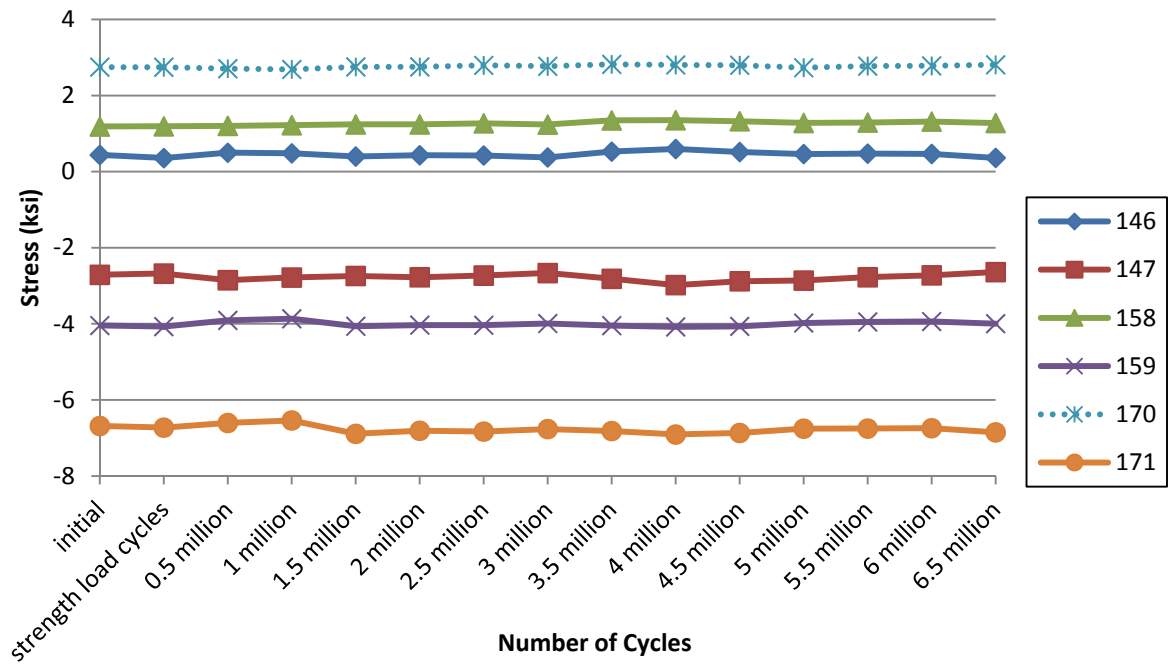


Figure 3-33: Transverse splice #1 north cross bar stresses

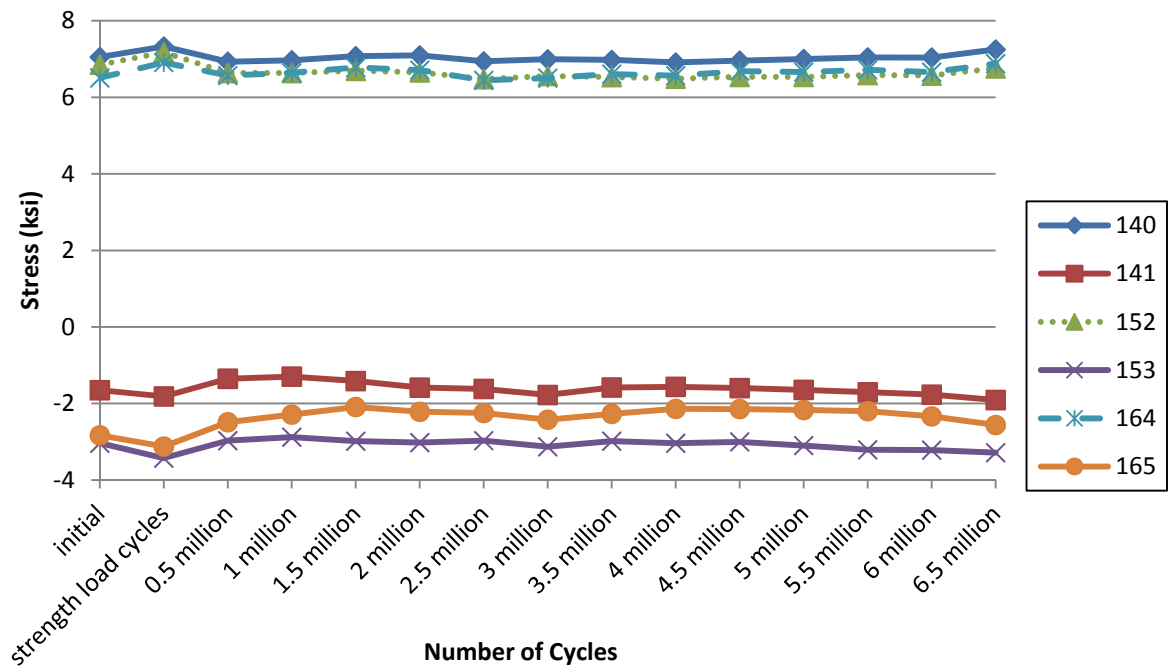


Figure 3-34: Transverse splice #1 south cross bars stresses

The main bar stresses on the north side of the transverse splice (i.e. opposite side of loading) are shown in Figure 3-35. This figure displays the stresses on the top (odd numbered gages) and bottom (even numbered gages) of the main bars. The stresses on the main bars near the transverse splice test position were found to stay fairly constant during testing.

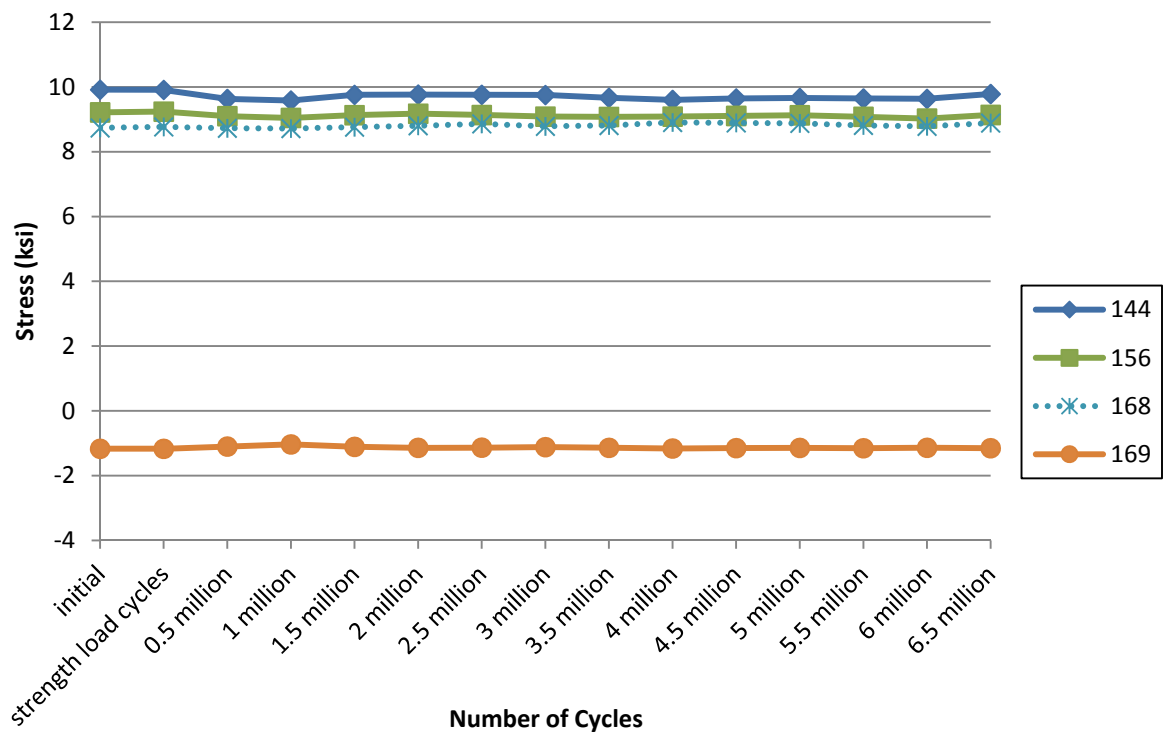


Figure 3-35: Transverse splice #1 main bar stresses

Although the cross bars and main bar stresses near the transverse splice did not change during the test, the stresses in the reinforcing steel crossing the splice did show a trend of increasing stresses as the test progressed. Three reinforcing bars with two strain gages on each bar were monitored during the testing. All six strain gages showed that the average stress in the reinforcing steel increased steadily throughout the cyclic load test. The stresses increased by approximately 0.5 ksi from the stresses measured at the start of the test as shown in Figure 3-36. If damage was to occur in the transverse splice due to concrete cracking, the stress in the reinforcing steel crossing the splice would be expected to increase since more of the load would be carried across the splice by the reinforcing steel.

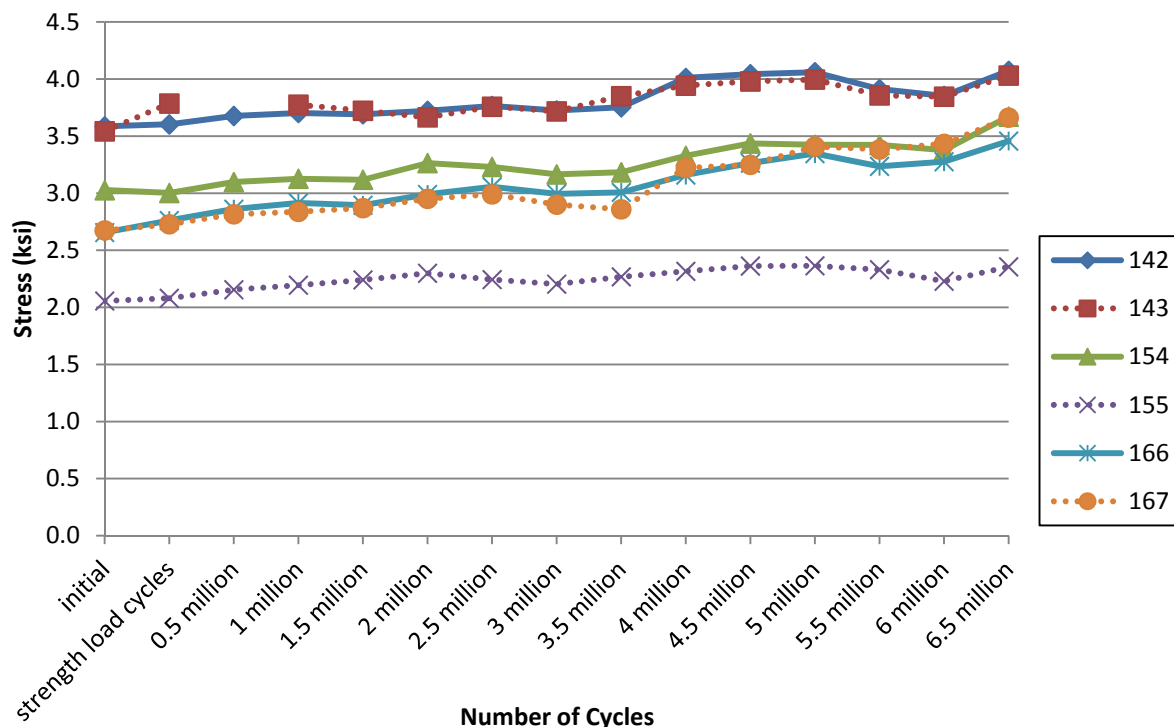


Figure 3-36: Transverse splice #1 reinforcing steel stresses

Strain gage data from the initial static tests when the actuator applied a load of 29.1 kips to the load patch. The tables only give the stresses for the strain gages in critical locations in the bridge which were hooked up to the data logger and functioning properly during the transverse splice #1 static tests.

Concrete Cracking. Only a slight amount of crack growth was found at the splice during the testing with the majority of this cracking occurring during the beginning of the testing. Very small longitudinal cracks were found running across the bottom of the concrete at the transverse splice. Most of these cracks were present at the beginning of the test, but the cracks did seem to open up slightly during testing. A number of the cracks would “pump” when water was sprayed on them while the deck was loaded cyclically. Figure 3-37(left) shows the underside of the transverse splice with the form pan removed after the conclusion of the cyclic test. Small longitudinal cracks (marked in black) were spaced at approximately 4”, which corresponds to the cross bar spacing in the gird deck. Since the cross bars were located just above the form pan, only very minor concrete cover (< 1 ”) was found below these bars. Therefore, these cracks form due to the very thin layer of concrete at the location of the cross bars. Figure 3-37(right) shows the load patch area on the top of the deck after the conclusion of the cyclic test. Most of the cracking seen in this figure was present prior to the cyclic testing.

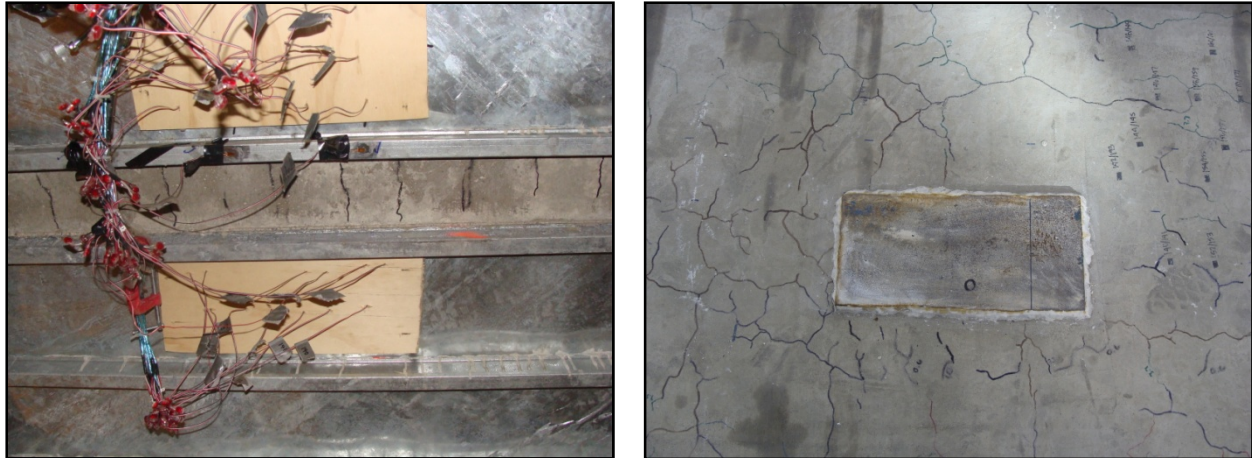


Figure 3-37: (Left) bottom of transverse splice; (right) transverse splice load patch (note steel plate is still in place)

3.3.15 Transverse Splice Cyclic Load Test #2

As discussed in Section 2.6.4, a second transverse splice position was tested due to the findings of transverse splice cyclic load test #1. The stresses measured by the strain gages on the reinforcing steel crossing the transverse splice increased throughout transverse splice cyclic load test #1. Therefore, another test was conducted to determine if the results would be repeatable.

Comparison to Roll Test Data. A similar stress comparison was made for transverse splice test #2 as was done for transverse splice test #1. The stress measured in the reinforcing steel crossing the transverse splice at the testing location from a 10 kip static test was compared to the maximum stresses caused by the truck roll tests as shown in Table 3-11. It was found that the stresses measured by these strain gages were similar for both the roll tests and 10 kip static load. Based on this, it was concluded the loading used for the cyclic load test reasonably represented the response produced by the truck tires.

Table 3-11: Transverse splice cyclic test #2 roll test comparison

Gage	Maximum Stress from Truck Roll Tests (ksi)	Stress from 10 Kip Static Load (ksi)
130T	0.93	1.08
131B	1.05	0.91

The stresses in transverse splice cyclic test #1 were compared to transverse splice cyclic test #2 as shown in Table 3-12. As seen in this table, the stresses at the reinforcing steel for transverse splice test #2 are comparable to transverse splice test #1 during the initial 30 kip static tests for each test.

Table 3-12: Comparison of transverse splice cyclic tests

Initial 30 Kip Static Tests		
	Gage	Stress (ksi)
Transverse Splice Test #1	142T	3.59
	143B	3.54
	154T	3.03
	155B	2.06
	166T	2.66
	167B	2.67
Transverse Splice Test #2	130T	3.42
	131B	2.38

Strain Gage Data. Static test data for the critical strain gages near the transverse splice were collected at the beginning of the test, after the application of the 100 strength load cycles, and at half million cycle intervals as discussed in Section 2.6.4.

Stresses from some of the strain gages near transverse splice test #1 were also collected during testing. These data were used to verify that the transverse splice test #1 did not cause any initial fatigue damage at the transverse splice test #2 position. All of the strain gages on the cross bars and reinforcing steel in the transverse splice test #1 position were found to cycle in compression with a maximum stress less than 1 ksi during the 29.1 kip static tests. The strain gages on the main bars at the transverse splice test #1 region were found to have a maximum tensile stress of less than 1 ksi and a maximum compression stress of less than 1.5 ksi during the 29.1 kip static tests. Because tensile stresses were found to be very low or nonexistent, no damage at the transverse splice test #2 position was expected to have occurred from the transverse splice test #1.

The stresses in the cross bars during the transverse splice test #2 are shown in Figure 3-38. These stresses did not seem to change greatly as the test progressed. This is similar to the results found for the cross bar strain gages during transverse splice test #1 shown in Figure 3-33 and Figure 3-34.

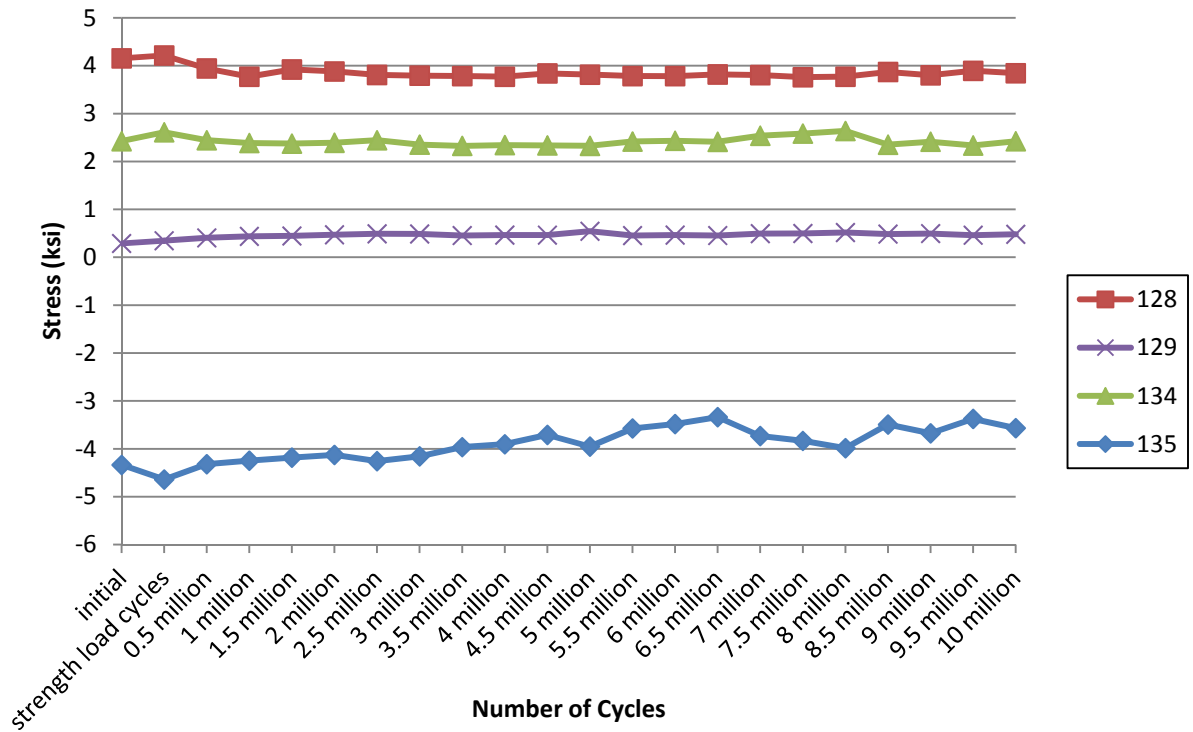


Figure 3-38: Transverse splice #2 cross bar stresses

The stresses in the main bars during transverse splice test #2 were found to have slightly different results than in test #1. The stresses in the main bars on the north side of the transverse splice (i.e. opposite of the load patch) were monitored throughout the test. These strain gage locations were similar to those monitored on the main bars during the first transverse splice test. It was found that the stresses in the main bars at this location decreased slightly during the second transverse splice test as shown in Figure 3-39. Channels 132 and 136 were strain gages located on the bottom of the first two main bars on the north side of the transverse splice. As can be seen, there was a slight decrease in tensile stress in these gages from the initial static tests to the final static tests. This decrease in stress was also found in Channel 133, located on the top of the main bar at the same location as Channel 132. Channel 133 displayed a slight decrease in compressive stress from the initial to the final static tests. If there was any degradation of the concrete in the splice, the damage would cause a change in the stiffness of the splice. A softening of the splice would result in a decrease in the amount of load transferred across the splice to the main bars on the other side. The drop in measured stress (load) in these main bars would explain the slight decrease in stress found in these members during the test.

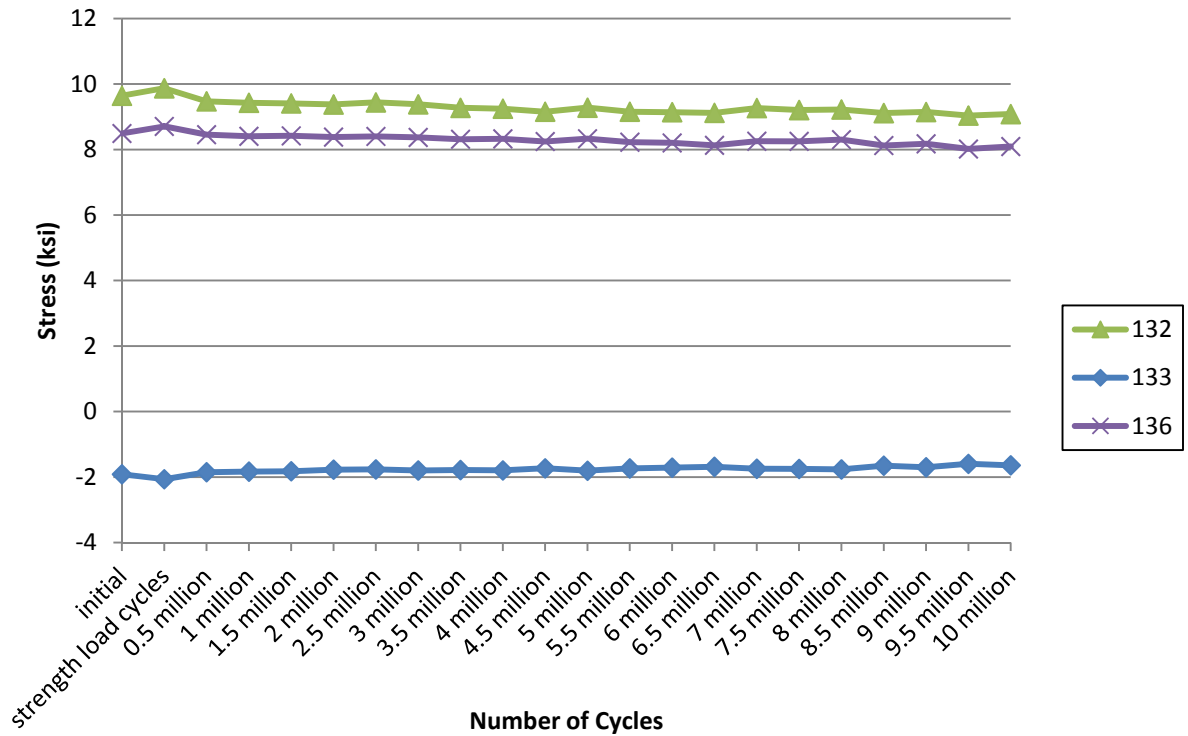


Figure 3-39: Transverse splice test #2 main bar stresses

The changes in stress of a reinforcing bar crossing the transverse splice near the testing location were monitored throughout the transverse splice test. These stresses are shown in Figure 3-40. From this figure, it can be seen that Channel 130T, which was on the top of a reinforcing steel bar, followed the same increasing trend as the stresses from transverse splice test #1 shown in Figure 3-36. Channel 131B, which was on the bottom of the reinforcing steel, displayed two trends. The stress decreased for the first 2.5 million cycles and then increased for the rest of the test such that it ended at a stress similar to that measured at the beginning of the test.

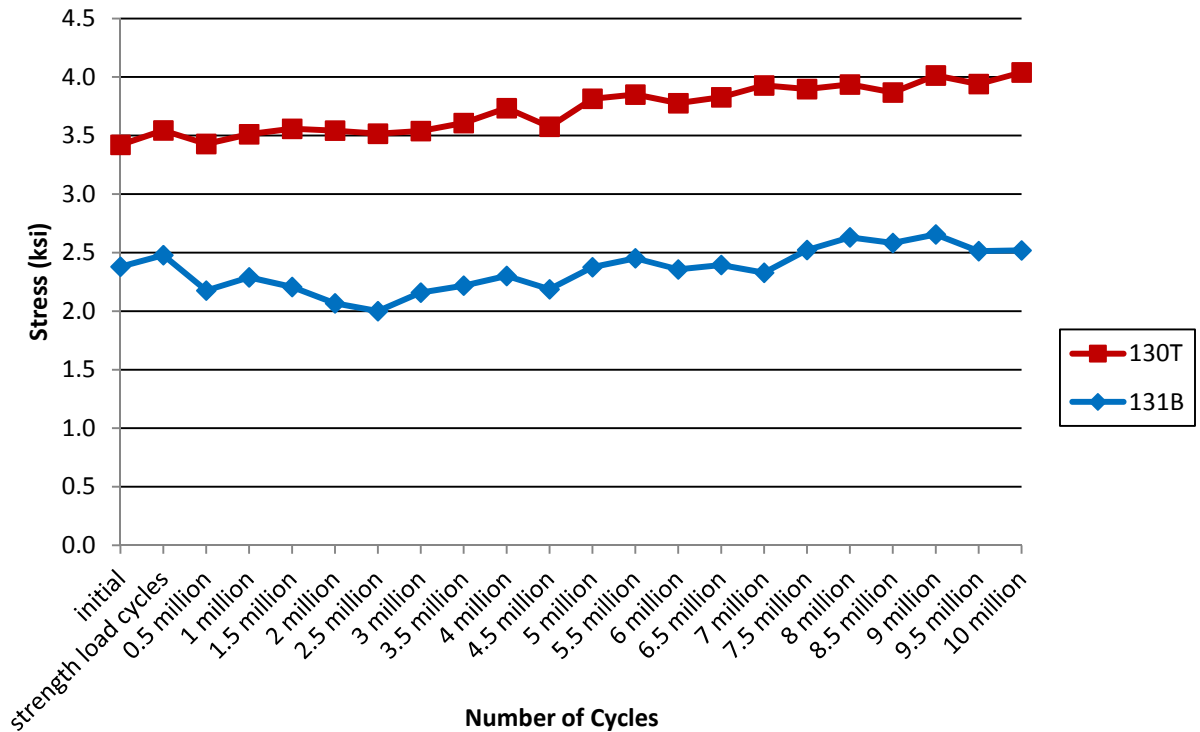


Figure 3-40: Transverse splice test #2 reinforcing steel stresses

Because of the slight change in stresses in both the reinforcing steel crossing the transverse splice and the main bars across the splice from the load patch in transverse splice test #2, it seems that there might be a slight amount of damage occurring in the splice due to the transverse splice cyclic test. The reinforcing steel stress increased in both the transverse splice test #1 and #2 while the main bar stress decrease was only found in the transverse splice test #2. The stress increase in the reinforcing steel would result due to any degradation in the concrete within the splice. This would result in a change in local behavior as well as cause the neutral axis of the section to shift. It is postulated that the observed changes in measured stress were the result of this degradation. Although the observed changes are interesting, they are primarily academic as the changes during the test were found to be relatively small compared to the total stress in these strain gages.

Strain gage data from the initial static tests when the actuator applied a load of 29.1 kips to the load patch. The tables only give the stresses for the strain gages in critical locations in the bridge which were hooked up to the data logger and functioning properly during the transverse splice #2 static tests.

Concrete Cracking. Small longitudinal cracks were found in the concrete at the bottom of the transverse splice prior to the start of the test. These cracks were similar to those shown in Figure 3-37(left) from the first transverse splice test location. Early in the testing procedure, some crack growth was observed as these cracks extended across the bottom of the transverse splice. In addition to the small longitudinal cracks, a diagonal crack across the bottom of the transverse splice was observed approximately 1 million cycles into the cyclic test. This crack, shown in Figure 3-41, was found in a similar location to a crack on the top surface of the deck

near the load patch. Measurements were made to verify that the crack was in the same location on the top and bottom of the transverse splice, which it did confirm. Therefore, concrete cores were taken in this region to determine if this crack penetrated through the depth of the splice. These cores are shown and discussed in the following section.

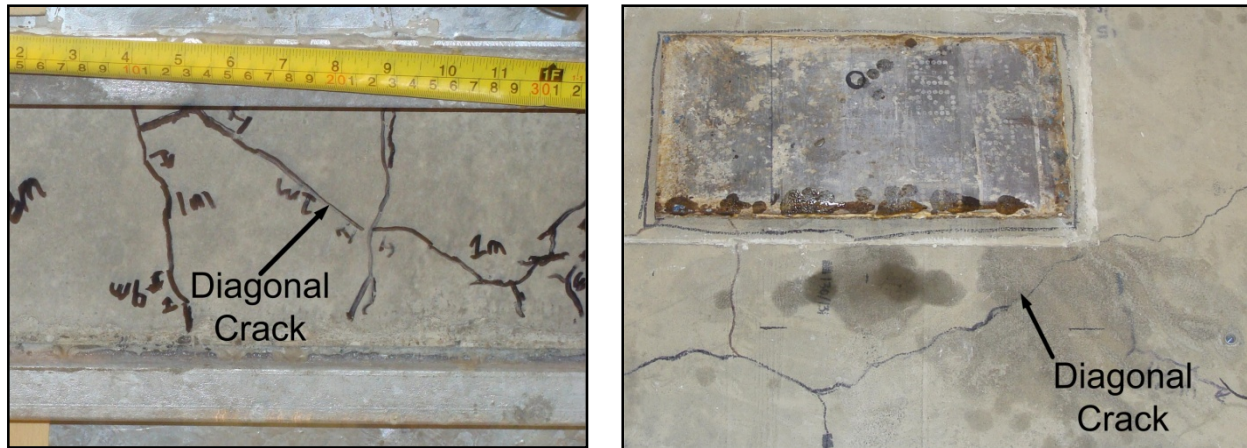


Figure 3-41: Diagonal crack transverse splice test #2 (left) bottom; (right) top

3.3.16 Application Summary - Transverse Splice Tests

The transverse splice cyclic test was used to develop the subassembly transverse splice cyclic tests. The findings and applications of this test are summarized as follows:

- The stresses in the transverse splice reinforcing steel during the test compared well to the roll tests. Therefore this test represented similar damage as repeated tire loading.
- Cross bar stresses on both sides of the transverse splice did not undergo much stress changes throughout testing.
- The transverse splice reinforcing steel stresses increased throughout both of the transverse splice cyclic tests along with some slight concrete cracking initially. These results reinforce that this test should be able to distinguish poor splice details which would sustain more damage and greater stress changes.
- The concrete cracking in the transverse splice was able to be evaluated through the use of fluorescent epoxy and concrete cores. These cores gave a good indication of the depth of the concrete cracks and the possibility of infiltration of deicing salts into the deck which could cause durability issues and corrosion of the steel bars.
- The results of the transverse splice cyclic tests were found to be repeatable and consistent.

3.4 Subassembly Stiffness Tests

This section discusses the findings of the subassembly stiffness tests for the strong (D_x) and weak (D_y) directions as well as in torsion (D_{xy}). Comparisons of the experimentally measured and theoretically computed stiffness's are also described herein. The findings of these tests were incorporated into the appropriate standard test methods.

3.4.1 Strong Axis Stiffness

Each subassembly specimen was tested to isolate and determine the stiffness of the deck in strong axis direction. This would create one way bending, similar to a beam, rather than the two-way plate behavior that a deck typically exhibits when loaded. The results were then used to determine the experimentally measure the strong axis direction stiffness, which was computed as:

$$D_x = \frac{P'L^3}{48\Delta_{CL}} \quad (3-9)$$

where:

D_x = Strong axis direction stiffness (kip-in.²/in.)

P' = The applied point load divided by the width of the deck specimen

L = Span length of the deck (in.)

Δ_{CL} = Net vertical deflection at the centerline of the deck.

To ensure that measured stiffness of the specimen was reasonable, a model of the strong axis direction was developed and the theoretical stiffness was computed as:

$$D_x = \frac{EI}{w_{\text{cross-section}}} \quad (3-10)$$

where:

E = Modulus of elasticity (ksi);

I = Moment of inertia (in.⁴); and

$w_{\text{cross-section}}$ = Width of the cross-section from which the moment of Inertia was determined (in).

It was desirable to ensure that the measured and theoretical strong axis stiffness were within 15% of one another. If this was not the case, the theoretical model of the deck was adjusted and the stiffness was recalculated to ensure the behavior of the deck was understood for this direction.

Open Grid Deck Specimen #1. After analyzing the data obtained from the subassembly strong axis stiffness test for this specimen, it was found that the results of the testing were very consistent. Small deflections at mid span of the specimen (i.e., where the load was applied) were measured throughout testing. This specimen behaved linearly as shown by CH_34 (i.e., a displacement location underneath the line load) in Figure 3-42. Therefore, the measured stiffness was computed for each test run and averaged as shown in Table 3-13.

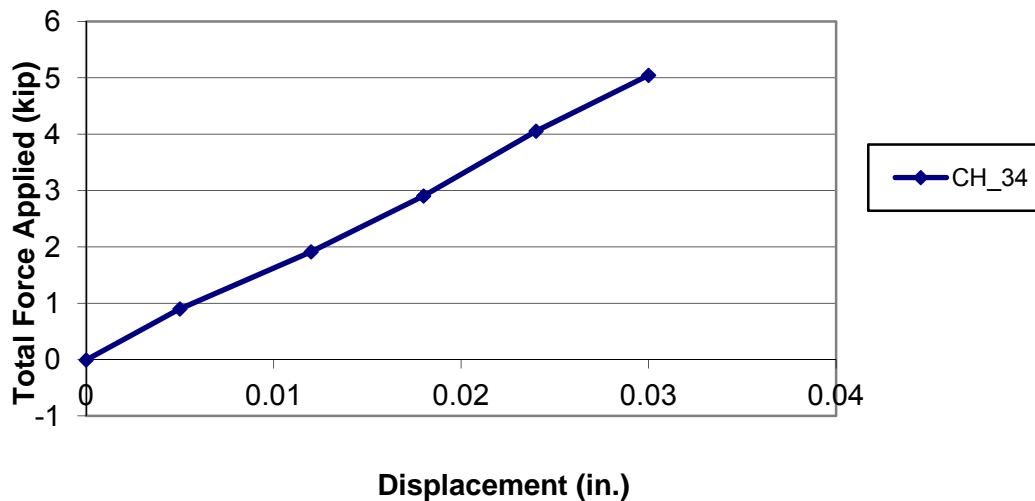


Figure 3-42: Linear deflection underneath line load

Open Grid Deck Specimen #2. The results of the subassembly strong axis stiffness test for this specimen were also consistent for all runs of the test. Again, small deflections were observed throughout testing. As shown in Table 3-13, this specimen was slightly more flexible than open grid deck specimen #1 in the strong axis because not all bar intersections were welded (i.e., main-cross bar and supplemental-cross bar) and there were not any diagonal bars in this specimen. Puddle welds were not included at all bar intersections because this specimen was intended to be encased in concrete for the partially filled grid deck specimen. The fabricator typically only includes enough welds necessary for fabrication, shipping and construction when the grid decks are to be encased in concrete.

Partially Filled Grid Deck Specimen. Again, the results for the subassembly strong axis stiffness test for this specimen were consistent for all runs of the test. Extremely small deflections, compared to those of the open grid deck specimens, were measured at the mid span of the specimen. Therefore, the measured stiffness, shown in Table 3-13, was much greater than those of the open grid deck specimens.

Comparison to Theoretical. The measured stiffness for each of the deck panels tested was compared to the theoretical stiffness for this direction. The theoretical stiffness was determined by using the transformed section of a 10 inch wide cross-section representative of the specimen in the strong axis direction. The theoretical stiffness was computed for this representative section of a bridge deck panel and converted to stiffness per unit width (i.e., per inch). When necessary to determine a theoretical stiffness more comparable with measured stiffness, adjustments were made to the model of the deck and reanalyzed. For example, it was found that the stiffness of open grid deck specimen #2 could be modeled more accurately in the strong direction by including only the main bars. The supplemental bars were very small compared to the main bars and not all welded to the cross bars. Therefore, the supplemental bars provided negligible contribution to the stiffness of the deck, making this is a reasonable assumption. However, this assumption was not appropriate to use for open grid deck specimen #1 since the cross bars were connected to the main and supplemental bars using puddle welds at

each intersection point. Rather, the transformed section of the deck was used to determine the appropriate theoretical value of the strong axis stiffness (D_x) of open grid deck specimen #1.

The subassembly partially filled grid deck specimen model was also adjusted to create a more accurate model. Specifically, once the neutral axis of the specimen was determined, the concrete in the tension region (i.e., below the neutral axis) was excluded from the moment of inertia. This assumption was reasonable because concrete is essentially ineffective in tension. Therefore, this region would not contribute to the stiffness of the deck.

Table 3-13 shows a comparison of the average measured and computed theoretical stiffness in the strong axis direction. The ratios of theoretical to average measured stiffness for each deck show that the model could reasonably represent the deck stiffness.

Table 3-13: Comparison of measured and theoretical stiffness in strong axis direction (D_x)

Deck Panel	Strong Direction Stiffness, D_x (kip-in. ² /in.)					<u>Theoretical Measured</u>
	Test #1	Test #2	Test #3	Average Measured	Theoretical $D_x=EI$	
Open Grid #1	23,652	22,840	23,288	23,260	21,866	0.94
Open Grid #2	16,060	15,570	16,218	15,950	14,812	0.93
Partially Filled Grid	67,900	75,500	71,700	71,700	68,324	0.95

3.4.2 Weak Axis Stiffness

In a similar manner to the strong axis stiffness test, each subassembly specimen was tested to isolate and determine the stiffness of the deck in weak axis direction. From the experimentally measured response, the weak axis direction stiffness was computed as:

$$D_y = \frac{P'L^3}{48\Delta_{CL}} \quad (3-11)$$

where:

D_y = Weak axis direction stiffness (kip-in.²/in.)

As was done for the strong axis stiffness test, a model of the weak axis direction was developed and the theoretical stiffness was computed as:

$$D_y = \frac{EI}{w_{\text{cross-section}}} \quad (3-12)$$

It was desirable to ensure that the measured and theoretical weak axis stiffness were within 15% of one another. If this was not the case, the theoretical model of the deck was adjusted and the stiffness was recalculated to ensure the behavior of the deck was understood for this direction.

Open Grid Deck Specimen #1. After analyzing the data obtained from the subassembly weak axis stiffness test for this specimen, it was found that the results of the testing were very consistent. Relatively small deflections at mid span of the specimen (i.e., where the load was applied) were measured throughout testing. However, these deflections were much greater than those measured in the strong axis stiffness test, indicating the deck was much more flexible in the weak axis direction as expected. In fact, the average measured weak axis stiffness

for this specimen, shown in Table 3-14, was approximately 17 times less than that of the strong axis direction.

Open Grid Deck Specimen #2. The results of the subassembly weak axis stiffness test for this specimen were also consistent for all runs of the test. Again, relatively small deflections were observed throughout testing. As shown in Table 3-14, the stiffness of this specimen was similar to that of open grid deck specimen #1 because the configuration of steel resisting the load in this direction is the same for both specimens.

Partially Filled Grid Deck Specimen. The results for the subassembly weak axis stiffness test for this specimen were consistent for all runs of the test. Small deflections were measured at the mid span of the specimen compared to those of the open grid deck specimens. Therefore, the stiffness of the partially filled grid deck specimen, shown in Table 3-14, was much greater than those of the open grid deck specimens. In fact, the weak axis stiffness of this specimen was greater than the strong axis stiffness of open grid deck specimen #2.

Comparison to Theoretical. The average stiffness measured for each of the deck panels tested was compared to the estimated theoretical stiffness for this direction as was done for the strong axis stiffness. The theoretical stiffness was determined by using the transformed section of the specimen in the weak axis direction. For the open grid deck specimens, the analysis was rather simple because the cross bars were the only components resisting the applied load in this direction. However, the partially filled grid deck specimen was modeled similar to that of its' stiffness in the strong axis direction (D_x). Only the cross bars and concrete in compression were used when computing the moment of inertia because the concrete in tension would contribute negligibly to the stiffness of the deck.

Table 3-14 shows a comparison of the measured and theoretical stiffness in the weak axis direction. The ratios of theoretical to average measured stiffness show that each deck were well modeled for this direction.

Table 3-14: Comparison of measured and theoretical stiffness in weak axis direction (D_y)

Deck Panel	Test #1 (kip-in ² /in)	Test #2 (kip-in ² /in)	Test #3 (kip-in ² /in)	Average Measured (kip-in ² /in)	Theoretical (kip-in ² /in)	<u>Theoretical</u> Measured
Open Grid #1	1,346	1,345	,1341	1,344	1,450	1.08
Open Grid #2	1,396	1,420	1,430	1,415	1,450	1.02
Partially Filled Grid	19,440	20,400	20,140	19,990	22,011	1.10

3.4.3 Torsion Stiffness

Each subassembly specimen was also tested to isolate and determine the stiffness of the deck in torsion. Unlike the strong and weak axis stiffness tests, this test evaluated the ability of the entire system to resist a point load at the free corner of the specimen. The results were then used to determine the experimentally measured torsional stiffness, which was computed as:

$$D_{xy} = \frac{PL^2}{4\Delta_L} \quad (3-13)$$

where:

D_{xy} = Torsion stiffness (kip-in²/in);

P = Applied point load at the free corner of the deck (kips); and

Δ_L = Vertical deflection of the deck under the point load.

Open Grid Deck Specimen #1. During the torsion stiffness test set-up, it was immediately observed that this open grid deck was extremely flexible in torsion. As shown in Figure 3-43, the free corner of the specimen underwent significant deflection before any load was applied at the free corner.



Figure 3-43: Torsion stiffness test set-up for open grid deck specimen #1

Since the deck was so flexible, loading was applied at the free corner using calibrated steel plates. After analyzing the data obtained from testing of this specimen, it was found that the results were very consistent. Therefore, the measured stiffness was computed for each test run and averaged as shown in Table 3-15.

Open Grid Deck Specimen #2. Similar to open grid deck specimen #1, it was immediately observed that this specimen was very flexible in torsion. Open grid deck specimen #2 was even more flexible since not all intersections of bars were welded and the strong axis stiffness, which controls torsion stiffness, was less than that of open grid deck specimen #1. This indicated that the contribution of the strong axis stiffness controlled the torsion stiffness of the deck. Once again, calibrated steel plates were used for loading and the measured stiffness was computed for each test run as shown in Table 3-15.

Partially Filled Grid Deck Specimen. This deck specimen was also much more flexible in torsion than in the strong and weak axis directions. (It is noted that this specimen was much stiffer in torsion than the open grid deck specimens tested.) Unlike the open grid deck specimens, the partially filled grid deck specimen did not experience significant deflection prior to loading as shown in Figure 3-44. Despite the increased torsion stiffness provided by the concrete, calibrated steel plates were still reasonable to use for loading. The measured stiffness was computed for each test run and averaged as shown in Table 3-15.



Figure 3-44: Torsion stiffness test set-up for partially filled grid deck specimen

Comparison of Deck Torsion Stiffness's. Table 3-15 shows the measured torsion stiffness of each of the subassembly specimens tested. Again, it can be seen that the partially filled grid deck is extremely stiff in torsion compared to the open grid deck specimens. Since the stiffness of most decks in torsion, including steel grid decks, is difficult to model, the theoretical and average measured torsion stiffness of the deck were not compared. Furthermore, it was assumed that if the results of the D_x and D_y tests were reasonable, the results of the D_{xy} test would also be accurate. It should be noted that each rotation of the torsion stiffness test consisted of multiple tests, which were averaged. Although open grid deck specimen #2 was only tested for one rotation, rotations 2 and 3 were not necessary since they would have produced similar results as shown by open grid deck specimen #1 and the partially filled grid deck specimen.

Table 3-15: Measured torsion stiffness

Deck Panel	Rotation #1 (kip-in ² /in)	Rotation #2 (kip-in ² /in)	Rotation #3 (kip-in ² /in)	Average Measured (kip-in ² /in)
Open Grid #1	135	125	141	134
Open Grid #2	68	-	-	68
Partially Filled Grid	12,968	13,155	13,448	13,190

3.4.4 Overall Stiffness Properties

The flexural stiffness (or orthotropic) ratio, D (D_x/D_y), and torsion stiffness parameter, α , for each subassembly stiffness specimen were computed based on both the average measured and theoretical stiffness properties. As shown in Table 3-16, the addition of concrete to open grid deck specimen #2 (i.e., the partially filled grid deck) caused the deck to become closer to isotropy (i.e., same stiffness in D_x and D_y) as expected. It should be noted that an increase in the orthotropic ratio, D , would cause an increase in the load to be applied for the subassembly strength verification test as can be seen from Equations 2-1 to 2-4 in Section 2.1.2.

Table 3-16: Comparison of measured and theoretical orthotropic ratios (D)

Deck Panel	Measured D $D = \frac{D_x}{D_y}$	Theoretical D $D = \frac{D_{x-theor.}}{D_{y-theor.}}$	Theoretical D $\frac{\text{Theoretical D}}{\text{Measured D}}$
Open Grid Deck #1	17.3	15.1	0.87
Open Grid Deck #2	11.3	10.2	0.90
Partially Filled Grid	3.6	2.1	0.86

The relative torsion stiffness parameter, α , of a given deck type is defined as:

$$\alpha = \frac{2D_{xy}}{\sqrt{D_x D_y}} \quad (3-14)$$

The measured D_{xy} stiffness was used in combination with the theoretical D_x and D_y stiffness values to determine the theoretical torsion stiffness parameter, α . The theoretical and experimentally measured twisting parameter values, α , were all equal as shown in Table 3-17. This was not surprising since the same D_{xy} was used for the calculation of both the theoretical and experimentally measured values of α and, as previously discussed, the much larger theoretical and measured values of D_x and D_y were in good comparison for each specimen. It should be noted that an increase in α would cause a decrease in the load to be applied for the strength verification tests as can be seen from Equations 2-1 to 2-4 in Section 2.1.2.

Table 3-17: Comparison of measured and theoretical twisting stiffness parameters (α)

Deck Panel	Measured α	Theoretical α	Theoretical α $\frac{\text{Theoretical } \alpha}{\text{Measured } \alpha}$
Open Grid Deck #1	0.05	0.05	1.0
Open Grid Deck #2	0.03	0.03	1.0
Partially Filled Grid	0.70	0.70	1.0

The experimentally measured values (D and α) were used to determine the load to be applied for the strength verification tests of the subassembly longitudinal and transverse splice specimens discussed in sections 3.5.1 and 3.7.1, respectively. Since the differences between the measured and theoretical orthotropic ratio and twisting stiffness parameter were minor, there was no need to compare load to be applied based on the theoretical deck parameters. Moreover, since the only difference was that the experimentally determined orthotropic ratio was slightly greater than the theoretically computed orthotropic ratio, the computed applied loads would be slightly conservative. Therefore, total loads of 40 kips and 59 kips were chosen to be applied to the subassembly transverse and longitudinal splice specimens, respectively, for the strength verification tests as shown in Table 3-18.

Table 3-18: Comparison of strength verification load computed

Strength Verification Test	Computed Minimum Load (kips)	Load Applied (kip)
Transverse Splice	38.5	40
Longitudinal Splice	58.1	59

3.4.5 Standard Test Methods

The standard test methods for the subassembly stiffness tests (D_x , D_y , and D_{xy}), included in Appendices G, H and I, were developed and verified during the testing program. Open grid deck specimen #1 was tested first primarily to develop test procedures, create test set-ups, verify that the test was reasonable and make adjustments to improve the proposed test methods (i.e., D_x , D_y , D_{xy}). Open grid specimen #2 and the partially filled grid deck specimen were then tested to determine the stiffness properties of the panels. These properties could then be used to determine the loads to be applied to the subassembly longitudinal and transverse splice and deck-to-superstructure connection strength verification tests since the same type of decks would be used. The testing of these two specimens was also used to further develop, verify, and make adjustments to these proposed test methods.

3.4.6 Application Summary

The subassembly stiffness tests were found to produce accurate results when compared to the theoretical stiffness for each of the decks tested. The stiffness properties of the partially filled grid deck can be used to determine the loads for the strength verification tests of the subassembly longitudinal and transverse splice specimens discussed in sections 3.5.1 and 3.7.1, respectively. Based on the findings of these test, the following were incorporated into the subassembly stiffness test methods and commentary:

- Multiple displacement measurements shall be taken at the supports and location of maximum displacement (i.e., under the load) so that rigid body movement may be accounted for during computation of the stiffness properties.
- The theoretical and experimentally measured stiffness of the deck in the strong (D_x) and weak (D_y) directions shall be within 15% of each other to be deemed acceptable. If this is not the case, the theoretical model shall be adjusted until this criterion is met so that the behavior of the deck is understood.
- It is reasonable to assume that if the experimental and theoretical stiffness in the strong (D_x) and weak (D_y) directions are in good comparison, the experimental and theoretical torsion stiffness (D_{xy}) should also compare well. Furthermore, modeling the torsion stiffness (D_{xy}) would be complex for bridge decks with orthotropic properties. Therefore, a theoretical model of the torsion stiffness (D_{xy}) is not required.

3.5 Subassembly Longitudinal Splice Test

This section describes the findings of the subassembly longitudinal splice test. Two configurations of the strength verification tests are described and compared to one another. Furthermore the results of the cyclic loading test and their significance are described herein. The subassembly longitudinal splice data and results are compared to those of the longitudinal splice and roll tests of the large-scale specimen. The findings of these tests were incorporated into the appropriate standard test method to ensure that the subassembly test reasonably represented a “slice” of the large-scale bridge deck.

3.5.1 Strength Verification Test Performance

As expected, cracks developed in the concrete deck during the strength verification test, as can be seen in Figure 3-45. Prior to the strength verification test, low level load tests were conducted to ensure data were reasonable and repeatable. Some hairline cracking of the concrete

was found during inspections after these low load level tests. The strength verification test was then carried out with flexible stringers, which induced further cracking of the concrete. The strength verification test was then repeated with rigid supports, which caused the most cracking of the concrete. As can be seen in the highlighted regions of Figure 3-45, these hairline cracks were developed predominately in the negative moment region (i.e., over the middle stringer) with some at the location of the patch loads. Although cracks were developed in the concrete, the strength of the deck was verified without any significant damage to the structure.

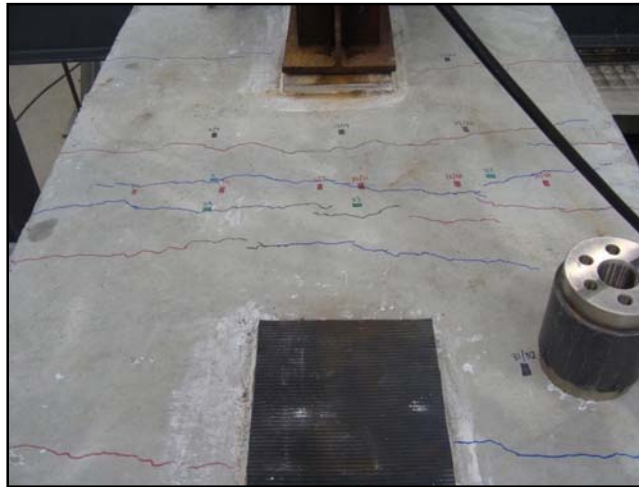


Figure 3-45: Cracks on subassembly longitudinal splice deck specimen

Strength Verification Test with Flexible Girders. One strength verification test was first conducted with flexible girders and data were collected. A load of 59 kips was applied to the deck through two 20" x 10" patches spaced at 4 ft. on center as discussed in Section 2.8.4.

The stresses measured in the reinforcing steel at the centerline of the longitudinal splice displayed non-linear behavior due to cracking of the concrete during this strength test. However, the deck deflection displayed linear behavior because the cracking of the concrete was relatively localized and limited such that it did not affect the overall stiffness of the deck. The largest deflections, approximately 0.17 in. as shown in Figure 3-46, were measured underneath the load patches (CH_45 and CH_47) and at the interior girder (CH_48). The deflections at the exterior stringers were significantly less than at the location of the applied load. The deflections at the exterior stringers (CH_44 and CH_46) were approximately 0.025" as shown in Figure 3-46. Although these measurements seem reasonable, a greater negative moment was desired to test the longitudinal splice of the deck. Therefore, this test was repeated using rigid stringers to achieve the desired negative moment at the longitudinal splice.

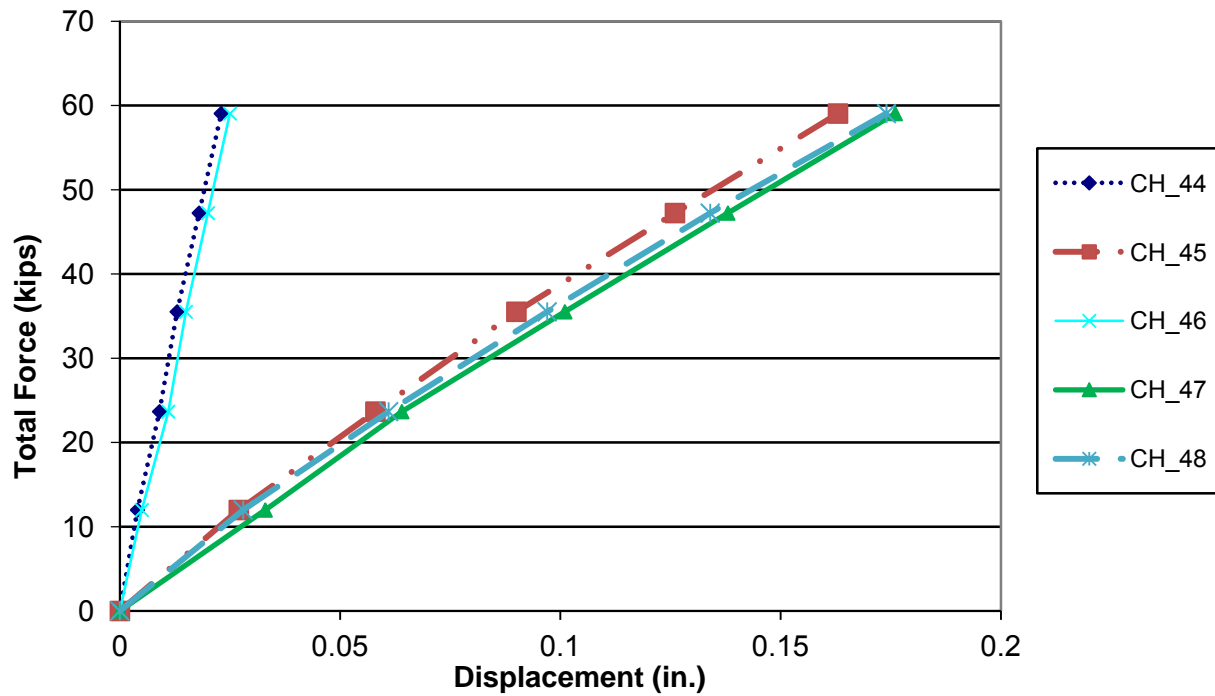


Figure 3-46: Displacements for strength verification load test with flexible stringers

Strength Verification Test with Rigid Girders. Concrete blocks and steel plates were used to support the stringers underneath the deck to simulate the effect of rigid girders as described in Section 2.8.4. The strength verification test was then repeated three times and data were collected.

Although the girders were more rigid, there was still some deflection at the stringers as shown in Figure 3-47. However, the deflection of all three stringers was significantly smaller and more uniform than for the strength verification test with flexible stringers as shown in

Table 3-19. Therefore, it was much easier to account for rigid body movement.

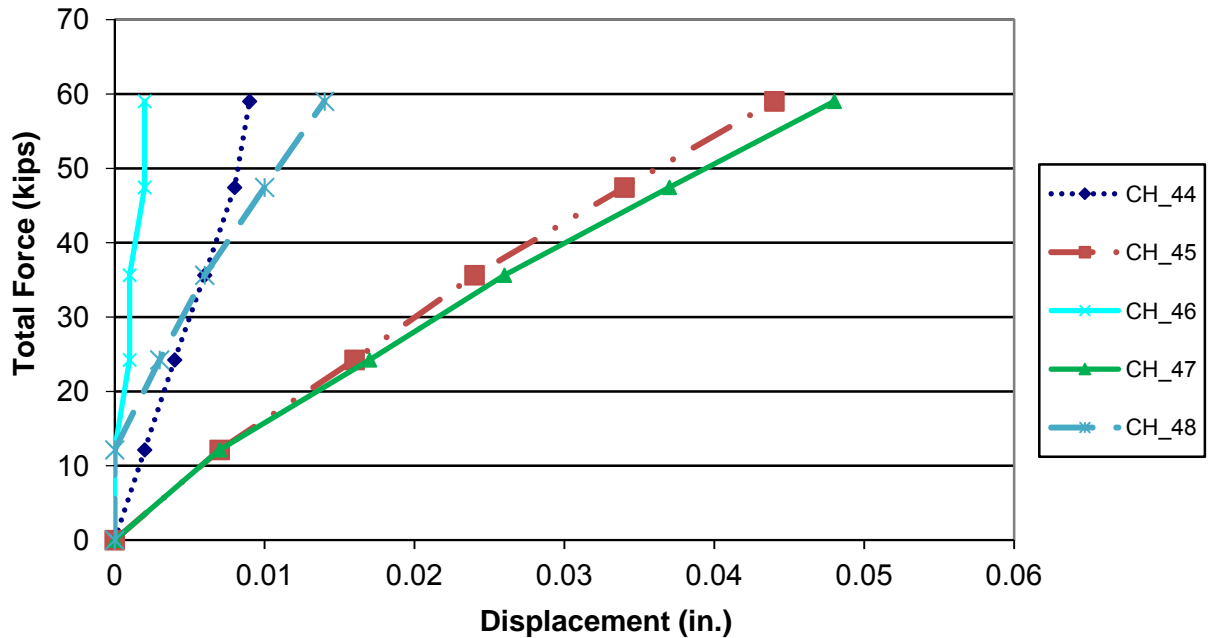


Figure 3-47: Displacements for strength verification load test with rigid stringers

The behavior of the deck remained essentially linear as shown in Figure 3-47. The largest deflections, measured underneath the load patches (CH_45 and CH_47), were reduced by a factor of 3.7 to approximately 0.05", as shown in

Table 3-19. The stresses were increased significantly in the negative moment region (i.e., reinforcing steel over the interior stringer) as expected, which induced further cracking of the concrete. However, the stresses in the positive moment region (i.e., under the patch loads) were reduced significantly. Therefore, since this test was developed to evaluate the strength of the longitudinal splice (i.e., reinforcing steel) located in the negative moment region (i.e., over the interior stringer), using rigid girders yields conservative results.

Table 3-19: Comparison of stress & displacement with flexible & rigid stringers

Location	Type	ID	Flexible Girders	Rigid Girders	<u>Flexible Rigid</u>
At North Load Patch	Displacement	CH_45	0.163	0.044	3.7
At South Load Patch	Displacement	CH_47	0.176	0.048	3.7
At Interior Stringer	Displacement	CH_48	0.174	0.014	12.5
At North Stringer	Displacement	CH_44	0.023	0.009	2.6
At South Stringer	Displacement	CH_46	0.025	0.002	12.5
Top of Interior Reinforcing Steel	Stress	CH_6	2.22	14.84	0.15
Bottom of Interior Reinforcing Steel	Stress	CH_7	1.59	12.05	0.13
Top of Main Bar under Patch	Stress	CH_15	-2.16	-1.65	1.31
Bottom of Main Bar under Patch	Stress	CH_16	16.38	9.78	1.67

3.5.2 Cyclic Load Test Performance

The only damage to the subassembly longitudinal splice specimen found during inspections throughout the cyclic load test was to the concrete in the deck. Once initiated, the cracks in the concrete opened slightly, but not significantly. The largest crack width found during inspection after termination of the cyclic load test (i.e., 6.75 million load cycles) was approximately 0.010 inches (0.25 mm) as shown in Figure 3-48.



Figure 3-48: Largest crack found in concrete at termination of subassembly longitudinal splice cyclic load test

The data also supported the finding that no significant damage was done to the longitudinal splice during testing. As shown in Figure 3-49, the displacements at the cyclic load (i.e., 27.6 kips) remained essentially unchanged throughout testing. The displacements at the location of the patch loads (CH_45 and CH_47) and the interior stringer (CH_48) were approximately equal. This implies that a significant amount of negative moment over the interior girder was lost. As will be discussed in the following section, this finding could be reasonably expected. The displacements at the exterior stringers (CH_44 and CH_46) were extremely small as expected.

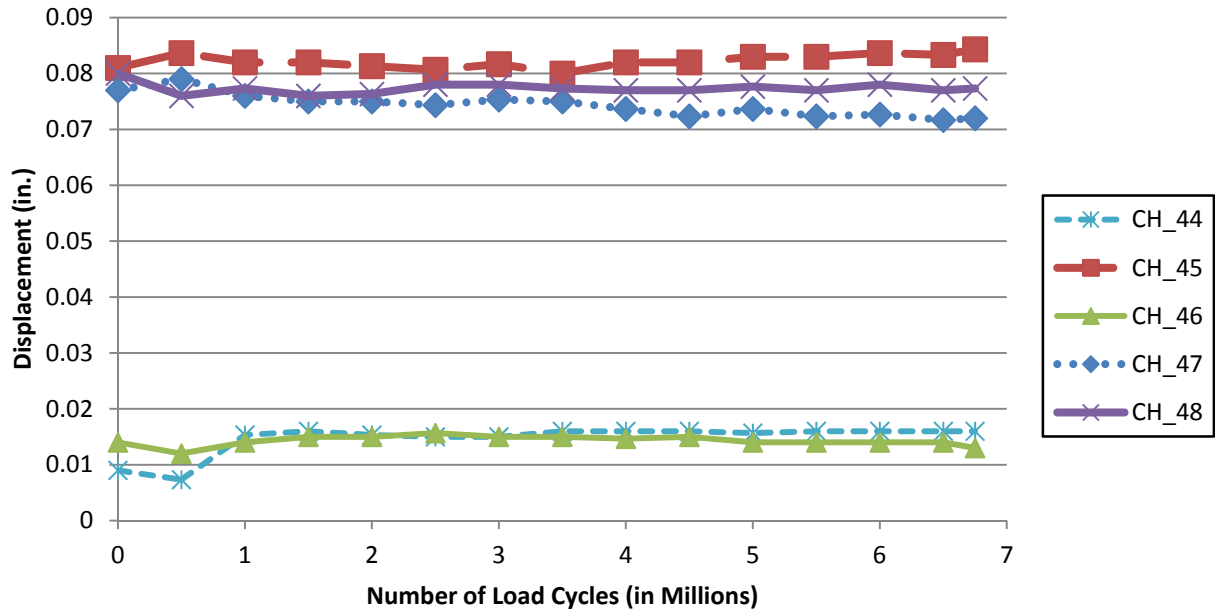


Figure 3-49: Displacements at fatigue load throughout cyclic load test

Similar to the large-scale longitudinal splice test, the stresses in the reinforcing steel showed essentially no change throughout the duration of the subassembly cyclic load test of the longitudinal splice as shown in Figure 3-50. The stress measured at the top of a reinforcing steel bar directly in between the patch loads (CH_6) was much greater than its counterpart on the bottom of the reinforcing steel (CH_7), which indicates a significant amount of negative bending locally as expected. The negative bending was significantly lower in the reinforcing steel away from the patches (CH_4 and CH_5). The reinforcing steel furthest away from the patches (i.e., close to the edge of the deck specimen) had the lowest stresses as expected. However, there was still some negative bending in this region as shown by the strain gage data from the top (CH_38) and bottom (CH_39) of the reinforcing steel.

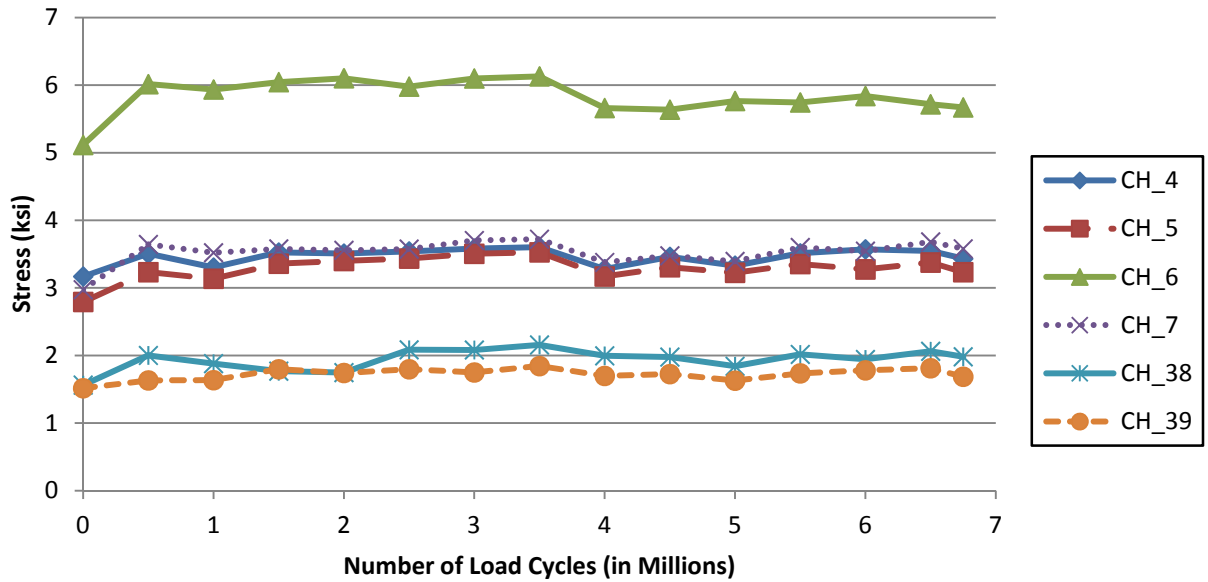


Figure 3-50: Reinforcing steel stresses at fatigue load throughout cyclic load test

As shown in Figure 3-51 and the other figures in this section, there appears to be slight changes to the stresses in the main bars under the load patches until approximately 2 to 3 million load cycles were applied. After this point, the magnitude of the stresses remained essentially consistent for the remainder of the cyclic load test. This change in stress was due to a “shake down” period during the first portion of the test when the deck was settling into place. This “shake down” period included initial cracking of the concrete and small internal changes in behavior. Since this “shake down” period lasted 2 to 3 million load cycles, it is recommended that the subassembly cyclic load test be carried out for a minimum of 3 million load cycles.

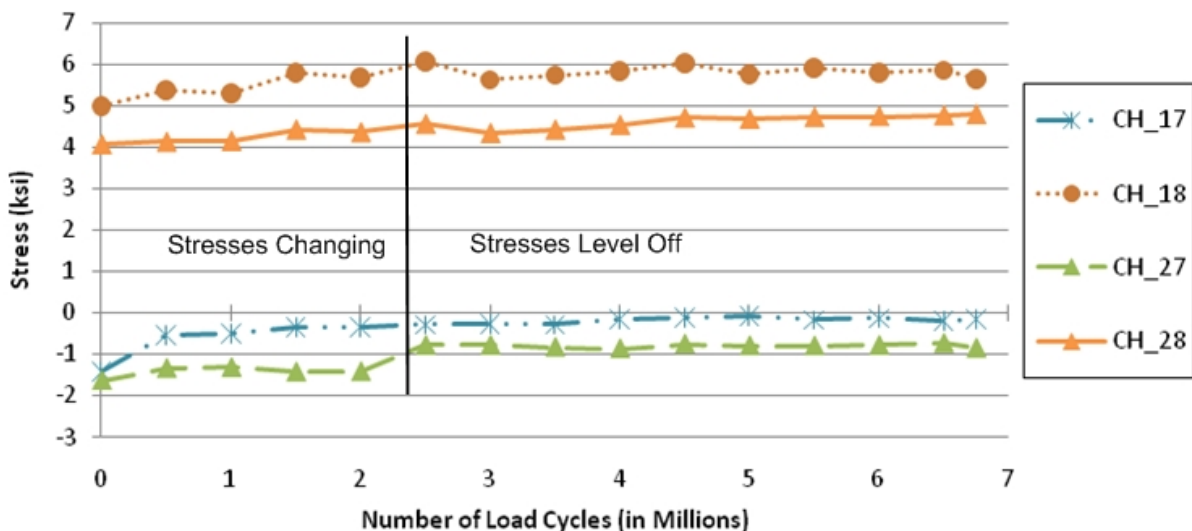


Figure 3-51: Stresses in main bars near patches leveling off after 2-3 million load cycles

If the cyclic load test had been run for less than 3 million load cycles, projecting the data past this number of load cycles would have been inaccurate since the slope changed after the initial “shake down” of the deck. As shown in Figure 3-52, the stresses in the main bar near the

stringer appear to change during the first 2-3 million load cycles of the cyclic load test. However, they did start to level out shortly after that point. Although the stresses shown in Figure 3-52 are very small and would not present a fatigue concern, this plot provides a good example of why cyclic tests should never be terminated before the application of 3 million load cycles if no significant damage is observed during inspections.

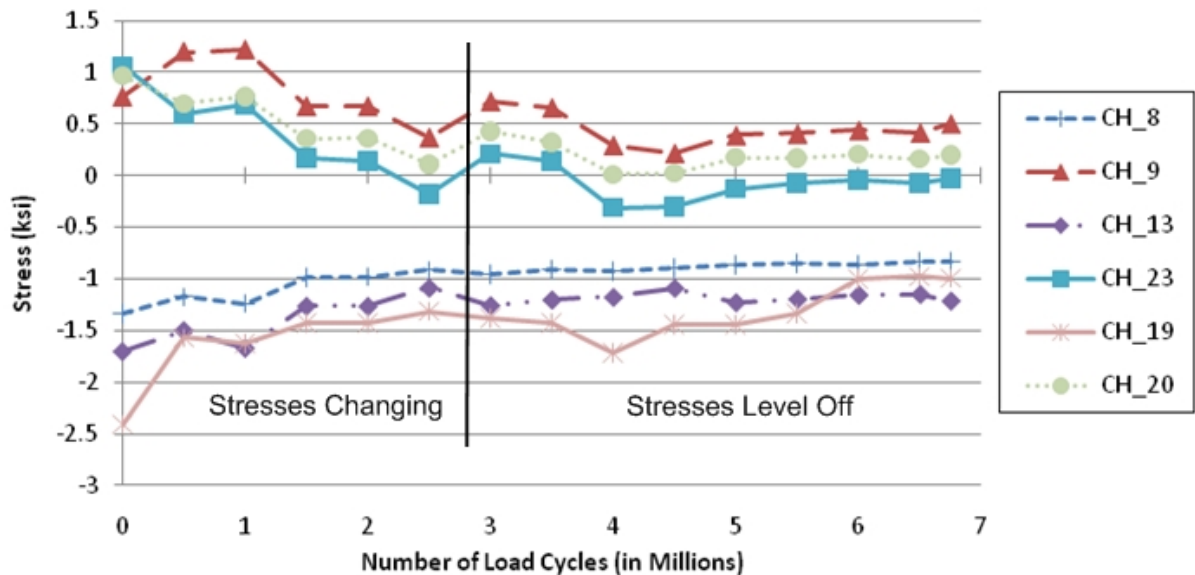


Figure 3-52: Main bar stresses near interior stringer

3.5.3 Comparison to Large-Scale Specimen

After completing the tests of the subassembly longitudinal splice, the displacements, stresses, and concrete cores taken from the subassembly longitudinal splice specimen were compared to those of the large-scale specimen. As discussed in Section 2.8, this was done to ensure the subassembly tests reasonably represented the large-scale bridge deck tested. The following sections discuss the comparison between results of these subassembly and large-scale longitudinal splice tests.

Displacements. LVDTs were placed underneath one of the load patches during the longitudinal splice test of the large-scale specimen. Another LVDT was placed on the interior girder close to the centerline of the longitudinal splice being tested. These locations were similar to those monitored throughout the subassembly longitudinal splice cyclic load test. As shown in Table 3-20, the deflections of the subassembly longitudinal splice specimen were slightly greater than those of the large-scale specimen. However, this was expected since the boundary conditions of the specimens were different. Because the large-scale specimen has more continuity than the subassembly specimen, one would expect the large-scale specimen to deflect less.

Despite this small difference in magnitude, the relative deflection of the deck to the girder was greater for the large-scale specimen than for the subassembly specimen as expected. This is due to the difference in the span of the deck between girders/stringers. The span of the large-scale deck between girders was 8 feet on center. This was larger than the 6 foot deck span

between stringers of the subassembly specimen. Therefore, the relative deflection of the deck to the girder should be greater for the large-scale specimen.

When modeling a deck, the support beams (i.e., stringers) are often considered to be rigid supports, which results in large negative moments over the interior support (i.e., stringer). However, Table 3-20 shows that the stringer/girder deflected almost as much as the deck during both the large-scale and subassembly longitudinal splice cyclic load tests (85% and 92%, respectively). This indicates that a significant portion of negative moment was lost at the longitudinal splice (i.e., over the interior stringer) due to the deflection of the support (i.e., stringer). As a result, little damage to the longitudinal splice would be expected.

Table 3-20: Comparison of displacements of subassembly test to large-scale test

Location	LVDT ID		Measured Displacement (in.)	
	Subassembly	Large-Scale Longitudinal Splice	Subassembly	Large-Scale Longitudinal Splice
Underneath Patch Load (max.)	CH_45	Deck	0.084	0.073
Stringer near centerline of splice	CH_48	Girder	0.077	0.062
Relative Deflection of the Deck	CH_45 – CH_48	Deck - Girder	0.007	0.011
Relative Deflection of Deck as a Percentage (%)	$\frac{\text{CH}_{45} - \text{CH}_{48}}{\text{CH}_{45}}$	$\frac{\text{Deck} - \text{Girder}}{\text{Deck}}$	8	15
Girder Deflection as Percentage of Deck Deflection (%)	$\frac{\text{CH}_{48}}{\text{CH}_{45}}$	$\frac{\text{Girder}}{\text{Deck}}$	92	85

Stresses. The measured stresses in the subassembly longitudinal splice specimen were also compared to those obtained during the large-scale specimen roll and static tests. As described in Section 2.6.2, the test consisted of rolling tandem axles, spaced at 4 feet center to center and weighing a total of 42 kips (i.e., 21 kips per axle), across the bridge in various transverse positions. This allowed the deck behavior of the deck and critical details to be understood at service level loading. As discussed in Section 3.3.13, a static test of approximately 25 kips was found to be comparable to the effect of one 21 kip axle during the roll test because there was also a minor contribution (i.e., 4 kips) from the other 21 kips axle since it was 4 feet away. Therefore, 25 kip load static tests conducted prior to the cyclic tests of the large-scale and subassembly specimens were used to compare the stresses measured.

Using the 25 kip static test prior to the cyclic test of the subassembly longitudinal splice specimen, it was found that the stresses in the bottom of the reinforcing steel were comparable to those experienced in the roll test as shown in Table 3-21. However, the stresses in the top of the reinforcing steel were much greater for the subassembly longitudinal splice test.

The tensile stress was expected to be greater in the top of the reinforcing steel during the subassembly longitudinal splice test because the patch loads were spaced at 4 feet on center for the subassembly specimen rather than 6 feet on center as used for the large-scale specimen. However, the observed difference in the response was considerably greater than expected and much more than the difference in patch spacing would produce. Based on the results of the static load test of the large-scale specimen, it was expected that the stress measured in the top of the reinforcing steel would be subjected to greater tensile stresses than at the bottom of the same reinforcing steel bar. This was because the main bars, which were one foot off the centerline of the splice, were experiencing negative bending. Unfortunately, the measured data in the large-

scale specimen did not support this assumption regarding simple bending behavior. Since those measurements in the reinforcing steel of the large-scale specimen were not consistent with the findings of the adjacent main bar data, it was concluded that local effects, though not fully characterized, were likely the cause.

Table 3-21: Comparison of stresses at 25 kips

	Strain Gage ID		Measured Stress (ksi)		
				Large-Scale Specimen	
Location	Subassembly Specimen	Large-Scale Specimen	Subassembly Specimen	Roll Test Position #2	Longitudinal Splice Cyclic Test
Top of Reinforcing Steel at Splice between load patches	CH_6	120T	3.22	1.43	1.53
Bottom of Reinforcing Steel at Splice between Load Patches	CH_7	121B	2.04	1.98	1.82
Top of Reinforcing Steel at Splice Away from Load	CH_4	94T	1.66	0.42	0.19
Bottom of Reinforcing Steel at Splice Away from Load	CH_5	95B	1.60	1.20	1.11

Concrete Cores. The concrete cores extracted from the subassembly and large-scale specimens exhibited similar damage from the cyclic loading tests. The following were found from the cores of the subassembly and large-scale specimens:

- The cyclic loading did not cause significant damage in addition to the initial damage (i.e., shrinkage of concrete in the large-scale specimen).
- Slightly more damage was found in the transverse positive moment region than in the transverse negative moment region.

It was evident that the large-scale deck had deeper cracks in the concrete than in the subassembly specimen. This was attributed to significant shrinkage cracking in the large-scale specimen, which was not present in the subassembly specimen.

3.5.4 Standard Test Method

The “Standard Test Method and Commentary for Subassembly Cyclic Loading Testing of Longitudinal Splices in Prefabricated Bridge Deck Panels,” included in Appendix H, was developed in parallel with the testing of subassembly longitudinal splice specimen. Overall, it was found that the results of this standard test method of a subassembly compared reasonably well to those of the large-scale specimen. There were some slight discrepancies due to the difference in deck span. However, the general behavior of the longitudinal splice and deck were

found to be very similar. Hence, the subassembly test can be used to accurately evaluate the performance of the longitudinal splice.

Since this was the first subassembly test developed to simulate critical details of a full bridge deck, it was used as a baseline for the other subassemblies, in which adjustments would be made to refine the proposed testing method. The results of the subassembly test were incorporated into the test method. For example, it was recommended that a cyclic load test never be terminated prior to the application of 3 million load cycles if no significant physical damage to the specimen had been observed. This was incorporated into the test method because there may be a “shake down” period during the early portion of the cyclic test during which the initial cracking of the deck and small internal changes in behavior occur. Hence, terminating the test too early may result in an overestimate of the durability of the splice. Also, considering the splice is subjected to individual wheel loads (and possibly hundreds of millions of cycles), it is not unreasonable to require a minimum number of cycles.

3.5.5 Application Summary

The subassembly longitudinal splice test method produced behavior, data and damage comparable to those of the large-scale specimen. The subassembly longitudinal splice test method will reveal any deficiencies of the longitudinal splice and deck specimen that may be present for an in-service bridge deck and longitudinal splice. Based on the findings of this subassembly test, the following was incorporated into the “Standard Test Method and Commentary for Subassembly Cyclic Loading Testing of Longitudinal Splices in Prefabricated Bridge Deck Panels,” included in Appendix H:

- A cyclic load test shall not be terminated prior to the application of three (3) million load cycles if no significant physical damage to the specimen had been observed. This was incorporated into the test method because there may be a “shake down” period during the early portion of the cyclic test during which the initial cracking of the concrete and small internal changes in behavior occur. Further, considering the number of cycles a deck will generally be exposed to, a lower bound seems reasonable. Through three million cycles is recommended, a larger value may be considered by the owner.
- This minimum required number of applied load cycles may be reduced if the total number of cycles that the in-service bridge deck is expected to undergo is less than 1.5 million load cycles.

The findings of the subassembly strength verification test of the longitudinal splice led to the following conclusion:

- Rigid stringers shall be used to test the strength of the longitudinal splice since it is in the negative moment region of a two span deck. This will yield a greater negative moment over the interior stringer and, thus, produce conservative results.
-

3.6 Subassembly Deck-to-Superstructure Connection Test Performance

This section describes the findings of the subassembly deck-to-superstructure connection test. The results of the cyclic loading and strength load test are described herein. The findings of

these tests were incorporated into the appropriate standard test method to ensure that the subassembly test reasonably represented a “slice” of a large-scale bridge deck.

3.6.1 Cyclic Load Test

Although the focus of the test was to evaluate the connection of the deck to the superstructure, a significant amount of fatigue damage was produced in the deck itself. Early in the test, it was observed that the open grid deck was significantly more flexible than the partially filled grid deck that was tested for the subassembly longitudinal splice test. This increase in flexibility was expected since the results of the subassembly stiffness tests found that open grid decks were much less stiff than partially filled grid decks.

Due to this flexibility, it was evident that damage would result at a low number of load cycles for this test. As a result, inspections and static tests were conducted more frequently than every 500,000 load cycles as was previously done for the subassembly longitudinal splice test. After approximately 230,000 load cycles, the first significant fatigue crack in a main bar was observed. Specifically, this crack was located in the central main bar, near the interior stringer. As can be seen in Figure 3-53, this crack initiated in a puddle weld that held the main and cross bars together, and propagated down into the main bar where it then entered the hole where a secondary bar passes through the main bar. The crack then reinitiated in the main bar and propagated through the remaining portion of the bar. The puddle weld was subjected to a very high stress range that was mainly in tension since it was located in the negative moment region (i.e., close to the interior stringer). The crack growth was marked at each inspection as shown in Table 3-21 (e.g. 241K=241,000 load cycles).

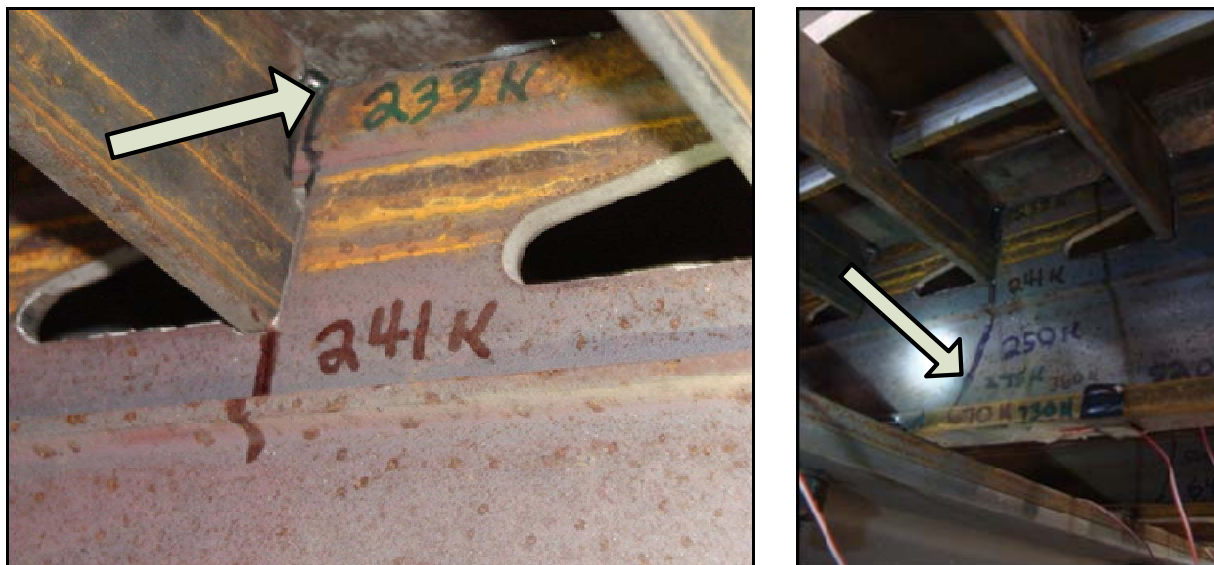


Figure 3-53: Fatigue cracking in central main bar near stringer (Left) Early crack growth; (Right) Crack growth at end of cyclic load test

After this crack initiated, the load and resulting stresses redistributed. Fortunately, strain gages were located within approximately 1-1/2” of this crack location and on the adjacent main bars at the same location, which allowed for this behavior to be analyzed in detail. Figure 3-54

shows the strain gages on the top of three adjacent main bars where fatigue cracking initiated. As previously discussed, fatigue cracking was first observed in the top of the center main bar near the interior stringer after approximately 230,000 load cycles. The load carried at that location dropped significantly and, consequently, so did the stress range (i.e., not absolute stress) as shown by CH_15 in Figure 3-54. The load then redistributed to the adjacent main bars approximately equally as shown by CH_13 and CH_17 in Figure 3-54 from about 230,000 cycles to about 350,000 cycles. At 225,000 load cycles, a visual inspection of the deck was completed before a metal fatigue crack was observed in the central main bar after approximately 230,000 load cycles. Therefore, the stress range data shown at 225,000 load cycles was projected from prior static tests. A static test was conducted shortly after this fatigue crack was observed.

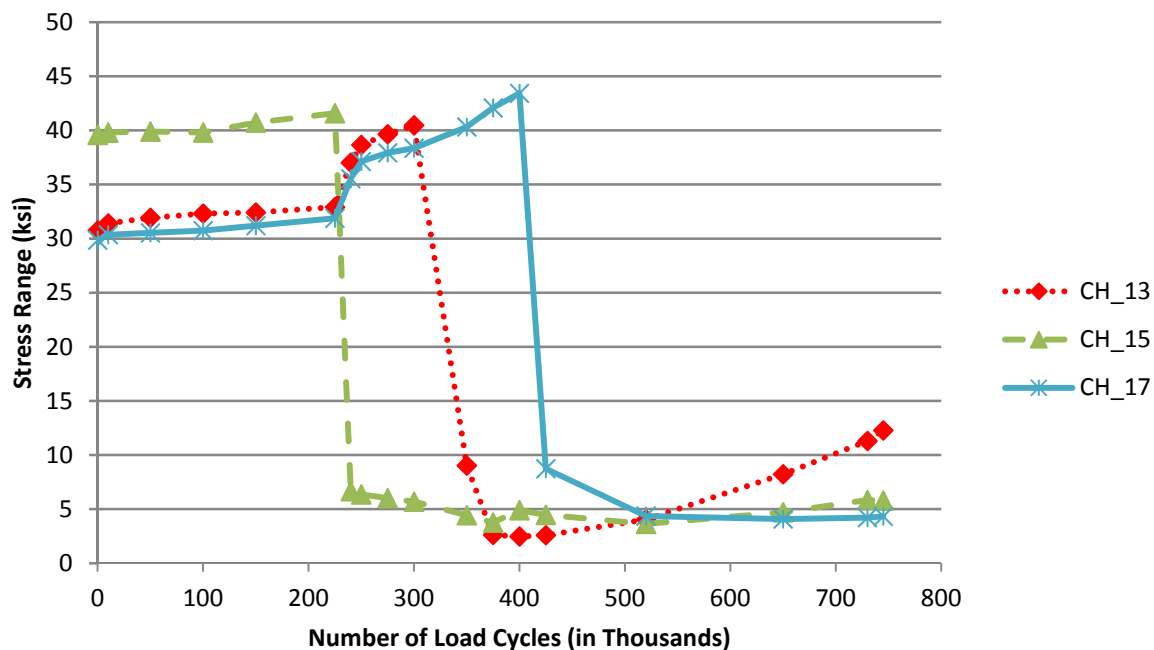


Figure 3-54: Stress range for top gages on main bars near interior stringer

Due to the redistribution of the load previously discussed, cracks initiated in the adjacent bars at the same location and propagated as shown in Figure 3-55. Again, the subsequent cracking of these adjacent bars is evident in Figure 3-54. Fatigue cracking in the top of the main bar near CH_13 (i.e., the main bar adjacent and to the east of the center main bar) was detected after approximately 350,000 load cycles. The east interior main bar (CH_13) experienced fatigue cracking before the west interior main bar, near CH_17. This, again, resulted in redistribution of the load to the remaining components of the deck, including the adjacent main bar to the west of the central main bar. As shown by Figure 3-54, the stress range in the top of the third interior main bar increased until cracking initiated. Again, the load was redistributed to the remaining components of the deck that were not cracked.



Figure 3-55: Fatigue cracks in other main bars (Left) East (second) main bar damaged; (Right) West (third) main bar damaged

The stress ranges measured by strain gages on the bottom of the main bars at the location of the cracking are shown in Figure 3-56. Of course, there are many similarities in the patterns of these stress ranges to the top of the main bars since they are essentially at the same locations on the deck. Once fatigue cracking initiated in the central main bar, the stress range in the bottom of the adjacent main bars to the east (CH_14) and west (CH_18) increased approximately equally in a very similar manner to the corresponding stresses at the top of the main bars (i.e., CH_13 and CH_17, respectively).

It can also be seen that there are some slight differences in behavior between the stress ranges measured at the top and bottom of these main bars. Unlike the stress ranges in the top of the main bars, the stress ranges in the bottom of the main bars increased when a crack first initiated before significantly reducing when the crack propagated into the bar further. It is also noted that the stress ranges at the bottom of the main bar generally did not drop off as much as at the top because, since these bars were still connected at the bottom, they could carry load across them. However, the stress range at the bottom of the main bar, CH_16, reduced again after approximately 730,000 load cycles because the fatigue crack propagated through the entire central main bar. This immediate reduction in stress range resembled that of the top of the main bars because the bottom portion of the main bar had been separated by a crack so that load could no longer pass across it. The stress range at bottom of this main bar also matched that at the top of the main bars at this location after it completely cracked through. It is noted that these stress ranges are not zero because the gages were located away from the actual location of the cracks.

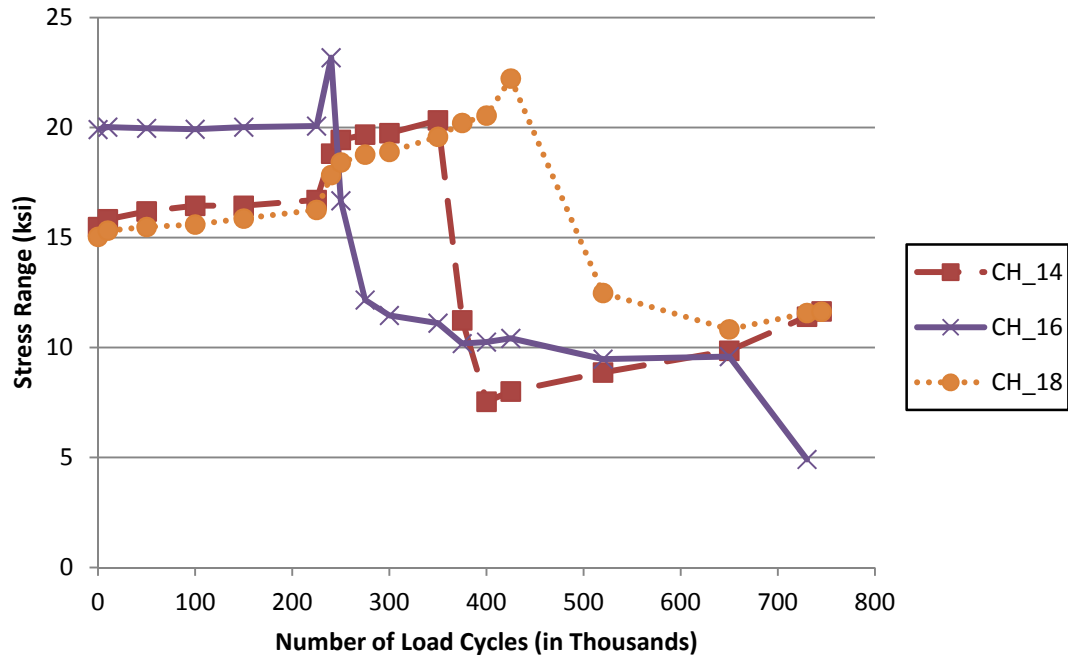


Figure 3-56: Stress range for bottom gages on main bars near interior stringer

Additional cracking in the main bars occurred near the location of the load patches. As shown in Figure 3-57, these cracks also initiated in the puddle welds and propagated down into the main bars. However, unlike the cracks developed near the interior stringer, these cracks were caused by the small tensile stresses in these puddle welds produced during the pulling portion of the load cycles (i.e., the upward portion of the load cycle that was intended to simulate rebound and reversal due to different wheel load positions). The applied stress range, though primarily compressive, is actually tensile at the weld due to the tensile residual stresses in the puddle welds themselves. This illustrates the importance of including the effect of stress reversal and the effects of even small applied tensile stresses in propagating a crack.



Figure 3-57: Main bar fatigue cracking near patch load

There was also cracking that initiated in the puddle welds joining together the main and cross bars that propagated into the cross bar rather than the main bar. As can be seen in Figure 3-58, this was very commonly found under the load patches.



Figure 3-58: Fatigue cracking in cross bars

Despite all of the metal fatigue cracking that occurred in the specimen during the cyclic load test, deflections only increased slightly until the test was terminated after approximately 750,000 load cycles. Figure 3-59 shows the gradual, and nearly linear, increase in displacement range underneath the load patches (CH_25 and CH_26) after the first significant fatigue crack (i.e., approximately 230,000 load cycles). Although the deflections at these two locations increased by almost 50%, the deflections remained small enough that passing traffic on a structure in service would likely not notice a difference in deflection and, therefore, would not create a serviceability issue. The deflections at the interior stringer (CH_27) decreased slightly throughout testing because the damage to the deck between the load patches and interior stringer caused load to be redistributed to the exterior stringers. Therefore, the deflections at the exterior stringers (CH_23 and CH_25) increased slightly throughout testing.

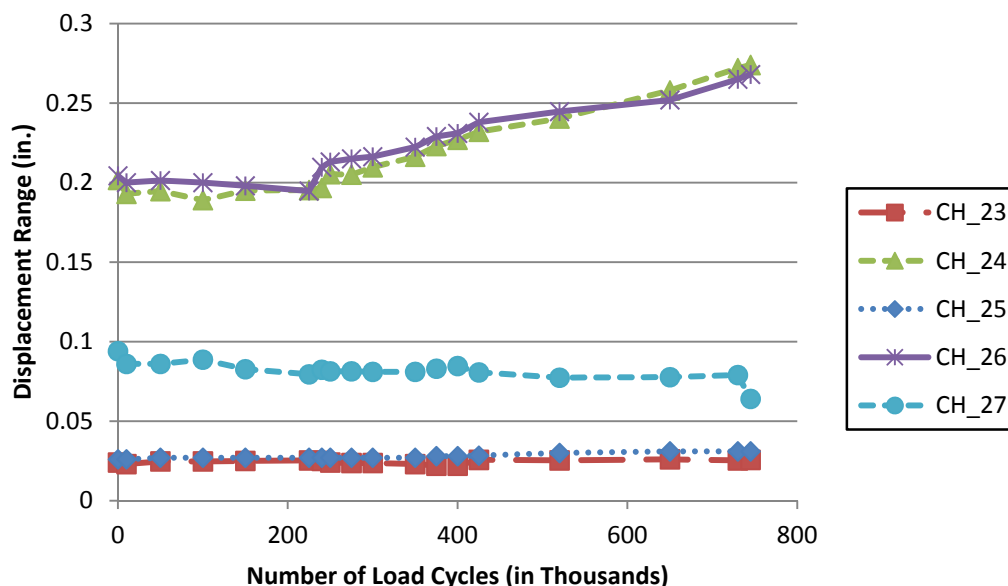


Figure 3-59: Measured displacement range at fatigue load range throughout testing

Despite the damage to the deck, no damage was observed to the welds or bolts of the deck-to-superstructure connection. Since the puddle welds are a lower fatigue category than that of the deck-to-superstructure connection, the cracking of these details is not surprising. Moreover, open grid decks have been well known for the “popping” or failure of puddle welds in the field as was found by Huang (2001) and GangaRao et al.(1988). Hence, this test also revealed similar deficiencies that would be expected to occur in the field on the deck itself.

A common deck-to-superstructure connection for an open grid deck consists of welding the main bars directly to the stringer in the field. Tensile residual stresses are always present in welded connections. Since there are imperfections in the fabrication of open grid decks, the deck is often “forced” together with the superstructure prior to field welding, which will create greater tensile residual stresses in these welds. These residual stresses, in combination with the tension stress from applied loads, commonly lead to fatigue cracking of the deck-to-superstructure connection even through the applied loads produce negative stress ranges. However, the deck-to-superstructure connection used for this test consisted of welding the main bars to bolt down plates which were, in turn, bolted to the stringer. In this case, this detail appeared to be quite resilient and not susceptible to damage. Obviously, the test would have revealed problems with less durable connections. Therefore, the proposed test method recommended that the deck-to-superstructure connection detail to be used for the in-service bridge deck be used for the subassembly tests.

3.6.2 Strength Load Test

After the cyclic load test was terminated, a load of 50 kips was applied to test the strength of the deck. Although the deck had relatively large deformations and experienced very high stresses no further physical damage was observed due to the application of the heavier load.

The behavior of the deck remained linear elastic as shown in Figure 3-60. The largest deflections, approximately 0.4 in., were measured underneath the load patches (CH_25 and

CH_26). The deflections at the stringers were significantly less than at the location of the applied load. The deflections at the measured exterior stringers (CH_23 and CH_25) were about one-tenth of the maximum deflections. The deflection measured at the interior stringer was approximately $\frac{1}{4}$ of the deflections at the load patches.

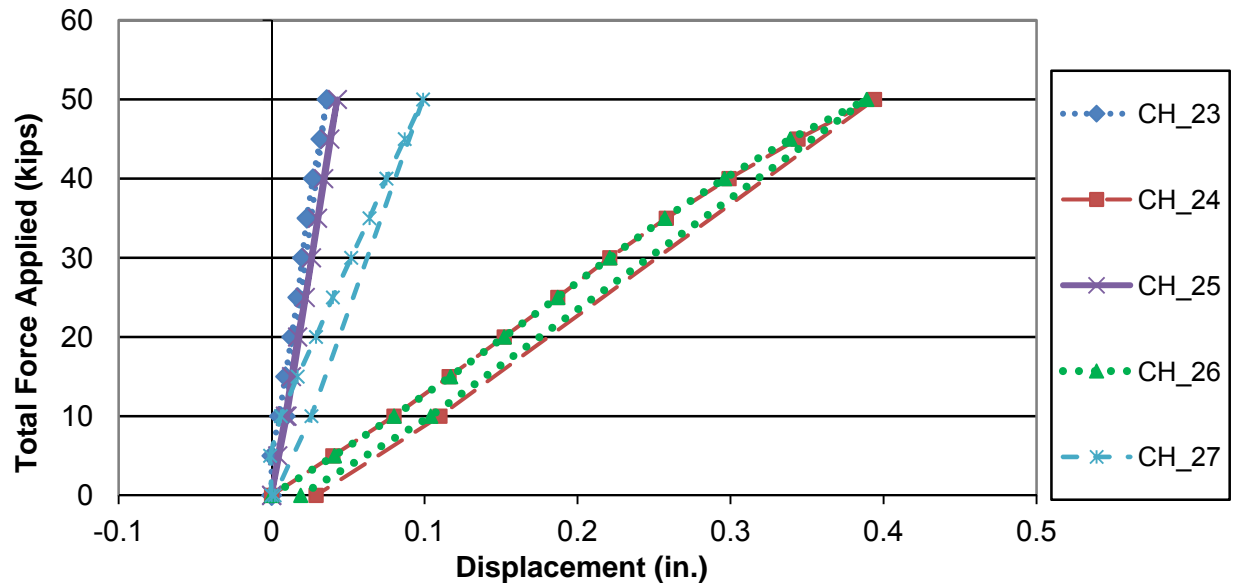


Figure 3-60: Displacements for strength verification load test

3.6.3 Standard Test Method

The “Standard Test Method and Commentary for Subassembly Cyclic Load Testing of Deck-to-Superstructure Connections for Prefabricated Bridge Deck Panels,” included in Appendix I, was developed in parallel with testing the subassembly deck-to-superstructure connection specimen. This test is slightly different than the other subassembly tests because it requires both pushing and pulling on the deck. Through this unique application of load, both compression and tension are created in the deck-to-superstructure connection at the interior stringer and in the deck itself.

The results of this test were incorporated into this test method. Moreover, the results of this test were also incorporated into the other subassembly standard test methods (i.e., longitudinal and transverse splice) when applicable. For example, commentary recommending engineers and technicians to conduct fatigue load static tests more frequently than every 500,000 load cycles for the first one million cycles and when significant damage was observed was added as a result of this test. This commentary was added to all of the standard subassembly cyclic testing methods. If this specimen was not closely monitored through frequent static tests and inspections, it would have been extremely difficult to evaluate what, when, and why this deck specimen deteriorated so quickly during this test.

3.6.4 Application

The subassembly deck-to-superstructure connection test method produced behavior and results consistent with those known to occur in the field. The “popping” of puddle welds is a

common failure that has been observed in many in-service open grid steel bridge decks. Therefore, this test method will also reveal any deficiencies of the deck itself that are likely to be observed in-service in addition to deficiencies with the deck-to-superstructure connection.

Based on the findings of this subassembly test, the following were incorporated into the subassembly testing methods and associated commentary for the deck-to-superstructure connection, as well as the longitudinal and transverse splice tests:

- The deck shall be attached to the superstructure using the same type of connections as will be used in the field so any deficiencies in the connection system may be revealed.
- Fatigue load static tests should be carried out more frequently in the first one million load cycles to verify the test set-up and specimen is performing as intended. This would also help to monitor whether damage is likely to occur or is occurring at a low number of load cycles.
- Fatigue load static tests should be carried out more frequently when significant damage to the deck has been observed.

3.7 Subassembly Transverse Splice Test Performance

This section describes the findings of the subassembly transverse splice test. The results of the strength verification test and cyclic load test are described herein. The subassembly transverse splice general behavior and results are compared to those of the transverse splice cyclic tests of the large-scale specimen. The findings of these tests were incorporated into the appropriate standard test method to ensure that the subassembly test reasonably represented a “slice” of the large-scale bridge deck.

3.7.1 Strength Verification Test

As discussed in Section 2.10.4, the strength verification test was conducted using flexible stringers since the subassembly transverse splice test used a single span deck and rigid body movement could easily be taken into account. Moreover, since the detail of concern (i.e., the transverse splice) was in the positive moment region in this case, it was conservative to use flexible stringers to induce higher stresses.

For all three runs of the strength verification test, the deck had relatively small deflections and high stresses. The behavior of the deck was linear elastic as shown in Figure 3-61. The largest deflection, approximately 0.175 in., was measured underneath the load patch (CH_48) at a load of 40 kips. The deflection near the load patch on the other side of the splice (CH_46) was slightly less than this. The deflections away from the patch on the side of loading (CH_45) and opposite side of the splice (CH_49) were approximately equal. This implied that the specimen was behaving as one deck panel with a similar stiffness across the transverse splice. The deflections at the stringers (CH_47 and CH_50) were also approximately equal as expected.

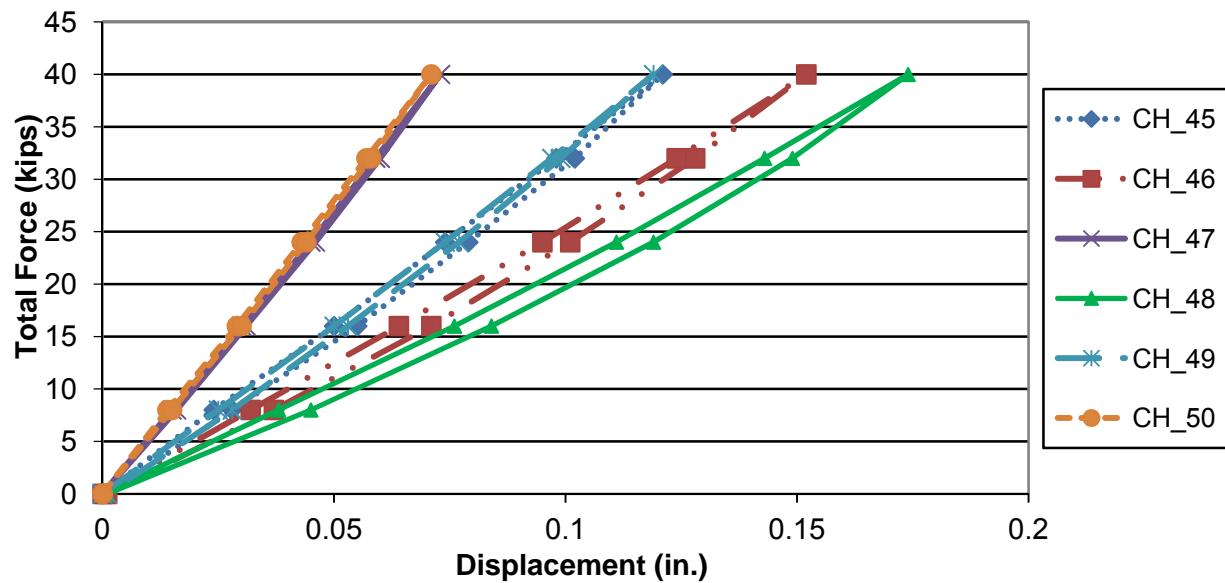


Figure 3-61: Displacements for strength verification load test

3.7.2 Cyclic Load Test

The subassembly transverse splice cyclic load test was terminated after over 10.5 million load cycles were applied. No significant damage to the structural components of the deck was found during inspections as a result of the cyclic loading test. As can be seen in Figure 3-62, some hairline cracking at the location of the transverse splice resulted from the cyclic load test.



Figure 3-62: Cracking on underside of subassembly transverse splice deck specimen

At the end of the test, fatigue cracking was observed in several of the form pans welded to the lower portion of main bars near the bolt down plates as shown in Figure 3-63. It is recognized that these cracks do not present any concern for the structural system of the deck specimen, but are reported for completeness.

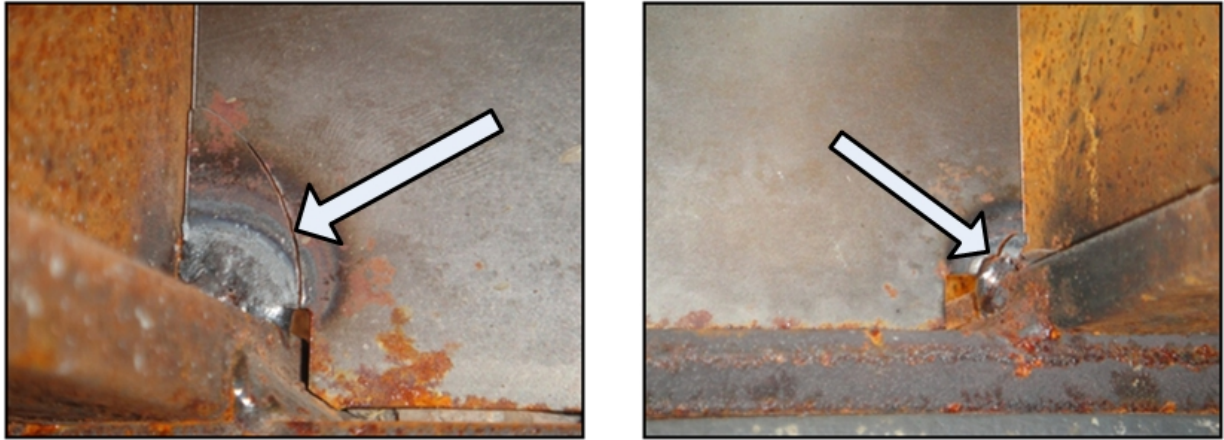


Figure 3-63: Fatigue cracking in form pans (Left) Typical crack observed; (Right) Other crack observed

In addition to not finding any physical evidence of damage to the deck specimen, the data obtained during the static tests showed signs of minimal damage to the deck. As previously discussed, a minimum of three static tests were conducted every 500,000 load cycles. Although the strength load (i.e., 40 kips) was applied during these static tests, data were also collected at 29.1 kips so that this test could be compared to the transverse splice tests of the large-scale specimen. The average displacements measured at 29.1 kips for these static tests are shown in Figure 3-64. As shown in this figure, there was essentially no change in the displacements measured throughout testing. Similar to the results of the strength verification test, the displacement under the patch load on the main bar closest to the centerline of the transverse splice (CH_48) was slightly greater than that measured on the other side of the splice (CH_46). Furthermore, the displacements measured away from the patch load on the side of loading (CH_45) and on the side of the splice not loaded (CH_49) were approximately equal as expected. Additionally, the displacements measured at the stringers near the centerline of the splice (CH_47 and CH_50) were also approximately equal.

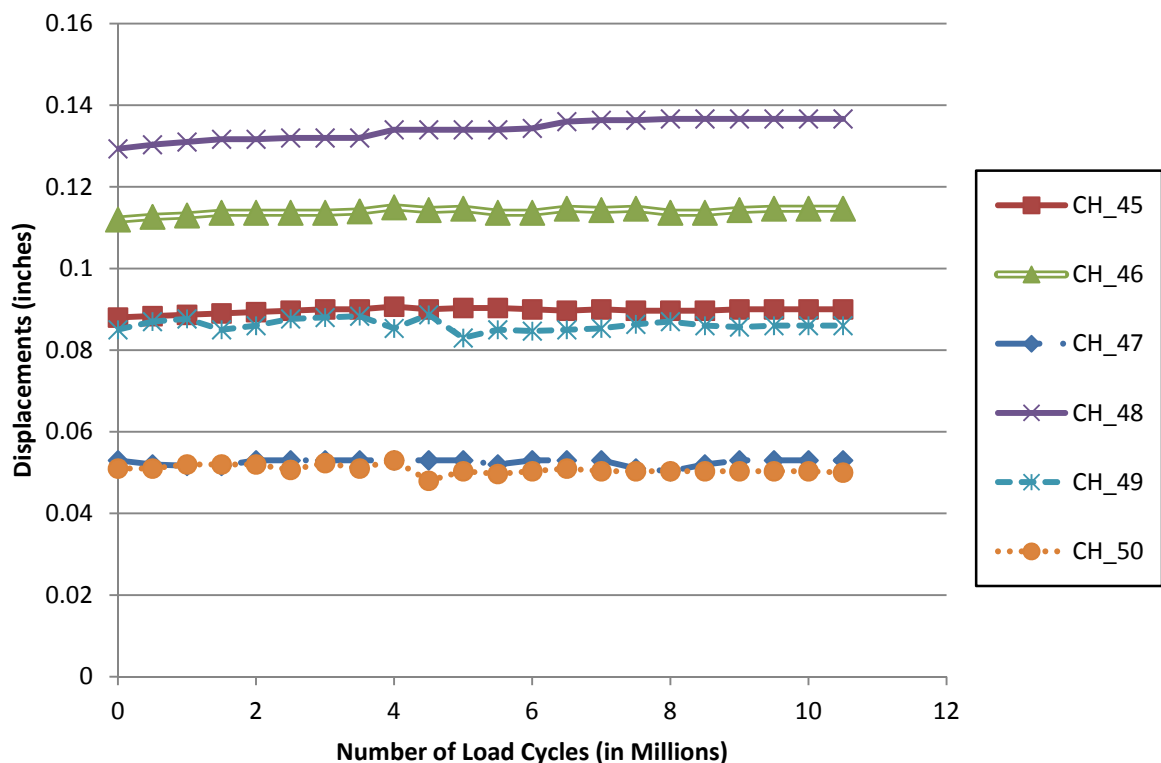


Figure 3-64: Displacements measured throughout testing at 29.1 kip load

Although there were no noticeable increases in the measured deflections of the deck specimen, there was evidence of a slight increase of stresses in the #4 reinforcing steel across the centerline of the transverse splice under the patch load. As shown in Figure 3-65, the stress in all the reinforcing steel that was instrumented across the centerline of the splice at 29.1 kips increased slightly over the duration of the cyclic load test.

CH_23 and CH_24 were strain gages located on the top and bottom, respectively, of a reinforcing steel bar under the patch load. CH_41 and CH_42 were strain gages located on the top and bottom, respectively, of another reinforcing steel bar approximately 8" away from the edge of the patch load (i.e., approximately halfway between the patch load and stringer). CH_43 and CH_44 were strain gages located on the top and bottom, respectively, of a reinforcing steel bar approximately 16" away from the edge of the patch load (i.e., close to the stringer). Figure 3-65 also shows that there was very little bending in the reinforcing steel of the transverse splice.

The measured stress was greatest in the reinforcing steel under the patch load (i.e., CH_23 and CH_24) and decreased in the reinforcing steel as the distance from the load patch increased as expected. The stress in the top of the reinforcing steel under the patch load (i.e., CH_23) increased steadily for the first portion of the cyclic load test (i.e., up to 4 million load cycles), then essentially leveled off. The trend of increasing stresses, especially CH_23, indicated that there was some, though minimal, damage to the specimen in this local region. Therefore, it was desirable to further investigate the stresses in reinforcing steel and main bars of the deck to understand the damage to the deck and resulting behavior.

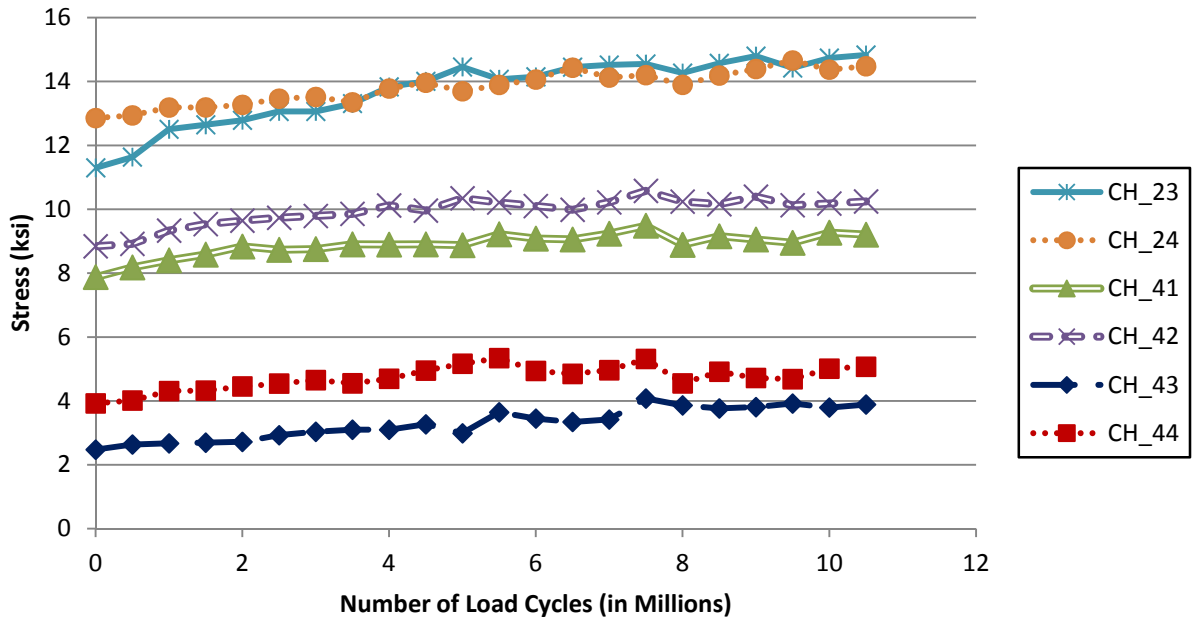


Figure 3-65: Reinforcing steel stresses measured throughout testing at 29.1 kip load

The average measured stresses at multiple reinforcing steel bars across the centerline of the transverse splice are shown in Table 3-22 for the initial and final static tests. The average main bar stresses are also shown so that the changes in stress and behavior may be compared to those of the reinforcing steel. These stresses correspond to an applied load of 29.1 kips rather than 40 kips (i.e., the strength verification load) so that a fair comparison may be made to those of the large-scale specimen cyclic load tests in the following section. The behavior corresponding to the 40 kip load was similar to that at an applied load of 29.1 kips.

Table 3-22 shows that that reinforcing steel underneath the patch load did experience a change in behavior as a result of the cyclic loading test. Initially, the stress at the bottom of the reinforcing steel is greater than that at the top of the reinforcing steel. However, by the end of the test (i.e., after 10.5 million load cycles), the stresses had increased such that the top of the reinforcing steel was experiencing a greater tensile stress than that of the bottom side of the reinforcing steel as shown in Figure 3-65. This indicates that the specimen was initially behaving as a single deck panel because the stiffness of the splice was the same as the rest of the deck. However, the splice was damaged due to the cyclic loading such that some stiffness was lost in the transverse splice. Despite this loss in stiffness at the splice, the panels still behaved as one deck panel because the damage was not significant. However, the local damage under the patch load caused a small amount of negative bending to occur in the reinforcing steel in this region.

Table 3-22: Initial and final stresses for transverse splice at 29.1 kip load

Location	Strain Gage ID	Stress (ksi)		
		Initial	Final	Increase
Reinforcing Steel Under Patch (Top of Bar)	CH_15	11.58	15.49	3.91
Reinforcing Steel Under Patch (Bottom of Bar)	CH_16	12.21	13.85	1.64
Reinforcing Steel Under Patch (Top of Bar)	CH_23	11.30	14.83	3.53
Reinforcing Steel Under Patch (Bottom of Bar)	CH_24	12.86	14.48	1.62
Reinforcing Steel Away from Patch (Top of Bar)	CH_1	3.58	5.33	1.75
Reinforcing Steel Away from Patch (Bottom of Bar)	CH_2	6.72	8.31	1.59
Reinforcing Steel Away from Patch (Top of Bar)	CH_41	7.88	9.21	1.33
Reinforcing Steel Away from Patch (Bottom of Bar)	CH_42	8.84	10.25	1.41
Reinforcing Steel Away from Patch (Top of Bar)	CH_43	2.48	3.89	1.41
Reinforcing Steel Away from Patch (Bottom of Bar)	CH_44	3.92	5.07	1.15
Main Bar Under Patch Load (Top of Bar)	CH_21	-1.91	-1.66	0.25
Main Bar Under Patch Load (Bottom of Bar)	CH_22	16.27	16.30	0.03
Main Bar on Other side of Splice (Top of Bar)	CH_39	-0.33	0.17	0.50
Main Bar on Other side of Splice (Bottom of Bar)	CH_40	13.12	13.62	0.50
Main Bar away from Load (Top of Bar)	CH_7	-2.10	-4.30	2.2
Main Bar away from Load (Bottom of Bar)	CH_8	10.50	11.78	1.28
Main Bar away from Load on Other Side of Splice (Top of Bar)	CH_29	-0.09	-0.14	0.05
Main Bar away from Load on Other Side of Splice (Bottom of Bar)	CH_30	8.76	9.32	0.56

Despite the change from positive to negative bending in the reinforcing steel underneath the patch load, the reinforcing steel away from the patch did not experience this change in bending as shown graphically in Figure 3-65 and numerically in Table 3-22. Although the stresses increased slightly due to damage in the splice under the load patch, the increase in stress at both the top and bottom of the reinforcing steel was approximately equal. This indicated that the damage was localized to under the patch load and that some of the stress from the damaged area was redistributed to the undamaged areas away from the patch. Moreover, the stresses experienced by the main bars generally did not increase. Again, this indicates that there was no damage at these locations.

3.7.3 Comparison to Large-Scale Specimen

After completing the tests of the subassembly transverse splice, the displacements, stresses, and concrete cores taken from the subassembly transverse splice specimen were compared to those of the large-scale specimen. As discussed in Section 2.10, this was done to ensure the subassembly tests reasonably represented the large-scale bridge deck tested. The following sections discuss the comparison between results of these subassembly and large-scale transverse splice tests.

Displacements. An LVDT was placed underneath the load patch on the main bar closest to the transverse splice during transverse splice test #2 of the large-scale specimen. Another LVDT was placed on the interior girder close to the centerline of the transverse splice being tested. These locations were similar to those monitored throughout the subassembly transverse splice cyclic load test.

As shown in Table 3-23, the relative deflection of the deck to the girder/stringer was greater for the large-scale specimen than for the subassembly specimen. Similarly to the longitudinal splice test, this was due to the use of a larger deck span for the large-scale specimen. The deflection of the girders/stringers, as a percentage of the deck deflection, was similar for both the large-scale and subassembly specimens. This indicates that the stiffness of the stringers chosen reasonably simulated the stiffness of the girders of the large-scale test.

Table 3-23: Comparison of displacements of subassembly test to large-scale test

Location	LVDT ID		Measured Displacement (in.)	
	Subassembly	Large-Scale Transverse Splice #2	Subassembly	Large-Scale Transverse Splice #2 (cycles)
Underneath Patch Load	CH_48	Deck	0.137	0.103 (1M)
Stringer near centerline of splice	CH_47	Girder	0.053	0.034 (1M)
Relative Deflection of the Deck	CH_48 – CH_47	Deck – Girder	0.084	0.069
Relative Deflection of Deck as a Percentage (%)	$\frac{CH_{48} - CH_{47}}{CH_{48}}$	$\frac{Deck - Girder}{Deck}$	61	67
Girder Deflection as Percentage of Deck Deflection (%)	$\frac{CH_{47}}{CH_{48}}$	$\frac{Girder}{Deck}$	39	33

Stresses. It was not possible to make a direct numerical comparison between the stresses measured by the subassembly transverse splice specimen and the large-scale specimen roll and cyclic load tests because the transverse splice details were significantly different. The main differences in configuration of the transverse splices are shown in Table 3-24.

Table 3-24: Comparison of transverse splice configuration

Detail	Subassembly	Large-Scale
Spacing of Main Bars at Transverse Splice	10 in.	6 in.
Splice Reinforcing Steel Length	3 ft. 4 in.	2 ft.
Splice Reinforcing Steel Size	#4	#3
Longest cross bar overhang past main bar in splice region	5-1/2 in.	3 in.

Since the patch load was applied such that the nearest edge of the patch was two inches from the centerline of the splice for both specimens, a greater proportion of the patch load was applied directly to the splice of the subassembly specimen. The patch load on the subassembly specimen extended 3-1/2 inches past the main bar closest to the splice, whereas the patch only extended 1 inch past the main bar closest to the splice on the large-scale specimen as shown in Figure 3-66. This would result in the subassembly transverse splice experiencing greater stresses and bending in the reinforcing steel than that of the large-scale specimen.

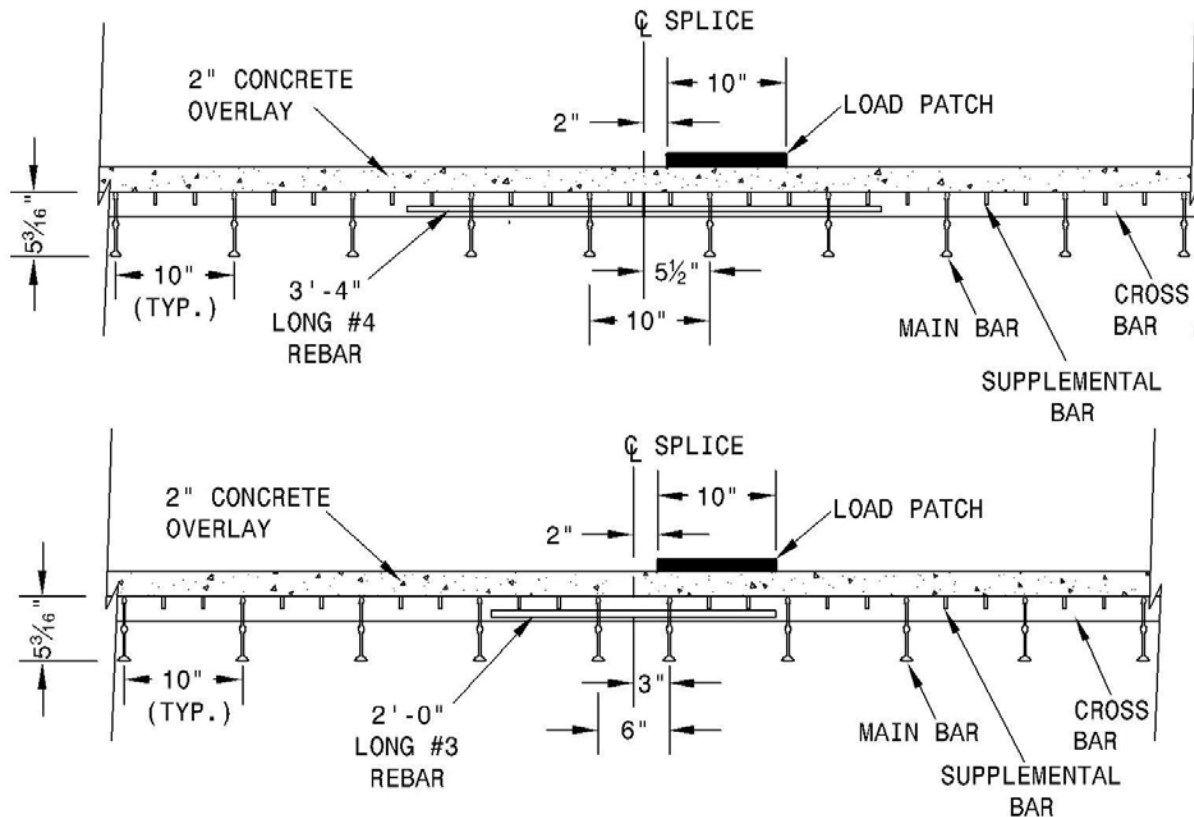


Figure 3-66: Transverse splice configurations (top) subassembly specimen; (bottom) large-scale specimen

Despite these differences, the splices and deck specimens were similar enough such that a comparison between general behavior and damage could be made. For the subassembly and large-scale specimens, only minor damage to the transverse splice was found. The data for each specimen showed that local damage of the transverse splice occurred throughout cyclic loading. Furthermore, the cyclic loading caused a reduced stiffness due to local damage such that a small negative moment was experienced by the reinforcing steel directly under the load patch. However, this damage was not considered to be significant for serviceability.

Based on visual inspections during testing, short surface cracks in the concrete were found on the underside of the deck at the splice. These cracks did not grow or open significantly throughout the cyclic load tests. Cracking was also found in the concrete at the top of the deck. For the large-scale specimen, this cracking was initiated due to shrinkage of the concrete (i.e., prior to any load being applied). For the subassembly specimen, since the concrete was placed in the deck without any restraint on the boundary of the specimen, there was not any shrinkage cracking of the concrete prior to the test set-up. However, upon bolting the deck to the superstructure (i.e., adding restraint) a large crack was initiated in the top of the concrete of the deck. This caused an effect similar to that of the shrinkage in the large-scale specimen; the deicing salts may be able to penetrate the steel through the concrete from the top of the deck. This similar damage to the concrete was shown in the cores taken from both the large-scale and subassembly specimens.

Although the stress data of the large-scale and subassembly transverse splice tests could not be directly compared, the general behavior observed during testing, damage observed during

visual inspections throughout testing and cores taken after termination showed that the subassembly test was representative of a similar large-scale bridge deck. The fact that different configurations were tested and similar behavior and damage was found demonstrated that the subassembly test could be used for different types of decks and produce representative results for a large-scale specimen.

Concrete Cores. The concrete cores extracted from the subassembly and large-scale specimens exhibited similar damage from the cyclic loading tests. The findings of the comparison of the cores of the subassembly and large-scale transverse splice specimens are shown as follows:

- The cyclic loading did not cause significant damage in addition to the initial damage (i.e., shrinkage of concrete in the large-scale specimen or initial cracking in subassembly specimen).
- Damage observed at the transverse splice was similar to that slightly away from the transverse splice. This indicated that the damage caused by the cyclic loading to the transverse splice was not significant.

Unlike the subassembly longitudinal splice specimen, a large initial crack was created in the subassembly transverse splice specimen by installing the deck-to-superstructure connection after curing. This, coincidentally, resulted in similar crack depths between the subassembly and large-scale transverse splice specimens.

3.7.4 Standard Test Methods

The “Standard Test Method and Commentary for Subassembly Cyclic Loading Testing of Transverse Splices in Prefabricated Bridge Deck Panels,” included in Appendix J, was developed in parallel with testing the subassembly transverse splice specimen. Overall, it was found that the results of this standard test method of a subassembly specimen compared well to those of the large-scale specimen. There were discrepancies in the magnitude of stresses produced at the splice due to the difference in deck configuration. However, the behavior of the transverse splice and deck were found to be very similar.

The results of testing the subassembly and large-scale specimens were incorporated into this test method. Additionally, the results were also incorporated into the other subassembly standard test methods (i.e., longitudinal splice and deck-to-superstructure connection) when applicable. For example, the load for the static tests conducted intermittently throughout the cyclic load test was that of the strength verification test. This load of 40 kips was used, rather than simply using fatigue load static tests, to simulate the effect of an overloaded truck axle mixed in with truck traffic every 500,000 load cycles. This was a more appropriate spectrum of loading because heavier trucks will pass over a bridge in the field occasionally. This change to the load applied for the static tests was applied to the other subassembly test methods as well.

3.7.5 Application Summary

The subassembly transverse splice test behavior and damage observed were comparable to those of the large-scale specimen despite the differences in the configuration of the splices. Therefore, this test can be used to evaluate the durability of different configurations of transverse splice details. Based on the findings of this subassembly test, the following was incorporated

into the subassembly testing methods and associated commentary for the deck-to-superstructure connection, as well as the longitudinal and transverse splice tests:

- The magnitude of the static load tests shall be determined from the “Proposed Recommended Method for Verifying Strength of Bridge Decks.” This simulates the effect of a heavy truck passing over a bridge mixed in with “typical” truck traffic and, thus, representing the load spectrum more accurately.

3.8 Proposed Changes to AASHTO-LRFD

This section describes proposed improvements to items currently included in AASHTO-LRFD based on the research described in this report.

3.8.1 Current Items

The present American Association of State Highway Officials Load and Resistance Factor Design Specification (AASHTO-LRFD 2010) accepts orthotropic plate analysis as a permissible technique for particular types of bridge decks. Section 4.6.2.1.8 of AASHTO LRFD prescribes live load design moment demands, based on an orthotropic thin plate theory formulation, for the following types of bridge decks:

- Partially filled steel grid decks;
- Fully filled steel grid decks; and
- Steel grid decks composite with reinforced concrete slabs.

As described earlier in Section 2.1.2, AASHTO defines two cases where orthotropic thin plate theory may be used to determine the design live load moments:

- Main bars perpendicular to the direction of traffic; and
- Main bars parallel to the direction of traffic.

The case where main bars are perpendicular to the direction of traffic is more commonly used because steel grid decks are much stiffer and stronger when placed with this orientation. As previously discussed in Section 2.1.2, for the case where the main bars of the deck are perpendicular to the direction of traffic, the live load design moment equations currently in AASHTO-LRFD (2010) are given as:

$$M_{\text{transverse-AASHTO}}(L \leq 120 \text{ in.}) = 1.28D^{0.197}L^{0.459}C \quad (3 - 15)$$

$$M_{\text{transverse-AASHTO}}(L > 120 \text{ in.}) = \frac{D^{0.188}(3.7L^{1.35} - 956.3)}{L}C \quad (3 - 16)$$

where:

L = span length of deck from center to center;

C = continuity factor (1.0 for simply supported and 0.8 for continuous spans);

D = orthotropic ratio (D_x/D_y);

D_x = strong direction stiffness; and

D_y = weak direction stiffness.

As also previously discussed, for the case where main bars of the deck are parallel to the direction of traffic, the live load design moment equations currently in AASHTO-LRFD (2010) are given as:

$$M_{\text{parallel-AASHTO}}(L \leq 120 \text{ in.}) = 0.73D^{0.123}L^{0.64}C \quad (3-17)$$

$$M_{\text{parallel-AASHTO}}(L > 120 \text{ in.}) = \frac{D^{0.138}(3.1L^{1.429} - 1088.5)}{L}C \quad (3-18)$$

These design equations envelope the load effects produced from the specified notional load combinations such as the design tandem and multiple truck tire patches (Higgins 2003).

3.8.2 Proposed New Items

Recently, semi-analytical solutions to the general orthotropic plate equations were developed (Turan 2009) that address the 3 orthotropic plate possibilities (Timoshenko and Woinowski-Krieger, 1959):

- Case #1 - relatively torsionally stiff, flexurally soft decks which correspond to partially and fully filled grid decks ($H > \sqrt{D_x D_y}$);
- Case #2 - relatively uniformly thick plate or typical reinforced concrete slab ($H = \sqrt{D_x D_y}$); and
- Case 3 - relatively torsionally soft, flexurally stiff decks which correspond to open steel grid deck ($H < \sqrt{D_x D_y}$).

Deck moments can be estimated from patch loads on the deck surface for Case 1 (i.e., torsionally stiff, flexurally soft decks) as:

$$M_x(y \geq \frac{v}{2}) = \frac{2L^2 q}{\pi^3} \sum_{m=1}^{\infty} \frac{1}{m^3} \sin\left(\frac{m\pi\zeta}{L}\right) \sin\left(\frac{m\pi u}{2L}\right) \sin\left(\frac{m\pi x}{L}\right) \times \left[\frac{t_1^2}{t_1^2 - t_2^2} \left(e^{\frac{-m\pi t_2(2y-v)}{2L}} - e^{\frac{-m\pi t_2(2y+v)}{2L}} \right) - \frac{t_2^2}{t_1^2 - t_2^2} \left(e^{\frac{-m\pi t_1(2y-v)}{2L}} - e^{\frac{-m\pi t_1(2y+v)}{2L}} \right) \right] \quad (3-19)$$

$$M_x(y = 0) = \frac{4L^2 q}{\pi^3} \sum_{m=1}^{\infty} \frac{1}{m^3} \sin\left(\frac{m\pi\zeta}{L}\right) \sin\left(\frac{m\pi u}{2L}\right) \sin\left(\frac{m\pi x}{L}\right) \times \left[1 + \frac{t_2^2}{t_1^2 - t_2^2} e^{\frac{-m\pi t_1 v}{2L}} - \frac{t_1^2}{t_1^2 - t_2^2} e^{\frac{-m\pi t_2 v}{2L}} \right] \quad (3-20)$$

$$\text{where } t_1 = \sqrt{\frac{H}{D_y} + \frac{\sqrt{H^2 - D_x D_y}}{D_y}} \text{ and } t_2 = \sqrt{\frac{H}{D_y} - \frac{\sqrt{H^2 - D_x D_y}}{D_y}}$$

For Case 2 (i.e., uniformly thick plate), the deck moments can be estimated in the same manner as:

$$M_x(y \geq \frac{v}{2}) = \frac{Lq}{\lambda \pi^2} \sum_{m=1}^{\infty} \frac{1}{m^2} \sin\left(\frac{m\pi \zeta}{L}\right) \sin\left(\frac{m\pi u}{2L}\right) \sin\left(\frac{m\pi x}{L}\right) \times \left[\left(\frac{2L\lambda}{m\pi} + y - \frac{v}{2} \right) e^{\frac{-m\pi(2y-v)}{2L\lambda}} - \left(\frac{2L\lambda}{m\pi} + y + \frac{v}{2} \right) e^{\frac{-m\pi(2y+v)}{2L\lambda}} \right] \quad (3-21)$$

$$M_x(y = 0) = \frac{4L^2 q}{\pi^3} \sum_{m=1}^{\infty} \frac{1}{m^3} \sin\left(\frac{m\pi \zeta}{L}\right) \sin\left(\frac{m\pi u}{2L}\right) \sin\left(\frac{m\pi x}{L}\right) \times \left[1 - \left(1 + \frac{m\pi v}{4L\lambda} \right) e^{\frac{-m\pi v}{2L\lambda}} \right] \quad (3-22)$$

where $\lambda = \left(\frac{D_y}{D_x} \right)^{0.25}$

For Case 3 (i.e., torsionally soft, flexurally stiff decks), the deck moments can, again, be estimated in the same manner as:

$$M_x(y \geq \frac{v}{2}) = \frac{2L^2 q}{\pi^3} \sum_{m=1}^{\infty} \frac{1}{m^3} \sin\left(\frac{m\pi \zeta}{L}\right) \sin\left(\frac{m\pi u}{2L}\right) \sin\left(\frac{m\pi x}{L}\right) \times \left[e^{\frac{-m\pi t_1(2y-v)}{2L}} \left(\cos\left(\frac{m\pi t_2(y-\frac{v}{2})}{L}\right) + \frac{t_1^2 - t_2^2}{2t_1 t_2} \sin\left(\frac{m\pi t_2(y-\frac{v}{2})}{L}\right) \right) - e^{\frac{-m\pi t_1(2y+v)}{2L}} \left(\cos\left(\frac{m\pi t_2(y+\frac{v}{2})}{L}\right) + \frac{t_1^2 - t_2^2}{2t_1 t_2} \sin\left(\frac{m\pi t_2(y+\frac{v}{2})}{L}\right) \right) \right] \quad (3-23)$$

$$M_x(y = 0) = \frac{4L^2 q}{\pi^3} \sum_{m=1}^{\infty} \frac{1}{m^3} \sin\left(\frac{m\pi \zeta}{L}\right) \sin\left(\frac{m\pi u}{2L}\right) \sin\left(\frac{m\pi x}{L}\right) \times e^{\frac{-m\pi t_1 v}{2L}} \left(1 - \left(\cos\left(\frac{m\pi t_2 v}{2L}\right) + \frac{t_1^2 - t_2^2}{2t_1 t_2} \sin\left(\frac{m\pi t_2 v}{2L}\right) \right) \right) \quad (3-24)$$

where $t_1 = \sqrt{\frac{\frac{D_x}{D_y} + \frac{H}{D_y}}{2}}$ and $t_2 = \sqrt{\frac{\frac{D_x}{D_y} - \frac{H}{D_y}}{2}}$

It should be noted that Case 2 is composed of the same equations used in Higgins (2003) to develop the present AASHTO-LRFD design equations. Using these general equations and considering the design truck (AASHTO-LRFD 2007, section 3.6.1.2.2) and design tandem

(AASHTO-LRFD 2007, section 3.6.1.2.3) live loads, Strength I live load factor, dynamic load allowance, and multiple presence factor, the Strength I design moments are described based on the stiffness properties of the decks. Therefore, as defined in Section 2.1.2, for the case where main bars are located transverse to traffic, the proposed maximum strong direction moments are:

$$M_{\text{transverse}}(L \leq 120 \text{ in.}) = \frac{1.17D^{0.214}L^{0.468}}{\alpha^{0.231}}C \quad (3 - 25)$$

$$M_{\text{transverse}}(L > 120 \text{ in.}) = \frac{D^{0.194}(1.3L^{1.55} - 857)}{L\alpha^{0.233}}C \quad (3 - 26)$$

where:

α = relative torsional stiffness parameter of the deck = $\frac{2D_{xy}}{\sqrt{D_x D_y}}$; and

D_{xy} = Torsional stiffness.

For the case when main bars are oriented parallel to traffic, the proposed maximum strong direction moments are:

$$M_{\text{parallel}}(L \leq 120 \text{ in.}) = \frac{0.91D^{0.12}L^{0.6}}{\alpha^{0.145}}C \quad (3 - 27)$$

$$M_{\text{parallel}}(L > 120 \text{ in.}) = \frac{D^{0.11}(1.136L^{1.62} - 725)}{L\alpha^{0.174}}C \quad (3 - 28)$$

The form of these proposed equations was selected to be similar to the current AASHTO-LRFD formulation in Section 4.6.2.1.8 but now include the influence of the relative torsional stiffness, α , of the deck. The inclusion of this relative stiffness parameter allows these proposed equations to be used for any type of deck rather than just the three currently included (Partially and fully filled grid decks and steel grid decks composite with reinforced concrete slabs).

To use the proposed formulas, the stiffness of a given bridge deck in the strong (D_x) and weak (D_y) directions, as well as in torsion (D_{xy}) are needed. AASHTO-LRFD (2007) prescribes that D_x and D_y can be determined experimentally or calculated using transformed area method as the moment of inertia times the modulus of elasticity for a unit width of deck. Cracked section properties should be considered in the calculation. Experimentally, for the strong direction flexural rigidity (D_x), the deck can be simply supported at the edges and a line load applied at the center, parallel to the supports. Since this load does not produce curvature in the orthogonal direction, the deck can be analyzed as a beam and the flexural stiffness of the beam (or unit width of the deck) can be calculated using the deflection and the applied load as described in Section 3.4. The same procedure can be followed for weak direction stiffness (D_y). The torsional stiffness (D_{xy}) should only be determined experimentally as described in Section 3.4. These three stiffness properties can then be used to determine the orthotropic ratio (D) and the relative stiffness parameter (α) so that the proposed equations may be used to determine the appropriate live load design moments for the given bridge deck.

CHAPTER 4 Conclusions and Suggested Research

The objectives of this research were to determine critical performance factors affecting bridge deck systems, develop testing protocols and criteria to evaluate these critical performance factors, and propose improvements to the existing AASHTO LRFD Bridge Design Specifications for Highway Bridges.

To complete this research, small-scale test methods were developed and validated in the laboratory to:

- Evaluate the resistance of a given wearing surfaces to combined cyclic temperatures, mechanical strains, and exposure to deicing chemicals (i.e., TMC test);
- Evaluate the resistance of a given wearing surface to sliding abrasion (e.g., effect of a snow plow); and
- Evaluate the resistance of a wearing surface and bridge deck to direct impact (e.g., freight falling off of a truck bed).

A large-scale bridge deck was also constructed, instrumented with strain gages and tested to understand the general behavior and identify critical performance factors of a partially filled steel grid bridge deck. A 42 kip tandem axle was rolled across the bridge (i.e., a roll test) at various transverse positions to understand the general behavior of the bridge deck, verify critical performance factors from a review of the literature and identify additional performance factors. Tests were then completed to evaluate the resistance of the critical details (i.e., longitudinal and transverse splice) to cyclic loading.

Subassembly test methods of bridge deck panels were developed and validated in the laboratory to:

- Determine the stiffness properties of bridge decks;
- Evaluate the resistance of critical performance factors to cyclic loading; and
- Validate the minimum required strength of bridge decks and critical details.

Subassembly open and partially filled grid deck panels were obtained and instrumented to determine the stiffness properties of these orthotropic decks. Additional subassembly specimens of critical details (i.e., longitudinal splice, transverse splice, and deck-to-superstructure connection) were obtained and instrumented to monitor displacements and stresses at critical locations throughout testing. The minimum required strength of critical details was determined based on analytical studies that led to the proposed changes to AASHTO from this research. The minimum strength of these critical details was then validated in the laboratory.

The subassembly specimens were also tested to evaluate the resistance of these critical details to cyclic loading. Static tests were conducted regularly throughout testing, as was done for the large-scale specimen, to collect data and monitor changes in behavior of the critical detail and deck. The general behavior, data and damage of the subassembly specimens were compared to the similar large-scale bridge deck specimen tested. Furthermore, the subassembly tests were also compared to the behavior and damage of similar bridge decks known to occur in-service.

4.1 Small-Scale Wearing Surface Tests

4.1.1 TMC Test

The TMC test was designed to evaluate the durability of thin epoxy concrete wear surfaces applied to steel or FRP plate type decks which are exposed to temperature cycles, mechanical strains, and attack from deicing chemicals. The test uses small 6"x20" specimens which are moved from a chemical bath to a temperature chamber and then to a mechanical tester before repeating the cycle again. The specimens are subjected to a total of 15 cycles, which include equal portions of the total loading of 7,500,000 strain cycles, 30 temperature cycles, and 15 chemical immersions. The test is run in cycles because failure of a wearing surface in the field is not the result of any one loading type, but a combination of mechanical strain, thermal strain, freeze/thaw expansion, and chemical attack.

At the completion of the loading phase of testing, the specimens are evaluated on a pass or fail basis using the ASTM 1583 pull-off test criteria. The wear surface passes the test if the pull-off tests achieve an average strength of at least 250 psi, with not more than one location debonding completely.

The TMC test has potential to be very useful for evaluating the durability of thin wearing surfaces on plate type decks. There were four sets of samples tested during development of this procedure. Both the Flexolith and T-48 wear surfaces qualified for use on steel decks with strain ranges up to 10 ksi. There was no delamination observed in either wear surface on the steel specimens. The Flexolith surface did not qualify for use on FRP plates at 900 microstrain because several of the specimens showed delaminations. The T-48 also failed on FRP at 900 microstrain, with large delaminations observed in four of six specimens. This procedure in its final form is ready to be used to evaluate wear surface products for use on plate type bridge decks. A complete technical specification has been included in Appendix C.

4.1.2 Sliding Abrasion Test

The Sliding Abrasion Test was designed to evaluate the resistance of wearing surfaces applied to bridge decks which are subjected to abrasive wear, specifically snow plow damage. The test uses a 3'x5' wear surface specimen which is clamped into a mechanical test frame. The loading is applied by a skid which reproduces the wear of a snow plow, using concrete weight blocks and a snow plow wear point. This skid is moved back and forth on the specimen by a long stroke actuator. As testing progresses, the skid wears a groove into the specimen, which is measured by laser sensors mounted on the skid, and recorded by a data logger. At the conclusion of testing, the wear pattern is plotted, and the average wear rate compared to an established baseline wear rate for a reinforced concrete deck. Following the concrete calibration, Steel Orthotropic specimens were tested with Euclid Chemical Flexolith, and Transpo T-48 epoxy concrete wear surfaces. Both of these surfaces were also tested on ZellComp FRP decks.

The Sliding Test was shown to create predictable wear patterns in the concrete calibration specimens with an average wear rate of 54,000 cycles/inch. A rating system was developed to compare the wear resistance of the other specimens to the average concrete wear resistance. The rating is called the wear resistance ratio (W_r). Under this system, concrete has a W_r of 1.0, and a W_r of 2.0 means that the specimen had twice the wear resistance of concrete.

The Flexolith and T-48 surfaces applied to Steel and FRP decks had an average W_r of 10. The high wear resistance is attributed to the hardness of the basalt aggregates used in both surfaces. There was no difference observed between the performance of the T-48 and Flexolith wear surfaces, likely because they used the same aggregates, and similar epoxy resin binders.

There was no significant difference between the average W_r of the surfaces applied to Steel Orthotropic and FRP specimens. It is concluded that the test results for a wear surface dependent on the wear surface, and not on the deck it is installed on provided there is sufficient bond to prevent the surface from being stripped from the deck during testing. The results of Sliding Abrasion testing on a given wear surface material are therefore an effective way to measure the performance of the wear surface under snow plow loading on any bridge deck system. A technical specification for this test is included in Appendix D.

4.1.3 Direct Impact Test

The Direct Impact Test was designed to evaluate the impact resistance of different types of bridge decks and compare the resistance of a given system to reinforced concrete. The test uses 3'x5' bridge deck specimens which are supported on the laboratory floor below a drop frame. The drop frame supports an Impact Head Assembly which has adjustable weight and drop height. The adjustments allow the impact energy to be controlled over a wide range. The Impact Head Assembly can be positioned on different areas of the specimen, allowing the impact resistance over deck elements such as ribs and stiffeners to be evaluated.

The testing engineer must complete a test plan which fully describes the behavior of the deck system under impact loads by varying the impact energy and location of each drop. After the behavior has been fully described, the performance of the deck is rated using two indices. For this test, significant damage is defined as damage which must receive a timely repair to prevent further degradation of the deck which would lead to premature replacement.

The Zero Damage Index compares the maximum energy a deck can withstand without sustaining significant damage from any individual drop to the maximum energy a reinforced concrete deck can withstand without sustaining significant damage from any individual drop. A zero damage score of 100 indicates that a deck has comparable resistance to a reinforced concrete deck, and a score of 50 indicates that a deck sustained damage at half the energy.

The Serviceability Index compares the minimum energy required to produce significant damage with every drop on a deck to the same energy criteria on a concrete deck. The energy level for this index is higher than the Zero Damage Index. A Serviceability Index score of 100 means that a deck was damaged by every drop at the same level as a reinforced concrete deck, and a score of 50 means that a deck was damaged by every drop at half the energy as concrete. A Serviceability Index score of greater than 200 means that it took twice the energy to damage the deck with every drop as it did for concrete.

The Direct Impact Test has shown consistent results during the calibration phase of testing and during the testing of FRP and Steel Orthotropic specimens. The test results have the potential to be confusing because the definition of significant damage is subjective. The results of the testing on steel specimens show that steel plate decks have excellent impact resistance, and that both indices are greater than 100. The results also show that the FRP had a Zero Damage Index score of 20 and a Serviceability Index score of 35. This test provides a useful rating scale for objectively evaluating the impact resistance of unfamiliar deck types.

4.2 Large-Scale Specimen Tests

The truck roll tests and the longitudinal and transverse cyclic tests of the large scale specimen resulted in the following conclusions:

- The partially filled grid deck was determined to be fully composite with the girders.
- AASHTO effective widths and distribution factors were a reasonable model for the composite behavior of the deck
- The truck roll tests were used to characterize the local and global behavior of the bridge deck subjected to rolling wheel loads. This relationship of the location of the truck tires to the load on a deck element was used to determine the location of the longitudinal and transverse splice cyclic tests.
- The stresses in the longitudinal and transverse splice reinforcing steel compared well to the truck roll tests.
- The longitudinal and transverse splice cyclic tests were used to develop subassembly longitudinal and transverse splice tests. The results of the subassembly cyclic tests were compared to the large scale cyclic tests to determine that the subassembly tests will yield similar behavior and results as the large scale tests.
- The steel stress and concrete crack length variation throughout the splice cyclic tests reinforced that these tests should be able to distinguish poor details without causing unrealistic damage.
- The depth of the concrete cracks near the test was able to be compared to control cracks, and the ability for the infiltration of deicing salts to the deck steel within the concrete could be evaluated.

4.3 Subassembly Stiffness Tests

The development and verification of the subassembly stiffness tests resulted in the following conclusions:

- The subassembly stiffness tests were found to produce accurate results when compared to the theoretical stiffness for each of the decks tested.
- The stiffness properties of the partially filled grid deck could be used to determine the loads for the strength verification tests of the subassembly longitudinal and transverse splice specimens.
- Multiple displacement measurements must be taken at the supports and location of maximum displacement (i.e., under the load) so that rigid body movement may be accounted for during computation of the stiffness properties.
- The theoretical and experimental stiffness of the deck in the strong (D_x) and weak (D_y) directions must be within 15 % of each other for the theoretical stiffness to be deemed acceptable.
- The theoretical models must be adjusted to meet the above criterion when necessary.
- A theoretical model is not necessary for the torsion stiffness (D_{xy}).

4.4 Subassembly Cyclic Tests

The development and verification of the subassembly longitudinal splice, transverse splice, and deck to superstructure connection cyclic load tests resulted in the following conclusions regarding each test method:

- The subassembly longitudinal splice test method produced behavior and results comparable to those of the large-scale specimen.
- The subassembly longitudinal splice test method will reveal any deficiencies of the longitudinal splice and deck specimen that may be present for an in-service bridge deck and longitudinal splice.
- Rigid stringers must be used to test the strength of the longitudinal splice if it is located in the negative moment region of a two span deck. However, flexible stringers that adequately model the stiffness of the in-service bridge may be used alternatively for the cyclic loading test.
- The subassembly deck to superstructure connection test method produced behavior and results consistent with those known to occur in the field.
- The subassembly deck to superstructure connection test method will reveal any deficiencies of the deck that are likely to be observed in-service.
- The subassembly transverse splice test behavior and damage observed were comparable to those of the large-scale specimen despite the differences in the configuration of the splices.

The findings of these tests also resulted in the following conclusions, which were incorporated into these test methods and associated commentary:

- A cyclic load test must not be terminated prior to the application of 3 million load cycles if no significant physical damage to the specimen had been observed. However, if the total number of cycles that the in-service bridge deck is expected to undergo is less than 1.5 million load cycles, this minimum number of load cycles may be reduced.
- The deck must be attached to the superstructure using the same type of connections as will be used in the field so any deficiencies in the connection system may be revealed.
- Fatigue load static tests should be carried out more frequently in the first one million load cycles to ensure the test set-up and data seem reasonable, and when significant damage to the deck has been observed.
- The magnitude of the static load tests must be determined from the “Proposed Recommended Method for Verifying Strength of Bridge Decks.”

4.5 Proposed Changes to AASHTO-LRFD

Section 4.6.2.1.8 of AASHTO-LRFD (2010) currently includes live load design moment demands, based on an orthotropic thin plate theory formulation, for the following types of bridge decks:

- Partially filled steel grid decks;
- Fully filled steel grid decks; and
- Steel grid decks composite with reinforced concrete slabs.

For these types of decks, AASHTO defines two cases where orthotropic thin plate theory may be used to determine the design live load moments:

- Main bars perpendicular (i.e., transverse) to the direction of traffic; and
- Main bars parallel to the direction of traffic.

The live load design moment equations currently included in Section 4.6.2.1.8 of AASHTO-LRFD (2010) are given as:

$$M_{\text{transverse-AASHTO}}(L \leq 120 \text{ in.}) = 1.28D^{0.197}L^{0.459}C \quad (4-1)$$

$$M_{\text{transverse-AASHTO}}(L > 120 \text{ in.}) = \frac{D^{0.188}(3.7L^{1.35} - 956.3)}{L}C \quad (4-2)$$

$$M_{\text{parallel-AASHTO}}(L \leq 120 \text{ in.}) = 0.73D^{0.123}L^{0.64}C \quad (4-3)$$

$$M_{\text{parallel-AASHTO}}(L > 120 \text{ in.}) = \frac{D^{0.138}(3.1L^{1.429} - 1088.5)}{L}C \quad (4-4)$$

where:

L = span length of deck from center to center;

C = continuity factor (1.0 for simply supported and 0.8 for continuous spans);

D = orthotropic ratio (D_x/D_y);

D_x = strong direction stiffness; and

D_y = weak direction stiffness.

Through this research, these equations were improved such that the relative torsional stiffness of a given deck is taken into account. The inclusion of torsional stiffness allows the live load moments for different types of bridge decks to be computed (i.e., not just those currently specified by AASHTO). These equations were also developed for the two cases currently in AASHTO (i.e., main bars perpendicular to traffic and main bars parallel to traffic) and were kept in a similar format to the existing equations in Section 4.6.2.1.8 of AASHTO-LRFD (i.e., the four equations above). Therefore, the improved live load design moment equations, proposed to replace those currently in Section 4.6.2.1.8 of AASHTO-LRFD, are given as:

$$M_{\text{transverse}}(L \leq 120 \text{ in.}) = \frac{1.17D^{0.214}L^{0.468}}{\alpha^{0.231}}C \quad (4-5)$$

$$M_{\text{transverse}}(L > 120 \text{ in.}) = \frac{D^{0.194}(1.3L^{1.55} - 857)}{L\alpha^{0.233}}C \quad (4-6)$$

$$M_{\text{parallel}}(L \leq 120 \text{ in.}) = \frac{0.91D^{0.12}L^{0.6}}{\alpha^{0.145}}C \quad (4-7)$$

$$M_{\text{parallel}}(L > 120 \text{ in.}) = \frac{D^{0.11}(1.136L^{1.62} - 725)}{L\alpha^{0.174}}C \quad (4-8)$$

where:

α = Relative torsional stiffness parameter of the deck = $\frac{2D_{xy}}{\sqrt{D_x D_y}}$; and
 D_{xy} = Torsional stiffness.

To use these improved formulations, experimental tests were required to determine the stiffness of a given bridge deck in the strong (D_x) and weak (D_y) directions, as well as in torsion (D_{xy}). The specific proposed changes are included in Appendix M.

4.6 Recommended Future Work

4.6.1 TMC Test

Further development of the TMC test has the potential to be very beneficial to the bridge industry. To date, there have only been four sets of samples run through the procedure. It would be advantageous for more identical sets of specimens to be tested to verify repeatability of the results.

The next step in verifying the usefulness of this test would be to correlate the TMC test results to the performance of a wear surface on a bridge. This could be achieved by a long-term study which would begin with the re-decking of a bridge. Several proposed wear surfaces could be tested prior to installation on the bridge and the performance of these surfaces could be periodically monitored in the future. This would allow the results of the TMC test to be compared to in-situ performance for all of the surfaces which were installed.

Another issue which should be investigated further is the relative contribution of the three types of loading. For example, of three sets of six identical specimens prepared, one could be subjected to the standard TMC test as a control, a second subjected to only mechanical cycling, and the third set to only chemical and temperature cycling. The results would give insight to how much of the sustained damage is a result of which types of loading, and how much damage is a result of the combination of the three loadings. There should be control pull off tests performed on a set of identical unconditioned specimens to establish the bond strength.

4.6.2 Sliding Abrasion Test

The Sliding Abrasion Test has potential to be useful for evaluating more types of wear surfaces which were not tested in this program. There were no asphalt decks tested in this program, and further testing is needed to ensure that the procedure is applicable to all types of wear surfaces.

A future project could evaluate the effects of using different aggregates on the abrasion resistance of a concrete wear surface. Such a project should include specimens fabricated from at least three test mixes using aggregates of varying hardness. The mixes should be identical with the exception of the coarse aggregate to allow that variable to be isolated. This testing would confirm the effect of aggregate hardness on the wear resistance of a deck surface.

The Sliding Abrasion Test also has the potential to help equipment manufacturers evaluate their products. It could be adapted to become a method for evaluating the lifespan of snowplow wear points. Wear points or blade prototypes could be mounted on the loading skid, run on a standard concrete surface, and the damage evaluated after a reasonable amount of cycles. This would allow a side by side comparison of wear points using an identical loading, which would be impossible to achieve in the field.

4.6.3 Direct Impact Test

The Direct Impact Test has the potential to be useful as a standard test method for materials other than bridge decks. It could, for example, be adapted for use as an inexpensive means of evaluating highway crash attenuators subject to vehicle impact without the use of actual test vehicles. The impact test could also be used to evaluate the resistance of guard rail components and pier supports used on bridges to vehicle crashes. A test specimen would need to be constructed such that the vertical impact would produce the same load effect as a horizontal vehicle collision. The expansion of this test to include bridge works other than the deck would provide a simple method for evaluating the resistance of various components to crash loading without the need to perform actual crash tests. This could reduce the cost of development by eliminating the need for crash tests.

4.6.4 Large-Scale and Subassembly Specimen Tests

The research discussed in this report also warrants further investigation to:

- Develop and verify a method for simulating the effect of concrete shrinkage or other problems that may not be encountered for large-scale specimens, but not in subassembly specimens;
- Develop and verify a test method for evaluating transverse splices located in negative moment regions (i.e., over a floorbeam) which would include the application of two patch loads (i.e., one on each side of the floorbeam) to simulate the effect of a tandem axle of a truck passing over this detail;
- Verify standard testing methods of subassembly specimens for deck panels with significantly different properties or characteristics than open or partially filled steel grid decks (e.g., FRP decks)

REFERENCES

- American Association of State and Highway Transportation Officials (2010). AASHTO LRFD Bridge Design Specifications. Fifth Edition. American Association of State and Highway Transportation Officials, Washington, DC.
- American Association of State and Highway Transportation Officials (2007). AASHTO LRFD Bridge Design Specifications. Fourth Edition. American Association of State and Highway Transportation Officials, Washington, DC.
- American Society for Testing and Materials (ASTM). (2003). "C 666 Standard Test Method for Resistance of Concrete to Rapid Freezing and Thawing."
- American Society for Testing and Materials (ASTM). (2004). "C 1583 Standard Test Method for Tensile Strength of Concrete Surfaces and the Bond Strength or Tensile Strength of Concrete Repair and Overlay Materials by Direct Tension."
- American Society for Testing and Materials (ASTM). (2005). "C 884 Standard test method for thermal compatibility between concrete and an epoxy resin overlay."
- ASTM. (2003). "C 672 Standard Test Method for Scaling Resistance of Concrete Surfaces Exposed to Deicing Chemicals ".
- ASTM. (2004). "C 1583 Standard Test Method for Tensile Strength of Concrete Surfaces and the Bond Strength or Tensile Strength of Concrete Repair and Overlay Materials by Direct Tension."
- Connor, R.J., Liu, Judy, and Higgins, C. (2007). "Interim Report: Bridge Deck Design Criteria and Testing Procedures." Prepared for NCHRP Project 10-72. Purdue University, West Lafayette, IN, March 2007.
- GangaRao, H., Seifert, W., and Kevork, H., (1988). "Behavior and Design of Open Steel Grid Decks for Highway Bridges", West Virginia University, Prepared for the West Virginia Department of Highways, Final Report, Vol. 1., June 1988.
- Gangarao, H. V. S., P. R. Raju, and R. Kannekanti, (1993). *Final Report: Static and Fatigue Behavior of Filled and Unfilled Composite Grid Bridge Decks*, Report CFC92-150. West Virginia University, Constructed Facilities Center, Morgantown, WV, December 1993, Volume III.
- Gopalaratnam, V. S., Baldwin, J. W., Hartnagel, B.A., and Rigdon, R. L. "Evaluation of Wearing Surface Systems for Orthotropic Steel-plate-bridge Decks," Missouri Cooperative Highway Research Program Report. 89-2, University of Missouri-Columbia, Columbia, Missouri.

- Higgins, C., (2003). "LRFD Orthotropic Plate Model for Live Load Moment in Filled Grid Decks." *ASCE, Journal of Bridge Engineering*, Vol. 8, No. 1, 20-28.
- Higgins, C., Turan, O. T., Connor, R.J., and Liu, J. "A Unified Approach for LRFD Live Load Moments in Bridge Decks." *Journal of Bridge Engineering*. American Society of Civil Engineers, posted ahead of print January 5, 2011.
- Huang, H., "Behavior of Steel Grid Decks for Bridges" (2001). Dissertation Submitted for the Degree of Doctor of Philosophy, University of Delaware.
- Indiana Department of Transportation. (2009). "Special Provision for Polymer Concrete Overlay for Bridge decks."
- L.B. Foster Company (2010).
<http://www.lbfoster.com/Fabricated/pdf/FAB_BridgeProducts_Brochure.pdf>.
"L.B. Foster Fabricated Bridge Products." Viewed April 22, 2010.
- Liu, Z. (2007). "Testing and Analysis of a Fiber Reinforced Polymer Bridge," Virginia Polytechnic Institute and State University, Blacksburg, VA.
- McEntire, J., and Nelson, L. (2006). "Flexural Performance of GFRP Bridge Decks." North Carolina State University, Raleigh, NC.
- Stenko, M. S., and Chawalwala, A. J. (2001). "Thin polysulfide epoxy bridge deck overlays." *Transportation Research Record*(1749), 64-67.
- Tsakopoulos, P. (1999). "Laboratory Fatigue Study of Full-Scale Closed-Rib Steel Orthotropic Deck Panels for Williamsburg Bridge Rehabilitation," Lehigh University, Bethlehem, PA.
- Turan O. T. (2009) "Design, Analysis and Evaluation of Bridge Superstructures for Live Loads" PhD Thesis, Oregon State University, Corvallis, OR.
- Turan, O. T., and Higgins, C. (2011). "Analytical Solutions to General Orthotropic Plates under Patch Loading." *Journal of Engineering Mechanics*. American Society of Civil Engineers, posted ahead of print January 13, 2011.
- Wattanadechachan, P., Aboutaha, R., Hag-Elsafi, O., and Alampalli, S. (2006). "Thermal Compatibility and Durability of Wearing Surfaces on GFRP Bridge Decks." *Journal of Bridge Engineering*, 11(465).
- Xi, Y., Chang, S., Asiz, A., and Li, Y. "Long-Term Durability of Fiber Reinforced Polymers (FRPs) and In-Situ Monitoring of FRP Bridge Decks in O'Fallon Park Bridge," Report CDOT-DTD-R-2004-03, Denver, CO., April 2004.

Zhao, L., Ansley, M., and Richards, D. (2006). "A Low-Profile FRP Composite Deck as Replacement for Open Steel Grid Decks." American Composites Manufacturers Association Convention and Trade Show, St Louis, MO.

ATTACHMENTS

**ATTACHMENT A - Proposed Test Method and Commentary for
TMC Resistance of Bridge Deck Wearing Surfaces**

Proposed Test Method and Commentary for TMC Resistance of Bridge Deck Wearing Surfaces

<p>1.0 General</p> <p>1.1 Scope</p> <p>This test method provides a procedure to determine the acceptance of a thin Wearing Surface for use on a FRP or steel plate type bridge deck when the wearing surface is exposed to thermal cycles (T), mechanical strains (M), and exposure to deicing chemicals (C), or other specified chemicals. A minimum of six (6) specimens are to be tested in one set.</p>	<p>C1.0 General</p> <p>C1.1 Scope</p> <p>This test is intended to simulate the loading (<i>i.e., thermal, chemical, and mechanical loads</i>) that a given deck surface is exposed to in the field during its lifetime. Research has shown that there is often an interaction between these various loads on a wearing surface. The test methodology described herein is intended to assess the durability and bond of a given wearing surface when subjected to various loads.</p>
<p>2.0 Referenced Documents</p> <p>2.1 General</p> <p>ASTM C 1583 Standard Test Method for the Tensile Strength of Concrete Surfaces and the Bond Strength of Tensile Strength of Concrete Repair and Overlay Materials by Direct Tension (Pull-off Method) (2007)</p>	<p>C2.0 Referenced Documents</p> <p>C2.1 General</p>
<p>3.0 Summary of Test Method</p> <p>3.1 General</p> <p>A layer of epoxy concrete, or similar thin Wearing Surface under investigation, is applied to six steel or Fiber Reinforced Polymer (FRP) Deck Plates. The plates are loaded in 15 sets of Thermal, Mechanical, and Chemical (TMC) cycles before being subjected to a pull-off test to determine if there is suitable remaining bond between Wearing Surface and substrate. The Wearing Surface is deemed 'acceptable' or 'unacceptable' based on the results of the Pull-off Tests.</p>	<p>C3.0 Summary of Test Method</p> <p>C3.1 General</p> <p>Since there are generally three common deicing agents used and to have replicate data, six specimens are required for the TMC tests. If an owner deems that only one or two types of deicing chemicals are appropriate for their agency, then only two or four specimens (2 per deicing compound) need be tested.</p>
<p>4.0 Significance of Use</p> <p>4.1 General</p> <p>This test applies to Wearing Surfaces applied to steel or FRP Deck Plates, with a maximum surface thickness of ½ inch. When debonding occurs between the Wearing Surface and substrate, the wearing surface is unsuitable for use on that deck at the temperature range, stress range, and deicing solutions at which the testing was conducted.</p>	<p>C4.0 Significance of Use</p> <p>C4.1 General</p>
<p>5.0 Apparatus</p> <p>5.1 Temperature Chamber</p> <p>The Temperature Chamber shall be capable of holding temperatures in the range between -10.0°F to 140°F with an accuracy of ±3.0°F. The chamber shall be programmable and automatically controlled during testing.</p>	<p>C5.0 Apparatus</p> <p>C5.1 Temperature Chamber</p> <p>A computer controlled programmable temperature chamber is required to ensure well controlled and documented temperature loading.</p>

Proposed Test Method and Commentary for TMC Resistance of Bridge Deck Wearing Surfaces

5.2 Mechanical Testing System

The Mechanical Testing System shall be capable of applying load to the samples in three-point bending to a specified strain range. The strain range on each sample shall be continuously monitored. It is acceptable to measure the strain at an offset from the loading point and to infer the maximum strain from moment and curvature calculations. Each specimen shall be subjected to the same strain range - within $\pm 10\%$. An example of a TMC Mechanical Testing System is shown in Figure 1. The specimens are supported at their top edges with angles and loaded from underneath by one inch rods at midspan. The fixture shall be capable of testing six (6) specimens simultaneously.

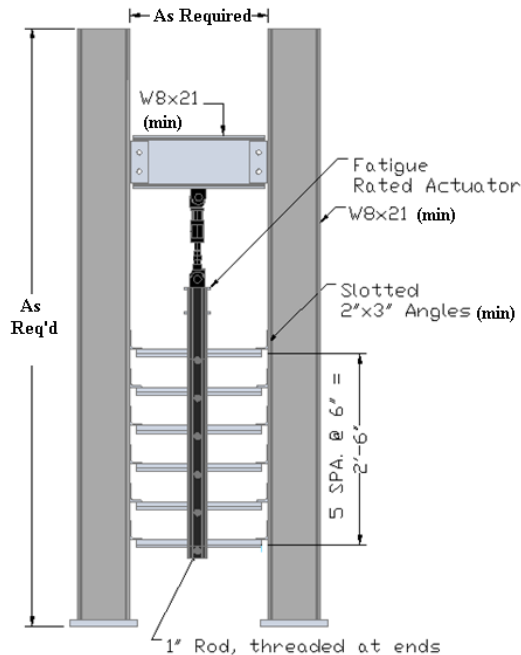


Figure 1: Example of a TMC Mechanical Testing System

C5.2 Mechanical Testing System

During the development of this test, it was found that a single actuator could be used to apply mechanical strain ranges on multiple specimens at once. With use of a fixture as described in Article 5.2, nearly identical strain ranges could be maintained on all specimens. The allowable tolerance of $\pm 10\%$ was selected to provide for some flexibility in the testing while still maintaining sufficient consistency among specimens.

Location of the loading rods at midspan will prevent placement of a strain gage at midspan. Therefore, strain gages will be placed at an offset and infer the maximum strain.

5.3 Pull-off Tester and Related Equipment

The Pull-off Tester, and drills etc. shall conform to the requirements of ASTM C 1583.

C5.3 Pull-off Tester and Related Equipment

6.0 Materials

6.1 Deck Plates

Deck Plates shall be the same material which is to be used on the bridge deck under consideration. Deck Plates shall be prepared per the recommendation of the Wearing Surface manufacturer.

C6.0 Materials

C6.1 Deck Plates

The Wearing Surface manufacturer may require sanding or other surface preparation of the Deck Plates prior to Wearing Surface application.

Proposed Test Method and Commentary for
TMC Resistance of Bridge Deck Wearing Surfaces

6.2 Wearing Surface The Wearing Surface shall be continuously bonded to the deck plate, and shall be less than ½ inch thick.	C6.2 Wearing Surface
6.3 Deicing Solutions There shall be three chemical solutions consisting of: 10% NaCl, 10% CaCl ₂ and 10% MgCl ₂ by weight mixed with water. The specific Deicing Solutions or fewer types of solutions may be deemed appropriate by the owner. The Deicing Solutions may be omitted at the discretion of the engineer or owner when the bridge under consideration is in a warm climate and not subject to deicing salts. In cases where Deicing Solutions are not used, at least three specimens shall still be tested where tap water is substituted for the Deicing Solution.	C6.3 Deicing Solutions It is recognized that some decks may be used in warmer climates and will not be subjected to deicing salts. In such cases it is permitted to conduct the test without the use of Deicing Solutions. However, moisture and water infiltration into a wearing surface can still result in degraded performance. Hence, since all bridge decks are exposed to rain, water is to be substituted when Deicing Solutions are not used. In environments where salt water is present naturally, such as a bridge near the ocean, such water should be substituted for tap water.
7.0 Sampling 7.1 Specimens Six identical Deck Plate specimens shall be prepared, and tested simultaneously, and considered to be one specimen set.	C7.0 Sampling C7.1 Specimens
7.2 Pull-off Tests A minimum of two Pull-off Tests shall be performed on each deck specimen.	C7.2 Pull-off Tests The combination of two Deck Plate specimens and two Pull-off tests per specimen results in four data. Assuming one data are invalid, a minimum of three valid data result.
8.0 Specimen Preparation 8.1 General The surface preparation of the Deck Specimens prior to Wearing Surface installation shall use the same methods planned for the field. The condition of the specimens in the lab shall be the same as the deck in the field with regards to cleanliness and surface roughness.	C8.0 Specimen Preparation C8.1 General
8.2 Size of Deck Specimens The Deck Specimens shall measure six inches by twenty inches. Any overhanging sections of Wearing Surface shall be removed prior to testing.	C8.2 Size of Deck Specimens
8.3 Instrumentation One uniaxial strain gage shall be installed on the bottom (i.e., face opposite to the wearing surface) of each Deck Plate specimen for measurement of mechanical strains in the location shown in Figure 2. The gage shall be sealed and protected against moisture and extreme temperatures experienced during the testing. A uniaxial strain gage with an active grid length appropriate for the material shall be selected.	C8.3 Instrumentation

Proposed Test Method and Commentary for TMC Resistance of Bridge Deck Wearing Surfaces

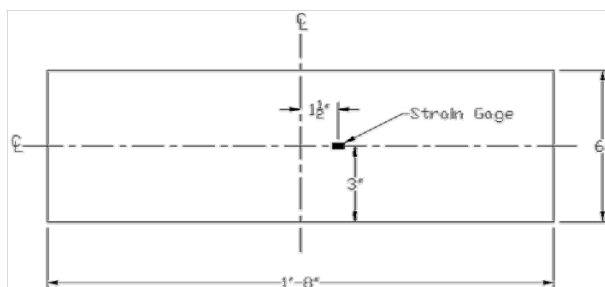


Figure 2: Strain Gage Location

9.0 Test Procedure

9.1 Exposure to Deicing Solution

Two Deck Specimens shall be immersed in each of the three specified Deicing Solutions for at least two minutes. Each specimen shall be immersed in the same solution for each cycle.

9.2 Transfer to Temperature Chamber

The Deck Specimens shall be removed from the Deicing Solutions, and excess solution shall be allowed to drip off of the specimens. Specimens shall not be permitted to dry and shall be placed in the Temperature Chamber within ten (10) minutes of being removed from the bath.

9.3 Temperature Cycles

The Temperature Chamber shall be programmed to make two complete cycles from room temperature, to -100°F, then to 140°F with each temperature held for a minimum of five hours, as shown in Figure 3. At the discretion of the engineer or owner, a different temperature range may be used which is deemed suitable for the region. However, the temperature range shall comply with the following provisions.

1. The maximum low temperature that may be used is 20°F.
2. The temperature range must exceed 100°F.
3. The soak time (time for which maximum or minimum temperature is held constant) shall remain at five hours.

C9.0 Test Procedure

C9.1 Exposure to Deicing Solution

Immersion of the specimen may appear to be overly harsh. However, one must consider that a deck may be exposed to wet conditions where deicing solutions are used for days at a time. Since the specimen is very small and edges are exposed, a duration of two minutes was deemed reasonable.

C9.2 Transfer to Temperature Chamber

Specimens must not be permitted to dry to ensure any freeze thaw effects that may result from the presence of deicing solution or water are incorporated in the test.

C9.3 Temperature Cycles

In some climates, different temperature ranges than specified herein may be more appropriate.

The limits on temperature range and minimum temperature were set to ensure that all wearing surfaces meet at least a minimum set of temperature requirements. The maximum lower limit of 20°F is to ensure that all decks can tolerate below-freezing temperatures. This was deemed important in areas where deicing chemicals are not normally used, but where temperatures could occasionally fall below freezing. Hence, the effect of expanding, freezing water would be captured.

Proposed Test Method and Commentary for TMC Resistance of Bridge Deck Wearing Surfaces

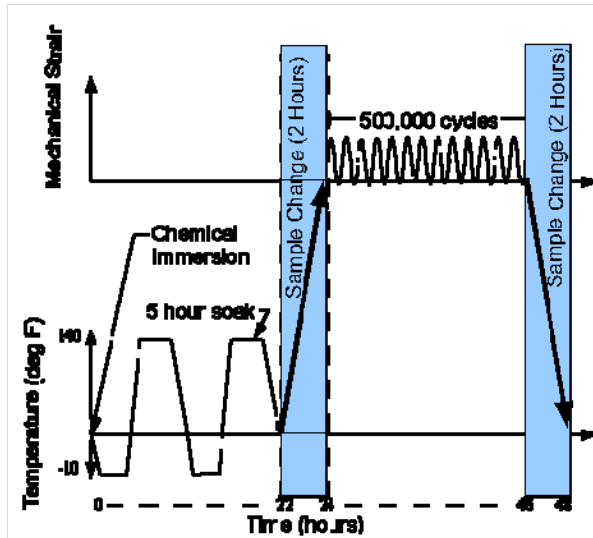


Figure 3: TMC Load Cycle

9.4 Transfer to Mechanical Testing System

The Deck Plate specimens shall then be removed from the Temperature Chamber, rinsed to remove any excess chemical solution using normal tap water, and installed in the Mechanical Testing System. The Deck Plate specimens shall be placed with the wearing surface oriented such that it is subjected to the target tensile strain range.

C9.4 Transfer to Mechanical Testing System

9.5 Mechanical Strain Cycles

The Mechanical Testing System shall be run for 500,000 cycles at the Target Strain Range. The Target Strain Range is defined as the strain range for which the Wearing Surface and/or bond between Wearing Surface and Deck Plate is to be qualified. The strain profile shall be sinusoidal and applied automatically using displacement control. The strain range in each specimen shall be periodically checked at intervals not exceeding 100,000 cycles throughout the test, and the measured strains must be within 10% of the Target Strain Range and recorded in the test log.

C9.5 Mechanical Strain Cycles

9.6 Completion of one TMC Cycle

After completion of the strain cycles, the Deck Plate specimens shall be removed from the Mechanical Testing System.

C9.6 Completion of one TMC Cycle

9.7 Inspection

Following the mechanical testing, the Deck Plate specimens shall be visually examined. Any visible delamination cracks between wear surface and substrate shall be measured and noted in the test log.

C9.7 Inspection

Proposed Test Method and Commentary for
TMC Resistance of Bridge Deck Wearing Surfaces

<p>9.8 Duration of Test</p> <p>Repeat Steps 9.1 through 9.7 fourteen more times unless failure in the form of significant debonding occurs prior to the completion of all fifteen cycles.</p>	<p>C9.8 Duration of Test</p> <p>The target number of total cycles of 7,500,000 is not intended to represent any specific number of trucks. Rather, it is a target value that should reveal any potential weaknesses in a given wearing surface. Assuming an ADTT of 2,500, and 4.5 axles per truck, this produces nearly two years of service. This assumes all trucks apply the maximum design strain range at the exact same location under the worst temperature and deicing conditions. Considering the number loading rates that most labs can accommodate (i.e., cycles/second) this also permits the test to be completed in a reasonable amount of time.</p>
<p>9.9 Pull-off Tests</p> <p>Two Pull-off Tests shall be performed on each Deck Specimen according to ASTM C1583. The tests shall use a two inch steel disk, and each disk shall be positioned such that the tested areas of both tests cross the center line of the specimen in the 20 inch direction. The test results shall be based on a minimum of ten individual pull-off tests; this allows for discard of results from one specimen, or two individual pull-off tests.</p>	<p>C9.9 Pull-off Tests</p>
<p>10.0 Report</p>	<p>C10.0 Report</p>
<p>10.1 Required Information and Results</p> <p>The test report shall include the following:</p> <ul style="list-style-type: none"> • Purpose of the test; • Type of Wearing Surface and Deck Plate; • Manufacturers of Wearing Surface and Deck Plate; • Date of Wearing Surface application; • Deck Plate surface preparation condition and methods; • Target Strain Range used for mechanical testing; • Basis for selecting the Target Strain Range; • Results of each Pull-off Test including failure mode, strength, and Deck Plate specimen number; • Types of Deicing Solutions, manufacturer names and the Deck Plate specimens to which they were applied. • Location and size of any delamination observed during testing; • Cycle number at time of observation; and • Sketches describing delamination location. 	<p>C10.1 Required Information and Results</p>

Proposed Test Method and Commentary for
TMC Resistance of Bridge Deck Wearing Surfaces

11.0 Interpretation of Results	C11.0 Interpretation of Results
11.1 Mechanical Strain Range The results of one set of Deck Plate specimens shall only be applicable to the tested Wearing Surface, on the tested Deck Plate, at service strains comparable to the Target Strain Range.	C11.1 Mechanical Strain Range
11.2 Pull-off Test The result of an individual Pull-off Test shall be considered invalid if the failure occurs within the adhesive or at the bond to the steel disk at a stress of less than 250 psi or if the Deck Plate specimen is damaged during testing. If during preparation for the Pull-off Test (using methods described in ASTM C1583), the Wearing Surface de-bonds from the Deck Plate, the bond strength shall be reported as 0 psi.	C11.2 Pull-off Test
11.3 Pass Criterion A Deck Plate and Wearing Surface combination shall be considered acceptable if no more than one individual Pull-off Test fails at a strength less than 50 psi and the average of nine successful Pull-off Tests is at least 250 psi.	C11.3 Pass Criterion
11.4 Failure Criterion Failure of the Wearing Surface on any single Deck Plate specimen prior to the completion of all 15 cycles shall cause the Wearing Surface to be deemed a failure and unacceptable for that Deck Plate.	C11.4 Failure Criterion

**ATTACHMENT B - Proposed Test Method and Commentary for
Sliding Abrasion Wear Resistance of Bridge Deck Wearing Surfaces**

Proposed Test Method and Commentary for Sliding Abrasion Wear Resistance of Bridge Deck Wearing Surfaces

<p>1.0 General</p> <p>1.1 Scope</p> <p>This test method is used to determine the relative wear rate of wearing surfaces applied to a specific bridge deck type which is subjected to abrasion from general wear, snow plows, etc. The wear rate of the deck and wearing surface(s) under study is compared to that of a standard reinforced concrete bridge deck.</p>	<p>C1.0 General</p> <p>C1.1 Scope</p> <p>This test method is used to determine the relative wear rate of wearing surfaces applied to a specific bridge deck type which is subjected to abrasion from general wear, snow plows, etc. The objective of the test is to make a relative comparison of wear rates of the wearing surface under investigation to that of a traditional concrete bridge deck. The method presumes that the user has a basic understanding of the past performance of traditional concrete decks on bridges in their inventory, in particular, the wear resistance. Hence, the relative comparison of the wear rate of the deck being tested to that of a typical deck will provide an indication of the durability of the wearing surface under consideration. Wearing surfaces that are not as resistance to abrasion as traditional reinforced concrete decks will be identified.</p>
<p>2.0 Summary of Test Method</p> <p>2.1 General</p> <p>A representative section of bridge deck that includes the wearing surface under consideration is subjected to cyclic mechanical abrasion over a defined area to determine the wear rate. The wear rate is then compared to an established wear rate value for a standard reinforced concrete bridge deck.</p>	<p>C2.0 Summary of Test Method</p> <p>C2.1 General</p> <p>The specimen is considered to be comprised of the deck and wearing surface together. In flexible deck systems, such as some FRP and orthotropic decks, local deformations under the wheel loads has led to delamination. If the deck used in the test is stiffer or softer than that to be used in the field, erroneous results can be obtained. Hence, the local stiffness of the deck plate and global stiffness of the test specimen must be reasonably comparable to that to be used in the field. If a previously tested wearing surface is to be used on a deck system for which the stiffness is markedly different than used in the previously tests, this test shall be repeated.</p>
<p>3.0 Significance of Use</p> <p>3.1 General</p> <p>This test applies to any wearing surface which is subject to abrasion wear in the field. The test is not intended to predict in-situ service life but rather give a relative indication of the performance of the pavement surface compared to traditional reinforced concrete or other wearing surfaces.</p>	<p>C3.0 Significance of Use</p> <p>C3.1 General</p> <p>The test method can only be used to establish relative abrasion resistance of the wearing surface under study compared to a traditional reinforced concrete deck. Hence, there is no prescribed conversion from the applied cycles, wear rate, etc. that can be applied to infer the actual in-situ life of the deck. The test method is only intended to identify wearing surfaces that will not perform as well as traditional reinforced concrete decks in terms of abrasion resistance. As stated in the Scope, it presumes owners are familiar with the wear performance of their current inventory of reinforced concrete decks.</p>

Proposed Test Method and Commentary for Sliding Abrasion Wear Resistance of Bridge Deck Wearing Surfaces

4.0 Apparatus

4.1 Loading Skid

The Loading Skid used to hold the weight blocks and Wear Point shall be fabricated with two rear wheels which run on guide tracks to ensure the single Wear Point runs in the center of the specimen. There shall be total 625 lbs of weight over the Wear Point (± 25 lbs). There shall be mounting points for displacement sensors in line with the Wear Point. A suggested assembly for the Loading Skid is shown in Figure 1.

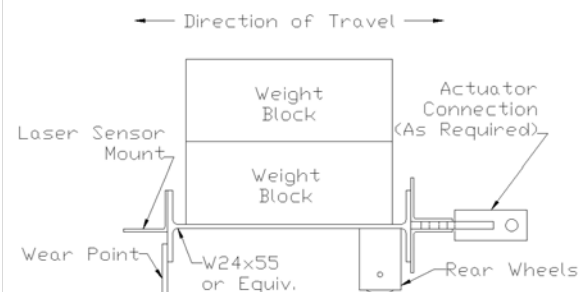


Figure 1: Suggested Loading Skid Assembly (Side Elevation)

4.2 Wear Point

The Wear Point shall be 9 inches long (transverse direction) and at least 1 inch wide (longitudinal direction). The contact surface shall be reinforced with carbide welds. The wear point shall bolt onto the loading skid to facilitate replacement if required.

4.3 Hydraulic Actuator

The actuator used to move the Loading Skid shall be capable of moving at a maximum of six inches per second. The actuator shall have sufficient stroke to be capable of producing a minimum wear path of 24 inches. The actuator shall be programmable and capable of running in

C4.0 Apparatus

C4.1 Loading Skid

The loading skid is a simple device used to apply force to the wear point. The value of the 625 lbs at the wear point is based research conducted as part of NCHRP 10-72 and corresponds to the weight on one shoe of full-size truck-mounted snow plow. Considering the many different types of plows that are available, the value could be debated. It is acceptable to use a heavier load only if unique calibration data from a reinforced concrete deck using the same load is obtained using the procedures described herein. Since the data obtained are evaluated on a relative scale, increasing the load should not affect the results. According to several manufacturers, the 625lbs is a reasonably representative of an average load on a typical shoe. A photograph of a suggested loading skid setup with a specimen is shown in Figure C1

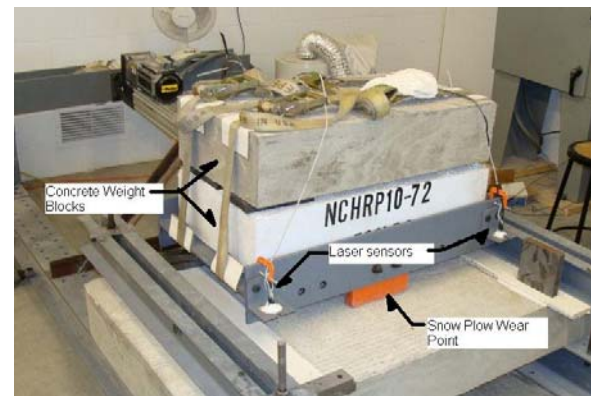


Figure C1 - Photograph of Suggest Loading Skid Setup

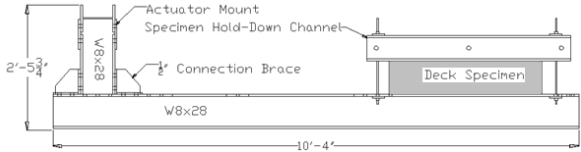
C4.2 Wear Point

The Wear Point itself corresponds to the typical snow-plow wear shoes found on large truck-mounted plows. In most cases, these shoes are reinforced with carbide welds. To ensure a more severe loading condition, it is specified the shoe be reinforced with carbide welds. In addition, the abrasion resistance of the carbide shoes is very high. Hence, wear of the shoe is negligible in a given test.

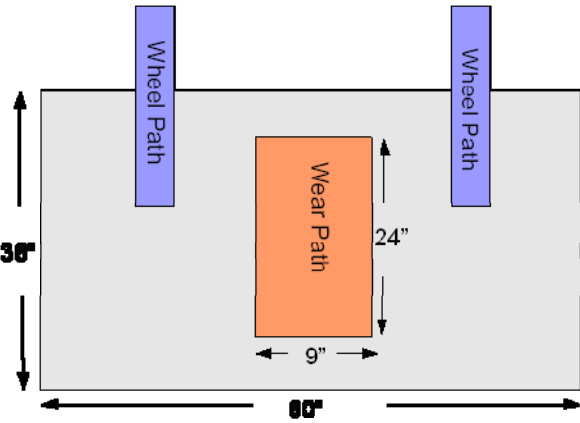
C4.3 Hydraulic Actuator

During the course of the research, various loading rates (in/second) were evaluated. A balance was struck between loading rates that were prohibitively slow and those that created too much "chatter" and vibration as the wear point slid across the deck. The rate of six inches per second

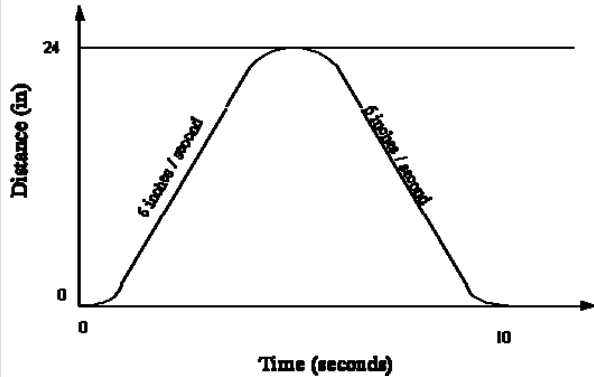
Proposed Test Method and Commentary for Sliding Abrasion Wear Resistance of Bridge Deck Wearing Surfaces

<p>cyclic displacement control.</p>	<p>appeared to be a reasonable upperbound. Faster rates may be considered if it can be shown that the results are not biased and that excessive heat, that may affect some epoxy resins, is not generated. The minimum wear path of 24 inches ensures that a sufficient length of the deck is tested. At the extreme limits of the stroke, the wear will usually be uneven at each end. Hence, if the wear path is too short, invalid data will be generated. It was found that 24 inches provides at least 18 inches of evenly worn wearing surface.</p>
<p>4.4 Load Frame</p> <p>A loading frame shall be used to connect the actuator to the Loading Skid. A suggested design is shown in Figure 2. The actuator shall be mounted with uni-directional clevises to prevent uplift of the skid. The actuator shall be mounted horizontally and be vertically aligned with the skid. The deck specimen shall be secured to the reaction beams and may be tied down using structural channels and rods. A suggested set-up is shown in Figure 2.</p>  <p style="text-align: center;">Figure 2: Sliding Abrasion Test Frame</p>	<p>C4.4 Load Frame</p> <p>The suggested loading frame was found to provide sufficient stiffness while still being economical to fabricate and erect most laboratories. It is also self-reacting such that the test can be conducted in facilities without a strong floor.</p>
<p>4.5 Instrumentation</p> <p>Two non-contact displacement sensors shall be mounted to the Loading Skid at two points outside of the Wear Point path to measure vertical displacement (wear). The sensors shall be capable of measuring displacement with a minimum accuracy of 1/16 inch at a measurement rate no less than 10 Hz. A data acquisition system shall be used to record the number of cycles, displacement, and time of day. A smooth and level surface should be glued to the deck surface on each side to provide a uniform and constant elevation reference for each sensor.</p>	<p>C4.5 Instrumentation</p>
<p>4.6 Run-off Tracks</p> <p>The rear wheels of the Loading Skid shall be supported beyond the rear edge of the specimen if the specimen is not long enough. The Run-off Tracks shall be smooth and free from irregularities which could cause the Loading Skid to bounce or vibrate. The tracks may be clamped onto the specimen using threaded rod.</p>	<p>C4.6 Run-off Tracks</p> <p>During the course of the NCHRP research, it was found that the use of freely rolling guide wheels, rather than additional wear points, greatly improved the consistency of the observed wear, provided for smoother operation of the skid, and more consistent application of the load.</p>

Proposed Test Method and Commentary for Sliding Abrasion Wear Resistance of Bridge Deck Wearing Surfaces

<p>5.0 Materials</p> <p>5.1 Specimen Size</p> <p>The wearing surface shall be integral with or installed on a five foot wide, by minimum three foot long, bridge deck section. Specimens shall be prepared such that they can be installed in the loading frame. The specimen shall be sufficiently stiff to prevent any noticeable “bouncing” from the motion of the wear skid.</p>	<p>C5.0 Materials</p> <p>C5.1 Specimen Size</p>
<p>5.2 Installation of Wearing Surface</p> <p>The installation procedures for the wearing surface on the bridge deck specimen shall be the same as will be used in the field.</p>	<p>C5.2 Installation of Wearing Surface</p>
<p>6.0 Test Preparation</p> <p>6.1 Specimen Placement</p> <p>Place the surface specimen in the loading frame, and fasten securely to the frame.</p>	<p>C6.0 Test Preparation</p> <p>C6.1 Specimen Placement</p>
<p>6.2 Wear Path</p> <p>Run-off tracks may be required on some specimens to provide a continuous support for the wheels on the skid. It is noted that Run-off Tracks may not be necessary if the specimen is long enough to allow a full 24 inch actuator stroke without the wear path coming within three inches of the edge of the specimen. A diagram of the wear path is shown in Figure 3.</p>  <p style="text-align: center;">Figure 3: Sliding Abrasion Test Wear Path</p>	<p>C6.2 Wear Path</p>
<p>6.3 Load Application</p> <p>Install the Loading Skid and any required weight blocks to achieve the target weight over the Wear Point. After attaching the skid to the actuator, it must be ensured that the actuator is aligned properly and will only provide horizontal force to the loading skid.</p>	<p>C6.3 Load Application</p> <p>The load applied by the wear point can be measured using a scale beneath the wear point or other device while supporting the skid at the other supports. This may be done prior to installing the skid in the frame. It must be ensured that the actuator does not apply any vertical force to the loading skid as this will result in an increase or</p>

Proposed Test Method and Commentary for
Sliding Abrasion Wear Resistance of Bridge Deck Wearing Surfaces

	decrease in the applied vertical load at the wear point.
7.0 Test Procedure	C7.0 Test Procedure
7.1 Motion Profile <p>The actuator shall be programmed to run the motion profile in Figure 4. The ramping portion of the loading curve shall not occur faster than six inches per second. The average wear depth measured by the displacement sensor shall be measured and recorded by the data acquisition system at least once every 100 cycles.</p>  <p style="text-align: center;">Figure 4: Motion Profile</p>	C7.1 Motion Profile
7.2 Number of Load Cycles <p>The actuator shall be operated using an automated controller for a minimum of 35,000 cycles to establish a stable wear pattern for the surface. At the conclusion of testing, the wear created by the Wear Point shall be measured manually to verify the measurements of the displacement sensors.</p>	C7.2 Number of Load Cycles <p>The minimum number of cycles was set at 35,000 as it has been found to be a reasonable limit at which a stable wear pattern and rate is confidently produced. Generally, significant non-linear wear occurs during the first few thousand cycles of the test.</p> <p>It is noted that the 35,000 cycles does not correspond to the number of passes of a snow plow, ADTT or any other measure of in-situ performance. Rather, it is simply the number of cycles at which a stable wear rate can be determined.</p>
8.0 Calculations	C8.0 Calculations
8.1 Wear Resistance to Sliding Abrasion <p>The relative Wear Resistance of the specimen (W_r) shall be calculated as a ratio of the average Wear Rate from the two displacement sensors (W) in cycles per inch, divided by 53,000 cycles /inch, as shown in Equation 1.</p> $W_r = \frac{W}{53,000 \text{ cycles/inch}} \text{ Eq. 1}$	C8.1 Wear Resistance to Sliding Abrasion <p>The 53,000 cycle/inch Wear Rate used in Equation 1 is the average Wear Rate observed in reinforced concrete specimens during development of the test. The owner may use this wear rate for calculation of the Wear Resistance of the specimens, or an alternate calibration may be used by testing a reinforced concrete deck using steps 7.1 to 7.4.</p>

Proposed Test Method and Commentary for
Sliding Abrasion Wear Resistance of Bridge Deck Wearing Surfaces

9.0 Report	C9.0 Report
9.1 Required Information and Results The test report shall include the following: <ul style="list-style-type: none"> • Deck type; • Type of wearing surface; • Manufacturer; • Installation procedure. • Two dimensional plot showing the average wear depth readings from the displacement sensors plotted on the vertical axis, and the cycle count on the horizontal axis; • The relative Wear Resistance of the specimen; • The Wear Rate; and • Deck type tested for calibration (if applicable). 	C9.1 Required Information and Results
10.0 Interpretation of Results	C10.0 Interpretation of Results
10.1 Wear Resistance to Sliding Abrasion The relative Wear Resistance calculated in this test shall be used as a relative indicator of the field life of a given pavement surface. For example, if W_r has a value less than one, then the surface is more susceptible to abrasion wear than a standard concrete deck. The deck may also be more susceptible to damage from snowplows. If the value of W_r is greater than one (1.0), then the surface has abrasion resistance greater than standard concrete.	C10.1 Wear Resistance to Sliding Abrasion

**ATTACHMENT C - Proposed Test Method and Commentary for
Qualitative Comparison of Various Deck Types Subjected to Direct Impact**

Proposed Test Method and Commentary for Qualitative Comparison of Various Deck Types Subjected to Direct Impact

<p>1.0 General</p> <p>1.1 Scope</p> <p>This test method describes a procedure for assessing the durability of bridge decks subjected to direct impacts. The impact resistance is rated using comparative indices calibrated to the resistance of a traditional reinforced concrete bridge deck.</p>	<p>C1.0 General</p> <p>C1.1 Scope</p> <p>This test method was developed as part of NCHRP Project 10-72 "Bridge Deck Design Criteria and Testing Procedures". On occasion, decks are subjected to vertical impact from an object striking the deck surface nearly perpendicular to the plane of the deck. Examples would include an object falling off a vehicle or a trailer hitch coming loose and striking the deck, or impact due to vehicular collision. These impacts, although uncommon, can result in damage to the deck system. If a deck type is difficult to repair, or the damage leads to subsequent environmental or fatigue degradation, possible consequences include lane closures, axle weight restrictions, or costly remediation. Hence, in order to provide owners with a comparative performance measure for a deck under direct vertical impact, the direct impact test was developed.</p>
<p>2.0 Summary of Test Method</p> <p>2.1 General</p> <p>This test is intended to rate the relative durability of different types of bridge decks subjected to direct impact loads. The test uses a standard Impact Head to establish the level of energy the deck can withstand without requiring major repairs. For owners considering an unfamiliar deck type, the test is intended to provide an indicator as to the relative soundness and durability of the deck as compared to traditional reinforced concrete.</p>	<p>C2.0 Summary of Test Method</p> <p>C2.1 General</p> <p>The test evaluations are made on a comparative scale. Specifically, impact damage of specimens is evaluated and compared to that of a conventional reinforced concrete deck. This approach allows an owner to compare performance of a given deck system to that of a traditional and familiar deck system, such as reinforced concrete. It is noted that the test is not intended to represent any specific damage but rather to provide a method to compare the resistance of various deck types to direct impact.</p>
<p>3.0 Significance and Use</p> <p>3.1 General</p> <p>This test is applicable to any bridge deck type that can be produced to fit within the test frame and may be subject to impact loading. The test method was developed to be applicable to any deck system other than FRP or orthotropic decks.</p>	<p>C3.0 Significance and Use</p> <p>C3.1 General</p> <p>During the course of the research performed as part of NCHRP 10-72, tests were conducted on FRP decks with wearing surface and orthotropic decks with wearing surfaces. The control tests were performed on reinforced concrete decks designed and detailed to typical Indiana Department of Transportation specifications. The mix design was also consistent with standard Indiana requirements. The size of the specimen was selected such that it sufficiently represented an in-situ deck, while still being small enough to fit in most testing laboratories. In addition, specimens of the sizes required are more easily maneuvered in the lab and not as costly.</p>

Proposed Test Method and Commentary for Qualitative Comparison of Various Deck Types Subjected to Direct Impact

4.0 Apparatus

4.1 Drop Tower

The Drop Tower (Figure 1) shall be fabricated to hoist the Impact Head to a minimum of 15 feet over the specimen. The design shall allow for the specimen to be secured to the laboratory strong floor. The Drop Tower shall permit the Impact Head to be moved relative to the specimen. The Drop Tower also shall include guide tracks (not shown) for the Impact Head that permit it to be raised and dropped freely, with a minimum of friction. The guide tracks shall be capable of being positioned over any area of the specimen. The guide tracks shall allow the impact tip to be guided to within 1 inch of the desired location.

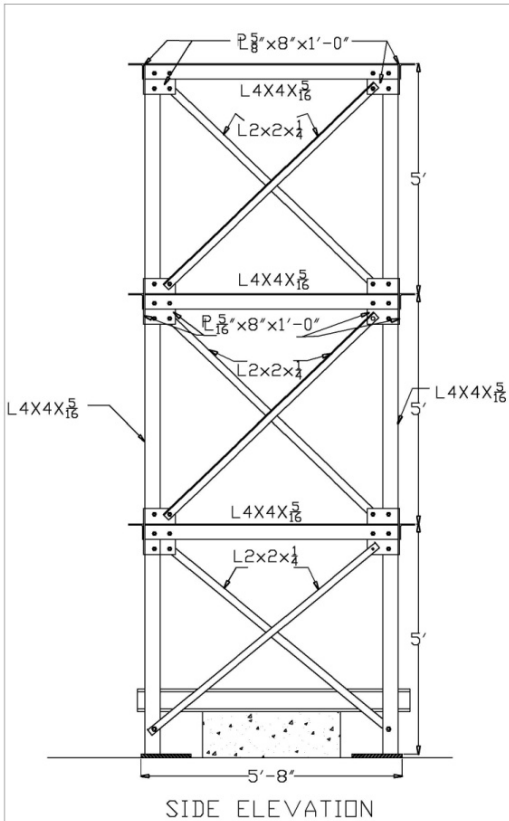


Figure 1: Drop Tower

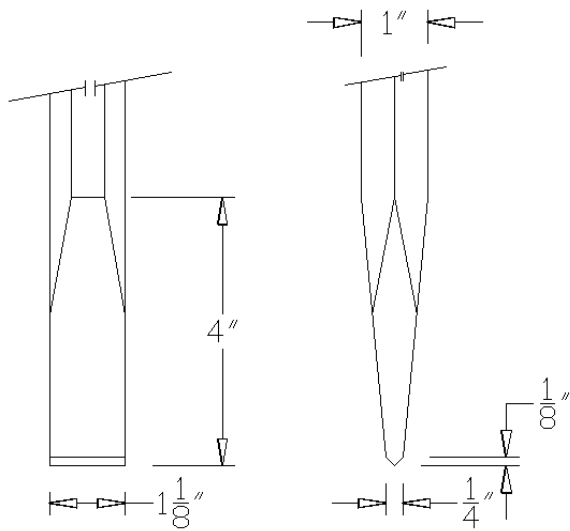
C4.0 Apparatus

4.1 Drop Tower

Proposed Test Method and Commentary for Qualitative Comparison of Various Deck Types Subjected to Direct Impact

4.1 Impact Head

The Impact Head shall be fabricated to run along lubricated guide tracks within the Drop Tower. The Impact Head shall be lifted by a steel cable, securely fastened at the top of the assembly. It shall be dropped from the lift cable by a quick release mechanism. The Impact Head shall securely hold the Impact Tip in a vertical position, and allow for replacement should the Impact Tip become blunted. The Impact Head shall have adjustable weights in increments of 50 lbs to bring the total weight to a minimum of 350 lbs. Any Impact Head bolts shall be fully pre-tensioned to prevent slip during impact. Impact Tip – The Impact Tip shall be a commercially available steel jack hammer spade bit. The tip shall be 1.125 inches wide as shown in Figure 2.



C4.1 Impact Head

A suggested impact head detail is shown in Figure C4.1



Proposed Test Method and Commentary for
Qualitative Comparison of Various Deck Types Subjected to Direct Impact

5.0 Materials	C5.0 Materials
5.1 Specimens Deck specimens shall be fabricated and the wearing surface (if any) applied and prepared in a manner consistent with field applications. The deck specimen should be large enough to include all potentially impact sensitive details. The specimens must fit below the Drop Tower, and be able to be secured to the laboratory floor using channels and post-tensioning rods as shown in Figure 1. The deck specimens shall measure 30 in by 60 in or larger.	C5.1 Specimens
6.0 Test Preparation	C6.0 Test Preparation
6.1 Test Setup The test specimen shall be placed below the Drop Tower, and a layer of mortar or Hydrostone shall be poured between the specimen and the floor to provide uniform support. After the mortar has cured, the specimen shall be secured to the floor using post-tensioning rods and structural channels.	C6.1 Test Setup
7.0 Test Procedure	C7.0 Test Procedure
7.1 Target Drop Energy Calculate the required weight (W) and height (H) to achieve the target drop energy, as shown in Equation 1. The head shall have a minimum height of 12 inches, and a minimum weight of 100 lbs. It is recommended that the testing program begin at a target drop energy of 250 ft-lbs and gradually increase in increments of 250 ft-lbs. The height (H) shall be measured from the deck surface to the lowest point on the impact tip. $\text{Energy (ft*lbs)} = H \text{ (ft)} * W \text{ (lbs)} \text{ (Eq.1)}$	C7.1 Target Drop Energy During the course of the research conducted as part of NCHRP 10-72, it was found that little damage was ever produced at energy levels less than about 250 ft-lbs. Based on the review of all the data obtained during the NCHRP research, 250 ft-lbs was found to be reasonable increment that would ensure an estimate of the energy is calculated to sufficient resolution applied at a given damage level while not being unrealistically precise or too small. However, smaller increments may be more appropriate for some deck systems not considered in the research.
7.2 Impact Head Position Position the Impact Head over the detail under consideration. Each impact must be performed on an undamaged portion of the specimen. The distance shall be sufficiently large to ensure no interaction of multiple impacts	C7.2 Impact Head Position The distance between impacts is not specified prescriptively as it will vary for various specimens and energy values. The user is expected to be able to determine the appropriate distance to ensure no interaction. If the user is unsure, a conservative estimate should be used.
7.3 Impact Head Weight Height Adjust Impact Head weight to the desired level.	C7.3 Impact Head Weight Height
7.4 Quick Release Mechanism Install the quick release mechanism between the Impact Head and the lift cable.	C7.4 Quick Release Mechanism

Proposed Test Method and Commentary for
Qualitative Comparison of Various Deck Types Subjected to Direct Impact

<p>7.5 Impact Head Weight Height Tolerance The head shall be raised and positioned within ½ inch of the correct height (H), a minimum of 12 inches above the deck.</p>	<p>C7.5 Impact Head Weight Height Tolerance</p>
<p>7.6 Release of Impact Head Release the Impact Head using the quick release mechanism.</p>	<p>C7.6 Release of Impact Head</p>
<p>7.7 Inspection The results of the impact, including length, width, and depth of damaged area, and type of damage shall be thoroughly recorded and photographed. The weight of the Impact Head and height of the drop shall also be recorded.</p>	<p>C7.7 Inspection</p>
<p>7.8 Repetition Repeat steps 7.1 through 7.7, increasing the energy in increments of 250 ft-lbs. The test plan must consider all potentially impact sensitive details. For some deck types, this may include performing impact drops directly over deck ribs if present, as well as at mid-span between the ribs. A range of impacts with energies ranging from 250 to 4,000 ft-lbs shall be performed over each potentially impact sensitive detail. Note that more than one test specimen may be needed.</p> $I_0 = \frac{\text{Energy}}{2400 \text{ ft}\cdot\text{lb}} * 100 \text{ (Eq 2)}$	<p>C7.8 Repetition</p>

Proposed Test Method and Commentary for
Qualitative Comparison of Various Deck Types Subjected to Direct Impact

<p>8.0 Calculations</p> <p>8.1 Significant Damage</p> <p>For the purposes of this test, Significant Damage shall be defined as damage to a bridge deck resulting from an individual Impact Drop which, if it had occurred in the field, would present an immediate hazard to the motoring public and must be repaired in a timely manner to prevent further degradation of the deck. The specific characteristics of Significant Damage will depend on the deck system and the details of the bridge under consideration; these characteristics are to be defined by the owner or agency.</p>	<p>C8.0 Calculations</p> <p>C8.1 Significant Damage</p> <p>The calculations included in article eight are intended to provide very simplified quantifiable comparisons of the resistance of various bridge deck types to a known standard, such as reinforced concrete.</p> <p>The determination of what is Significant Damage is recognized to be somewhat subjective. However, during the development of this testing method, it was felt that what constitutes significant damage to a bridge deck may be reliably based upon reasonable engineering judgment. Meanwhile, since different owners may have differing opinions on what constitutes significant damage, a list of various damage scenarios should be developed by the owner prior to beginning the testing so that pass/fail criteria may be defined. In addition, this will also assist in determining the locations for impact prior to the beginning of the test. For new deck types where there is no experience, unforeseen failure modes may occur.</p>
<p>8.2 Evaluation of Damage</p> <p>To establish if damage has occurred in deck types such as FRP or orthotropic steel plate, it is convenient to check for water leakage at the point of impact. This can be performed by flooding the portion of the deck where damage is observed with approximately one to two inches of standing water. The water should be allowed to stand for no less than 20 minutes to ensure enough time for the water to migrate through the deck. After 20 minutes, if no water is observed to have leaked through the deck at the point of impact, it should be concluded that the damage was not significant.</p>	<p>C8.2 Evaluation of Damage</p> <p>During the course of the research, it was found that for FRP and steel orthotropic decks, leakage of water through the top surface layer was an effective and convenient indicator of damage. Leakage of water is also a mode of failure that can result in further damage in the field. For example, water leakage within a cellular FRP deck system could result in future problems due to freeze-thaw cycles, deicer intrusion, etc. Hence, the water leakage check is presented as a reasonable way to determine if damage to the deck has occurred.</p>
<p>8.3 Zero Damage Index</p> <p>The Zero Damage Index (I_0) shall be calculated from the maximum impact energy that the deck can withstand without showing signs of Significant Damage from any individual drop over any of the details or locations under consideration. I_0 shall be calculated as the ratio of that energy compared to 2400 ft-lbs, which is the energy a reinforced concrete bridge deck can withstand without Significant Damage. The formula is given in Equation 2. If multiple details are tested on a given deck type, the lowest value of I_0 shall govern. Alternately, the owner may elect to use a different energy level for calibration of the Zero Damage Index. If a different calibration value is to</p>	

Proposed Test Method and Commentary for
Qualitative Comparison of Various Deck Types Subjected to Direct Impact

<p>be used, the alternate energy level for the Zero Damage Index shall be determined from testing a reinforced concrete bridge deck using steps 7.1 through 7.8.</p>	
<p>8.4 Serviceability Index</p> <p>The Serviceability Index (I_s) shall be calculated from the <u>minimum</u> energy required to create Significant Damage over every detail, with every impact. I_s shall be calculated as the ratio of that energy compared to 3600 ft-lbs, which is the energy required to produce Significant Damage in a reinforced concrete bridge deck with every drop. The formula is given in Equation 3. The owner may also elect to use a different energy level for calibration of the Serviceability Index. The alternate energy level for the Serviceability Index shall be determined from testing a reinforced concrete bridge deck using steps 7.1 through 7.8.</p> $I_s = \frac{\text{Energy}}{3600 \text{ ft}\cdot\text{lb}} * 100 \text{ (Eq. 3)}$	<p>C8.4 Serviceability Index</p>
<p>9.0 Report</p>	<p>C9.0 Report</p>
<p>9.1 Required Information and Results</p> <p>The test report shall include the following:</p> <ul style="list-style-type: none"> • Type of wearing surface; • Deck type on which it was installed; • Manufacturer; • Installation procedure; • cross sectional drawing indicating details which were considered in testing and their locations; • Chart showing the Significant Damage characteristics defined for the deck; • Energy required to produce Significant Damage at each location within the deck; • Photographs that clearly show the damage from each drop; • Dimensions of the damaged regions. • Zero Damage and Serviceability Indices and the criteria used to define and calculate them; and • If baseline values other than those recommended herein are used, the details pertaining to the testing associated with obtaining those values shall also be reported. 	<p>C9.1 Required Information and Results</p>

Proposed Test Method and Commentary for
Qualitative Comparison of Various Deck Types Subjected to Direct Impact

10.0 Interpretation of Results	C10.0 Interpretation of Results
<p>10.1 Indices</p> <p>The Zero Damage and Serviceability Indices are intended to give bridge owners an indication of the relative durability of an unfamiliar deck subjected to impact loading. If both indices, are high (scoring 100 or above) and then the deck is as or more durable than a reinforced concrete deck and has excellent impact resistance. If both indices are low (less than 100) then the deck is less durable than concrete. If the I_0 is less than 100, and the I_s greater than 100, then the damage behavior of the deck is variable, and there are areas which are less durable than concrete. If the I_0 is less than 25, use of the deck is not recommended where vertical impacts are a potential concern.</p>	<p>C10.1 Indices</p>

**ATTACHMENT D - Proposed Recommended Method for Verifying Strength of Bridge
Decks**

Proposed Recommended Method for Verifying Strength of Bridge Decks

1.1 Scope

This test method describes a procedure for verifying the AASHTO_LRFD Strength I limit state of a prefabricated bridge deck. To determine the required maximum test load, the deck flexural stiffness ratio, D (D_x/D_y), and twisting stiffness, D_{xy} , must be established according to the methods described in the standard test methods and commentary for determining flexural stiffness (D_x , D_y , and D_{xy}) of bridge decks.

1.2 Summary

This test procedure is used to verify the strength of a bridge deck to achieve the AASHTO-LRFD Strength I limit state. The test is conducted with a single patch load applied at midspan of the deck specimen. The load magnitude applied to the patch is established based on the width and stiffness properties of the deck sample. Data to be reported include the applied test load (P_t) at prescribed force increments and net centerline displacements (Δ_{CL}). Each test is conducted only once.

1.3 Approach

The deck specimen is placed on parallel, continuous, and rigid supports that provide vertical support only. Force is applied to the specimen through a rectangular load patch placed at midspan. The patch orientation is positioned so as to reflect the operating conditions of the deck (either supports transverse or parallel to traffic). Five equal load intervals are applied to the maximum load specified and at each interval, the centerline displacement of the specimen under the patch is measured. The specimen need not be tested to destruction and after the maximum load is achieved, the load can be removed.

2.0 Specimens

2.1 Components – General

Specimens shall be representative deck assemblies of a typical portion of a bridge deck and contain all the relevant detailing and connections used for both deck orientations as would be used for field applications. The specimen width dimension is established so that the minimum width is at least 3 times the patch dimension that is parallel to the supports. The minimum deck width must also contain at least three (3) load carrying ribs or bars. The specimen is to be supported continuously on rigid supports along two sides of the specimen such that it is simply supported for bending about its strong axis as shown in Figure 1. The span dimension between the centerline of lines of support shall be established by the manufacturer. For a selected span and the established stiffness parameters, D_x , D_y , and D_{xy} , the applied force on the patch is determined according to Tables 1F and Figures 1F. Linear interpolation may be used for cases that are in between those listed in the tables and figures.

Prior to testing, the specimen shall be visually inspected for flaws or defects that could affect the measured strength of the bridge deck being considered. Defects and flaws shall be defined as per the appropriate governing specification (e.g. contract documents, relevant ASTM

standards, etc.). Specimens containing flaws and defects that are deemed sufficient to affect strength shall not be used for testing. If a specimen with minor defects is tested (i.e. those deemed to not significantly affect the strength of the deck), the defects and their locations shall be documented and included in the report.

2.2 Instrumentation

The test specimen shall be instrumented to measure the vertical displacements of the specimen at three locations. The measurements shall be taken over the supports (2 sensors) and at the center of the specimen directly under the load patch. The measurements shall be along a line of symmetry as illustrated in Figure 2. Displacements shall be measured to a resolution of 0.001 inches (25 μm). Sensors and instrumentation for accurately measuring the applied force shall also be used. The resolution of the load measuring device shall be 1% of maximum test load applied, P_{max} defined in section 2.1. Calibrations of all sensors shall be reported.

3.0 Fixtures

3.1 Fixture Details

Fixtures capable of adequately supporting and loading the specimen during the test shall be provided. The fixtures shall be fabricated such that no additional displacements or stresses are generated as a result of fixture misalignments or movements. In addition, fabrication tolerances in the specimen shall be corrected or compensated for using non-mechanical means (i.e., shimming) and where required shall be reported. Dimensional tolerances of support locations shall be within $\pm 1/8$ in. (3 mm)

The supporting fixtures shall be sufficiently stiff to ensure vertical displacement of the fixture is less than 0.005 inches (127 μm) under the maximum applied load. Vertical displacement of the supports shall be measured as described in section 2.2. Measured vertical displacement of the supports at each load step shall be reported.

4.0 Test Procedure

4.1 General

One (1) data set is required to establish the strength of a prototype bridge deck panel.

4.2 Loads

Loads shall be applied to the specimen with a hydraulic jack or actuator. The magnitude of the load will be increased in five (5) equal increments pre-determined for the test. The load shall be applied in a pseudo-static manner and shall be maintained for a minimum of sixty (60) seconds within $\pm 2\%$ at each load increment to allow for the collection of data and inspection of the specimen. The load and displacements shall be monitored continuously throughout the test using a data acquisition system.

4.2.1 Application of Load

Load shall be applied through a single patch located at midspan of the specimen. The rectangular patch size shall be 10x20 in. (254x508 mm). The patch shall be a stiffened hot-rolled W shape that can provide uniform contact pressure over the patch area as illustrated in Figure 3. A ½ in. (13 mm) thick bearing pad with a minimum hardness of 50 durometer shall be placed between the steel patch and the specimen to account for surface unevenness. The long patch dimension shall be oriented either parallel or transverse to the supports so as to represent the field application for the deck considered.

4.2.2 Preloading

The Maximum Test Load, determined in section 2.1, shall be divided into five equal increments (i.e. $P_{\max}/5$). The specimen shall be initially loaded to the first increment ($P_{\max}/5$) to ensure proper seating of the fixtures, specimen, and patch load as well as insure the sensors and measuring system are functioning properly. During this preload phase, displacement data shall be recorded and the deck response (load vs. net centerline displacement) should exhibit linear response in the upper 1/3 portion of the loading curve. If the measurements indicate nonlinear response over the entire preloading history, then the sources of nonlinearity shall be determined and corrected. After initial preload, the applied load shall be removed and all sensors reset to zero.

The preloading can be reapplied as many times as necessary to position/seat the specimen and ensure proper operation of the data collection system.

4.2.4 Strength Test

Once preloading has been performed and the load and displacements are reset to zero, the strength test can be conducted. Force shall be slowly applied to the load patch at the predetermined load increments. At each increment, the force shall be held for a minimum of 60 seconds to collect data and inspect the specimen. Inspection of the specimen during testing shall note and report the load at which any crack initiation and propagation, slip, or other visible distortions or distress are observed. After each increment is achieved and the load maintained, the load shall be increased to the next higher increment. The process shall be repeated until the maximum load is achieved and maintained for at least 5 minutes. Then the load can be removed and the test concluded. Alternatively, the load can be increased until specimen failure.

5.0 Results

5.1. Interpretation of Results

The deck shall be considered to achieve the AASHTO-LRFD Strength I limit state if the Maximum Test Load can be sustained as described in the previous section.

The data obtained from the strength test shall be used to demonstrate the overall load-deformation response of the specimen. Rigid body support deformations shall be removed by

averaging the support settlements at each load interval and subtracting from the gross centerline deformation measurement. The net load-deformation response shall be reported.

6.0 Reporting of Data

6.1 Strength Test Results and Observations

The following data shall be reported:

1. Vertical displacements (at all locations), and the Test Load (P_t), shall be reported in tabular format for each load increment.
2. The net vertical displacement at midspan shall also be plotted with respect to the Test Load (P_t).
3. Visible distress observed during testing shall be reported and images or sketches showing the conditions shall be provided with reference to the load at which the conditions were first observed.

6.2 Miscellaneous Required Information

The following additional information shall also be reported.

- Deck type and fabricator.
- Material properties of deck components (both nominal and tested).
- Any deviations from specified properties or tolerances.
- A drawing showing the shape, size and orientation of the specimen and test fixtures.
- A drawing showing the location of all instrumentation and the load patch.
- Section properties and detailed dimensions of the specimens and supports/fixtures.

COMMENTARY

To develop a test method that can be reasonably performed in most laboratory settings, a single patch load placed at midspan on a finite width deck sample placed on simple supports is considered. The span length is specified by the manufacturer and the sample width is selected to be representative of in-situ deck elements shipped to the field. The deck must be at least 3 times the width of the patch orientation parallel to supports and contain a minimum of 3 main direction load carrying elements (ribs or bars for example) with the same connecting details used in-situ. For main bars transverse to direction of traffic, the patch length is positioned parallel to main bar direction, as shown in Figure 1a and for main bars parallel to direction of the traffic, the patch width is positioned parallel to main bar direction as shown in Figure 1b. The load magnitude to be applied to the sample will depend on the deck span, deck sample width, deck orientation relative to the direction of traffic, and the deck stiffness properties. As described previously, the deck section properties are required to determine the internal moment distribution. Different load amplitudes are required to demonstrate strength, serviceability, and fatigue limit states.

To capture the load effects present in a continuous deck with a single patch on a finite width deck requires the internal moment distribution be considered. To determine these effects, an unfactored truck patch load (16 kips) was placed at the center of the span length and strong direction moments (M_{Patch}) were calculated from $y=-4L$ to $y=4L$ with 1 in. increments using Turan (2009). Since the equations proposed by Turan (2009) are valid for $y \geq \frac{v}{2}$ and $y = 0$; for strong direction moments under the patch, superposition principle was used as shown in Figure 2. For the strong direction moment which is $\frac{t}{2}$ away from the x axis, where $\frac{t}{2}$ is less than $\frac{v}{2}$; two patches with lengths t and $(v-t)$ were superposed and the strong direction moments under the patch load were obtained. In order to verify these results, finite element analyses were performed using ABAQUS 6.8-2. The element type used was S4R (4 node, reduced integration, conventional stress, thin or thick shell element) and elastic analysis was performed consistent with the analytical derivations. Excellent correlation with a maximum discrepancy of 0.5% was observed between the finite element analyses and the superposed analytical solutions as shown in Figure 3.

Equations were developed to calculate the AASHTO-LRFD Strength I level strong direction design moments ($M_{AASHTO LRFD}$) for main bars transverse to traffic and parallel to traffic as:

$$M_{transverse}(L \leq 120 \text{ in.}) = \frac{1.17 D^{0.214} L^{0.468}}{\alpha^{0.231}} C \quad (F-1)$$

$$M_{transverse}(L > 120 \text{ in.}) = \frac{D^{0.194} (1.3 L^{1.55} - 857)}{L \alpha^{0.233}} C \quad (F-2)$$

$$M_{parallel}(L \leq 120 \text{ in.}) = \frac{0.91 D^{0.12} L^{0.6}}{\alpha^{0.145}} C \quad (F-3)$$

$$M_{parallel}(L > 120 \text{ in.}) = \frac{D^{0.11} (1.136 L^{1.62} - 725)}{L \alpha^{0.174}} C \quad (F-4)$$

where C is the continuity factor, L is the span length, D is the relative stiffness ratio (D_x/D_y) and α is the deck twisting stiffness. For simply supported $C=1.0$ and for continues spans $C=0.8$. For this study, simply supported values were used ($C=1.0$).

For different span widths (from 3 ft to 8 ft with 1 ft increments), α values ($\alpha=0.25, 0.5, 0.75, 1.0, 2.0, 4.0, 8.0$), orthotropic stiffness ratios ($D=2.0, 2.5, 5.0, 8.0, 10.0$), and span lengths (from 3 ft to 20 ft with 1 ft increments); required test load was calculated as:

$$P = 16 \text{ kips} \frac{M_{AASHTO LRFD}}{M_{Max patch}} \frac{M_{Span width}}{M_{Total}} \quad (F-5)$$

where M_{Total} is the total static moment (Eq. 6), $M_{Span width}$ is the static moment calculated for the specified deck sample width (Eq. 7), and $M_{Max patch}$ is the maximum value of M_{Patch} for the specified span length.

$$M_{Total} = 2 \int_0^{4L} M_{Patch} dy \quad (F-6)$$

$$M_{Span\ width} = 2 \int_0^{Span\ width} M_{Patch} dy \quad (F-7)$$

Since $M_{AASHTO\ LRFD}$ is a piecewise function, the behavior of P is different for $L \leq 120$ in. and $L > 120$ in. as shown in Figure 4a. Thus the local maximum value in the second part of the function was used as a threshold value and combined with the first part as shown in Figure 4b.

For main bars transverse to direction of traffic results are shown in Figures 1F-5F and were tabulated in Table 1F-5F. For main bars parallel to direction of traffic results are shown in Fig 6F-10F and were tabulated in Table 6F-10F.

Figures:

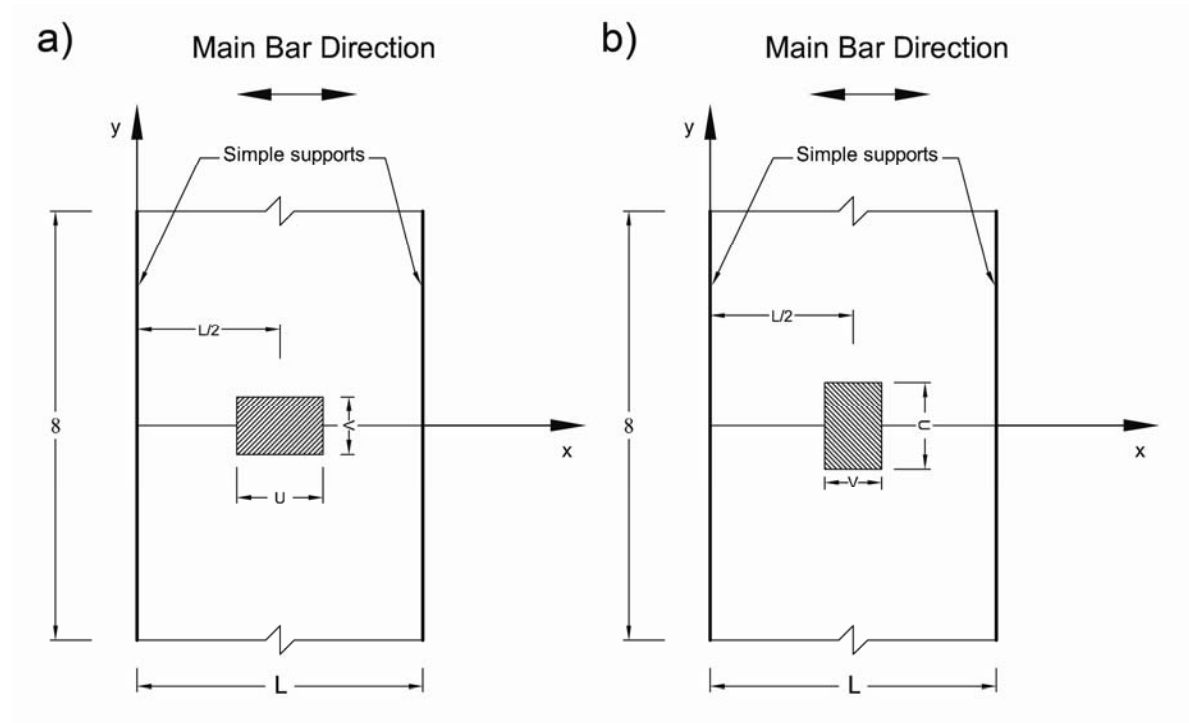


Figure 1: Patch load orientations a) main bars transverse to direction of traffic b) main bars parallel to direction of traffic

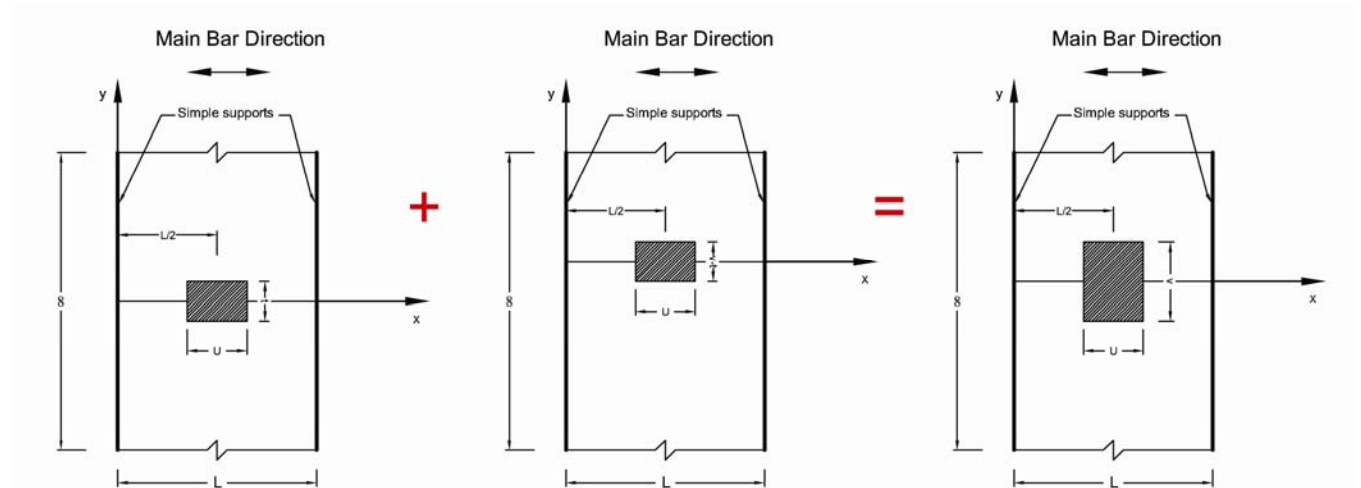


Figure 2: Strong direction moment under the patch.

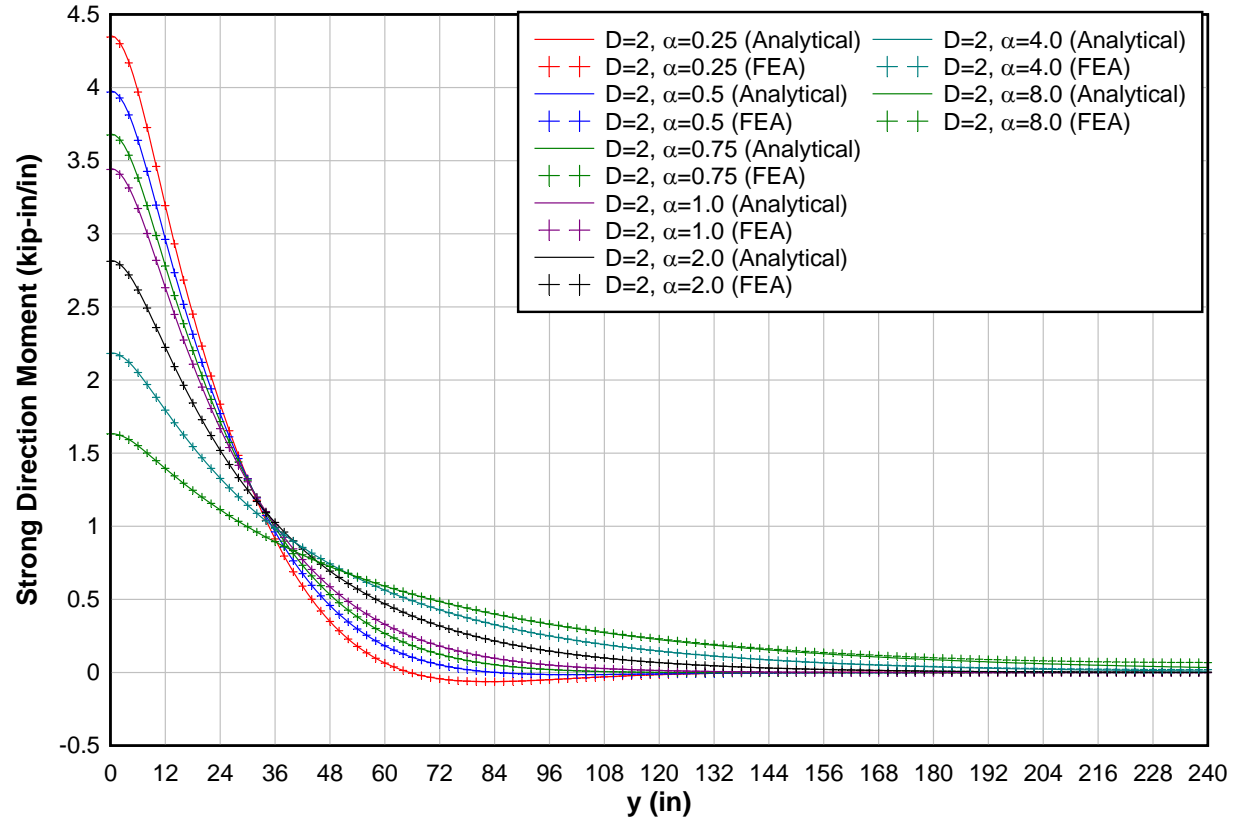


Figure 3: Comparison of strong direction moment along y for a single patch at midspan with $D=2, L=60$ in.

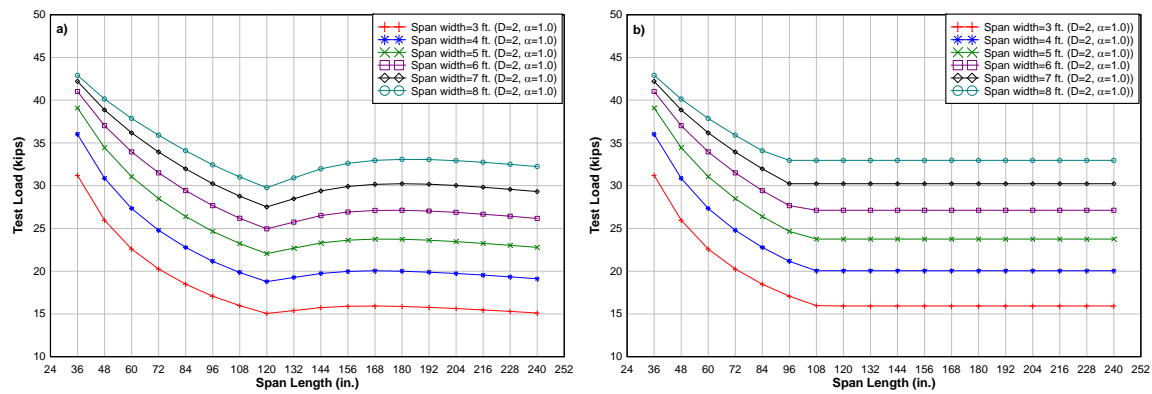


Figure 4: Test Load (P) a) without the threshold b) with the threshold.

Plots

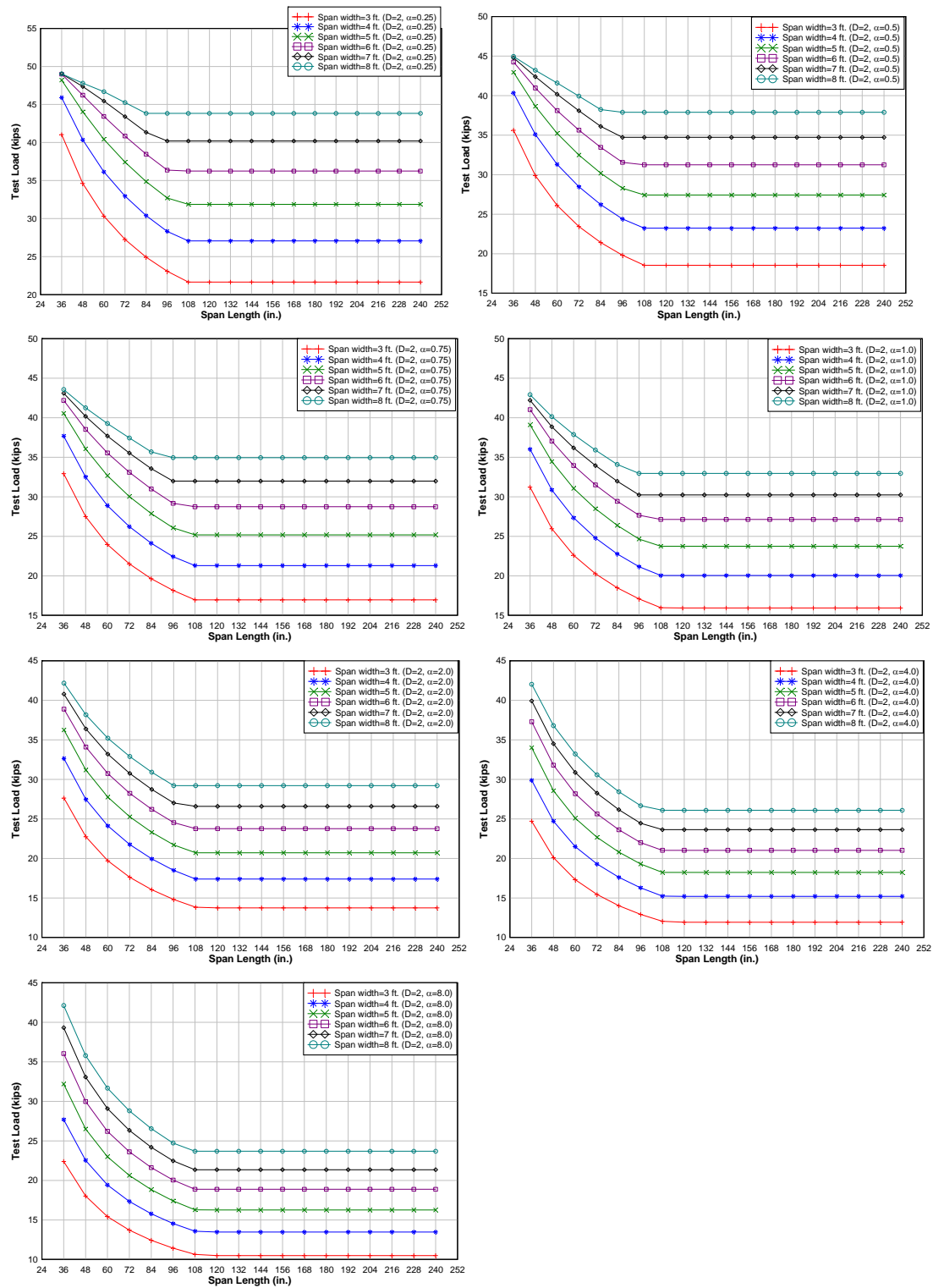


Figure 1F: Main bars transverse to traffic, $D=2.0$.

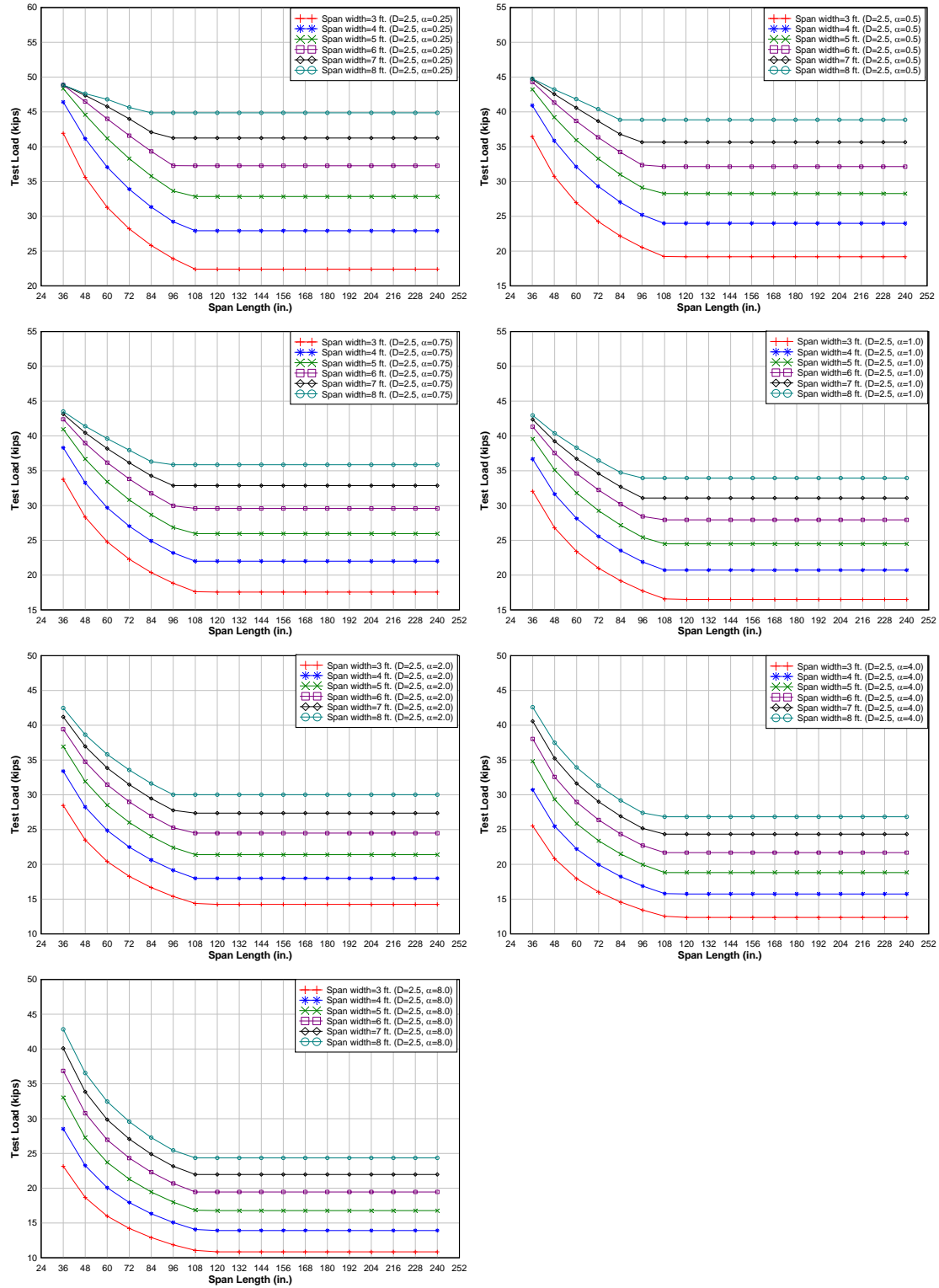


Figure 2F: Main bars transverse to traffic, D=2.5.

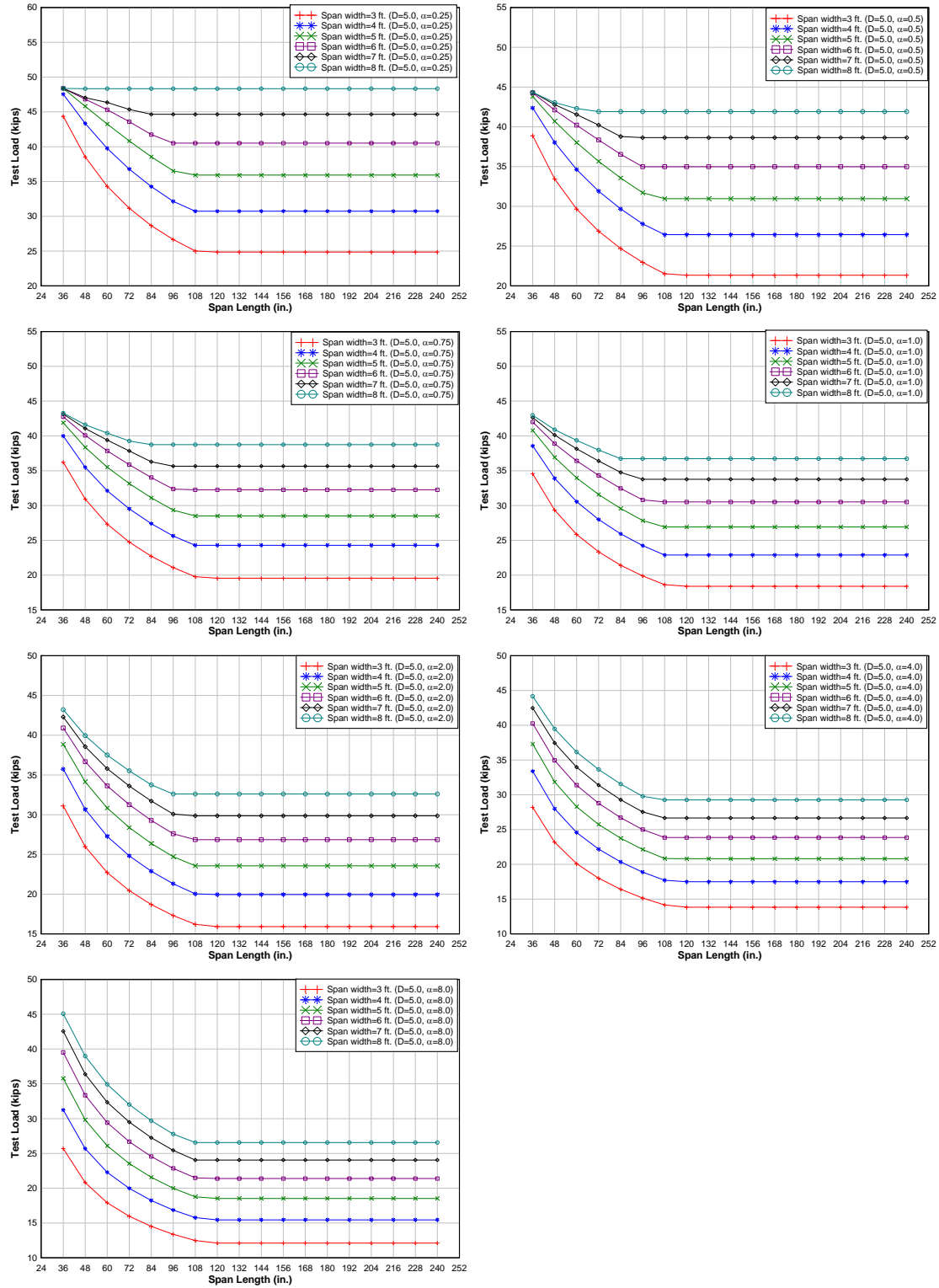


Figure 3F: Main bars transverse to traffic, $D=5.0$.

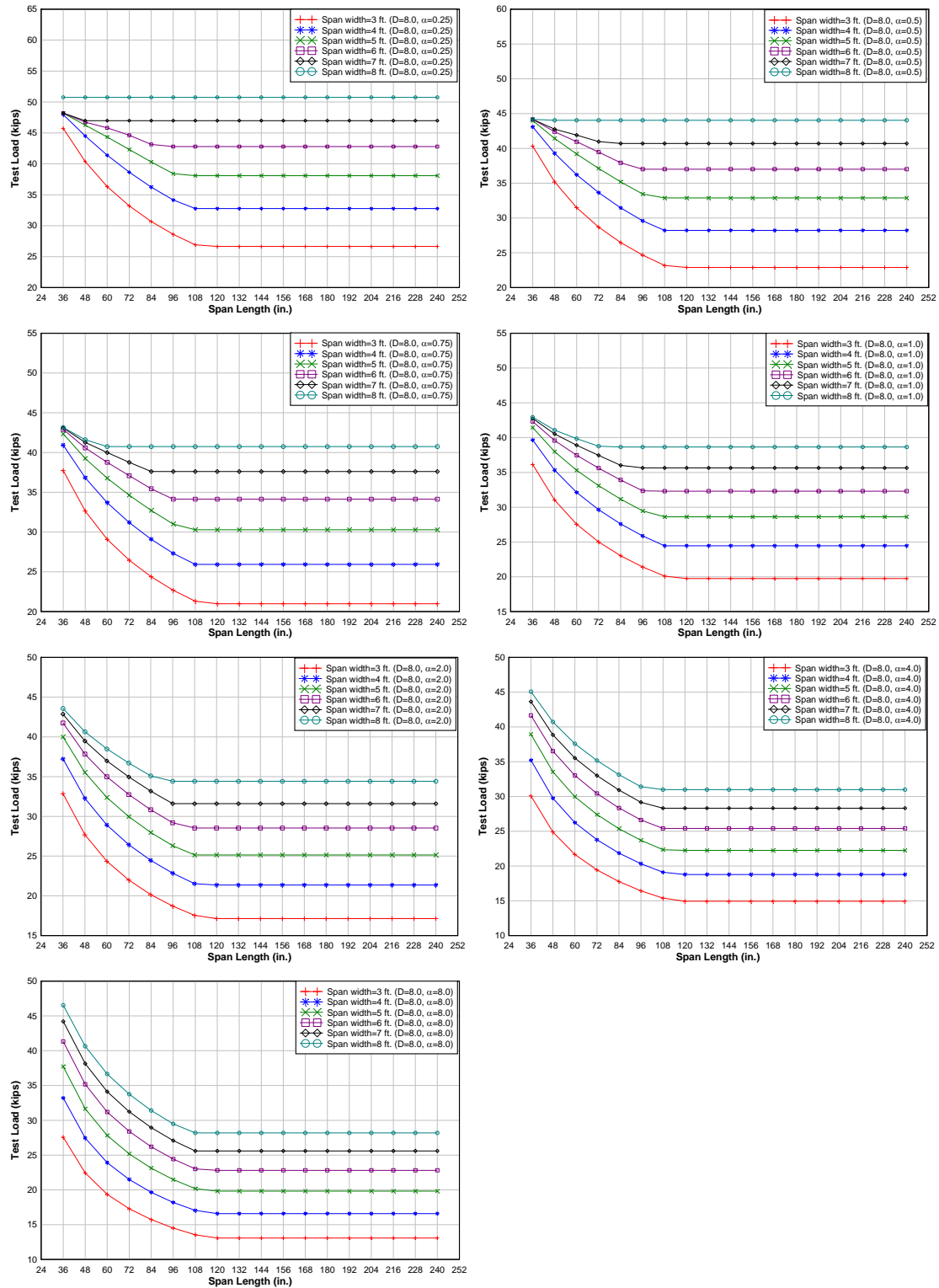


Figure 4F: Main bars transverse to traffic, $D=8.0$.

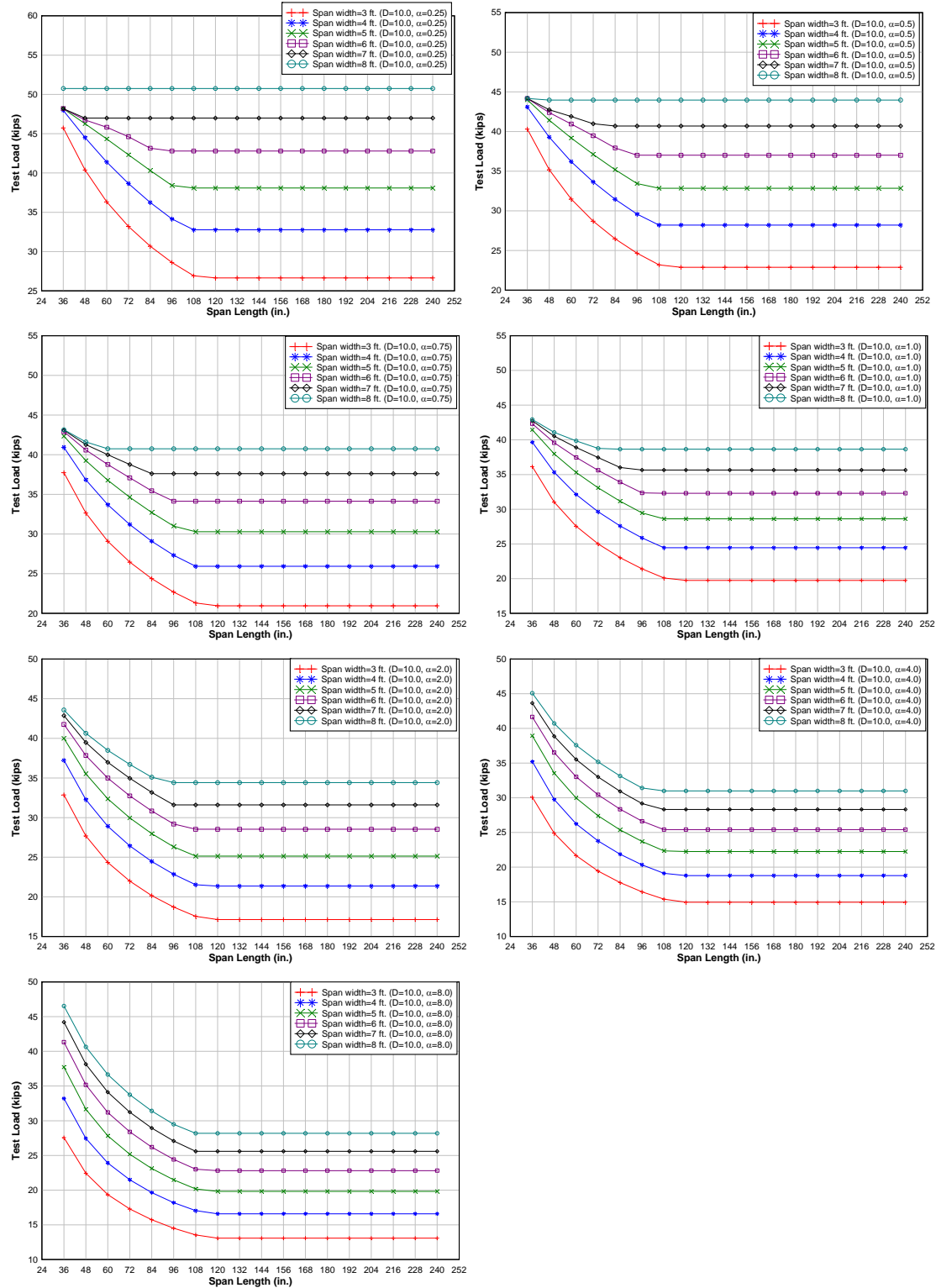


Figure 5F: Main bars transverse to traffic, $D=10.0$.

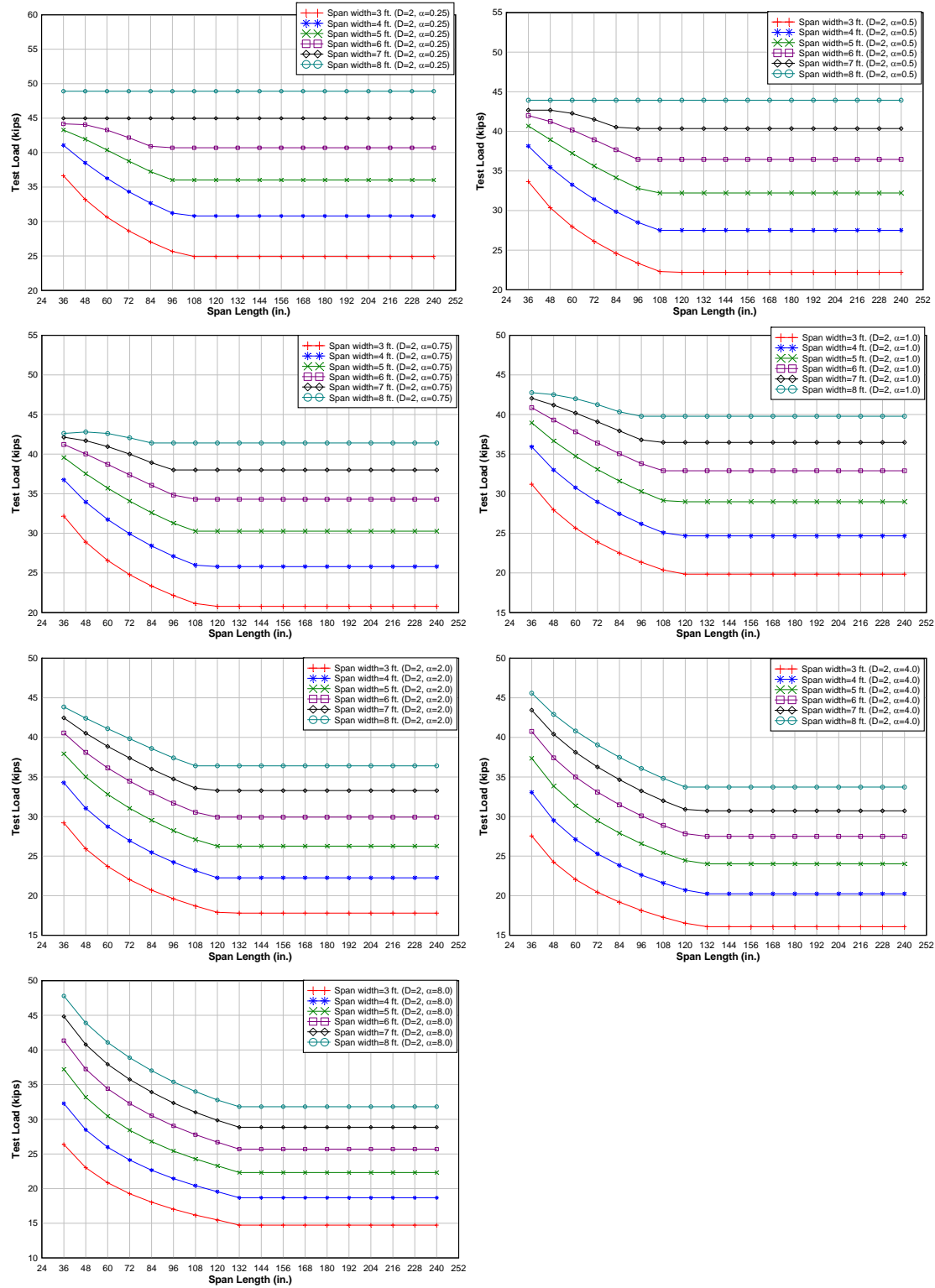


Figure 6F: Main bars parallel to traffic, D=2.0.

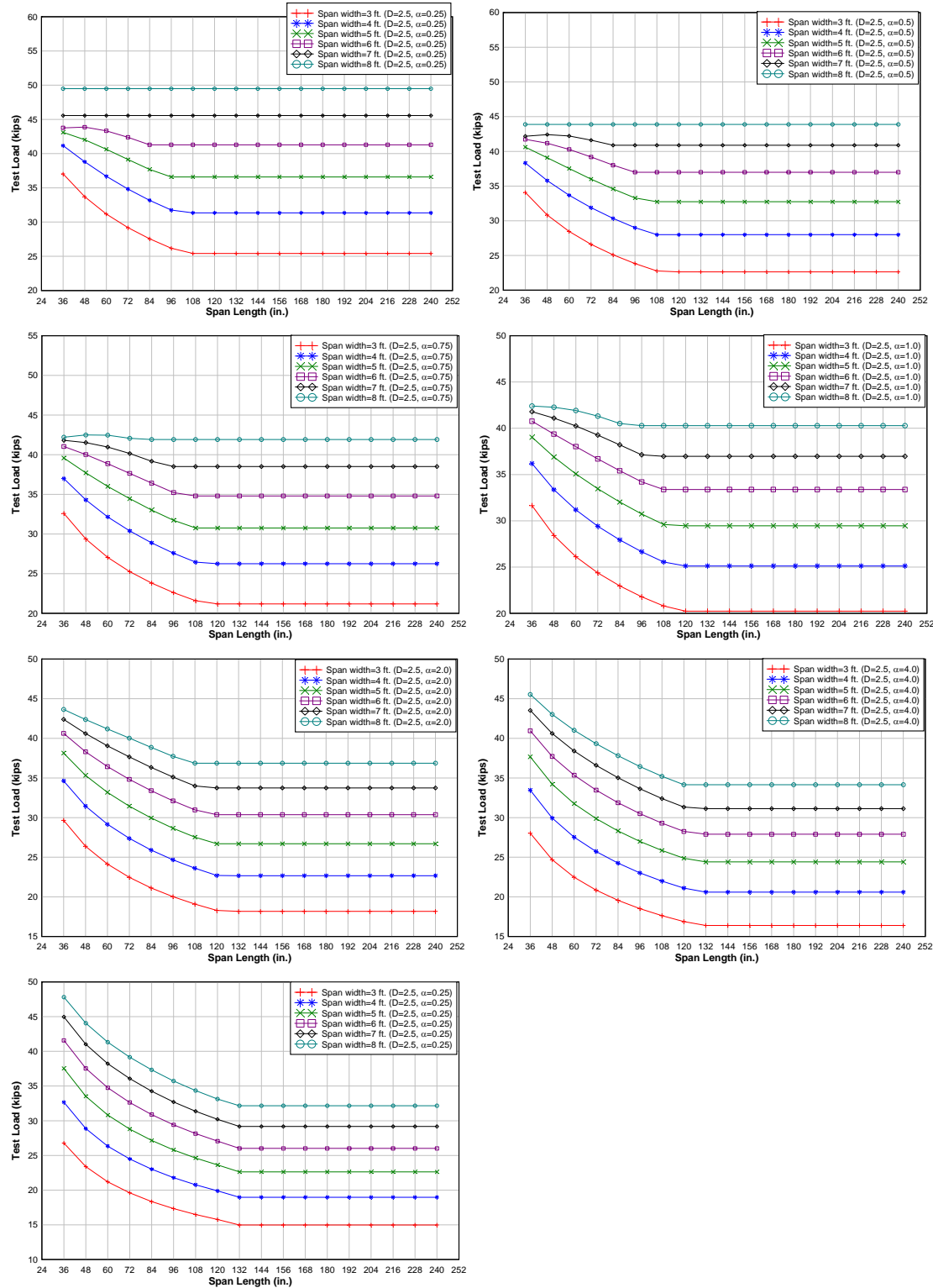


Figure 7F: Main bars parallel to traffic, $D=2.5$.

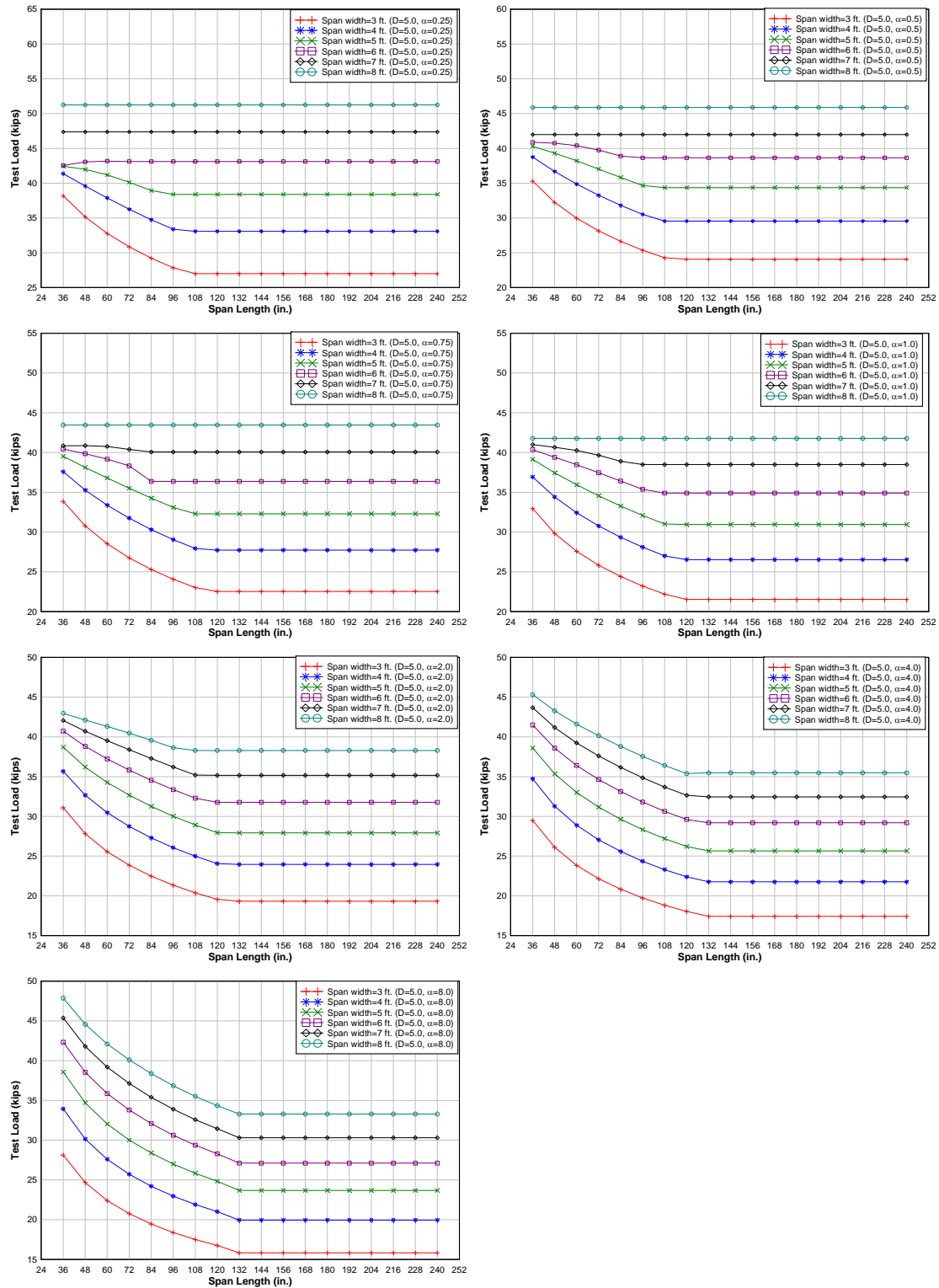


Figure 8F: Main bars parallel to traffic, D=5.0.

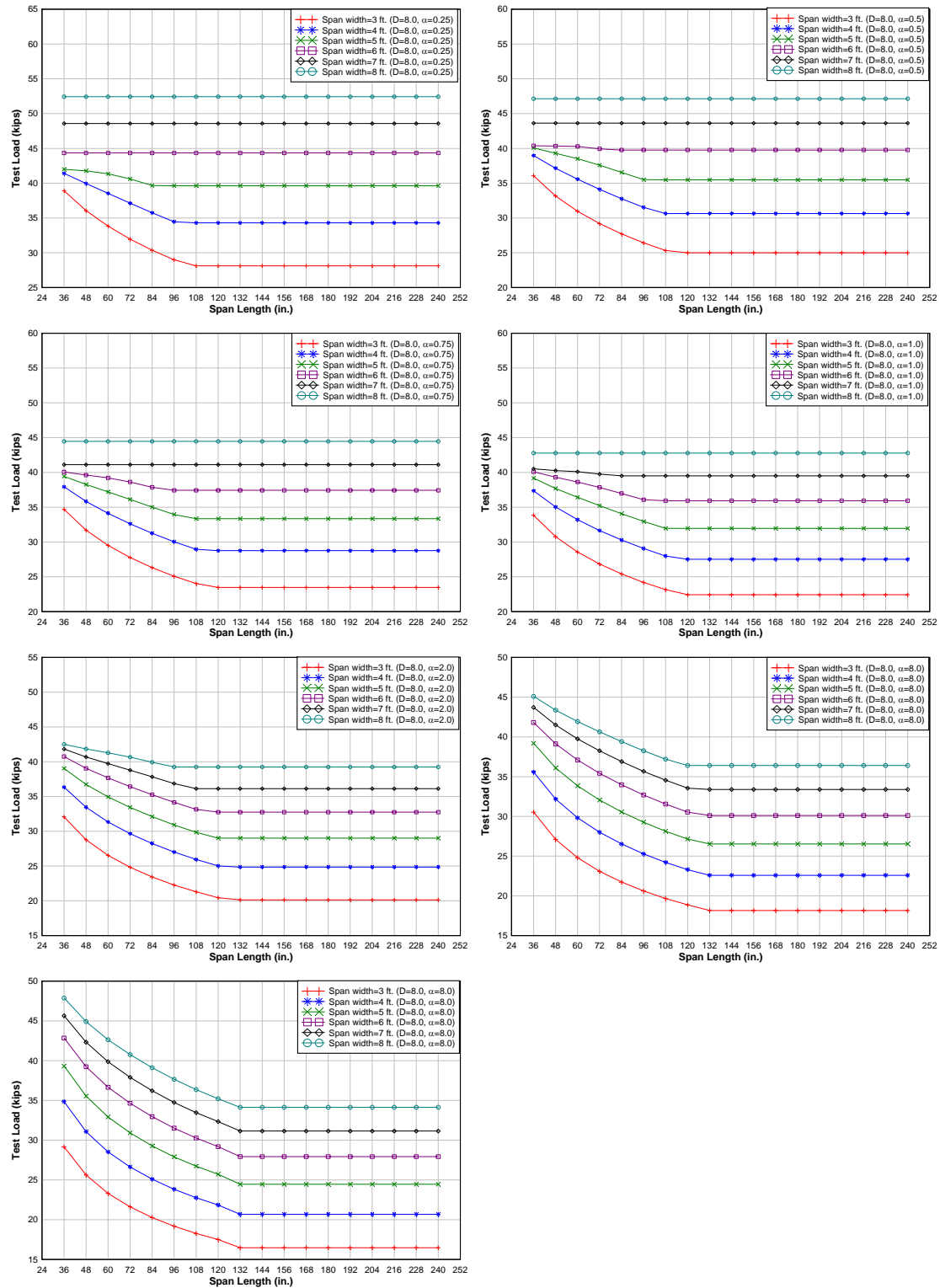


Figure 9F: Main bars parallel to traffic, $D=8.0$.

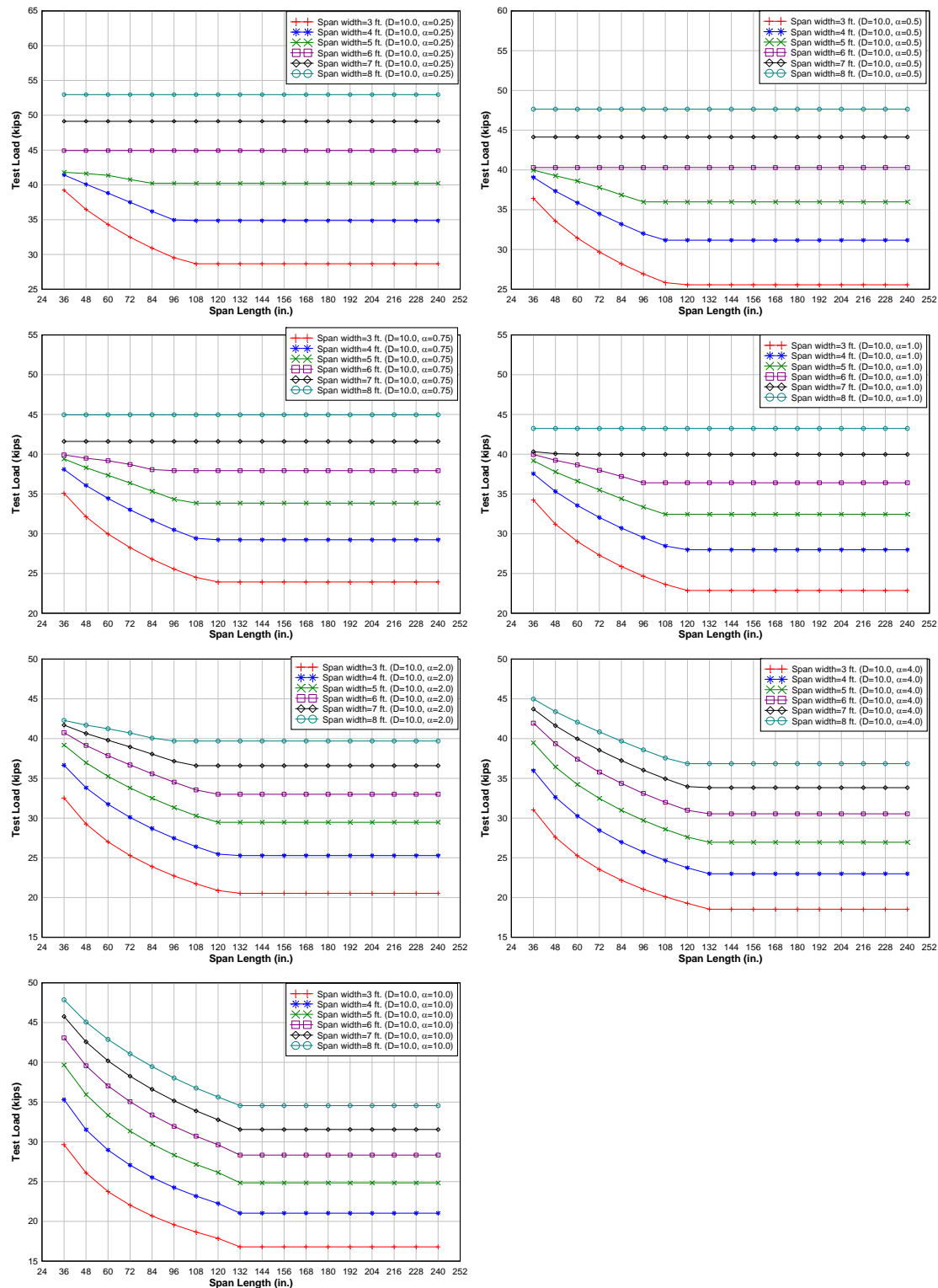


Figure 10F: Main bars parallel to traffic, $D=10.0$.

Tables

Table 1F-1. Main bars transverse to traffic, D=2.

D	α	L (in)	P (3ft)	P (4ft)	P (5ft)	P (6ft)	P (7ft)	P (8ft)
2	0.25	36	41.0	45.9	48.2	49.0	49.0	49.0
		48	34.6	40.3	44.0	46.2	47.4	47.8
		60	30.3	36.1	40.4	43.4	45.4	46.7
		72	27.3	32.9	37.4	40.8	43.4	45.3
		84	24.9	30.4	34.9	38.5	41.3	43.8
		96	23.1	28.3	32.7	36.4	40.2	43.8
		108	21.6	27.1	31.9	36.2	40.2	43.8
		120	21.6	27.1	31.9	36.2	40.2	43.8
		132	21.6	27.1	31.9	36.2	40.2	43.8
		144	21.6	27.1	31.9	36.2	40.2	43.8
		156	21.6	27.1	31.9	36.2	40.2	43.8
		168	21.6	27.1	31.9	36.2	40.2	43.8
		180	21.6	27.1	31.9	36.2	40.2	43.8
		192	21.6	27.1	31.9	36.2	40.2	43.8
		204	21.6	27.1	31.9	36.2	40.2	43.8
		216	21.6	27.1	31.9	36.2	40.2	43.8
		228	21.6	27.1	31.9	36.2	40.2	43.8
		240	21.6	27.1	31.9	36.2	40.2	43.8
	0.50	36	35.6	40.3	42.9	44.2	44.8	44.9
		48	29.9	35.1	38.6	41.0	42.4	43.2
		60	26.1	31.3	35.2	38.1	40.2	41.6
		72	23.4	28.5	32.5	35.6	38.1	39.9
		84	21.4	26.2	30.2	33.5	36.1	38.2
		96	19.8	24.4	28.3	31.6	34.7	37.9
		108	18.5	23.2	27.4	31.2	34.7	37.9
		120	18.5	23.2	27.4	31.2	34.7	37.9
		132	18.5	23.2	27.4	31.2	34.7	37.9
		144	18.5	23.2	27.4	31.2	34.7	37.9
		156	18.5	23.2	27.4	31.2	34.7	37.9
		168	18.5	23.2	27.4	31.2	34.7	37.9
		180	18.5	23.2	27.4	31.2	34.7	37.9
		192	18.5	23.2	27.4	31.2	34.7	37.9
		204	18.5	23.2	27.4	31.2	34.7	37.9
		216	18.5	23.2	27.4	31.2	34.7	37.9
		228	18.5	23.2	27.4	31.2	34.7	37.9
		240	18.5	23.2	27.4	31.2	34.7	37.9

Table 1F-2. Main bars transverse to traffic, D=2.

D	α	L (in)	P (3ft)	P (4ft)	P (5ft)	P (6ft)	P (7ft)	P (8ft)
2	0.75	36	32.9	37.7	40.5	42.2	43.1	43.6
		48	27.5	32.5	36.1	38.5	40.2	41.2
		60	24.0	28.9	32.7	35.5	37.7	39.3
		72	21.5	26.2	30.0	33.1	35.5	37.4
		84	19.6	24.1	27.9	31.0	33.6	35.7
		96	18.2	22.4	26.1	29.2	32.0	35.0
		108	17.0	21.3	25.2	28.7	32.0	35.0
		120	17.0	21.3	25.2	28.7	32.0	35.0
		132	17.0	21.3	25.2	28.7	32.0	35.0
		144	17.0	21.3	25.2	28.7	32.0	35.0
		156	17.0	21.3	25.2	28.7	32.0	35.0
		168	17.0	21.3	25.2	28.7	32.0	35.0
		180	17.0	21.3	25.2	28.7	32.0	35.0
		192	17.0	21.3	25.2	28.7	32.0	35.0
		204	17.0	21.3	25.2	28.7	32.0	35.0
		216	17.0	21.3	25.2	28.7	32.0	35.0
		228	17.0	21.3	25.2	28.7	32.0	35.0
		240	17.0	21.3	25.2	28.7	32.0	35.0
	1.00	36	31.2	36.0	39.1	41.0	42.2	42.9
		48	26.0	30.9	34.4	37.0	38.9	40.1
		60	22.6	27.3	31.1	34.0	36.2	37.9
		72	20.3	24.8	28.5	31.5	33.9	35.9
		84	18.5	22.8	26.4	29.4	32.0	34.1
		96	17.1	21.2	24.7	27.7	30.2	33.0
		108	16.0	20.0	23.7	27.1	30.2	33.0
		120	15.9	20.0	23.7	27.1	30.2	33.0
		132	15.9	20.0	23.7	27.1	30.2	33.0
		144	15.9	20.0	23.7	27.1	30.2	33.0
		156	15.9	20.0	23.7	27.1	30.2	33.0
		168	15.9	20.0	23.7	27.1	30.2	33.0
		180	15.9	20.0	23.7	27.1	30.2	33.0
		192	15.9	20.0	23.7	27.1	30.2	33.0
		204	15.9	20.0	23.7	27.1	30.2	33.0
		216	15.9	20.0	23.7	27.1	30.2	33.0
		228	15.9	20.0	23.7	27.1	30.2	33.0
		240	15.9	20.0	23.7	27.1	30.2	33.0

Table 1F-3. Main bars transverse to traffic, D=2.

D	α	L (in)	P (3ft)	P (4ft)	P (5ft)	P (6ft)	P (7ft)	P (8ft)
2	2.00	36	27.6	32.6	36.2	38.9	40.8	42.2
		48	22.7	27.5	31.2	34.1	36.4	38.2
		60	19.7	24.1	27.7	30.7	33.2	35.2
		72	17.6	21.8	25.3	28.2	30.8	32.9
		84	16.0	19.9	23.3	26.2	28.7	30.9
		96	14.8	18.5	21.7	24.5	27.0	29.2
		108	13.8	17.4	20.7	23.8	26.6	29.2
		120	13.7	17.4	20.7	23.8	26.6	29.2
		132	13.7	17.4	20.7	23.8	26.6	29.2
		144	13.7	17.4	20.7	23.8	26.6	29.2
		156	13.7	17.4	20.7	23.8	26.6	29.2
		168	13.7	17.4	20.7	23.8	26.6	29.2
		180	13.7	17.4	20.7	23.8	26.6	29.2
		192	13.7	17.4	20.7	23.8	26.6	29.2
		204	13.7	17.4	20.7	23.8	26.6	29.2
		216	13.7	17.4	20.7	23.8	26.6	29.2
		228	13.7	17.4	20.7	23.8	26.6	29.2
		240	13.7	17.4	20.7	23.8	26.6	29.2
	4.00	36	24.7	29.9	34.0	37.3	39.9	42.0
		48	20.1	24.7	28.6	31.8	34.5	36.8
		60	17.3	21.5	25.1	28.2	30.9	33.2
		72	15.4	19.3	22.7	25.6	28.3	30.6
		84	14.0	17.6	20.8	23.6	26.2	28.4
		96	12.9	16.3	19.3	22.0	24.4	26.7
		108	12.0	15.2	18.2	21.0	23.6	26.1
		120	11.9	15.2	18.2	21.0	23.6	26.1
		132	11.9	15.2	18.2	21.0	23.6	26.1
		144	11.9	15.2	18.2	21.0	23.6	26.1
		156	11.9	15.2	18.2	21.0	23.6	26.1
		168	11.9	15.2	18.2	21.0	23.6	26.1
		180	11.9	15.2	18.2	21.0	23.6	26.1
		192	11.9	15.2	18.2	21.0	23.6	26.1
		204	11.9	15.2	18.2	21.0	23.6	26.1
		216	11.9	15.2	18.2	21.0	23.6	26.1
		228	11.9	15.2	18.2	21.0	23.6	26.1
		240	11.9	15.2	18.2	21.0	23.6	26.1

Table 1F-4. Main bars transverse to traffic, D=2.

D	α	L (in)	P (3ft)	P (4ft)	P (5ft)	P (6ft)	P (7ft)	P (8ft)
2	8.00	36	22.4	27.7	32.2	36.0	39.3	42.1
		48	18.0	22.5	26.5	30.0	33.1	35.8
		60	15.4	19.4	23.0	26.2	29.1	31.7
		72	13.7	17.3	20.6	23.6	26.3	28.8
		84	12.4	15.8	18.8	21.6	24.2	26.5
		96	11.4	14.5	17.4	20.0	22.5	24.7
		108	10.6	13.6	16.3	18.9	21.4	23.7
		120	10.5	13.5	16.3	18.9	21.4	23.7
		132	10.5	13.5	16.3	18.9	21.4	23.7
		144	10.5	13.5	16.3	18.9	21.4	23.7
		156	10.5	13.5	16.3	18.9	21.4	23.7
		168	10.5	13.5	16.3	18.9	21.4	23.7
		180	10.5	13.5	16.3	18.9	21.4	23.7
		192	10.5	13.5	16.3	18.9	21.4	23.7
		204	10.5	13.5	16.3	18.9	21.4	23.7
		216	10.5	13.5	16.3	18.9	21.4	23.7
		228	10.5	13.5	16.3	18.9	21.4	23.7
		240	10.5	13.5	16.3	18.9	21.4	23.7

Table 2F-1. Main bars transverse to traffic, D=2.5.

D	α	L (in)	P (3ft)	P (4ft)	P (5ft)	P (6ft)	P (7ft)	P (8ft)
2.5	0.25	36	41.9	46.4	48.3	48.9	48.9	48.9
		48	35.6	41.1	44.6	46.5	47.4	47.6
		60	31.3	37.1	41.2	44.0	45.8	46.8
		72	28.2	33.9	38.3	41.6	44.0	45.7
		84	25.8	31.3	35.8	39.3	42.1	44.9
		96	23.9	29.2	33.6	37.3	41.3	44.9
		108	22.4	27.9	32.8	37.3	41.3	44.9
		120	22.4	27.9	32.8	37.3	41.3	44.9
		132	22.4	27.9	32.8	37.3	41.3	44.9
		144	22.4	27.9	32.8	37.3	41.3	44.9
		156	22.4	27.9	32.8	37.3	41.3	44.9
		168	22.4	27.9	32.8	37.3	41.3	44.9
		180	22.4	27.9	32.8	37.3	41.3	44.9
		192	22.4	27.9	32.8	37.3	41.3	44.9
		204	22.4	27.9	32.8	37.3	41.3	44.9
		216	22.4	27.9	32.8	37.3	41.3	44.9
		228	22.4	27.9	32.8	37.3	41.3	44.9
		240	22.4	27.9	32.8	37.3	41.3	44.9
	0.50	36	36.5	40.9	43.2	44.3	44.7	44.8
		48	30.8	35.9	39.2	41.3	42.6	43.2
		60	27.0	32.1	36.0	38.7	40.6	41.8
		72	24.3	29.3	33.3	36.4	38.7	40.4
		84	22.2	27.1	31.0	34.2	36.8	38.9
		96	20.5	25.2	29.1	32.4	35.6	38.9
		108	19.2	24.0	28.3	32.1	35.6	38.9
		120	19.2	24.0	28.3	32.1	35.6	38.9
		132	19.2	24.0	28.3	32.1	35.6	38.9
		144	19.2	24.0	28.3	32.1	35.6	38.9
		156	19.2	24.0	28.3	32.1	35.6	38.9
		168	19.2	24.0	28.3	32.1	35.6	38.9
		180	19.2	24.0	28.3	32.1	35.6	38.9
		192	19.2	24.0	28.3	32.1	35.6	38.9
		204	19.2	24.0	28.3	32.1	35.6	38.9
		216	19.2	24.0	28.3	32.1	35.6	38.9
		228	19.2	24.0	28.3	32.1	35.6	38.9
		240	19.2	24.0	28.3	32.1	35.6	38.9

Table 2F-2. Main bars transverse to traffic, D=2.5.

D	α	L (in)	P (3ft)	P (4ft)	P (5ft)	P (6ft)	P (7ft)	P (8ft)
2.5	0.75	36	33.8	38.3	40.9	42.4	43.1	43.5
		48	28.3	33.3	36.7	39.0	40.5	41.4
		60	24.8	29.7	33.4	36.2	38.2	39.6
		72	22.3	27.0	30.8	33.8	36.2	38.0
		84	20.4	24.9	28.7	31.8	34.3	36.3
		96	18.8	23.2	26.9	30.0	32.9	35.9
		108	17.6	22.0	26.0	29.6	32.9	35.9
		120	17.6	22.0	26.0	29.6	32.9	35.9
		132	17.6	22.0	26.0	29.6	32.9	35.9
		144	17.6	22.0	26.0	29.6	32.9	35.9
		156	17.6	22.0	26.0	29.6	32.9	35.9
		168	17.6	22.0	26.0	29.6	32.9	35.9
		180	17.6	22.0	26.0	29.6	32.9	35.9
		192	17.6	22.0	26.0	29.6	32.9	35.9
		204	17.6	22.0	26.0	29.6	32.9	35.9
		216	17.6	22.0	26.0	29.6	32.9	35.9
		228	17.6	22.0	26.0	29.6	32.9	35.9
		240	17.6	22.0	26.0	29.6	32.9	35.9
	1.00	36	32.0	36.7	39.6	41.3	42.4	43.0
		48	26.8	31.6	35.1	37.5	39.2	40.4
		60	23.4	28.1	31.8	34.6	36.7	38.3
		72	21.0	25.6	29.3	32.2	34.6	36.5
		84	19.2	23.5	27.2	30.2	32.7	34.7
		96	17.7	21.9	25.4	28.4	31.1	34.0
		108	16.6	20.7	24.5	27.9	31.1	34.0
		120	16.5	20.7	24.5	27.9	31.1	34.0
		132	16.5	20.7	24.5	27.9	31.1	34.0
		144	16.5	20.7	24.5	27.9	31.1	34.0
		156	16.5	20.7	24.5	27.9	31.1	34.0
		168	16.5	20.7	24.5	27.9	31.1	34.0
		180	16.5	20.7	24.5	27.9	31.1	34.0
		192	16.5	20.7	24.5	27.9	31.1	34.0
		204	16.5	20.7	24.5	27.9	31.1	34.0
		216	16.5	20.7	24.5	27.9	31.1	34.0
		228	16.5	20.7	24.5	27.9	31.1	34.0
		240	16.5	20.7	24.5	27.9	31.1	34.0

Table 2F-3. Main bars transverse to traffic, D=2.5.

D	α	L (in)	P (3ft)	P (4ft)	P (5ft)	P (6ft)	P (7ft)	P (8ft)
2.5	2.00	36	28.5	33.4	36.9	39.4	41.2	42.5
		48	23.5	28.2	31.9	34.8	37.0	38.7
		60	20.4	24.9	28.5	31.5	33.9	35.8
		72	18.3	22.5	26.0	29.0	31.5	33.6
		84	16.7	20.6	24.0	27.0	29.5	31.6
		96	15.4	19.1	22.4	25.3	27.8	30.0
		108	14.4	18.0	21.4	24.5	27.4	30.0
		120	14.3	18.0	21.4	24.5	27.4	30.0
		132	14.3	18.0	21.4	24.5	27.4	30.0
		144	14.3	18.0	21.4	24.5	27.4	30.0
		156	14.3	18.0	21.4	24.5	27.4	30.0
		168	14.3	18.0	21.4	24.5	27.4	30.0
		180	14.3	18.0	21.4	24.5	27.4	30.0
		192	14.3	18.0	21.4	24.5	27.4	30.0
		204	14.3	18.0	21.4	24.5	27.4	30.0
		216	14.3	18.0	21.4	24.5	27.4	30.0
		228	14.3	18.0	21.4	24.5	27.4	30.0
		240	14.3	18.0	21.4	24.5	27.4	30.0
	4.00	36	25.5	30.7	34.8	38.0	40.6	42.6
		48	20.8	25.5	29.3	32.6	35.2	37.5
		60	18.0	22.2	25.8	29.0	31.6	33.9
		72	16.0	20.0	23.4	26.4	29.0	31.3
		84	14.6	18.2	21.5	24.4	26.9	29.2
		96	13.4	16.9	20.0	22.7	25.2	27.4
		108	12.5	15.8	18.8	21.7	24.3	26.8
		120	12.4	15.7	18.8	21.7	24.3	26.8
		132	12.4	15.7	18.8	21.7	24.3	26.8
		144	12.4	15.7	18.8	21.7	24.3	26.8
		156	12.4	15.7	18.8	21.7	24.3	26.8
		168	12.4	15.7	18.8	21.7	24.3	26.8
		180	12.4	15.7	18.8	21.7	24.3	26.8
		192	12.4	15.7	18.8	21.7	24.3	26.8
		204	12.4	15.7	18.8	21.7	24.3	26.8
		216	12.4	15.7	18.8	21.7	24.3	26.8
		228	12.4	15.7	18.8	21.7	24.3	26.8
		240	12.4	15.7	18.8	21.7	24.3	26.8

Table 2F-4. Main bars transverse to traffic, D=2.5.

D	α	L (in)	P (3ft)	P (4ft)	P (5ft)	P (6ft)	P (7ft)	P (8ft)
2.5	8.00	36	23.2	28.5	33.0	36.9	40.1	42.8
		48	18.7	23.3	27.3	30.8	33.9	36.6
		60	16.0	20.1	23.7	27.0	29.9	32.4
		72	14.2	17.9	21.3	24.3	27.1	29.6
		84	12.9	16.3	19.5	22.3	24.9	27.3
		96	11.9	15.1	18.0	20.7	23.2	25.4
		108	11.1	14.1	16.8	19.5	22.0	24.3
		120	10.9	13.9	16.8	19.5	22.0	24.3
		132	10.9	13.9	16.8	19.5	22.0	24.3
		144	10.9	13.9	16.8	19.5	22.0	24.3
		156	10.9	13.9	16.8	19.5	22.0	24.3
		168	10.9	13.9	16.8	19.5	22.0	24.3
		180	10.9	13.9	16.8	19.5	22.0	24.3
		192	10.9	13.9	16.8	19.5	22.0	24.3
		204	10.9	13.9	16.8	19.5	22.0	24.3
		216	10.9	13.9	16.8	19.5	22.0	24.3
		228	10.9	13.9	16.8	19.5	22.0	24.3
		240	10.9	13.9	16.8	19.5	22.0	24.3

Table 3F-1. Main bars transverse to traffic, D=5.0.

D	α	L (in)	P (3ft)	P (4ft)	P (5ft)	P (6ft)	P (7ft)	P (8ft)
5	0.25	36	44.4	47.5	48.4	48.4	48.4	48.4
		48	38.5	43.3	45.8	46.8	47.0	48.3
		60	34.3	39.8	43.3	45.3	46.4	48.3
		72	31.2	36.8	40.8	43.6	45.4	48.3
		84	28.7	34.3	38.6	41.8	44.6	48.3
		96	26.7	32.1	36.5	40.5	44.6	48.3
		108	25.0	30.7	35.9	40.5	44.6	48.3
		120	24.9	30.7	35.9	40.5	44.6	48.3
		132	24.9	30.7	35.9	40.5	44.6	48.3
		144	24.9	30.7	35.9	40.5	44.6	48.3
		156	24.9	30.7	35.9	40.5	44.6	48.3
		168	24.9	30.7	35.9	40.5	44.6	48.3
		180	24.9	30.7	35.9	40.5	44.6	48.3
		192	24.9	30.7	35.9	40.5	44.6	48.3
		204	24.9	30.7	35.9	40.5	44.6	48.3
		216	24.9	30.7	35.9	40.5	44.6	48.3
		228	24.9	30.7	35.9	40.5	44.6	48.3
		240	24.9	30.7	35.9	40.5	44.6	48.3
	0.50	36	38.9	42.4	43.8	44.3	44.3	44.3
		48	33.4	38.0	40.7	42.1	42.8	43.0
		60	29.7	34.6	38.0	40.2	41.5	42.3
		72	26.9	31.9	35.7	38.4	40.2	41.9
		84	24.7	29.7	33.6	36.5	38.8	41.9
		96	22.9	27.8	31.7	35.0	38.6	41.9
		108	21.5	26.4	31.0	35.0	38.6	41.9
		120	21.3	26.4	31.0	35.0	38.6	41.9
		132	21.3	26.4	31.0	35.0	38.6	41.9
		144	21.3	26.4	31.0	35.0	38.6	41.9
		156	21.3	26.4	31.0	35.0	38.6	41.9
		168	21.3	26.4	31.0	35.0	38.6	41.9
		180	21.3	26.4	31.0	35.0	38.6	41.9
		192	21.3	26.4	31.0	35.0	38.6	41.9
		204	21.3	26.4	31.0	35.0	38.6	41.9
		216	21.3	26.4	31.0	35.0	38.6	41.9
		228	21.3	26.4	31.0	35.0	38.6	41.9
		240	21.3	26.4	31.0	35.0	38.6	41.9

Table 3F-2. Main bars transverse to traffic, D=5.0.

D	α	L (in)	P (3ft)	P (4ft)	P (5ft)	P (6ft)	P (7ft)	P (8ft)
5	0.75	36	36.2	40.0	41.9	42.8	43.1	43.3
		48	30.9	35.5	38.4	40.1	41.1	41.6
		60	27.3	32.1	35.5	37.9	39.4	40.4
		72	24.7	29.5	33.2	35.9	37.8	39.3
		84	22.7	27.4	31.1	34.0	36.3	38.7
		96	21.1	25.6	29.3	32.4	35.7	38.7
		108	19.8	24.3	28.5	32.3	35.7	38.7
		120	19.5	24.3	28.5	32.3	35.7	38.7
		132	19.5	24.3	28.5	32.3	35.7	38.7
		144	19.5	24.3	28.5	32.3	35.7	38.7
		156	19.5	24.3	28.5	32.3	35.7	38.7
		168	19.5	24.3	28.5	32.3	35.7	38.7
		180	19.5	24.3	28.5	32.3	35.7	38.7
		192	19.5	24.3	28.5	32.3	35.7	38.7
		204	19.5	24.3	28.5	32.3	35.7	38.7
		216	19.5	24.3	28.5	32.3	35.7	38.7
		228	19.5	24.3	28.5	32.3	35.7	38.7
		240	19.5	24.3	28.5	32.3	35.7	38.7
	1.00	36	34.5	38.6	40.8	42.0	42.6	43.0
		48	29.3	33.9	36.9	38.9	40.1	40.9
		60	25.9	30.5	34.0	36.4	38.2	39.4
		72	23.4	28.0	31.6	34.3	36.4	38.0
		84	21.4	25.9	29.6	32.5	34.8	36.7
		96	19.9	24.2	27.8	30.8	33.8	36.7
		108	18.6	22.9	26.9	30.5	33.8	36.7
		120	18.4	22.9	26.9	30.5	33.8	36.7
		132	18.4	22.9	26.9	30.5	33.8	36.7
		144	18.4	22.9	26.9	30.5	33.8	36.7
		156	18.4	22.9	26.9	30.5	33.8	36.7
		168	18.4	22.9	26.9	30.5	33.8	36.7
		180	18.4	22.9	26.9	30.5	33.8	36.7
		192	18.4	22.9	26.9	30.5	33.8	36.7
		204	18.4	22.9	26.9	30.5	33.8	36.7
		216	18.4	22.9	26.9	30.5	33.8	36.7
		228	18.4	22.9	26.9	30.5	33.8	36.7
		240	18.4	22.9	26.9	30.5	33.8	36.7

Table 3F-3. Main bars transverse to traffic, D=5.0.

D	α	L (in)	P (3ft)	P (4ft)	P (5ft)	P (6ft)	P (7ft)	P (8ft)
5	2.00	36	31.1	35.7	38.8	40.9	42.3	43.2
		48	26.0	30.7	34.1	36.7	38.6	39.9
		60	22.7	27.3	30.8	33.6	35.8	37.5
		72	20.4	24.8	28.4	31.3	33.6	35.5
		84	18.7	22.9	26.4	29.3	31.7	33.8
		96	17.3	21.3	24.7	27.6	30.1	32.6
		108	16.2	20.0	23.6	26.9	29.9	32.6
		120	15.9	20.0	23.6	26.9	29.9	32.6
		132	15.9	20.0	23.6	26.9	29.9	32.6
		144	15.9	20.0	23.6	26.9	29.9	32.6
		156	15.9	20.0	23.6	26.9	29.9	32.6
		168	15.9	20.0	23.6	26.9	29.9	32.6
		180	15.9	20.0	23.6	26.9	29.9	32.6
		192	15.9	20.0	23.6	26.9	29.9	32.6
		204	15.9	20.0	23.6	26.9	29.9	32.6
		216	15.9	20.0	23.6	26.9	29.9	32.6
		228	15.9	20.0	23.6	26.9	29.9	32.6
		240	15.9	20.0	23.6	26.9	29.9	32.6
	4.00	36	28.2	33.4	37.3	40.3	42.5	44.2
		48	23.2	28.0	31.8	34.9	37.5	39.5
		60	20.1	24.6	28.3	31.4	34.0	36.1
		72	18.0	22.2	25.7	28.8	31.4	33.6
		84	16.4	20.4	23.8	26.7	29.3	31.6
		96	15.2	18.9	22.1	25.0	27.5	29.8
		108	14.2	17.7	20.8	23.9	26.7	29.3
		120	13.8	17.5	20.8	23.9	26.7	29.3
		132	13.8	17.5	20.8	23.9	26.7	29.3
		144	13.8	17.5	20.8	23.9	26.7	29.3
		156	13.8	17.5	20.8	23.9	26.7	29.3
		168	13.8	17.5	20.8	23.9	26.7	29.3
		180	13.8	17.5	20.8	23.9	26.7	29.3
		192	13.8	17.5	20.8	23.9	26.7	29.3
		204	13.8	17.5	20.8	23.9	26.7	29.3
		216	13.8	17.5	20.8	23.9	26.7	29.3
		228	13.8	17.5	20.8	23.9	26.7	29.3
		240	13.8	17.5	20.8	23.9	26.7	29.3

Table 3F-4. Main bars transverse to traffic, D=5.0.

D	α	L (in)	P (3ft)	P (4ft)	P (5ft)	P (6ft)	P (7ft)	P (8ft)
5	8.00	36	25.7	31.2	35.8	39.5	42.6	45.1
		48	20.8	25.7	29.8	33.4	36.4	39.0
		60	17.9	22.3	26.1	29.4	32.4	34.9
		72	16.0	20.0	23.5	26.7	29.5	32.0
		84	14.5	18.2	21.6	24.6	27.3	29.7
		96	13.4	16.9	20.0	22.8	25.4	27.8
		108	12.5	15.8	18.8	21.5	24.1	26.6
		120	12.1	15.5	18.5	21.4	24.1	26.6
		132	12.1	15.5	18.5	21.4	24.1	26.6
		144	12.1	15.5	18.5	21.4	24.1	26.6
		156	12.1	15.5	18.5	21.4	24.1	26.6
		168	12.1	15.5	18.5	21.4	24.1	26.6
		180	12.1	15.5	18.5	21.4	24.1	26.6
		192	12.1	15.5	18.5	21.4	24.1	26.6
		204	12.1	15.5	18.5	21.4	24.1	26.6
		216	12.1	15.5	18.5	21.4	24.1	26.6
		228	12.1	15.5	18.5	21.4	24.1	26.6
		240	12.1	15.5	18.5	21.4	24.1	26.6

Table 4F-1. Main bars transverse to traffic, D=8.0.

D	α	L (in)	P (3ft)	P (4ft)	P (5ft)	P (6ft)	P (7ft)	P (8ft)
8	0.25	36	45.7	48.0	48.2	48.2	48.2	50.8
		48	40.4	44.5	46.3	46.7	47.0	50.8
		60	36.3	41.4	44.3	45.8	47.0	50.8
		72	33.2	38.7	42.3	44.6	47.0	50.8
		84	30.7	36.2	40.3	43.2	47.0	50.8
		96	28.6	34.2	38.4	42.8	47.0	50.8
		108	26.9	32.8	38.1	42.8	47.0	50.8
		120	26.6	32.8	38.1	42.8	47.0	50.8
		132	26.6	32.8	38.1	42.8	47.0	50.8
		144	26.6	32.8	38.1	42.8	47.0	50.8
		156	26.6	32.8	38.1	42.8	47.0	50.8
		168	26.6	32.8	38.1	42.8	47.0	50.8
		180	26.6	32.8	38.1	42.8	47.0	50.8
		192	26.6	32.8	38.1	42.8	47.0	50.8
		204	26.6	32.8	38.1	42.8	47.0	50.8
		216	26.6	32.8	38.1	42.8	47.0	50.8
		228	26.6	32.8	38.1	42.8	47.0	50.8
		240	26.6	32.8	38.1	42.8	47.0	50.8
	0.50	36	40.3	43.1	44.0	44.2	44.2	44.2
		48	35.2	39.3	41.4	42.4	42.8	44.0
		60	31.5	36.2	39.2	41.0	41.9	44.0
		72	28.7	33.6	37.1	39.5	41.0	44.0
		84	26.5	31.5	35.2	37.9	40.7	44.0
		96	24.7	29.6	33.4	37.0	40.7	44.0
		108	23.2	28.2	32.9	37.0	40.7	44.0
		120	22.9	28.2	32.9	37.0	40.7	44.0
		132	22.9	28.2	32.9	37.0	40.7	44.0
		144	22.9	28.2	32.9	37.0	40.7	44.0
		156	22.9	28.2	32.9	37.0	40.7	44.0
		168	22.9	28.2	32.9	37.0	40.7	44.0
		180	22.9	28.2	32.9	37.0	40.7	44.0
		192	22.9	28.2	32.9	37.0	40.7	44.0
		204	22.9	28.2	32.9	37.0	40.7	44.0
		216	22.9	28.2	32.9	37.0	40.7	44.0
		228	22.9	28.2	32.9	37.0	40.7	44.0
		240	22.9	28.2	32.9	37.0	40.7	44.0

Table 4F-2. Main bars transverse to traffic, D=8.0.

D	α	L (in)	P (3ft)	P (4ft)	P (5ft)	P (6ft)	P (7ft)	P (8ft)
8	0.75	36	37.7	40.9	42.3	42.9	43.1	43.1
		48	32.6	36.8	39.3	40.6	41.3	41.6
		60	29.1	33.7	36.8	38.8	40.0	40.7
		72	26.5	31.2	34.6	37.1	38.8	40.7
		84	24.4	29.1	32.7	35.4	37.6	40.7
		96	22.7	27.3	31.0	34.1	37.6	40.7
		108	21.3	25.9	30.3	34.1	37.6	40.7
		120	21.0	25.9	30.3	34.1	37.6	40.7
		132	21.0	25.9	30.3	34.1	37.6	40.7
		144	21.0	25.9	30.3	34.1	37.6	40.7
		156	21.0	25.9	30.3	34.1	37.6	40.7
		168	21.0	25.9	30.3	34.1	37.6	40.7
		180	21.0	25.9	30.3	34.1	37.6	40.7
		192	21.0	25.9	30.3	34.1	37.6	40.7
		204	21.0	25.9	30.3	34.1	37.6	40.7
		216	21.0	25.9	30.3	34.1	37.6	40.7
		228	21.0	25.9	30.3	34.1	37.6	40.7
		240	21.0	25.9	30.3	34.1	37.6	40.7
	1.00	36	36.1	39.7	41.4	42.3	42.7	42.9
		48	31.0	35.3	38.0	39.6	40.5	41.1
		60	27.6	32.1	35.3	37.5	38.9	39.9
		72	25.0	29.6	33.1	35.6	37.5	38.8
		84	23.0	27.6	31.2	33.9	36.0	38.7
		96	21.4	25.9	29.5	32.4	35.6	38.7
		108	20.1	24.5	28.6	32.3	35.6	38.7
		120	19.8	24.5	28.6	32.3	35.6	38.7
		132	19.8	24.5	28.6	32.3	35.6	38.7
		144	19.8	24.5	28.6	32.3	35.6	38.7
		156	19.8	24.5	28.6	32.3	35.6	38.7
		168	19.8	24.5	28.6	32.3	35.6	38.7
		180	19.8	24.5	28.6	32.3	35.6	38.7
		192	19.8	24.5	28.6	32.3	35.6	38.7
		204	19.8	24.5	28.6	32.3	35.6	38.7
		216	19.8	24.5	28.6	32.3	35.6	38.7
		228	19.8	24.5	28.6	32.3	35.6	38.7
		240	19.8	24.5	28.6	32.3	35.6	38.7

Table 4F-3. Main bars transverse to traffic, D=8.0.

D	α	L (in)	P (3ft)	P (4ft)	P (5ft)	P (6ft)	P (7ft)	P (8ft)
8	2.00	36	32.9	37.2	40.0	41.8	42.9	43.6
		48	27.7	32.3	35.5	37.8	39.5	40.6
		60	24.3	28.9	32.4	35.0	37.0	38.5
		72	22.0	26.4	30.0	32.7	35.0	36.7
		84	20.2	24.5	28.0	30.8	33.2	35.1
		96	18.7	22.9	26.3	29.2	31.6	34.4
		108	17.5	21.5	25.1	28.5	31.6	34.4
		120	17.1	21.4	25.1	28.5	31.6	34.4
		132	17.1	21.4	25.1	28.5	31.6	34.4
		144	17.1	21.4	25.1	28.5	31.6	34.4
		156	17.1	21.4	25.1	28.5	31.6	34.4
		168	17.1	21.4	25.1	28.5	31.6	34.4
		180	17.1	21.4	25.1	28.5	31.6	34.4
		192	17.1	21.4	25.1	28.5	31.6	34.4
		204	17.1	21.4	25.1	28.5	31.6	34.4
		216	17.1	21.4	25.1	28.5	31.6	34.4
		228	17.1	21.4	25.1	28.5	31.6	34.4
		240	17.1	21.4	25.1	28.5	31.6	34.4
	4.00	36	30.1	35.2	38.9	41.7	43.6	45.1
		48	24.9	29.7	33.5	36.5	38.9	40.7
		60	21.7	26.2	30.0	33.0	35.5	37.6
		72	19.4	23.8	27.4	30.4	33.0	35.2
		84	17.8	21.9	25.4	28.4	30.9	33.1
		96	16.4	20.3	23.7	26.6	29.2	31.4
		108	15.4	19.1	22.4	25.4	28.3	31.0
		120	14.9	18.8	22.2	25.4	28.3	31.0
		132	14.9	18.8	22.2	25.4	28.3	31.0
		144	14.9	18.8	22.2	25.4	28.3	31.0
		156	14.9	18.8	22.2	25.4	28.3	31.0
		168	14.9	18.8	22.2	25.4	28.3	31.0
		180	14.9	18.8	22.2	25.4	28.3	31.0
		192	14.9	18.8	22.2	25.4	28.3	31.0
		204	14.9	18.8	22.2	25.4	28.3	31.0
		216	14.9	18.8	22.2	25.4	28.3	31.0
		228	14.9	18.8	22.2	25.4	28.3	31.0
		240	14.9	18.8	22.2	25.4	28.3	31.0

Table 4F-4. Main bars transverse to traffic, D=8.0.

D	α	L (in)	P (3ft)	P (4ft)	P (5ft)	P (6ft)	P (7ft)	P (8ft)
8	8.00	36	27.6	33.2	37.7	41.3	44.2	46.5
		48	22.4	27.5	31.7	35.2	38.1	40.6
		60	19.4	23.9	27.8	31.2	34.1	36.7
		72	17.3	21.5	25.2	28.4	31.2	33.8
		84	15.7	19.7	23.1	26.2	29.0	31.4
		96	14.5	18.2	21.5	24.4	27.1	29.5
		108	13.6	17.0	20.2	23.0	25.6	28.2
		120	13.1	16.6	19.8	22.8	25.6	28.2
		132	13.1	16.6	19.8	22.8	25.6	28.2
		144	13.1	16.6	19.8	22.8	25.6	28.2
		156	13.1	16.6	19.8	22.8	25.6	28.2
		168	13.1	16.6	19.8	22.8	25.6	28.2
		180	13.1	16.6	19.8	22.8	25.6	28.2
		192	13.1	16.6	19.8	22.8	25.6	28.2
		204	13.1	16.6	19.8	22.8	25.6	28.2
		216	13.1	16.6	19.8	22.8	25.6	28.2
		228	13.1	16.6	19.8	22.8	25.6	28.2
		240	13.1	16.6	19.8	22.8	25.6	28.2

Table 5F-1. Main bars transverse to traffic, D=10.0.

D	α	L (in)	P (3ft)	P (4ft)	P (5ft)	P (6ft)	P (7ft)	P (8ft)
10	0.25	36	45.7	48.0	48.2	48.2	48.2	50.8
		48	40.4	44.5	46.3	46.7	47.0	50.8
		60	36.3	41.4	44.3	45.8	47.0	50.8
		72	33.2	38.7	42.3	44.6	47.0	50.8
		84	30.7	36.2	40.3	43.2	47.0	50.8
		96	28.6	34.2	38.4	42.8	47.0	50.8
		108	26.9	32.8	38.1	42.8	47.0	50.8
		120	26.6	32.8	38.1	42.8	47.0	50.8
		132	26.6	32.8	38.1	42.8	47.0	50.8
		144	26.6	32.8	38.1	42.8	47.0	50.8
		156	26.6	32.8	38.1	42.8	47.0	50.8
		168	26.6	32.8	38.1	42.8	47.0	50.8
		180	26.6	32.8	38.1	42.8	47.0	50.8
		192	26.6	32.8	38.1	42.8	47.0	50.8
		204	26.6	32.8	38.1	42.8	47.0	50.8
		216	26.6	32.8	38.1	42.8	47.0	50.8
		228	26.6	32.8	38.1	42.8	47.0	50.8
		240	26.6	32.8	38.1	42.8	47.0	50.8
	0.50	36	40.3	43.1	44.0	44.2	44.2	44.2
		48	35.2	39.3	41.4	42.4	42.8	44.0
		60	31.5	36.2	39.2	41.0	41.9	44.0
		72	28.7	33.6	37.1	39.5	41.0	44.0
		84	26.5	31.5	35.2	37.9	40.7	44.0
		96	24.7	29.6	33.4	37.0	40.7	44.0
		108	23.2	28.2	32.8	37.0	40.7	44.0
		120	22.9	28.2	32.8	37.0	40.7	44.0
		132	22.9	28.2	32.8	37.0	40.7	44.0
		144	22.9	28.2	32.8	37.0	40.7	44.0
		156	22.9	28.2	32.8	37.0	40.7	44.0
		168	22.9	28.2	32.8	37.0	40.7	44.0
		180	22.9	28.2	32.8	37.0	40.7	44.0
		192	22.9	28.2	32.8	37.0	40.7	44.0
		204	22.9	28.2	32.8	37.0	40.7	44.0
		216	22.9	28.2	32.8	37.0	40.7	44.0
		228	22.9	28.2	32.8	37.0	40.7	44.0
		240	22.9	28.2	32.8	37.0	40.7	44.0

Table 5F-2. Main bars transverse to traffic, D=10.0.

D	α	L (in)	P (3ft)	P (4ft)	P (5ft)	P (6ft)	P (7ft)	P (8ft)
10	0.75	36	37.7	40.9	42.3	42.9	43.1	43.1
		48	32.6	36.8	39.3	40.6	41.3	41.6
		60	29.1	33.7	36.8	38.8	40.0	40.7
		72	26.5	31.2	34.6	37.1	38.8	40.7
		84	24.4	29.1	32.7	35.4	37.6	40.7
		96	22.7	27.3	31.0	34.1	37.6	40.7
		108	21.3	25.9	30.3	34.1	37.6	40.7
		120	21.0	25.9	30.3	34.1	37.6	40.7
		132	21.0	25.9	30.3	34.1	37.6	40.7
		144	21.0	25.9	30.3	34.1	37.6	40.7
		156	21.0	25.9	30.3	34.1	37.6	40.7
		168	21.0	25.9	30.3	34.1	37.6	40.7
		180	21.0	25.9	30.3	34.1	37.6	40.7
		192	21.0	25.9	30.3	34.1	37.6	40.7
		204	21.0	25.9	30.3	34.1	37.6	40.7
		216	21.0	25.9	30.3	34.1	37.6	40.7
		228	21.0	25.9	30.3	34.1	37.6	40.7
		240	21.0	25.9	30.3	34.1	37.6	40.7
	1.00	36	36.1	39.7	41.4	42.3	42.7	42.9
		48	31.0	35.3	38.0	39.6	40.5	41.1
		60	27.6	32.1	35.3	37.5	38.9	39.9
		72	25.0	29.6	33.1	35.6	37.5	38.8
		84	23.0	27.6	31.2	33.9	36.0	38.7
		96	21.4	25.9	29.5	32.4	35.6	38.7
		108	20.1	24.5	28.6	32.3	35.6	38.7
		120	19.8	24.5	28.6	32.3	35.6	38.7
		132	19.8	24.5	28.6	32.3	35.6	38.7
		144	19.8	24.5	28.6	32.3	35.6	38.7
		156	19.8	24.5	28.6	32.3	35.6	38.7
		168	19.8	24.5	28.6	32.3	35.6	38.7
		180	19.8	24.5	28.6	32.3	35.6	38.7
		192	19.8	24.5	28.6	32.3	35.6	38.7
		204	19.8	24.5	28.6	32.3	35.6	38.7
		216	19.8	24.5	28.6	32.3	35.6	38.7
		228	19.8	24.5	28.6	32.3	35.6	38.7
		240	19.8	24.5	28.6	32.3	35.6	38.7

Table 5F-3. Main bars transverse to traffic, D=10.0.

D	α	L (in)	P (3ft)	P (4ft)	P (5ft)	P (6ft)	P (7ft)	P (8ft)
10	2.00	36	32.9	37.2	40.0	41.8	42.9	43.6
		48	27.7	32.3	35.5	37.8	39.5	40.6
		60	24.3	28.9	32.4	35.0	37.0	38.5
		72	22.0	26.4	30.0	32.7	35.0	36.7
		84	20.2	24.5	28.0	30.8	33.2	35.1
		96	18.7	22.9	26.3	29.2	31.6	34.4
		108	17.5	21.5	25.1	28.5	31.6	34.4
		120	17.1	21.4	25.1	28.5	31.6	34.4
		132	17.1	21.4	25.1	28.5	31.6	34.4
		144	17.1	21.4	25.1	28.5	31.6	34.4
		156	17.1	21.4	25.1	28.5	31.6	34.4
		168	17.1	21.4	25.1	28.5	31.6	34.4
		180	17.1	21.4	25.1	28.5	31.6	34.4
		192	17.1	21.4	25.1	28.5	31.6	34.4
		204	17.1	21.4	25.1	28.5	31.6	34.4
		216	17.1	21.4	25.1	28.5	31.6	34.4
		228	17.1	21.4	25.1	28.5	31.6	34.4
		240	17.1	21.4	25.1	28.5	31.6	34.4
	4.00	36	30.1	35.2	38.9	41.7	43.6	45.1
		48	24.9	29.7	33.5	36.5	38.9	40.7
		60	21.7	26.2	30.0	33.0	35.5	37.6
		72	19.4	23.8	27.4	30.4	33.0	35.2
		84	17.8	21.9	25.4	28.4	30.9	33.1
		96	16.4	20.3	23.7	26.6	29.2	31.4
		108	15.4	19.1	22.4	25.4	28.3	31.0
		120	14.9	18.8	22.2	25.4	28.3	31.0
		132	14.9	18.8	22.2	25.4	28.3	31.0
		144	14.9	18.8	22.2	25.4	28.3	31.0
		156	14.9	18.8	22.2	25.4	28.3	31.0
		168	14.9	18.8	22.2	25.4	28.3	31.0
		180	14.9	18.8	22.2	25.4	28.3	31.0
		192	14.9	18.8	22.2	25.4	28.3	31.0
		204	14.9	18.8	22.2	25.4	28.3	31.0
		216	14.9	18.8	22.2	25.4	28.3	31.0
		228	14.9	18.8	22.2	25.4	28.3	31.0
		240	14.9	18.8	22.2	25.4	28.3	31.0

Table 5F-4. Main bars transverse to traffic, D=10.0.

D	α	L (in)	P (3ft)	P (4ft)	P (5ft)	P (6ft)	P (7ft)	P (8ft)
10	8.00	36	27.6	33.2	37.7	41.3	44.2	46.5
		48	22.4	27.5	31.7	35.2	38.1	40.6
		60	19.4	23.9	27.8	31.2	34.1	36.7
		72	17.3	21.5	25.2	28.4	31.2	33.8
		84	15.7	19.7	23.1	26.2	29.0	31.4
		96	14.5	18.2	21.5	24.4	27.1	29.5
		108	13.6	17.0	20.2	23.0	25.6	28.2
		120	13.1	16.6	19.8	22.8	25.6	28.2
		132	13.1	16.6	19.8	22.8	25.6	28.2
		144	13.1	16.6	19.8	22.8	25.6	28.2
		156	13.1	16.6	19.8	22.8	25.6	28.2
		168	13.1	16.6	19.8	22.8	25.6	28.2
		180	13.1	16.6	19.8	22.8	25.6	28.2
		192	13.1	16.6	19.8	22.8	25.6	28.2
		204	13.1	16.6	19.8	22.8	25.6	28.2
		216	13.1	16.6	19.8	22.8	25.6	28.2
		228	13.1	16.6	19.8	22.8	25.6	28.2
		240	13.1	16.6	19.8	22.8	25.6	28.2

Table 6F-1. Main bars parallel to traffic, D=2.0.

D	α	L (in)	P (3ft)	P (4ft)	P (5ft)	P (6ft)	P (7ft)	P (8ft)
2	0.25	36	36.6	41.1	43.3	44.2	45.0	48.9
		48	33.2	38.5	42.0	44.1	45.0	48.9
		60	30.6	36.3	40.4	43.3	45.0	48.9
		72	28.6	34.3	38.8	42.2	45.0	48.9
		84	27.0	32.7	37.2	40.9	45.0	48.9
		96	25.7	31.2	36.0	40.7	45.0	48.9
		108	24.9	30.8	36.0	40.7	45.0	48.9
		120	24.9	30.8	36.0	40.7	45.0	48.9
		132	24.9	30.8	36.0	40.7	45.0	48.9
		144	24.9	30.8	36.0	40.7	45.0	48.9
		156	24.9	30.8	36.0	40.7	45.0	48.9
		168	24.9	30.8	36.0	40.7	45.0	48.9
		180	24.9	30.8	36.0	40.7	45.0	48.9
		192	24.9	30.8	36.0	40.7	45.0	48.9
		204	24.9	30.8	36.0	40.7	45.0	48.9
		216	24.9	30.8	36.0	40.7	45.0	48.9
		228	24.9	30.8	36.0	40.7	45.0	48.9
		240	24.9	30.8	36.0	40.7	45.0	48.9
	0.50	36	33.7	38.1	40.7	42.0	42.7	43.9
		48	30.4	35.5	39.0	41.2	42.7	43.9
		60	28.0	33.3	37.2	40.2	42.3	43.9
		72	26.1	31.4	35.6	38.9	41.5	43.9
		84	24.6	29.9	34.2	37.7	40.5	43.9
		96	23.4	28.5	32.8	36.5	40.4	43.9
		108	22.3	27.5	32.2	36.5	40.4	43.9
		120	22.2	27.5	32.2	36.5	40.4	43.9
		132	22.2	27.5	32.2	36.5	40.4	43.9
		144	22.2	27.5	32.2	36.5	40.4	43.9
		156	22.2	27.5	32.2	36.5	40.4	43.9
		168	22.2	27.5	32.2	36.5	40.4	43.9
		180	22.2	27.5	32.2	36.5	40.4	43.9
		192	22.2	27.5	32.2	36.5	40.4	43.9
		204	22.2	27.5	32.2	36.5	40.4	43.9
		216	22.2	27.5	32.2	36.5	40.4	43.9
		228	22.2	27.5	32.2	36.5	40.4	43.9
		240	22.2	27.5	32.2	36.5	40.4	43.9

Table 6F-2. Main bars parallel to traffic, D=2.0.

D	α	L (in)	P (3ft)	P (4ft)	P (5ft)	P (6ft)	P (7ft)	P (8ft)
2	0.75	36	32.2	36.8	39.6	41.2	42.1	42.6
		48	28.9	34.0	37.5	40.0	41.7	42.8
		60	26.6	31.7	35.7	38.7	41.0	42.6
		72	24.8	29.9	34.1	37.4	40.0	42.1
		84	23.3	28.4	32.6	36.1	38.9	41.4
		96	22.1	27.1	31.3	34.8	38.0	41.4
		108	21.1	26.0	30.3	34.3	38.0	41.4
		120	20.8	25.8	30.3	34.3	38.0	41.4
		132	20.8	25.8	30.3	34.3	38.0	41.4
		144	20.8	25.8	30.3	34.3	38.0	41.4
		156	20.8	25.8	30.3	34.3	38.0	41.4
		168	20.8	25.8	30.3	34.3	38.0	41.4
		180	20.8	25.8	30.3	34.3	38.0	41.4
		192	20.8	25.8	30.3	34.3	38.0	41.4
		204	20.8	25.8	30.3	34.3	38.0	41.4
		216	20.8	25.8	30.3	34.3	38.0	41.4
		228	20.8	25.8	30.3	34.3	38.0	41.4
		240	20.8	25.8	30.3	34.3	38.0	41.4
	1.00	36	31.2	35.9	39.0	40.9	42.0	42.8
		48	28.0	33.0	36.7	39.3	41.2	42.5
		60	25.7	30.8	34.7	37.8	40.2	42.0
		72	23.9	29.0	33.1	36.4	39.1	41.2
		84	22.5	27.5	31.6	35.1	37.9	40.3
		96	21.3	26.2	30.3	33.8	36.8	39.8
		108	20.4	25.1	29.1	32.9	36.5	39.8
		120	19.8	24.7	29.0	32.9	36.5	39.8
		132	19.8	24.7	29.0	32.9	36.5	39.8
		144	19.8	24.7	29.0	32.9	36.5	39.8
		156	19.8	24.7	29.0	32.9	36.5	39.8
		168	19.8	24.7	29.0	32.9	36.5	39.8
		180	19.8	24.7	29.0	32.9	36.5	39.8
		192	19.8	24.7	29.0	32.9	36.5	39.8
		204	19.8	24.7	29.0	32.9	36.5	39.8
		216	19.8	24.7	29.0	32.9	36.5	39.8
		228	19.8	24.7	29.0	32.9	36.5	39.8
		240	19.8	24.7	29.0	32.9	36.5	39.8

Table 6F-3. Main bars parallel to traffic, D=2.0.

D	α	L (in)	P (3ft)	P (4ft)	P (5ft)	P (6ft)	P (7ft)	P (8ft)
2	2.00	36	29.2	34.3	37.9	40.6	42.5	43.8
		48	25.9	31.0	35.0	38.1	40.5	42.4
		60	23.7	28.7	32.8	36.1	38.9	41.1
		72	22.0	26.9	31.0	34.5	37.4	39.8
		84	20.7	25.5	29.5	33.0	36.0	38.6
		96	19.6	24.2	28.2	31.7	34.7	37.4
		108	18.7	23.2	27.1	30.5	33.6	36.4
		120	17.9	22.3	26.3	29.9	33.3	36.4
		132	17.8	22.3	26.3	29.9	33.3	36.4
		144	17.8	22.3	26.3	29.9	33.3	36.4
		156	17.8	22.3	26.3	29.9	33.3	36.4
		168	17.8	22.3	26.3	29.9	33.3	36.4
		180	17.8	22.3	26.3	29.9	33.3	36.4
		192	17.8	22.3	26.3	29.9	33.3	36.4
		204	17.8	22.3	26.3	29.9	33.3	36.4
		216	17.8	22.3	26.3	29.9	33.3	36.4
		228	17.8	22.3	26.3	29.9	33.3	36.4
		240	17.8	22.3	26.3	29.9	33.3	36.4
	4.00	36	27.6	33.1	37.4	40.7	43.4	45.6
		48	24.2	29.5	33.8	37.4	40.4	42.9
		60	22.1	27.1	31.4	35.0	38.1	40.8
		72	20.5	25.3	29.5	33.1	36.3	39.0
		84	19.2	23.8	27.9	31.5	34.7	37.5
		96	18.1	22.6	26.6	30.1	33.2	36.1
		108	17.3	21.6	25.4	28.9	32.0	34.8
		120	16.5	20.7	24.5	27.8	30.9	33.7
		132	16.1	20.2	24.0	27.5	30.7	33.7
		144	16.1	20.2	24.0	27.5	30.7	33.7
		156	16.1	20.2	24.0	27.5	30.7	33.7
		168	16.1	20.2	24.0	27.5	30.7	33.7
		180	16.1	20.2	24.0	27.5	30.7	33.7
		192	16.1	20.2	24.0	27.5	30.7	33.7
		204	16.1	20.2	24.0	27.5	30.7	33.7
		216	16.1	20.2	24.0	27.5	30.7	33.7
		228	16.1	20.2	24.0	27.5	30.7	33.7
		240	16.1	20.2	24.0	27.5	30.7	33.7

Table 6F-4. Main bars parallel to traffic, D=2.0.

D	α	L (in)	P (3ft)	P (4ft)	P (5ft)	P (6ft)	P (7ft)	P (8ft)
2	8.00	36	26.4	32.3	37.2	41.3	44.8	47.8
		48	23.0	28.5	33.2	37.2	40.8	43.9
		60	20.8	26.0	30.5	34.4	37.9	41.1
		72	19.3	24.1	28.4	32.3	35.7	38.9
		84	18.0	22.7	26.8	30.5	33.9	37.0
		96	17.0	21.4	25.4	29.0	32.4	35.4
		108	16.2	20.4	24.3	27.8	31.0	34.0
		120	15.5	19.6	23.3	26.7	29.8	32.8
		132	14.7	18.7	22.3	25.7	28.8	31.8
		144	14.7	18.7	22.3	25.7	28.8	31.8
		156	14.7	18.7	22.3	25.7	28.8	31.8
		168	14.7	18.7	22.3	25.7	28.8	31.8
		180	14.7	18.7	22.3	25.7	28.8	31.8
		192	14.7	18.7	22.3	25.7	28.8	31.8
		204	14.7	18.7	22.3	25.7	28.8	31.8
		216	14.7	18.7	22.3	25.7	28.8	31.8
		228	14.7	18.7	22.3	25.7	28.8	31.8
		240	14.7	18.7	22.3	25.7	28.8	31.8

Table 7F-1. Main bars parallel to traffic, D=2.5.

D	α	L (in)	P (3ft)	P (4ft)	P (5ft)	P (6ft)	P (7ft)	P (8ft)
2.5	0.25	36	37.0	41.2	43.1	43.8	45.6	49.5
		48	33.7	38.8	42.0	43.9	45.6	49.5
		60	31.2	36.7	40.6	43.3	45.6	49.5
		72	29.2	34.8	39.1	42.4	45.6	49.5
		84	27.5	33.2	37.7	41.3	45.6	49.5
		96	26.2	31.7	36.6	41.3	45.6	49.5
		108	25.4	31.3	36.6	41.3	45.6	49.5
		120	25.4	31.3	36.6	41.3	45.6	49.5
		132	25.4	31.3	36.6	41.3	45.6	49.5
		144	25.4	31.3	36.6	41.3	45.6	49.5
		156	25.4	31.3	36.6	41.3	45.6	49.5
		168	25.4	31.3	36.6	41.3	45.6	49.5
		180	25.4	31.3	36.6	41.3	45.6	49.5
		192	25.4	31.3	36.6	41.3	45.6	49.5
		204	25.4	31.3	36.6	41.3	45.6	49.5
		216	25.4	31.3	36.6	41.3	45.6	49.5
		228	25.4	31.3	36.6	41.3	45.6	49.5
		240	25.4	31.3	36.6	41.3	45.6	49.5
	0.50	36	34.1	38.3	40.6	41.7	42.2	43.9
		48	30.8	35.8	39.1	41.2	42.4	43.9
		60	28.5	33.7	37.5	40.3	42.2	43.9
		72	26.6	31.9	36.0	39.2	41.6	43.9
		84	25.1	30.3	34.6	38.0	40.9	43.9
		96	23.8	29.0	33.3	37.0	40.9	43.9
		108	22.8	28.0	32.7	37.0	40.9	43.9
		120	22.6	28.0	32.7	37.0	40.9	43.9
		132	22.6	28.0	32.7	37.0	40.9	43.9
		144	22.6	28.0	32.7	37.0	40.9	43.9
		156	22.6	28.0	32.7	37.0	40.9	43.9
		168	22.6	28.0	32.7	37.0	40.9	43.9
		180	22.6	28.0	32.7	37.0	40.9	43.9
		192	22.6	28.0	32.7	37.0	40.9	43.9
		204	22.6	28.0	32.7	37.0	40.9	43.9
		216	22.6	28.0	32.7	37.0	40.9	43.9
		228	22.6	28.0	32.7	37.0	40.9	43.9
		240	22.6	28.0	32.7	37.0	40.9	43.9

Table 7F-2. Main bars parallel to traffic, D=2.5.

D	α	L (in)	P (3ft)	P (4ft)	P (5ft)	P (6ft)	P (7ft)	P (8ft)
2.5	0.75	36	32.6	37.0	39.6	41.0	41.8	42.2
		48	29.4	34.3	37.7	40.0	41.5	42.5
		60	27.0	32.2	36.0	38.9	41.0	42.5
		72	25.3	30.4	34.4	37.6	40.1	42.1
		84	23.8	28.9	33.0	36.4	39.2	41.9
		96	22.6	27.6	31.7	35.2	38.5	41.9
		108	21.6	26.5	30.8	34.8	38.5	41.9
		120	21.2	26.3	30.8	34.8	38.5	41.9
		132	21.2	26.3	30.8	34.8	38.5	41.9
		144	21.2	26.3	30.8	34.8	38.5	41.9
		156	21.2	26.3	30.8	34.8	38.5	41.9
		168	21.2	26.3	30.8	34.8	38.5	41.9
		180	21.2	26.3	30.8	34.8	38.5	41.9
		192	21.2	26.3	30.8	34.8	38.5	41.9
		204	21.2	26.3	30.8	34.8	38.5	41.9
		216	21.2	26.3	30.8	34.8	38.5	41.9
		228	21.2	26.3	30.8	34.8	38.5	41.9
		240	21.2	26.3	30.8	34.8	38.5	41.9
	1.00	36	31.6	36.2	39.0	40.8	41.8	42.4
		48	28.4	33.4	36.9	39.4	41.1	42.3
		60	26.1	31.2	35.1	38.0	40.3	41.9
		72	24.4	29.4	33.5	36.7	39.3	41.3
		84	23.0	27.9	32.0	35.4	38.2	40.5
		96	21.8	26.7	30.7	34.2	37.1	40.3
		108	20.8	25.5	29.6	33.4	37.0	40.3
		120	20.2	25.1	29.5	33.4	37.0	40.3
		132	20.2	25.1	29.5	33.4	37.0	40.3
		144	20.2	25.1	29.5	33.4	37.0	40.3
		156	20.2	25.1	29.5	33.4	37.0	40.3
		168	20.2	25.1	29.5	33.4	37.0	40.3
		180	20.2	25.1	29.5	33.4	37.0	40.3
		192	20.2	25.1	29.5	33.4	37.0	40.3
		204	20.2	25.1	29.5	33.4	37.0	40.3
		216	20.2	25.1	29.5	33.4	37.0	40.3
		228	20.2	25.1	29.5	33.4	37.0	40.3
		240	20.2	25.1	29.5	33.4	37.0	40.3

Table 7F-3. Main bars parallel to traffic, D=2.5.

D	α	L (in)	P (3ft)	P (4ft)	P (5ft)	P (6ft)	P (7ft)	P (8ft)
2.5	2.00	36	29.7	34.6	38.1	40.6	42.4	43.6
		48	26.4	31.4	35.3	38.3	40.6	42.4
		60	24.1	29.2	33.2	36.4	39.1	41.2
		72	22.5	27.4	31.4	34.8	37.7	40.0
		84	21.1	25.9	30.0	33.4	36.3	38.9
		96	20.0	24.7	28.7	32.1	35.1	37.7
		108	19.1	23.6	27.5	31.0	34.0	36.9
		120	18.3	22.7	26.7	30.4	33.7	36.9
		132	18.2	22.7	26.7	30.4	33.7	36.9
		144	18.2	22.7	26.7	30.4	33.7	36.9
		156	18.2	22.7	26.7	30.4	33.7	36.9
		168	18.2	22.7	26.7	30.4	33.7	36.9
		180	18.2	22.7	26.7	30.4	33.7	36.9
		192	18.2	22.7	26.7	30.4	33.7	36.9
		204	18.2	22.7	26.7	30.4	33.7	36.9
		216	18.2	22.7	26.7	30.4	33.7	36.9
		228	18.2	22.7	26.7	30.4	33.7	36.9
		240	18.2	22.7	26.7	30.4	33.7	36.9
	4.00	36	28.0	33.5	37.7	40.9	43.5	45.5
		48	24.7	29.9	34.2	37.7	40.6	43.0
		60	22.5	27.5	31.8	35.3	38.4	41.0
		72	20.9	25.7	29.9	33.5	36.6	39.3
		84	19.6	24.3	28.3	31.9	35.0	37.8
		96	18.5	23.0	27.0	30.5	33.6	36.4
		108	17.6	22.0	25.9	29.3	32.4	35.2
		120	16.9	21.1	24.9	28.3	31.3	34.1
		132	16.4	20.6	24.4	27.9	31.1	34.1
		144	16.4	20.6	24.4	27.9	31.1	34.1
		156	16.4	20.6	24.4	27.9	31.1	34.1
		168	16.4	20.6	24.4	27.9	31.1	34.1
		180	16.4	20.6	24.4	27.9	31.1	34.1
		192	16.4	20.6	24.4	27.9	31.1	34.1
		204	16.4	20.6	24.4	27.9	31.1	34.1
		216	16.4	20.6	24.4	27.9	31.1	34.1
		228	16.4	20.6	24.4	27.9	31.1	34.1
		240	16.4	20.6	24.4	27.9	31.1	34.1

Table 7F-4. Main bars parallel to traffic, D=2.5.

D	α	L (in)	P (3ft)	P (4ft)	P (5ft)	P (6ft)	P (7ft)	P (8ft)
2.5	8.00	36	26.8	32.7	37.5	41.6	45.0	47.8
		48	23.4	28.9	33.5	37.5	41.0	44.1
		60	21.2	26.3	30.8	34.7	38.2	41.3
		72	19.6	24.5	28.8	32.6	36.1	39.2
		84	18.4	23.0	27.2	30.9	34.3	37.3
		96	17.3	21.8	25.8	29.4	32.7	35.7
		108	16.5	20.8	24.6	28.1	31.4	34.3
		120	15.8	19.9	23.6	27.1	30.2	33.1
		132	15.0	19.0	22.6	26.0	29.2	32.2
		144	15.0	19.0	22.6	26.0	29.2	32.2
		156	15.0	19.0	22.6	26.0	29.2	32.2
		168	15.0	19.0	22.6	26.0	29.2	32.2
		180	15.0	19.0	22.6	26.0	29.2	32.2
		192	15.0	19.0	22.6	26.0	29.2	32.2
		204	15.0	19.0	22.6	26.0	29.2	32.2
		216	15.0	19.0	22.6	26.0	29.2	32.2
		228	15.0	19.0	22.6	26.0	29.2	32.2
		240	15.0	19.0	22.6	26.0	29.2	32.2

Table 8F-1. Main bars parallel to traffic, D=5.0.

D	α	L (in)	P (3ft)	P (4ft)	P (5ft)	P (6ft)	P (7ft)	P (8ft)
5	0.25	36	38.2	41.4	42.4	42.5	47.4	51.3
		48	35.2	39.6	42.0	43.1	47.4	51.3
		60	32.8	37.9	41.2	43.2	47.4	51.3
		72	30.8	36.3	40.1	43.1	47.4	51.3
		84	29.2	34.7	38.9	43.1	47.4	51.3
		96	27.8	33.4	38.4	43.1	47.4	51.3
		108	27.0	33.1	38.4	43.1	47.4	51.3
		120	27.0	33.1	38.4	43.1	47.4	51.3
		132	27.0	33.1	38.4	43.1	47.4	51.3
		144	27.0	33.1	38.4	43.1	47.4	51.3
		156	27.0	33.1	38.4	43.1	47.4	51.3
		168	27.0	33.1	38.4	43.1	47.4	51.3
		180	27.0	33.1	38.4	43.1	47.4	51.3
		192	27.0	33.1	38.4	43.1	47.4	51.3
		204	27.0	33.1	38.4	43.1	47.4	51.3
		216	27.0	33.1	38.4	43.1	47.4	51.3
		228	27.0	33.1	38.4	43.1	47.4	51.3
		240	27.0	33.1	38.4	43.1	47.4	51.3
	0.50	36	35.3	38.8	40.3	40.9	42.0	45.9
		48	32.3	36.7	39.3	40.8	42.0	45.9
		60	30.0	34.9	38.2	40.4	42.0	45.9
		72	28.2	33.3	37.0	39.8	42.0	45.9
		84	26.6	31.8	35.8	38.9	42.0	45.9
		96	25.4	30.5	34.7	38.7	42.0	45.9
		108	24.3	29.6	34.4	38.7	42.0	45.9
		120	24.1	29.6	34.4	38.7	42.0	45.9
		132	24.1	29.6	34.4	38.7	42.0	45.9
		144	24.1	29.6	34.4	38.7	42.0	45.9
		156	24.1	29.6	34.4	38.7	42.0	45.9
		168	24.1	29.6	34.4	38.7	42.0	45.9
		180	24.1	29.6	34.4	38.7	42.0	45.9
		192	24.1	29.6	34.4	38.7	42.0	45.9
		204	24.1	29.6	34.4	38.7	42.0	45.9
		216	24.1	29.6	34.4	38.7	42.0	45.9
		228	24.1	29.6	34.4	38.7	42.0	45.9
		240	24.1	29.6	34.4	38.7	42.0	45.9

Table 8F-2. Main bars parallel to traffic, D=5.0.

D	α	L (in)	P (3ft)	P (4ft)	P (5ft)	P (6ft)	P (7ft)	P (8ft)
5	0.75	36	33.9	37.6	39.5	40.4	40.9	43.5
		48	30.8	35.3	38.1	39.9	40.9	43.5
		60	28.5	33.4	36.8	39.2	40.8	43.5
		72	26.8	31.7	35.5	38.3	40.4	43.5
		84	25.3	30.3	34.3	36.4	40.1	43.5
		96	24.1	29.1	33.1	36.4	40.1	43.5
		108	23.0	27.9	32.3	36.4	40.1	43.5
		120	22.5	27.7	32.3	36.4	40.1	43.5
		132	22.5	27.7	32.3	36.4	40.1	43.5
		144	22.5	27.7	32.3	36.4	40.1	43.5
		156	22.5	27.7	32.3	36.4	40.1	43.5
		168	22.5	27.7	32.3	36.4	40.1	43.5
		180	22.5	27.7	32.3	36.4	40.1	43.5
		192	22.5	27.7	32.3	36.4	40.1	43.5
		204	22.5	27.7	32.3	36.4	40.1	43.5
		216	22.5	27.7	32.3	36.4	40.1	43.5
		228	22.5	27.7	32.3	36.4	40.1	43.5
		240	22.5	27.7	32.3	36.4	40.1	43.5
	1.00	36	33.0	36.9	39.1	40.4	41.0	41.8
		48	29.8	34.4	37.4	39.4	40.7	41.8
		60	27.6	32.4	35.9	38.5	40.3	41.8
		72	25.8	30.8	34.6	37.5	39.7	41.8
		84	24.4	29.3	33.3	36.4	38.9	41.8
		96	23.2	28.1	32.1	35.4	38.5	41.8
		108	22.2	27.0	31.0	34.9	38.5	41.8
		120	21.5	26.5	30.9	34.9	38.5	41.8
		132	21.5	26.5	30.9	34.9	38.5	41.8
		144	21.5	26.5	30.9	34.9	38.5	41.8
		156	21.5	26.5	30.9	34.9	38.5	41.8
		168	21.5	26.5	30.9	34.9	38.5	41.8
		180	21.5	26.5	30.9	34.9	38.5	41.8
		192	21.5	26.5	30.9	34.9	38.5	41.8
		204	21.5	26.5	30.9	34.9	38.5	41.8
		216	21.5	26.5	30.9	34.9	38.5	41.8
		228	21.5	26.5	30.9	34.9	38.5	41.8
		240	21.5	26.5	30.9	34.9	38.5	41.8

Table 8F-3. Main bars parallel to traffic, D=5.0.

D	α	L (in)	P (3ft)	P (4ft)	P (5ft)	P (6ft)	P (7ft)	P (8ft)
5	2.00	36	31.1	35.7	38.7	40.7	42.1	43.0
		48	27.8	32.7	36.2	38.8	40.7	42.1
		60	25.6	30.5	34.3	37.2	39.5	41.3
		72	23.9	28.7	32.7	35.8	38.4	40.5
		84	22.5	27.3	31.3	34.5	37.3	39.6
		96	21.3	26.1	30.0	33.4	36.2	38.6
		108	20.4	25.0	28.9	32.3	35.2	38.3
		120	19.6	24.1	27.9	31.8	35.2	38.3
		132	19.3	24.0	27.9	31.8	35.2	38.3
		144	19.3	24.0	27.9	31.8	35.2	38.3
		156	19.3	24.0	27.9	31.8	35.2	38.3
		168	19.3	24.0	27.9	31.8	35.2	38.3
		180	19.3	24.0	27.9	31.8	35.2	38.3
		192	19.3	24.0	27.9	31.8	35.2	38.3
		204	19.3	24.0	27.9	31.8	35.2	38.3
		216	19.3	24.0	27.9	31.8	35.2	38.3
		228	19.3	24.0	27.9	31.8	35.2	38.3
		240	19.3	24.0	27.9	31.8	35.2	38.3
	4.00	36	29.5	34.7	38.6	41.5	43.7	45.3
		48	26.1	31.3	35.3	38.6	41.2	43.3
		60	23.8	28.9	33.0	36.4	39.2	41.6
		72	22.2	27.1	31.2	34.6	37.6	40.1
		84	20.8	25.6	29.6	33.1	36.2	38.8
		96	19.7	24.4	28.3	31.8	34.9	37.5
		108	18.8	23.3	27.2	30.6	33.7	36.4
		120	18.0	22.4	26.2	29.6	32.6	35.4
		132	17.4	21.8	25.6	29.2	32.5	35.5
		144	17.4	21.8	25.6	29.2	32.5	35.5
		156	17.4	21.8	25.6	29.2	32.5	35.5
		168	17.4	21.8	25.6	29.2	32.5	35.5
		180	17.4	21.8	25.6	29.2	32.5	35.5
		192	17.4	21.8	25.6	29.2	32.5	35.5
		204	17.4	21.8	25.6	29.2	32.5	35.5
		216	17.4	21.8	25.6	29.2	32.5	35.5
		228	17.4	21.8	25.6	29.2	32.5	35.5
		240	17.4	21.8	25.6	29.2	32.5	35.5

Table 8F-4. Main bars parallel to traffic, D=5.0.

D	α	L (in)	P (3ft)	P (4ft)	P (5ft)	P (6ft)	P (7ft)	P (8ft)
5	8.00	36	28.1	33.9	38.6	42.3	45.4	47.9
		48	24.7	30.1	34.7	38.5	41.8	44.6
		60	22.4	27.6	32.0	35.9	39.2	42.1
		72	20.8	25.7	30.0	33.8	37.1	40.1
		84	19.5	24.2	28.4	32.1	35.4	38.4
		96	18.4	23.0	27.0	30.6	33.9	36.9
		108	17.5	21.9	25.8	29.4	32.6	35.5
		120	16.8	21.0	24.8	28.3	31.4	34.3
		132	15.8	19.9	23.7	27.1	30.3	33.3
		144	15.8	19.9	23.7	27.1	30.3	33.3
		156	15.8	19.9	23.7	27.1	30.3	33.3
		168	15.8	19.9	23.7	27.1	30.3	33.3
		180	15.8	19.9	23.7	27.1	30.3	33.3
		192	15.8	19.9	23.7	27.1	30.3	33.3
		204	15.8	19.9	23.7	27.1	30.3	33.3
		216	15.8	19.9	23.7	27.1	30.3	33.3
		228	15.8	19.9	23.7	27.1	30.3	33.3
		240	15.8	19.9	23.7	27.1	30.3	33.3

Table 9F-1. Main bars parallel to traffic, D=8.0.

D	α	L (in)	P (3ft)	P (4ft)	P (5ft)	P (6ft)	P (7ft)	P (8ft)
8	0.25	36	38.9	41.4	42.0	44.3	48.6	52.4
		48	36.1	40.0	41.8	44.3	48.6	52.4
		60	33.8	38.5	41.3	44.3	48.6	52.4
		72	32.0	37.1	40.6	44.3	48.6	52.4
		84	30.4	35.7	39.7	44.3	48.6	52.4
		96	29.0	34.5	39.6	44.3	48.6	52.4
		108	28.1	34.3	39.6	44.3	48.6	52.4
		120	28.1	34.3	39.6	44.3	48.6	52.4
		132	28.1	34.3	39.6	44.3	48.6	52.4
		144	28.1	34.3	39.6	44.3	48.6	52.4
		156	28.1	34.3	39.6	44.3	48.6	52.4
		168	28.1	34.3	39.6	44.3	48.6	52.4
		180	28.1	34.3	39.6	44.3	48.6	52.4
		192	28.1	34.3	39.6	44.3	48.6	52.4
		204	28.1	34.3	39.6	44.3	48.6	52.4
		216	28.1	34.3	39.6	44.3	48.6	52.4
		228	28.1	34.3	39.6	44.3	48.6	52.4
		240	28.1	34.3	39.6	44.3	48.6	52.4
	0.50	36	36.1	39.0	40.1	40.4	43.6	47.1
		48	33.2	37.2	39.3	40.3	43.6	47.1
		60	31.0	35.6	38.5	40.3	43.6	47.1
		72	29.2	34.1	37.6	39.9	43.6	47.1
		84	27.7	32.8	36.6	39.8	43.6	47.1
		96	26.4	31.5	35.5	39.8	43.6	47.1
		108	25.3	30.6	35.5	39.8	43.6	47.1
		120	25.0	30.6	35.5	39.8	43.6	47.1
		132	25.0	30.6	35.5	39.8	43.6	47.1
		144	25.0	30.6	35.5	39.8	43.6	47.1
		156	25.0	30.6	35.5	39.8	43.6	47.1
		168	25.0	30.6	35.5	39.8	43.6	47.1
		180	25.0	30.6	35.5	39.8	43.6	47.1
		192	25.0	30.6	35.5	39.8	43.6	47.1
		204	25.0	30.6	35.5	39.8	43.6	47.1
		216	25.0	30.6	35.5	39.8	43.6	47.1
		228	25.0	30.6	35.5	39.8	43.6	47.1
		240	25.0	30.6	35.5	39.8	43.6	47.1

Table 9F-2. Main bars parallel to traffic, D=8.0.

D	α	L (in)	P (3ft)	P (4ft)	P (5ft)	P (6ft)	P (7ft)	P (8ft)
8	0.75	36	34.7	37.9	39.4	40.1	41.1	44.5
		48	31.7	35.8	38.3	39.6	41.1	44.5
		60	29.5	34.1	37.2	39.2	41.1	44.5
		72	27.8	32.6	36.1	38.6	41.1	44.5
		84	26.3	31.3	35.0	37.9	41.1	44.5
		96	25.1	30.0	34.0	37.4	41.1	44.5
		108	24.0	28.9	33.3	37.4	41.1	44.5
		120	23.5	28.8	33.3	37.4	41.1	44.5
		132	23.5	28.8	33.3	37.4	41.1	44.5
		144	23.5	28.8	33.3	37.4	41.1	44.5
		156	23.5	28.8	33.3	37.4	41.1	44.5
		168	23.5	28.8	33.3	37.4	41.1	44.5
		180	23.5	28.8	33.3	37.4	41.1	44.5
		192	23.5	28.8	33.3	37.4	41.1	44.5
		204	23.5	28.8	33.3	37.4	41.1	44.5
		216	23.5	28.8	33.3	37.4	41.1	44.5
		228	23.5	28.8	33.3	37.4	41.1	44.5
		240	23.5	28.8	33.3	37.4	41.1	44.5
	1.00	36	33.8	37.4	39.2	40.1	40.5	42.8
		48	30.8	35.0	37.7	39.3	40.3	42.8
		60	28.6	33.2	36.4	38.6	40.1	42.8
		72	26.8	31.7	35.2	37.8	39.8	42.8
		84	25.4	30.3	34.1	37.0	39.5	42.8
		96	24.2	29.1	33.0	36.1	39.5	42.8
		108	23.2	28.0	32.0	35.9	39.5	42.8
		120	22.4	27.5	32.0	35.9	39.5	42.8
		132	22.4	27.5	32.0	35.9	39.5	42.8
		144	22.4	27.5	32.0	35.9	39.5	42.8
		156	22.4	27.5	32.0	35.9	39.5	42.8
		168	22.4	27.5	32.0	35.9	39.5	42.8
		180	22.4	27.5	32.0	35.9	39.5	42.8
		192	22.4	27.5	32.0	35.9	39.5	42.8
		204	22.4	27.5	32.0	35.9	39.5	42.8
		216	22.4	27.5	32.0	35.9	39.5	42.8
		228	22.4	27.5	32.0	35.9	39.5	42.8
		240	22.4	27.5	32.0	35.9	39.5	42.8

Table 9F-3. Main bars parallel to traffic, D=8.0.

D	α	L (in)	P (3ft)	P (4ft)	P (5ft)	P (6ft)	P (7ft)	P (8ft)
8	2.00	36	32.1	36.3	39.0	40.7	41.8	42.5
		48	28.8	33.4	36.7	39.0	40.7	41.8
		60	26.5	31.3	34.9	37.7	39.7	41.3
		72	24.8	29.7	33.4	36.4	38.8	40.7
		84	23.4	28.2	32.1	35.3	37.8	39.9
		96	22.3	27.0	30.9	34.2	36.9	39.2
		108	21.3	25.9	29.8	33.1	36.1	39.2
		120	20.4	25.0	29.0	32.7	36.1	39.2
		132	20.1	24.8	29.0	32.7	36.1	39.2
		144	20.1	24.8	29.0	32.7	36.1	39.2
		156	20.1	24.8	29.0	32.7	36.1	39.2
		168	20.1	24.8	29.0	32.7	36.1	39.2
		180	20.1	24.8	29.0	32.7	36.1	39.2
		192	20.1	24.8	29.0	32.7	36.1	39.2
		204	20.1	24.8	29.0	32.7	36.1	39.2
		216	20.1	24.8	29.0	32.7	36.1	39.2
		228	20.1	24.8	29.0	32.7	36.1	39.2
		240	20.1	24.8	29.0	32.7	36.1	39.2
	4.00	36	30.5	35.6	39.2	41.8	43.7	45.1
		48	27.1	32.2	36.1	39.1	41.5	43.4
		60	24.8	29.8	33.8	37.1	39.7	41.9
		72	23.1	28.0	32.1	35.4	38.2	40.6
		84	21.7	26.5	30.6	34.0	36.9	39.4
		96	20.6	25.3	29.3	32.7	35.7	38.3
		108	19.7	24.2	28.1	31.5	34.5	37.2
		120	18.9	23.3	27.2	30.5	33.5	36.4
		132	18.2	22.6	26.5	30.1	33.4	36.4
		144	18.2	22.6	26.5	30.1	33.4	36.4
		156	18.2	22.6	26.5	30.1	33.4	36.4
		168	18.2	22.6	26.5	30.1	33.4	36.4
		180	18.2	22.6	26.5	30.1	33.4	36.4
		192	18.2	22.6	26.5	30.1	33.4	36.4
		204	18.2	22.6	26.5	30.1	33.4	36.4
		216	18.2	22.6	26.5	30.1	33.4	36.4
		228	18.2	22.6	26.5	30.1	33.4	36.4
		240	18.2	22.6	26.5	30.1	33.4	36.4

Table 9F-4. Main bars parallel to traffic, D=8.0.

D	α	L (in)	P (3ft)	P (4ft)	P (5ft)	P (6ft)	P (7ft)	P (8ft)
8	8.00	36	29.2	34.9	39.3	42.8	45.6	47.9
		48	25.6	31.1	35.5	39.2	42.3	44.9
		60	23.3	28.5	32.9	36.7	39.9	42.6
		72	21.6	26.6	30.9	34.6	37.9	40.8
		84	20.3	25.1	29.3	33.0	36.2	39.1
		96	19.2	23.8	27.9	31.5	34.7	37.7
		108	18.3	22.8	26.7	30.3	33.5	36.4
		120	17.5	21.8	25.7	29.2	32.3	35.2
		132	16.5	20.7	24.5	27.9	31.1	34.1
		144	16.5	20.7	24.5	27.9	31.1	34.1
		156	16.5	20.7	24.5	27.9	31.1	34.1
		168	16.5	20.7	24.5	27.9	31.1	34.1
		180	16.5	20.7	24.5	27.9	31.1	34.1
		192	16.5	20.7	24.5	27.9	31.1	34.1
		204	16.5	20.7	24.5	27.9	31.1	34.1
		216	16.5	20.7	24.5	27.9	31.1	34.1
		228	16.5	20.7	24.5	27.9	31.1	34.1
		240	16.5	20.7	24.5	27.9	31.1	34.1

Table 10F-1. Main bars parallel to traffic, D=10.0.

D	α	L (in)	P (3ft)	P (4ft)	P (5ft)	P (6ft)	P (7ft)	P (8ft)
10	0.25	36	39.2	41.4	41.8	44.9	49.1	53.0
		48	36.5	40.1	41.6	44.9	49.1	53.0
		60	34.3	38.8	41.4	44.9	49.1	53.0
		72	32.5	37.5	40.8	44.9	49.1	53.0
		84	30.9	36.2	40.2	44.9	49.1	53.0
		96	29.5	34.9	40.2	44.9	49.1	53.0
		108	28.7	34.9	40.2	44.9	49.1	53.0
		120	28.7	34.9	40.2	44.9	49.1	53.0
		132	28.7	34.9	40.2	44.9	49.1	53.0
		144	28.7	34.9	40.2	44.9	49.1	53.0
		156	28.7	34.9	40.2	44.9	49.1	53.0
		168	28.7	34.9	40.2	44.9	49.1	53.0
		180	28.7	34.9	40.2	44.9	49.1	53.0
		192	28.7	34.9	40.2	44.9	49.1	53.0
		204	28.7	34.9	40.2	44.9	49.1	53.0
		216	28.7	34.9	40.2	44.9	49.1	53.0
		228	28.7	34.9	40.2	44.9	49.1	53.0
		240	28.7	34.9	40.2	44.9	49.1	53.0
	0.50	36	36.4	39.1	40.0	40.3	44.1	47.6
		48	33.6	37.3	39.3	40.3	44.1	47.6
		60	31.4	35.9	38.6	40.3	44.1	47.6
		72	29.7	34.5	37.8	40.3	44.1	47.6
		84	28.2	33.2	36.9	40.3	44.1	47.6
		96	26.9	32.0	36.0	40.3	44.1	47.6
		108	25.8	31.2	36.0	40.3	44.1	47.6
		120	25.6	31.2	36.0	40.3	44.1	47.6
		132	25.6	31.2	36.0	40.3	44.1	47.6
		144	25.6	31.2	36.0	40.3	44.1	47.6
		156	25.6	31.2	36.0	40.3	44.1	47.6
		168	25.6	31.2	36.0	40.3	44.1	47.6
		180	25.6	31.2	36.0	40.3	44.1	47.6
		192	25.6	31.2	36.0	40.3	44.1	47.6
		204	25.6	31.2	36.0	40.3	44.1	47.6
		216	25.6	31.2	36.0	40.3	44.1	47.6
		228	25.6	31.2	36.0	40.3	44.1	47.6
		240	25.6	31.2	36.0	40.3	44.1	47.6

Table 10F-2. Main bars parallel to traffic, D=10.0.

D	α	L (in)	P (3ft)	P (4ft)	P (5ft)	P (6ft)	P (7ft)	P (8ft)
10	0.75	36	35.1	38.1	39.4	39.9	41.6	45.0
		48	32.1	36.1	38.3	39.5	41.6	45.0
		60	30.0	34.4	37.4	39.2	41.6	45.0
		72	28.2	33.0	36.4	38.7	41.6	45.0
		84	26.8	31.7	35.4	38.1	41.6	45.0
		96	25.6	30.5	34.3	37.9	41.6	45.0
		108	24.5	29.4	33.9	37.9	41.6	45.0
		120	23.9	29.2	33.9	37.9	41.6	45.0
		132	23.9	29.2	33.9	37.9	41.6	45.0
		144	23.9	29.2	33.9	37.9	41.6	45.0
		156	23.9	29.2	33.9	37.9	41.6	45.0
		168	23.9	29.2	33.9	37.9	41.6	45.0
		180	23.9	29.2	33.9	37.9	41.6	45.0
		192	23.9	29.2	33.9	37.9	41.6	45.0
		204	23.9	29.2	33.9	37.9	41.6	45.0
		216	23.9	29.2	33.9	37.9	41.6	45.0
		228	23.9	29.2	33.9	37.9	41.6	45.0
		240	23.9	29.2	33.9	37.9	41.6	45.0
	1.00	36	34.2	37.6	39.2	40.0	40.3	43.2
		48	31.2	35.3	37.8	39.2	40.1	43.2
		60	29.0	33.6	36.6	38.7	40.0	43.2
		72	27.3	32.1	35.5	38.0	40.0	43.2
		84	25.9	30.7	34.4	37.2	40.0	43.2
		96	24.7	29.5	33.4	36.4	40.0	43.2
		108	23.6	28.5	32.4	36.4	40.0	43.2
		120	22.9	28.0	32.4	36.4	40.0	43.2
		132	22.9	28.0	32.4	36.4	40.0	43.2
		144	22.9	28.0	32.4	36.4	40.0	43.2
		156	22.9	28.0	32.4	36.4	40.0	43.2
		168	22.9	28.0	32.4	36.4	40.0	43.2
		180	22.9	28.0	32.4	36.4	40.0	43.2
		192	22.9	28.0	32.4	36.4	40.0	43.2
		204	22.9	28.0	32.4	36.4	40.0	43.2
		216	22.9	28.0	32.4	36.4	40.0	43.2
		228	22.9	28.0	32.4	36.4	40.0	43.2
		240	22.9	28.0	32.4	36.4	40.0	43.2

Table 10F-3. Main bars parallel to traffic, D=10.0.

D	α	L (in)	P (3ft)	P (4ft)	P (5ft)	P (6ft)	P (7ft)	P (8ft)
10	2.00	36	32.5	36.6	39.2	40.7	41.7	42.3
		48	29.3	33.8	37.0	39.1	40.6	41.7
		60	27.0	31.7	35.2	37.8	39.8	41.2
		72	25.3	30.1	33.8	36.7	38.9	40.7
		84	23.9	28.7	32.5	35.6	38.1	40.1
		96	22.7	27.5	31.3	34.5	37.2	39.7
		108	21.7	26.4	30.3	33.5	36.6	39.7
		120	20.9	25.5	29.5	33.0	36.6	39.7
		132	20.5	25.3	29.5	33.0	36.6	39.7
		144	20.5	25.3	29.5	33.0	36.6	39.7
		156	20.5	25.3	29.5	33.0	36.6	39.7
		168	20.5	25.3	29.5	33.0	36.6	39.7
		180	20.5	25.3	29.5	33.0	36.6	39.7
		192	20.5	25.3	29.5	33.0	36.6	39.7
		204	20.5	25.3	29.5	33.0	36.6	39.7
		216	20.5	25.3	29.5	33.0	36.6	39.7
		228	20.5	25.3	29.5	33.0	36.6	39.7
		240	20.5	25.3	29.5	33.0	36.6	39.7
	4.00	36	31.0	36.0	39.5	41.9	43.7	45.0
		48	27.6	32.6	36.4	39.4	41.6	43.4
		60	25.3	30.3	34.2	37.4	40.0	42.1
		72	23.5	28.5	32.5	35.8	38.5	40.8
		84	22.2	27.0	31.0	34.4	37.2	39.7
		96	21.0	25.7	29.7	33.1	36.0	38.6
		108	20.1	24.7	28.6	32.0	34.9	37.6
		120	19.3	23.7	27.6	31.0	34.0	36.8
		132	18.5	23.0	27.0	30.5	33.8	36.8
		144	18.5	23.0	27.0	30.5	33.8	36.8
		156	18.5	23.0	27.0	30.5	33.8	36.8
		168	18.5	23.0	27.0	30.5	33.8	36.8
		180	18.5	23.0	27.0	30.5	33.8	36.8
		192	18.5	23.0	27.0	30.5	33.8	36.8
		204	18.5	23.0	27.0	30.5	33.8	36.8
		216	18.5	23.0	27.0	30.5	33.8	36.8
		228	18.5	23.0	27.0	30.5	33.8	36.8
		240	18.5	23.0	27.0	30.5	33.8	36.8

Table 10F-4. Main bars parallel to traffic, D=10.0.

D	α	L (in)	P (3ft)	P (4ft)	P (5ft)	P (6ft)	P (7ft)	P (8ft)
10	8.00	36	29.6	35.3	39.7	43.1	45.8	47.9
		48	26.1	31.5	35.9	39.6	42.6	45.1
		60	23.8	29.0	33.3	37.0	40.2	42.9
		72	22.0	27.1	31.4	35.0	38.3	41.1
		84	20.7	25.5	29.7	33.4	36.6	39.5
		96	19.6	24.3	28.3	31.9	35.2	38.0
		108	18.7	23.2	27.2	30.7	33.9	36.8
		120	17.9	22.3	26.1	29.6	32.8	35.6
		132	16.8	21.0	24.8	28.3	31.6	34.6
		144	16.8	21.0	24.8	28.3	31.6	34.6
		156	16.8	21.0	24.8	28.3	31.6	34.6
		168	16.8	21.0	24.8	28.3	31.6	34.6
		180	16.8	21.0	24.8	28.3	31.6	34.6
		192	16.8	21.0	24.8	28.3	31.6	34.6
		204	16.8	21.0	24.8	28.3	31.6	34.6
		216	16.8	21.0	24.8	28.3	31.6	34.6
		228	16.8	21.0	24.8	28.3	31.6	34.6
		240	16.8	21.0	24.8	28.3	31.6	34.6

**ATTACHMENT E - Proposed Test Method and Commentary for Determining
Strong Axis Flexural Stiffness (D_x) of Bridge Decks**

Proposed Test Method and Commentary for Determining Strong Axis Flexural Stiffness (D_x) of Bridge Decks

<p>1.0 General</p> <p>1.1 Scope</p> <p>This test method describes a procedure for determining the flexural stiffness of a prefabricated bridge deck about the strong axis for non-isotropic decks. This test may also be used to determine the flexural stiffness of isotropic decks.</p>	<p>C1.0 General</p> <p>C1.1 Scope</p> <p>The strong axis of a bridge deck is that which will produce a greater flexural stiffness. For cases where the bridge deck is isotropic, the orientation of the specimen is not a concern. Therefore, this test procedure is applicable to any type of bridge deck.</p>
<p>1.2 Summary</p> <p>This test procedure is used to determine the flexural stiffness of a prefabricated bridge deck. Data reported includes total force applied (P) at pre-determined force increments, area over which force is applied (A), and displacements at defined locations (Δ). Each test shall be repeated a minimum of three times to ensure repeatability. For each test run, the force shall be applied at a minimum of five (5) levels and the corresponding displacement data shall be recorded. The data collected shall be used to determine the flexural stiffness of the bridge deck about its strong axis (D_x).</p>	<p>C1.2 Summary</p> <p>Flexural stiffness of a bridge deck can be determined through this test method. Full-scale testing of a representative subassembly sample is required. The test results generate the needed data that are used to design the bridge deck per the AASHTO LRFD Bridge Design Specifications. The test results can also be used to gain a better understanding of force distribution through the deck itself. Required data to be reported includes the flexural stiffness, relationship between displacements and force applied as well as stress and force applied.</p>
<p>1.3 Approach</p> <p>Force is to be applied as a line load at midspan of the deck specimen. Resulting vertical displacements are measured and recorded at prescribed locations. The specimen shall be supported continuously along the two edges that are parallel to the applied line load. The deck is effectively subjected to one way bending/flexure. This permits direct measurement of the flexural stiffness of the deck in the orientation transverse to the line load. To determine the stiffness, the applied load, maximum displacement and length/span of the deck must be known. The strong axis flexural stiffness (D_x) can then be computed using an appropriate mathematical expression for the particular type of bridge deck under investigation.</p>	<p>C1.3 Approach</p> <p>The behavior of many bridge decks can not be simplified or idealized using simple beam models because they possess orthotropic properties. Hence, it is difficult to evaluate their stiffness properties without conducting full-scale testing.</p> <p>To isolate the stiffness in a single direction so it can be computed from the experimental measurements, a line load is applied transverse to the strong direction so that the contribution of the weak direction stiffness is negligible to the measured response. The resulting response of the deck is, therefore, flexural deformation in only one direction.</p>
<p>2.0 Specimens</p> <p>2.1 Components – General</p> <p>Specimens shall be representative full-scale subassemblies of a typical portion of the bridge deck. The specimen shall include all components of an in-service bridge deck panel which affect load distribution. The same deck specimen may be used to determine the bending stiffness in the weak direction (D_y) and the torsional stiffness (D_{xy}) that are described in other documents. The specimen is to be supported on rigid supports along two sides of the specimen such that it is simply supported for bending about its strong axis</p>	<p>C2.0 Specimens</p> <p>C2.1 Components –General</p> <p>The range of specimen size was selected such that it would provide practical dimensions while maintaining an accurate representation of the bridge deck. Testing of a specimen with dimensions smaller than the recommended minimum may produce inaccurate results.</p>

Proposed Test Method and Commentary for Determining Strong Axis Flexural Stiffness (D_x) of Bridge Decks

as shown in Figure 1. The span between the two supports shall be a minimum of five (5) feet (1.5 m). The transverse dimension shall be sufficiently wide to include at least three of the primary load carrying members, but shall not be less than one half the span length. *(It is noted that a square specimen is required for the D_{xy} tests and hence, it may be desirable to use a square specimen for the D_x and D_y tests.)*

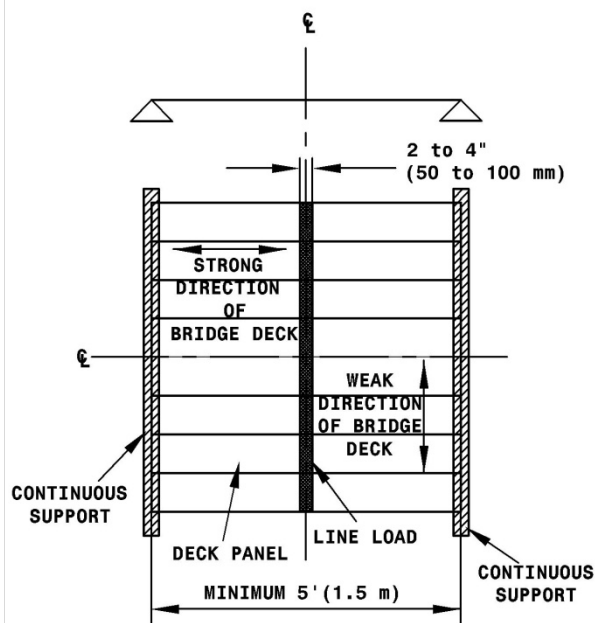


Figure 1: Strong Axis Stiffness (D_x) Test Set-up

Prior to testing, the specimen shall be visually inspected for any flaws or defects that could possibly affect the measured flexural stiffness of the bridge deck being considered. Defects and flaws shall be defined as per the appropriate governing specification (e.g., contract documents, ASTM documents, etc.). Specimens containing flaws and defects that are deemed to significantly affect the flexural stiffness of the specimen shall not be used for stiffness testing and data collection. Specimens that meet specifications but exhibit minor defects can be tested but such defects and their locations shall be documented and reported.

2.2 Instrumentation

The test specimen shall be instrumented to measure the vertical displacements of the specimen to a minimum resolution of 0.001 inches (25 μ m). Vertical displacements shall be measured over each support at three locations; at the mid-

C2.2 Instrumentation

Strain gages are required to ensure that yielding of the specimen does not occur at locations where the stress is expected to be greatest. However, exceeding the yield stress is unlikely since the applied loading will be relatively

Proposed Test Method and Commentary for Determining Strong Axis Flexural Stiffness (D_x) of Bridge Decks

length location and at the ends. These measurements allow rigid body movement of the supports to be accounted for in the calculation of the strong-axis bending stiffness. Vertical displacements of the deck specimen shall be measured at a minimum of three locations (i.e. one in the middle and two close to the edges of the specimen) along the length of the line load to ensure that the deck is displacing uniformly. Limited strain gaging is required to monitor stresses at critical locations during testing and to understand the behavior of the deck panels. As a minimum, specimens shall be instrumented as illustrated in Figure 2.

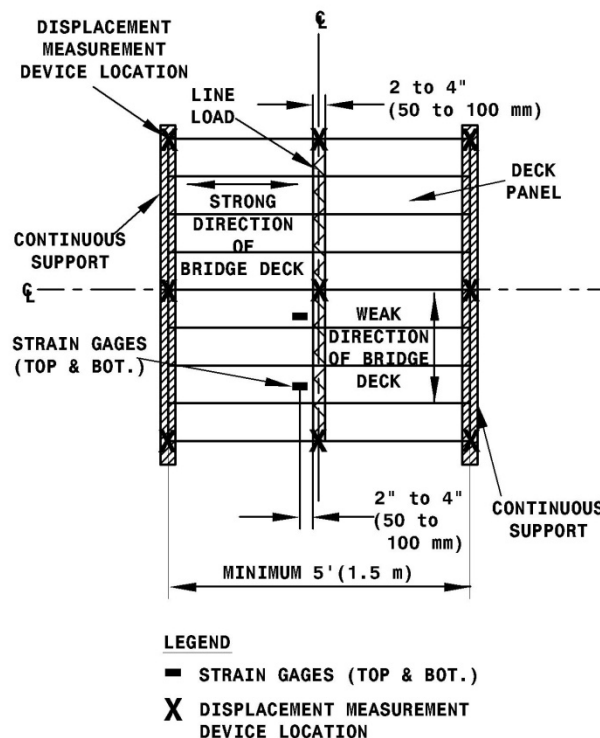


Figure 2: Minimum Instrumentation Required for Strong Axis Stiffness (D_x) Test

Instrumentation for accurately measuring applied force shall also be used. The resolution of the load measuring device shall be calibrated such that it has a resolution to 1% of maximum test load applied, P_t , as defined in 4.2.3. All sensor calibrations shall be reported.

3.0 Fixtures

3.1 Fixture Details

Fixtures capable of adequately supporting and loading the specimen during the test shall be provided. The fixtures shall be sufficiently stiff such that no additional displacements or stresses

low. Strain gages can also be used to gain a greater understanding of the deck behavior.

Accurate displacement and force measurements are critical to the success of this test. It is imperative that the devices used to measure the displacements and applied forces are calibrated accurately before testing. Vertical displacement measurements are to be taken at mid-span of the specimen where the load is applied and other locations to gain a sufficiently detailed profile of the bridge panel. Vertical displacements are also to be measured at the supports to ensure there is not any rigid-body movement of the specimen as this would skew the results of the test.

C3.0 Fixtures

C3.1 Fixture Details

Proposed Test Method and Commentary for Determining Strong Axis Flexural Stiffness (D_x) of Bridge Decks

are generated as a result of fixture misalignment or movement. In addition, fabrication tolerances in the specimen shall be corrected or compensated for using non-mechanical means (i.e., shimming) and where required shall be reported. Dimensional tolerances of support locations shall be within $\pm 1/8$ in. (3 mm)

The supporting fixtures shall be sufficiently stiff to ensure vertical displacement of the fixture is less than 0.010 inches (250 μm) under the maximum applied load. Vertical displacement of the supports shall be measured as described in 2.2. Vertical displacement of the supports under each load step shall be included in the report.

4.0 Test Procedure

4.1 General

A minimum of three (3) data sets are required to establish the flexural stiffness of a bridge deck panel. All data may be obtained from a single subassembly. Additionally, the same deck specimen may also be used for other stiffness tests (i.e. D_y and D_{xy}) as long as it is not damaged in any previous test. If, however, the specimen is damaged during testing, it shall not be used for any future testing.

4.2 Loads

Loads shall be applied using a hydraulic jack or actuator. The magnitude of the load shall be increased in equal increments pre-determined for the test (i.e. "load control"). The load shall be maintained within $\pm 2\%$ of the target value for each load increment for a minimum of ten (10) seconds to allow for the collection of data. The load shall be monitored throughout the test to ensure that the desired load intervals are achieved.

4.2.1 Application of Load

Load shall be applied as a line load at the midspan location of the specimen and oriented parallel to the supports using a single loading mechanism. The width of the line load (parallel to the span) shall be a minimum of 2 in. (50 mm) and maximum of 4 in. (100 mm). If a bearing pad is used, it shall have a minimum hardness of 50 durometer and a maximum thickness of 1 inch.

C4.0 Test Procedure

C4.1 General

A single bridge deck specimen may be used for data collection. The specimen is not to be damaged during the strong direction flexural stiffness (D_x) testing. The deck specimen used for this test may also be used to determine the flexural stiffness of the deck in the weak (D_y) direction and the torsional stiffness (D_{xy}). If a panel is damaged such that it affects the stiffness properties of the specimen, it shall be removed, and the testing shall be repeated with an undamaged specimen.

C4.2 Loads

Loads shall be applied through the use of hydraulic jacks or other similar loading devices. Displacements and stresses shall be monitored continuously throughout the test to ensure displacements and stresses remain below the desired level (*to be determined by the individual conducting the test*).

C4.2.1 Application of Load

The patch is typically a 1" (25 mm) thick steel plate on top of a hard rubber bearing pad, placed in contact with the deck as shown in Figure 3.

Proposed Test Method and Commentary for Determining Strong Axis Flexural Stiffness (D_x) of Bridge Decks

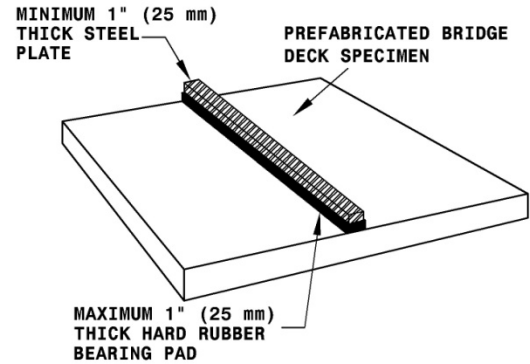


Figure 3: Typical Line Load on Bridge Deck

4.2.2 Preloading

The specimen shall be preloaded to ensure proper seating of the fixtures, specimen, and patch load. During the preload phase, displacement data shall be recorded. The response of the deck (load vs. displacement) shall be verified for linearity in the upper 1/3 portion of the loading curve. The magnitude of the preload, P_s , shall be of sufficient magnitude to ensure seating of the fixtures and specimen, but shall not exceed $1/3 P_{max}$ as defined in 4.2.3. If measurements indicate nonlinear response over the entire preloading history, then the cause(s) for the nonlinearity shall be determined and corrected. Once the specimen is seated, the preload, P_s , shall be reapplied and considered the starting point (i.e., zero point) for the actual stiffness test.

4.2.3 Load Parameters

The maximum load (P_{max}) to be applied shall be determined as 50% of the minimum estimated load which produces any one of the following conditions in the strong axis direction:

1. Cracking in any portion of the specimen
2. Yielding in any portion of the specimen
3. Debonding or slip of the concrete
4. Any non-linear behavior not caused by bringing the test specimen and fixtures into contact (i.e. preloading described in 4.2.2).

The Test Load, P_t , shall be computed as the difference between the maximum load, P_{max} , and the preload, P_s , (i.e. $P_t = P_{max} - P_s$).

C4.2.2 Preloading

Preloading of the specimen is an effective method to “shake down” the setup and identify potential issues that could affect the testing results.

C4.2.3 Load Parameters

The limit states described in 4.2.3 and calculated value of P_{max} (set equal to 50% of the load which could produce these limit states) were established to ensure no non-linear response is produced and to ensure the specimen is not damaged.

The load which would produce cracking, yielding, debonding, or any other non-linear behavior may be calculated using any methodology that relies on traditional mechanics solutions.

Proposed Test Method and Commentary for Determining Strong Axis Flexural Stiffness (D_x) of Bridge Decks

<p>4.2.4 Stiffness Test</p> <p>The Test Load, determined in 4.2.3, is to be divided into five equal load increments (i.e. $P_t/5$). Once the Test Load is determined and the operation of the instrumentation and data acquisition has been verified, all load shall be removed from the specimen. The preload (P_s) shall then be reapplied.</p> <p>Next, all strain gages, load, and displacement measuring devices shall be rebalanced to zero while the preload is maintained. Then, the Test Load (P_t) shall be applied in equal increments as pre-determined and shall be held at each increment for a minimum of 10 seconds to collect data. P_t shall be of sufficient magnitude to obtain accurate and meaningful load displacement data. P_t shall not exceed P_{max} as defined in 4.2.3. This test shall be repeated a minimum of three times to assess repeatability and average results.</p>	<p>C4.2.4 Stiffness Test</p>
<p>5.0 Results</p> <p>5.1 Interpretation of Results</p> <p>The data obtained from each of the flexural stiffness tests shall be plotted and the data examined to determine if the response of the specimen is linear elastic. It shall be verified that the three measured displacements at midspan were within 10% of each other throughout the testing phase. The standard deviation of the displacements measured shall be no more than 5% of the average displacement measured. If this criterion is not met, corrections may be made to the set-up/instrumentation and the tests shall be repeated. Once it is verified that the response of the deck is linear elastic, the flexural stiffness of the deck in the strong direction (D_x) shall be computed as per 5.1.1.</p>	<p>C5.0 Results</p> <p>C5.1 Interpretation of Results</p> <p>The measured displacement for all runs of the test should be approximately equal. If a single data is an outlier resulting in this criterion not being met, another run of the test shall be conducted. If the criterion is still not met, all tests shall be included in computing the average displacement and the standard deviation shall be reported for that location.</p>
<p>5.1.1 Calculation of Measured Strong Axis Flexural Stiffness</p> <p>The flexural stiffness of the deck in the strong direction (D_x) shall be based on calculated results from the best fit linear curve developed from the experimental data. The data used to develop the best fit curve shall be corrected to remove any rigid body support deformations. Once the best fit curve is determined, individual experimental displacement data shall be checked to be within +/- 15% of that predicted by the best fit curve at the respective load steps. Data that fall outside of this band shall be discarded and another test performed using the same specimen.</p> <p>From the experimentally measured response of the deck specimen, the strong-direction stiffness parameter D_x (kip-in²/in) can be calculated using</p>	<p>C5.1.1 Calculation of Measured Strong Axis Flexural Stiffness</p>

Proposed Test Method and Commentary for Determining Strong Axis Flexural Stiffness (D_x) of Bridge Decks

Eq. 1 as:

$$D_x = \frac{P' L^3}{48 \Delta_{CL}} \quad (1)$$

Where P' is the applied point load, P , divided by the deck specimen width (e.g., kip/in), L is the span length (e.g., in), and Δ_{CL} is the net vertical deflection at the center of the deck (e.g., in).

The load P' and the deflection Δ_{CL} shall be determined for any P' using the best fit linear curve.

5.1.2 Comparison of Measured Flexural Stiffness to Theoretical Flexural Stiffness

The measured flexural stiffness shall be compared to the theoretical flexural stiffness of the strong axis direction (D_x). The theoretical flexural stiffness in the strong axis (D_x) direction may be computed using the transformed area method as the elastic modulus, E , times the moment of inertia, I , for a unit width of deck.

If the measured and theoretical flexural stiffness differ by more than 15%, potential reasons for the discrepancy shall be discussed in the testing report and the measured value may be used directly. If the measured and theoretical flexural stiffness differ by more than 15%, the reasons for the discrepancy shall be investigated and adjustments made to the theoretical model to better reflect the actual behavior of the deck.

C5.1.2 Comparison of Measured Flexural Stiffness to Theoretical Flexural Stiffness

The comparison of the measured and theoretical response is intended to ensure the deck producer has a reasonable understanding as to the behavior and load distribution characteristics of the given deck. Differences of 15% or less are deemed acceptable. However, larger differences suggest the theoretical model developed by the producer is inaccurate and not capable of accurately predicting the actual response of the deck. To avoid potential problems in service due to this lack of understanding as to the actual response characteristics of the deck, it is required that the theoretical model be refined to ensure the producer more fully understands the actual behavior of the deck.

6.0 Reporting of Data

6.1 Stiffness Test Results and Observations

The following data shall be reported:

1. The displacement (at all locations), measured stresses, and the Test Load (P_t), shall be reported in tabular format for each load step.
2. The average vertical displacement at mid-span shall also be plotted vs. the Test Load (P_t).
3. The computed bridge deck strong axis flexural stiffness (D_x).
4. Theoretical bridge deck strong axis flexural stiffness (D_x) shall be reported.
5. Comparison between the measured and theoretical bridge deck strong axis flexural stiffness.

C6.0 Reporting of Data

C6.1 Stiffness Test Results and Observations

Displacements at the support locations shall be reported as well as at the load to ensure rigid body movement during testing is accounted for when determining the strong axis flexural stiffness (D_x) of the bridge deck.

Proposed Test Method and Commentary for Determining
Strong Axis Flexural Stiffness (D_x) of Bridge Decks

6.2 Miscellaneous Required Information

The following additional information shall also be reported:

- Deck type and fabricator.
- Material properties for deck components.
- Visible deviations or defects from specified.
- A drawing showing the shape, size and orientation of the specimen and the fixtures.
- A drawing showing the location of all instrumentation and the load patch.
- Section properties and detail dimensions of the specimens and supports/fixtures.
- All sensor calibrations

C6.2 Miscellaneous Required Information

**ATTACHMENT F - Proposed Test Method and Commentary for Determining
Weak Axis Flexural Stiffness (D_y) of Bridge Decks**

Proposed Test Method and Commentary for Determining Weak Axis Flexural Stiffness (D_y) of Bridge Decks

<p>1.0 General</p> <p>1.1 Scope</p> <p>This test method describes a procedure for determining the flexural stiffness of a prefabricated bridge deck about the weak axis for non-isotropic decks. This test may also be used to determine the flexural stiffness of isotropic decks.</p>	<p>C1.0 General</p> <p>C1.1 Scope</p> <p>The weak axis of a bridge deck is that which will produce a lesser flexural stiffness than that of the strong direction. However, the stiffness is significant for design and, therefore, must be known. For cases where the bridge deck is isotropic, the orientation is not a concern. Therefore, this test procedure is applicable to any type of bridge deck.</p>
<p>1.2 Summary</p> <p>This test procedure is used to determine the flexural stiffness of a prefabricated bridge deck. Data reported includes total force applied (P) at pre-determined force increments, area over which force is applied (A), and displacements at defined locations (Δ). Each test shall be repeated a minimum of three times to ensure repeatability. For each test run, the force shall be applied at a minimum of five (5) levels and the corresponding displacement data shall be recorded. The data collected shall be used to determine the flexural stiffness of the bridge deck about its weak axis (D_y).</p>	<p>C1.2 Summary</p> <p>Flexural stiffness of a bridge deck can be determined through this test method. Full-scale testing of a representative subassembly is required. The test results generate the needed data that are used to design the bridge deck per the AASHTO LRFD Bridge Design Specifications. The test results also can be used to gain a better understanding of force distribution through the deck itself. Required data to be reported includes the flexural stiffness, relationship between displacements and force applied as well as stress and force applied.</p>
<p>1.3 Approach</p> <p>Force is to be applied as a line load at midspan of the deck specimen. Resulting vertical displacements are measured and recorded at prescribed locations. The specimen shall be supported continuously along the two edges that are parallel to the applied line load. The deck is effectively subjected to one way bending/flexure. This permits direct measurement of the flexural stiffness of the deck in the orientation transverse to the line load. To determine the stiffness, the applied load, maximum displacement and length/span of the deck must be known. The weak axis flexural stiffness (D_y) can then be computed using an appropriate mathematical expression for the particular type of bridge deck under investigation.</p>	<p>C1.3 Approach</p> <p>The behavior of many bridge decks can not be simplified or idealized using simple beam models because they possess orthotropic properties. Hence, it is difficult to evaluate their stiffness properties without conducting full-scale testing.</p> <p>To isolate the stiffness in a single direction so it can be computed from the experimental measurements, a line load is applied transverse to the weak direction so that the contribution of the strong direction stiffness is negligible to the measured response. The resulting response of the deck is, therefore, bending in only one direction.</p>
<p>2.0 Specimens</p> <p>2.1 Components – General</p> <p>Specimens shall be representative full-scale subassemblies of a typical portion of a bridge deck. The specimen shall contain all components of an in-service bridge deck panel which affect load distribution. The same deck specimen may be used to determine the bending stiffness in the strong direction (D_x) and the torsional stiffness (D_{xy}) that are described in other documents. The specimen is to be supported on rigid supports</p>	<p>C2.0 Specimens</p> <p>C2.1 Components – General</p> <p>The range of specimen size was selected such that it would provide practical dimensions while maintaining an accurate representation of the full-scale bridge deck. Testing of a specimen with dimensions smaller than the recommended minimum may produce inaccurate results.</p>

Proposed Test Method and Commentary for Determining Weak Axis Flexural Stiffness (D_y) of Bridge Decks

along two sides of the specimen such that it is simply supported for bending about its weak axis as shown in Figure 1. The span between the two supports shall be a minimum of five (5) feet (1.5 m). The transverse dimension shall be sufficiently wide to include at least three of the primary load carrying members, but shall not be less than one half the span length. *(It is noted that a square specimen is required for the D_{xy} tests and hence, it may be desirable to use a square specimen for the D_y tests.)*

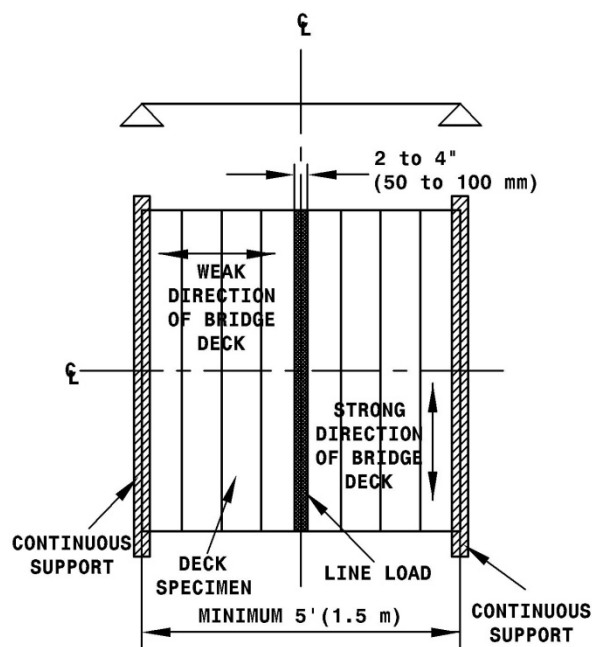


Figure 1: Weak Axis Stiffness (D_y) Test Set-up

Prior to testing, the specimen shall be visually inspected for any flaws or defects that could possibly affect the measured flexural stiffness of the bridge deck being considered. Defects and flaws shall be defined as per the appropriate governing specification (e.g. contract documents, ASTM documents, etc.). Specimens containing flaws and defects that are deemed to significantly affect the flexural stiffness of the specimen shall not be used for stiffness testing and data collection. Specimens that meet specifications but exhibit minor defects can be tested but such defects and their locations shall be documented and reported.

2.2 Instrumentation

The test specimen shall be instrumented to measure the vertical displacements of the specimen to a minimum resolution of 0.001 inches

C2.2 Instrumentation

Strain gages are required to ensure that yielding of the specimen does not occur at locations where the stress is expected to be

Proposed Test Method and Commentary for Determining Weak Axis Flexural Stiffness (D_y) of Bridge Decks

(25 μ m). Vertical displacements shall be measured over each support at three locations; at the mid-length location and at the ends. These measurements allow rigid body movement of the supports to be accounted for in the calculation of the weak-axis bending stiffness. Vertical displacements of the deck specimen shall be measured at a minimum of three locations (i.e. one in the middle and two close to the edges of the specimen) along the length of the line load to ensure that the deck is displacing uniformly. Limited strain gaging is required to monitor stresses at critical locations during testing and to understand the behavior of the deck panels. As a minimum, specimens shall be instrumented as illustrated in Figure 2.

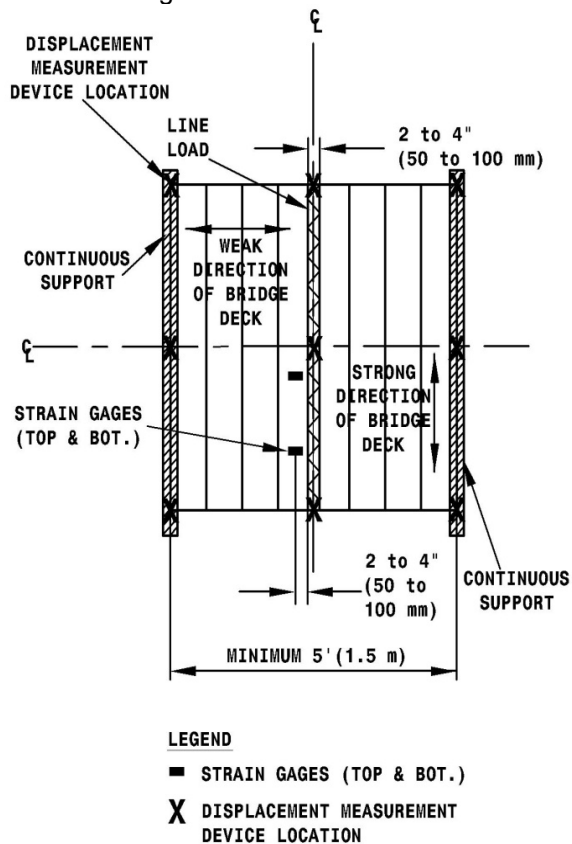


Figure 2: Minimum Instrumentation Required for Weak Axis Stiffness (D_y) Test

Instrumentation for accurately measuring applied force shall also be used. The resolution of the load measuring device shall be calibrated such that it has a resolution to 1% of maximum test load applied, P_t , as defined in 4.2.3. All sensor calibrations shall be reported.

greatest. However, exceeding the yield stress is unlikely since the applied loading will be relatively low. Strain gages can also be used to gain a greater understanding of the deck behavior.

Accurate displacement and force measurements are critical to the success of this test. It is imperative that the devices used to measure the displacements and applied forces are calibrated accurately before testing. Vertical displacement measurements are to be taken at mid-span of the specimen where the load is applied and other locations to gain a sufficiently detailed profile of the bridge panel. Vertical displacements are also to be measured at the supports to ensure there is not any rigid-body movement of the specimen as this would skew the results of the test.

Proposed Test Method and Commentary for Determining
Weak Axis Flexural Stiffness (D_y) of Bridge Decks

<p>3.0 Fixtures</p> <p>3.1 Fixture Details</p> <p>Fixtures capable of adequately supporting and loading the specimen during the test shall be provided. The fixtures shall be sufficiently stiff such that no additional displacements or stresses are generated as a result of fixture misalignments or movements. In addition, fabrication tolerances in the specimen shall be corrected or compensated for using non-mechanical means (i.e., shimming) and where required shall be reported. Dimensional tolerances of support locations shall be within +/- 1/8 in. (3 mm)</p> <p>The supporting fixtures shall be sufficiently stiff to ensure vertical displacement of the fixture is less than 0.010 inches (250 μm) under the maximum applied load. Vertical displacement of the supports shall be measured as described in 2.2. Vertical displacement of the supports under each load step shall be included in the report.</p>	<p>C3.0 Fixtures</p> <p>C3.1 Fixture Details</p>
<p>4.0 Test Procedure</p> <p>4.1 General</p> <p>A minimum of three (3) data sets are required to establish the flexural stiffness of a bridge deck panel. All data may be obtained from a single subassembly. Additionally, the same deck specimen may also be used for other stiffness tests (i.e. D_x and D_{xy}) as long as it is not damaged in any previous test. If, however, the specimen is damaged during testing, it shall not be used for any future testing.</p>	<p>C4.0 Test Procedure</p> <p>C4.1 General</p> <p>A single bridge deck panel may be used for data collection. The specimen is not to be damaged during the weak direction flexural stiffness (D_y) testing. The deck specimen used for this test may also be used to determine the flexural stiffness of the deck in the strong (D_x) direction and the torsional stiffness (D_{xy}). If a panel is damaged such that it affects the stiffness properties of the specimen, it shall be removed, and the testing shall be repeated with an undamaged specimen.</p>
<p>4.2 Loads</p> <p>Loads shall be applied using a hydraulic jack or actuator. The magnitude of the load shall be increased in equal increments pre-determined for the test. The load shall be maintained within +/- 2% at each load increment for a minimum of ten (10) seconds to allow for the collection of data. The load shall be monitored throughout the test to ensure that the desired load intervals are achieved.</p>	<p>C4.2 Loads</p> <p>Loads shall be applied through the use of hydraulic jacks or other similar loading devices. Displacements and stresses shall be monitored continuously throughout the test to ensure displacements and stresses remain below the desirable level (<i>to be determined by the individual conducting the test</i>).</p>
<p>4.2.1 Application of Load</p> <p>Load shall be applied as a line load at the midspan location of the specimen and oriented parallel to the supports using a single loading mechanism. The width of the line load (parallel to the span) shall be a minimum of 2 in. (50 mm) and maximum of 4 in. (100 mm). If a bearing pad is used, it shall have a minimum hardness of 50 durometer and a maximum thickness of 1 inch (25 mm).</p>	<p>C4.2.1 Application of Load</p> <p>The patch is typically a 1" (25 mm) thick steel plate on top of a hard rubber bearing pad, placed in contact with the deck as shown in Figure 3.</p>

Proposed Test Method and Commentary for Determining Weak Axis Flexural Stiffness (D_y) of Bridge Decks

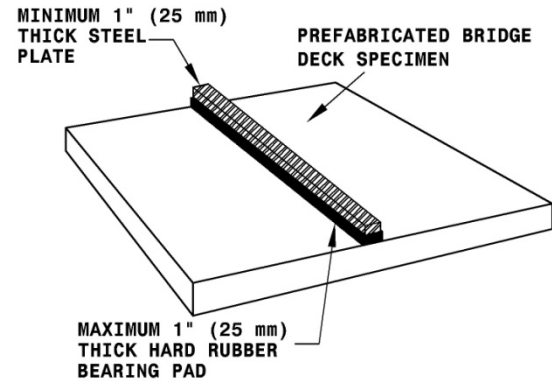


Figure 3: Typical Line Load on Bridge Deck

4.2.2 Preloading

The specimen shall be preloaded to ensure proper seating of the fixtures, specimen and patch load. During the preload phase, displacement data shall be recorded. The response of the deck (load vs. displacement) shall be verified for linearity in the upper 1/3 portion of the loading curve. The magnitude of the preload, P_s , shall be of sufficient magnitude to ensure seating of the fixtures and specimen, but shall not exceed $1/3 P_{max}$ as defined in 4.2.3. If measurements indicate nonlinear response over the entire preloading history, then the cause(s) for the nonlinearity shall be determined and corrected. Once the specimen is seated, the preload, P_s , shall be reapplied and considered the starting point (i.e., zero point) for the actual stiffness test.

C4.2.2 Preloading

4.2.3 Load Parameters

The maximum load (P_{max}) to be applied shall be determined as 50% of the minimum estimated load which produces any one the following conditions in the weak axis direction:

1. Cracking in any portion of the specimen
2. Yielding in any portion of the specimen
3. Debonding or slip of the concrete
4. Any non-linear behavior not caused by bringing the test specimen and fixtures into contact (i.e. preloading described in 4.2.2).

The Test Load, P_t , shall be computed as the difference between the maximum load, P_{max} , and the preload, P_s , (i.e. $P_t = P_{max} - P_s$).

C4.2.3 Load Parameters

The limit states described in 4.2.3 and calculated value of P_{max} (set equal to 50% of the load which could produce these limit states) were established to ensure no non-linear response is produced and to ensure the specimen is not damaged.

The load which would produce cracking, yielding, debonding, or any other non-linear behavior may be calculated using any methodology that relies on traditional mechanics solutions.

Proposed Test Method and Commentary for Determining Weak Axis Flexural Stiffness (D_y) of Bridge Decks

<p>4.2.4 Stiffness Test</p> <p>The Test Load, determined in 4.2.3, is to be divided into five equal load increments (i.e. $P_t/5$). Once the Test Load is determined and the operation of the instrumentation and data acquisition has been verified, all load shall be removed from the specimen. The preload (P_s) shall then be reapplied.</p> <p>Next, all strain gages, load, and displacement measuring devices shall be rebalanced to zero while the preload is maintained. Then, the Test Load (P_t) shall be applied in equal increments as pre-determined and shall be held at each increment for a minimum of 10 seconds to collect data. P_t shall be of sufficient magnitude to obtain accurate and meaningful load displacement data. P_t shall not exceed P_{max} as defined in 4.2.3. This test shall be repeated a minimum of three times to assess repeatability and average results.</p>	<p>C4.2.4 Stiffness Test</p>
<p>5.0 Results</p> <p>5.1 Interpretation of Results</p> <p>The data obtained from each of the flexural stiffness tests shall be plotted and the data examined to determine if the response of the specimen is linear elastic. It shall be verified that the three measured displacements at midspan were within 10% of each other throughout the testing phase. The standard deviation of the displacements measured shall be no more than 5% of the average displacement measured. If this criterion is not met, corrections may be made to the set-up/instrumentation and the test shall be repeated. Once it is verified that the response of the deck is linear elastic, the flexural stiffness of the deck in the weak direction (D_y) shall be computed as per 5.1.1.</p>	<p>C5.0 Results</p> <p>C5.1 Interpretation of Results</p> <p>The measured displacement for all runs of the test should be approximately equal. If a single data is an outlier resulting in this criterion not being met, another run of the test shall be conducted. If the criterion is still not met, all tests shall be included in computing the average displacement and the standard deviation shall be reported for that location.</p>
<p>5.1.1 Calculation of Measured Weak Axis Flextural Stiffness</p> <p>The flexural stiffness of the deck in the weak direction (D_y) shall be based on calculated results from the best fit linear curve developed from the experimental data. The data used to develop the best fit curve shall be corrected to remove any rigid body support deformations. Once the best fit curve is determined, individual experimental displacement data shall be checked to be within +/- 15% of that predicted by the best fit curve at the respective load steps. Data that fall outside of this band shall be discarded and another test performed using the same specimen.</p> <p>From the experimentally measured response of the deck specimen, the weak-direction stiffness parameter D_y (kip-in²/in) can be calculated using</p>	<p>C5.1.1 Calculation of Measured Weak Axis Flextural Stiffness</p>

Proposed Test Method and Commentary for Determining Weak Axis Flexural Stiffness (D_y) of Bridge Decks

Eq. 1 as:

$$D_y = \frac{P'L^3}{48\Delta_{CL}} \quad (1)$$

where P' is the applied point load, P , divided by the deck specimen width (e.g., kip/in), L is the span length (e.g., in), and Δ_{CL} is the net vertical deflection at the center of the deck (e.g., in).

The load P' and the deflection Δ_{CL} shall be determined for any P' using the best fit linear curve.

5.1.2 Comparision of Measured Flexural Stiffness to Theoretical Flexural Stiffness

The measured flexural stiffness shall be compared to the theoretical flexural stiffness of the weak axis direction (D_y). The theoretical flexural stiffness in the weak axis (D_y) direction may be computed using the transformed area method as the elastic modulus, E , times the moment of inertia, I , for a unit width of deck.

If the measured and theoretical flexural stiffness differ by more than 15%, potential reasons for the descrepance shall be discussed in the testing report and the measured value may be used directly. If the measured and theoretical flexural stiffness differ by more than 15%, the reasons for the descrepancy shall be investigated and adjustments made to the theoretical model to better reflect the actual behavior of the deck.

6.0 Reporting of Data

6.1 Stiffness Test Results and Observations

The following data shall be reported:

1. The displacement (at all locations), measured stresses, and the Test Load (P_t), shall be reported in tabular format for each load step.
2. The average vertical displacement at mid-span shall also be plotted vs. the Test Load (P_t).
3. The computed bridge deck weak axis flexural stiffness (D_y).
4. Theoretical bridge deck weak axis flexural stiffness (D_y) shall be reported.
5. Comparison between the measured and theoretical bridge deck weak axis flexural stiffness.

C5.1.2 Comparision of Measured Flexural Stiffness to Theoretical Flexural Stiffness

The comparison of the measured and theoretical response is intended to ensure the deck producer has a reasonable understanding as to the behavior and load distribution characteristics of the given deck. Differences of 15% or less are deemed acceptable. However, larger differences suggest the theoretical model developed by the producer is inaccurate and not cpable of accurately predicting the actual response of the deck. To avoid potential problems in service due this lack of understanding as to the actual response characteristics of the deck, it is required that the theoretical model be refined to ensure the producer more fully understands the actual behavior of the deck.

C6.0 Reporting of Data

C6.1 Stiffness Test Results and Observations

Displacements at the support locations shall be reported as well as at the load to ensure rigid body movement during testing is accounted for when determining the weak axis flexural stiffness (D_y) of the bridge deck.

Proposed Test Method and Commentary for Determining
Weak Axis Flexural Stiffness (D_y) of Bridge Decks

6.2 Miscellaneous Required Information

The following additional information shall also be reported.

- Deck type and fabricator.
- Material properties for deck components.
- Visible deviations or defects from specified.
- A drawing showing the shape, size and orientation of the specimen and the fixtures.
- A drawing showing the location of all instrumentation and the load patch.
- Section properties and detail dimensions of the specimens and supports/fixtures.
- All sensor calibrations

C6.2 Miscellaneous Required Information

**ATTACHMENT G - Proposed Test Method and Commentary for Determining
Torsional Stiffness (D_{xy}) of Bridge Decks**

Proposed Test Method and Commentary for Determining Torsional Stiffness (D_{xy}) of Bridge Decks

<p>1.0 General</p> <p>1.1 Scope</p> <p>This test method describes a procedure for determining the torsional stiffness of prefabricated bridge decks (i.e. stiffness for loading that induces simultaneous bending about both the strong axis and weak axis).</p>	<p>C1.0 General</p> <p>C1.1 Scope</p> <p>Bridge deck panels typically do not have a significant torsional stiffness. For design, it is useful to determine the stiffness of the bridge deck in all loading directions. This test method is applicable to any type of prefabricated bridge deck.</p>
<p>1.2 Summary</p> <p>This test procedure is used to determine the torsional stiffness of a prefabricated bridge deck. Data reported includes total force applied (P) at pre-determined load increments, area over which force is applied (A), and displacements at defined locations (Δ). Each test shall be repeated a minimum of three times to ensure repeatability. For each run of a test, a minimum of five (5) force levels shall be applied to the specimen and the corresponding displacement data shall be recorded. The data collected shall be used to determine the torsional stiffness (D_{xy}) of the bridge deck specimen.</p>	<p>C1.2 Summary</p> <p>Torsional stiffness of a bridge deck can be determined through this test method. Full-scale testing of a representative subassembly sample is required. The test results generate the needed data that are used to design the bridge deck per the AASHTO LRFD Bridge Design Specifications. The test results can also be used to gain a better understanding of force distribution through the deck itself. Data reported includes displacements, total force applied, area and location of load application, dimensions and details of deck specimen, relationship between displacements and total force applied as well as stress and total force applied.</p>
<p>1.3 Approach</p> <p>The deck is to be supported at three of the four corners of the deck. Force is to be applied as a point load at the free corner of the bridge deck and displacements of the specimen are recorded at prescribed locations.</p> <p>To determine the torsional stiffness, the applied load, maximum displacement and length/span of the deck are required. The torsional stiffness (D_{xy}) can then be computed using an appropriate mathematical expression for the particular type of bridge deck.</p>	<p>C1.3 Approach</p> <p>Although bridge decks are not typically loaded in torsion alone, the torsional stiffness of many prefabricated deck types is required to ensure an accurate estimate of the bending in the strong and weak axis directions as many decks do not act as a simple beam and have unique properties that make them difficult to evaluate.</p> <p>The applied load and length of the specimen are required to compute the torsional stiffness.</p>
<p>2.0 Specimens</p> <p>2.1 Components – General</p> <p>Specimens shall be representative, full-scale subassemblies of a typical portion of a bridge deck. The specimen shall contain all components of an in-service bridge deck panel which affect load distribution. The same deck specimen may be used for the bending stiffness in the strong direction (D_x) and weak direction (D_y) that are described in other documents. The specimen is to be supported on a rigid point support at opposite corners. A third corner of the specimen, opposite to the free corner where the loading is applied, shall also be placed on a point support as shown in Figure 1.</p>	<p>C2.0 Specimens</p> <p>C2.1 Components – General</p> <p>The range of specimen size was selected such that it would be practical while maintaining an accurate representation of the full bridge deck. Testing of a specimen with dimensions smaller than the recommended minimum may produce inaccurate results.</p>

Proposed Test Method and Commentary for Determining Torsional Stiffness (D_{xy}) of Bridge Decks

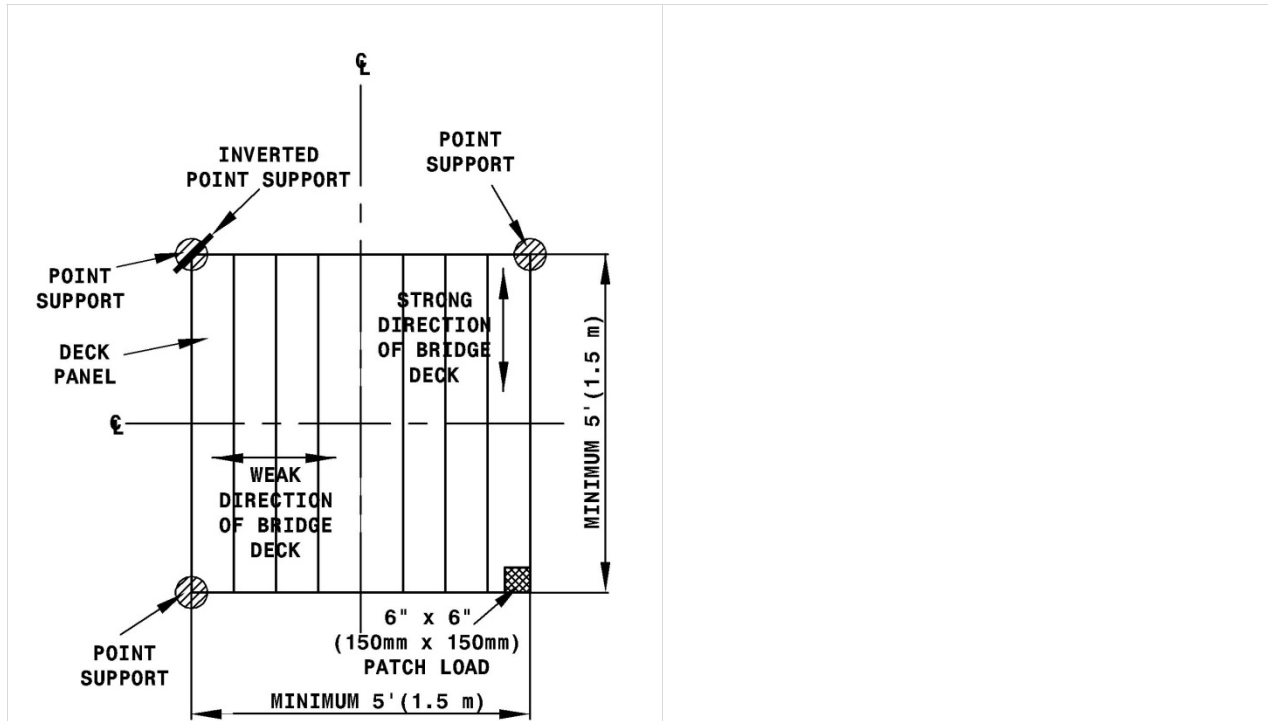


Figure 1: Torsional Stiffness (D_{xy}) Test Set-up

In addition, the third corner shall also have an inverted point support at the corner (i.e., the support must be able to resist uplift of the specimen). The span between any two adjacent point supports shall be a minimum of 5 feet (1.5 m). The deck specimen shall have equal length and width dimensions (i.e. a square).

Prior to testing, the specimen shall be visually inspected for any flaws or defects that could possibly affect the torsional stiffness of the bridge deck being considered. Defects and flaws shall be defined as per the appropriate governing specification (e.g., contract specifications, ASTM's, etc.). Specimens containing flaws and defects that are deemed to significantly affect the torsional stiffness of the specimen shall not be used for stiffness testing and data collection. Specimens that meet the specifications but exhibit minor defects can be tested but such defects and their locations shall be documented and reported.

2.2 Instrumentation

The test specimen shall be instrumented to measure the vertical displacement of the specimen to a minimum resolution of 0.001 inches (25 μ m). Vertical displacements shall be measured over each support. These measurements allow rigid body movement to be accounted for in the

C2.2 Instrumentation

Strain gages are not required because significant stress will not be produced during this test. However, it is suggested to use the same strain gage recommendations as per the proposed Bridge Deck Strong (D_x) and Weak (D_y) Axis Stiffness Test Specification. This will ensure that

Proposed Test Method and Commentary for Determining Torsional Stiffness (D_{xy}) of Bridge Decks

calculation of the torsional stiffness. Vertical displacements shall be measured at a minimum of two additional locations; the center of the specimen and the location of maximum displacement (i.e. at the free corner of the deck where the load is applied).

Strain gaging is not required to monitor stresses during testing of the deck panels. As a minimum, specimens shall be instrumented as illustrated in Figure 2.

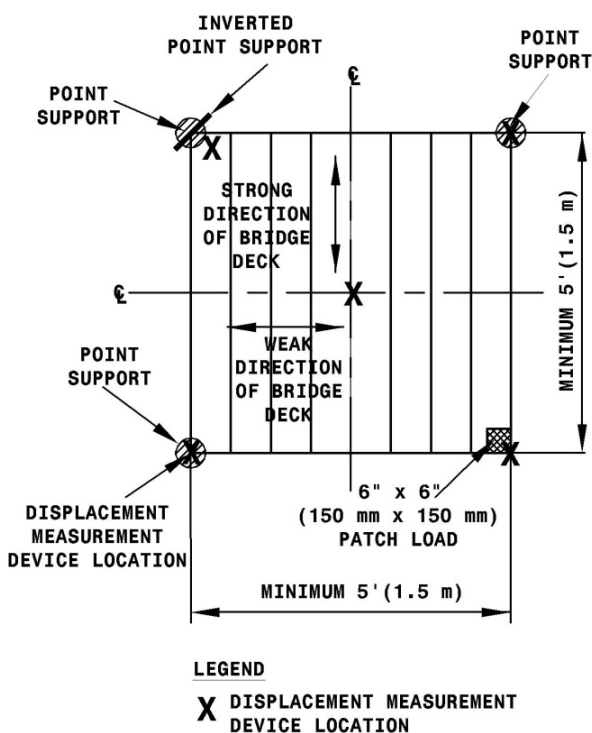


Figure 2: Minimum Instrumentation Required for Torsional Stiffness (D_{xy}) Test

Instrumentation for accurately measuring the applied force shall also be used. The resolution of the load measuring device shall be calibrated such that it has a resolution to 1% of maximum test load applied, P_t , as defined in 4.2.3. All sensor calibrations shall be reported.

yielding of the specimen does not occur. However, as previously discussed, exceeding the yield stress should not be a great concern since the loading will be relatively low. Strain gages can also be used to gain a greater understanding of the deck behavior.

The displacement and force measurements are critical to success of this test. It is imperative that the devices used to measure the displacements are calibrated accurately before testing. Vertical displacement measurements are to be taken at the free corner of the specimen where the load is applied, the center of the specimen and other locations to gain a sufficiently detailed profile of the bridge panel. Vertical displacements are also to be measured at the supports to ensure there is not any rigid-body movement of the specimen as this would skew the results of the test.

It is noted that the required force to induce significant displacement is rather low in some types of open grid decks and partially filled grid decks. In such cases, it may be preferable to use calibrated weights (e.g., steel plates) to apply the load.

3.0 Fixtures

3.1 Fixture Details

Fixtures capable of adequately supporting and securing the specimen during the test shall be provided. The fixtures shall be fabricated such that no additional displacements or stresses are generated as a result of fixture misalignments or movements. In addition, fabrication errors in the specimen shall be corrected or compensated for using non-mechanical means (i.e., shimming) and where required shall be reported. Dimensional

C3.0 Fixtures

Proposed Test Method and Commentary for Determining Torsional Stiffness (D_{xy}) of Bridge Decks

<p>tolerances of support locations shall be within +/- 1/8 in. (3 mm).</p> <p>The supporting fixtures shall be sufficiently stiff to ensure vertical displacement of the fixture is less than 0.010 inches (250 μm) under the maximum applied load. Vertical displacement of the supports shall be measured as described in 2.2. Vertical displacement of the supports under each load step shall be included in the report.</p>	
<p>4.0 Test Procedure</p> <p>4.1 General</p> <p>A minimum of three (3) data sets are required to establish the torsional stiffness of a bridge deck panel. All data may be obtained from a single subassembly. Additionally, the same deck specimen may also be used for the bending stiffness tests (D_x and D_y) as long as it is not damaged in any previous test. If, however, the specimen is damaged during testing, it shall not be used for any future testing.</p>	<p>C4.0 Test Procedure</p> <p>C4.1 General</p> <p>A single bridge deck panel may be used for data collection. The specimen is not to be damaged during the torsional stiffness testing. The deck specimen used for this test may also be used to determine the flexural stiffness of the deck in the strong (D_x) and weak (D_y) directions. If a panel is damaged so that it affects the stiffness properties of the specimen, it shall be removed and the testing shall be repeated with an undamaged specimen.</p>
<p>4.2 Loads</p> <p>Load shall may be applied through various means included calibrated weights, a hydraulic jack or actuator. The magnitude of the load shall be increased in equal increments pre-determined for the test. The load shall be maintained within +/- 2% at each load increment for a minimum of ten (10) seconds to allow for the collection of data. The load shall be recorded and monitored throughout the test to ensure that the desired load intervals are achieved.</p>	<p>C4.2 Loads</p> <p>The torsional stiffness of bridge deck panels is typically extremely low. Steel plates of known weight can be used for loading to control the loading at a very low magnitude. Displacements and stresses shall be monitored continuously throughout the test to ensure displacements and stresses remain below a desirable level.</p>
<p>4.2.1 Application of Load</p> <p>Load shall be applied through a single 6"x 6" (150 x 150 mm) patch. The patch is typically a steel plate. It can be placed on top of a hard rubber bearing pad, having a minimum hardness of 50 durometer and maximum thickness of 1/2" (13 mm), to improve distribution of the patch load. The patch is applied as the first load interval on the deck and then used as the base on which to apply more load with additional plates. The patch load shall be placed at the free corner of the specimen.</p>	<p>C4.2.1 Application of Load</p> <p>It is noted that the bearing pad also increases the friction between applied load and the specimen which helps to ensure that the applied load does not slide as the deck deflects. This is particularly important in grid decks if calibrated weights are used.</p>
<p>4.2.2 Preloading</p> <p>Since bridge decks are typically very flexible in torsion, it may not be necessary for the specimen to be preloaded to ensure proper seating of the fixtures, specimen and patch load. If it is deemed that a preload is necessary, displacement data shall be recorded during the preload phase. The response of the deck (load vs. displacement) shall</p>	<p>C4.2.2 Preloading</p> <p>Preloading of the specimen is an effective method to "shake down" the setup and identify potential issues that could affect the testing results.</p>

Proposed Test Method and Commentary for Determining Torsional Stiffness (D_{xy}) of Bridge Decks

<p>be verified for linearity in the upper 1/3 portion of the loading curve. The magnitude of the preload, P_s, shall be enough to ensure seating of the fixtures and specimen, but shall not exceed 1/3 P_{max} as defined in 4.2.3. If measurements indicate nonlinear response over the entire preloading history, then the cause(s) for the nonlinearity shall be determined and corrected. Once the specimen is seated, the preload, P_s, shall be reapplied and considered the starting point (i.e., zero point) for the actual stiffness test.</p>	
<p>4.2.3 Load Parameters</p> <p>The maximum load, P_{max}, shall be determined as 50% of the minimum estimated load which produces any one the following conditions in torsion:</p> <ol style="list-style-type: none"> 1. Cracking in any portion of the specimen 2. Yielding in any portion of the specimen 3. Debonding or slip of concrete 4. Any non-linear behavior not caused by bringing the test specimen and fixtures into contact (i.e. preloading). <p>The Test Load, P_t, shall be computed as the difference between the maximum load, P_{max}, and the preload, P_s (i.e. $P_t = P_{max} - P_s$).</p>	<p>4.2.3 Load Parameters</p> <p>The limit states described in 4.2.3 and calculated value of P_{max} (set equal to 50% of the load which could produce these limit states) were established to ensure no non-linear response is produced and to ensure the specimen is not damaged.</p> <p>The load which would produce cracking, yielding, debonding, or any other non-linear behavior may be calculated using any methodology that relies on traditional mechanics solutions.</p>
<p>4.2.4 Stiffness Test</p> <p>The Test Load (P_t), determined in 4.2.3, is to be divided into five equal load increments (i.e. $P_t/5$). Once the Test Load is determined and the instrumentation and data acquisition have been verified, all load shall be removed from the specimen. The preload (P_s) shall then be reapplied (if required).</p> <p>Next, all strain gages, load, and displacement measuring devices shall be rebalanced to zero while the preload is maintained. Then, the Test Load (P_t) shall be applied in equal increments as pre-determined and shall be held at each increment for a minimum of ten seconds to collect data. P_t shall be of sufficient magnitude to obtain accurate and meaningful load displacement data. P_t shall not exceed P_{max} as defined in 4.2.3. This test shall be repeated a minimum of three times to assess repeatability and average results.</p>	<p>C4.2.4 Stiffness Test</p>
<p>5.0 Results</p> <p>5.1 Interpretation of Results</p> <p>The data obtained from each run of the torsional stiffness test shall be plotted and the data</p>	<p>C5.0 Results</p> <p>C5.1 Interpretation of Results</p> <p>The measured displacement for all runs of the test should be approximately equal. Any single</p>

Proposed Test Method and Commentary for Determining Torsional Stiffness (D_{xy}) of Bridge Decks

<p>examined to determine if the response of the specimen is linear elastic. The standard deviation of the displacements measured shall be no more than 5% of the average displacement measured. Once it is verified that the response of the deck is linear elastic, the torsional stiffness (D_{xy}) of the deck shall be computed as per 5.1.1.</p>	<p>data not meeting this requirement results in this criterion not being met, another run of the test shall be conducted. If the criterion is still not met, all tests shall be included in computing the average displacement and the standard deviation shall be reported for that location.</p>
<p>5.1.1 Calculation of Measured Torsional Stiffness</p> <p>The torsional stiffness (D_{xy}) of the deck shall be based on calculated results from the best fit linear curve fit of the data. The data used to develop the best fit curve shall be corrected to remove any rigid body support deformations. Once the best fit curve is determined, individual experimental displacement data shall be checked to be within +/- 15% of that predicted by the best fit curve at the respective load steps. Data that fall outside of this band shall be discarded and another test performed using the same specimen.</p> <p>From the experimentally measured response of the deck specimen, the torsional stiffness parameter D_{xy} (kip-in²/in) can be calculated using Eq. 1 as:</p> $D_{xy} = \frac{P L^2}{4\Delta_L} \quad (1)$ <p>where P is the point load applied at the corner (kips), Δ_L is the vertical deflection the corner under the point load (in), and L is the span length (in). The resulting α values can be computed as:</p> $\alpha = \frac{2D_{xy}}{\sqrt{D_x D_y}} \quad (2)$ <p>where D_x is the strong-direction stiffness of the deck and D_y is the weak-direction stiffness of the deck defined in other documents.</p>	<p>D_x shall be determined in accordance with the "Proposed Recommended Method for Determining Strong Axis Flexural Stiffness (D_x) of Bridge Decks."</p> <p>D_y shall be determined in accordance with the "Proposed Recommended Method for Determining Weak Axis Flexural Stiffness (D_y) of Bridge Decks."</p>
<p>6.0 Reporting of Data</p> <p>6.1 Stiffness Test Results and Observations</p> <p>The following data shall be reported:</p> <ol style="list-style-type: none"> 1. The displacement (at all locations), measured stresses, and the Test Load (P_t), shall be reported in tabular format for each load step. 2. The vertical displacement under the point load shall also be plotted vs. the Test Load (P_t). 3. The computed bridge deck torsional stiffness (D_{xy}) and resulting α value. 	<p>C6.0 Reporting of Data</p> <p>C6.1 Stiffness Test Results and Observations</p> <p>Displacements at the support locations as well as at the load shall be reported to ensure that rigid body movement during testing is accounted for when determining the torsional stiffness (D_{xy}) of the bridge deck.</p>

Proposed Test Method and Commentary for Determining
Torsional Stiffness (D_{xy}) of Bridge Decks

6.2 Miscellaneous Required Information

The following additional information shall also be reported.

- Deck type and fabricator
- Material properties for deck components.
- Visible defects or deviations from specified.
- A drawing showing the shape, size and orientation of the specimen and the fixtures.
- A drawing showing the locations of all instrumentation and the load patch.
- Section properties and detail dimensions of the specimens and supports/fixtures.
- All sensor calibrations

**ATTACHMENT H - Proposed Test Method and Commentary for Subassembly Cyclic
Load Testing of Longitudinal Splices in Prefabricated Bridge Deck Panels**

Proposed Test Method and Commentary for Subassembly Cyclic Load Testing of Longitudinal Splices in Prefabricated Bridge Deck Panels

<p>1.0 General</p> <p>1.1 Scope</p> <p>This test method describes a procedure for assessing the fatigue resistance of longitudinal splices of prefabricated bridge deck panels. Longitudinal splices are structural details in bridge decks that join together two prefabricated panels transverse to the direction of traffic.</p>	<p>C1.0 General</p> <p>C1.1 Scope</p> <p>Longitudinal splice details are typically located over a stringer/girder where two prefabricated deck panels meet. Hence, this testing specification was developed with that type of detailing in mind. The specimen could easily be adapted to other longitudinal splice locations. The centerline of the longitudinal splice, as defined herein, runs parallel to the direction of traffic.</p>
<p>1.2 Summary</p> <p>This test procedure can be used to evaluate the resistance and durability of a longitudinal splice connecting prefabricated deck panels subjected to cyclic (i.e., fatigue) loading. Data reported includes the load range (ΔP), nominal stress range at selected locations (S_r), and the number of cycles (N_f) at test termination.</p>	<p>C1.2 Summary</p> <p>The applied cyclic loading is intended to reveal and identify potential metal fatigue as well as other durability issues which occur under repeated loading. The procedures described herein are applicable to both shop and field splices.</p>
<p>1.3 Approach</p> <p>A subassembly specimen representative of the in-service bridge deck shall be used to evaluate the durability and cyclic load (i.e., fatigue) resistance of the longitudinal splice. Occasional heavy loads mixed in with normal traffic are also simulated intermittently through the use of static tests. Stresses and displacement shall be monitored to evaluate the changes in behavior throughout the test. This test is intended to reveal and identify deficiencies in the longitudinal splice and deck that would be likely to occur for the in-service bridge deck.</p>	<p>C1.3 Approach</p> <p>The load is applied through two load patches in full contact with the deck. This is intended to simulate a typical truck axle.</p> <p>The application of a heavier load is intended to incorporate a wider load spectrum and the effects of heavier vehicles that are part of normal traffic.</p> <p>Stresses are monitored mainly in the area of the critical detail (i.e., longitudinal splice).</p> <p>Visual inspections are to be carried out regularly throughout the test to identify any damage to the subassembly.</p>
<p>2.0 Specimens</p> <p>2.1 Components – General</p> <p>Specimens shall be representative full-scale subassemblies of the bridge deck type under investigation. The specimen shall contain all components of the bridge deck panel which affect in-service load distribution. The width dimension of each deck panel shall be sufficiently wide to include at least three of the primary load carrying members, but shall not be less than one half the span length of the test specimen.</p> <p>The deck specimen shall be carried on three support beams (e.g., stringers) which provide similar stiffness and deflections of those expected for the in-service bridge. Further, the supporting members shall be sized so that the resulting stress ranges in those members are comparable to those that would be observed in the field. The beams shall be placed on rigid supports at each end. The orientation of the deck and beams shall represent that of the in-service bridge, as shown in Figure 1.</p>	<p>C2.0 Specimens</p> <p>C2.1 Components –General</p> <p>All components effecting load distribution must be included in the test to ensure that the test accurately simulates all localized behavior of the in-service bridge deck.</p> <p>The width dimension of the deck shall be sufficiently wide to ensure the load distribution is such that the failure mode of the specimen is not altered.</p> <p>Supports are not required to be the same cross section as used in the field, but should be proportioned such that the expected deformations and stresses in the deck and supports that would be observed in the real structure shall be reasonably represented.</p> <p>Supporting beams that are too flexible will sometimes produce misleading results. Three support beams are used since the splice detail,</p>

Proposed Test Method and Commentary for Subassembly Cyclic Load Testing of Longitudinal Splices in Prefabricated Bridge Deck Panels

Prior to testing, the specimen shall be visually inspected for any flaws or defects that could possibly affect the fatigue resistance of the longitudinal splice and bridge deck being considered. Defects and flaws shall be defined as per the appropriate governing specification (e.g., contract documents, ASTM standards, etc.). Specimens containing flaws and defects that are deemed to affect the performance and/or resistance of the specimen shall not be used. Specimens that meet the appropriate governing specifications but exhibit minor defects can be tested but such defects and their locations shall be documented and reported.

located in the transverse negative moment region of the deck (i.e., of the interior support beam), is the only area of concern for this test.

It is noted that the same deck specimen may be used for the test method described in the "Proposed Recommended Method for Verifying Strength of Bridge Decks" if the specimen is not damaged such that it would produce unreliable/unrealistic data for a test.

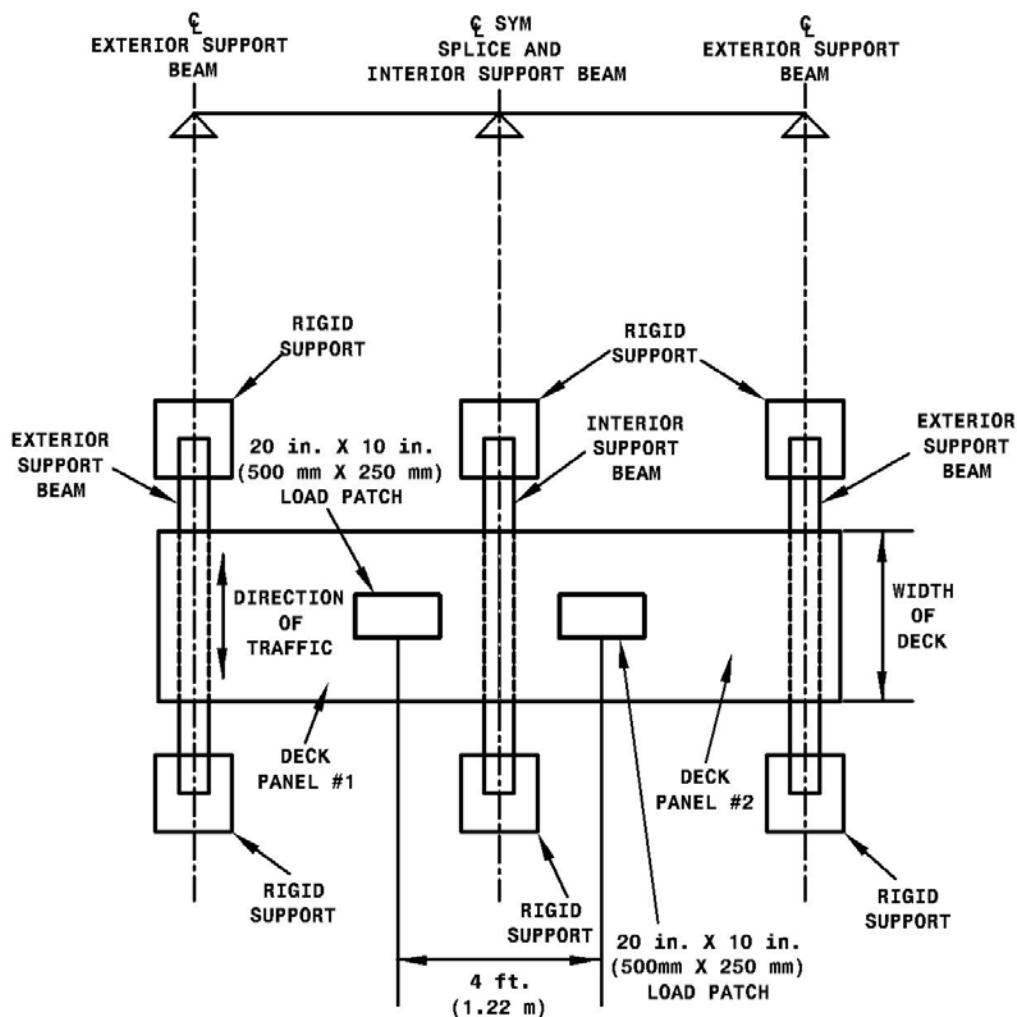


Figure 1: Longitudinal Splice Test Set-up

Proposed Test Method and Commentary for Subassembly Cyclic Load Testing of Longitudinal Splices in Prefabricated Bridge Deck Panels

2.2 Instrumentation

The test specimen shall be instrumented to measure the vertical displacement of the specimen to a minimum resolution of 0.001 in. (25 μm). Vertical displacements shall be measured at mid width of the deck at each support (e.g., midspan of each support beam). Vertical displacements shall also be measured under each load patch as shown in Figure 2.

Sufficient strain gaging is required to monitor stresses at critical locations (i.e., the longitudinal splice) during testing and to understand the behavior of the longitudinal splice and deck panels. The data collected at these locations shall be used to determine the behavior and stresses at the longitudinal splice

The applied force shall also be measured. The resolution of the load measuring device shall be calibrated such that it has a resolution to 1% of the maximum load in the load range. All sensor calibrations shall be reported.

C2.2 Instrumentation

A total of five vertical displacement measurement locations are required to obtain a profile of the deck displacements.

Strain gages are required mainly in the area of the longitudinal splice to determine the stress range of the detail of concern. For example, on the reinforcing steel, grid deck members, or other components. The detail(s) shall be instrumented at sufficient locations along the splice with strain gages to ensure that relevant data is obtained. This test method assumes the user has sufficient knowledge regarding the deck type under consideration to formulate a meaningful instrumentation plan. The owner and manufacturer should agree upon the amount and location of instrumentation.

Proposed Test Method and Commentary for Subassembly Cyclic Load Testing of Longitudinal Splices in Prefabricated Bridge Deck Panels

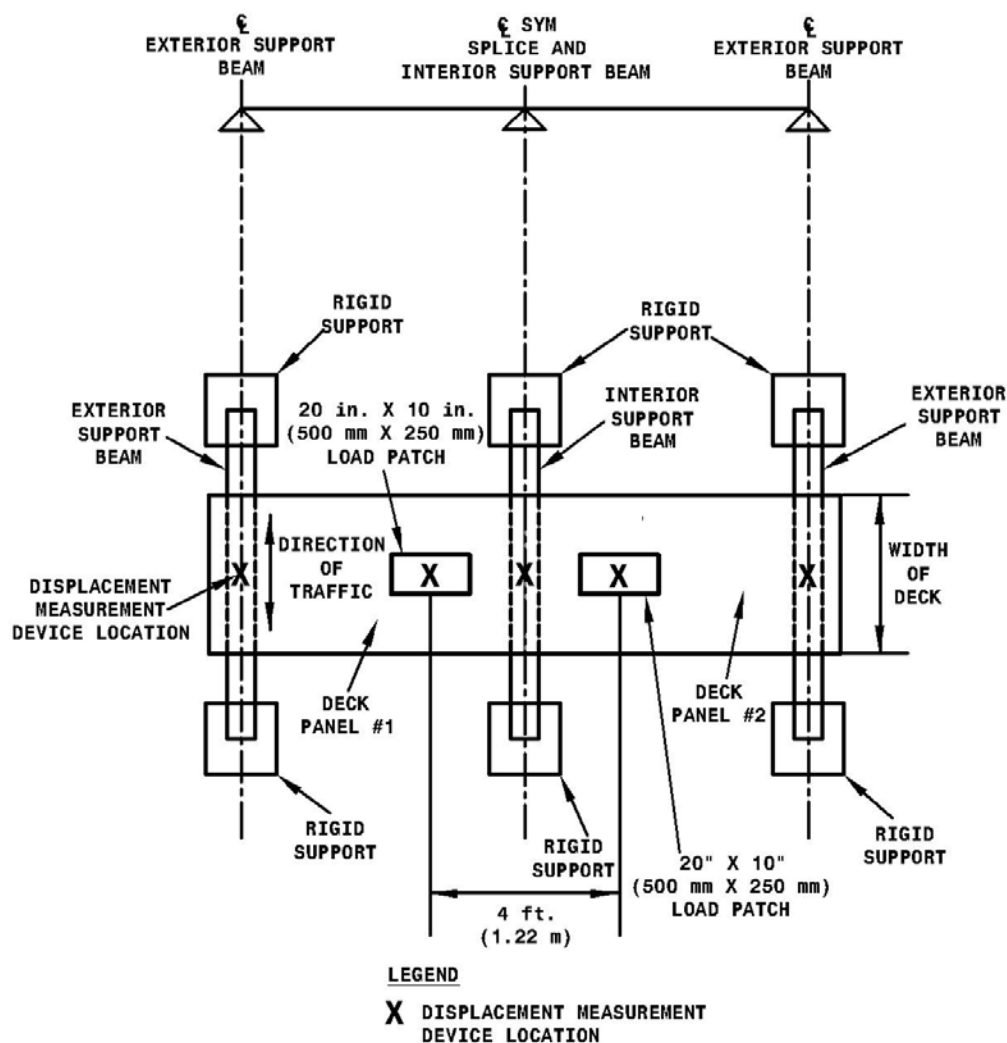


Figure 2: Minimum Instrumentation Required for Longitudinal Splice Test

3.0 Fixtures

3.1 Fixture Details

Fixtures capable of adequately supporting and securing the specimen during the test shall be provided. The fixtures shall be fabricated such that no additional displacements or stresses are generated as a result of fixture misalignments or movements. In addition, fabrication errors in the specimen shall be corrected or compensated for using non-mechanical means (i.e., shimming) and where required shall be reported. Dimensional tolerances of support locations shall be within $\pm 1/8$ in. (3 mm).

3.2 Support Beams/Stringers

The support beams or stringers shall be designed such that they adequately model the stiffness and stresses that are expected to be experienced for the in-service bridge.

C3.0 Fixtures

C3.1 Fixture Details

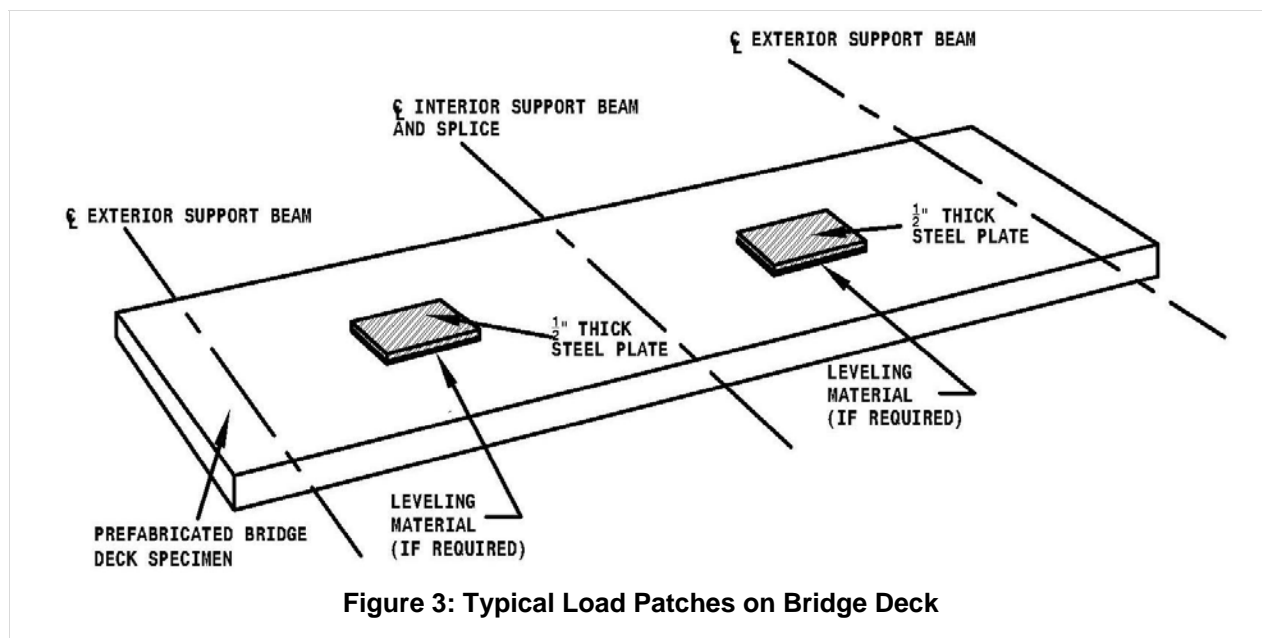
C3.2 Support Beams/Stringers

The support beams or stringers shall reasonably simulate the support conditions that are used for the actual bridge. Using supports that are excessively flexible is not permitted as this will

Proposed Test Method and Commentary for Subassembly Cyclic Load Testing of Longitudinal Splices in Prefabricated Bridge Deck Panels

	<p>significantly alter the negative moment over the interior support beam and may lead to unconservative results. Use of support beams that are slightly stiffer than needed will generally result in conservative results for the negative moment at the longitudinal splice.</p>
<p>3.3 Deck Connection to Superstructure</p> <p>The deck shall be attached to the superstructure (i.e., the support beams) using the same type of connections as will be used in the field.</p>	<p>C3.3 Deck Connection to Superstructure</p> <p>The deck-to-superstructure connection is an important component that affects the overall performance of the assembly. Since, this test is intended to reveal any deficiencies of the entire deck system, it is appropriate to accurately simulate this connection.</p>
<p>4.0 Cyclic Load Test Procedure</p> <p>4.1 General</p> <p>When multiple data sets are required, the deck specimen(s) themselves may not be reused. The fixtures and support beams may be reused as long as they are not damaged. Damaged fixtures and support beams shall be replaced and meet the requirements of 3.1 and 3.2.</p>	<p>C4.0 Cyclic Load Test Procedure</p> <p>C4.1 General</p> <p>For short span bridges or those with limited deck areas, it may not be necessary to perform more than one test. However, for bridges with large deck areas containing numerous longitudinal splices, the owner may wish to consider requiring more than one test (e.g., 3 to 5) to obtain additional confidence in the performance of the deck system and ensure repeatability of results.</p>
<p>4.2 Loads</p> <p>Load shall be applied through a hydraulic actuator or other similar loading device. The magnitude of the load range (ΔP) shall be maintained throughout the entire test (i.e., "load control"). The load range shall be monitored throughout testing to ensure that the target maximum and minimum load, and load range are being maintained. The load shall only be applied vertically (i.e., no horizontal component).</p>	<p>C4.2 Loads</p>
<p>4.2.1 Application of Load</p> <p>Load shall be applied equally through two load patches 20 in. (500 mm) long and 10 in. (250 mm) wide. The patches typically consist of steel plates placed in contact with the deck as shown in Figure 3.</p> <p>The load patches shall be oriented on the deck such that they represent wheel loads travelling in the direction of traffic. A spacing of 4 ft. (1.22 m) on center shall be used with each patch an equal distance away from the centerline of the splice, as previously shown in Figure 2, to produce the desired negative moment.</p>	<p>C4.2.1 Application of Load</p> <p>A spacing of 4 ft. (1.22 m) on center between patch loads corresponds to the lateral spacing between two trucks side by side. Leveling material (e.g., hydro stone) may be used to bring the load patches into full contact with the deck, if necessary.</p>

Proposed Test Method and Commentary for Subassembly Cyclic Load Testing of Longitudinal Splices in Prefabricated Bridge Deck Panels



4.2.2 Magnitude of Cyclic Load Range

For fatigue, the applied cyclic axle load range is 13.8 kips (61.4 kN). This load range, ΔP , is the minimum effective axle load that shall be applied. The axle load may be increased by a factor, S_{amp} , to decrease the time that it takes to complete the cyclic load test. The maximum value of S_{amp} shall be less than or equal to 3.0.

C4.2.2 Magnitude of Cyclic Load Range

The minimum applied load range is determined by applying a load factor of 0.75 to a single rear axle of the HS20 design truck tandem. In performing this test, it must be recognized that the individual rear axles of the HS20 actually simulate a tandem axle.

Multiplying the HS20 load by the factor of 0.75 yields the same effective load range and hence, effective stress range, S_{reff} prescribed by the AASHTO LRFD Bridge Design Specifications for finite life fatigue design.

The impact factor is set at 1.15 and is the dynamic load allowance for the fatigue limit state as specified by the AASHTO LRFD Bridge Design Specifications. Hence, the actual axle load is $(0.75 \times 32 \text{ kips} \times 1.15IF)/2 \text{ axles} = 13.8 \text{ kips/axle}$ (61.4 kN).

The limitation of 3.0 for S_{amp} is to prevent the user from selecting a load that is unrealistically high and may result in a different failure mode than what would be observed under service conditions. S_{amp} will commonly be set to 2.0 as that corresponds to the upper bound fatigue limit state load for infinite life prescribed in the AASHTO LRFD Bridge Design Specifications and is a realistic axle load.

Proposed Test Method and Commentary for Subassembly Cyclic Load Testing of Longitudinal Splices in Prefabricated Bridge Deck Panels

The projected ADTT shall be used to determine the required number of cycles to be applied for the cyclic load test of the subassembly. To compute the number of cycles to be applied for the cyclic load test:

$$N = (365 \text{ days/year})(75 \text{ years})(4.5 \text{ cycles/truck})(ADTT)_{SL}$$

where:

N = total number of cycles of stress range to be applied to the in-service bridge deck over its design life

$(ADTT)_{SL}$ = the single lane ADTT determined using the projected ADTT for the bridge.

The total number of cycles is assumed to be inversely proportional to the cube of the load range. Therefore, the number of cycles to be applied for the cyclic load test may be computed as:

$$N_f = N / (S_{amp})^3$$

where:

N_f = number of cycles at the desired load range to be applied for the cyclic load test

S_{amp} = factor by which load range is increased (i.e., amplified) from the HS15 axle

The load range applied shall not be so large as to alter the failure mode that would be observed in service conditions. The applied load shall not cause the yield stress to be exceeded in any portion of the specimen.

4.2.3 Vibration of Bridge Deck

A high frequency pneumatic vibrator or similar device shall be used to simulate the effect of vibrations caused by trucks passing over the bridge. The vibrator shall be rigidly attached to a support beam nearest to the longitudinal splice no more than two feet (610 mm) away from the outside edge of the deck. The vibrator shall be excited after the application of every 500,000 load cycles. The vibrator shall apply 50,000 cycles each interval and shall preferably be applied simultaneously with the application of the load cycles. The vibrator shall be excited prior to conducting the static tests at these intervals. The vibrator shall be capable of operating between 80 Hz and 120 Hz and produce a force range of 8 kips to 12 kips.

If the cyclic load test is terminated prior to any

The projected ADTT shall be acquired from the owner (e.g., DOT). This number of cycles shall be used and proportioned based on the increase in load range for the cyclic load test according to the relationship shown.

If a design life other than 75 years is desired, the appropriate design life may be used to compute the total number of cycles of stress range to be applied over the design life, N. It is noted that the 75 year life may be too excessive for most bridge decks.

The single lane ADTT shall be determined as :

$$(ADTT)_{SL} = p \times (ADTT)$$

where:

$(ADTT)$ = projected number of trucks per day in one direction averaged over the design life.

p = fraction of traffic in a single lane (Table 3.6.1.4.2-1 (AASHTO LRFD))

It is assumed that the S-N cubic relationship used for metal fatigue can be used for this application.

C4.2.3 Vibration of Bridge Deck

Vibrations caused by the passing of trucks and wheel impacts can play a role in the stresses/deflections experienced by the bridge deck and connections to the superstructure. Some connection details may also loosen or fail in service due to vibrations from passing trucks. The application of the load range alone would not truly represent the full spectrum of dynamic loading of truck traffic. Although it is not essential the vibratory cycles and load cycles be applied concurrently, it is preferred. The 50,000 vibratory cycles every 500,000 load cycles was arbitrarily set as 10% of the load cycles. A greater percentage should be considered if the joints are located near traffic metering devices such as toll facilities, traffic signals, etc. However, it would seem that there would be no need to apply more than 25% of the

Proposed Test Method and Commentary for Subassembly Cyclic Load Testing of Longitudinal Splices in Prefabricated Bridge Deck Panels

damage and the desired number of cycles is reached, the vibrator shall be excited for a minimum of 50,000 cycles prior to conducting the final static test.	load cycles. The vibrator shall be excited prior to conducting the static tests at these intervals to simulate the vibrations from trucks passing over the deck. The vibrator used during the development of this test was a Vibco model number SVRLS 8000.
5.0 Static Test Procedure	C5.0 Static Test Procedure
5.1 General Static tests shall be conducted regularly throughout the cyclic load test to monitor the change in stress range, displacements, and to infer if there is any damage of the longitudinal splice and deck.	C5.1 General
5.2 Loads for Static Tests The strength load shall be applied for the static tests. The magnitude of the strength load shall be as defined in 5.2.2. The static loads shall be applied in a minimum of five increasing and approximately equal steps until the target static load (i.e., strength load) is achieved. A load interval equal to the load used in the cyclic load testing portion of the test shall be included in the load steps. The load shall be maintained within +/- 2% at each load increment for a minimum of ten seconds to allow for the collection of data. The load shall be monitored throughout the test to ensure that the desired load intervals are achieved.	C5.2 Loads for Static Tests The maximum load to be applied for the static tests is larger than that of the cyclic load test to simulate the effect of a heavy truck passing over the bridge. A load interval equal to the load used in the cyclic load test shall be used to understand the behavior of the deck at both the cyclic and strength loads.
5.2.1 Application of Load for Static Tests Application of load for the static tests shall be the same as that during the cyclic load test, as per 4.2.1.	C5.2.1 Application of Load for Static Tests
5.2.2 Magnitude of Load for Static Tests The maximum load to be applied, P_{max} , shall be that determined from the "Proposed Recommended Method for Verifying Strength of Bridge Decks".	C5.2.2 Magnitude of Load for Static Tests
5.3 Data Collection for Static Tests Static tests shall be conducted prior to the start of the cyclic load test, after every 500,000 cycles, and after termination of the test if the target number of cycles is achieved. Each static test shall be repeated a minimum of three times and data collected to assess repeatability and average results. Data from the three tests shall produce displacements and stress measurements within 15% of each other. If the measurements for the three static tests are outside of this range, the reasons shall be determined and corrected if	C5.3 Data Collection for Static Tests Intervals less the 500,000 cycles can also be used if deemed appropriate by the owner. However, it is recommended to conduct cyclic load range static tests more frequently during the first 1,000,000 cycles of the test to identify any changes in behavior that occur early in the test. It is also recommended to conduct cyclic load static tests more frequently when damage to the deck is observed.

Proposed Test Method and Commentary for Subassembly Cyclic Load Testing of Longitudinal Splices in Prefabricated Bridge Deck Panels

possible.	
6.0 Inspection and Termination of Test	C6.0 Inspection and Termination of Test
6.1 General The specimen, support beams or stringers, fixtures and connection details shall be inspected, at a minimum, <ol style="list-style-type: none"> 1) prior to commencement of the cyclic load test; 2) after completion of each set of static tests; and 3) after termination of the cyclic load test (if applicable). 	C6.1 General The specimen shall be inspected for defects including crack development and propagation, delamination, and failures as defined in 6.2.1. The support beams and fixtures shall also be inspected for damage and movement.
6.2 Duration of Test A test shall be terminated after the application of the desired number of cycles, N_f , at a given load range, ΔP . In such cases, the longitudinal splice is adequate. The test shall also be terminated if any of the failure criteria defined in 6.2.1 is met. In such cases, the longitudinal splice does not have sufficient fatigue resistance. The test shall be run a minimum of three million cycles unless the actual number of heavy axles anticipated to cross the deck in a given travel lane has been shown to be less than or equal to 50% of this value. In such cases, twice the actual number of cycles that are anticipated to cross the joint shall be applied.	C6.2 Duration of Test During the research used to develop this test, various approaches were evaluated to establish the minimum duration of the test. Considering the uncertainties associated with in-situ loading, assumptions built-in to the test method, potential ramifications of deck failure, and the cost of testing, a minimum duration of three million cycles was selected. The requirement that the minimum number of applied cycles be the lesser of the minimum specified (i.e., three million) or twice the actual number of heavy axles (if the actual number of load cycles in a given travel lane is less than 50% of the minimum specified) crossing the joint is a conservative approach to ensure a minimum number of cycles are applied even for low-volume roads. For example, if it is estimated that 1,000,000 axles will cross the joint during the design life of the deck, a minimum of 2,000,000 cycles shall be applied during the test.
6.2.1 Definitions of Failure The following shall be used to define failure of a given longitudinal splice: <ul style="list-style-type: none"> • Yielding in any portion of the specimen; • Significant changes in behavior (i.e., nonlinear response) or difference in measured response greater than 15% from the start of the test at critical locations; • Fatigue cracking of steel that would compromise the performance of the deck during its intended service life; • Debonding or slip of concrete; • Cracking of the concrete that will likely result in corrosion of the encased steel; or • Any other damage that would result in premature durability or strength failure of 	C6.2.1 Definitions of Failure Although the deck may not experience collapse, large deflections creating a serviceability limit state may be produced. If a specimen experiences deflections that would be undesirable for service, the test shall be terminated.

Proposed Test Method and Commentary for Subassembly Cyclic Load Testing of
Longitudinal Splices in Prefabricated Bridge Deck Panels

the specimen or supporting members.	
7.0 Results	C7.0 Results
7.1 Interpretation of Results A longitudinal splice shall be deemed suitable for service if the test is terminated after the specimen has survived the desired number of cycles, N_f , at the appropriate load range, ΔP , and does not satisfy any of the failure criteria in 6.2.1	C7.1 Interpretation of Results
8.0 Reporting of Data	C8.0 Reporting of Data
8.1 Cyclic Load Test Results and Observations The following data shall be reported: <ol style="list-style-type: none"> 1. The average displacement (at all locations), measured stress, and load from the static tests shall be reported in tabular format at all load levels for the initial and final static tests. 2. The average measured stresses and displacement at the cyclic and strength loads from each set of static tests shall be plotted against the number of cycles completed (i.e., 0, 500,000, 1,000,000, etc). These values shall also be reported in tabular format. 3. Load range, ΔP, and the corresponding desired number of cycles, N_f, for the cyclic load test. 4. Number of cycles and reason for termination of the cyclic load test. 5. Details of failure (if applicable). 	C8.1 Cyclic Load Test Results and Observations The measured displacements and stresses are to be monitored throughout the test. The average displacements and stresses from the sets of static tests carried out every 500,000 cycles are to be plotted against the number of cycles to determine whether there are significant changes in the behavior of the deck (e.g., increased deflections, stresses, etc).
8.2 Miscellaneous Required Information The following information shall also be reported: <ul style="list-style-type: none"> • Deck type and fabricator; • Section properties and dimensions of the specimens and supports/fixtures; • Material properties for deck components; • Visible deviations or defects; • A drawing showing the shape, size and orientation of the specimen and the fixtures; • A drawing showing the location of all instrumentation and the load patches; and • All sensor calibrations. 	C8.2 Miscellaneous Required Information

**ATTACHMENT I - Proposed Test Method and Commentary for Subassembly Cyclic Load
Testing of Deck-to-Superstructure Connections for Prefabricated Bridge Decks**

Proposed Test Method and Commentary for Subassembly Cyclic Load Testing of Deck-to-Superstructure Connections for Prefabricated Bridge Decks

1.0 General	C1.0 General
1.1 Scope <p>This test method describes a procedure for assessing the cyclic loading resistance of the connection of prefabricated bridge deck panels to the superstructure.</p>	C1.1 Scope <p>The deck-to-superstructure connection details are important structural details in bridges. These details often consist of welds, bolted connections, shear studs, etc.</p>
1.2 Summary <p>This test procedure can be used to evaluate the cyclic (i.e., fatigue) loading resistance and durability of a deck-to-superstructure connection. Data reported includes the load range (ΔP), nominal stress range (S_r) at selected locations, and the number of cycles (N_f) at test termination.</p>	C1.2 Summary <p>The applied cyclic loading is intended to reveal and identify potential metal fatigue as well as other durability issues with these connections which occur under repeated loading.</p>
1.3 Approach <p>A subassembly specimen representative of the in-service bridge deck shall be used to evaluate the durability and cyclic load (i.e., fatigue) resistance of the deck-to-superstructure connection. Occasional heavy loads mixed in with normal traffic are also simulated through the use of intermittent static tests performed at higher loads. Stresses and displacement shall be monitored to evaluate the changes in behavior throughout the test. This test is intended to reveal and identify deficiencies in the deck-to-superstructure connection and deck that would be likely to occur for the in-service bridge deck.</p>	C1.3 Approach <p>The load is applied through two load patches in full contact with the deck. This is intended to simulate a typical truck axle. Additionally, the load patches are connected to the deck such that the deck may be pulled upward to simulate the tension induced in the deck-to-superstructure connection by truck traffic passing on adjacent spans.</p> <p>The application of a heavier load is intended to incorporate a wider load spectrum and the effects of heavier vehicles that are part of normal traffic.</p> <p>Stresses are monitored mainly in the area of the critical detail (i.e., deck-to-superstructure connection).</p> <p>Visual inspections are to be carried out regularly throughout the test to identify any damage to the subassembly.</p>
2.0 Specimens	C2.0 Specimens
2.1 Components – General <p>Specimens shall be representative full-scale subassemblies of the bridge deck type under investigation. The specimen shall contain all components of an in-service bridge deck panel which affect in-service load distribution. The width dimension of a deck panel shall be sufficiently wide to include at least three of the primary load carrying members, but shall not be less than one half the span length of the test specimen.</p> <p>The deck specimen shall be carried on three support beams (i.e., stringers) which provide similar stiffness and deflections to those expected for the in-service bridge. Further, the supporting members shall be sized so that the resulting stress ranges in those members are comparable to those that would be observed in the field. The beams shall be placed on rigid supports at each end. The orientation of the deck and beams shall represent that of the in-service bridge, as shown in Figure 1.</p>	C2.1 Components –General <p>All components effecting load distribution must be included in the test to ensure that the test accurately simulates all localized behavior of the in-service bridge deck.</p> <p>The width dimension of the deck shall be sufficiently wide to ensure the load distribution is such that the failure mode of the specimen is not altered.</p> <p>Supports are not required to be the same cross section as used in the field, but should be proportioned such that the expected deformations and stresses in the deck and supports that would be observed in the real structure shall be reasonably represented.</p> <p>Supporting beams that are too flexible will produce misleading results. Three support beams are used to produce a negative transverse moment at the location of the interior stringer.</p>

Proposed Test Method and Commentary for Subassembly Cyclic Load Testing of Deck-to-Superstructure Connections for Prefabricated Bridge Decks

Prior to testing, the specimen shall be visually inspected for any flaws or defects that could possibly affect the cyclic loading resistance of the deck-to-superstructure connection and bridge deck being considered. Defects and flaws shall be defined as per the appropriate governing specification (e.g., contract documents, ASTM standards, etc.). Specimens containing flaws and defects that are deemed to affect the performance of the specimen shall not be used. Specimens that meet the appropriate governing specifications but exhibit minor defects can be tested but such defects and their locations shall be documented and reported.

It is noted that the same deck specimen may be used for the test method described in the "Proposed Recommended Method for Verifying Strength of Bridge Decks" if the specimen is not damaged such that it would produce unreliable/unrealistic data for a test.

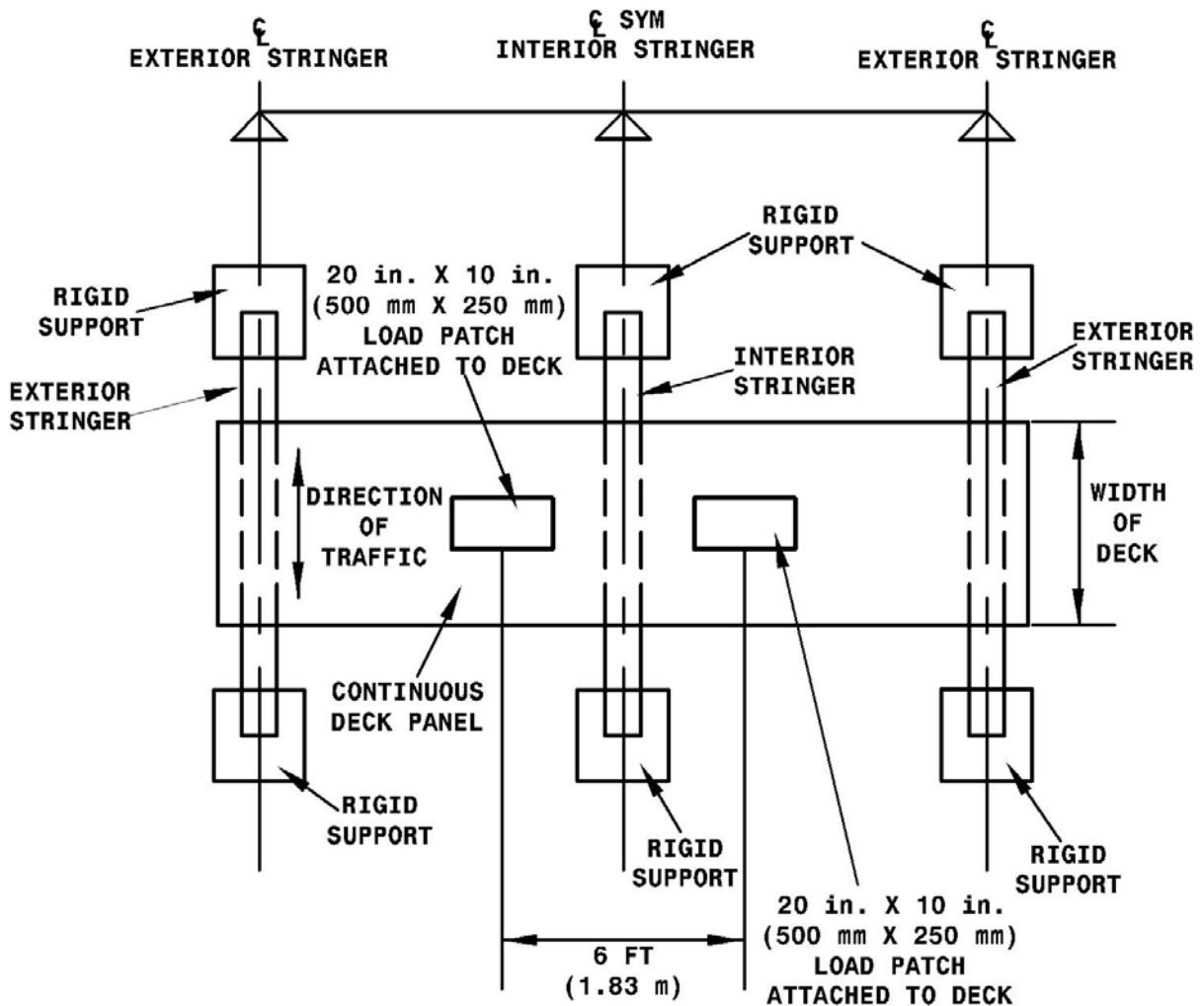


Figure 1: Deck-to-Superstructure Connection Cyclic Test Set-up

Proposed Test Method and Commentary for Subassembly Cyclic Load Testing of Deck-to-Superstructure Connections for Prefabricated Bridge Decks

2.2 Instrumentation

The test specimen shall be instrumented to measure the vertical displacement of the specimen to a minimum resolution of 0.001 in. (25 μ m). Vertical displacements shall be measured at mid width of the deck at each support (e.g., stringer) so that rigid body movement of the structural system (i.e., deck and stringers) can be recorded. Vertical displacements shall also be measured under each load patch as shown in Figure 2.

Sufficient strain gaging is required to monitor stresses at critical locations (e.g., the deck-to-superstructure connection) during testing and to understand the behavior of the deck-to-superstructure connection and deck panel(s). The data collected at these locations shall be used to determine the behavior and stresses at the deck-to-superstructure connection.

The applied force shall also be measured. The resolution of the load measuring device shall be calibrated such that it has a resolution to 1% of the maximum load in the load range. All sensor calibrations shall be reported.

C2.2 Instrumentation

A total of five vertical displacement measurement locations are required to obtain a profile of the deck displacements.

Strain gages are required mainly in the area of the deck-to-superstructure connection to determine the stress range of the detail of concern (e.g., welds or other components). The detail(s) shall be instrumented at sufficient locations along the connection with strain gages to ensure that relevant data is obtained. This test method assumes the user has sufficient knowledge regarding the deck type under consideration to formulate a meaningful instrumentation plan. The owner and manufacturer should agree upon the amount and location of instrumentation.

Proposed Test Method and Commentary for Subassembly Cyclic Load Testing of
Deck-to-Superstructure Connections for Prefabricated Bridge Decks

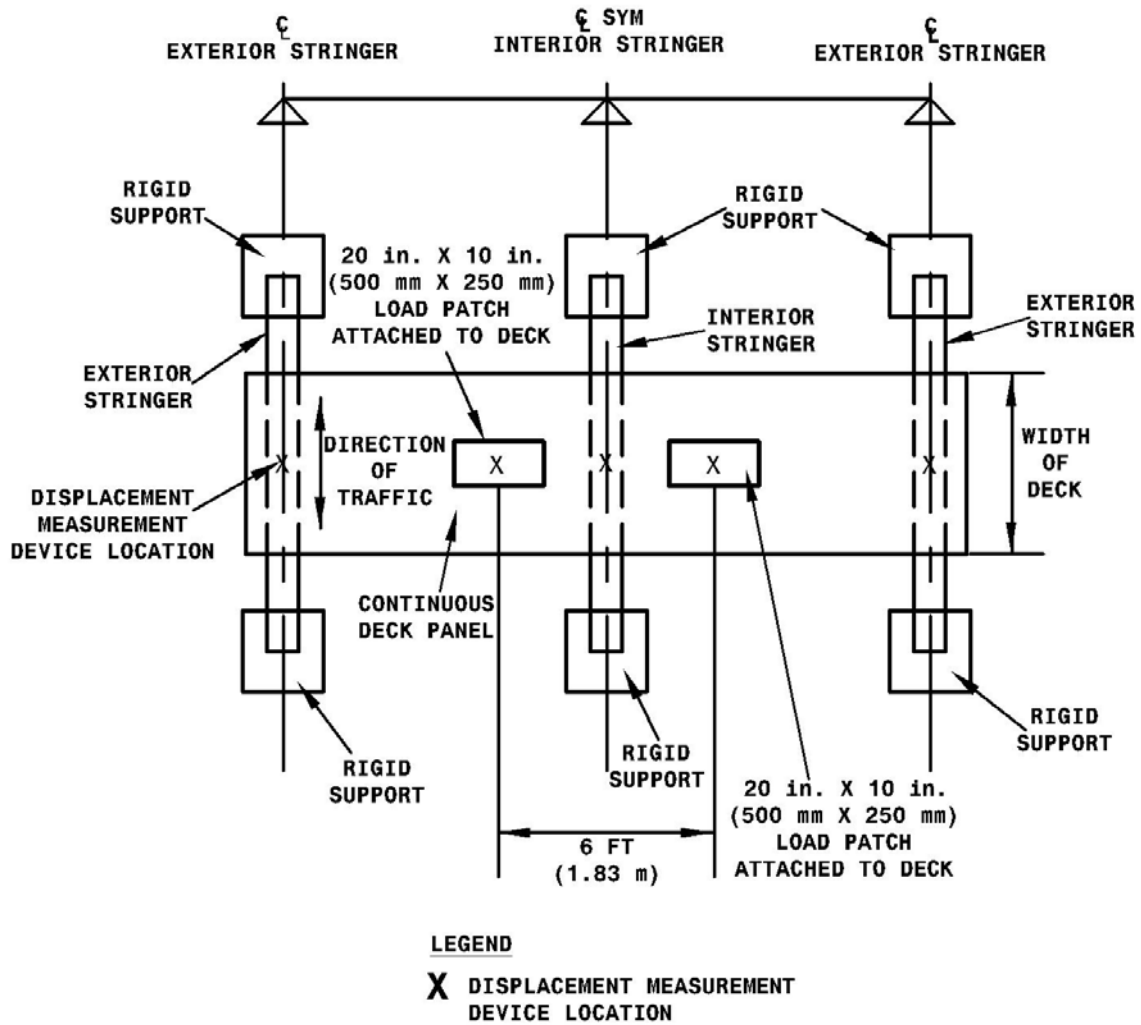


Figure 2: Minimum Instrumentation Required for Deck-to-Superstructure Connection Cyclic Test

3.0 Fixtures

3.1 Fixture Details

Fixtures capable of adequately supporting and securing the specimen during the test shall be provided. The fixtures shall be fabricated such that no additional displacements or stresses are generated as a result of fixture misalignments or movements. In addition, fabrication errors in the specimen shall be corrected or compensated for using non-mechanical means (i.e., shimming) and where required shall be reported. Dimensional tolerances of support locations shall be within $\pm 1/8$ in. (3 mm).

Fixtures shall also be designed to resist uplift of the fixtures and stringers when the specimen is pulled upward.

C3.0 Fixtures

C3.1 Fixture Details

Proposed Test Method and Commentary for Subassembly Cyclic Load Testing of Deck-to-Superstructure Connections for Prefabricated Bridge Decks

<p>3.2 Support Beams/Stringers</p> <p>The support beams or stringers shall be designed such that they adequately model the stiffness and stresses that are expected to be experienced for the in-service bridge.</p>	<p>C3.2 Stringers</p> <p>The support beams or stringers shall reasonably simulate the support conditions that are used for the actual bridge. Using supports that are excessively flexible is not permitted as this will significantly alter the negative moment over the interior support beam and may lead to unconservative results.</p>
<p>3.3 Deck Connection to Superstructure</p> <p>The deck shall be attached to the superstructure (i.e., the support beams) using the same type of connections as will be used in the field.</p>	<p>C3.3 Deck Connection to Superstructure</p> <p>This testing method is intended to reveal any weaknesses in the connection system.</p>
<p>4.0 Cyclic Load Test Procedure</p> <p>4.1 General</p> <p>When multiple data sets are required, the deck specimen(s) themselves may not be reused. The fixtures and stringers may be reused as long as they are not damaged. Damaged fixtures and stringers shall be replaced and meet the requirements of 3.1 and 3.2.</p>	<p>C4.0 Cyclic Load Test Procedure</p> <p>C4.1 General</p> <p>For short span bridges or those with small deck areas, it may not be necessary to perform more than one of these tests. However, for bridges with large deck areas, the owner may wish to consider requiring more than one test (e.g., 3 to 5) to obtain additional confidence in the performance of the deck system and ensure repeatability of results.</p>
<p>4.2 Loads</p> <p>Load shall be applied through a hydraulic actuator or other similar loading device. The magnitude of the load range (ΔP) shall be maintained throughout the entire test (i.e., "load control"). The load range shall be monitored throughout testing to ensure that the target maximum and minimum load, and load range are being maintained. The load shall only be applied vertically (i.e., no horizontal component).</p>	<p>C4.2 Loads</p>
<p>4.2.1 Application of Load</p> <p>Load shall be applied equally through two load patches 20 in. (500 mm) long and 10 in. (250 mm) wide. The patches typically consist of steel plates placed in contact with the deck as shown in Figure 3.</p> <p>The load patches shall be oriented on the deck such that they represent wheel loads travelling in the direction of traffic. A spacing of 6 ft. (1.83 m) on center shall be used with each patch an equal distance away from the centerline of the interior stringer, as previously shown in Figure 2, to produce the desired negative moment.</p> <p>Load shall be applied to produce both compression and tension in the deck-to-superstructure connection at the interior stringer (i.e., uplift will need to be applied). This shall be achieved by pushing down and pulling up on the deck at the location of the load patches. A</p>	<p>C4.2.1 Application of Load</p> <p>A spacing of 6 ft. (1.83 m) on center between the patch loads corresponds to the lateral spacing of the tires on the standard fatigue truck. Leveling material (e.g., hydro stone) may be used to bring the load patches into full contact with the deck, if necessary.</p> <p>The requirement for an uplift component in the load is intended to simulate the effects of stress reversals that have been observed in the field due to support deflection and the effect of vehicles in adjacent lanes.</p>

Proposed Test Method and Commentary for Subassembly Cyclic Load Testing of Deck-to-Superstructure Connections for Prefabricated Bridge Decks

spreader beam is used to distribute the applied force to the load patches at the desired locations. The spreader beam shall also be attached to the deck at the load patch locations to achieve uplift of the bridge deck at these locations.

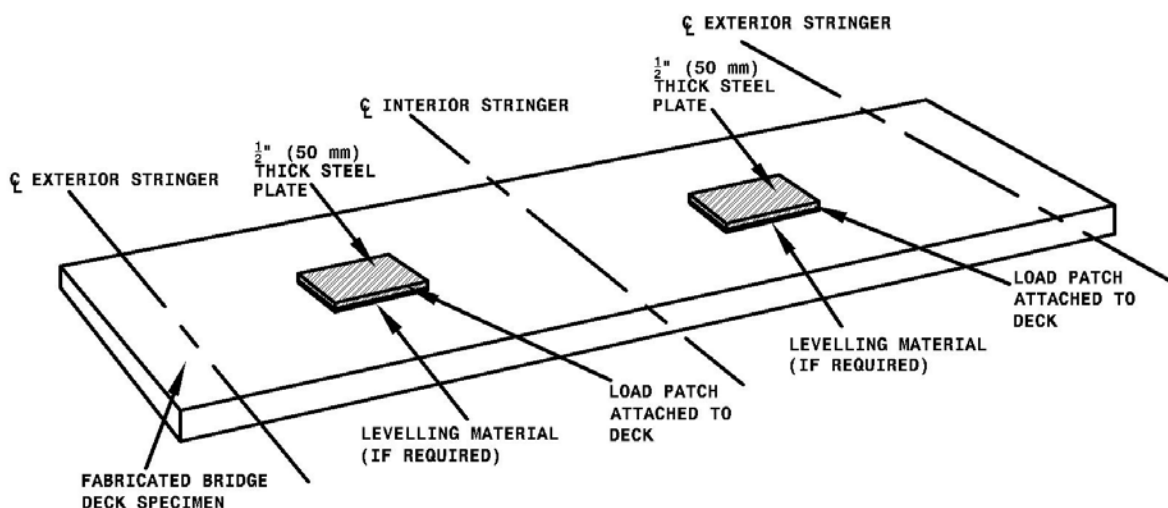


Figure 3: Typical Load Patches on Bridge Deck

4.2.2 Magnitude of Cyclic Load Range

For fatigue, the applied cyclic axle load range is 13.8 kips (61.4 kN). Additionally, the deck will be pulled-up with one-third of this load [i.e., 4.6 kips (20.5 kN)]. Therefore, the total cyclic load range is 18.4 kips (81.9 kN). This load range, ΔP , is the minimum effective axle load that shall be applied. The axle load may be increased by a factor, S_{amp} , to decrease the time that it takes to complete the cyclic load test. The maximum value of S_{amp} shall be less than or equal to 3.0. If increased load ranges are used, the proportions of the downward and upward loads shall be maintained.

C4.2.2 Magnitude of Cyclic Load Range

The minimum applied load range is determined by applying a load factor of 0.75 to a single rear axle of the HS20 design truck tandem. In performing this test, it must be recognized that the individual rear axles of the HS20 actually simulate a tandem axle.

Multiplying the HS 20 load by a factor of 0.75 yields the same effective load range and hence, effective stress range, S_{eff} , prescribed by the AASHTO LRFD Bridge Design Specifications for finite life fatigue design.

The impact factor is set at 1.15 and is the dynamic load allowance for the fatigue limit state as specified by the AASHTO LRFD Bridge Design Specification. Hence, the actual axle load is $(0.75 \times 32 \text{ kips}) \times \frac{1}{2} \times 1.15 = 13.8 \text{ kips (61.4 kN)}$.

Proposed Test Method and Commentary for Subassembly Cyclic Load Testing of Deck-to-Superstructure Connections for Prefabricated Bridge Decks

<p>The projected ADTT shall be used to determine the required number of cycles to be applied for the cyclic load test of the subassembly. To compute the number of cycles to be applied for the cyclic load test:</p> $N = (365 \text{ days/year})(75 \text{ years})(4.5 \text{ cycles/truck})(ADTT)_{SL}$ <p>where:</p> <p>N = total number of cycles of stress range to be applied to the in-service bridge deck over its design life $(ADTT)_{SL}$ = the single lane ADTT determined using the projected ADTT for the bridge.</p> <p>The total number of cycles is assumed to be inversely proportional to the cube of the load range. Therefore, the number of cycles to be applied for the cyclic load test may be computed as:</p> $N_f = N / (S_{amp})^3$ <p>where:</p> <p>N_f = number of cycles at the desired load range to be applied for the cyclic load test S_{amp} = factor by which load range is increased (i.e., amplified) from the HS15 axle</p>	<p>It is also required to pull the deck up at the locations of the patch loads for this test to induce tension in the deck-to-superstructure connection(s) at the interior stringer. Although pulling the deck upward is not the actual in-service loading, the tension produced in the deck-to-superstructure connection is intended to simulate the effect of trucks traveling on adjacent deck spans. This loading is set as one-third of the axle load (i.e., $1/3 \times 13.8 = 4.6$ kips (20.5 kN)).</p> <p>Therefore, combining the applied axle loading (i.e., pushing) and the pulling loading, the total load range is $13.8 + 4.6 = 18.4$ kips (81.9 kN).</p> <p>The limitation of 3.0 for S_{amp} is to prevent the user from selecting a load that is unrealistically high and may result in a different failure mode than what would be observed under service conditions. S_{amp} will commonly be set to 2.0 as that corresponds to the upper bound fatigue limit state load for infinite life prescribed in the AASHTO LRFD Bridge Design Specifications and is a realistic axle load.</p> <p>The projected ADTT shall be acquired from the owner (e.g., DOT). This number of cycles shall be used and proportioned based on the increase in load range for the cyclic load test according to the relationship shown.</p> <p>If a design life other than 75 years is desired, the appropriate design life may be used to compute the total number of cycles of stress range to be applied over the design life, N. It is noted that the 75 year life may be too excessive for most bridge decks.</p> <p>The single lane ADTT shall be determined as :</p> $(ADTT)_{SL} = p \times (ADTT)$ <p>where:</p> <p>$(ADTT)$ = projected number of trucks per day in one direction averaged over the design life. p = fraction of traffic in a single lane (Table 3.6.1.4.2-1 (AASHTO LRFD))</p> <p>It is assumed that the S-N cubic relationship used for metal fatigue can be used for this application.</p>
---	---

Proposed Test Method and Commentary for Subassembly Cyclic Load Testing of Deck-to-Superstructure Connections for Prefabricated Bridge Decks

<p>The load range applied shall not be so large as to alter the failure mode that would be observed in service conditions. The applied load shall not cause the yield stress to be exceeded in any portion of the specimen.</p>	
<p>4.2.3 Vibration of Bridge Deck</p> <p>A high frequency pneumatic vibrator or similar device shall be used to simulate the effect of vibrations caused by trucks passing over the bridge. The vibrator shall be rigidly attached to a support beam nearest to the deck-to-superstructure connection being tested no more than two feet (610 mm) away from the outside edge of the deck. The vibrator shall be excited after the application of every 500,000 load cycles. The vibrator shall apply 50,000 cycles each interval and shall preferably be applied simultaneously with the application of the load cycles. The vibrator shall be excited prior to conducting the static tests at these intervals. The vibrator shall be capable of operating between 80 Hz and 120 Hz and produce a force range of 8 to 12 kips.</p> <p>If the cyclic load test is terminated prior to any damage and the desired number of cycles is reached, the vibrator shall be excited for a minimum of 50,000 cycles prior to conducting final static test.</p>	<p>C4.2.3 Vibration of Bridge Deck</p> <p>Vibrations caused by the passing of trucks and wheel impacts can play a role in the stresses/deflections experienced by the bridge deck and connections to the superstructure. Some connection details may also loosen or fail in service due to vibrations from passing trucks. The application of the load range alone would not truly represent the full spectrum of dynamic loading of truck traffic. Although it is not essential the vibratory cycles and load cycles be applied concurrently, it is preferred. The 50,000 vibratory cycles every 500,000 load cycles was arbitrarily set as 10% of the load cycles. A greater percentage should be considered if the joints are located near traffic metering devices such as toll facilities, traffic signals, etc. However, it would seem that there would be no need to apply more than 25% of the load cycles.</p> <p>The vibrator shall be excited prior to conducting the static tests at these intervals to simulate the vibrations from trucks passing over the deck.</p> <p>The vibrator used during the development of this test was a Vibco model number SVRLS 8000.</p>
<p>5.0 Static Tests</p>	<p>C5.0 Static Tests</p>
<p>5.1 General</p> <p>Static tests shall be conducted regularly throughout the cyclic load test to monitor the change in stress range, displacements and to infer if there is any damage of the deck-to-superstructure connection and deck.</p>	<p>C5.1 General</p>
<p>5.2 Loads for Static Tests</p> <p>The strength load shall be applied for the static tests. The magnitude of the load shall be as defined in 5.2.2.</p> <p>The static loads shall be applied in a minimum of eight approximately equal steps until the target static load is achieved. Load intervals equal to the maximum and minimum (i.e pushing and pulling) loads used in the cyclic load testing portion of the test shall also be included in the load steps.</p> <p>The load shall be maintained within +/- 2% at each load increment for a minimum of ten seconds to allow for the collection of data. The load shall be monitored throughout the test to ensure that the desired load intervals are achieved.</p>	<p>C5.2 Loads for Static Tests</p> <p>The maximum load to be applied for the static tests is larger than that of the cyclic load test to simulate the effect of a heavy truck passing over the bridge.</p> <p>Load intervals equal to the maximum (i.e pushing) and minimum (i.e., pulling) loads used in the cyclic load testing portion of the test shall be included to understand the behavior of the deck at both the fatigue and strength loads.</p>

Proposed Test Method and Commentary for Subassembly Cyclic Load Testing of
Deck-to-Superstructure Connections for Prefabricated Bridge Decks

<p>5.2.1 Application of Load for Static Tests Application of load for the static tests shall be the same as that during the cyclic load test, as per 4.2.1.</p>	<p>C5.2.1 Application of Load for Static Tests</p>
<p>5.2.2 Magnitude of Load for Static Tests The maximum (i.e pushing) load to be applied, P_{max}, shall be that determined from the “Proposed Recommended Method for Verifying Strength of Bridge Decks”. The minimum (i.e., pulling) load to be applied shall be the same magnitude as that used in the cyclic load test, as per 1.3.</p>	<p>C5.2.2 Magnitude of Load for Static Tests</p>
<p>5.3 Data Collection for Static Tests Static tests shall be conducted prior to the start of the cyclic load test, after every 500,000 cycles, and after termination of the test if the target number of cycles is achieved. Each static test shall be repeated a minimum of three times and data collected to assess repeatability and average results. Data from the three tests shall produce displacements and stress measurements within 15% of each other. If the measurements for the three static tests are outside of this range, the reasons shall be determined and corrected if possible.</p>	<p>C5.3 Data Collection for Static Tests Intervals less the 500,000 cycles can also be used if deemed appropriate by the owner. However, it is recommended to conduct cyclic load range static tests more frequently during the first 1,000,000 cycles of the test to identify any changes in behavior that occur early in the test. It is also recommended to conduct cyclic load static tests more frequently when damage to the deck is observed.</p>
<p>6.0 Inspection and Termination of Test</p>	<p>C6.0 Inspection and Termination of Test</p>
<p>6.1 General The specimen, support beams or stringers, fixtures and connection details shall be inspected, at a minimum,</p> <ol style="list-style-type: none"> 1) prior to commencement of the cyclic load test; 2) after completion of each set of static tests; and 3) after termination of the cyclic load test (if applicable). 	<p>C6.1 General The specimen shall be inspected for defects including crack development and propagation, delamination and failures as defined in 6.2.1. The support beams and fixtures shall also be inspected for damage and movement.</p>
<p>6.2 Duration of Test A test shall be terminated after the application of the desired number of cycles, N_f, at a given load range, ΔP. In such cases, the deck-to-superstructure connection is adequate. The test shall also be terminated if any of the failure criteria defined in 6.2.1 is met. In such cases, the deck-to-superstructure connection does not have sufficient cyclic loading resistance. The test shall be run a minimum of three million cycles unless the actual number of heavy axles anticipated to cross the deck in a given travel lane has been shown to be less than or equal to 50% of</p>	<p>C6.2 Duration of Test During the research used to develop this test, various approaches were evaluated to establish the minimum duration of the test. Considering the uncertainties associated with in-situ loading, assumptions built-in to the test method, potential ramifications of deck failure, and the cost of testing, a minimum duration of three million cycles was selected. The requirement that the minimum number of applied cycles be the lesser of the minimum specified (i.e., three million) or twice the actual number of heavy axles (if the actual number of</p>

Proposed Test Method and Commentary for Subassembly Cyclic Load Testing of Deck-to-Superstructure Connections for Prefabricated Bridge Decks

<p>this value. In such cases, twice the actual number of cycles that are anticipated to cross the joint shall be applied.</p>	<p>load cycles in a given travel lane is less than 50% of the minimum specified) crossing the joint is a conservative approach to ensure a minimum number of cycles are applied even for low-volume roads.</p> <p>For example, if it is estimated that 1,000,000 axles will cross the joint during the design life of the deck, a minimum of 2,000,000 cycles shall be applied during the test.</p>
<p>6.2.1 Definitions of Failure</p> <p>The following shall be used to define failure of a given deck-to-superstructure connection:</p> <ul style="list-style-type: none"> • Yielding in any portion of the specimen; • Significant changes in behavior (i.e., nonlinear response) or difference in measured response greater than 15% from the start of the test at critical locations; • Fatigue cracking of steel that would compromise the performance of the deck during its intended service life; • Debonding or slip of concrete; • Cracking of the concrete that will likely result in corrosion of the encased steel; or • Any other damage that would result in premature durability or strength failure of the specimen or supporting members. 	<p>C6.2.1 Definitions of Failure</p> <p>Although the deck may not experience collapse, large deflections creating a serviceability limit state may be produced. If a specimen experiences deflections that would be undesirable for service, the test shall be terminated.</p>
<p>7.0 Results</p> <p>7.1 Interpretation of Results</p> <p>A deck-to-superstructure connection shall be deemed suitable for service if the test is terminated after the specimen has survived the desired number of cycles, N_t, at the appropriate load range, ΔP, and does not satisfy any of the failure criteria presented in 6.2.1.</p>	<p>C7.0 Results</p> <p>C7.1 Interpretation of Results</p>

Proposed Test Method and Commentary for Subassembly Cyclic Load Testing of
Deck-to-Superstructure Connections for Prefabricated Bridge Decks

8.0 Reporting of Data	C8.0 Reporting of Data
8.1 Cyclic Load Test Results and Observations The following data shall be reported: <ol style="list-style-type: none"> 1. The displacements (at all locations), measured stresses, and load from the static tests shall be reported in tabular format at all load levels for the initial and final static tests. 2. The average measured stresses and displacement at the cyclic and strength loads from each set of static tests shall be plotted against the number of cycles completed (i.e., 0, 500,000, 1,000,000, etc). These values shall also be reported in tabular format. 3. Load range, ΔP, and the corresponding desired number of cycles, N_f, for the cyclic load test. 4. Number of cycles and reason for termination of the cyclic load test. 5. Details of failure (if applicable). 	C8.1 Cyclic Load Test Results and Observations The measured displacements and stresses are to be monitored throughout the test. The average displacements and stresses from the sets of static tests carried out every 500,000 cycles are plotted against the number of cycles to determine whether there are significant changes in the behavior of the deck (e.g., increased deflections, stresses, etc).
8.2 Miscellaneous Required Information The following information shall also be reported: <ul style="list-style-type: none"> • Deck type and fabricator; • Section properties and detail dimensions of the specimens and supports/fixtures; • Material properties for deck components; • Visible deviations or defects; • A drawing showing the shape, size and orientation of the specimen and the fixtures; • A drawing showing the locations of all instrumentation and the load patches; and • All sensor calibrations. 	C8.2 Miscellaneous Required Information

**ATTACHMENT J - Proposed Test Method and Commentary for Subassembly Cyclic
Load Testing of Transverse Splices in Prefabricated Bridge Deck Panels**

Standard Test Method and Commentary for Subassembly Cyclic Load Testing of Transverse Splices in Prefabricated Bridge Deck Panels

<p>1.0 General</p> <p>1.1 Scope</p> <p>This test method describes a procedure for assessing the fatigue resistance of transverse splices of prefabricated bridge deck panels. Transverse splices are structural details in bridge decks that join together two panels in the direction of traffic.</p>	<p>C1.0 General</p> <p>C1.1 Scope</p> <p>Transverse splice details are located where two prefabricated deck panels meet. The centerline of the transverse splice, as defined herein, runs perpendicular to the direction of traffic.</p>
<p>1.2 Summary</p> <p>This test procedure can be used to assess the resistance and durability of a transverse splice connecting prefabricated deck panels subjected to cyclic (i.e., fatigue) loading. Data reported includes the load range (ΔP), nominal stress range at selected locations (S_r), and the number of cycles (N_f) at test termination.</p>	<p>C1.2 Summary</p> <p>The applied cyclic loading is intended to reveal and identify potential metal fatigue as well as other durability issues which occur under repeated loading. The procedures described herein are applicable to both shop and field splices.</p>
<p>1.3 Approach</p> <p>A subassembly specimen representative of the in-service bridge deck shall be used to evaluate the durability and cyclic load (i.e., fatigue) resistance of the transverse splice. Heavy loads are also simulated intermittently through the use of static tests. Stresses and displacement shall be monitored to evaluate the changes in behavior throughout the test. This test will reveal and identify deficiencies in the transverse splice and deck that would be likely to occur for the in-service bridge deck.</p>	<p>C1.3 Approach</p> <p>The load is applied through a load patch in full contact with the deck. This is intended to simulate a typical truck tire.</p> <p>The application of a heavier load is intended to incorporate a wider load spectrum.</p> <p>Stresses are monitored mainly in the area of the critical detail (i.e., transverse splice).</p> <p>Visual inspections are to be carried out regularly throughout the test to identify any damage to the subassembly.</p>
<p>2.0 Specimens</p> <p>2.1 Components – General</p> <p>Specimens shall be representative full-scale subassemblies of the bridge deck type under investigation. The specimen shall contain all components of the bridge deck panel which affect in-service load distribution. The width dimension of each deck panel shall be sufficiently wide to include at least three of the primary load carrying members, but shall not be less than one half the span length of the test specimen.</p> <p>The deck specimen shall be carried on two support beams (e.g., stringers) which provide similar stiffness and deflections of those expected for the in-service bridge. Further, the supporting members shall be sized so that the resulting stress ranges in those members are comparable to those that would be observed in the field.</p> <p>The beams shall be placed on rigid supports at each end. The orientation of the deck and beams shall represent that of the in-service bridge, as shown in Figure 1.</p> <p>Prior to testing, the specimen shall be visually inspected for any flaws or defects that could</p>	<p>C2.0 Specimens</p> <p>C2.1 Components –General</p> <p>All components effecting load distribution must be included in the test to ensure that the test accurately simulates all localized behavior of the in-service bridge deck.</p> <p>The width dimension of each deck panel shall be sufficiently wide to ensure the load distribution is such that the failure mode of the specimen is not altered.</p> <p>Supports are not required to be the same cross section as used in the field, but should be proportioned such that the expected deformations and stresses in the deck and supports that would be observed in the real structure shall be reasonably represented.</p> <p>Supporting beams that are too flexible will sometimes produce misleading results. Only two support beams are used since the splice detail, located in the transverse positive moment region of the deck, is the only area of concern for this test.</p>

Standard Test Method and Commentary for Subassembly Cyclic Load Testing of Transverse Splices in Prefabricated Bridge Deck Panels

possibly affect the fatigue resistance of the transverse splice and bridge deck being considered. Defects and flaws shall be defined as per the appropriate governing specification (e.g., contract documents, ASTM documents, etc.). Specimens containing flaws and defects that are deemed to affect the performance and/or resistance of the specimen shall not be used. Specimens that meet the appropriate governing specifications but exhibit minor defects can be tested but such defects and their locations shall be documented and reported.

It is noted that the same deck specimen may be used for the test method described in the "Proposed Recommended Method for Verifying Strength of Bridge Decks" if the specimen is not damaged such that it would produce unreliable/unrealistic data for a test.

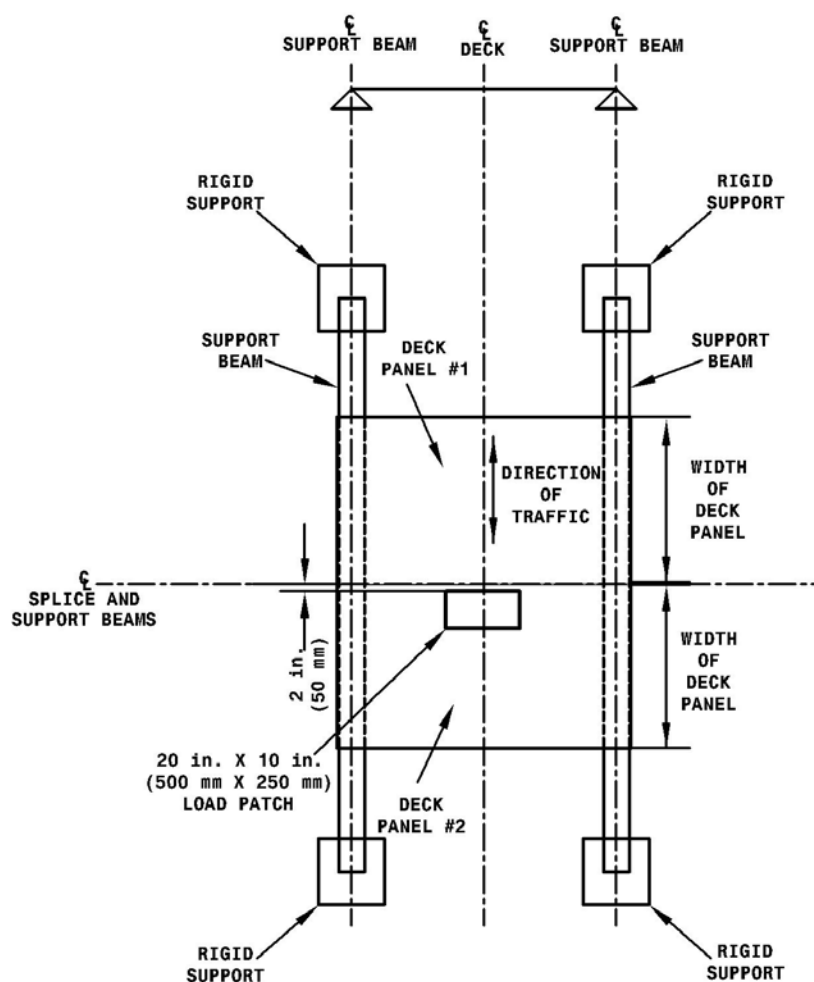


Figure 1: Plan View of Transverse Splice Test Set-up

2.2 Instrumentation

The test specimen shall be instrumented to measure the vertical displacement of the specimen to a minimum resolution of 0.001 in. (25 μ m). Vertical displacements shall be measured at the centerline of the splice at each support (e.g., support beam). Vertical displacements shall be

C2.2 Instrumentation

A total of six vertical displacement measurement locations are required to obtain a profile of the deck displacements.

Standard Test Method and Commentary for Subassembly Cyclic Load Testing of Transverse Splices in Prefabricated Bridge Deck Panels

also measured at a minimum of two additional locations; the location of maximum displacement (i.e., under the load patch); and near the splice and patch load, but on the side opposite to the patch load.

Sufficient strain gaging is required to monitor stresses at critical locations (i.e., the transverse splice) during testing and to understand the behavior of the transverse splice and deck panels. The data collected at these locations shall be used to determine the behavior and stresses at the transverse splice.

The applied load shall also be measured. The resolution of the load measuring device shall be calibrated such that it has a resolution to 1% of maximum load in the load range. All sensor calibrations shall be reported.

Strain gages are required mainly in the area of the transverse splice to determine the stress range of the detail of concern. For example, on the reinforcing steel, grid deck members, or other components. The detail(s) shall be instrumented at sufficient locations along the splice with strain gages to ensure that relevant data is obtained. This test method assumes the user has sufficient knowledge regarding the deck type under consideration to formulate a meaningful instrumentation plan. The owner and manufacturer should agree upon the amount and location of instrumentation.

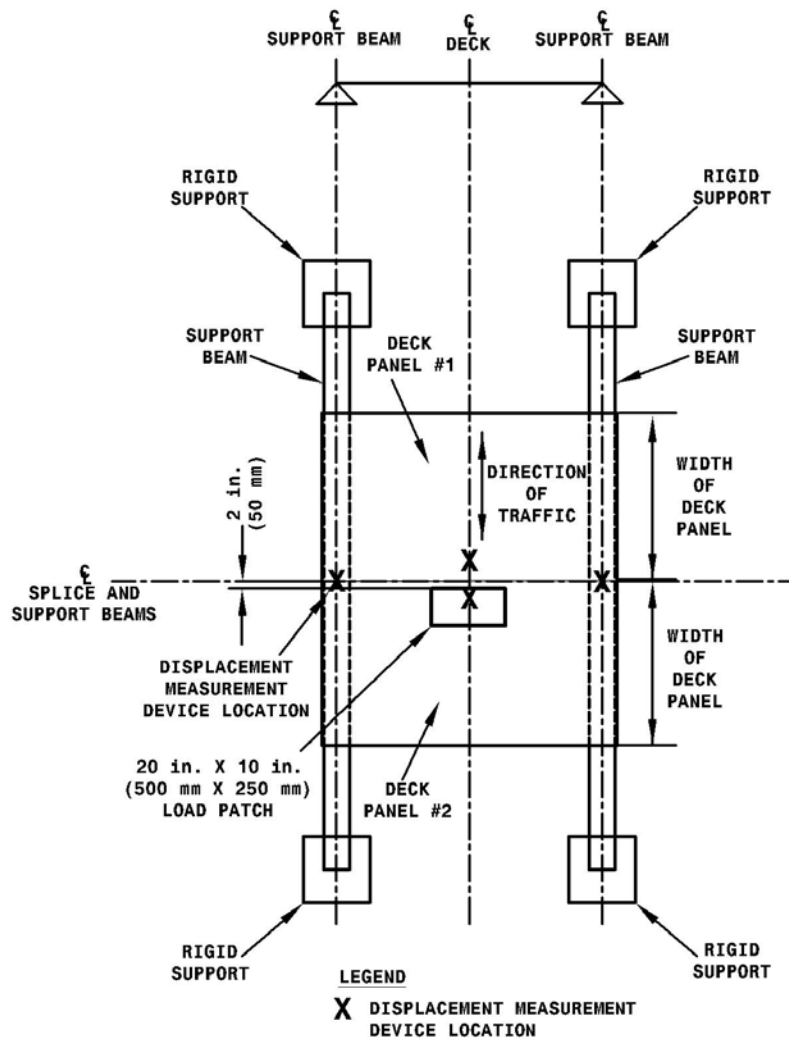


Figure 2: Minimum Instrumentation Required for Transverse Splice Test

Standard Test Method and Commentary for Subassembly Cyclic Load Testing of Transverse Splices in Prefabricated Bridge Deck Panels

<p>3.0 Fixtures</p> <p>3.1 Fixture Details</p> <p>Fixtures capable of adequately supporting and securing the specimen during the test shall be provided. The fixtures shall be fabricated such that no additional displacements or stresses are generated as a result of fixture misalignments or movements. In addition, fabrication errors in the specimen shall be corrected or compensated for using non-mechanical means (i.e., shimming) and where required shall be reported. Dimensional tolerances of support locations shall be within $\pm 1/8$ in. (3 mm).</p>	<p>C3.0 Fixtures</p> <p>C3.1 Fixture Details</p>
<p>3.2 Support Beams/Stringers</p> <p>The support beams or stringers shall be designed such that they adequately model the stiffness and stresses that are expected to be experienced for the in-service bridge.</p>	<p>C3.2 Support Beams/Stringers</p> <p>The support beams or stringers shall reasonably simulate the support conditions that are used for the bridge. Using supports that are excessively flexible is not permitted as this can lead to data that do not accurately represent the actual expected behavior of the deck panel. Use of support beams that are excessively stiff may result in unconservative results for the positive moment at the transverse splice.</p>
<p>3.3 Deck Connection to Superstructure</p> <p>The deck shall be attached to the superstructure (i.e., the support beams) using the same type of connections as will be used in the field.</p>	<p>C3.3 Deck Connection to Superstructure</p> <p>The deck-to-superstructure connection is an important component that affects the overall performance of the assembly. Since this test is intended to reveal any deficiencies of the entire deck system, it is appropriate to accurately simulate this connection.</p>
<p>4.0 Cyclic Load Test Procedure</p> <p>4.1 General</p> <p>When multiple data sets are required, the deck specimen(s) themselves may not be reused. The fixtures and support beams may be reused as long as they are not damaged. Damaged fixtures and support beams shall be replaced so they meet the requirements of 3.1 and 3.2.</p>	<p>C4.0 Cyclic Load Test Procedure</p> <p>C4.1 General</p> <p>For short span bridges or those with limited deck areas, it may not be necessary to perform more than one test. However, for bridges with large deck areas containing numerous transverse splices, the owner may wish to consider requiring more than one test (e.g., 3 to 5) to obtain additional confidence in the performance of the deck system and ensure repeatability of results.</p>
<p>4.2 Loads</p> <p>Load shall be applied through a hydraulic actuator or other similar loading device. The magnitude of the load range (ΔP) shall be maintained throughout the entire test (i.e., "load control"). The load range shall be monitored throughout testing to ensure that the target</p>	<p>C4.2 Loads</p>

Standard Test Method and Commentary for Subassembly Cyclic Load Testing of Transverse Splices in Prefabricated Bridge Deck Panels

maximum and minimum load, and load range are being maintained. The load shall only be applied vertically (i.e., no horizontal component).

4.2.1 Application of Load

Load shall be applied evenly through one load patch 20 in. (500 mm) long and 10 in. (250 mm) wide. The patch typically consists of a steel plate placed in contact with the deck as shown in Figure 3.

The load patch shall be oriented on the deck such that it represents a wheel load travelling in the direction of traffic. It shall be placed such that the edge of the patch nearest the splice is no more than two inches (50 mm) away from the centerline of the splice on the center of the deck, as previously shown in Figure 2.

C4.2.1 Application of Load

The location of the patch shall produce the greatest potential for differential displacements across the splice. Therefore, placement of the load patch directly over the splice shall not be used. Leveling material (e.g., hydro stone) may be used to bring the load patch into full contact with the deck, if necessary.

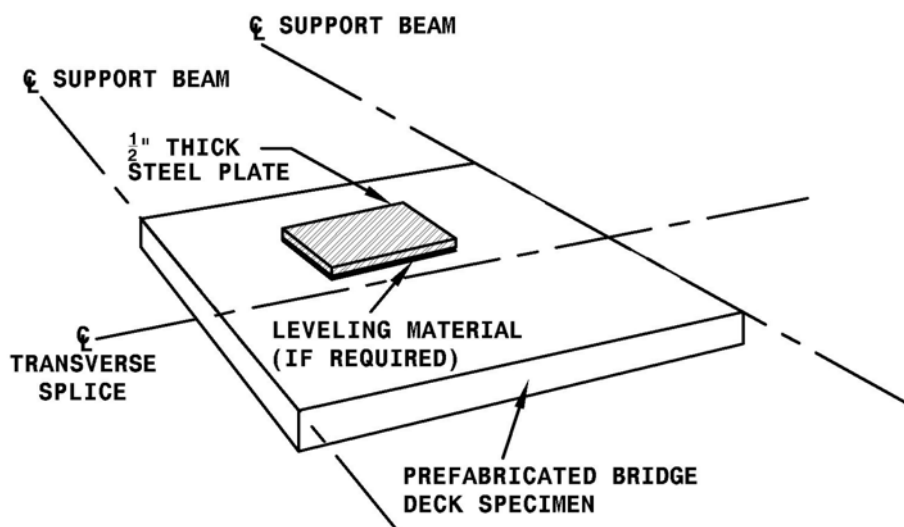


Figure 3: Typical Load Patch on Bridge Deck

4.2.2 Magnitude of Cyclic Load Range

For fatigue, the applied cyclic load range is 6.9 kips (30.7 kN). This load range, ΔP , is the minimum effective half axle load that shall be applied. The half axle load may be increased by a factor, S_{amp} , to decrease the time that it takes to complete the cyclic load test. The maximum value of S_{amp} shall be less than or equal to 3.0.

C4.2.2 Magnitude of Cyclic Load Range

A load factor of 0.75 is applied to an axle of the HS20 design truck to transform it to that of the HS15 fatigue truck. The HS15 yields the effective load range and hence, effective stress range, S_{reff} . In performing this test, it must be recognized that the individual rear axles of the HS20 truck are intended to simulate a tandem axle.

Only one half of the axle load is used to simulate a truck tire passing over the transverse

Standard Test Method and Commentary for Subassembly Cyclic Load Testing of Transverse Splices in Prefabricated Bridge Deck Panels

<p>The projected ADTT shall be used to determine the required number of cycles to be applied for the cyclic load test of the subassembly. To compute the number of cycles to be applied for the cyclic load test:</p> $N = (365^{\text{days}} / \text{year})(75 \text{ years})(4.5^{\text{cycles}} / \text{truck})(\text{ADTT})_{\text{SL}}$ <p>where:</p> <p>N = total number of cycles of stress range to be applied to the in-service bridge deck over its design life $(\text{ADTT})_{\text{SL}}$ = the single lane ADTT determined using the projected ADTT for the bridge.</p> <p>The total number of cycles is assumed to be inversely proportional to the cube of the load range. Therefore, the number of cycles to be applied for the cyclic load test may be computed as:</p> $N_f = N / (S_{\text{amp}})^3$ <p>where:</p> <p>N_f = number of cycles at the desired load range to be applied for the cyclic load test S_{amp} = factor by which load range is increased (i.e., amplified) from the HS15 axle</p> <p>The load range applied shall not be so large as to alter the failure mode that would be observed in service conditions. The applied load shall not cause the yield stress to be exceeded in any portion of the specimen.</p>	<p>splice detail. The tire is assumed to apply half the load of the given axle.</p> <p>The impact factor is set at 1.15 and is the dynamic load allowance for the fatigue limit state as specified by the AASHTO LRFD Bridge Design Specification. Hence, the actual half axle load is $(0.75 \times 32 \text{ kips}) \times \frac{1}{2} \times 1.15 \times \frac{1}{2} = 6.9 \text{ kips}$ (30.7 kN).</p> <p>The limitation of $3.0 S_{\text{amp}}$ is to prevent the user from selecting a load that is unrealistically high and may result in a different failure mode than that which would be observed under service conditions. S_{amp} will commonly be set to 2.0 as that corresponds to the upper bound fatigue limit state load for infinite life prescribed in the AASHTO LRFD Bridge Design Specifications and is a realistic axle load.</p> <p>The projected ADTT shall be acquired from the owner (e.g., DOT). This number of cycles shall be used and proportioned based on the increase in load range for the cyclic load test according to relationship shown.</p> <p>If a design life other than 75 years is desired, the appropriate design life may be used to compute the total number of cycles of stress range to be applied over the design life, N. It is noted that the 75 year life may be too excessive for most bridge decks.</p> <p>For decks, it is assumed that the front axle of a truck produces half of a load cycle while the remaining axles produce one (1) load cycle each. Therefore, the number of cycles assumed to be produced per truck passage for a deck is 4.5.</p> <p>The single lane ADTT shall be determined as :</p> $(\text{ADTT})_{\text{SL}} = p \times (\text{ADTT})$ <p>where:</p> <p>(ADTT) = projected number of trucks per day in one direction averaged over the design life. p = fraction of traffic in a single lane (Table 3.6.1.4.2-1 (AASHTO LRFD))</p> <p>It is assumed that the S-N cubic relationship used for metal fatigue can be used for this application.</p>
--	---

Standard Test Method and Commentary for Subassembly Cyclic Load Testing of Transverse Splices in Prefabricated Bridge Deck Panels

4.2.3 Vibration of Bridge Deck

A high frequency pneumatic vibrator or similar device shall be used to simulate the effect of vibrations caused by trucks passing over the bridge. The vibrator shall be rigidly attached to a support beam nearest to the transverse splice no more than two feet (610 mm) away from the outside edge of the deck. The vibrator shall be excited after the application of every 500,000 load cycles. The vibrator shall apply 50,000 cycles each interval and shall preferably be applied simultaneously with the application of the load cycles. The vibrator shall be excited prior to conducting the static tests at these intervals. The vibrator shall be capable of operating between 80 Hz and 120 Hz and produce a force range of 8 kips to 12 kips.

If the cyclic load test is terminated prior to any damage and the desired number of cycles is reached, the vibrator shall be excited for a minimum of 50,000 cycles prior to conducting the final static test.

C4.2.3 Vibration of Bridge Deck

Vibrations caused by the passing of trucks and wheel impacts can play a role in the stresses/deflections experienced by the bridge deck and connections to the superstructure. Some connection details may also loosen or fail in service due to vibrations from passing trucks. The application of the load range alone would not truly represent the full spectrum of dynamic loading of truck traffic. Although it is not essential the vibratory cycles and load cycles be applied concurrently, it is preferred. The 50,000 vibratory cycles every 500,000 load cycles was arbitrarily set as 10% of the load cycles. A greater percentage should be considered if the joints are located near traffic metering devices such as toll facilities, traffic signals, etc. However, it would seem that there would be no need to apply more than 25% of the load cycles.

The vibrator shall be excited prior to conducting the static tests at these intervals to simulate the vibrations from trucks passing over the deck.

The vibrator used during the development of this test was a Vibco model number SVRLS 8000.

5.0 Static Test Procedure

C5.0 Static Test Procedure

5.1 General

Static tests shall be conducted regularly throughout the cyclic load test to monitor the change in stress range, displacements, and to infer if there is any damage of the transverse splice and deck.

C5.1 General

5.2 Loads for Static Tests

The strength load shall be applied for the static tests. The magnitude of the strength load shall be as defined in 5.2.2.

The static loads shall be applied in a minimum of five increasing and approximately equal steps until the target static load (i.e., strength load) is achieved. A load interval equal to the load used in the cyclic testing portion of the test shall also be included in the load steps.

The load shall be maintained within +/- 2% at each load increment for a minimum of ten seconds to allow for the collection of data. The load shall be monitored throughout the test to ensure that the desired load intervals are achieved.

C5.2 Loads for Static Tests

The maximum load to be applied for the static tests is larger than that of the cyclic test to simulate the effect of a heavy truck passing over the bridge.

A load interval equal to the load used in the cyclic test shall also be included in the load steps. This is desirable to understand the behavior of the deck at both the cyclic and strength loads.

5.2.1 Application of Load for Static Tests

Application of load for the static tests shall be the same as that during the cyclic test, as per 4.2.1.

C5.2.1 Application of Load for Static Tests

Standard Test Method and Commentary for Subassembly Cyclic Load Testing of Transverse Splices in Prefabricated Bridge Deck Panels

<p>5.2.2 Magnitude of Load for Static Tests</p> <p>The maximum load to be applied, P_{max}, shall be that determined from the “Proposed Recommended Method for Verifying Strength of Bridge Decks”.</p>	<p>C5.2.2 Magnitude of Load for Static Tests</p>
<p>5.3 Data Collection for Static Tests</p> <p>Static tests shall be conducted prior to the start of the cyclic test, after every 500,000 cycles, and after termination of the test if the target number of cycles is achieved.</p> <p>Each static test shall be repeated a minimum of three times and data collected to assess repeatability and average results.</p> <p>Data from the three tests shall produce displacements and stress measurements within 15% of each other. If the measurements for the three static tests are outside of this range, the reasons shall be determined and corrected if possible.</p>	<p>C5.3 Data Collection for Static Tests</p> <p>Intervals less than 500,000 cycles can also be used if deemed appropriate by the owner. However, it is recommended to conduct cyclic load range static tests more frequently during the first 1,000,000 cycles of the test to identify any changes in behavior that occur early in the test. It is also recommended to conduct cyclic load range static tests more frequently when damage to the deck is observed.</p>
<p>6.0 Inspection and Termination of Test</p> <p>6.1 General</p> <p>The specimen, support beams or stringers, fixtures and connection details shall be inspected, at a minimum,</p> <ol style="list-style-type: none"> 1) prior to commencement of the cyclic load test; 2) after completion of each set of static tests; and 3) after termination of the cyclic load test (if applicable). 	<p>C6.0 Inspection and Termination of Test</p> <p>C6.1 General</p> <p>The specimen shall be inspected for defects including crack development and propagation, delamination, and failures as defined in 6.2.1.</p> <p>The support beams and fixtures shall also be inspected for damage and movement.</p>

Standard Test Method and Commentary for Subassembly Cyclic Load Testing of Transverse Splices in Prefabricated Bridge Deck Panels

<p>6.2 Duration of Test</p> <p>A test shall be terminated after the application of the desired number of cycles, N_f, at a given load range, ΔP. In such cases, the transverse splice is adequate.</p> <p>The test shall also be terminated if any of the failure criteria defined in 6.2.1 is met. In such cases, the transverse splice does not have sufficient fatigue resistance.</p> <p>The test shall be run a minimum of three million cycles unless the actual number of heavy axles anticipated to cross the joint in a given travel lane has been shown to be less than or equal to 50% of this value. In such cases, twice the actual number of cycles that are anticipated to cross the joint shall be applied.</p>	<p>C6.2 Duration of Test</p> <p>During the research used to develop this test, various approaches were evaluated to establish the minimum duration of the test. Considering the uncertainties associated with in-situ loading, assumptions built-in to the test method, potential ramifications of deck failure, and the cost of testing, a minimum duration of three million cycles was selected.</p> <p>The requirement that the minimum number of applied cycles be the lesser of the minimum specified (i.e., three million) or twice the actual number of heavy axles (if the actual number of load cycles in a given travel lane is less than 50% of the minimum specified) crossing the joint is a conservative approach to ensure a minimum number of cycles are applied even for low-volume roads.</p> <p>For example, if it is estimated that 1,000,000 axles will cross the joint during the design life of the deck, a minimum of 2,000,000 cycles shall be applied during the test.</p>
<p>6.2.1 Definitions of Failure</p> <p>The following shall be used to define failure of a given transverse splice:</p> <ul style="list-style-type: none"> • Yielding in any portion of the specimen; • Significant changes in behavior (i.e., nonlinear response) or difference in measured response greater than 15% from the start of the test at critical locations; • Fatigue cracking of steel that would compromise the performance of the deck during its intended service life. Debonding or slip of concrete; • Cracking of the concrete that will likely result in corrosion of the encased steel; or • Any other damage that would result in premature durability or strength failure of the specimen or supporting members. 	<p>C6.2.1 Definitions of Failure</p> <p>Although the deck may not experience collapse, large deflections creating a serviceability limit state may be produced. If a specimen experiences deflections that would be undesirable for service, the test shall be terminated.</p>
<p>7.0 Results</p> <p>7.1 Interpretation of Results</p> <p>A transverse splice shall be deemed suitable for service if the test is terminated after the specimen has survived the desired number of cycles, N_f, at the appropriate load range, ΔP, and does not satisfy any of the failure criteria in 6.2.1.</p>	<p>C7.0 Results</p> <p>C7.1 Interpretation of Results</p>

Standard Test Method and Commentary for Subassembly Cyclic Load Testing of Transverse Splices in Prefabricated Bridge Deck Panels

8.0 Reporting of Data	C8.0 Reporting of Data
8.1 Cyclic Load Test Results and Observations The following data shall be reported: <ol style="list-style-type: none"> 1. The average displacements (at all locations), measured stresses, and load shall be reported in tabular format at all load levels for the initial and final static tests. 2. The average measured stresses and displacement at the cyclic and strength loads from each set of static tests shall be plotted against the number of cycles completed (i.e., 0, 500,000, 1,000,000, etc). These values shall also be reported in tabular format. 3. Load range, ΔP, and the corresponding desired number of cycles, N_f, for the cyclic load test. 4. Number of cycles and reason for termination of the cyclic load test. 5. Details of failure (if applicable). 	C8.1 Cyclic Load Test Results and Observations The measured displacements and stresses are to be monitored throughout the test. The average displacements and stresses from the sets of static tests carried out every 500,000 cycles are to be plotted against the number of cycles to determine whether there are significant changes in the behavior of the deck (e.g., increased deflections, stresses, etc).
8.2 Miscellaneous Required Information The following information shall also be reported: <ul style="list-style-type: none"> • Deck type and fabricator; • Section properties and detail dimensions of the specimens and supports/fixtures; • Material properties for deck components. • Visible deviations or defects; • A drawing showing the shape, size and orientation of the specimen and the fixtures; • A drawing showing the location of all instrumentation and the load patch; and • All sensor calibrations. 	C8.2 Miscellaneous Required Information

ATTACHMENT K - Proposed Revisions to AASHTO LRFD Bridge Design Specifications

<p>4.6.2.1.8 Live Load Force Effects for Fully and Partially Filled Grids and for Unfilled Grid Decks Composite with Reinforced Concrete Slabs</p>	<p>C4.6.2.1.8</p>
<p>Moments in kip-in./in. of deck due to live load may be determined as:</p> <ul style="list-style-type: none"> Main bars perpendicular to traffic: <p>For $L \leq 120$ in.</p> $M_{transverse} = 1.28 D^{0.197} L^{0.459} C$ $M_{transverse} = \frac{1.17 D^{0.214} L^{0.468}}{\alpha^{0.231}} (C) \quad (4.6.2.1.8-1)$ <p>For $L > 120$ in.</p> $M_{transverse} = \frac{D^{0.188} (3.7 L^{1.35} - 956.3)}{L} (C)$ $M_{transverse} = \frac{D^{0.194} (1.3 L^{1.55} - 857)}{L \alpha^{0.233}} (C) \quad (4.6.2.1.8-2)$ <ul style="list-style-type: none"> Main bars parallel to traffic: <p>For $L \leq 120$ in.</p> $M_{parallel} = 0.73 D^{0.123} L^{0.64} C$ $M_{parallel} = \frac{0.91 D^{0.12} L^{0.6}}{\alpha^{0.145}} (C) \quad (4.6.2.1.8-3)$ <p>For $L > 120$ in.</p> $M_{parallel} = \frac{D^{0.138} (3.1 L^{1.429} - 1088.5)}{L} (C)$ $M_{parallel} = \frac{D^{0.11} (1.136 L^{1.62} - 725)}{L \alpha^{0.174}} (C) \quad (4.6.2.1.8-4)$	<p>The moment equations are based on orthotropic plate theory considering vehicular live loads specified in Article 3.6. The moment equations are based on analytical solutions to generalized orthotropic plate theory by Turan and Higgins (2011) considering vehicular patch loads specified in Article 3.6. The equations take into account relevant factored load combinations including truck and tandem loads. The moment equations also account for dynamic load allowance, multiple presence factors, and load positioning on the deck surface to produce the largest possible moment.</p> <p>Negative moment can be determined as maximum simple span positive moment times the continuity factor, C.</p> <p>The reduction factor of 3.0 in the last sentence of Article 4.6.2.1.8 accounts for smaller dynamic load allowance (15 percent vs. 33 percent), smaller load factor (0.75 vs. 1.75) and no multiple presence (1.0 vs. 1.2) when considering fatigue. Use of Eqs. 1 and 3 Eqs. 4.6.2.1.8-1 and 4.6.2.1.8-3 for all spans is appropriate as Eqs. 1 and 3 Eqs. 4.6.2.1.8-1 and 4.6.2.1.8-3 reflect an individual design truck on short-span lengths while Eqs. 2 and 4 Eqs. 4.6.2.1.8-2 and 4.6.2.1.8-4 reflect the influence of multiple design tandems that control moment envelope on longer span lengths. The approximations produce reasonable estimates of fatigue Strength I and Fatigue moments; however, improved estimates can be determined using design truck, tandem and fatigue truck patch loads in the infinite series formula provided by Higgins (2003) Higgins <i>et al.</i> (2011).</p>

<p>where:</p> <p>L = span length from center-to-center of supports (in.)</p> <p>C = continuity factor; 1.0 for simply supported and 0.8 for continuous spans</p> <p>$D = D_x/D_y$</p> <p>D_x = flexural rigidity of deck in main bar direction (kip-in.²/in.)</p> <p>D_y = flexural rigidity of deck perpendicular to main bar direction (kip-in.²/in.)</p> <p>α = relative torsional stiffness parameter of the deck = $\frac{2D_{xy}}{\sqrt{D_x D_y}}$; and</p> <p>$D_{xy}$ = torsional stiffness.</p>	
<p>For grid decks, D_x and D_y should be calculated as EI_x and EI_y where E is the modulus of elasticity and I_x and I_y are the moment of inertia per unit width of deck, considering the section as cracked and using the transformed area method for the main bar direction and perpendicular to main bar direction, respectively</p> <p>Moments for fatigue assessment may be estimated for all span lengths by reducing Eq. 4.6.2.1.8-1 for main bars perpendicular to traffic or Eq. 4.6.2.1.8-3 for main bars parallel to traffic by a factor of 3.</p>	<p>Actual D_x and D_y values can vary considerably depending on the specific deck design, and using assumed values based only on the general type of deck can lead to unconservative design moments. Flexural rigidity in each direction should be calculated analytically as EI considering the section as cracked and using the transformed area method. Flexural rigidity in the strong (D_x) and weak (D_y) directions should be established experimentally or calculated analytically as EI per unit width of deck considering the section as cracked and using the transformed area method. The torsional stiffness (D_{xy}) should be determined experimentally. Standard test methods to obtain D_x, D_y, and D_{xy} are presented in NCHRP Report 10-72.</p> <p>For deck systems with thick concrete plating such as fully and partially filled grid as well as uniformly thick decks, α can be taken as unity.</p>
<p>Deflection in units of in. due to vehicular live load may be determined as:</p> <ul style="list-style-type: none"> Main bars perpendicular to traffic: $\Delta_{transverse} = \frac{0.0052D^{0.19}L^3}{D_x} \quad (4.6.2.1.8-5)$ <ul style="list-style-type: none"> Main bars parallel to traffic: $\Delta_{parallel} = \frac{0.0072D^{0.11}L^3}{D_x} \quad (4.6.2.1.8-6)$	<p>The deflection equations permit calculation of the midspan displacement for a deck under service load. The equations are based on orthotropic plate theory and consider both truck and tandem loads on a simply supported deck.</p> <p>Deflection may be reduced for decks continuous over three or more supports. A reduction factor of 0.8 is conservative.</p> <p><u>The approximations produce reasonable estimates of Service I deflections; however, improved estimates can be determined for prescribed patch loads in the infinite series formula provided by Turan and Higgins (2011).</u></p>

4.6.2.1.9 Inelastic Analysis		
The inelastic finite element analysis or yield line analysis may be permitted by the Owner.		
<u>References</u> Turan, O.T., and C. Higgins, "Analytical Solutions to General Orthotropic Plates under Patch Loading," <i>ASCE Journal of Engineering Mechanics</i> , July 2011 Vol. 137, No. 7, pp. 504-508 Higgins, C., Turan, O. T., Connor, R. J., Liu, J., (2011) "A Unified Approach for LRFD Live Load Moments in Bridge Decks" <i>ASCE Journal of Bridge Engineering</i> . (doi:10.1061/(ASCE)BE.1943-5592.0000217)		

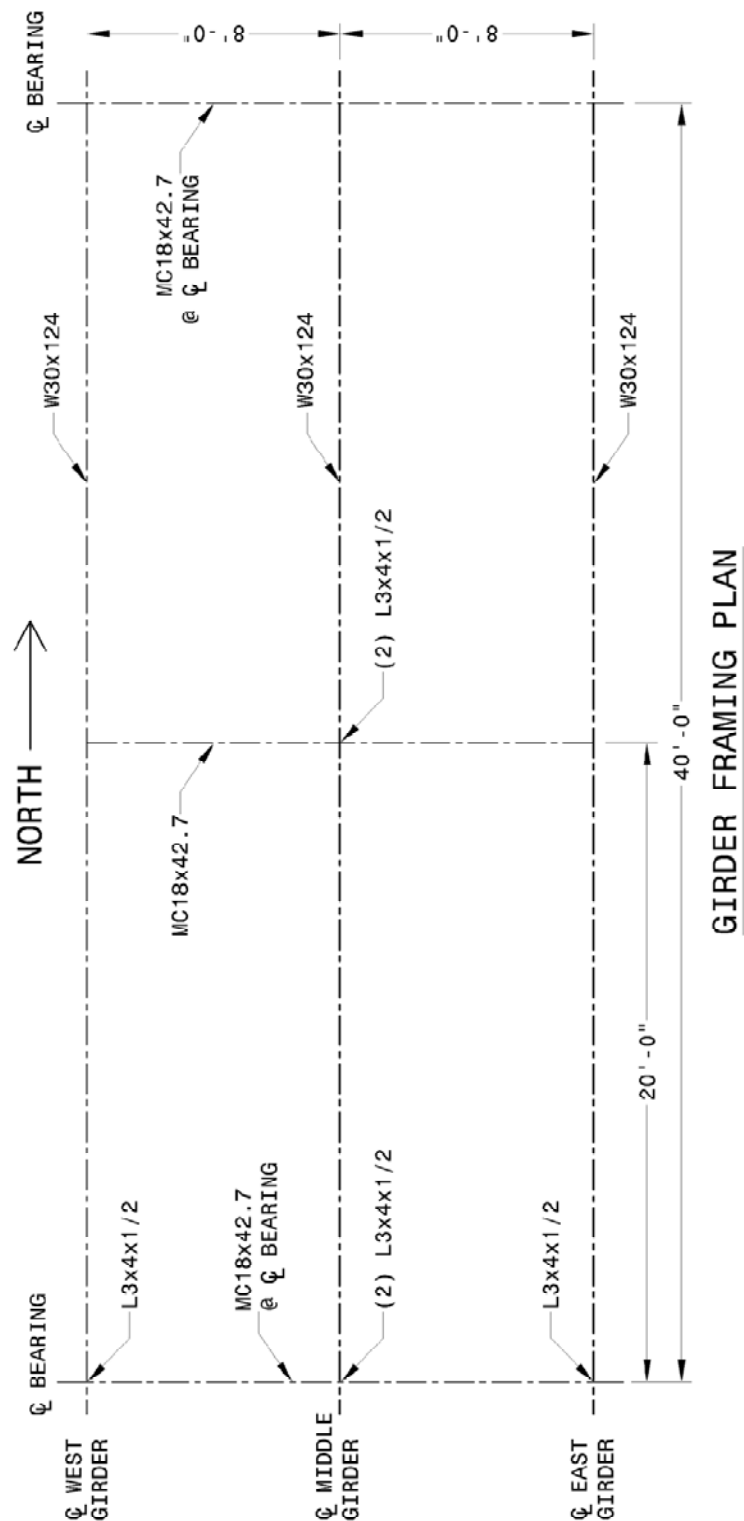
APPENDIX A Drawings

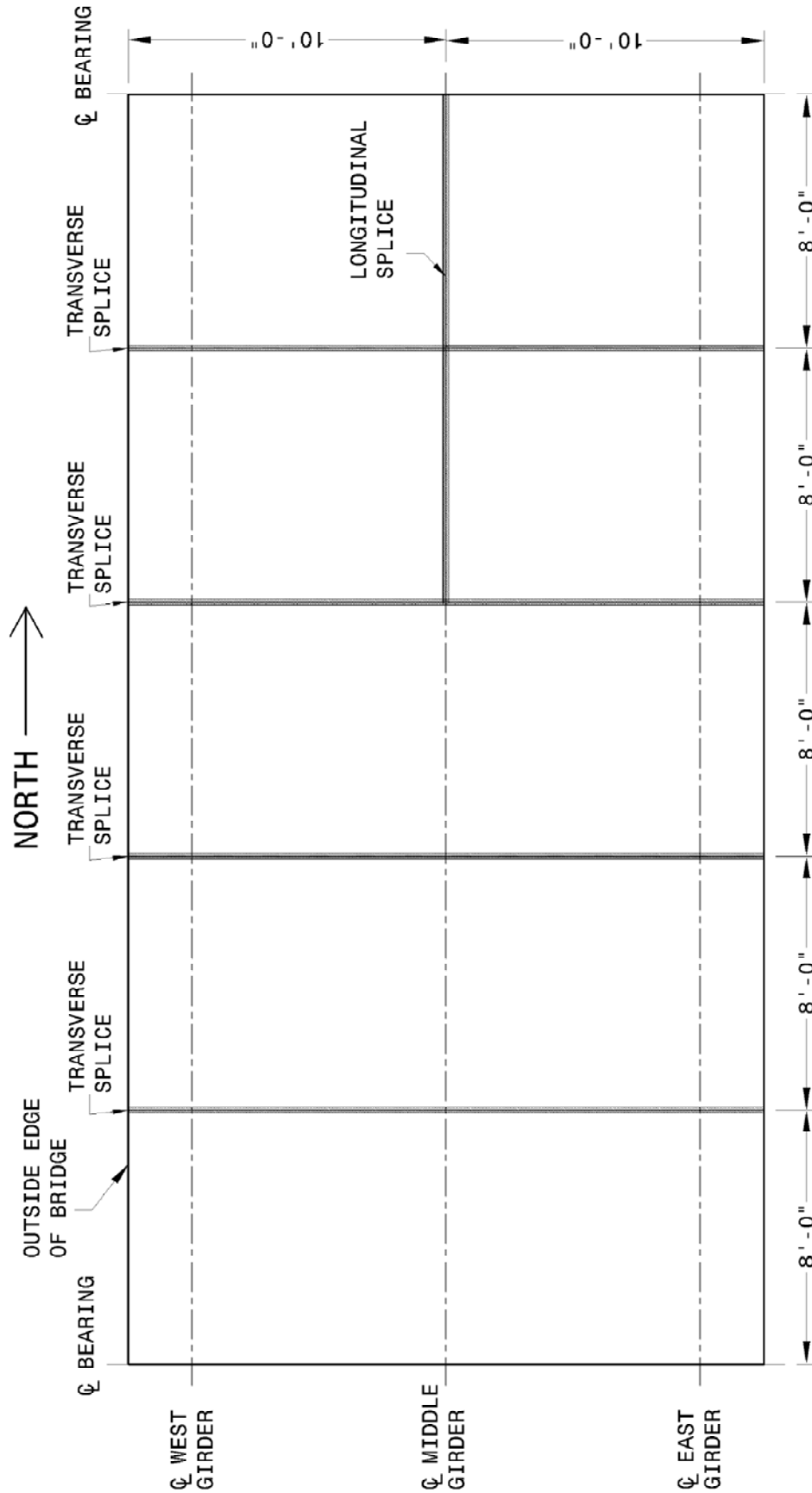
TABLE OF CONTENTS

A.1	Large Scale Specimen.....	A-1
A.1.1	Girder and Deck Layout	A-1
A.1.2	Main Bar Strain Gage Plans	A-4
A.1.3	Cross Bar Strain Gage Plans.....	A-8
A.1.4	Girder Strain Gage and LVDT Plans.....	A-13
A.2	Subassembly Open Grid Deck Specimen #1	A-17
A.2.1	Strong Direction Stiffness (D_x) Test.....	A-18
A.2.2	Weak Direction Stiffness (D_y) Test.....	A-22
A.2.3	Torsional Stiffness (D_{xy}) Test Rotation #1	A-26
A.2.4	Torsional Stiffness (D_{xy}) Test Rotation #2	A-30
A.2.5	Torsion Stiffness (D_{xy}) Test Rotation #3.....	A-34
A.2.6	Elevations of Steel with Strain Gages	A-36
A.3	Subassembly Open Grid Deck Specimen #2	A-40
A.3.1	Strong Direction Stiffness (D_x) Tests	A-41
A.3.2	Weak Direction Stiffness (D_y) Test.....	A-45
A.3.3	Torsion Stiffness (D_{xy}) Test Rotation #1	A-49
A.3.4	Elevations of Steel with Strain Gages	A-53
A.4	Subassembly Partially Filled Grid Deck Specimen.....	A-57
A.4.1	Torsion Stiffness (D_{xy}) Test Rotation #2.....	A-58
A.4.2	Torsion Stiffness (D_{xy}) Test Rotation #3.....	A-62
A.5	Subassembly Longitudinal Splice Specimen.....	A-65
A.5.1	Elevations of Steel Components with Strain Gages	A-68
A.6	Subassembly Deck-to-Superstructure Connection Specimen.....	A-70
A.6.1	Elevations of Steel Components with Strain Gages	A-74
A.7	Subassembly Transverse Splice Specimen.....	A-76
A.7.1	Elevations of Steel Components with Strain Gages	A-81

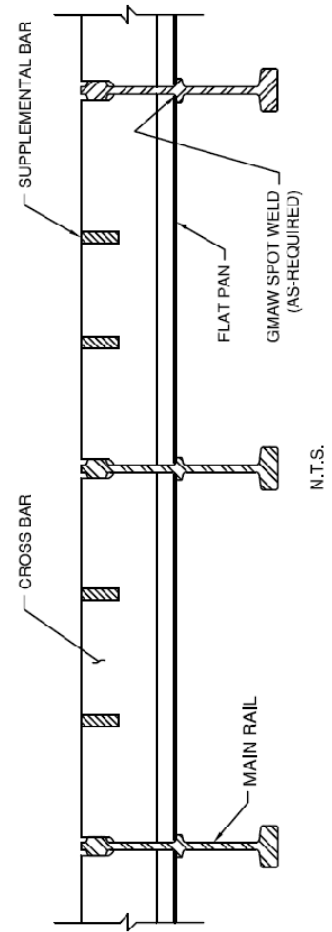
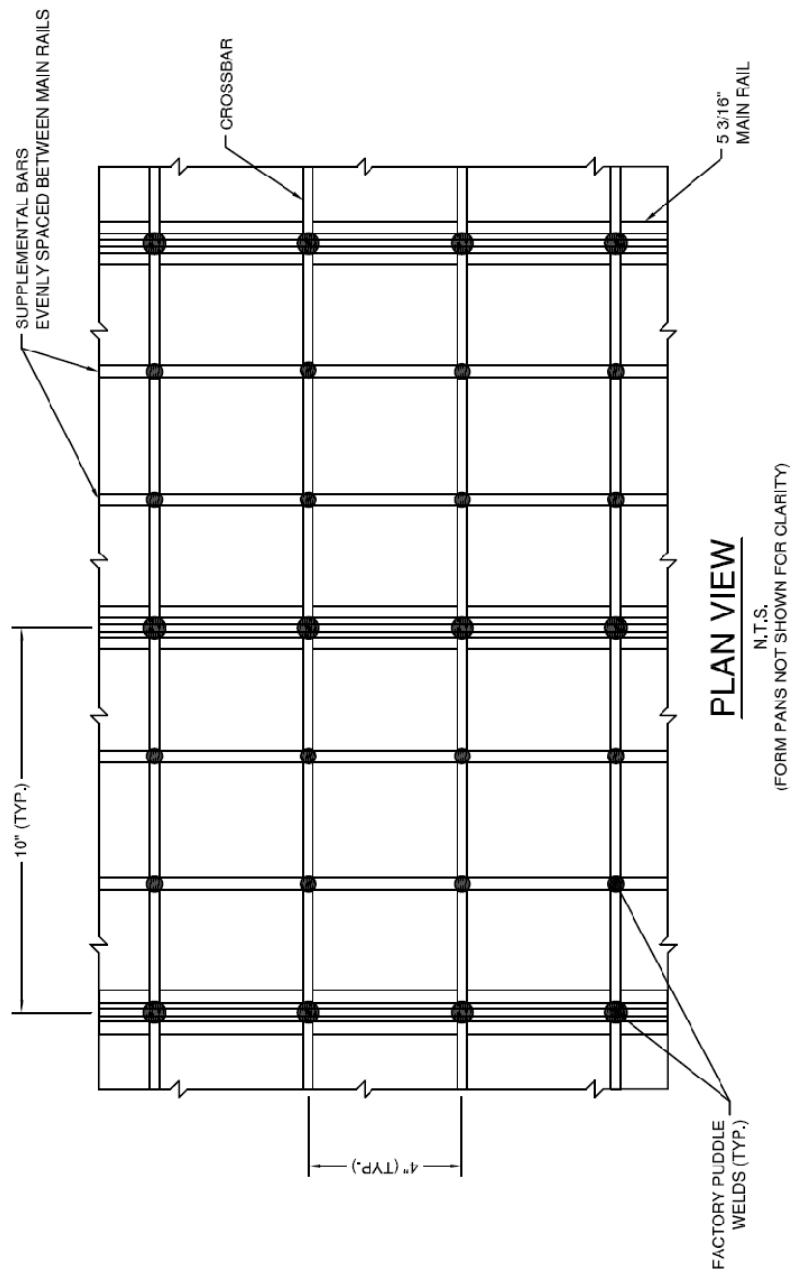
A.1 Large Scale Specimen

A.1.1 Girder and Deck Layout

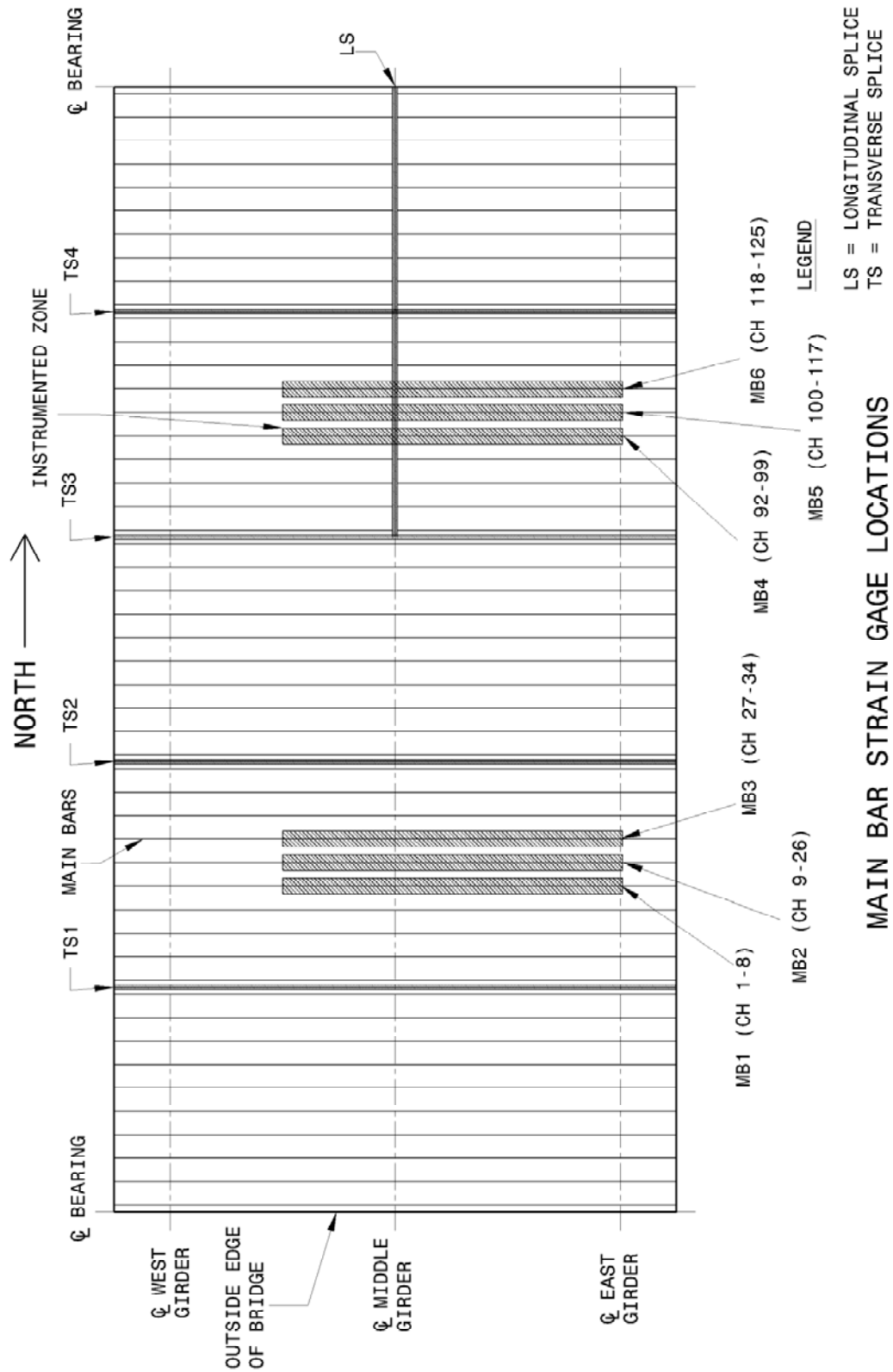


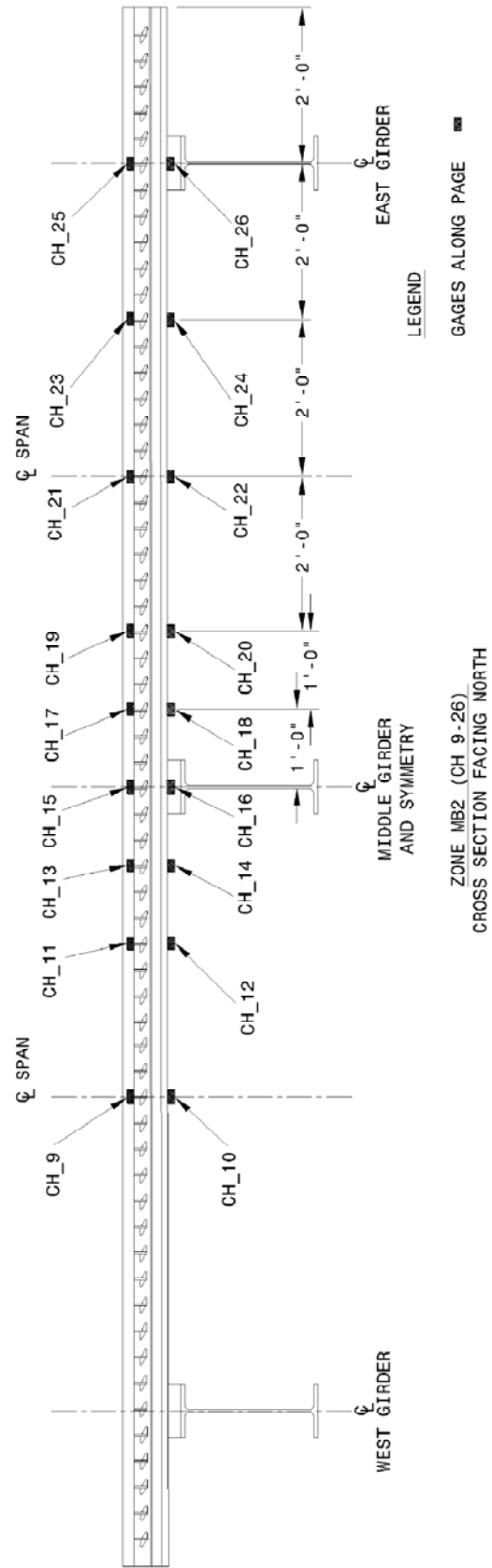
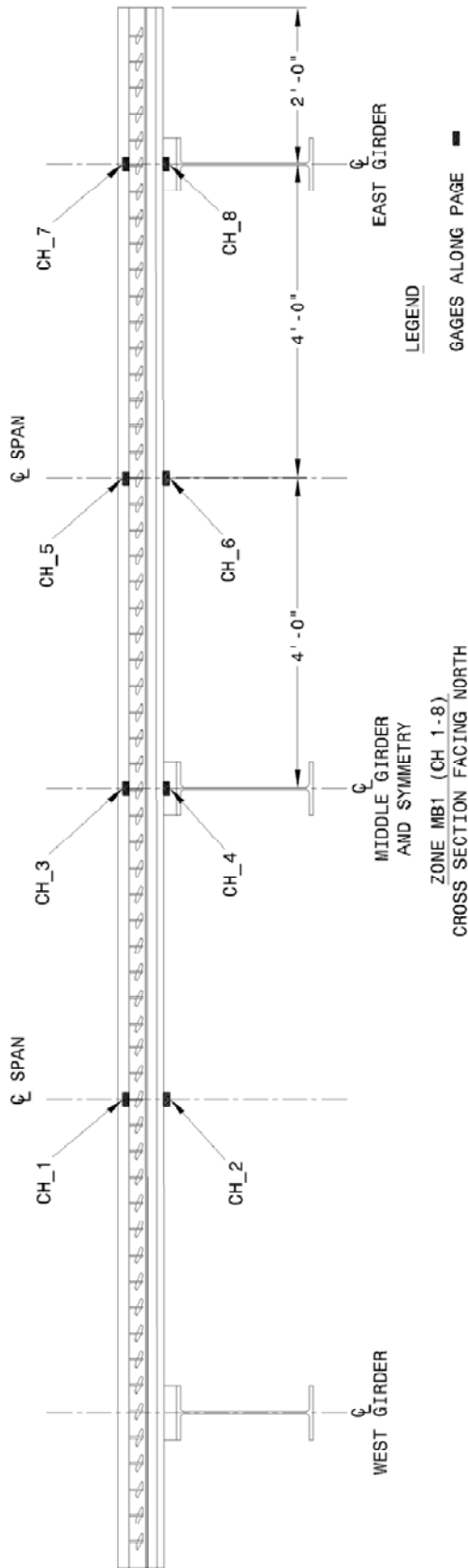


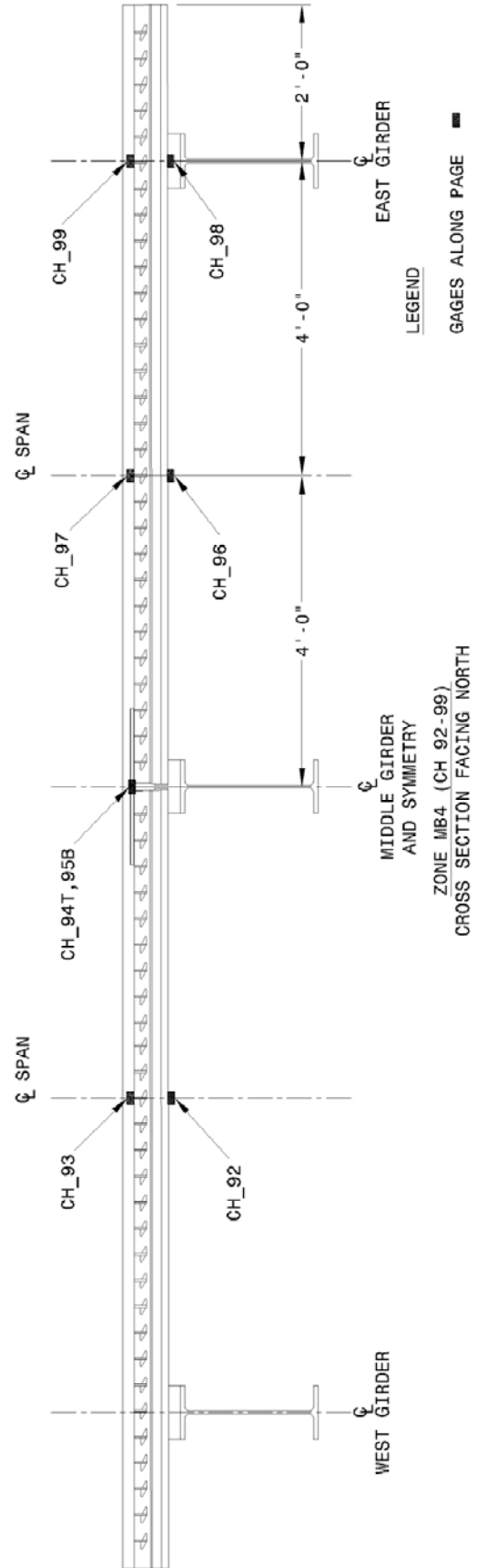
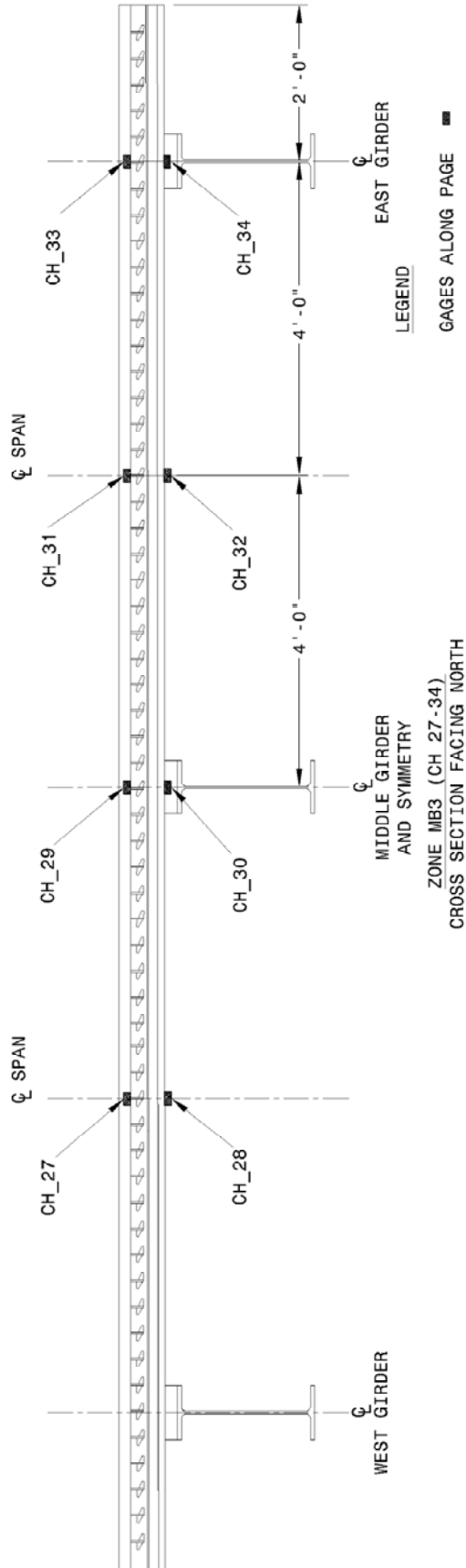
DECK PANEL LAYOUT



A.1.2 Main Bar Strain Gage Plans







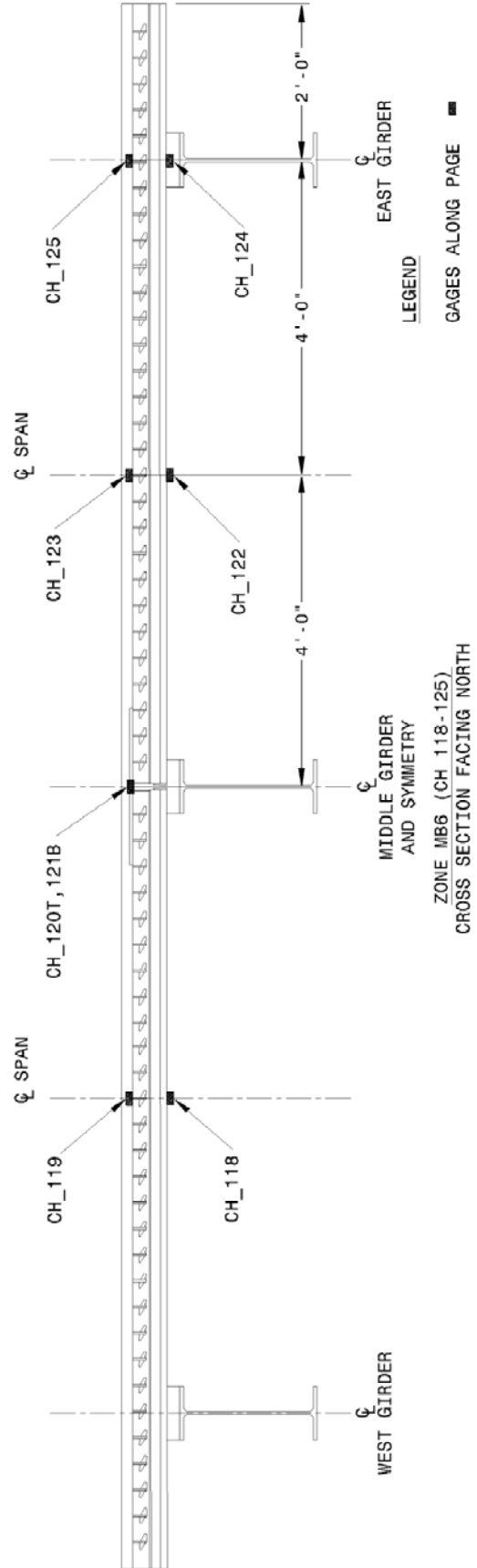
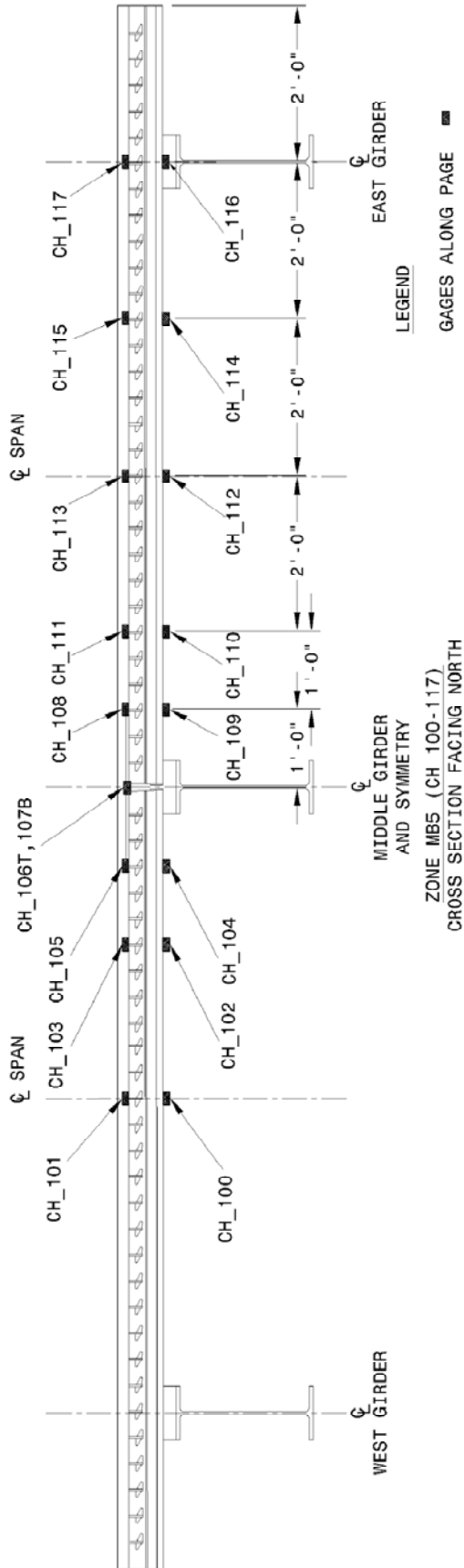


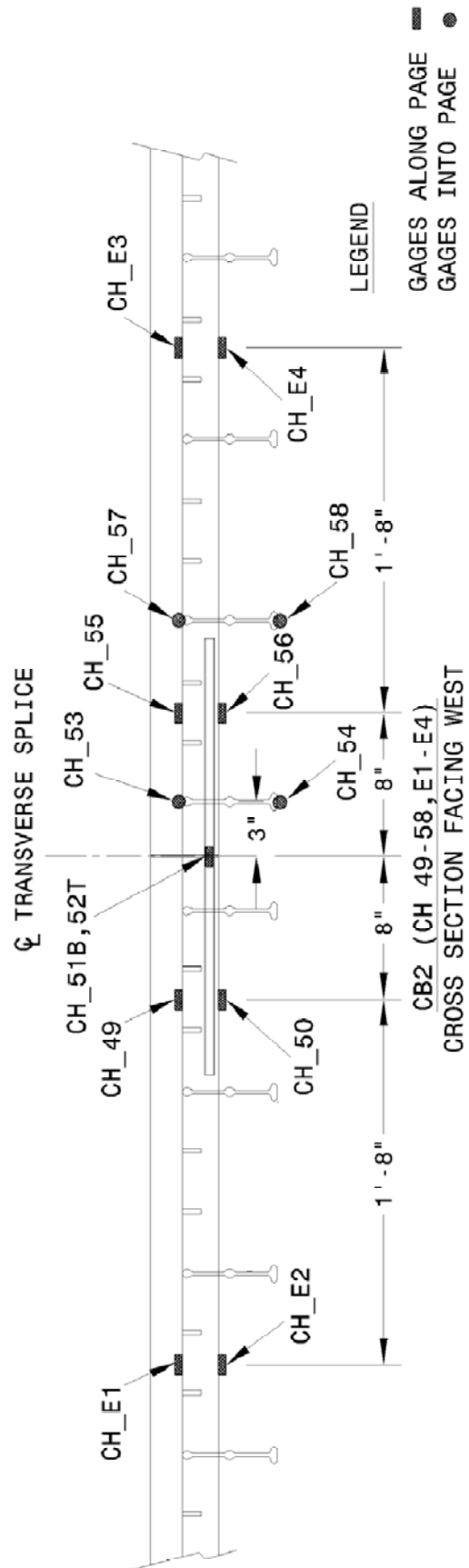
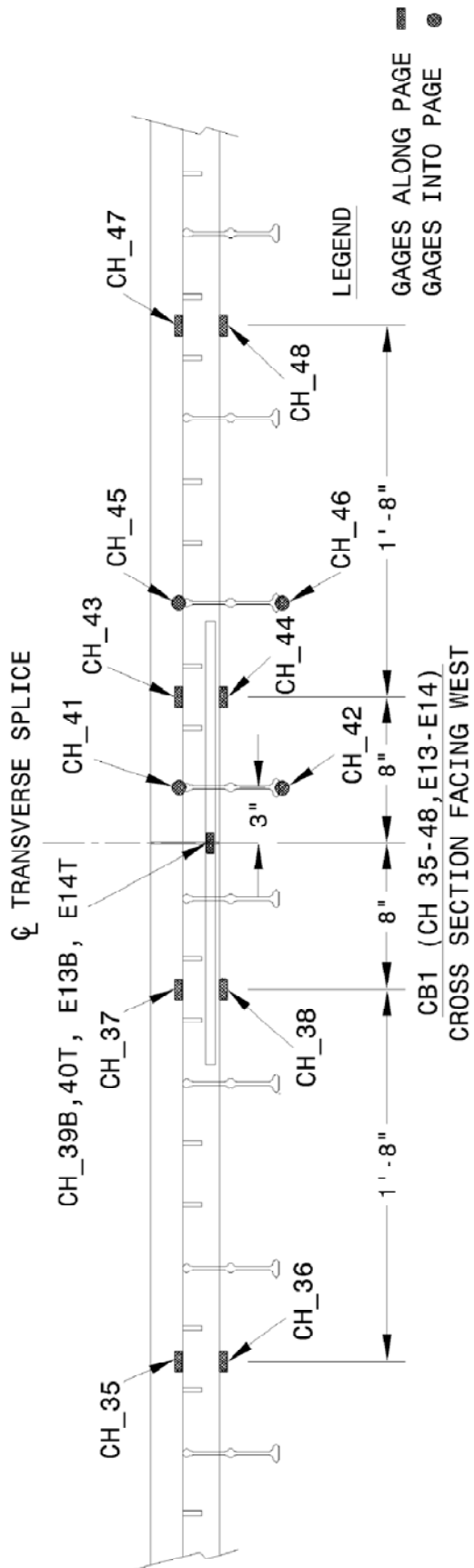
Diagram illustrating the locations of cross bar strain gages (CB) and transverse splice (TS) locations on a bridge deck. The diagram shows the layout of the bridge deck, including the West Girder, Middle Girder, and East Girder, and the locations of the cross bars (CB) and transverse splice (TS) locations.

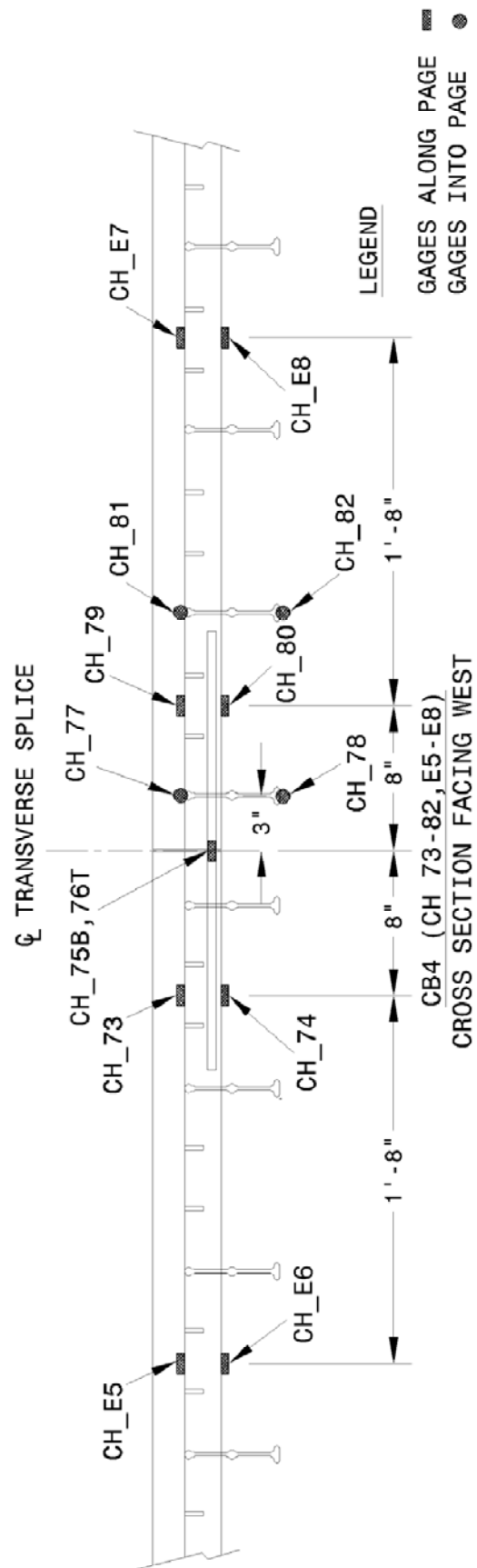
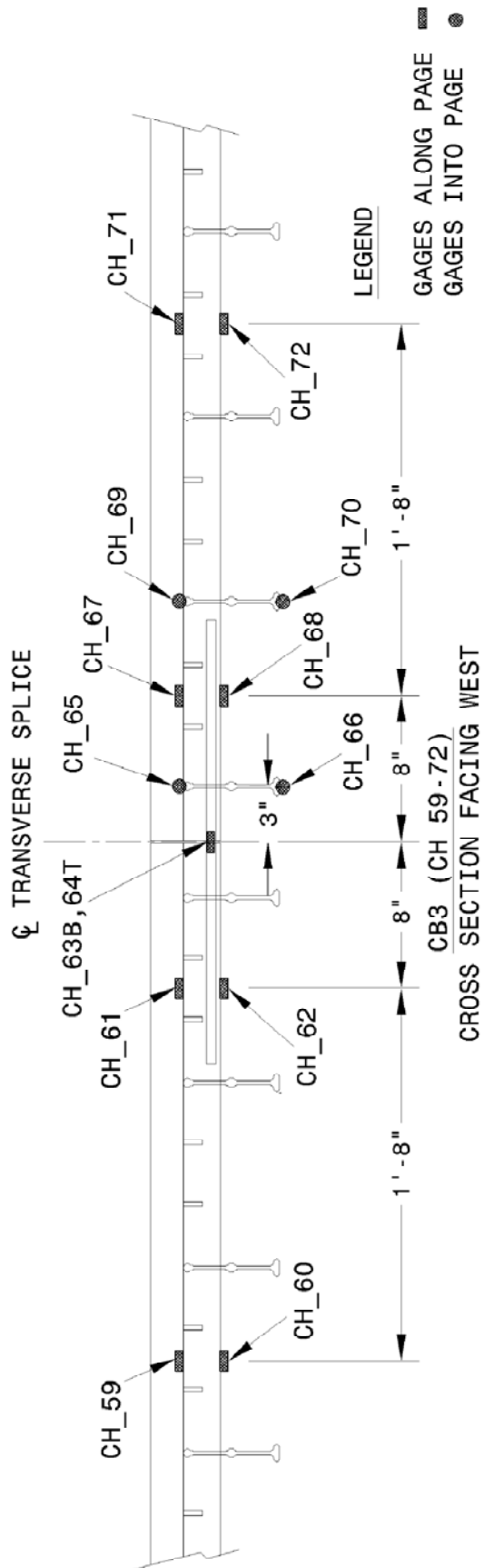
Legend:

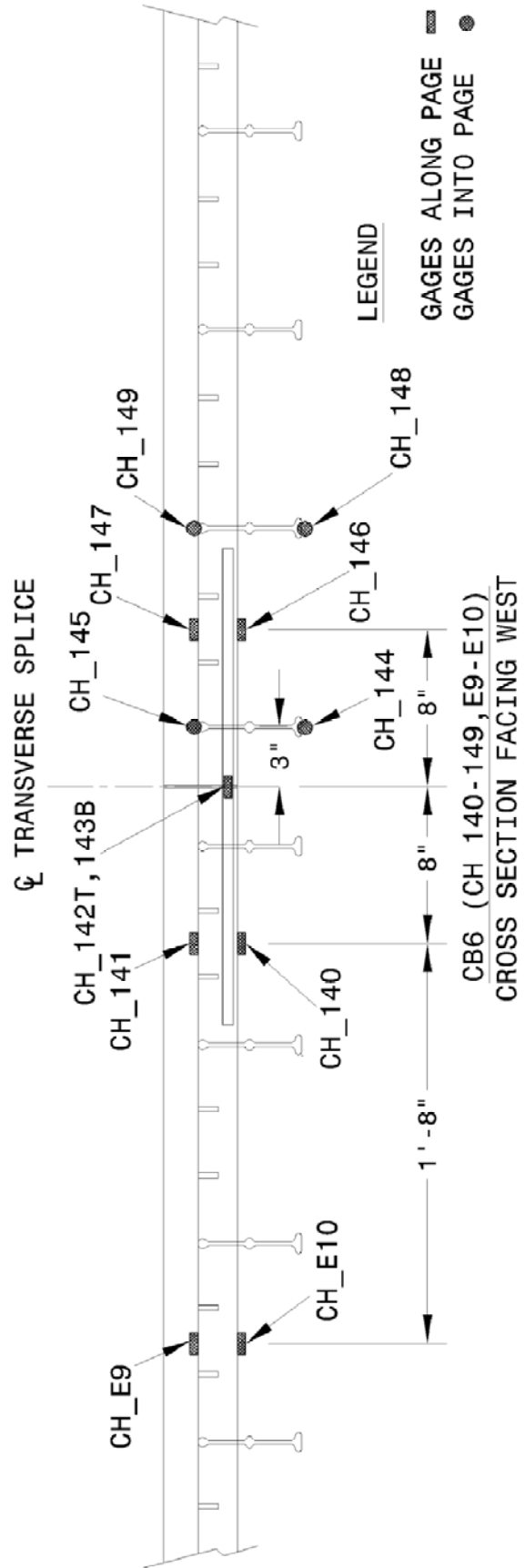
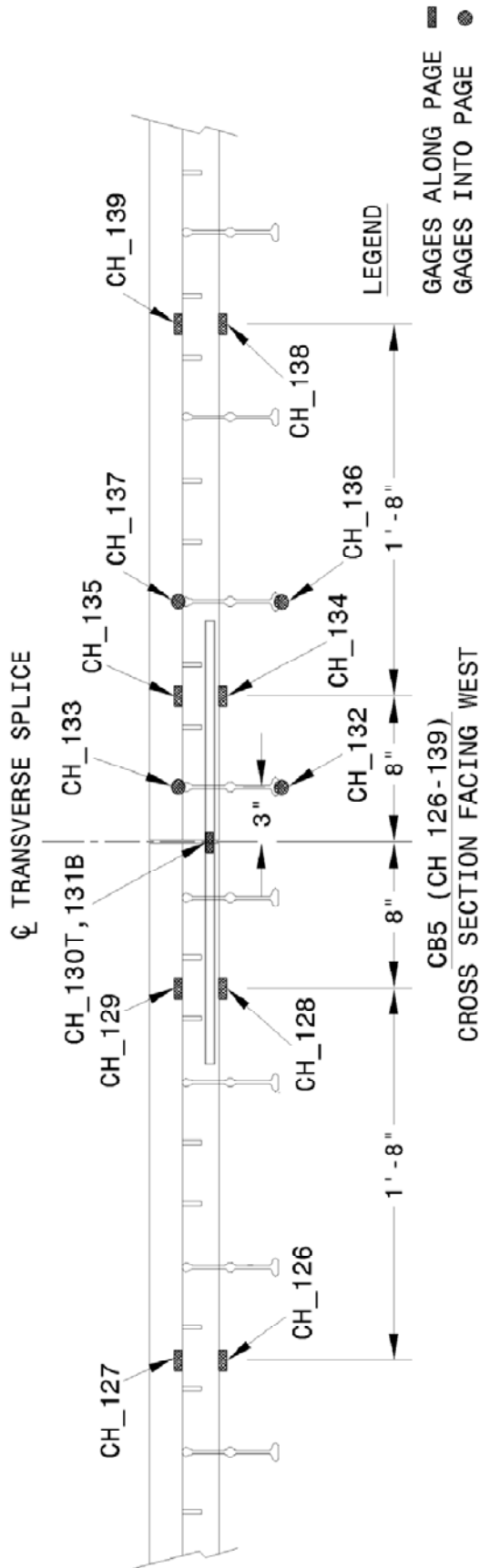
- LS = LONGITUDINAL SPLICE
- TS = TRANSVERSE SPLICE

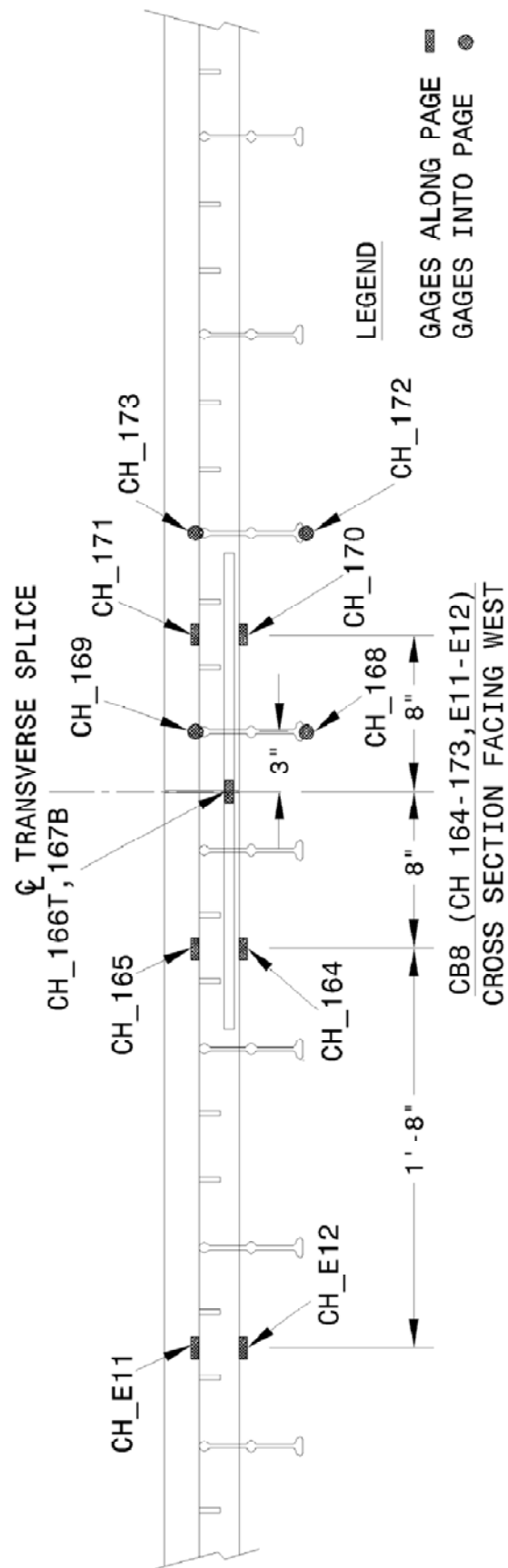
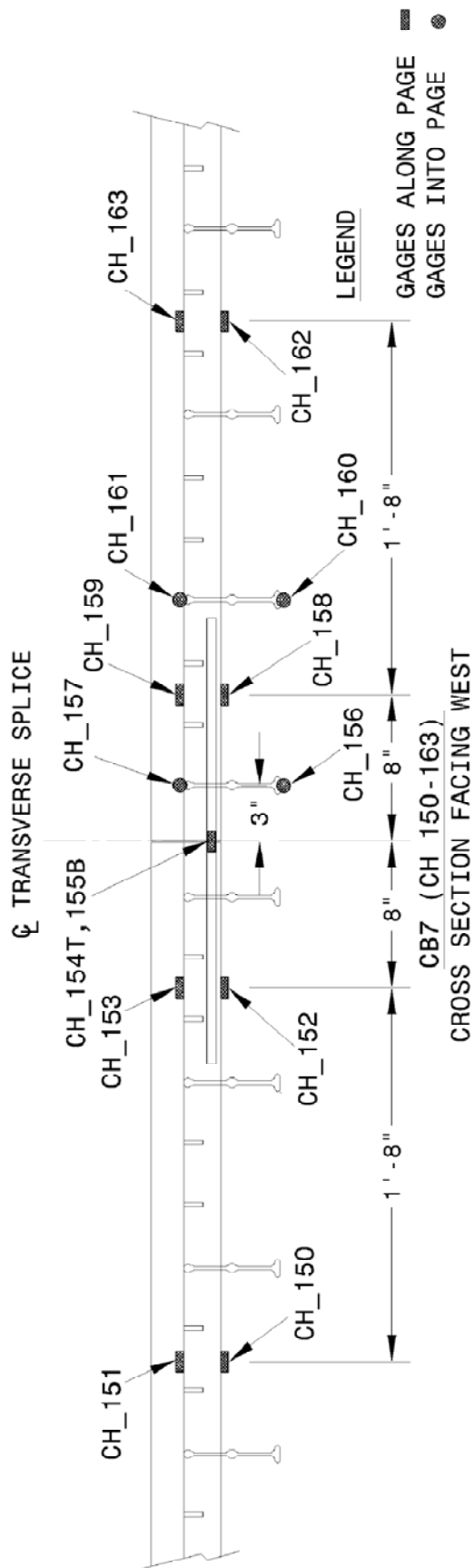
Diagram Labels:

- OUTSIDE EDGE OF BRIDGE
- TS4
- TS3
- TS2
- TS1
- CB1 (CH 35-48, E13-E14)
- CB2 (CH 49-58, E1-E4)
- CB3 (CH 59-72)
- CB4 (CH 73-82, E5-E8)
- CB5 (CH 126-139)
- CB6 (CH 140-149, E9-E10)
- CB7 (CH 150-163)
- CB8 (CH 164-173, E11-E12)
- INSTRUMENTED ZONE
- CROSS BARS (TYP)
- Q WEST GIRDER
- Q MIDDLE GIRDER
- Q EAST GIRDER
- Q BEARING
- LS

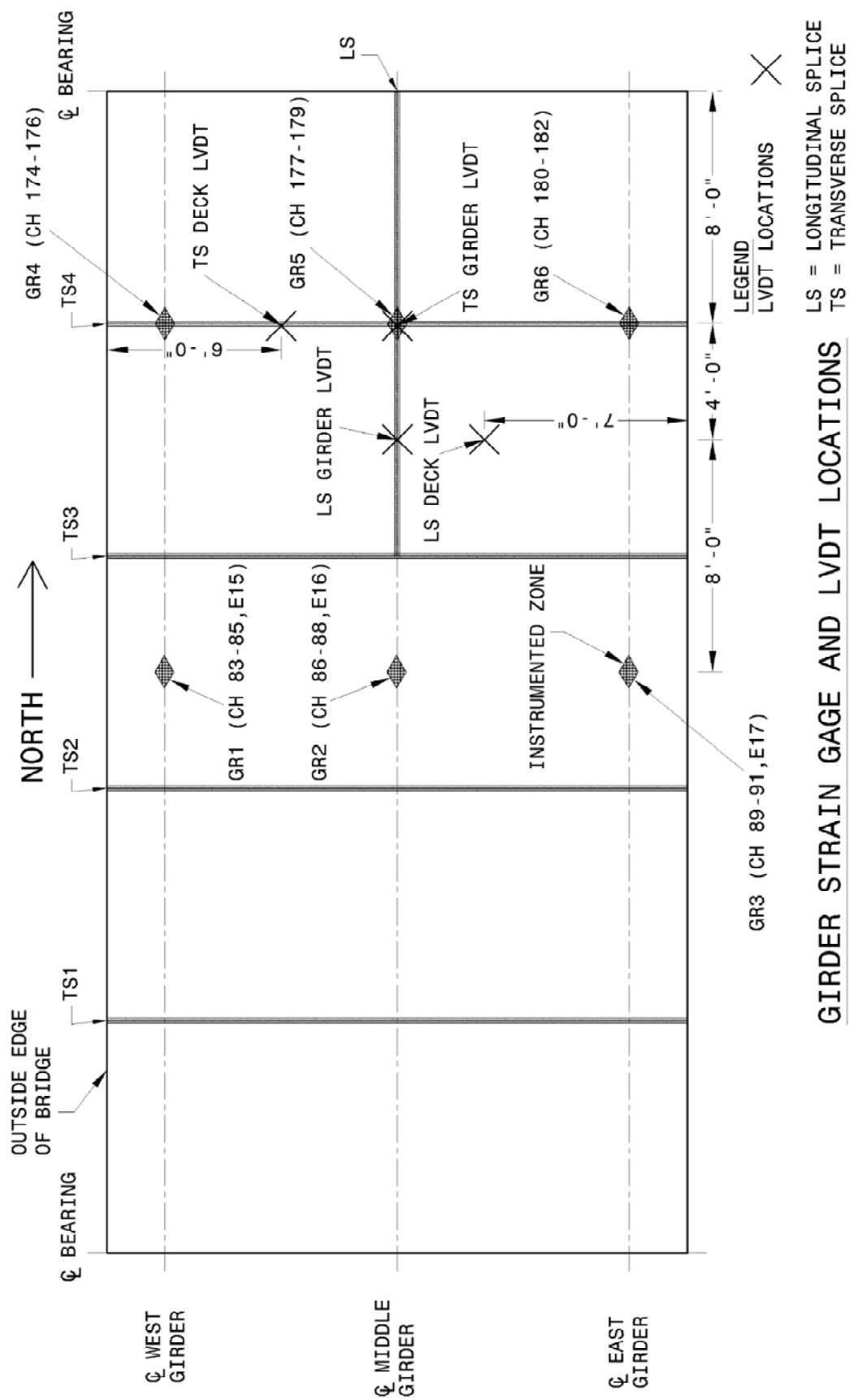


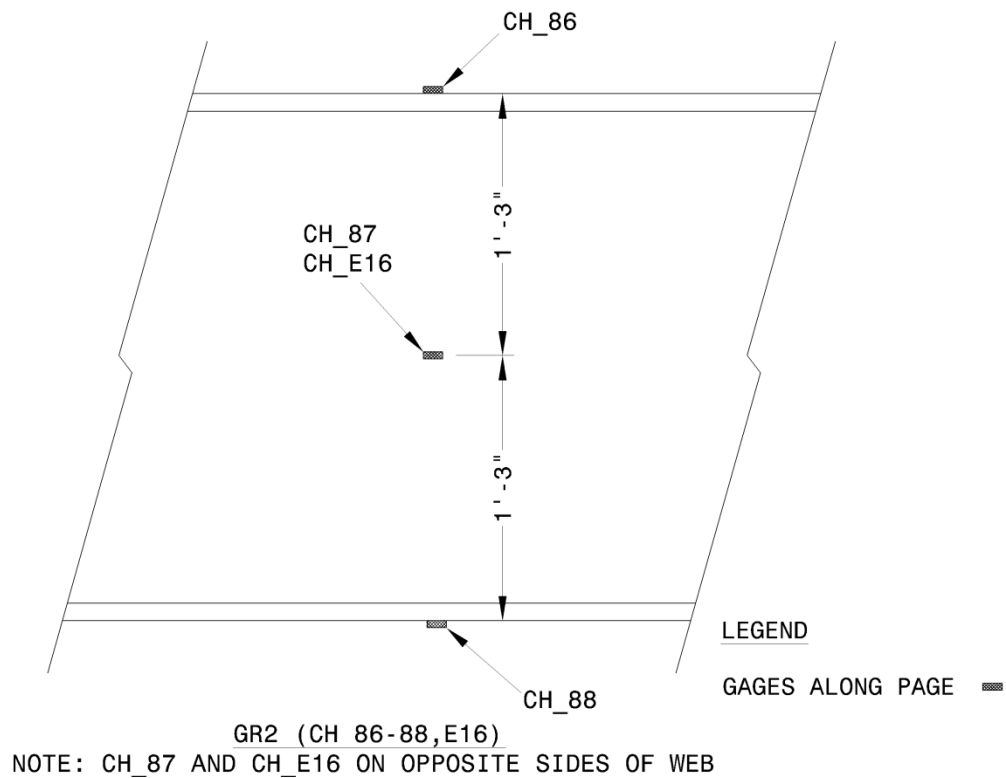
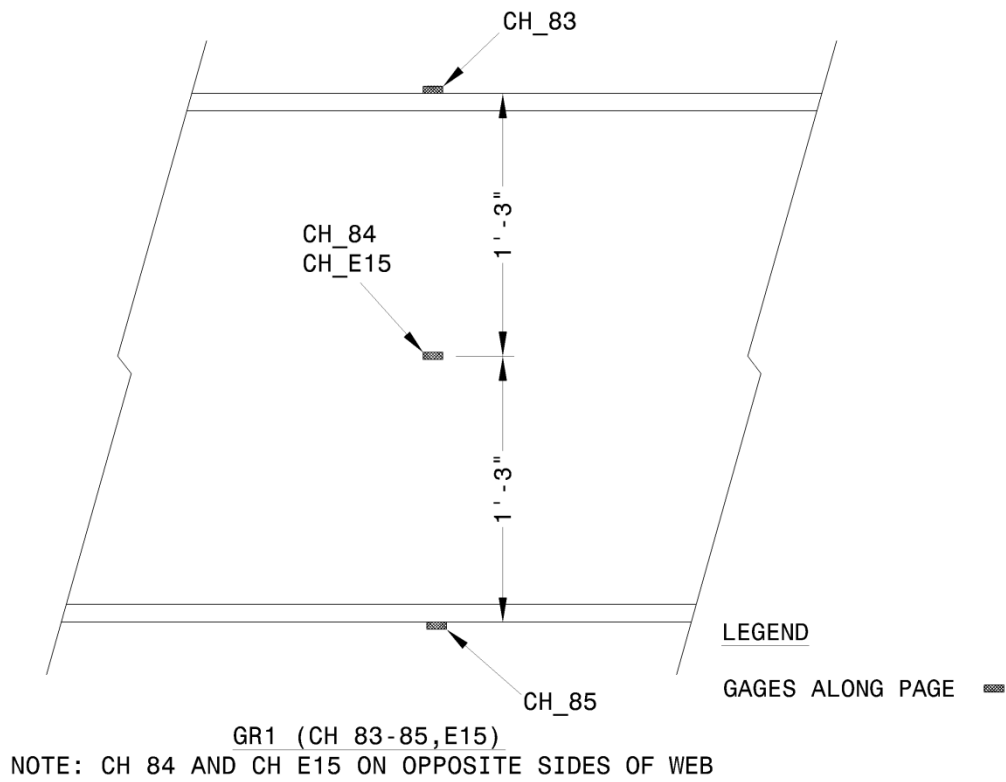


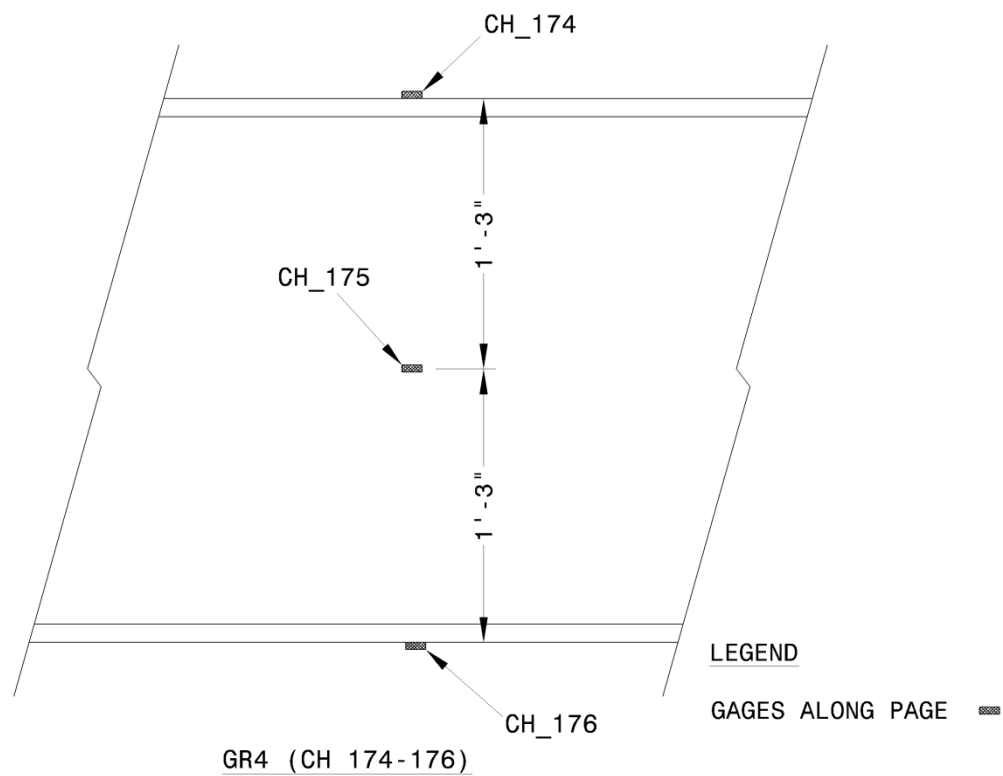
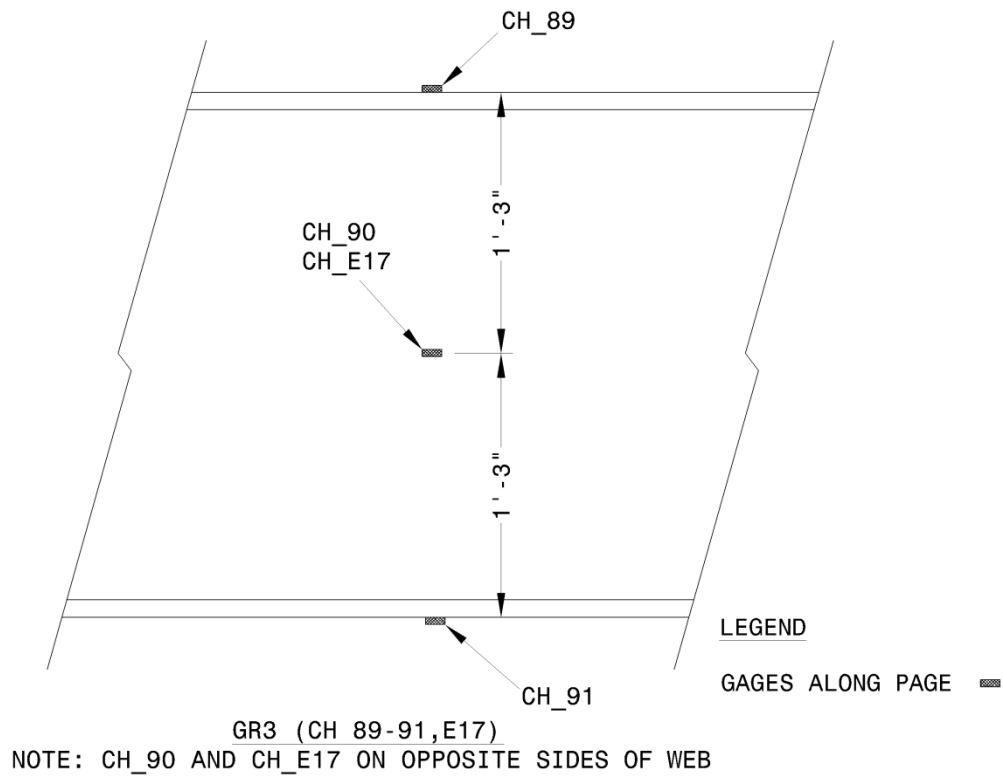


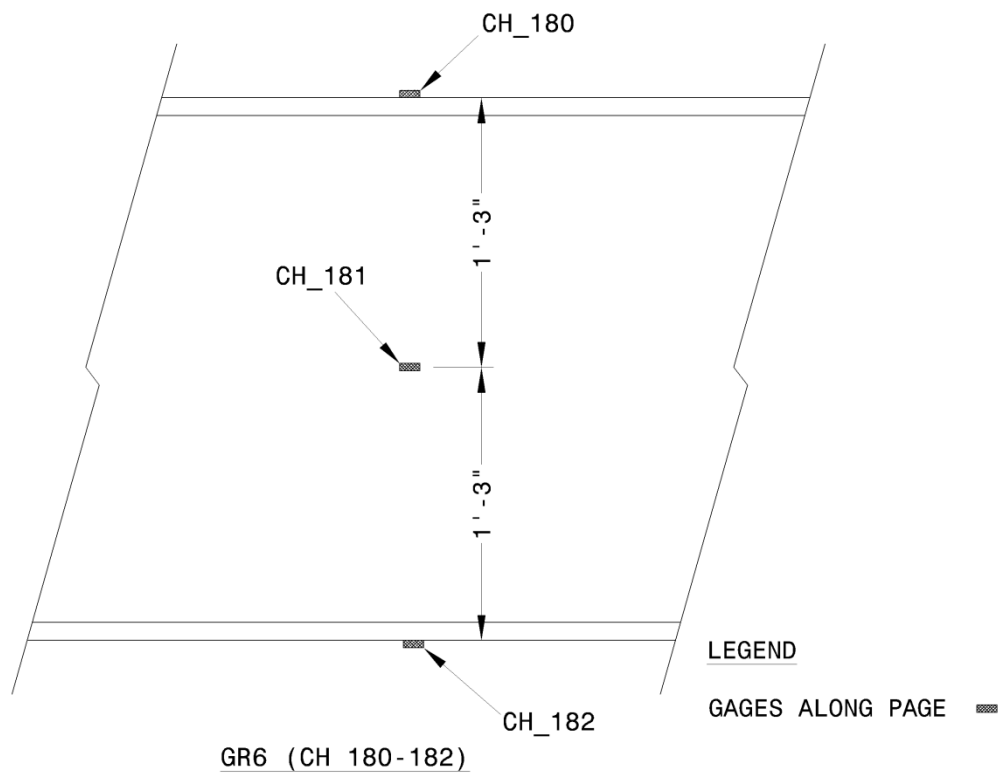
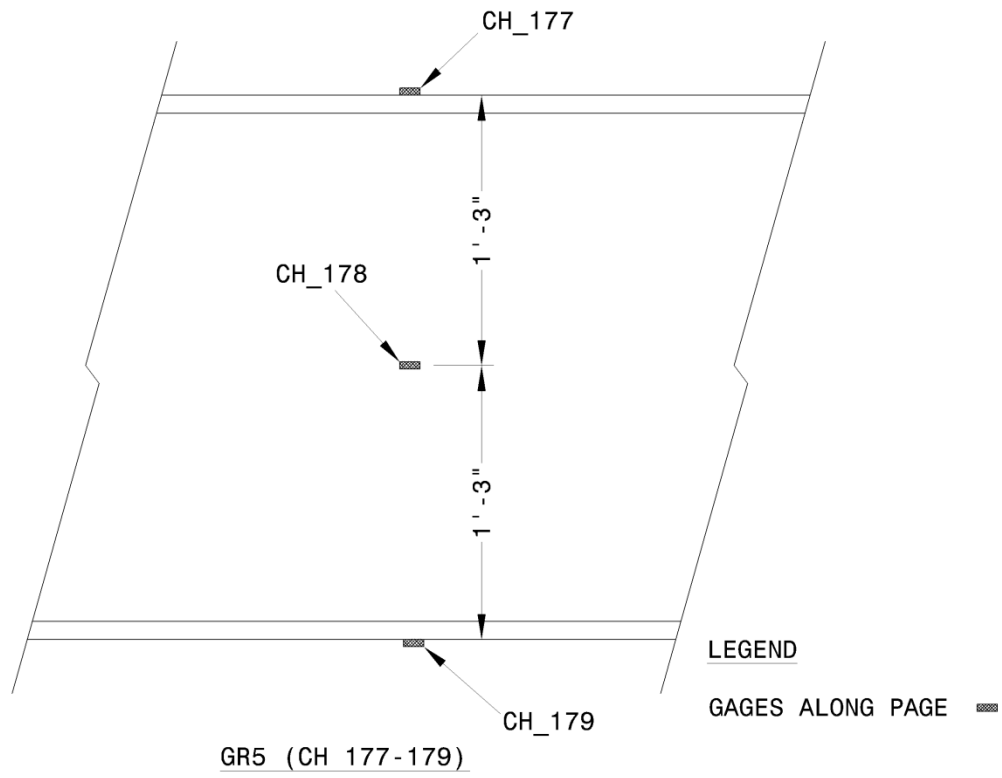


A.1.4 Girder Strain Gage and LVDT Plans

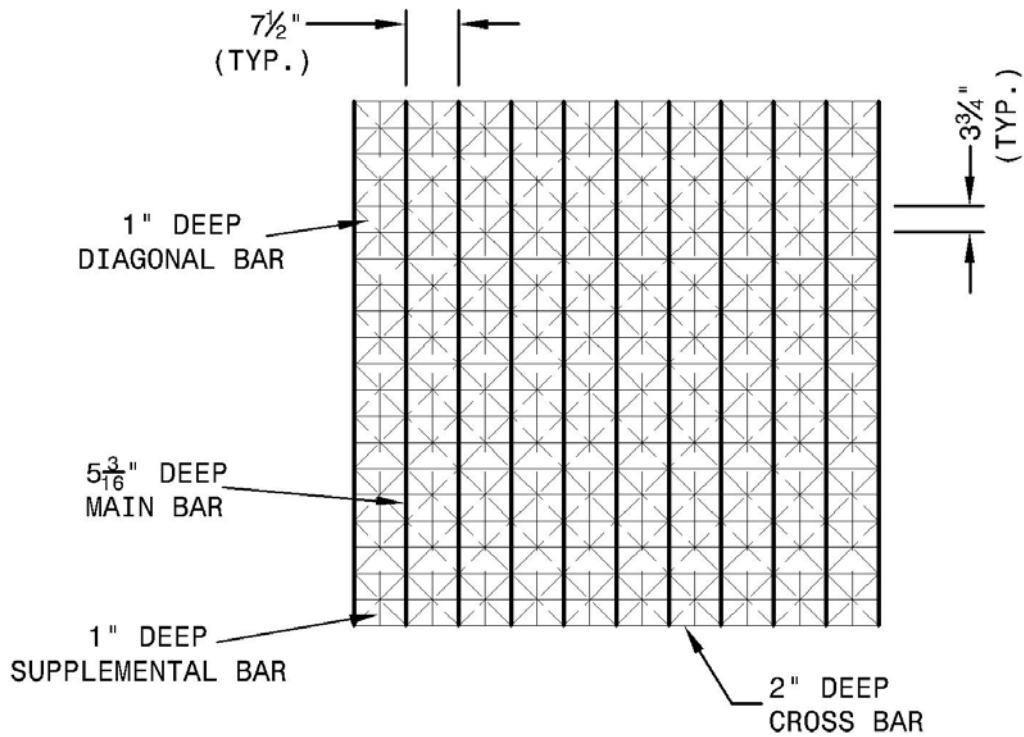




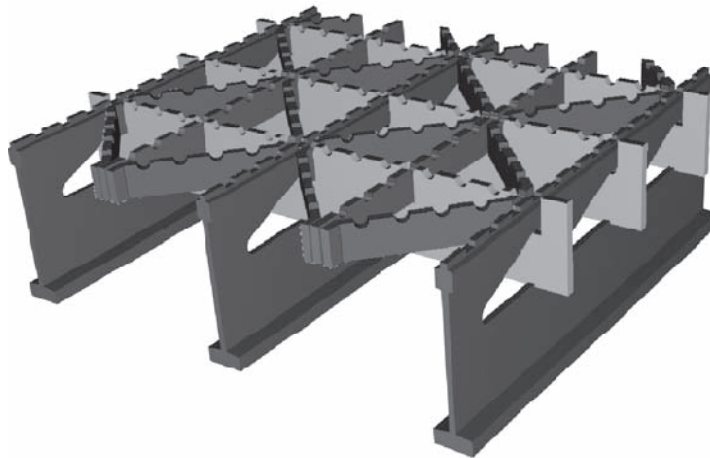




A.2 Subassembly Open Grid Deck Specimen #1

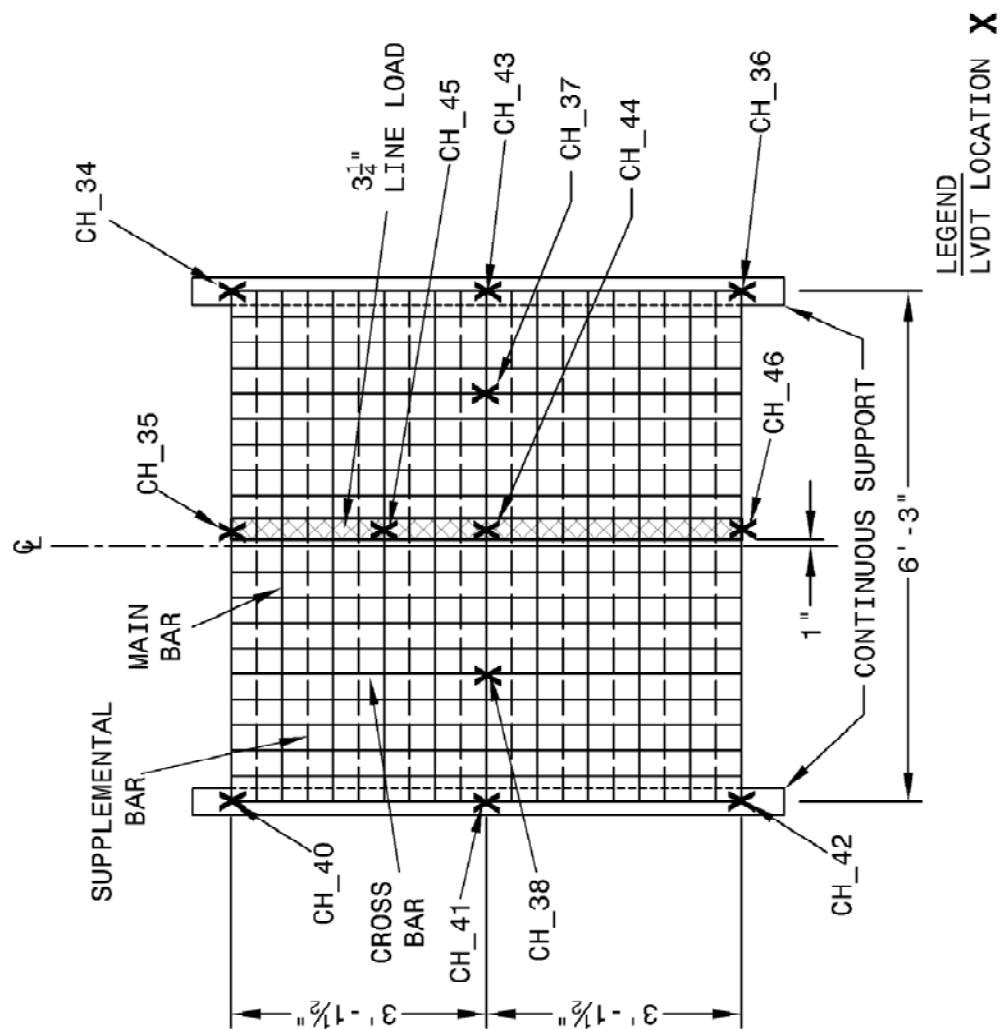


PLAN VIEW OF SUBASSEMBLY OPEN GRID DECK SPECIMEN #1



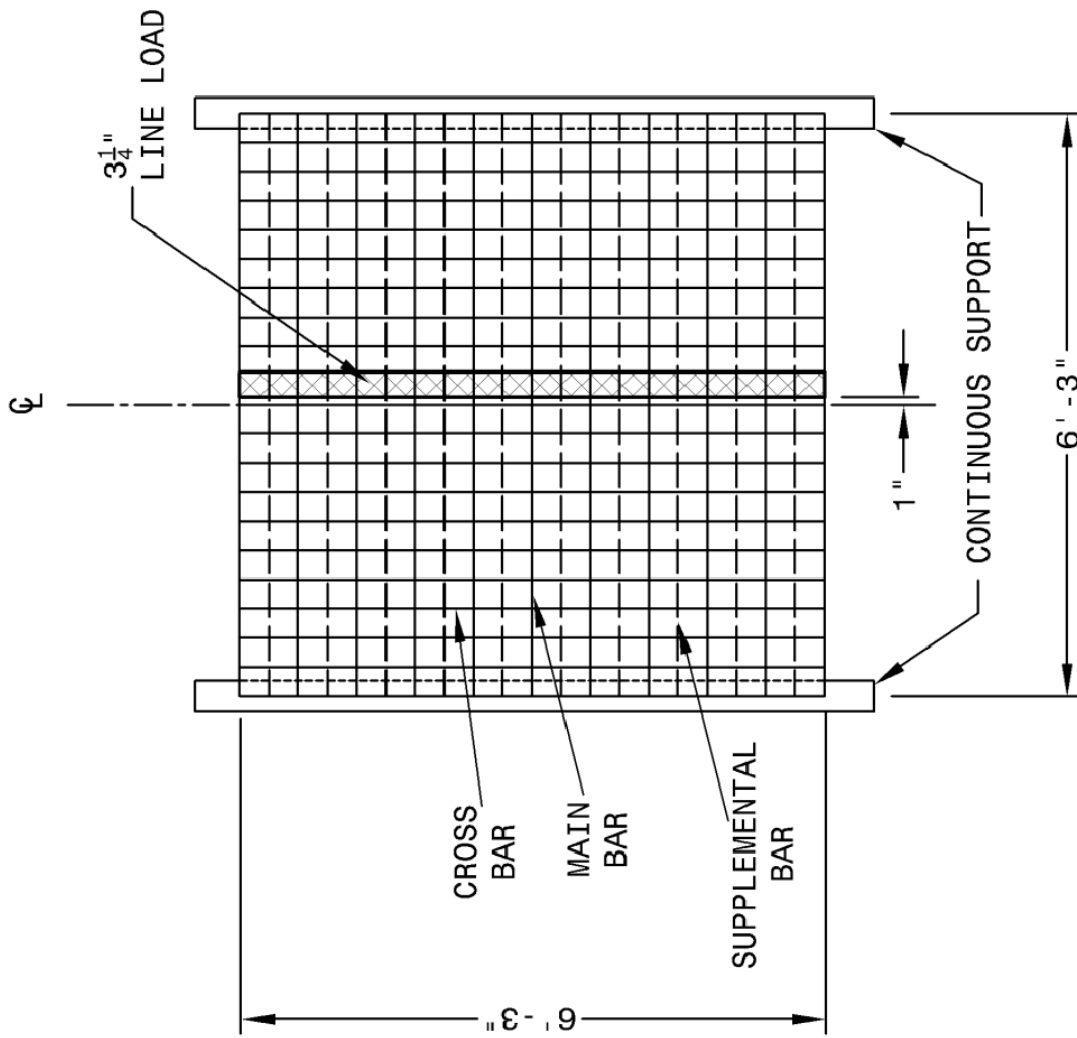
ISOTROPIC VIEW OF OPEN GRID DECK SPECIMEN #1 (L.B. FOSTER COMPANY 2010)

A.2.1 Strong Direction Stiffness (D_x) Test



LVDT PLAN FOR SUBASSEMBLY STRONG
DIRECTION STIFFNESS (D_x) TEST

NOTE: DIAGONAL BARS REMOVED FOR CLARITY

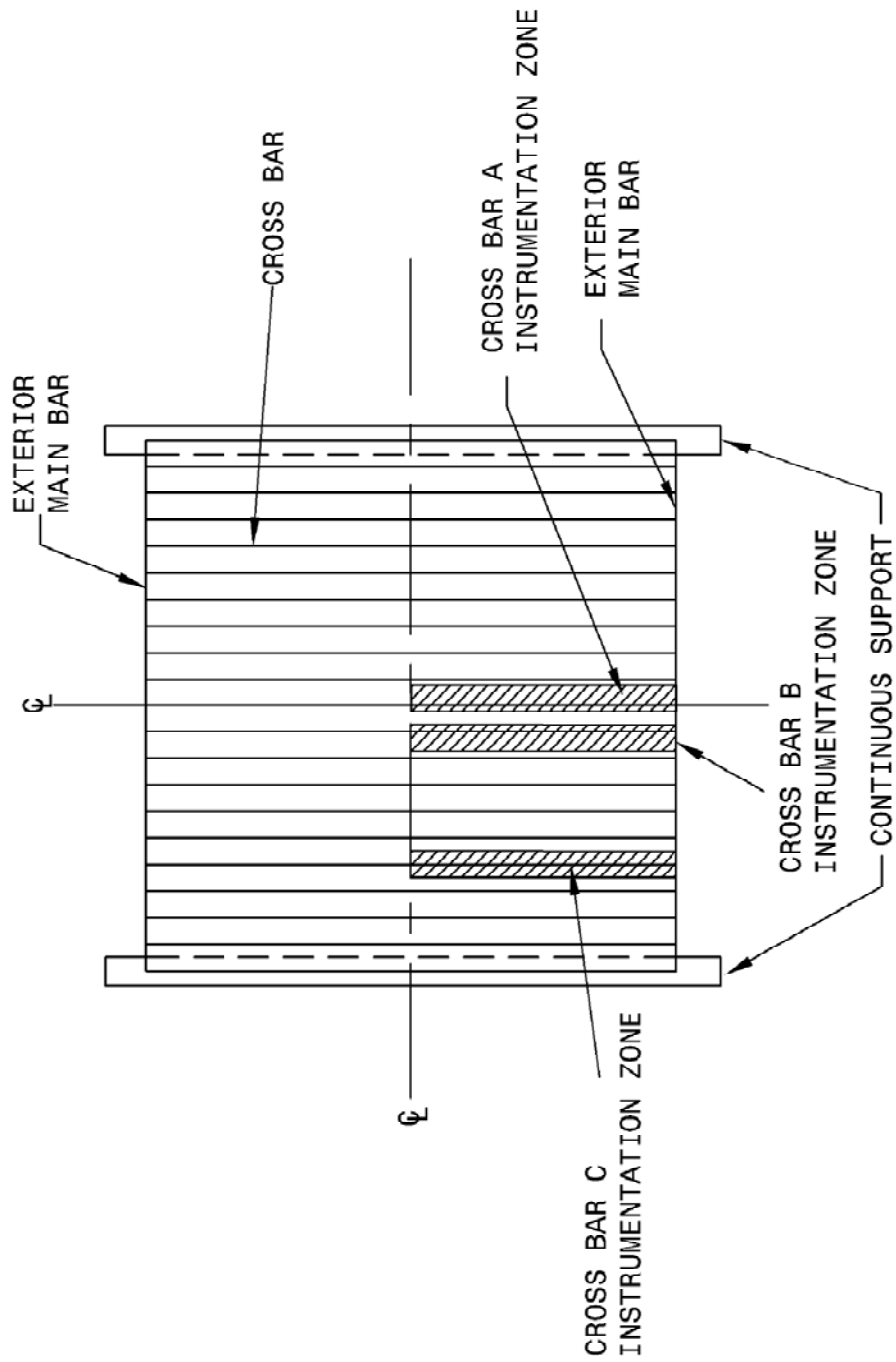


SUBASSEMBLY STRONG DIRECTION STIFFNESS
(DX) TEST

NOTE: DIAGONAL BARS REMOVED FOR CLARITY



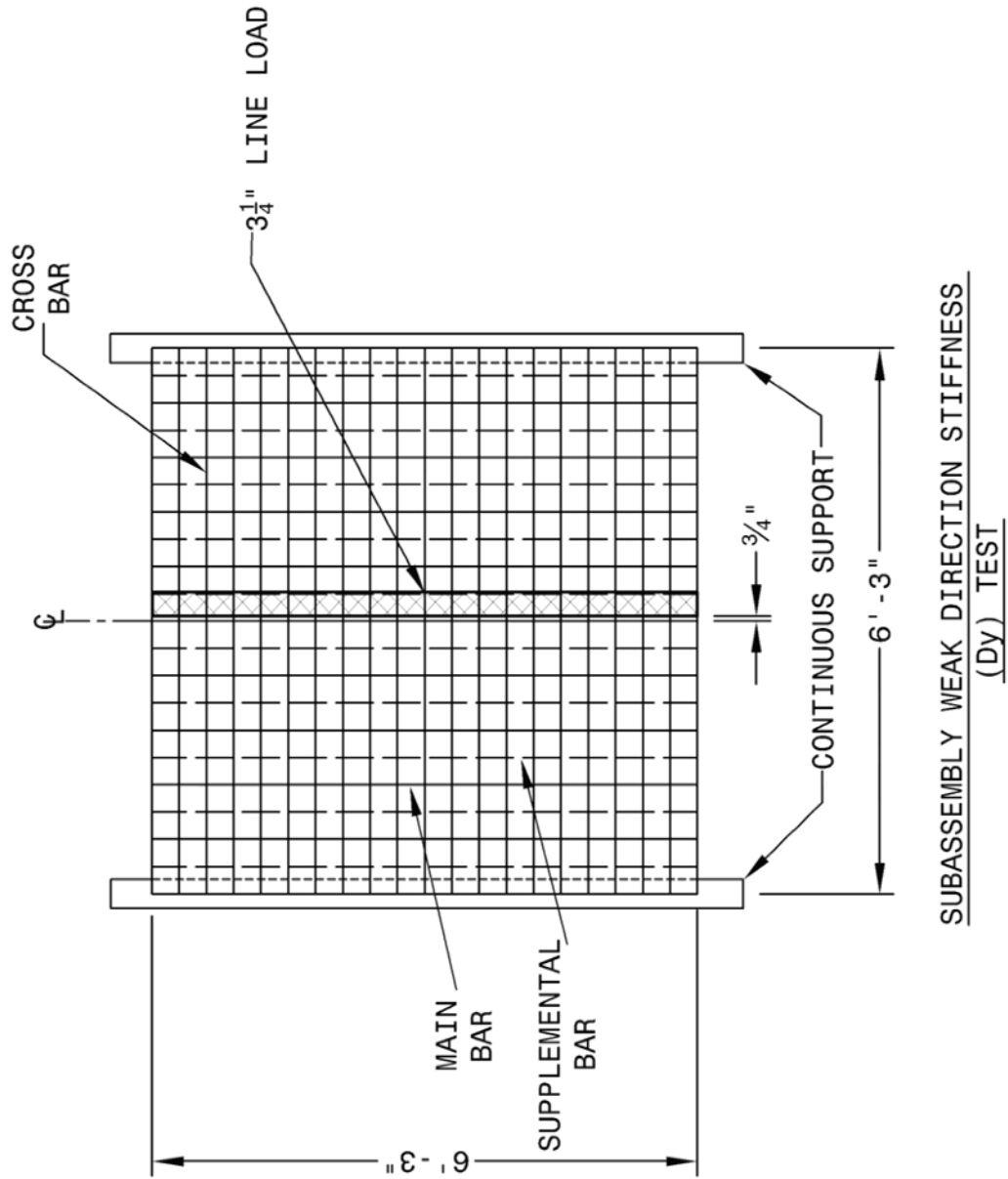
NOTE: 1) DIAGONAL BARS REMOVED FOR CLARITY
2) INTERIOR CROSS BARS REMOVED FOR CLARITY



CROSS BAR STRAIN GAGE PLAN FOR SUBASSEMBLY
STRONG DIRECTION STIFFNESS (Dx) TEST

- NOTE: 1) DIAGONAL BARS REMOVED FOR CLARITY
 2) INTERIOR MAIN AND SUPPLEMENTAL BARS REMOVED FOR CLARITY

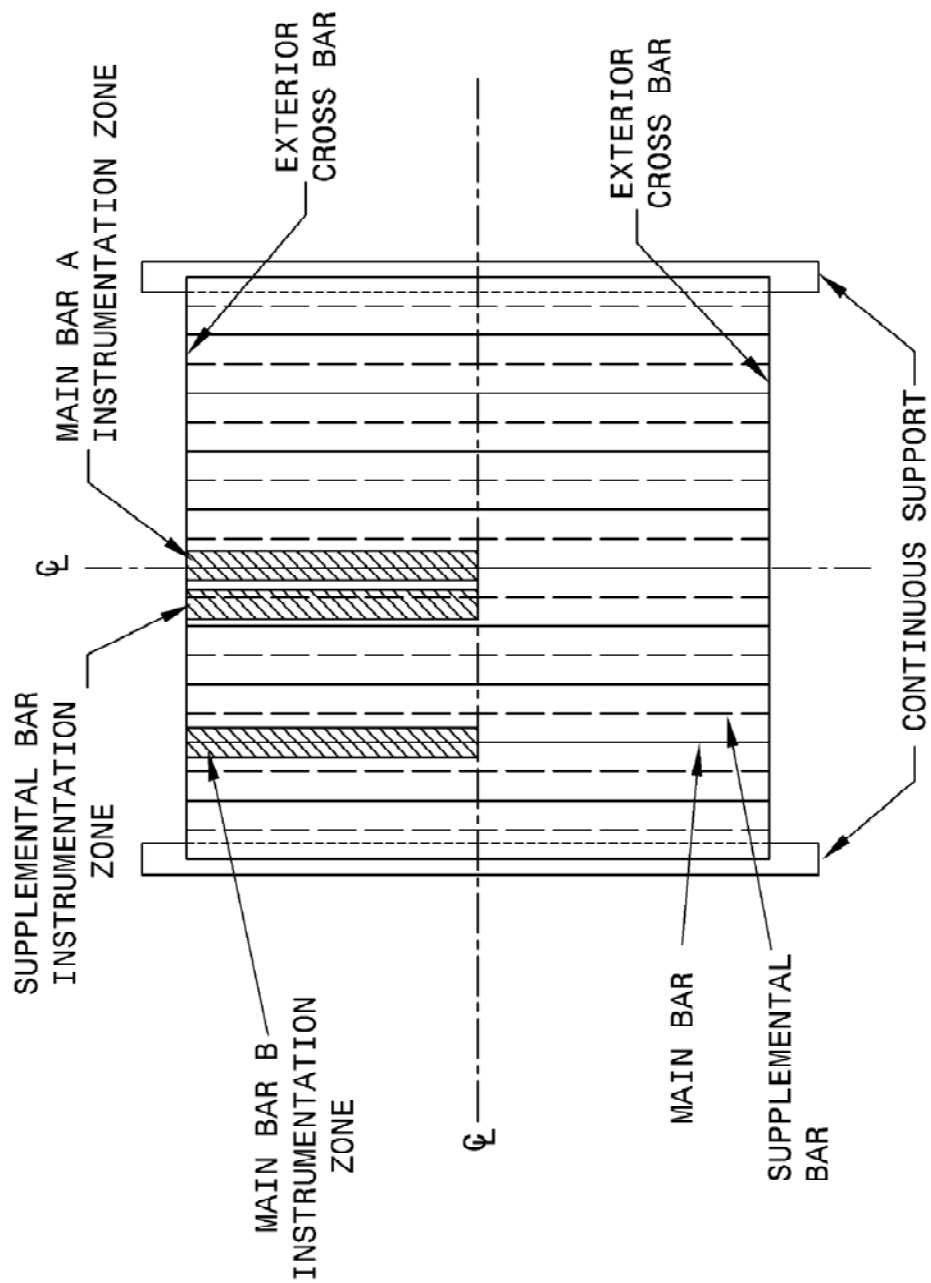
A.2.2 Weak Direction Stiffness (D_y) Test



NOTE: DIAGONAL BARS REMOVED FOR CLARITY

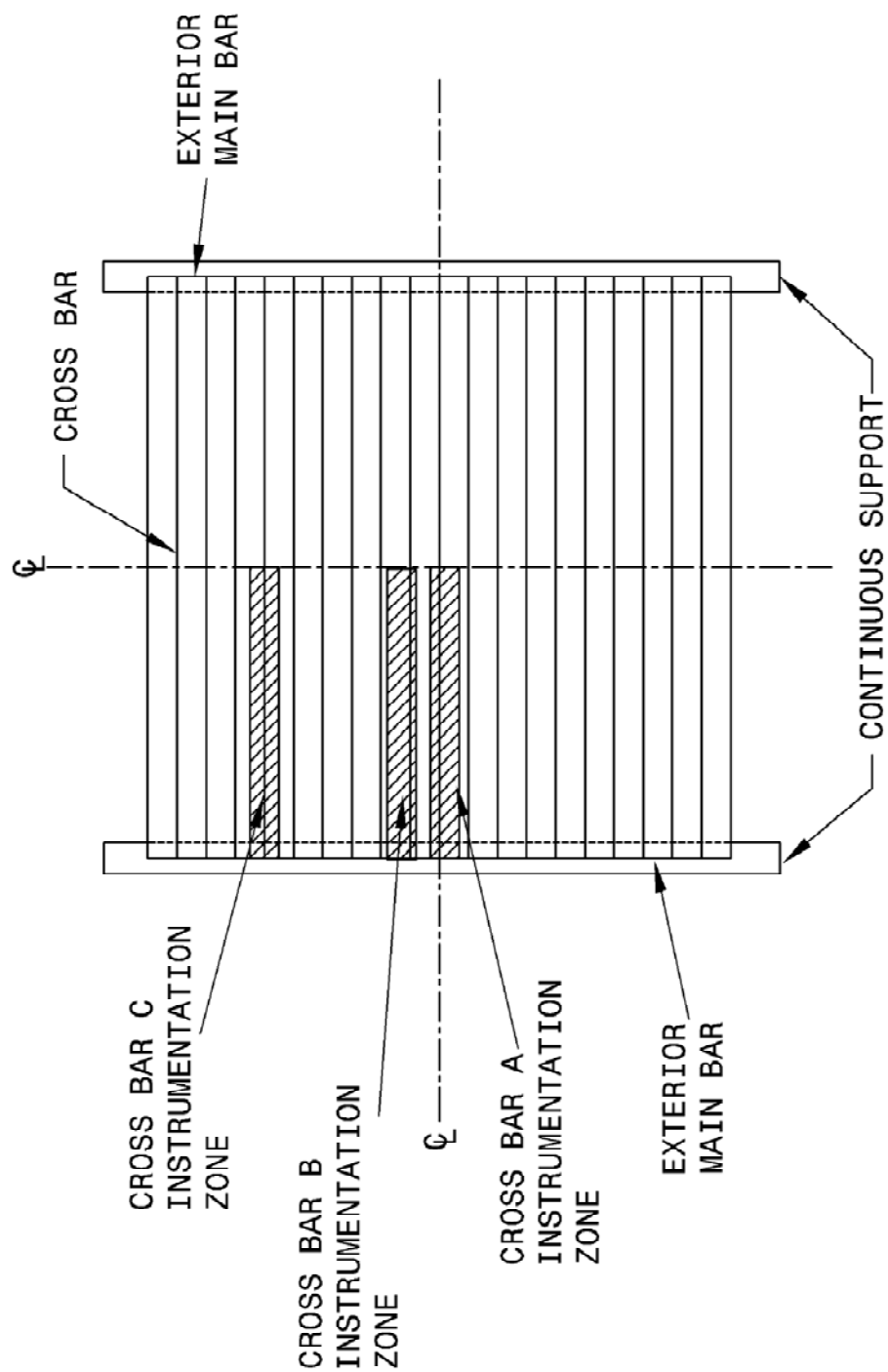


NOTE: DIAGONAL BARS REMOVED FOR CLARITY



MAIN AND SUPPLEMENTAL BAR STRAIN GAGE PLAN FOR
SUBASSEMBLY WEAK DIRECTION STIFFNESS (DY) TEST

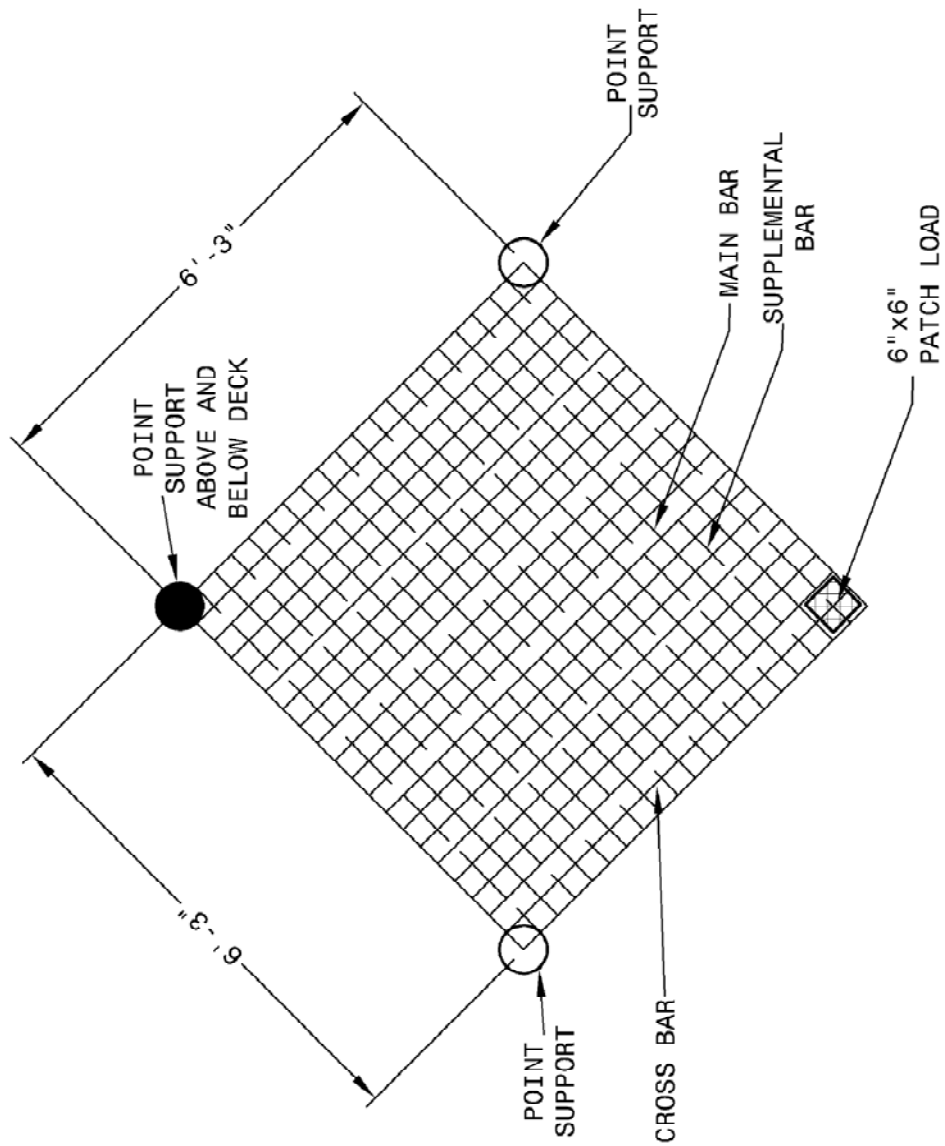
NOTE: 1) DIAGONAL BARS REMOVED FOR CLARITY
2) INTERIOR CROSS BARS REMOVED FOR CLARITY



CROSS BAR STRAIN GAGE PLAN FOR SUBASSEMBLY
WEAK DIRECTION STIFFNESS (Dy) TEST

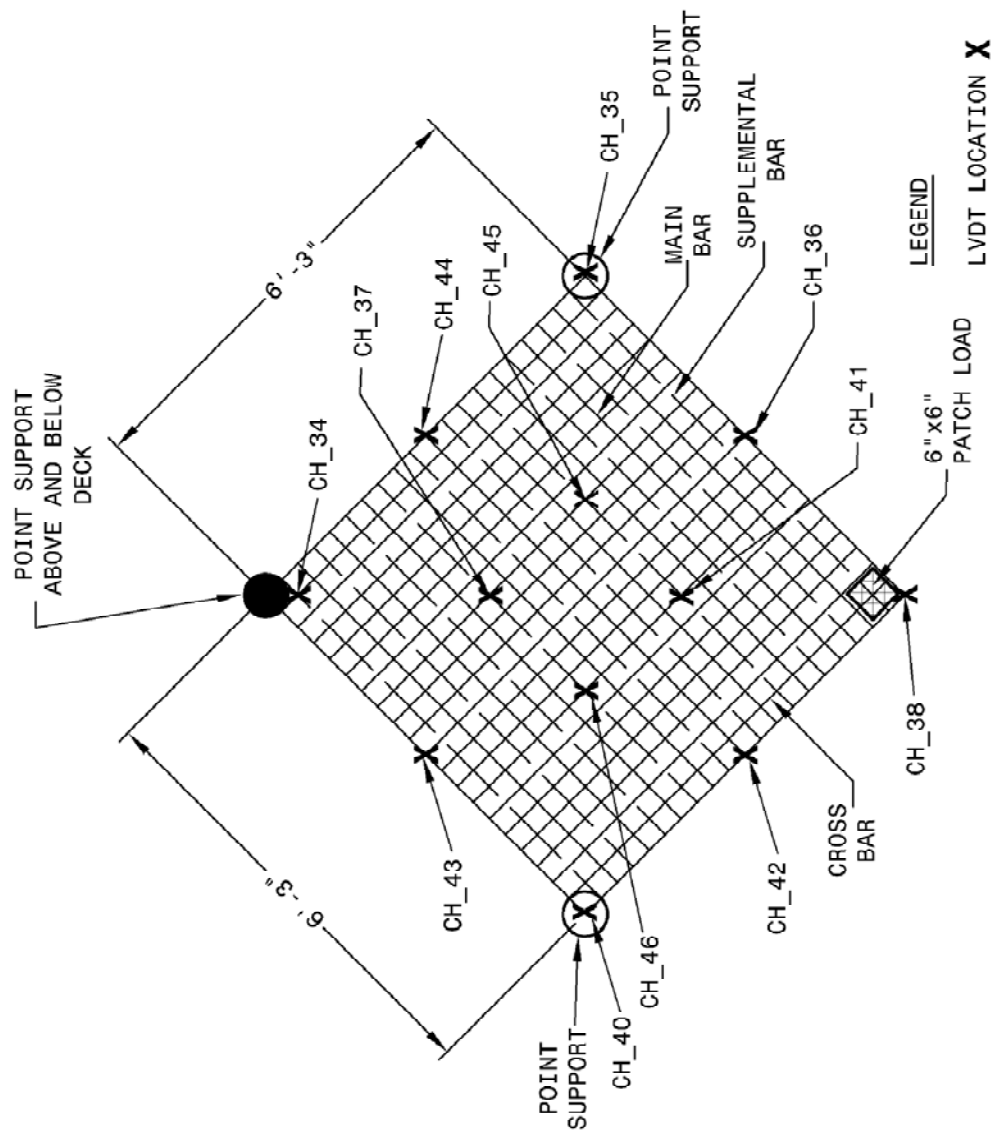
NOTE: 1) DIAGONAL BARS REMOVED FOR CLARITY
 2) INTERIOR MAIN AND SUPPLEMENTAL BARS REMOVED FOR CLARITY

A.2.3 Torsional Stiffness (D_{xy}) Test Rotation #1



SUBASSEMBLY TORSION STIFFNESS (D_{xy}) TEST SETUP
FOR TEST ROTATIONS #1 AND 3

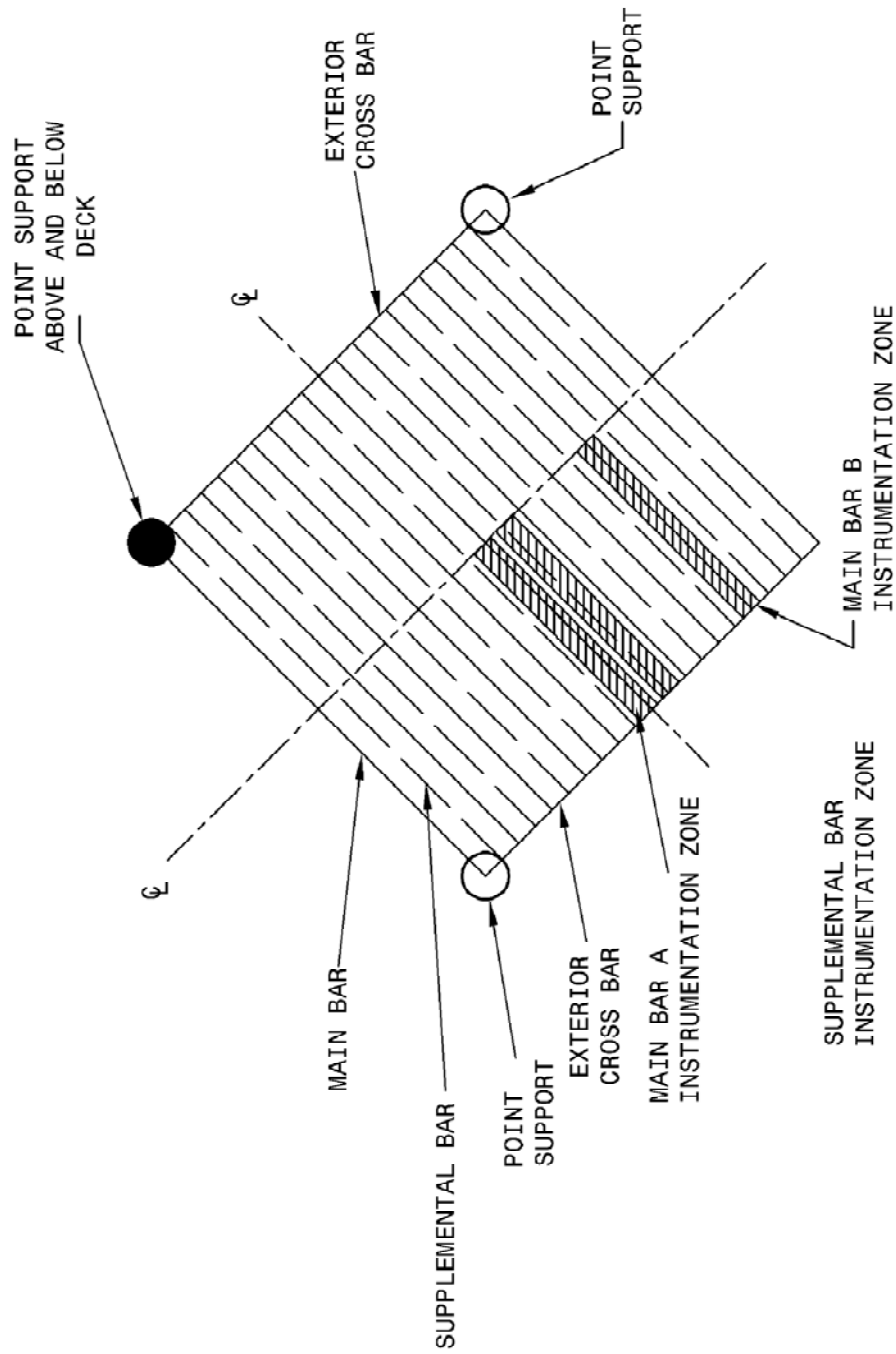
NOTE: DIAGONAL BARS REMOVED FOR CLARITY



LVDT PLAN FOR SUBASSEMBLY TORSION STIFFNESS

(Dxy) TEST ROTATIONS #1 AND 3

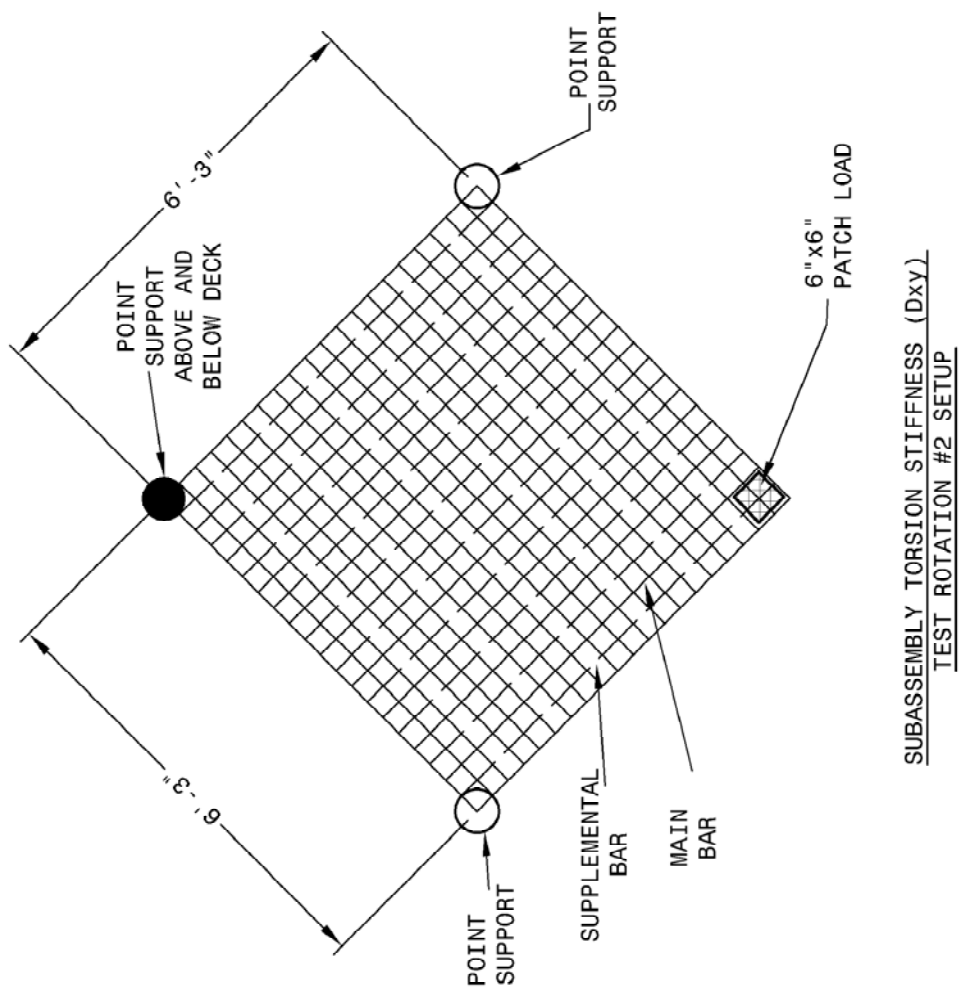
NOTE: DIAGONAL BARS REMOVED FOR CLARITY



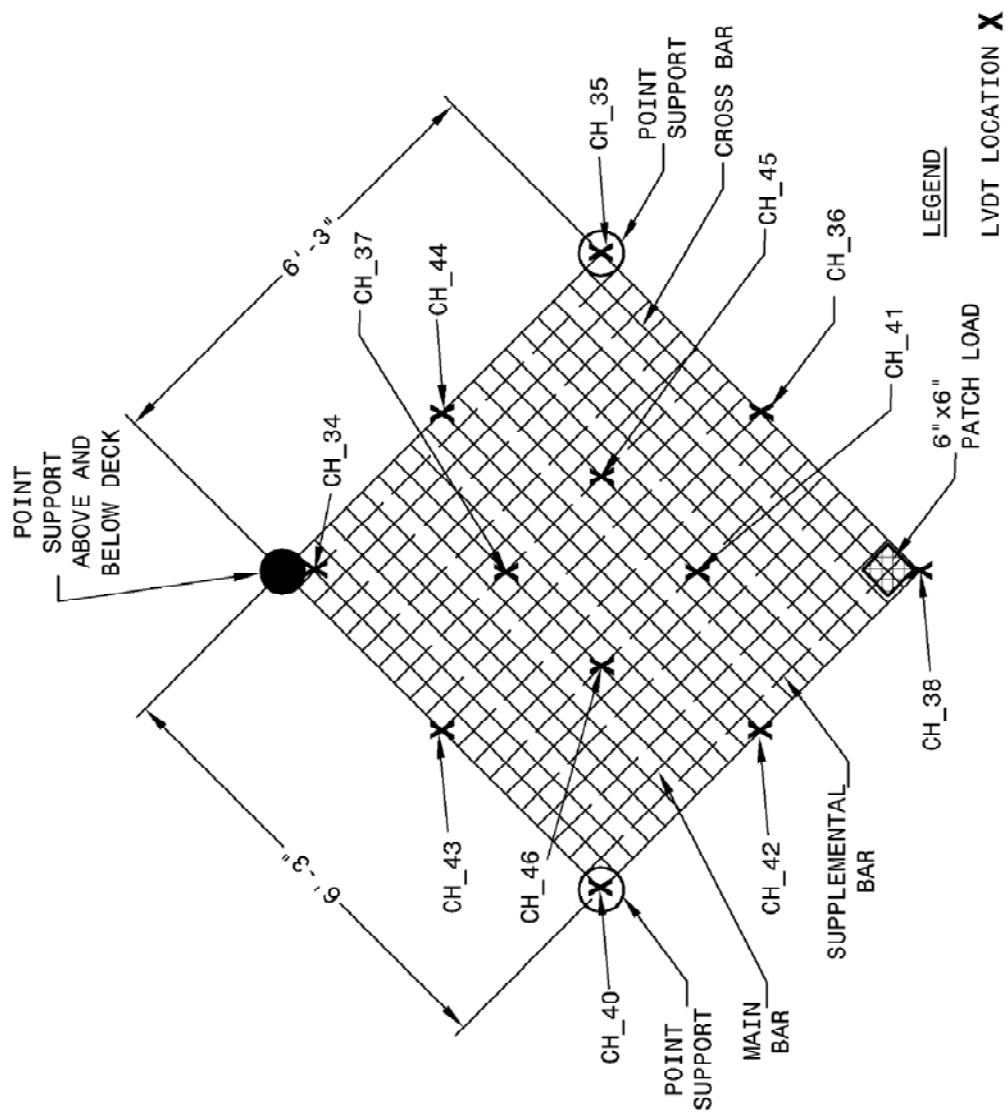
MAIN AND SUPPLEMENTAL STRAIN GAGE PLAN FOR
SUBASSEMBLY TORSION STIFFNESS (Dxy) TEST ROTATION #1

NOTE: 1) DIAGONAL BARS REMOVED FOR CLARITY
2) INTERIOR CROSS BARS REMOVED FOR CLARITY

A.2.4 Torsional Stiffness (D_{xy}) Test Rotation #2

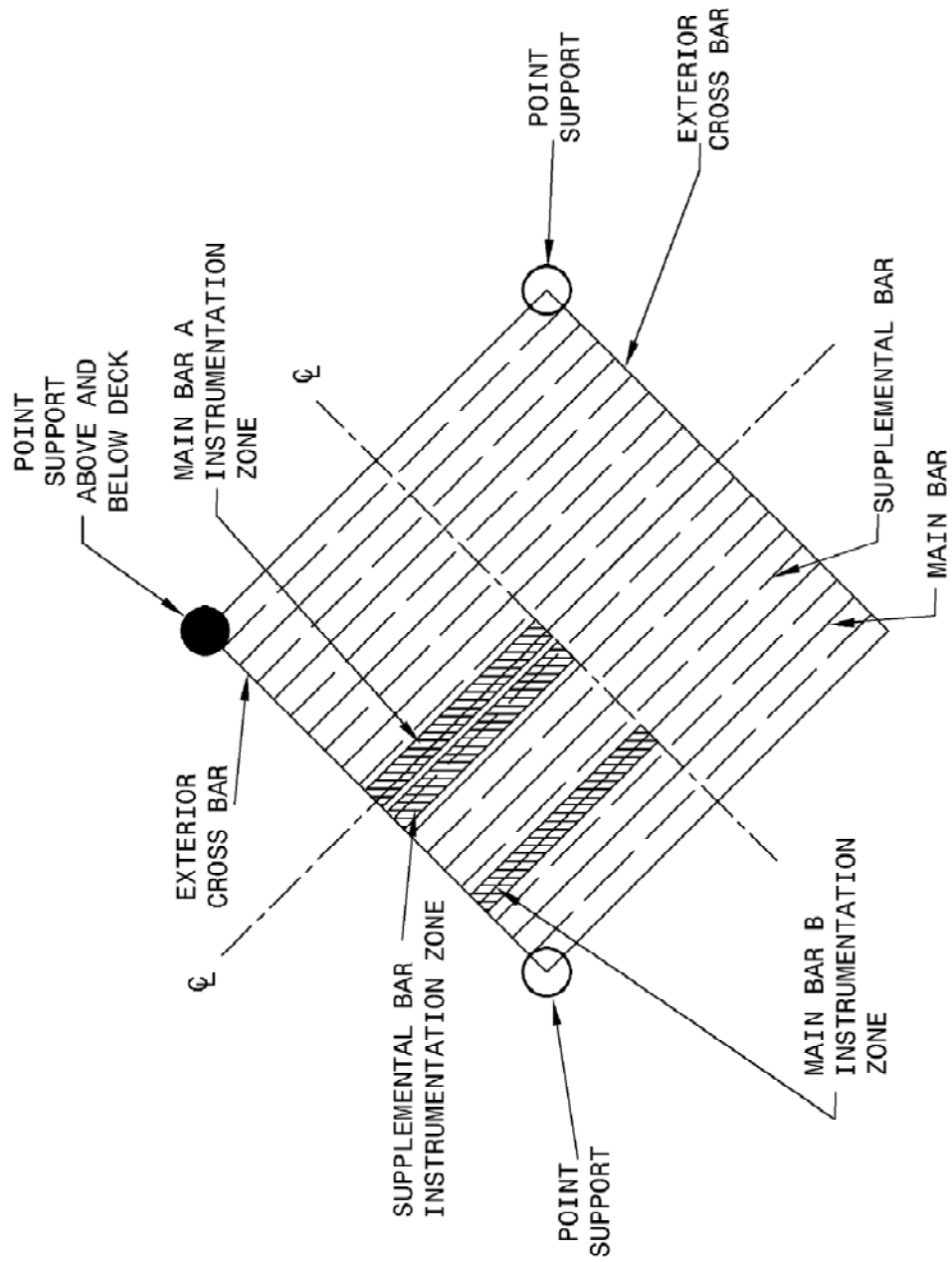


NOTE: DIAGONAL BARS REMOVED FOR CLARITY



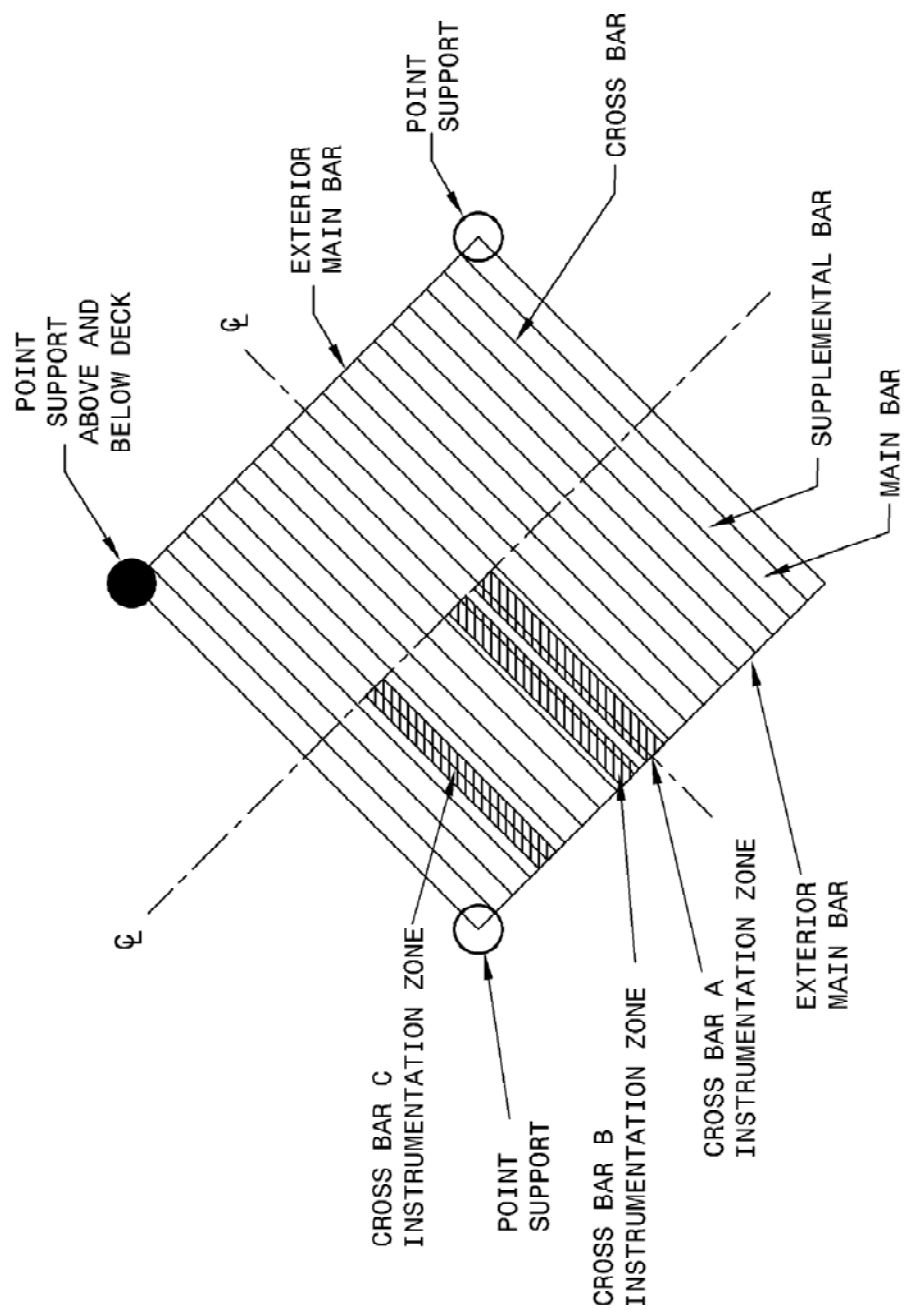
LVDT PLAN FOR SUBASSEMBLY TORSION STIFFNESS (Dxy)
TEST ROTATION #2

NOTE: DIAGONAL BARS REMOVED FOR CLARITY



MAIN AND SUPPLEMENTAL STRAIN GAGE PLAN FOR
SUBASSEMBLY TORSION STIFFNESS (Dxy) TEST ROTATION #2

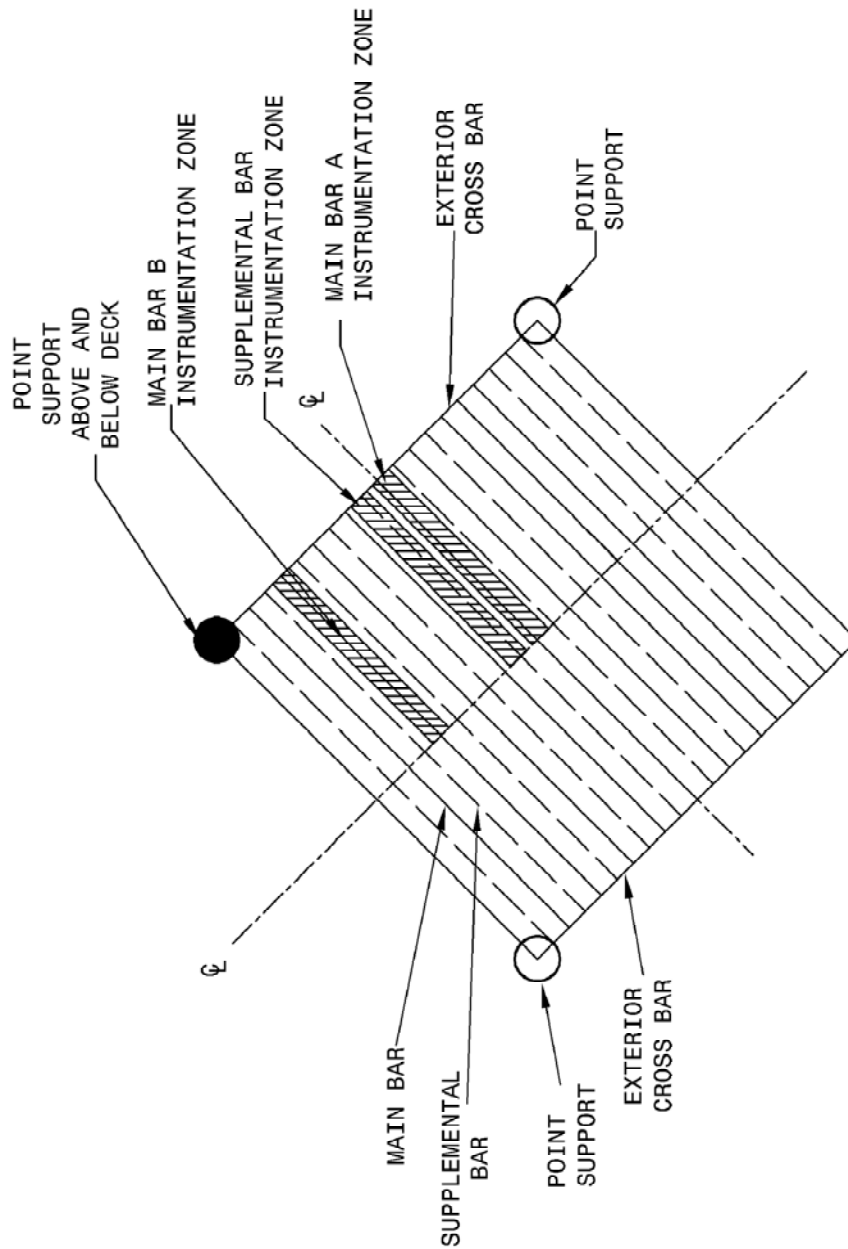
NOTE: 1) DIAGONAL BARS REMOVED FOR CLARITY
2) INTERIOR CROSS BARS REMOVED FOR CLARITY



CROSS BAR STRAIN GAGE PLAN FOR
SUBASSEMBLY TORSION STIFFNESS (Dxy) TEST ROTATION #2

NOTE: 1) DIAGONAL BARS REMOVED FOR CLARITY
2) INTERIOR MAIN AND SUPPLEMENTAL BARS REMOVED FOR CLARITY

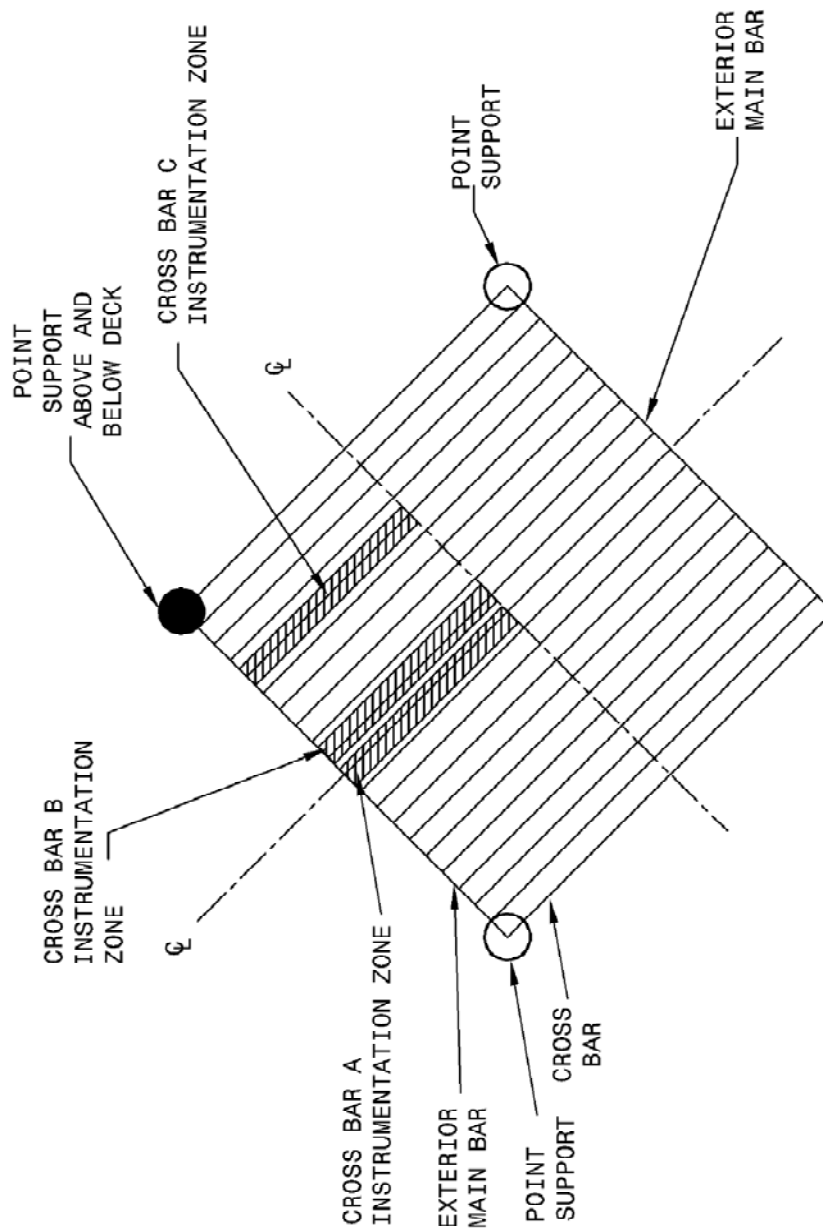
A.2.5 Torsion Stiffness (D_{xy}) Test Rotation #3



MAIN AND SUPPLEMENTAL BAR STRAIN GAGE PLAN FOR
SUBASSEMBLY TORSION STIFFNESS (D_{xy}) TEST ROTATION #3

NOTE: 1) DIAGONAL BARS REMOVED FOR CLARITY

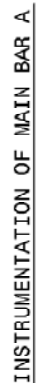
2) INTERIOR CROSS BARS REMOVED FOR CLARITY



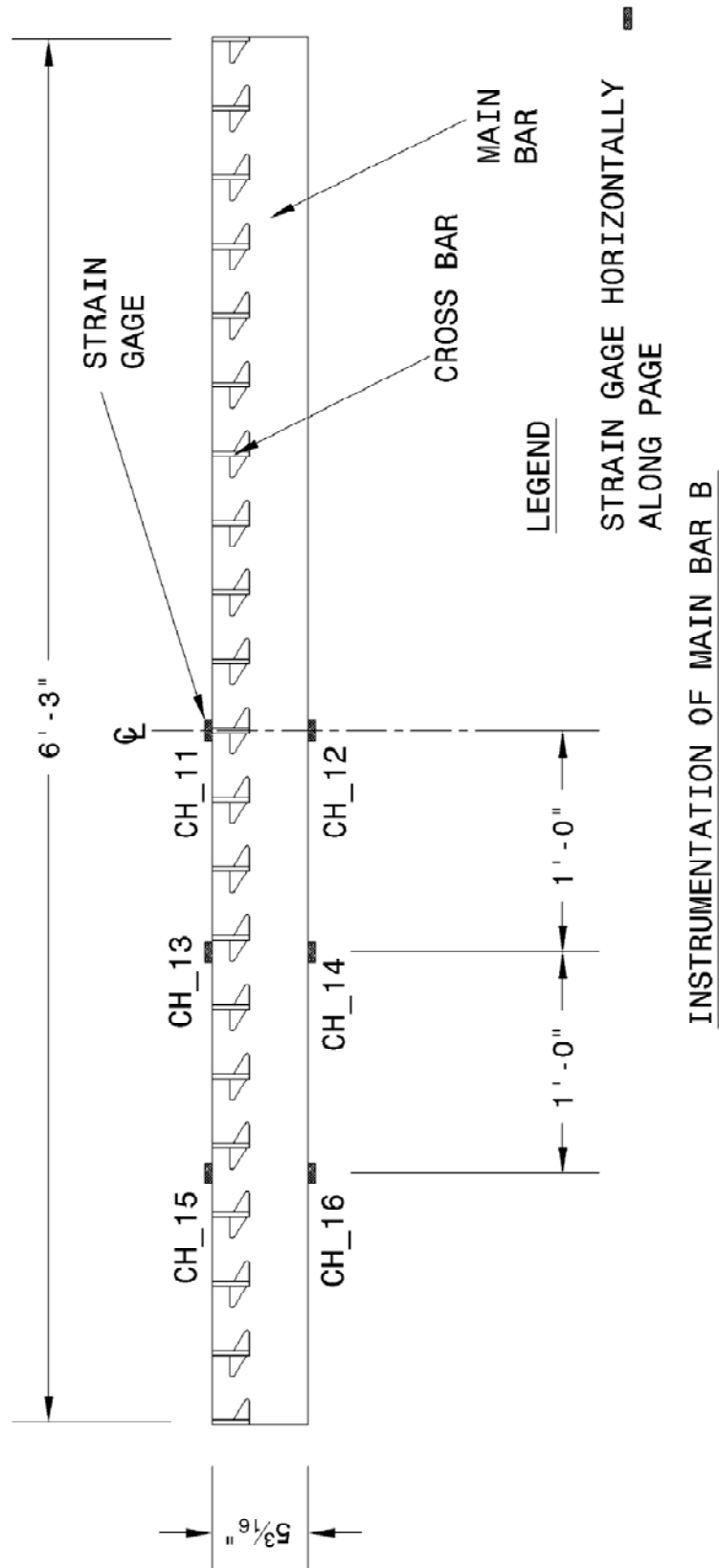
CROSS BAR STRAIN GAGE PLAN FOR SUBASSEMBLY TORSION
STIFFNESS (Dxy) TEST ROTATION #3

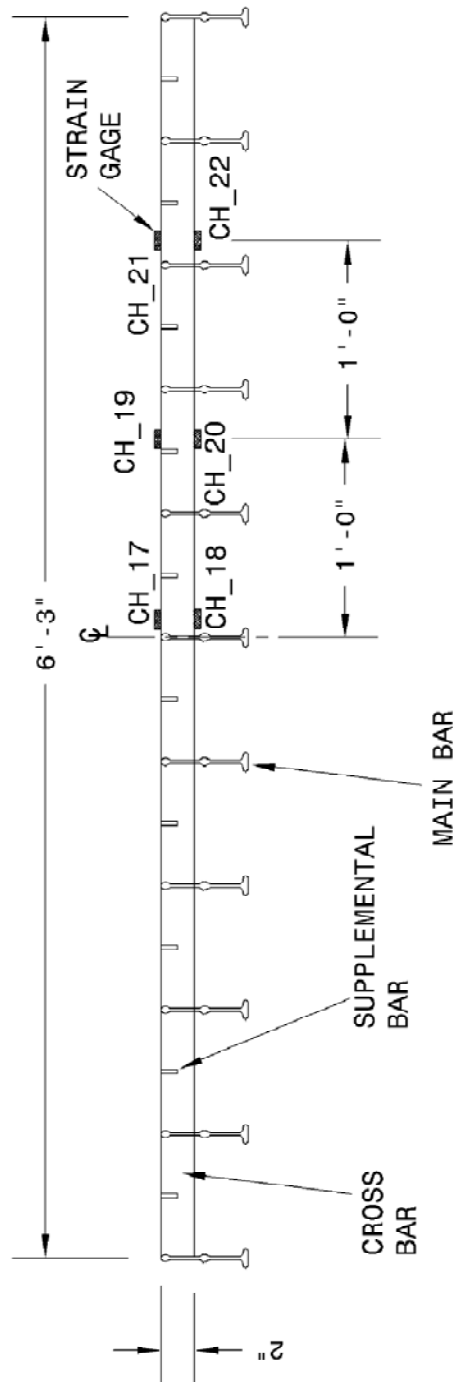
NOTE: 1) DIAGONAL BARS REMOVED FOR CLARITY
2) INTERIOR MAIN AND SUPPLEMENTAL BARS REMOVED FOR CLARITY

STRAIN GAGE HORIZONTALLY
ALONG PAGE

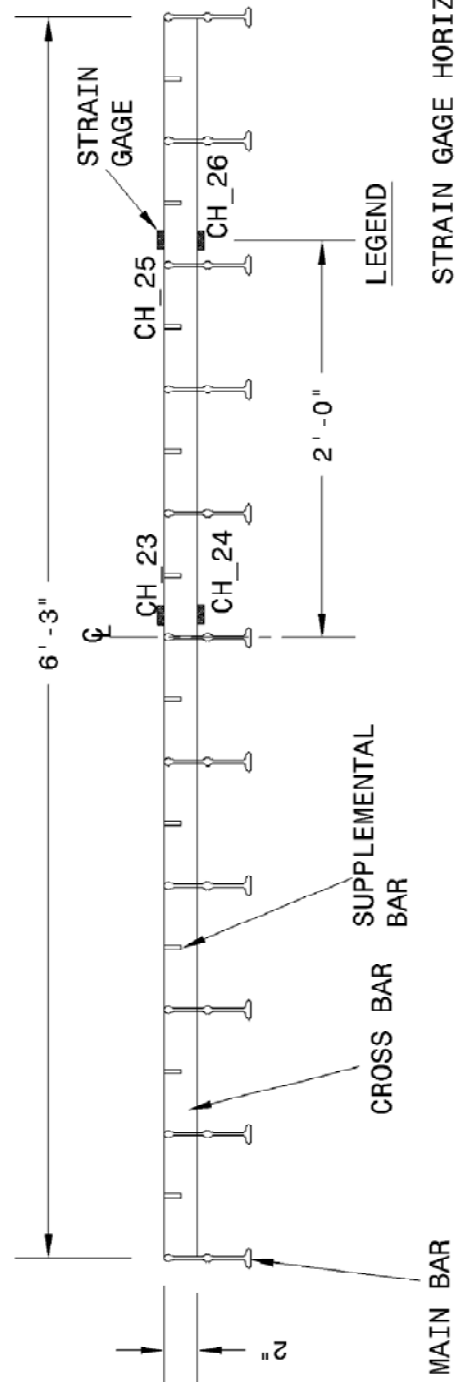


STRAIN GAGE HORIZONTALLY
ALONG PAGE

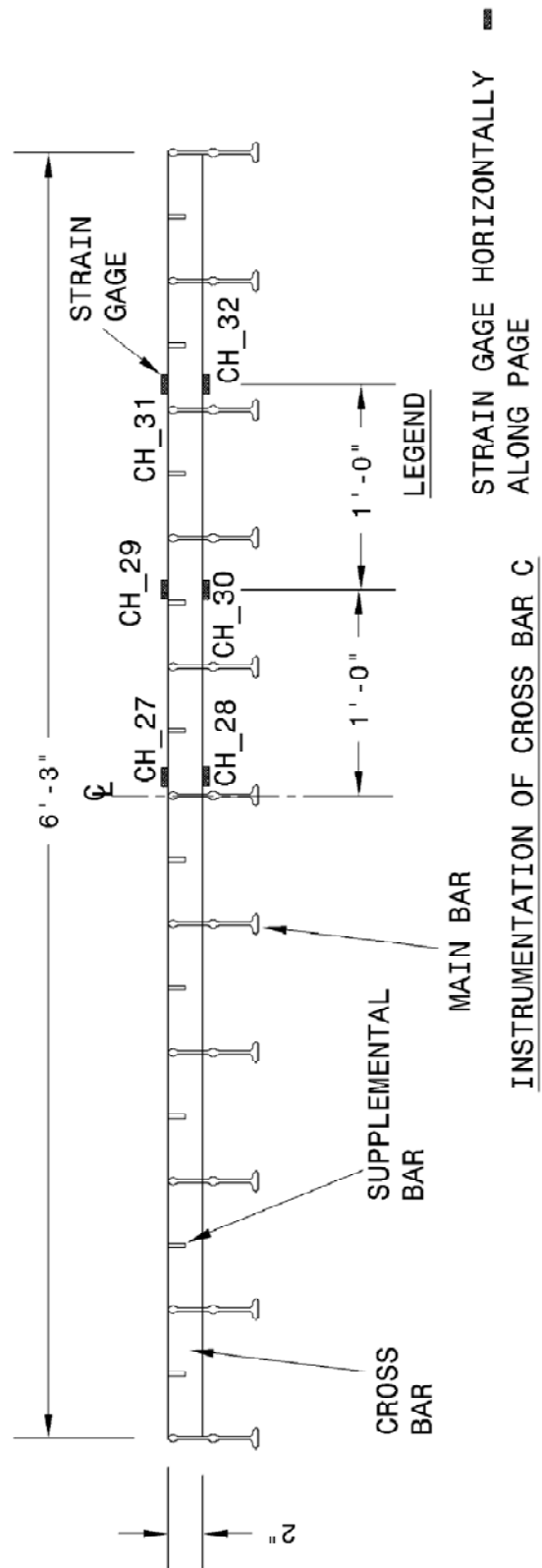




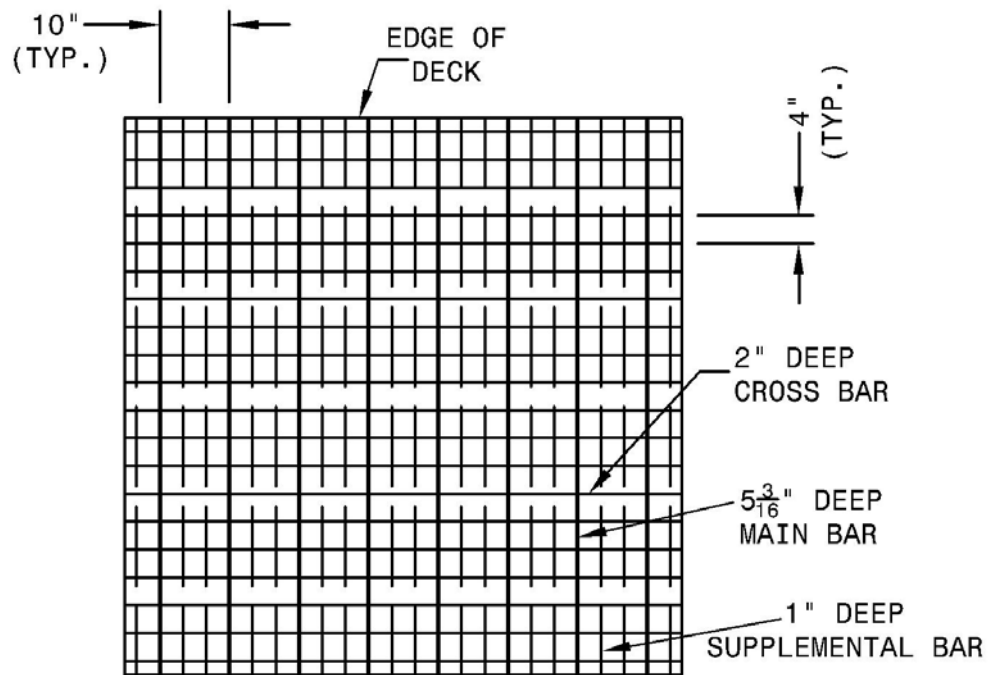
INSTRUMENTATION OF CROSS BAR A



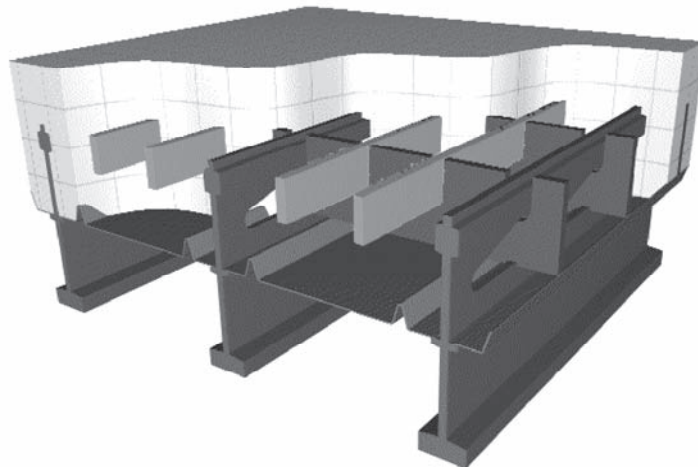
INSTRUMENTATION OF CROSS BAR B



A.3 Subassembly Open Grid Deck Specimen #2

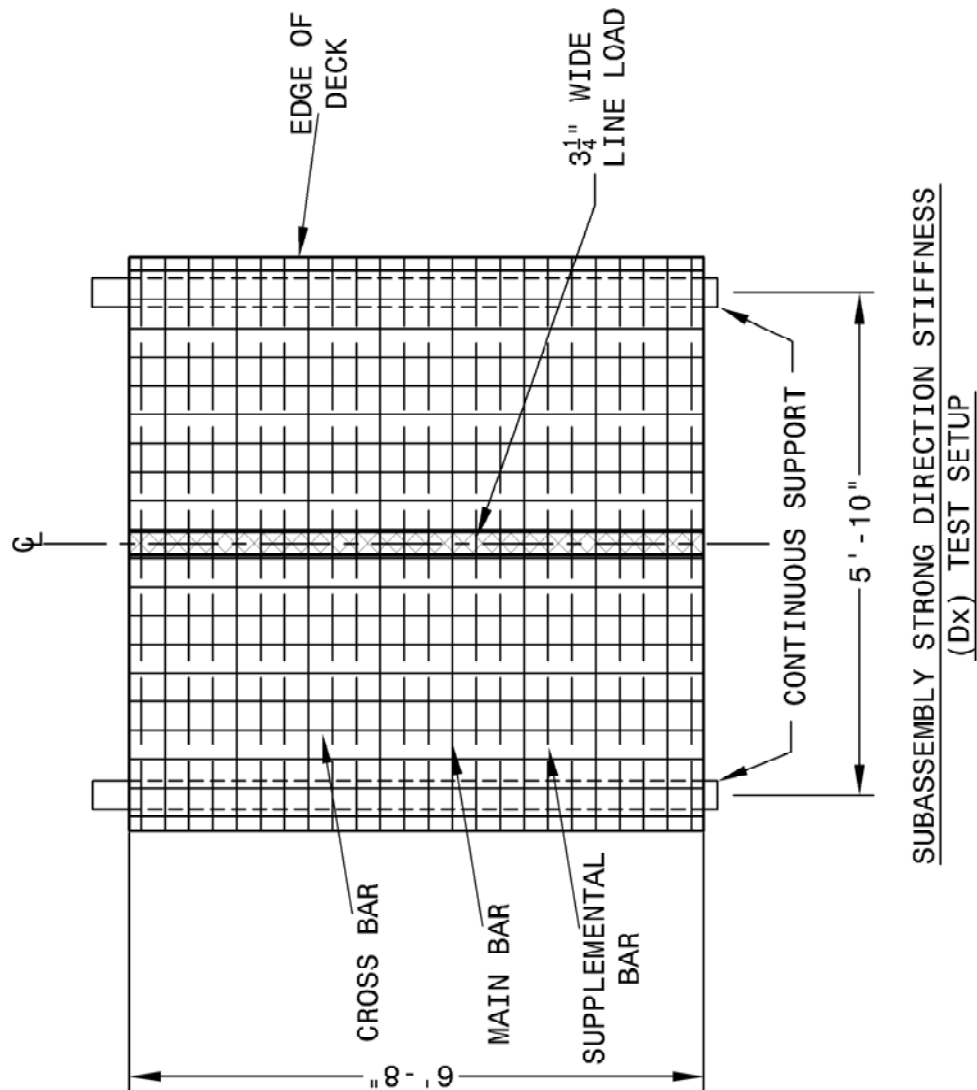


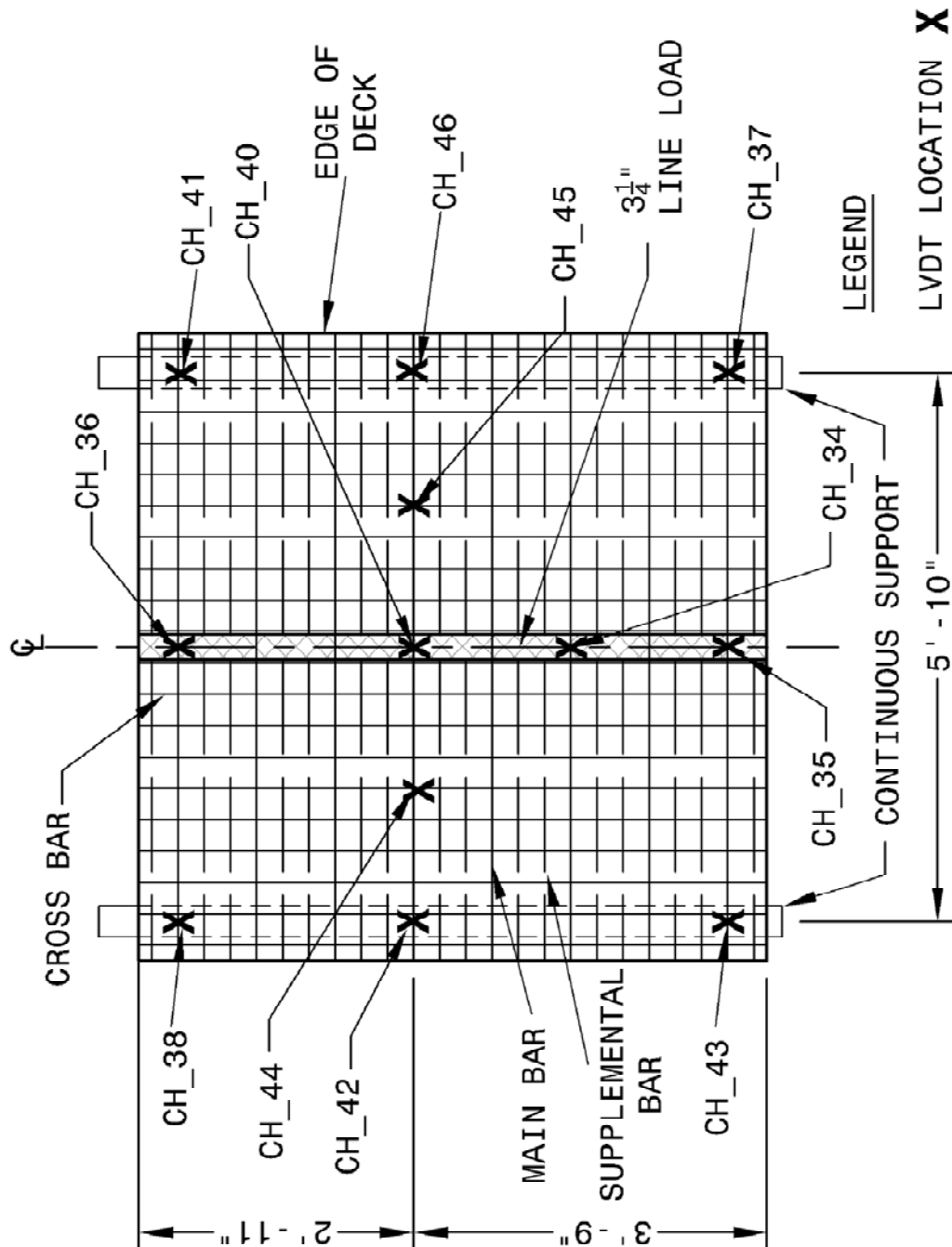
PLAN VIEW OF OPEN GRID DECK SPECIMEN #2 AND PARTIALLY
FILLED GRID DECK



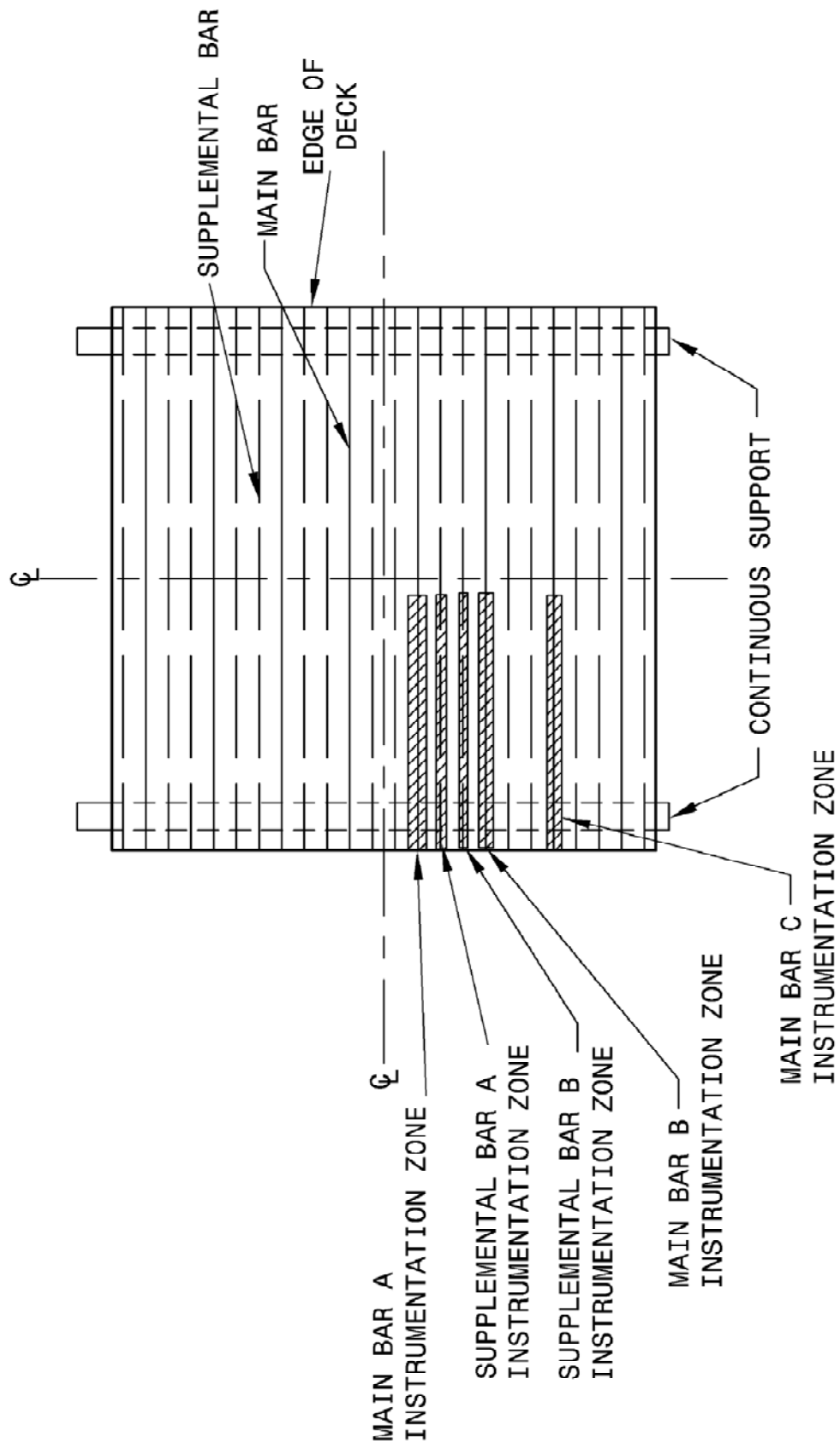
ISOTROPIC VIEW OF PARTIALLY FILLED GRID DECK SPECIMENS (L.B. FOSTER
COMPANY 2010)

A.3.1 Strong Direction Stiffness (D_x) Tests



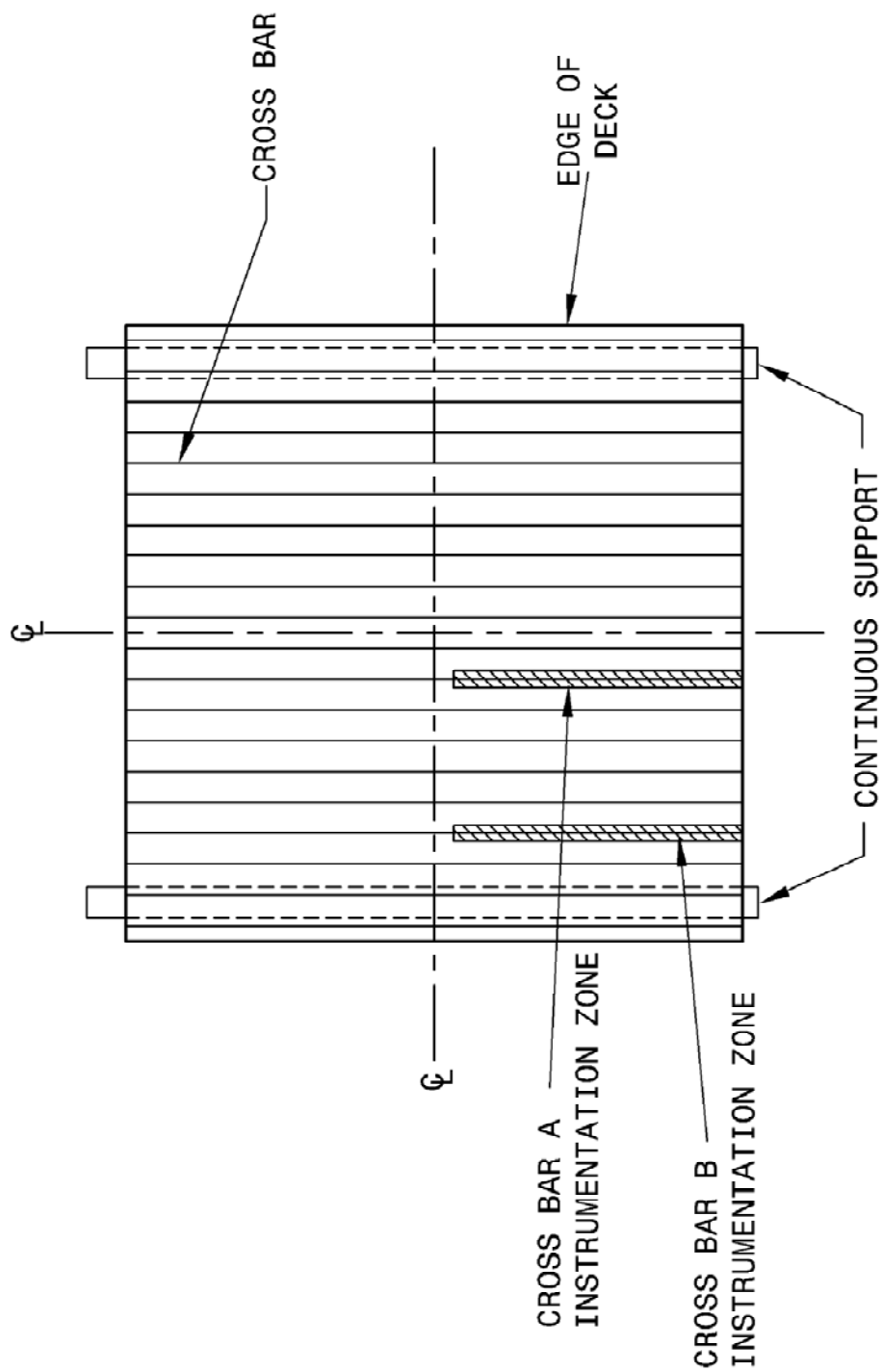


LVDT INSTRUMENTATION PLAN FOR SUBASSEMBLY
STRONG DIRECTION STIFFNESS (Dx) TEST



MAIN AND SUPPLEMENTAL BAR INSTRUMENTATION PLAN FOR
SUBASSEMBLY STRONG DIRECTION STIFFNESS (Dx) TEST

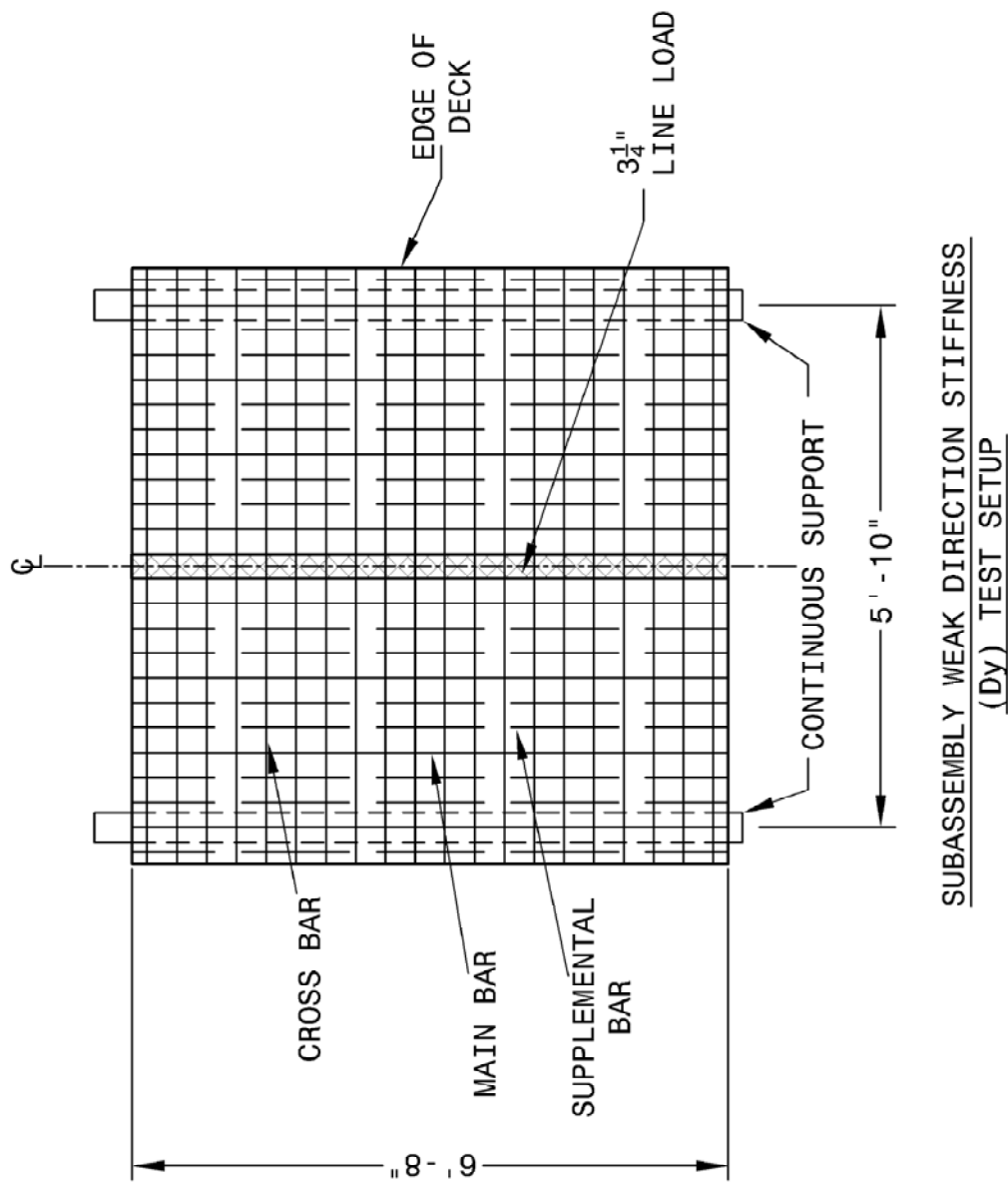
NOTE: CROSS BARS REMOVED FOR CLARITY

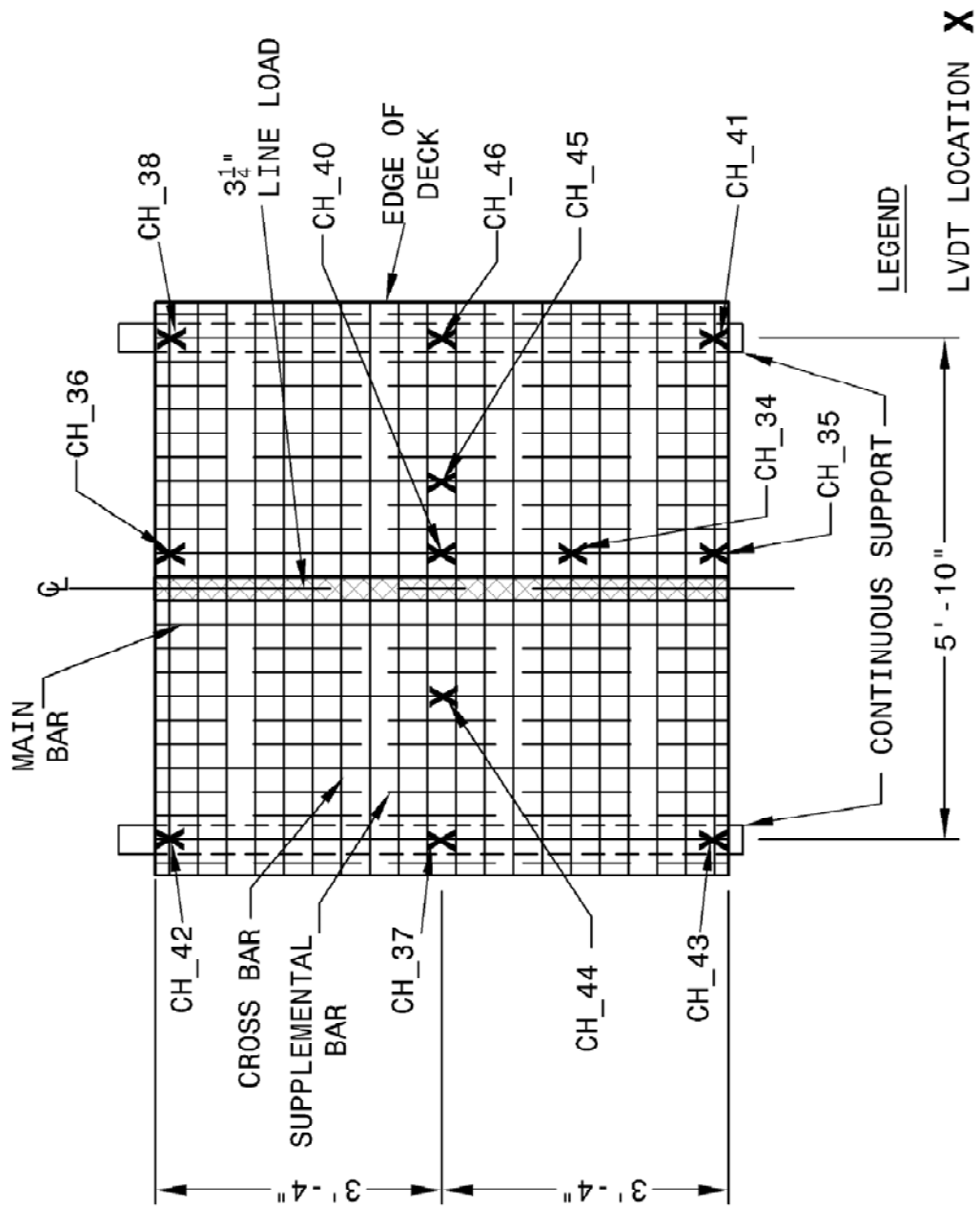


CROSS BAR INSTRUMENTATION PLAN FOR SUBASSEMBLY
STRONG DIRECTION STIFFNESS (Dx) TEST

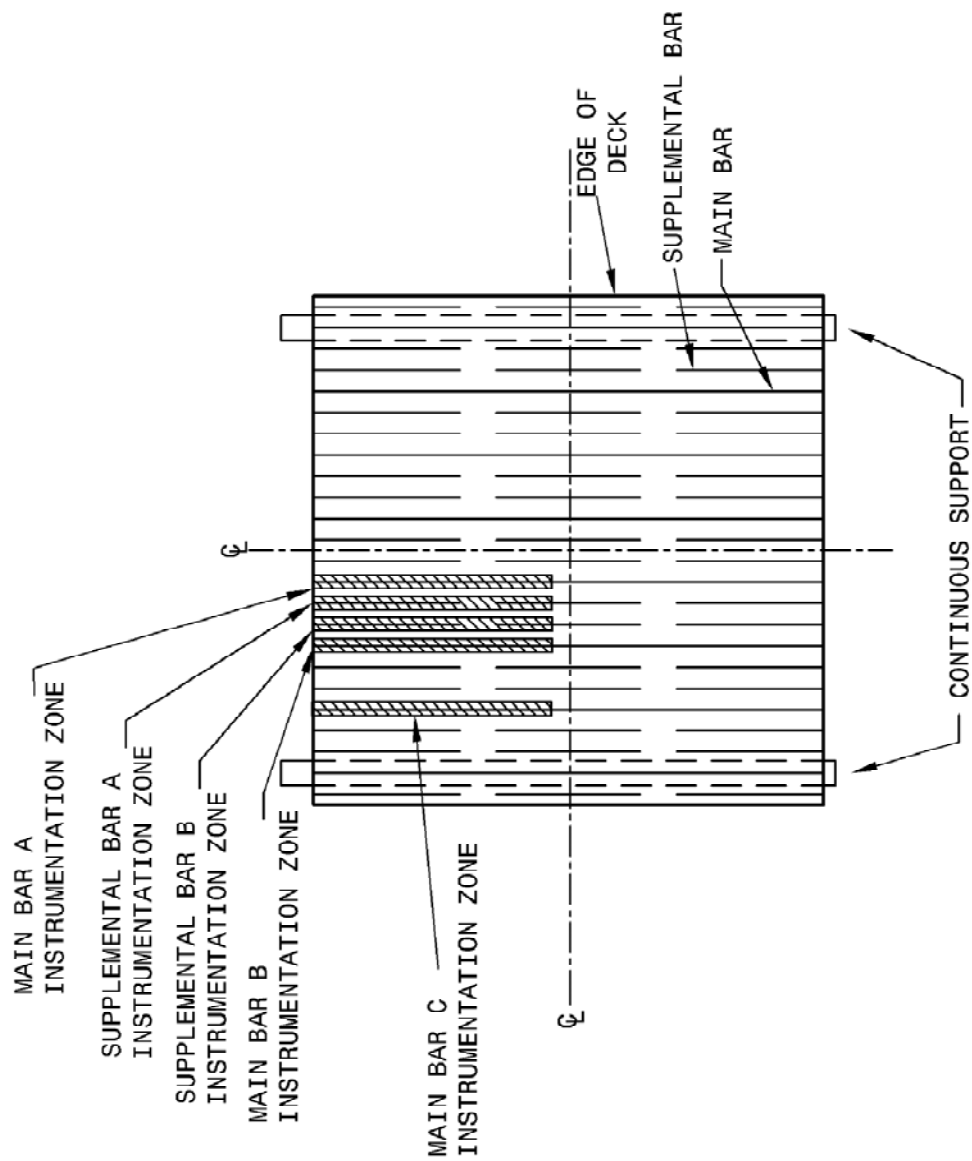
NOTE: MAIN AND SUPPLEMENTAL BARS REMOVED FOR CLARITY

A.3.2 Weak Direction Stiffness (D_y) Test



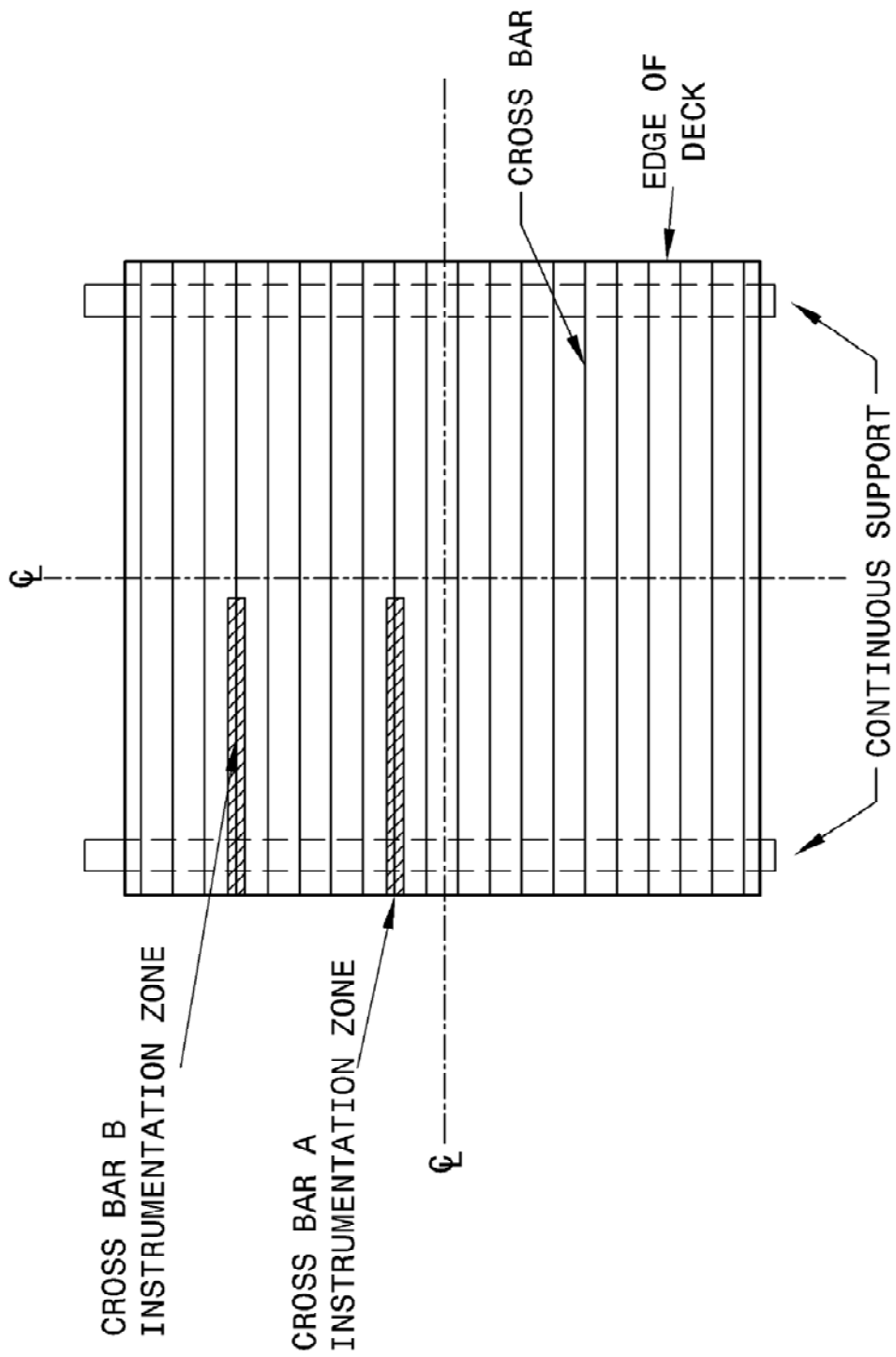


LVDT INSTRUMENTATION PLAN FOR SUBASSEMBLY
WEAK DIRECTION STIFFNESS (D_y) TEST



MAIN AND SUPPLEMENTAL BAR INSTRUMENTATION PLAN FOR
SUBASSEMBLY WEAK DIRECTION STIFFNESS (D_y) TEST

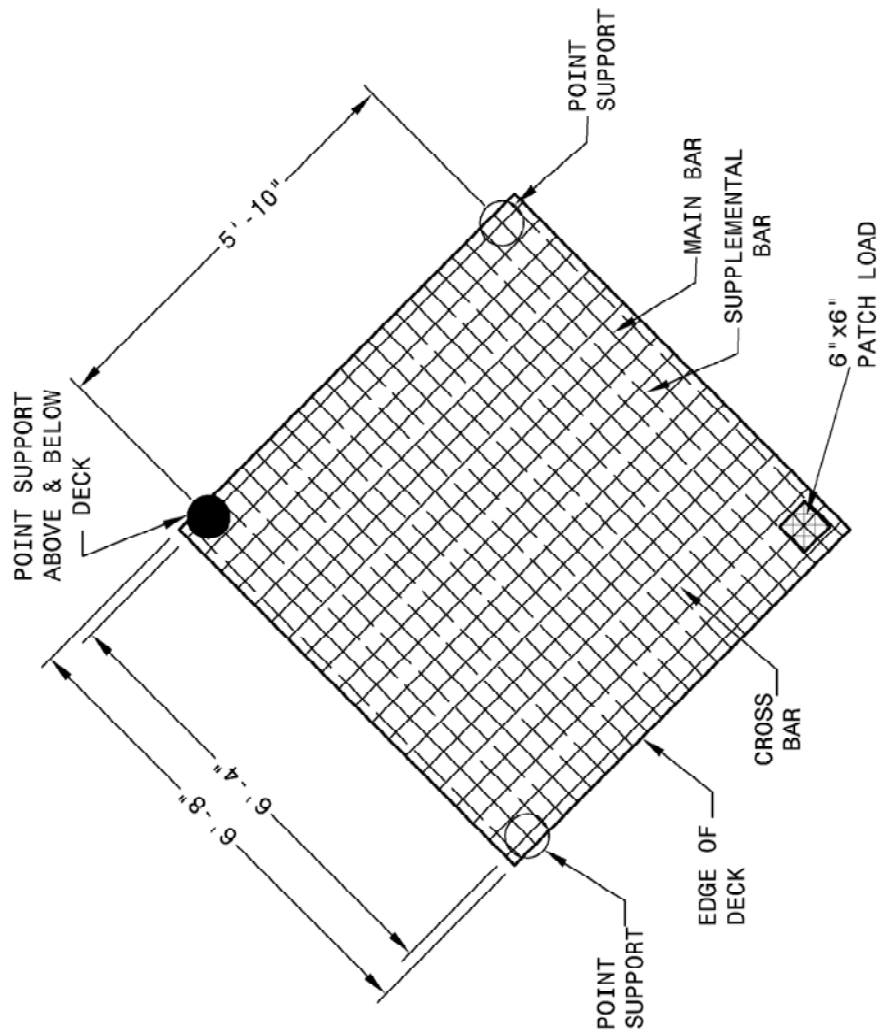
NOTE: CROSS BARS REMOVED FOR CLARITY



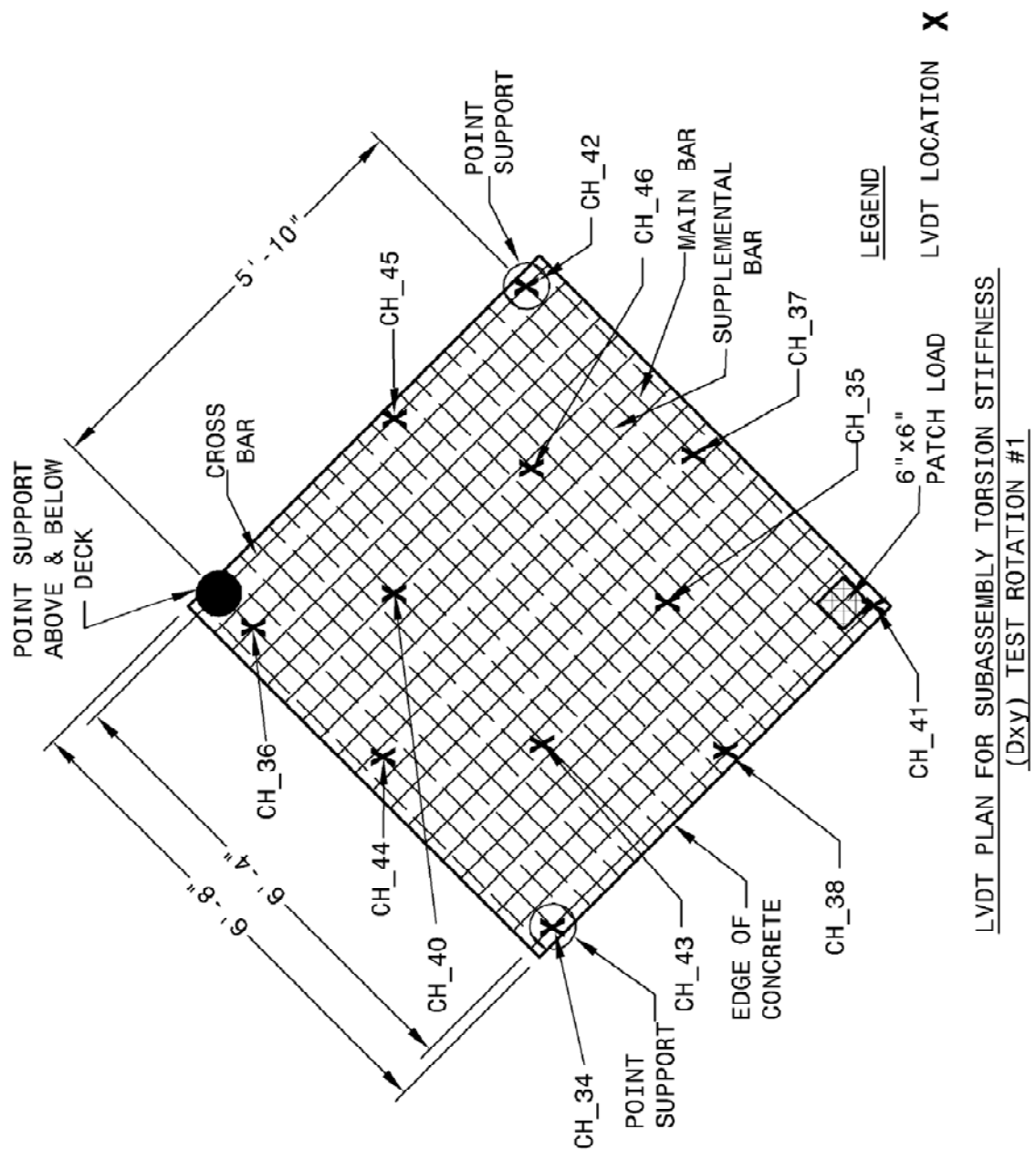
CROSS BAR GAGE PLAN FOR SUBASSEMBLY WEAK
DIRECTION (Dy) TEST

NOTE: MAIN AND SUPPLEMENTAL BARS REMOVED FOR CLARITY

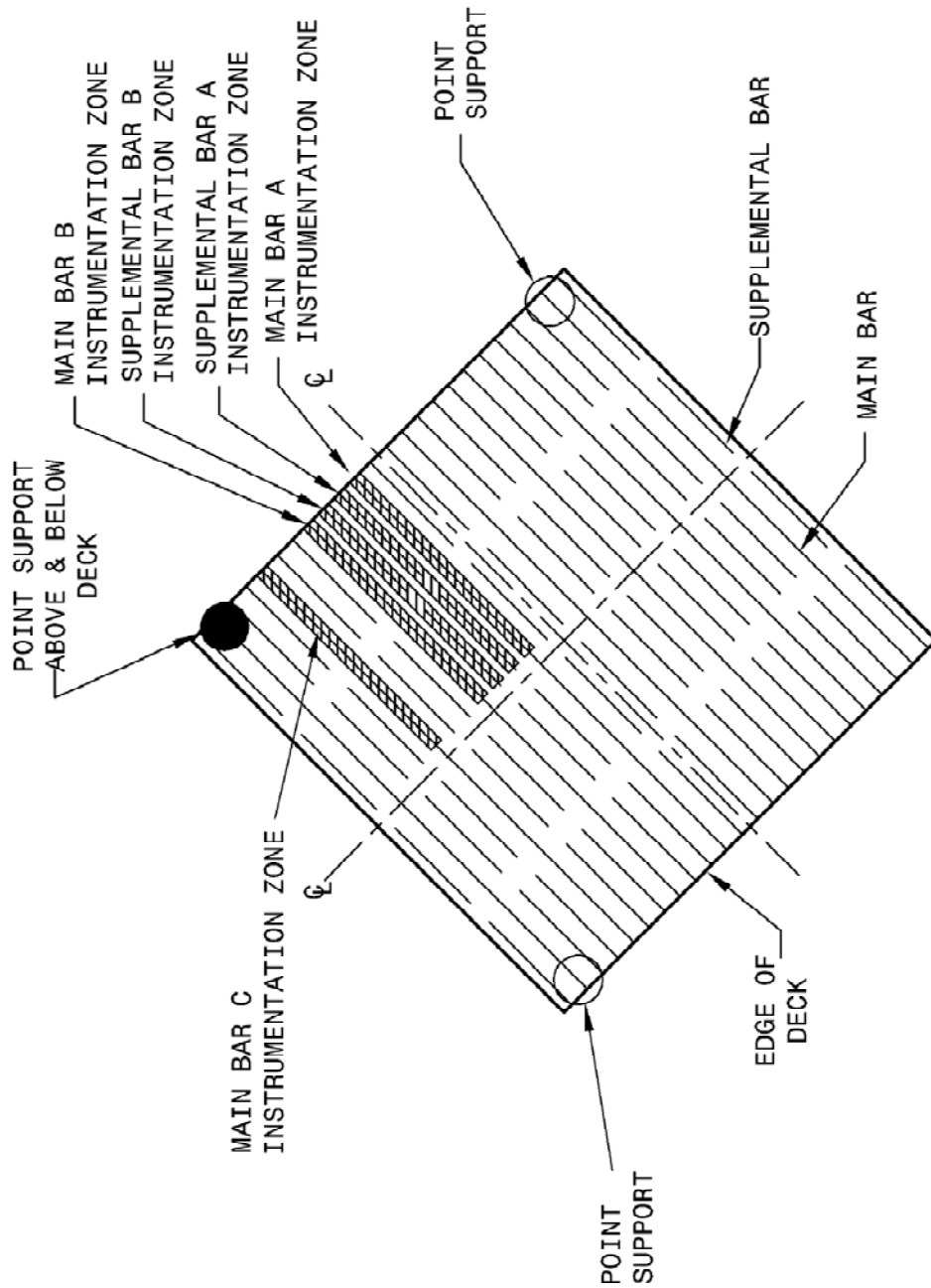
A.3.3 Torsion Stiffness (D_{xy}) Test Rotation #1



SUBASSEMBLY TORSION STIFFNESS (D_{xy}) TEST SETUP
FOR TEST ROTATION #1

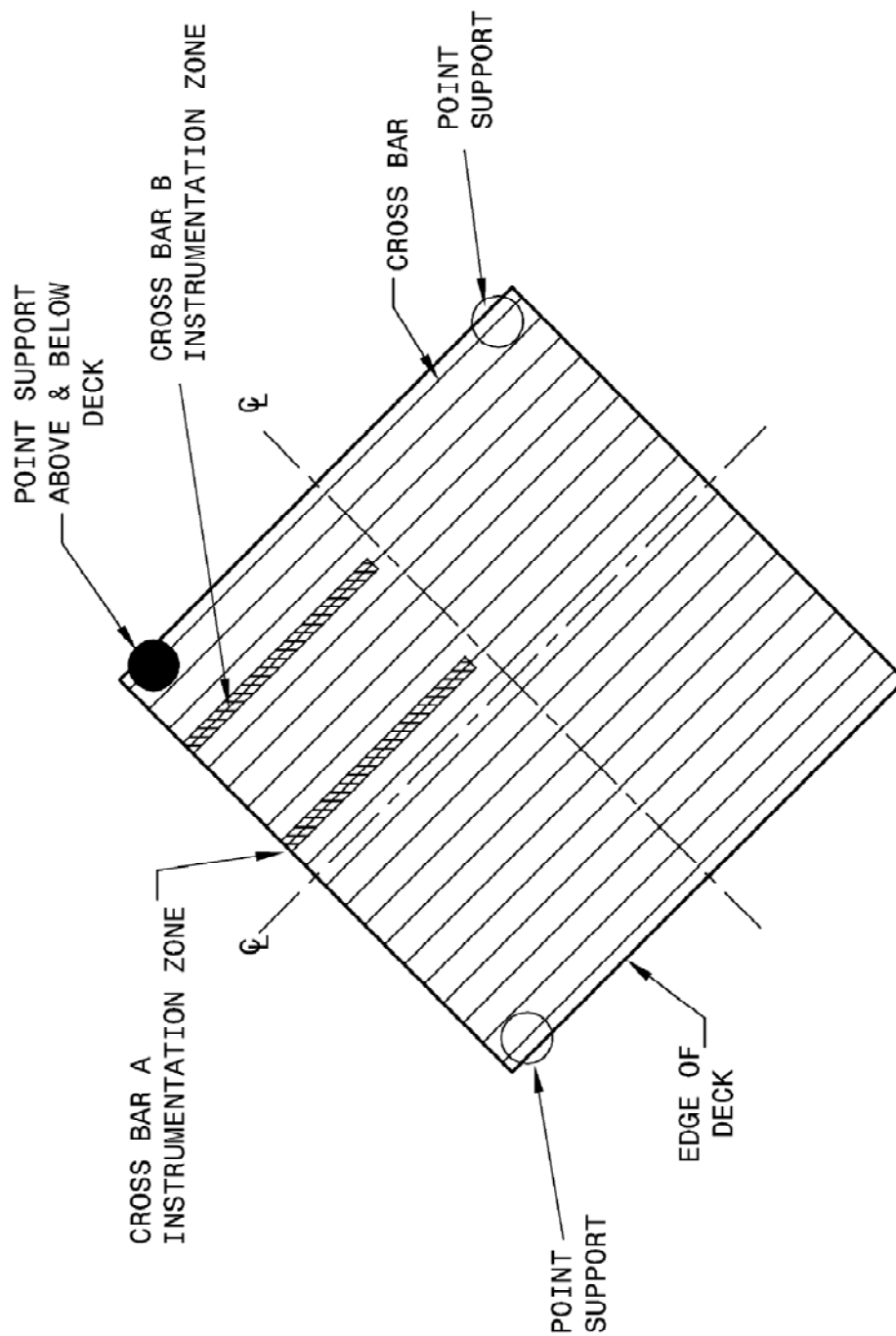


LVDT PLAN FOR SUBASSEMBLY TORSION STIFFNESS
(Dxy) TEST ROTATION #1



MAIN AND SUPPLEMENTAL BAR INSTRUMENTATION PLAN FOR TORSION
STIFFNESS (Dxy) TEST ROTATION #1

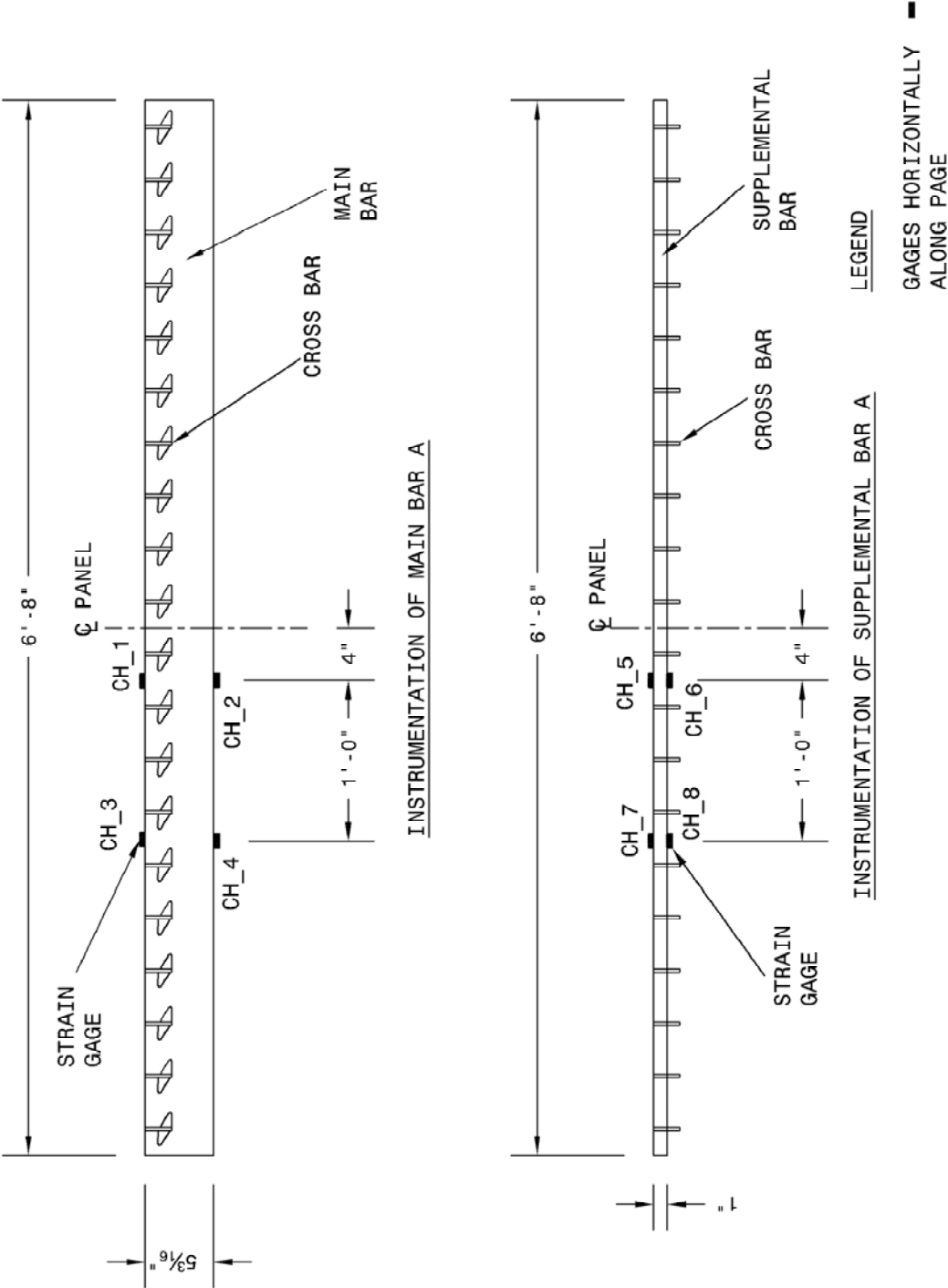
NOTE: CROSS BARS REMOVED FOR CLARITY

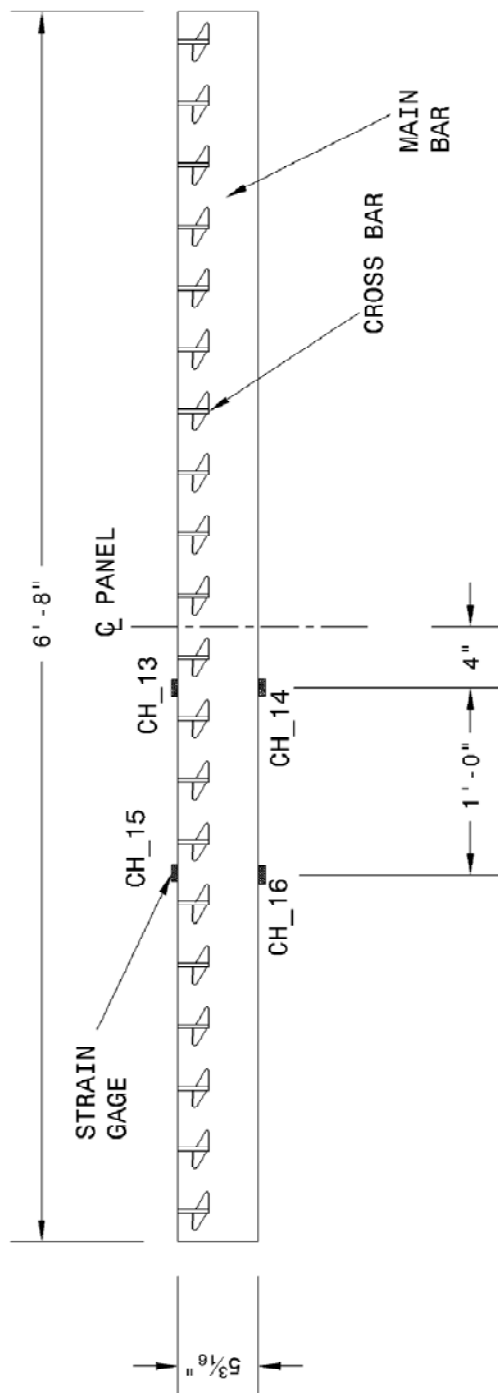


CROSS BAR INSTRUMENTATION PLAN FOR TORSION STIFFNESS
(Dxy) TEST ROTATION #1

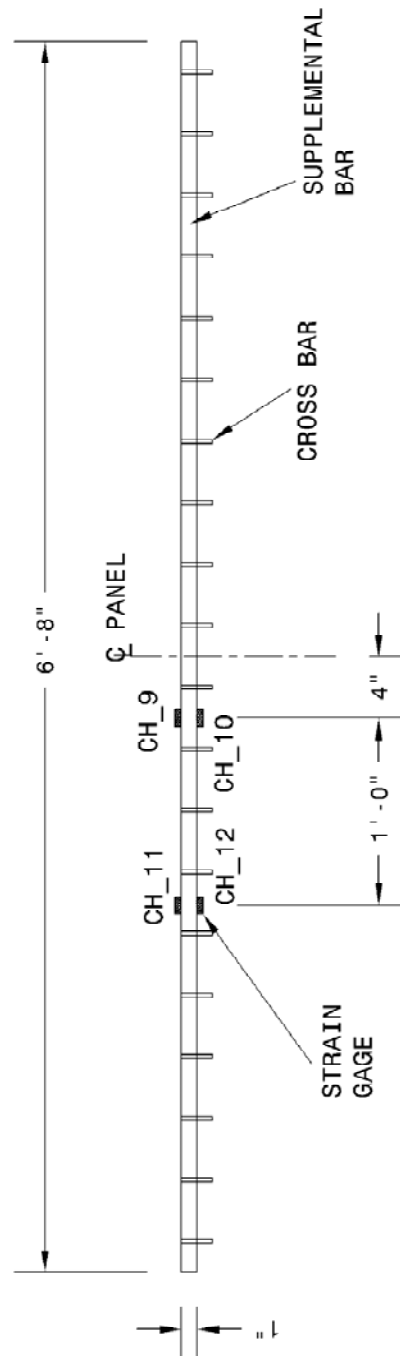
NOTE: MAIN AND SUPPLEMENTAL BARS REMOVED FOR CLARITY

A.3.4 Elevations of Steel with Strain Gages





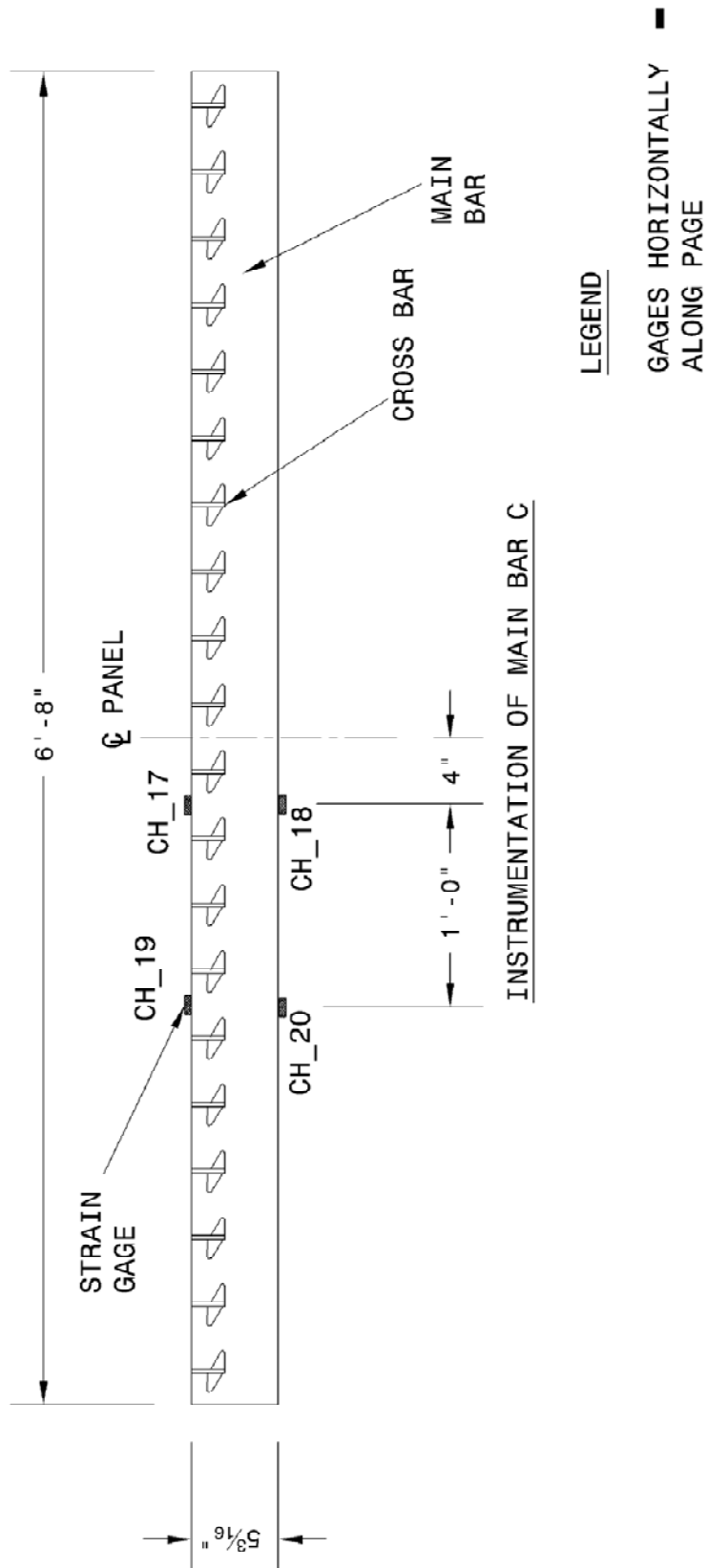
INSTRUMENTATION OF MAIN BAR B

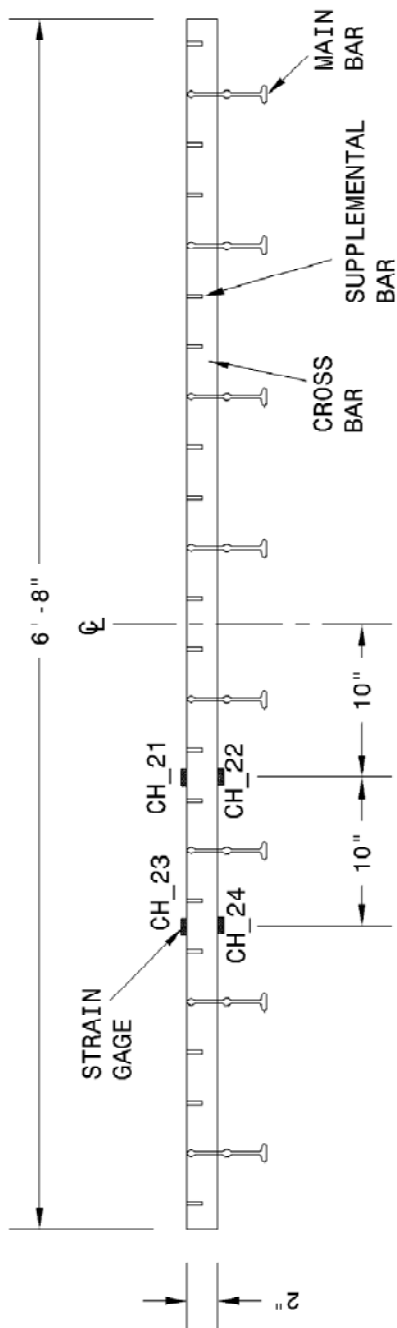


INSTRUMENTATION OF SUPPLEMENTAL BAR B

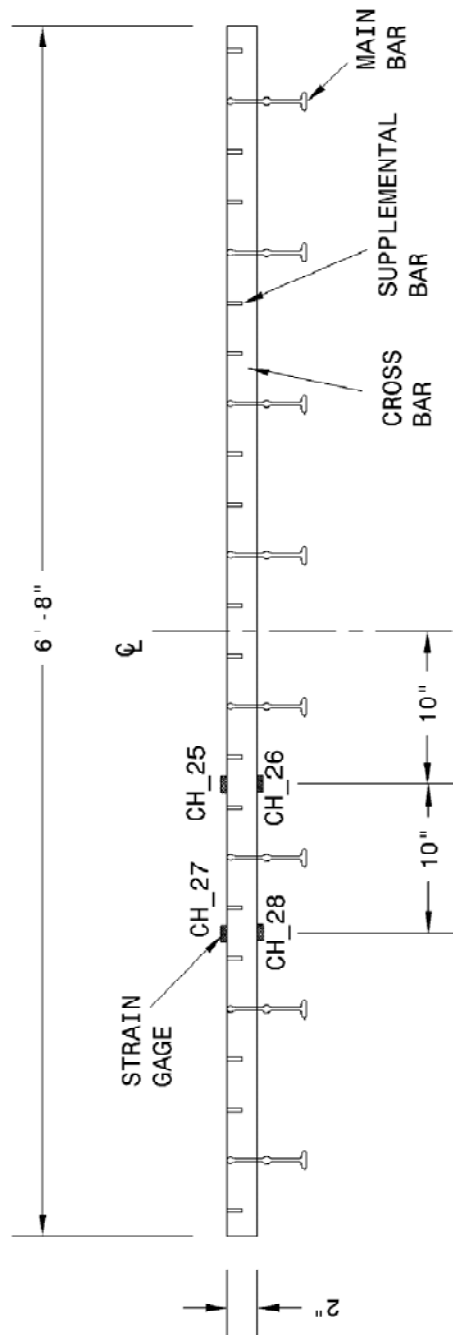
LEGEND

■
GAGES HORIZONTALLY
ALONG PAGE





INSTRUMENTATION OF CROSS BAR A



INSTRUMENTATION OF CROSS BAR B

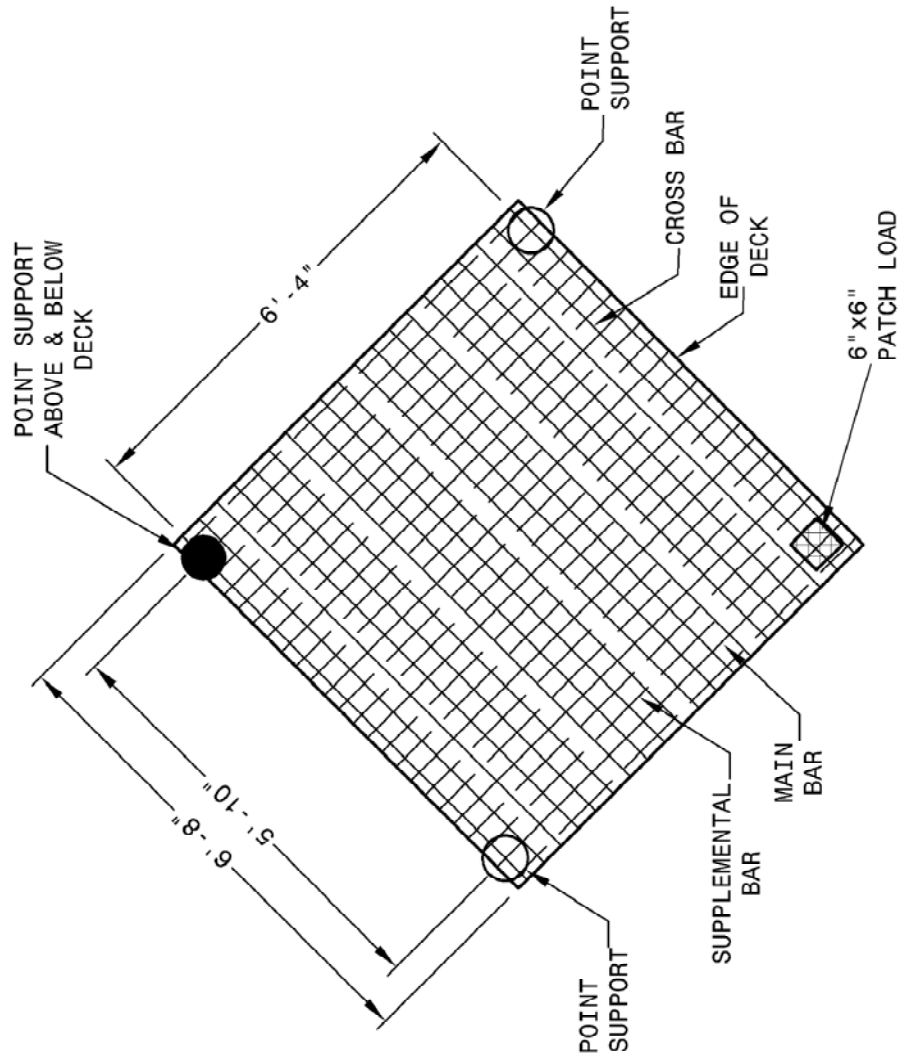
LEGEND
GAGES HORIZONTALLY
ALONG PAGE

A.4 Subassembly Partially Filled Grid Deck Specimen

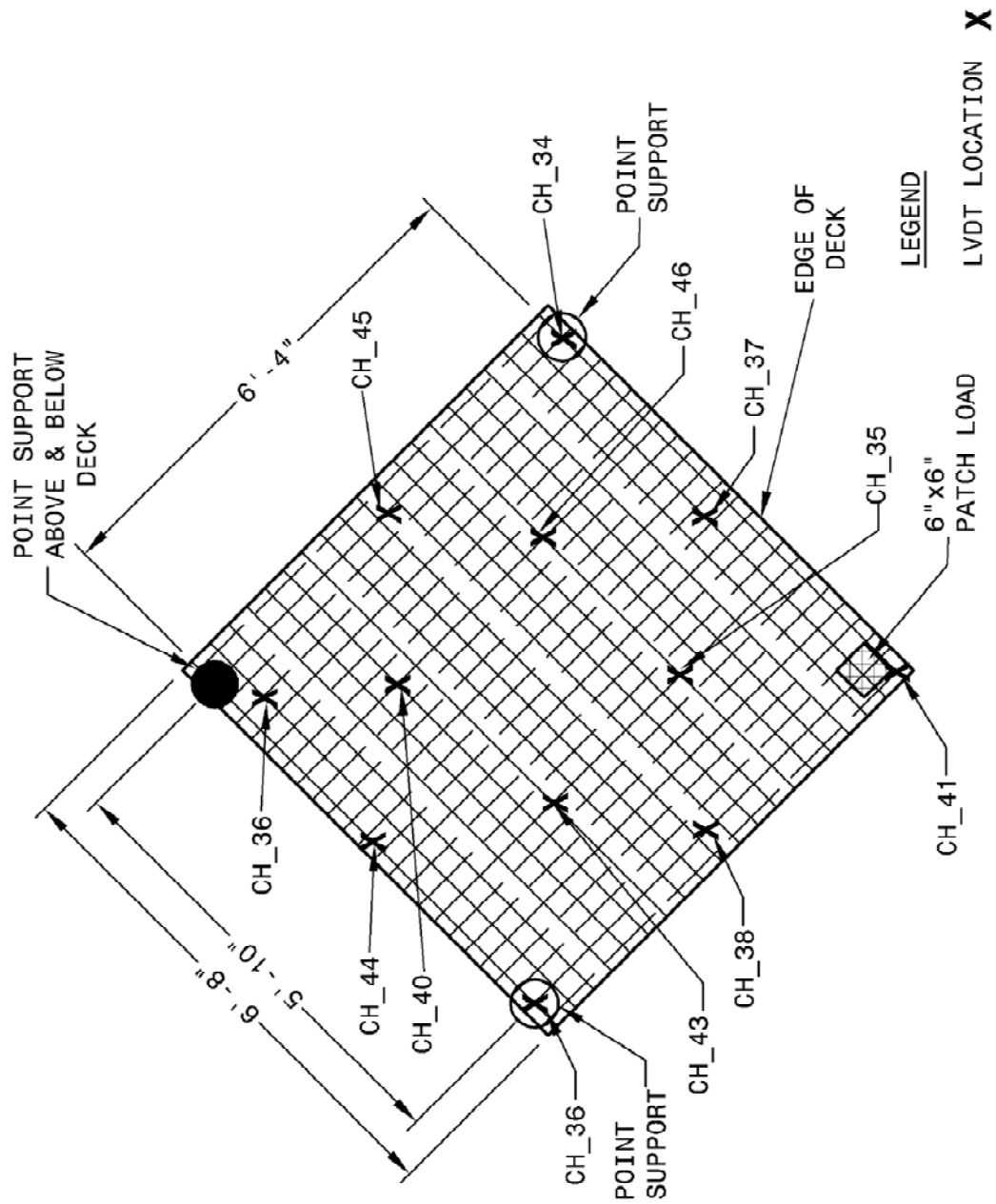
The test setup and instrumentation for the strong direction stiffness (D_x) and weak direction stiffness (D_y) tests were the same as those of subassembly open grid deck specimen #2. Test rotation #1 of the torsion stiffness (D_{xy}) test was also the same as that of open grid deck specimen #2. Therefore, please refer to A.3 for these test setups and associated instrumentation.

However, this chapter shows the test setup used for test rotations #2 and associated instrumentation plans. The instrumentation plans are also shown for test rotation #3, but the setup and LVDT plan was the same as that of open grid deck specimen #2 test rotation #1.

A.4.1 Torsion Stiffness (D_{xy}) Test Rotation #2

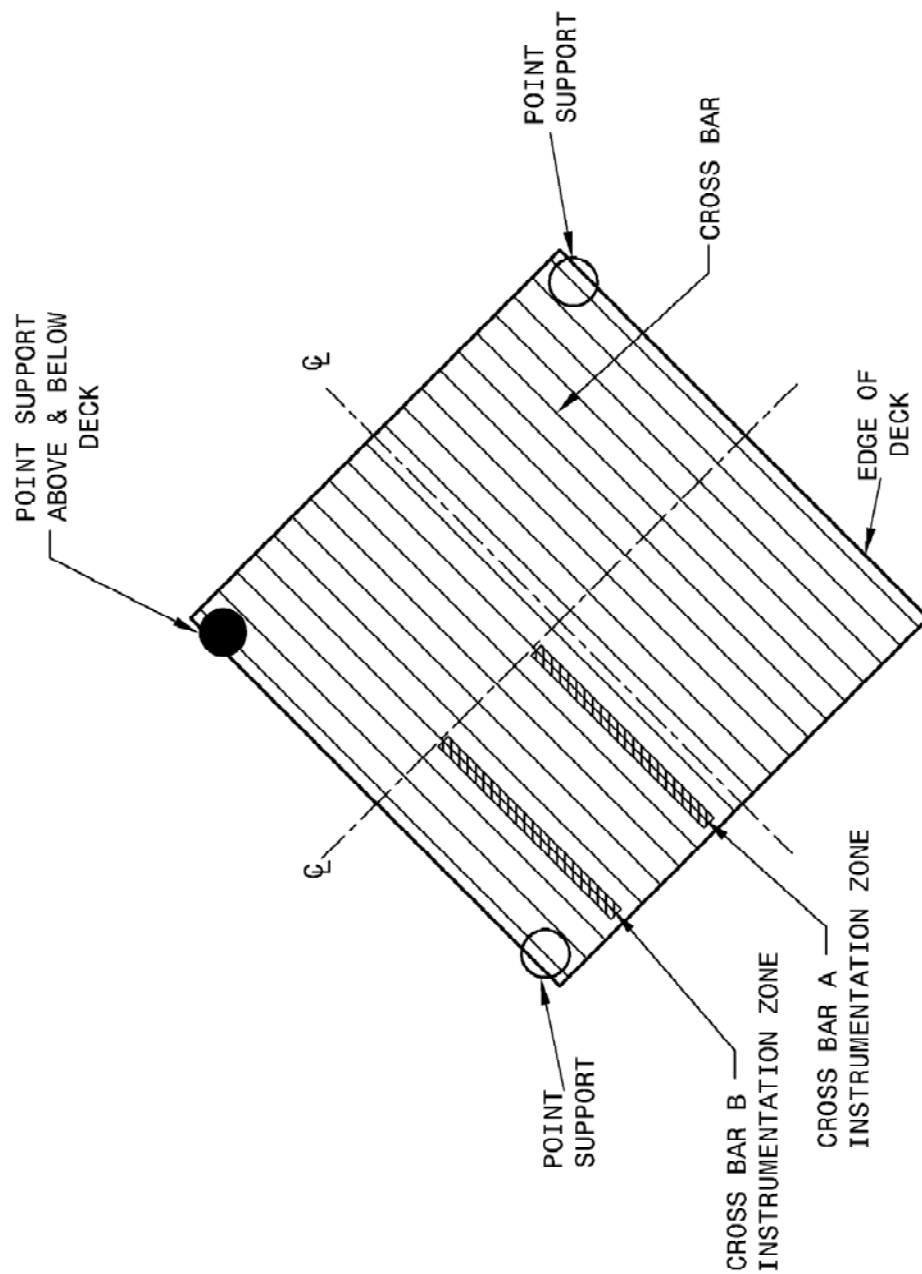


SUBASSEMBLY TORSION STIFFNESS (D_{xy}) TEST SETUP
FOR TEST ROTATION #2



INSTRUMENTATION PLAN FOR SUBASSEMBLY TORSION STIFFNESS

(Dxy) TEST ROTATION #2

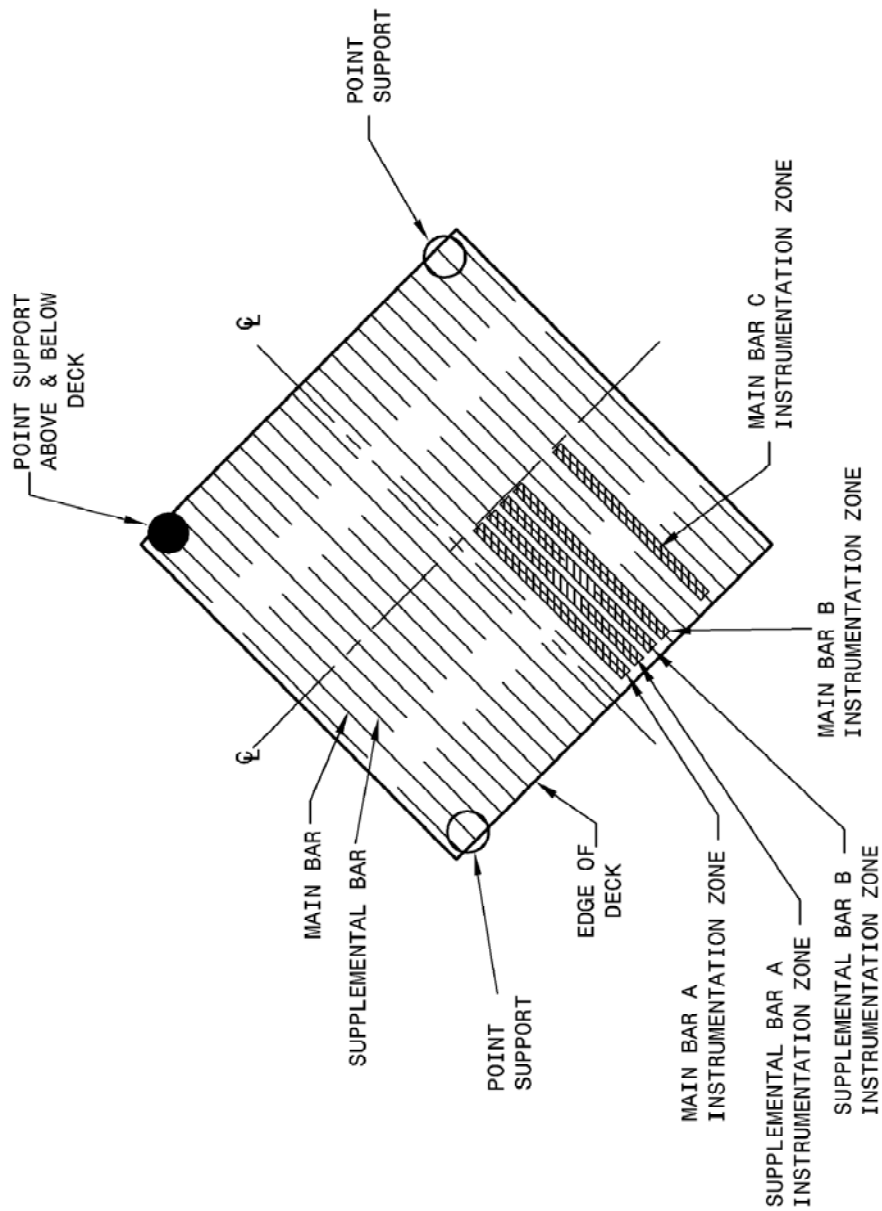


CROSS BAR STRAIN GAGE PLAN FOR SUBASSEMBLY TORSION
STIFFNESS (Dxy) TEST ROTATION #2

NOTE: MAIN AND SUPPLEMENTAL BARS REMOVED FOR CLARITY

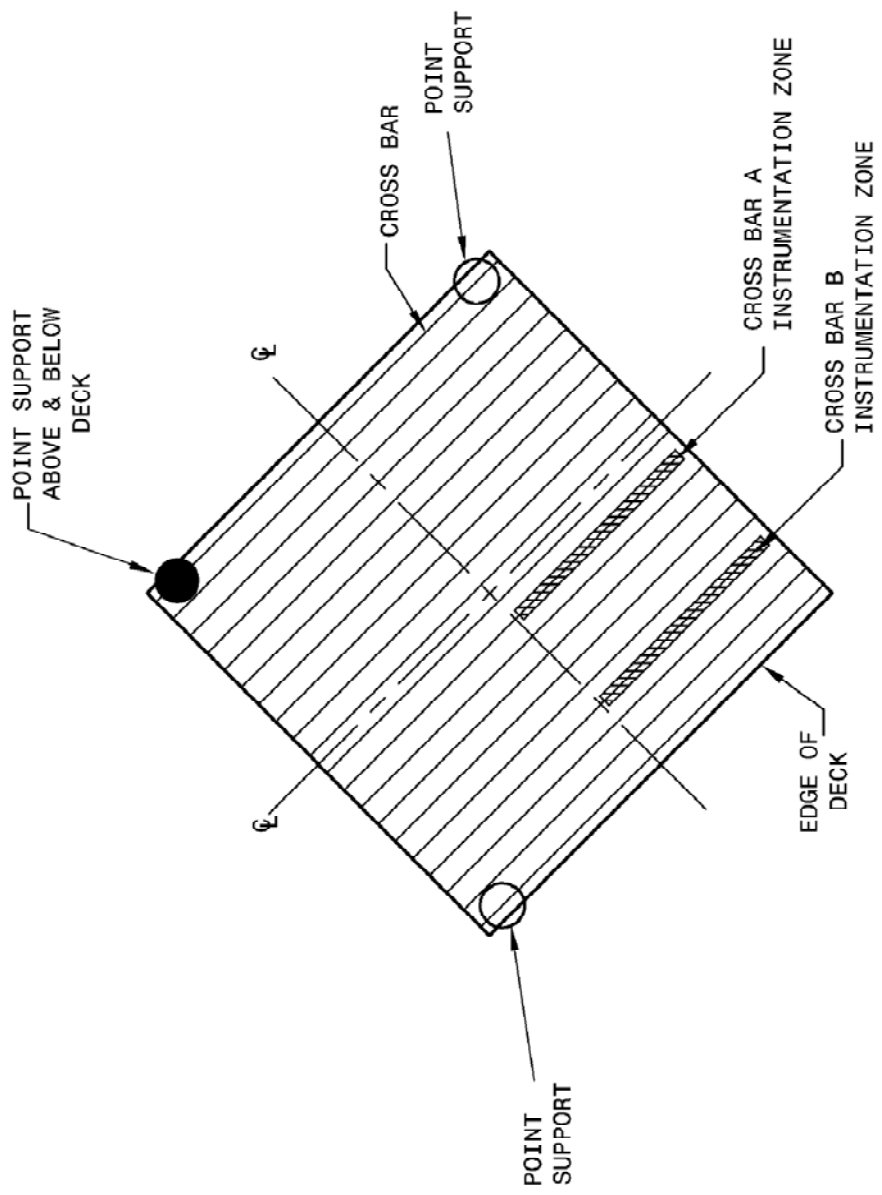
A.4.2 Torsion Stiffness (D_{xy}) Test Rotation #3

The test setup and LVDT locations were the same as those of Open Grid Deck Specimen Test Rotation #1. Therefore, please refer to A.3.



MAIN AND SUPPLEMENTAL BAR STRAIN GAGE PLAN FOR SUBASSEMBLY TORSION
STIFFNESS (Dxy) TEST ROTATION #3

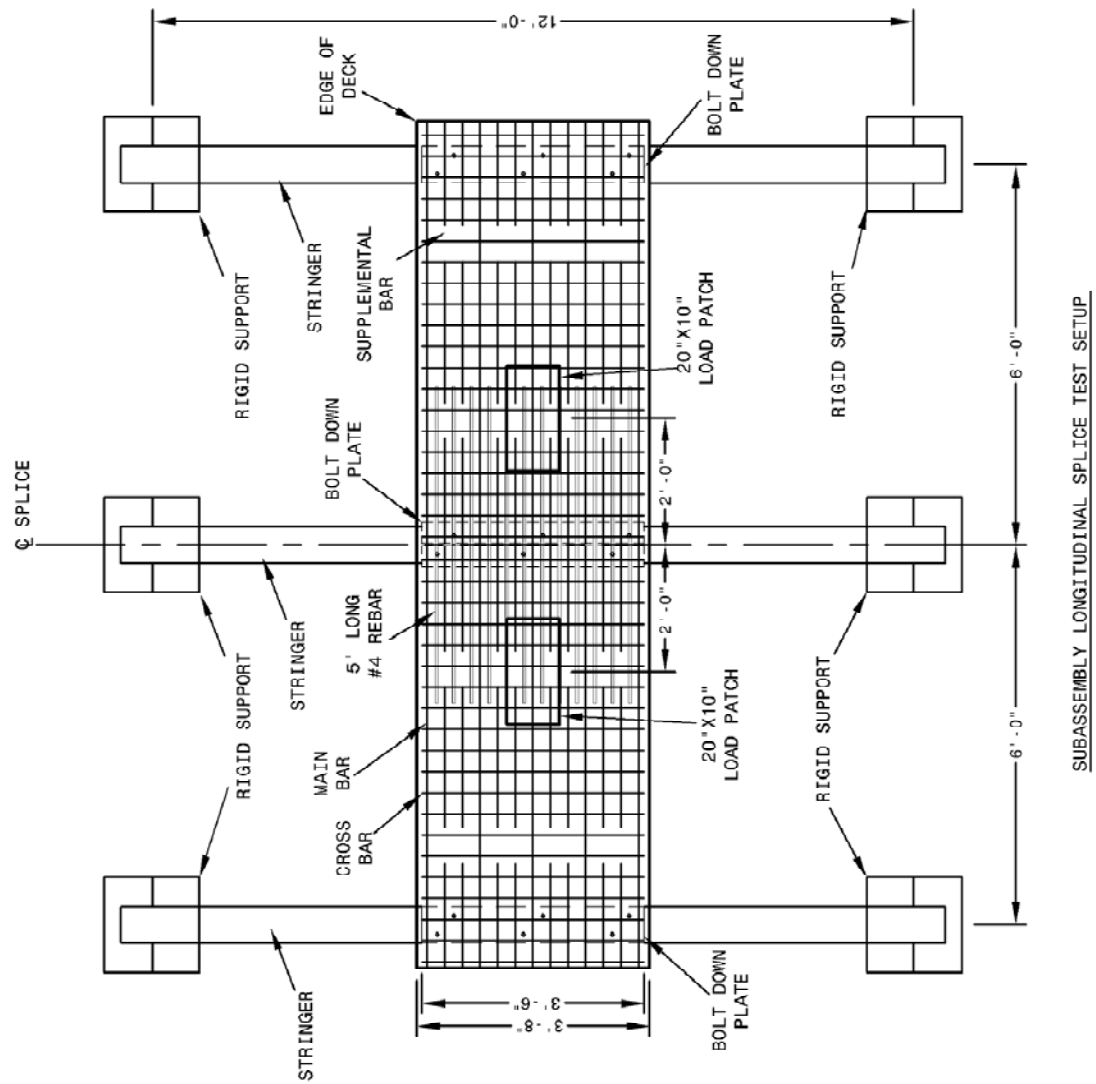
NOTE: CROSS BARS REMOVED FOR CLARITY

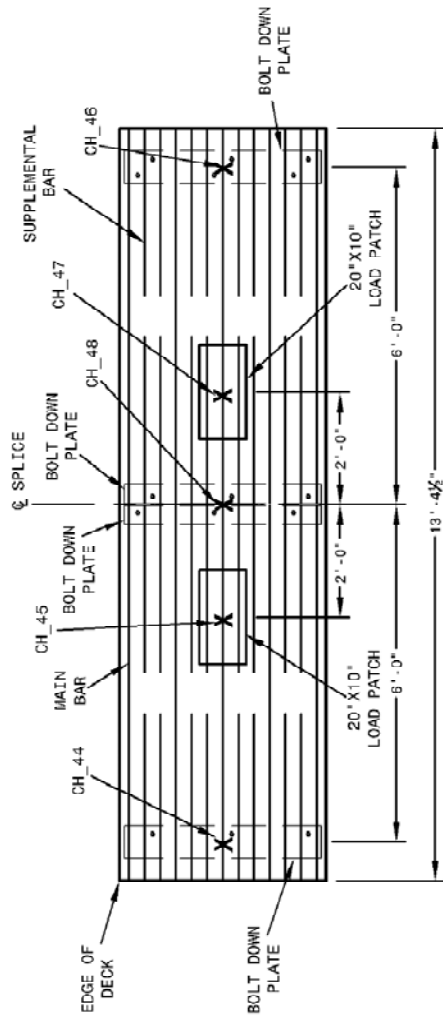


CROSS BAR GAGE PLAN FOR SUBASSEMBLY TORSION
STIFFNESS (Dxy) TEST ROTATION #3

NOTE: MAIN AND SUPPLEMENTAL BARS REMOVED FOR CLARITY

A.5 Subassembly Longitudinal Splice Specimen



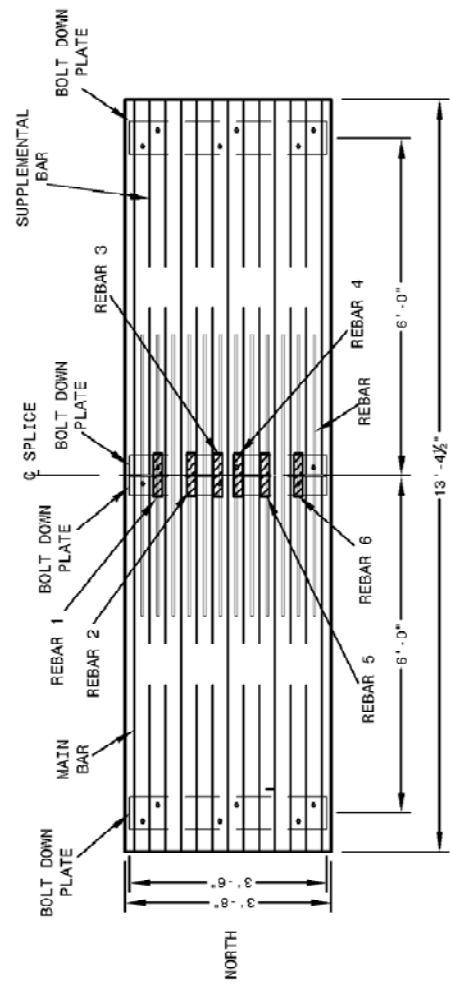


LVDT PLAN FOR SUBASSEMBLY LONGITUDINAL SPLICE TEST

NOTE: CROSS BARS AND REBAR REMOVED FOR CLARITY

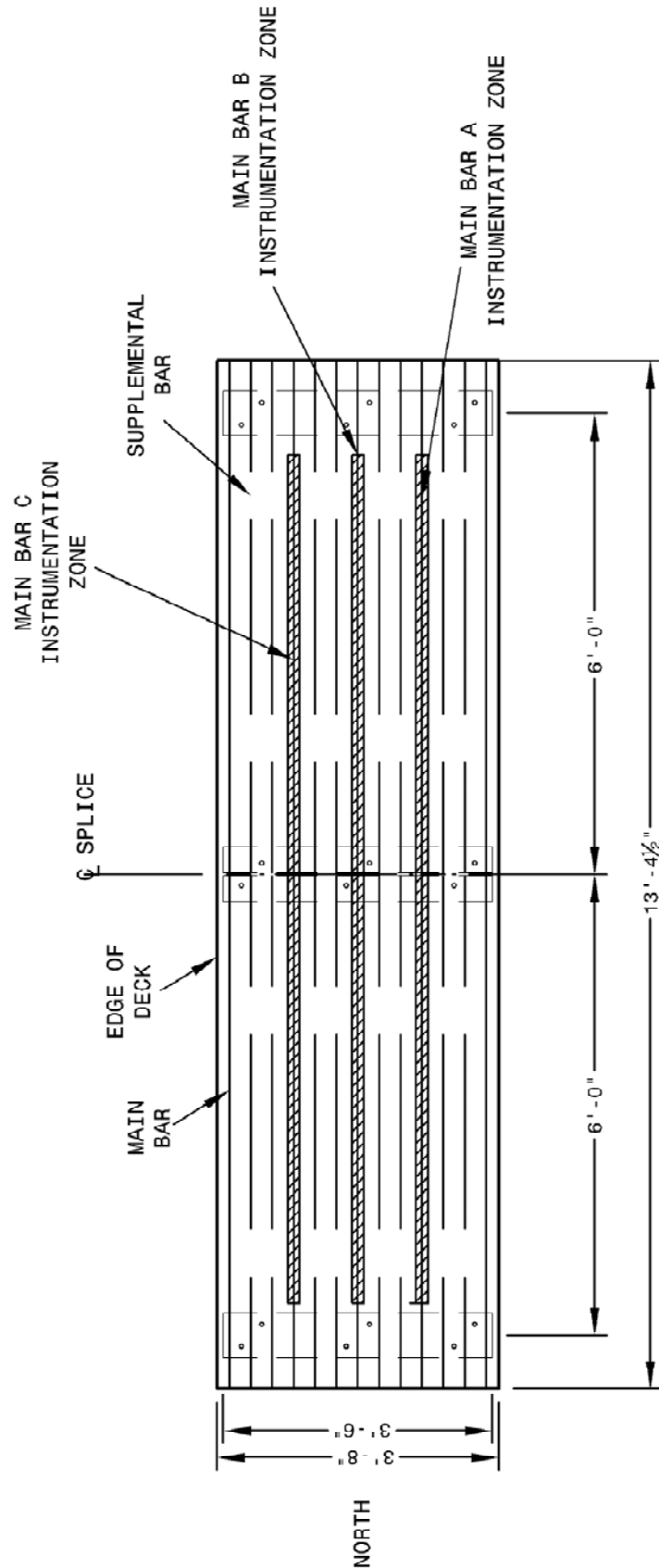
LEGEND

LVDT LOCATION X



REBAR STRAIN GAGE PLAN FOR SUBASSEMBLY LONGITUDINAL SPLICE TEST

NOTE: CROSS BARS REMOVED FOR CLARITY



MAIN BAR STRAIN GAGE PLAN FOR SUBASSEMBLY LONGITUDINAL SPLICE TEST

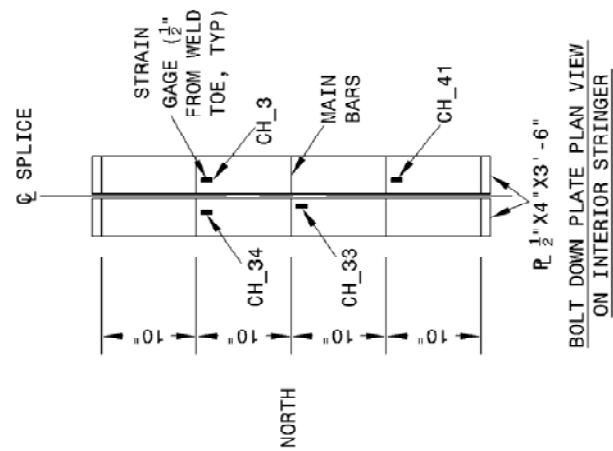
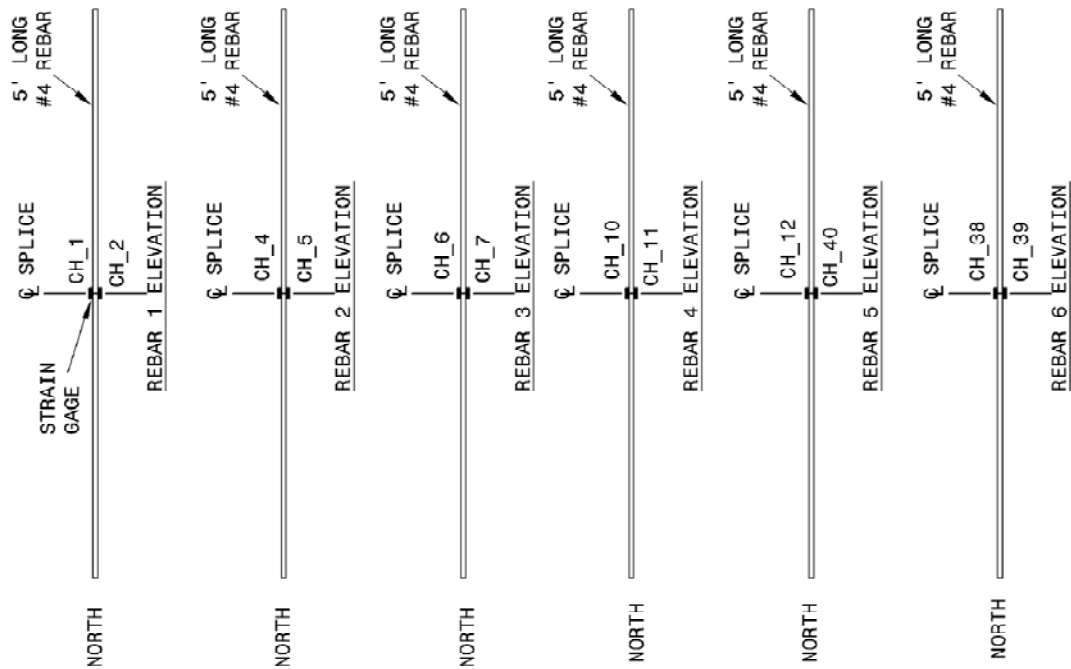
NOTE: CROSS BARS AND REBAR REMOVED FOR CLARITY

Figure 1 is an elevation view of the bridge deck cross-section. It shows a 2' concrete overlay on top of a main bar. A strain gage is located on the main bar. The main bar is composed of several segments: a 3'-0" segment on the left, followed by a 2'-11 1/2" segment, a 1'-7 1/2" segment, a 1'-5" segment, a 7 1/2" segment, a 6'-0" segment, and a 6'-8" segment on the right. The segments are separated by bolt down plates. The main bar is reinforced with #4 rebar. The segments are labeled CH_19, CH_20, CH_21, CH_22, CH_23, CH_24, CH_29, CH_30, CH_31, and CH_32. A 5' long #4 rebar is shown at the top. A splice is indicated at the 3'-0" segment. A north arrow is at the bottom left.

Figure 1 is a cross-sectional diagram of a bridge deck. It shows a 2" concrete overlay on top of a main reinforcement layer. The main reinforcement consists of #4 rebar spaced at 5' intervals. A central splice is shown with a 7 1/2" gap. The deck is supported by a central pier and two side piers. The total width of the deck is 6'-8". The main bar is labeled 'MAIN BAR' and the cross bar is labeled 'CROSS BAR'. The bolt down plates are labeled 'BOLT DOWN PLATE'.

LEGEND

A-68

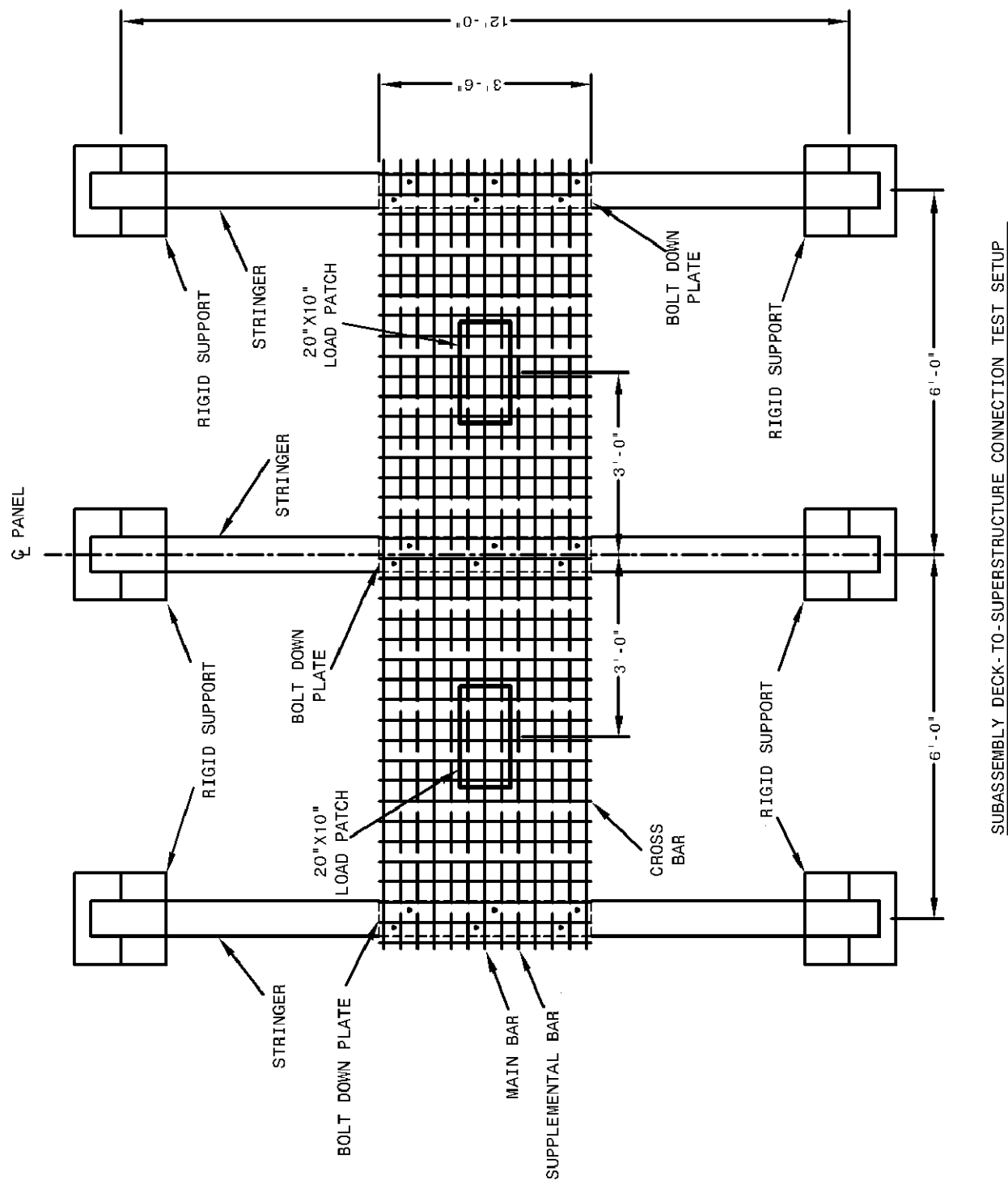


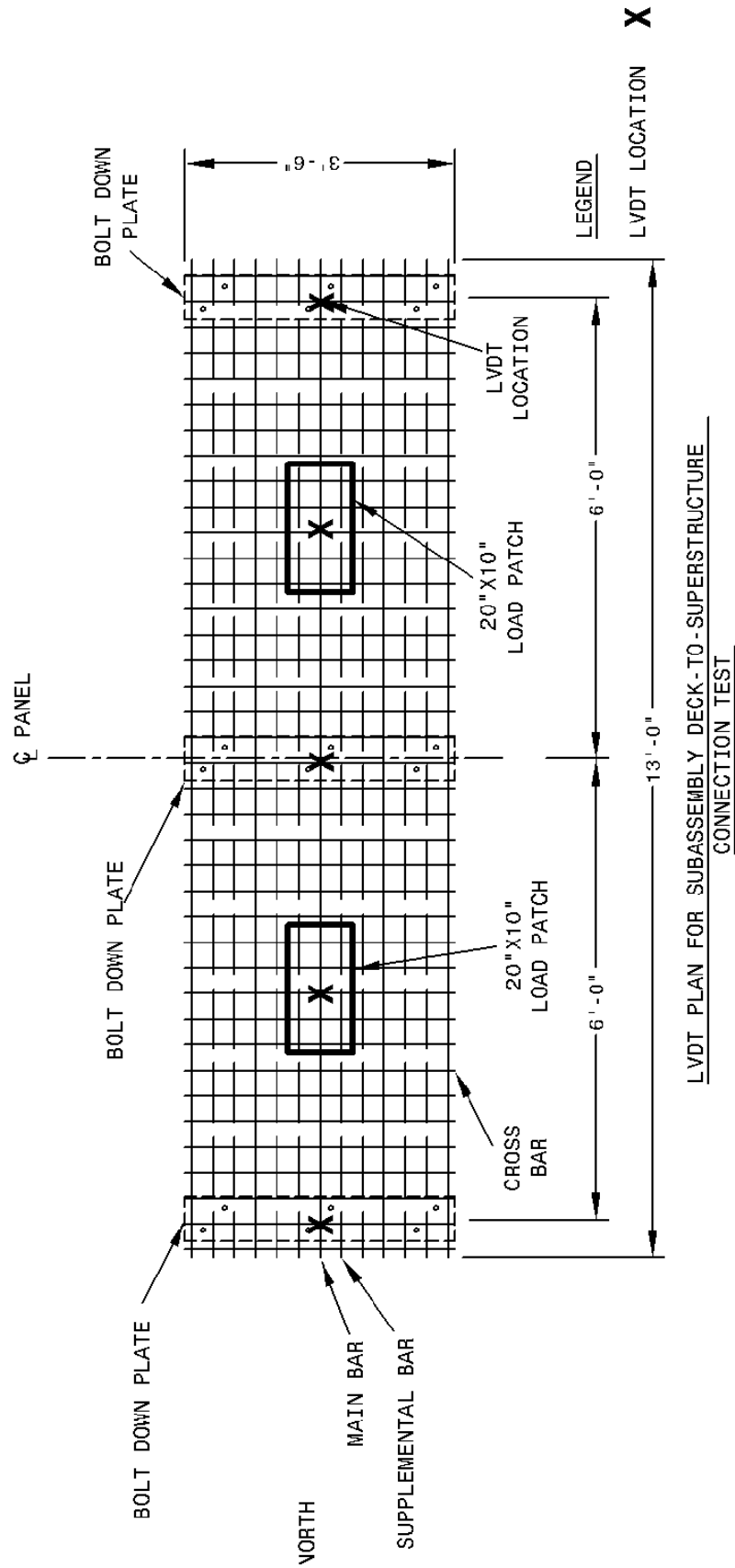
LEGEND

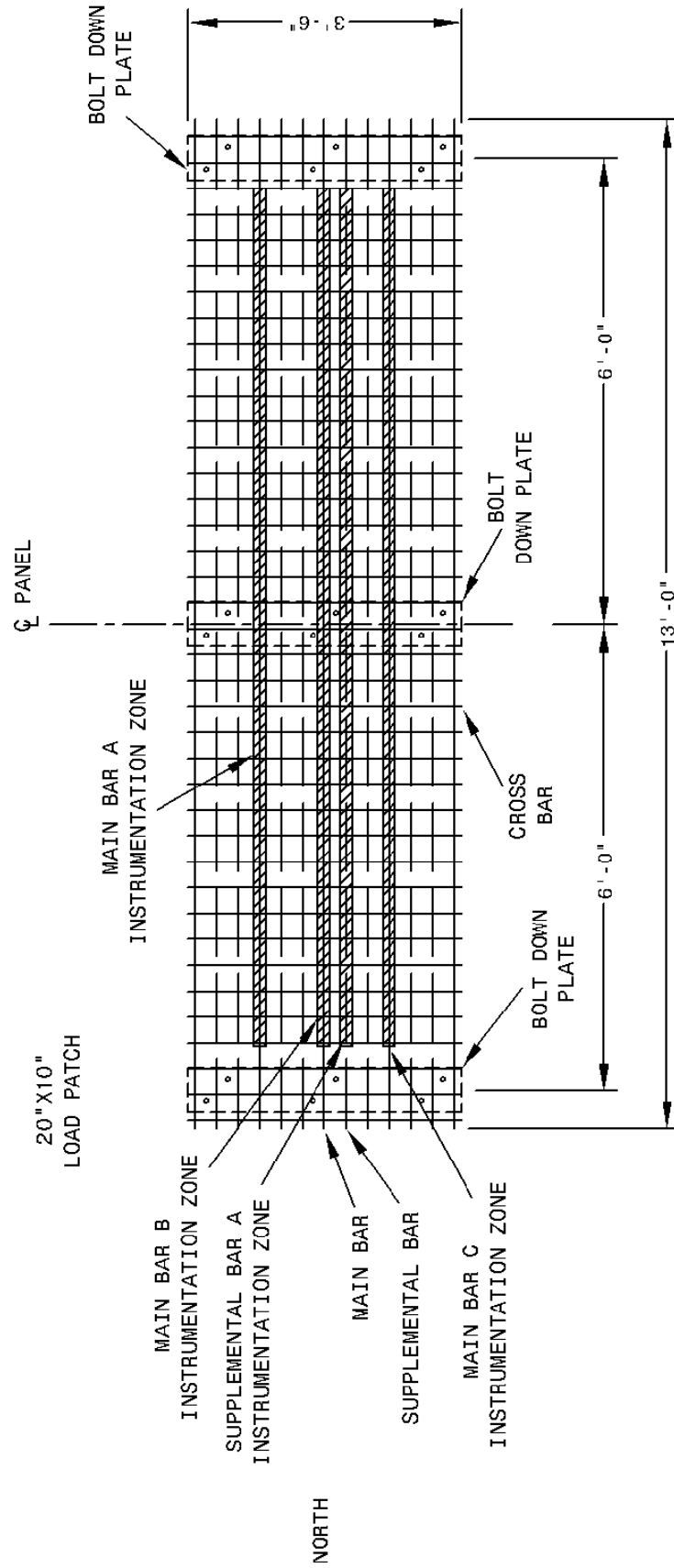
GAGES HORIZONTALLY ALONG PAGE -

GAGES VERTICALLY ALONG PAGE |

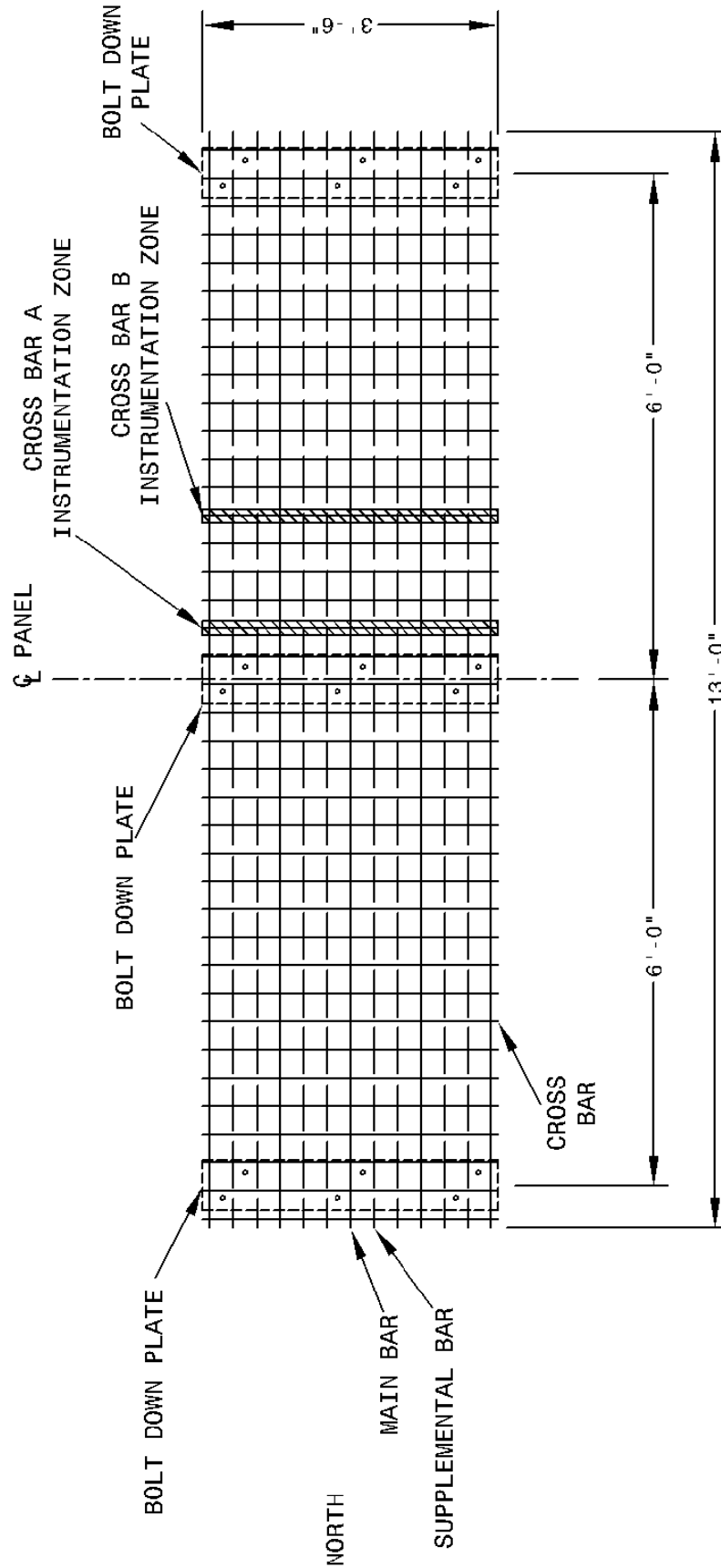
A.6 Subassembly Deck-to-Superstructure Connection Specimen





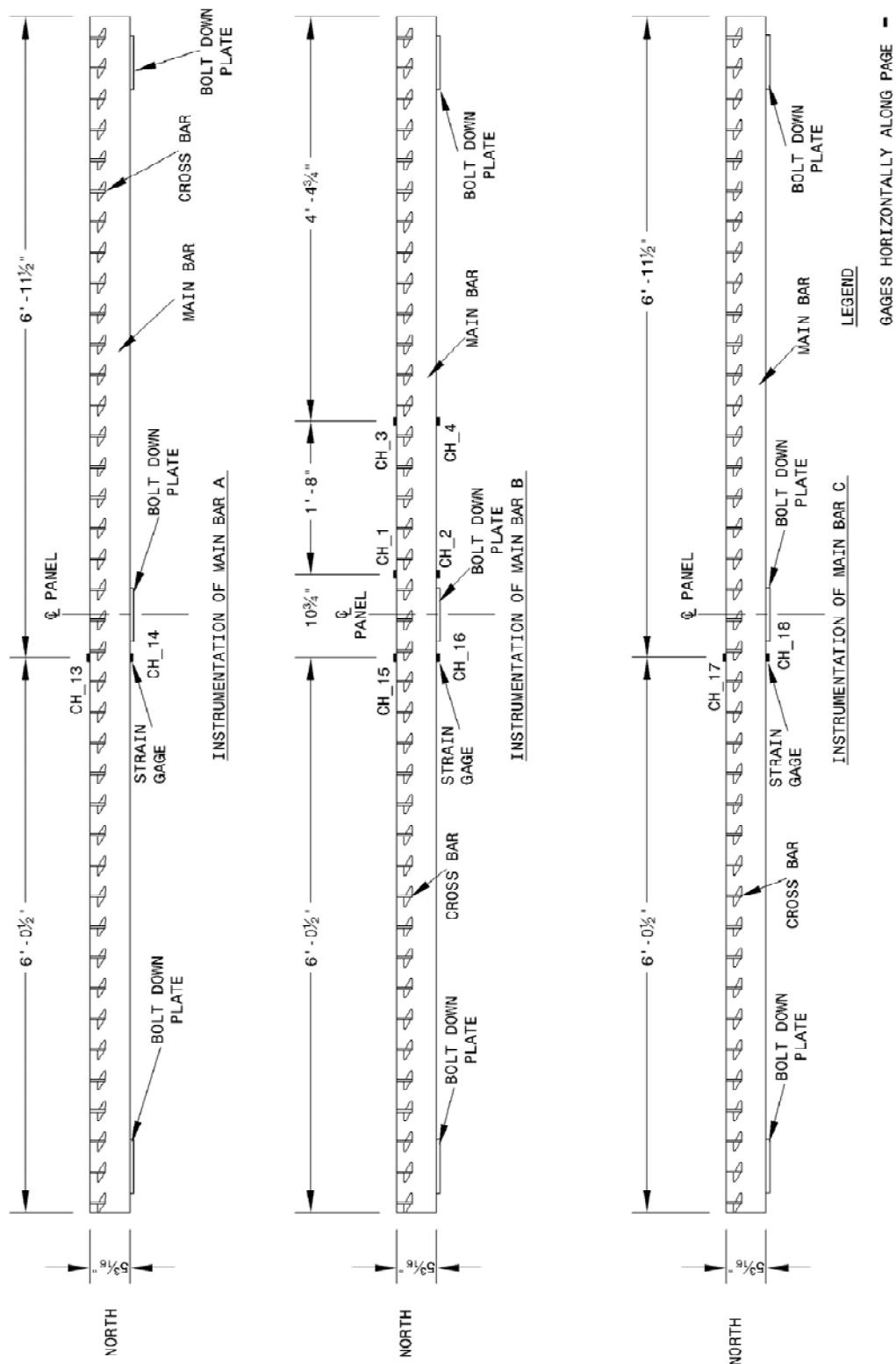


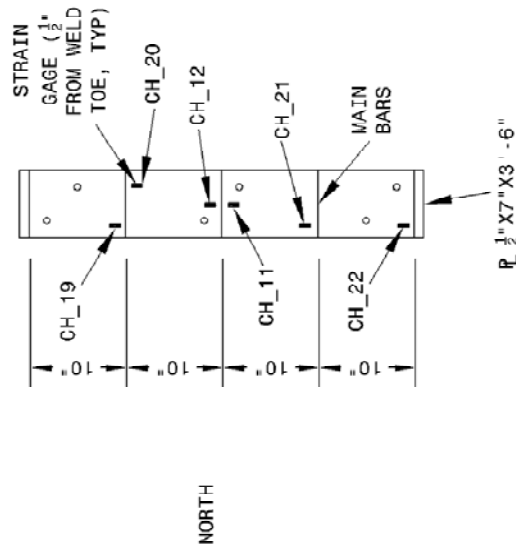
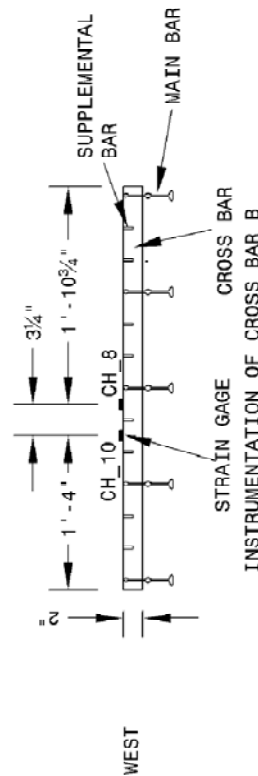
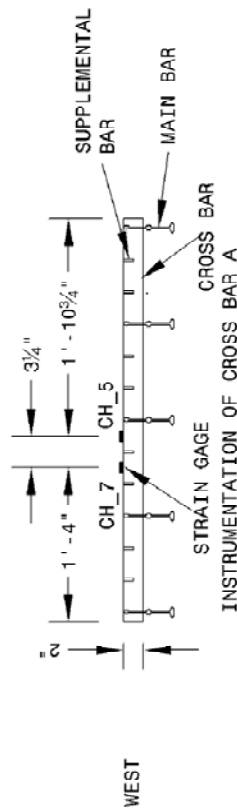
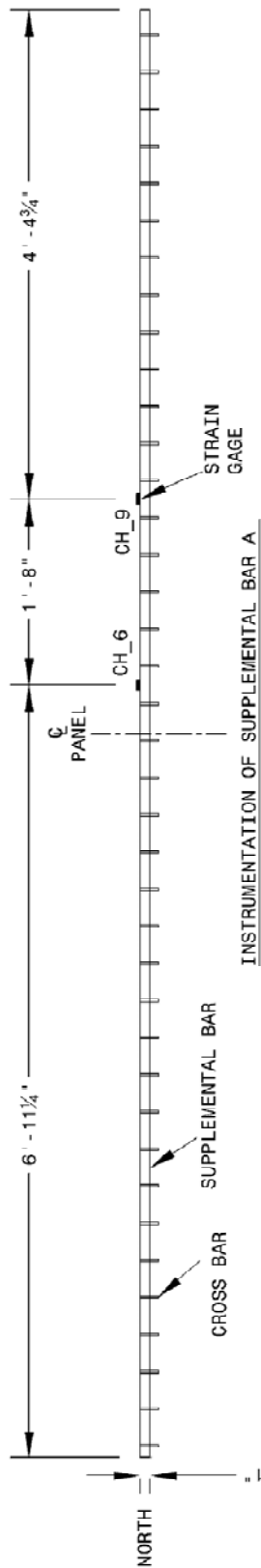
MAIN AND SUPPLEMENTAL BAR STRAIN GAGE PLAN FOR SUBASSEMBLY
DECK-T0-SUPERSTRUCTURE CONNECTION TEST



CROSS BAR STRAIN GAGE PLAN FOR SUBASSEMBLY
DECK-TO-SUPERSTRUCTURE CONNECTION TEST

A.6.1 Elevations of Steel Components with Strain Gages





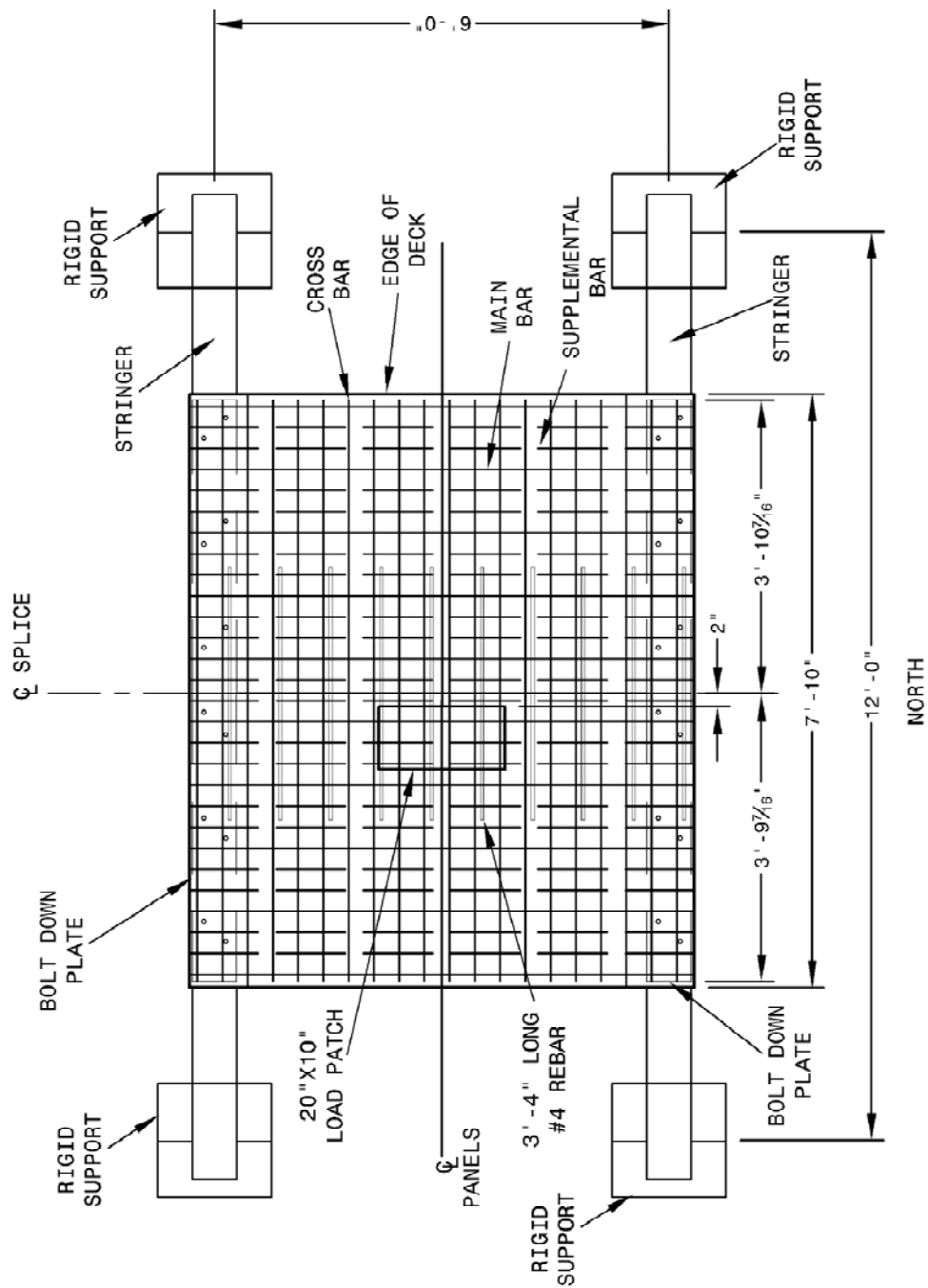
BOLT DOWN PLATE PLAN VIEW
ON INTERIOR STRINGER

LEGEND

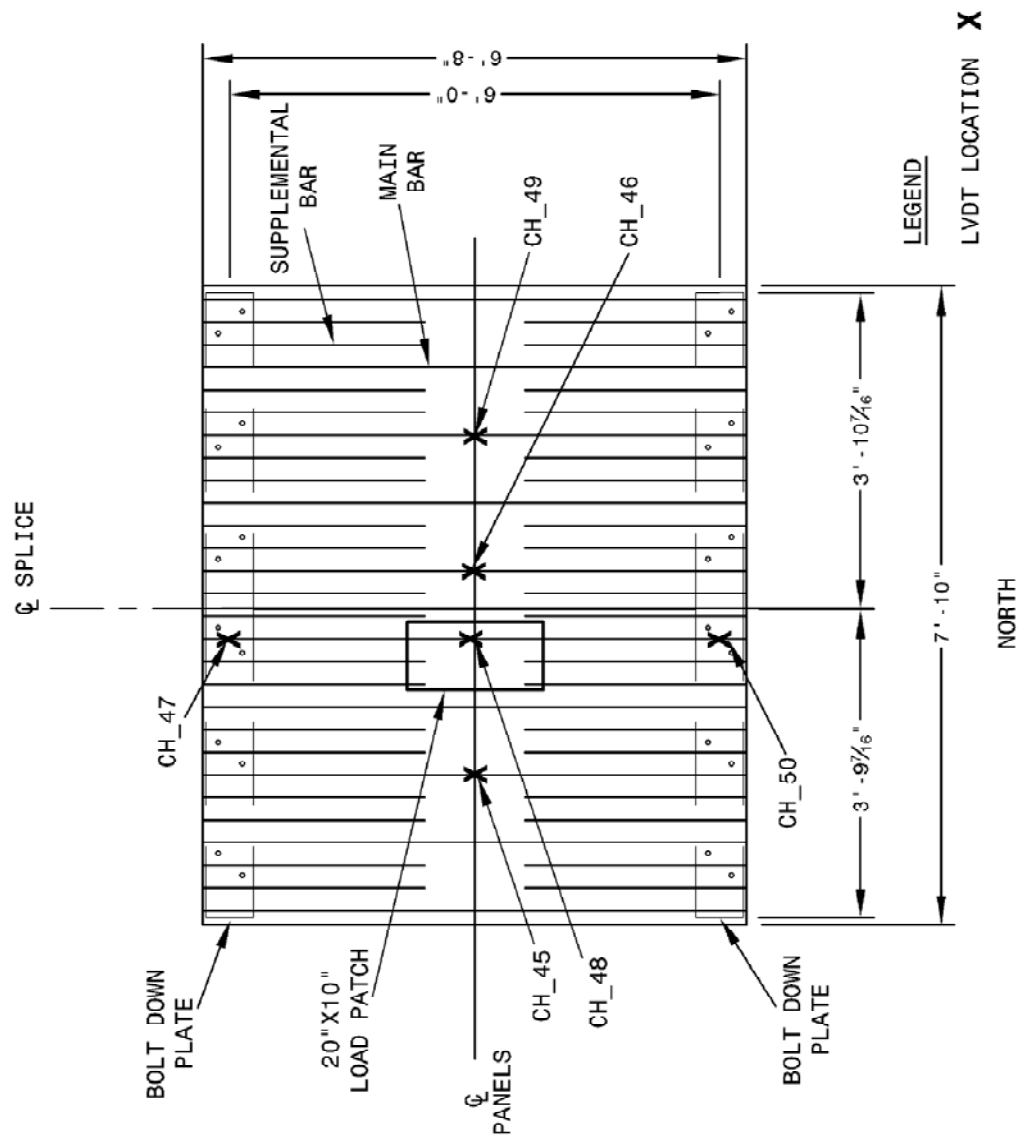
GAGES HORIZONTALLY ALONG PAGE -

GAGES VERTICALLY ALONG PAGE -

A.7 Subassembly Transverse Splice Specimen

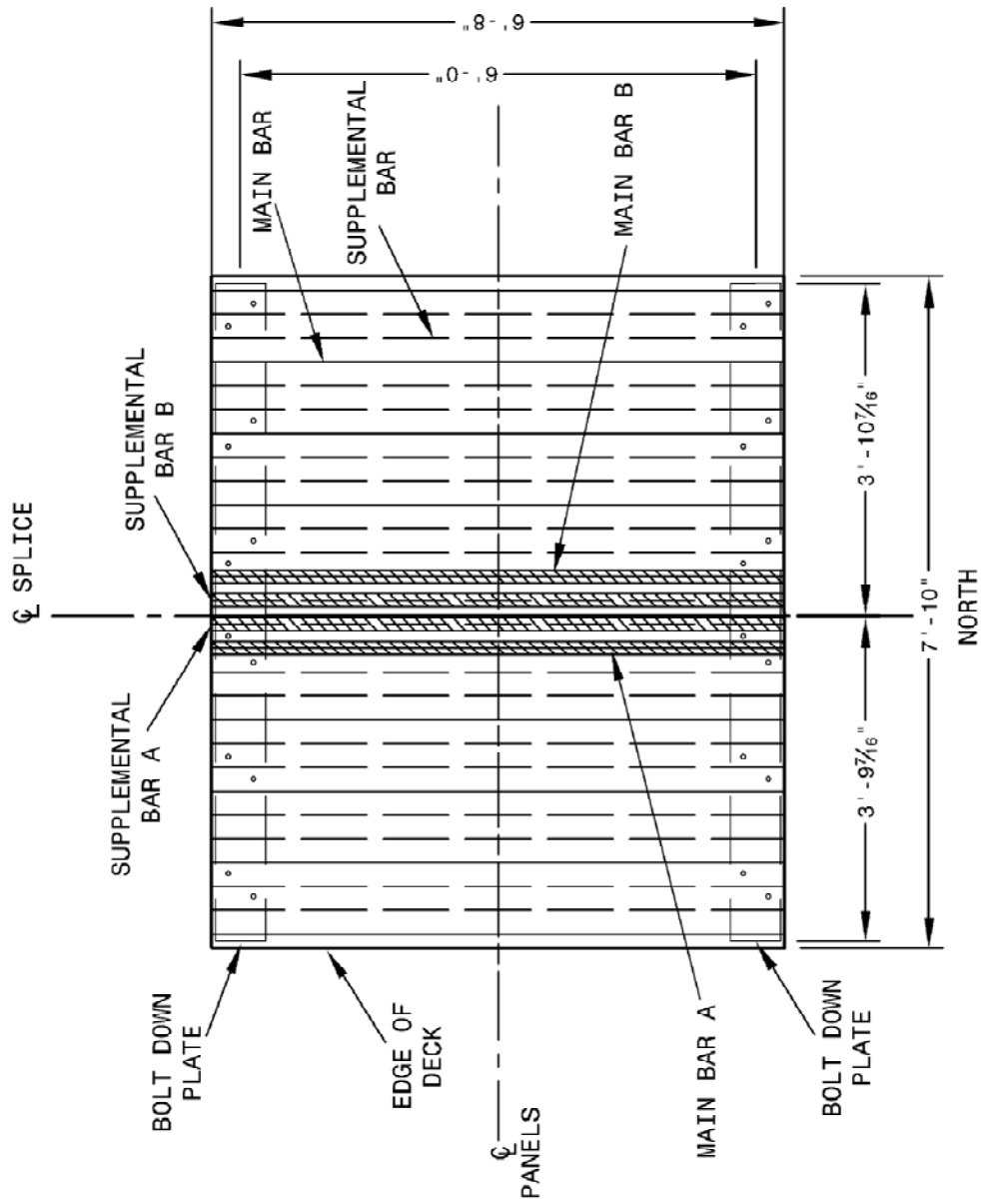


SUBASSEMBLY TRANSVERSE SPLICE TEST SETUP



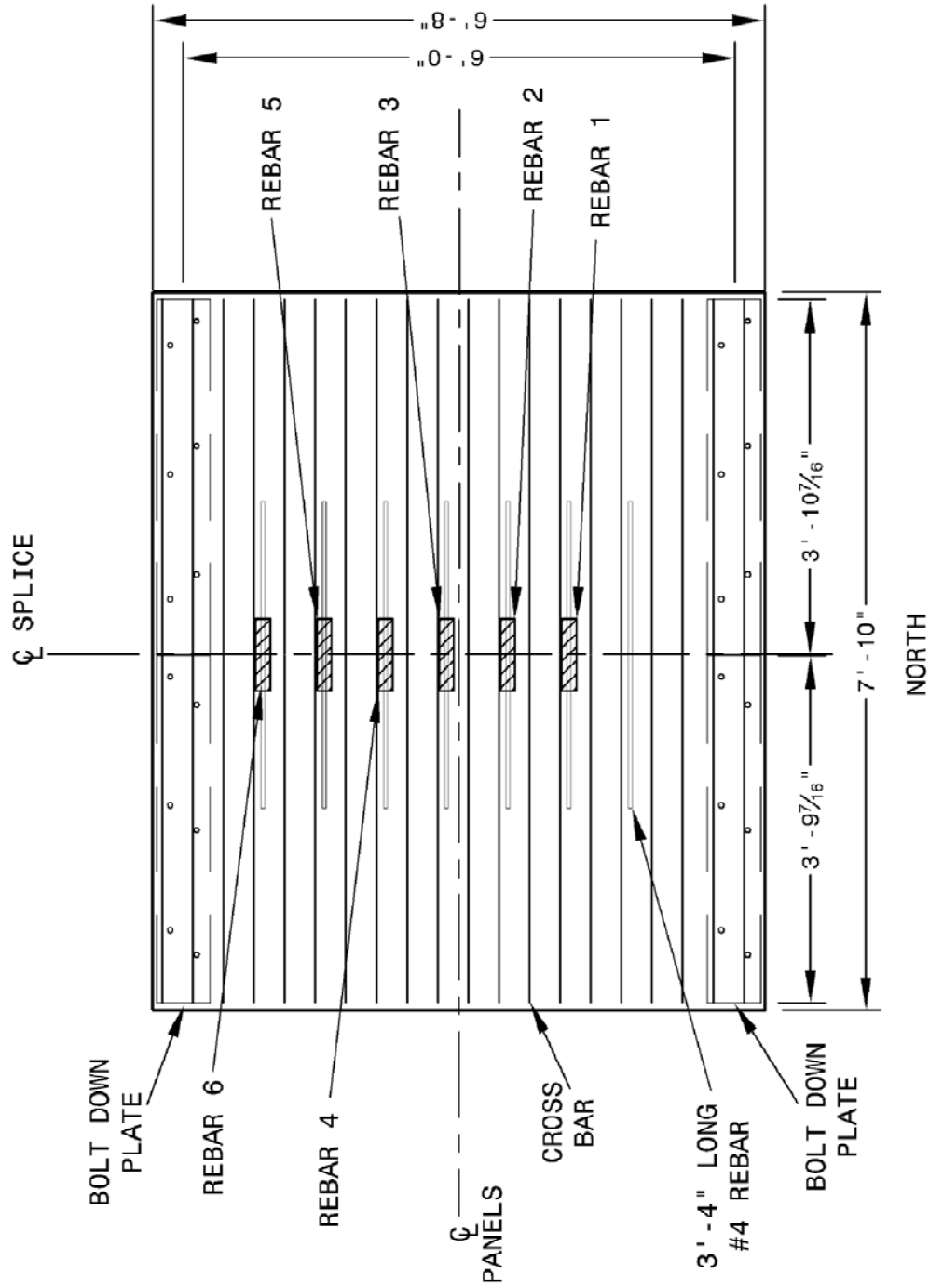
LVDT PLAN FOR SUBASSEMBLY TRANSVERSE SPLICE TEST

NOTE: CROSS BARS AND REBAR REMOVED FOR CLARITY



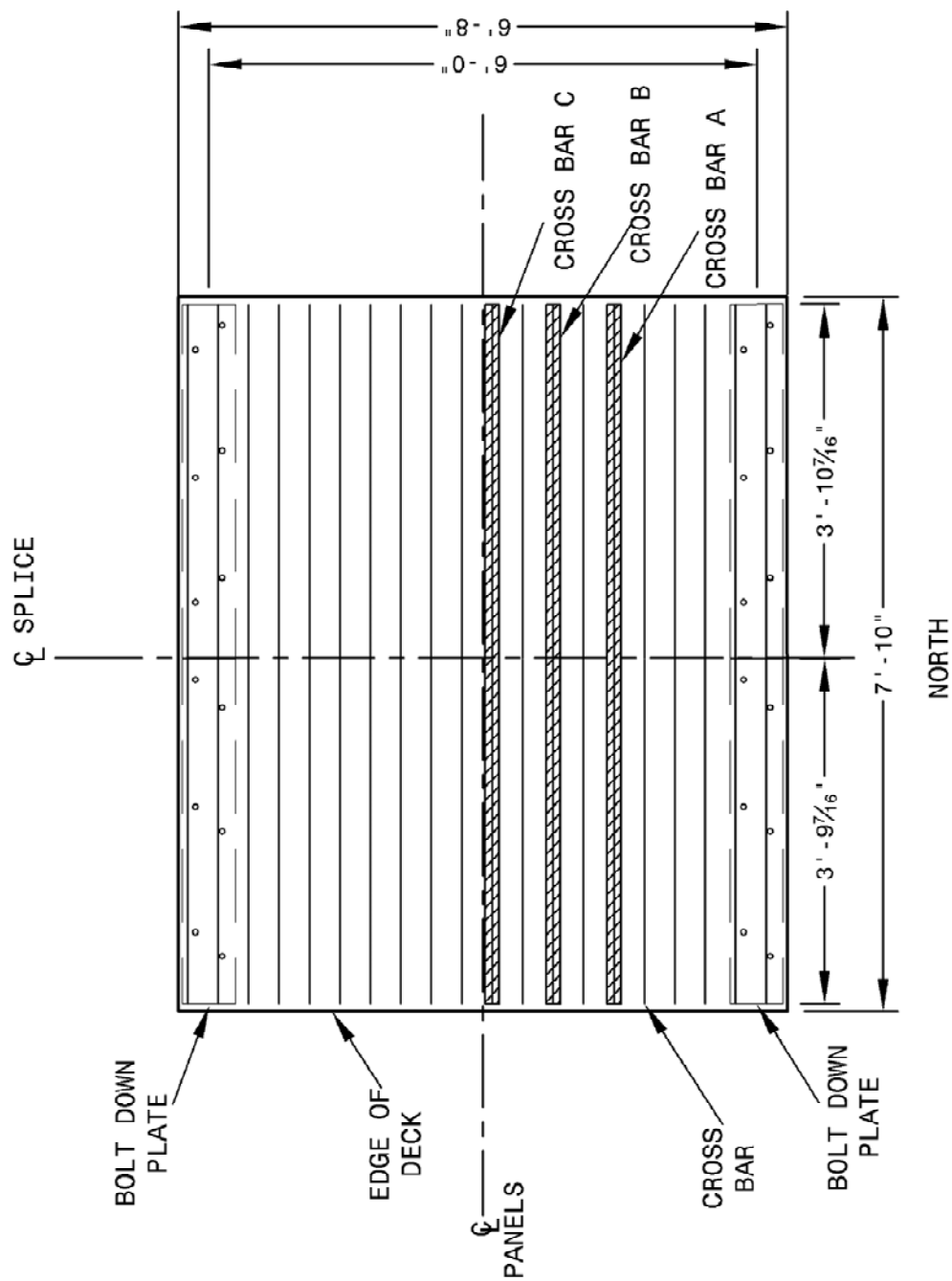
MAIN AND SUPPLEMENTAL BAR STRAIN GAGE PLAN FOR SUBASSEMBLY
TRANSVERSE SPLICE TEST

NOTE: CROSS BARS AND REBAR REMOVED FOR CLARITY



REBAR STRAIN GAGE PLAN FOR SUBASSEMBLY TRANSVERSE SPLICE
TEST

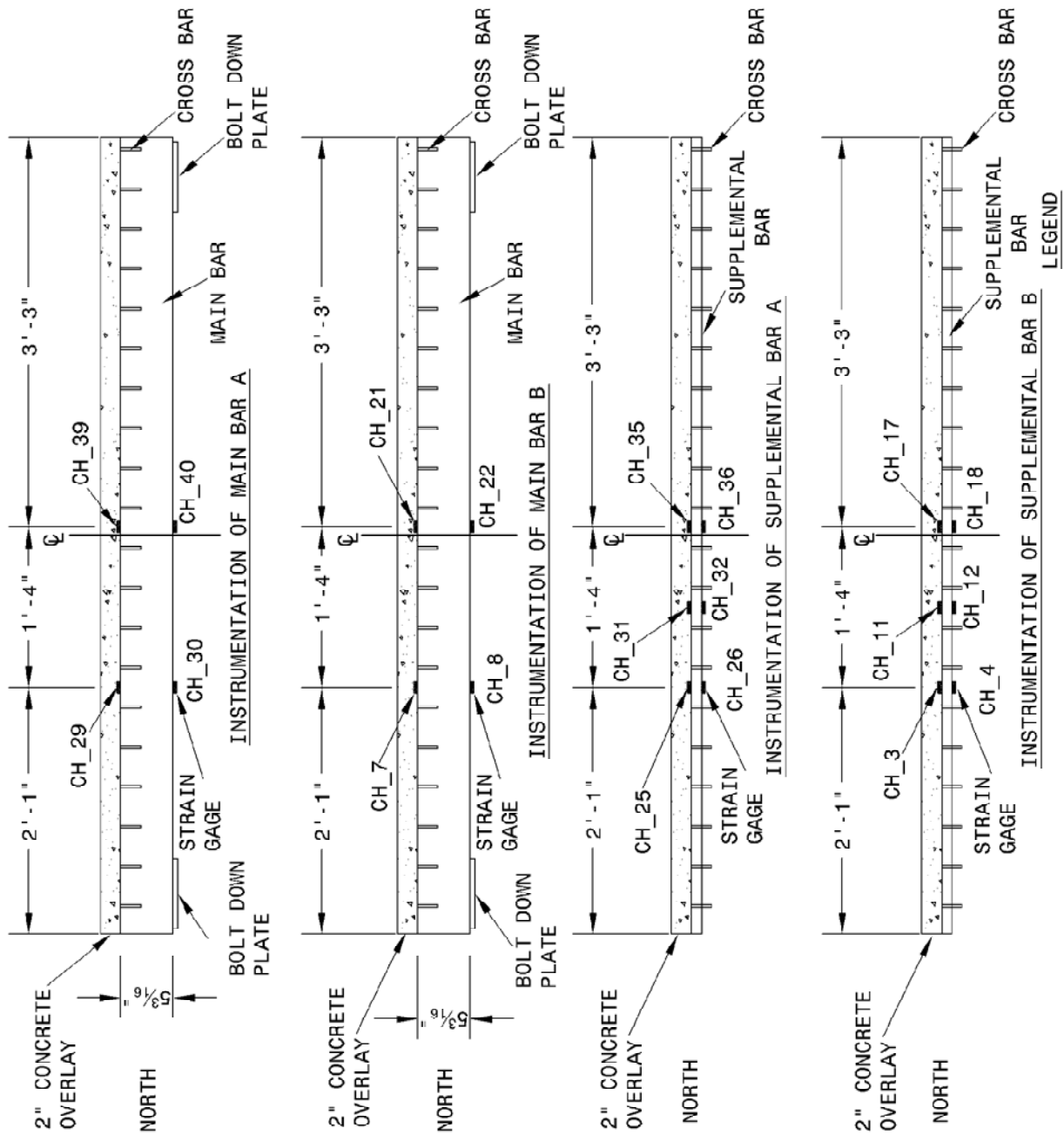
NOTE: MAIN BARS AND SUPPLEMENTAL BARS REMOVED FOR CLARITY



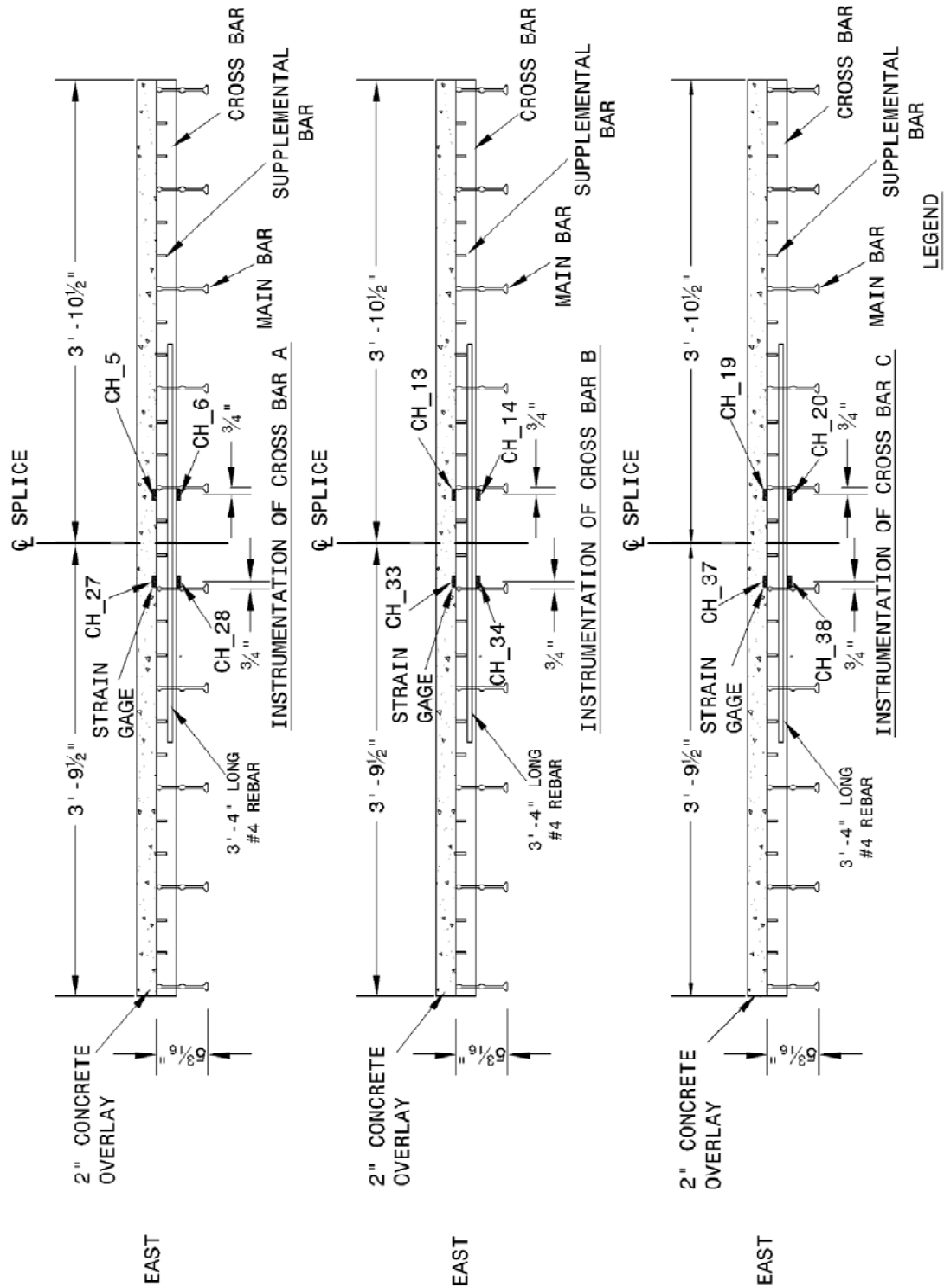
CROSS BAR STRAIN GAGE PLAN FOR SUBASSEMBLY TRANSVERSE
SPLICE TEST

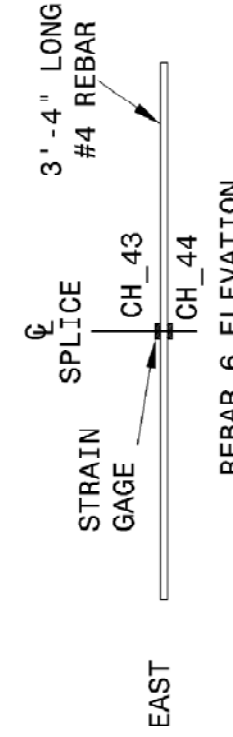
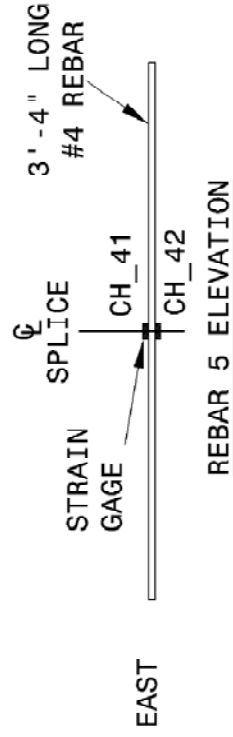
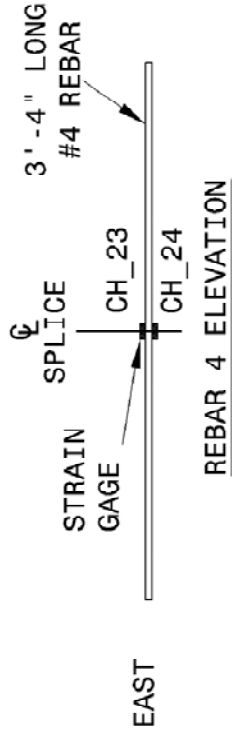
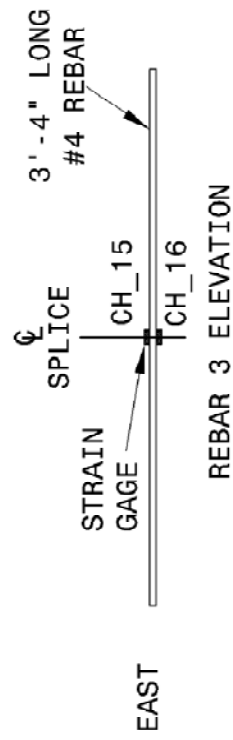
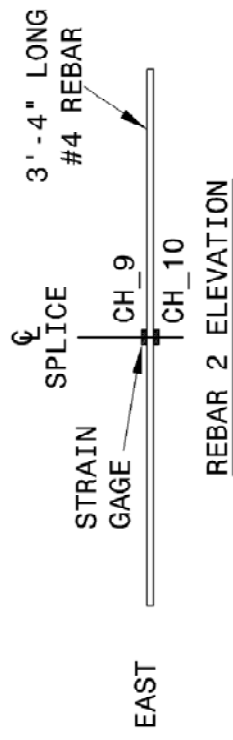
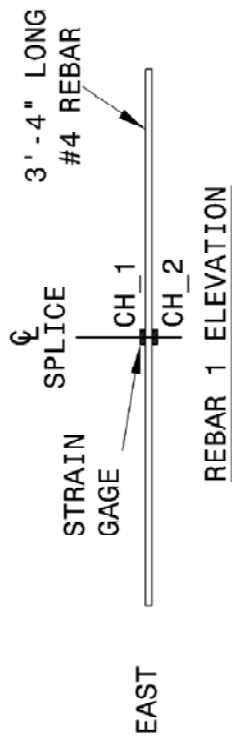
NOTE: MAIN BARS, SUPPLEMENTAL BARS AND REBAR REMOVED FOR CLARITY

A.7.1 Elevations of Steel Components with Strain Gages



GAGES HORIZONTALLY ALONG PAGE





LEGEND

GAGES HORIZONTALLY ALONG PAGE -

APPENDIX B Calculations and Data

TABLE OF CONTENTS

B.1	Large Scale Specimen.....	B-1
B.1.1	Midspan Girder Calculations.....	B-1
B.1.2	Maximum Stresses during Truck Roll Tests	B-8
B.1.3	Longitudinal Splice Test Static Load Stress Data	B-11
B.1.4	Transverse Splice Test #1 Static Load Stress Data	B-12
B.1.5	Transverse Splice Test #2 Static Load Stress Data	B-13
B.2	Subassembly Open Grid Deck Specimen #1 Experimentally Measured Stiffness.....	B-14
B.2.1	Strong Direction Stiffness (D_x) Test.....	B-14
B.2.2	Weak Direction Stiffness (D_y) Test.....	B-18
B.2.3	Torsional (D_{xy}) Stiffness Test.....	B-23
B.2.4	Measured Stiffness Properties of Subassembly Open Grid Deck Specimen #1.....	B-27
B.3	Subassembly Open Grid Deck Specimen #1 Theoretical Stiffness	B-29
B.3.1	Strong Direction Stiffness (D_x).....	B-29
B.3.2	Weak Direction Stiffness (D_y).....	B-31
B.4	Subassembly Open Grid Deck Specimen #2 Experimentally Measured Stiffness.....	B-33
B.4.1	Strong Direction Stiffness (D_x) Tests	B-33
B.4.2	Weak Direction Stiffness Tests (D_y)	B-37
B.4.3	Torsional Stiffness (D_{xy}) Test.....	B-43
B.4.4	Measured Stiffness Properties of Subassembly Open Grid Deck Specimen #2.....	B-46
B.5	Subassembly Open Grid Deck Specimen #2 Theoretical Stiffness	B-47
B.5.1	Strong Direction Stiffness (D_x).....	B-47
B.5.2	Weak Direction Stiffness (D_y).....	B-49
B.6	Subassembly Partially Filled Grid Deck Specimen Experimentally Measured Stiffness.....	B-50
B.6.1	Strong Direction Stiffness (D_x) Test.....	B-50
B.6.2	Weak Direction Stiffness (D_y) Test.....	B-54
B.6.3	Torsional Stiffness (D_{xy}) Test.....	B-60

B.6.4	Measured Stiffness Properties of Subassembly Partially Filled Grid Deck Specimen	B-63
B.7	Subassembly Partially Filled Grid Deck Specimen Theoretical Stiffness.....	B-65
B.7.1	Strong Direction Stiffness (D_x).....	B-65
B.7.2	Weak Direction Stiffness (D_y).....	B-70
B.8	Computing Loads to be Applied for Subassembly Strength Verification Tests.....	B-75
B.8.1	Subassembly Longitudinal Splice Strength Verification Test.....	B-75
B.8.2	Subassembly Transverse Splice Strength Verification Test.....	B-78
B.9	Stresses Measured During Strength Verification Tests	B-80
B.9.1	Subassembly Longitudinal Splice Strength Verification Test.....	B-80
B.9.2	Subassembly Deck-to-Superstructure Connection Strength Test.....	B-83
B.9.3	Subassembly Transverse Splice Strength Verification Test.....	B-83

B.1 Large Scale Specimen

B.1.1 Midspan Girder Calculations

Midspan Girder Composite Checks

$$\text{kip} := 1000\text{lb} \quad \text{Girder}_{\text{Spacing}} := 8\text{ft} \quad E := 29000 \frac{\text{kip}}{\text{in}^2} \quad f'_c := 6.9\text{ksi}$$

Composite Section Properties

Interior Girder

Effective width

$$b_e := 8\text{ft} \quad \text{Effective Width AASHTO 4.6.2.6}$$

$$E_c := 1820 \sqrt{f'_c} \cdot \text{ksi}^{0.5} \quad \text{AASHTO C5.4.2.4} \quad E_c = 4.781 \times 10^3 \cdot \text{ksi}$$

$$n := \frac{29000\text{ksi}}{E_c}$$

$$n = 6.066$$

W30x124 Girder

$$A_{\text{girder}} := 36.5n^2$$

$$d_{\text{girder}} := 30.2n$$

$$q_{\text{girder}} := \left[A_{\text{girder}} \cdot \left(\frac{d_{\text{girder}}}{2} \right) \right] \quad q_{\text{girder}} = 551.15 \text{in}^3$$

Longitudinal Steel in Deck

$$\text{No}_{\text{bars}} := 2 \cdot \left[\frac{\left(\frac{b_e}{2} - 2\text{in} \right)}{4\text{in}} + 1 \right]$$

$$\text{No}_{\text{bars}} = 25$$

$$\text{No}_{\text{bars}} := 24$$

Round down to nearest even integer

$$A_{\text{steel}} := \text{No}_{\text{bars}} \cdot 2.5\text{in} \cdot 2\text{in}$$

$$A_{\text{steel}} = 12 \text{in}^2$$

$$q_{\text{steel}} := A_{\text{steel}} \cdot (d_{\text{girder}} + 6.1875n)$$

$$q_{\text{steel}} = 436.65 \text{in}^3$$

Concrete Deck

$$\frac{b_e}{n} = 1.319\text{ft} \quad \text{Transformed Width Concrete Deck}$$

$$A_c := \left(\frac{b_e}{n} \right) \cdot 4.5\text{in} \quad \text{Transformed Area Concrete Deck}$$

$$A_c = 71.217 \text{in}^2$$

$$q_c := A_c \cdot (d_{\text{girder}} + 6.9375n)$$

$$q_c = 2.645 \times 10^3 \cdot \text{in}^3$$

Concrete Haunch

$$\frac{11.5n}{n} = 1.896 \text{ in}$$

Transformed Area Concrete Haunch

$$A_{\text{haunch}} := \left[\left(\frac{11.5n}{n} \right) \cdot \left[\left(4 + \frac{11}{16} \right) \text{in} \right] \right]$$

$$A_{\text{haunch}} = 8.887 \text{ in}^2$$

$$q_{\text{haunch}} := A_{\text{haunch}} \cdot \left[d_{\text{girder}} + \frac{\left[\left(4 + \frac{11}{16} \right) \text{in} \right]}{2} \right]$$

$$q_{\text{haunch}} = 289.204 \text{ in}^3$$

Centroid (from bottom of the girder)

$$y := \frac{q_{\text{girder}} + q_c + q_{\text{haunch}} + q_{\text{steel}}}{A_{\text{girder}} + A_c + A_{\text{haunch}} + A_{\text{steel}}}$$

$$y = 30.495 \text{ in}$$

Transformed Section Modulus

$$I_{\text{girder}} := 5360 \text{ in}^4 + A_{\text{girder}} \cdot \left(\frac{d_{\text{girder}}}{2} - y \right)^2$$

$$I_{\text{girder}} = 1.401 \times 10^4 \cdot \text{in}^4$$

$$I_{\text{conc}} := \left(\frac{1}{12} \right) \cdot \left(\frac{b_e}{n} \right) \cdot (4.5 \text{ in})^3 + A_c \cdot (d_{\text{girder}} + 6.9375n - y)^2$$

$$I_{\text{conc}} = 3.262 \times 10^3 \cdot \text{in}^4$$

$$I_{\text{haunch}} := \left(\frac{1}{12} \right) \cdot \left(\frac{11.5n}{n} \right) \cdot \left[\left(4 + \frac{11}{16} \right) \text{in} \right]^3 + A_{\text{haunch}} \cdot \left[d_{\text{girder}} + \frac{\left[\left(4 + \frac{11}{16} \right) \text{in} \right]}{2} - y \right]^2$$

$$I_{\text{haunch}} = 53.557 \text{ in}^4$$

$$I_{\text{steel}} := N_{\text{bars}} \cdot \left(\frac{1}{12} \right) \cdot (.25 \text{ in}) \cdot (2 \text{ in})^3 + A_{\text{steel}} \cdot (d_{\text{girder}} + 6.1875n - y)^2$$

$$I_{\text{steel}} = 420.597 \text{ in}^4$$

$$I_{\text{total}} := I_{\text{girder}} + I_{\text{conc}} + I_{\text{haunch}} + I_{\text{steel}}$$

$$I_{\text{total}} = 1.775 \times 10^4 \cdot \text{in}^4$$

$$S := \frac{I_{\text{total}}}{y}$$

$$S = 581.969 \text{ in}^3$$

Exterior Girder

Effective width

Effective Width AASHTO 4.6.2.6

$$b_{e2} := 6 \text{ ft}$$

AASHTO C5.4.2.4

$$E_{c2} := 1820 \sqrt{f'_c} \cdot \text{ksi}^{0.5}$$

$$E_{c2} = 4.781 \times 10^3 \cdot \text{ksi}$$

$$n_2 := \frac{29000 \text{ ksi}}{E_{c2}}$$

$$n_2 = 6.066$$

W30x124 Girder

$$A_{\text{girder2}} := 36.8 \text{ in}^2$$

$$d_{\text{girder2}} := 30.2 \text{ in}$$

$$q_{\text{girder2}} := \left[A_{\text{girder2}} \cdot \left(\frac{d_{\text{girder2}}}{2} \right) \right]$$

$$q_{\text{girder2}} = 555.68 \text{ in}^3$$

Longitudinal Steel in Deck

$$N_{\text{bars2}} := 2 \cdot \left[\frac{\left(\frac{b_{e2}}{2} - 2 \text{ in} \right)}{4 \text{ in}} + 1 \right]$$

$$N_{\text{bars2}} = 19$$

$$N_{\text{bars2}} := 18$$

Round down to nearest even integer

$$A_{\text{steel2}} := N_{\text{bars2}} \cdot .25 \text{ in} \cdot 2 \text{ in}$$

$$A_{\text{steel2}} = 9 \text{ in}^2$$

$$q_{\text{steel2}} := A_{\text{steel2}} \cdot (d_{\text{girder2}} + 6.1875 \text{ in})$$

$$q_{\text{steel2}} = 327.487 \text{ in}^3$$

Concrete Deck

$$\frac{b_{e2}}{n_2} = 0.989 \text{ ft}$$

Transformed Width Concrete Deck

$$A_{c2} := \left(\frac{b_{e2}}{n_2} \right) \cdot 4.5 \text{ in}$$

Transformed Area Concrete Deck

$$A_{c2} = 53.413 \text{ in}^2$$

$$q_{c2} := A_{c2} \cdot (d_{\text{girder2}} + 6.9375 \text{ in})$$

$$q_{c2} = 1.984 \times 10^3 \text{ in}^3$$

Concrete Haunch

$$\frac{11.5 \text{ in}}{n_2} = 1.896 \text{ in}$$

Transformed Area Concrete Haunch

$$A_{\text{haunch2}} := \left[\frac{11.5 \text{ in}}{n_2} \cdot \left[\left(4 + \frac{11}{16} \right) \text{ in} \right] \right]$$

$$A_{\text{haunch2}} = 8.887 \text{ in}^2$$

$$q_{\text{haunch2}} := A_{\text{haunch2}} \cdot \left[d_{\text{girder2}} + \frac{\left[\left(4 + \frac{11}{16} \right) \text{ in} \right]}{2} \right]$$

$$q_{\text{haunch2}} = 289.204 \text{ in}^3$$

Centroid (from bottom of the girder)

$$y_2 := \frac{q_{\text{girder2}} + q_{c2} + q_{\text{haunch2}} + q_{\text{steel2}}}{A_{\text{girder2}} + A_{c2} + A_{\text{haunch2}} + A_{\text{steel2}}}$$

$$y_2 = 29.195 \text{ in}$$

Transformed Moment of Inertia

$$I_{\text{girder2}} := 5360 \text{ in}^4 + A_{\text{girder2}} \cdot \left(\frac{d_{\text{girder2}}}{2} - y_2 \right)^2$$

$$I_{\text{girder2}} = 1.267 \times 10^4 \text{ in}^4$$

$$I_{\text{conc2}} := \left(\frac{1}{12} \right) \cdot \left(\frac{b_{e2}}{n_2} \right) \cdot (4.5 \text{ in})^3 + A_{c2} \cdot (d_{\text{girder2}} + 6.9375 \text{ in} - y_2)^2$$

$$I_{\text{conc2}} = 3.459 \times 10^3 \text{ in}^4$$

$$I_{\text{haunch2}} := \left(\frac{1}{12} \right) \cdot \left(\frac{11.5 \text{ in}}{n_2} \right) \cdot \left[\left(4 + \frac{11}{16} \right) \text{ in} \right]^3 + A_{\text{haunch2}} \cdot \left[d_{\text{girder2}} + \frac{\left[\left(4 + \frac{11}{16} \right) \text{ in} \right]}{2} - y_2 \right]^2$$

$$I_{\text{haunch2}} = 115.914 \text{ in}^4$$

$$I_{\text{steel2}} := N_{\text{bars2}} \cdot \left(\frac{1}{12} \right) \cdot (.25 \text{ in}) \cdot (2 \text{ in})^3 + A_{\text{steel2}} \cdot (d_{\text{girder2}} + 6.1875 \text{ in} - y_2)^2$$

$$I_{\text{steel2}} = 468.559 \text{ in}^4$$

$$I_{\text{total2}} := I_{\text{girder2}} + I_{\text{conc2}} + I_{\text{haunch2}} + I_{\text{steel2}}$$

$$I_{\text{total2}} = 1.672 \times 10^4 \text{ in}^4$$

$$S_2 := \frac{I_{\text{total2}}}{y_2}$$

$$S_2 = 572.529 \text{ in}^3$$

Experimental Longitudinal Splice Test Moments

30 Kip Static Load

West Girder

$$\sigma_{30\text{west}} := 0.88 \frac{\text{kip}}{\text{in}^2}$$

$$M_{30\text{west}} := \sigma_{30\text{west}} \cdot S_2$$

$$M_{30\text{west}} = 41.985 \text{ kip}\cdot\text{ft}$$

Middle Girder

$$\sigma_{30\text{mid}} := 1.77 \frac{\text{kip}}{\text{in}^2}$$

$$M_{30\text{mid}} := \sigma_{30\text{mid}} \cdot S$$

$$M_{30\text{mid}} = 85.84 \text{ kip}\cdot\text{ft}$$

East Girder

$$\sigma_{30\text{east}} := 0.88 \frac{\text{kip}}{\text{in}^2}$$

$$M_{30\text{east}} := \sigma_{30\text{east}} \cdot S_2$$

$$M_{30\text{east}} = 41.985 \text{ kip}\cdot\text{ft}$$

58 Kip Static Load

West Girder

$$\sigma_{58\text{west}} := 1.69 \frac{\text{kip}}{\text{in}^2}$$

$$M_{58\text{west}} := \sigma_{58\text{west}} \cdot S_2$$

$$M_{58\text{west}} = 80.631 \text{ kip}\cdot\text{ft}$$

Middle Girder

$$\sigma_{58\text{mid}} := 3.44 \frac{\text{kip}}{\text{in}^2}$$

$$M_{58\text{mid}} := \sigma_{58\text{mid}} \cdot S$$

$$M_{58\text{mid}} = 166.831 \text{ kip}\cdot\text{ft}$$

East Girder

$$\sigma_{58\text{east}} := 1.69 \frac{\text{kip}}{\text{in}^2}$$

$$M_{58\text{east}} := \sigma_{58\text{east}} \cdot S_2$$

$$M_{58\text{east}} = 80.631 \text{ kip}\cdot\text{ft}$$

Theoretical Longitudinal Splice Test Moments

30 Kip Static Load

Moment at midspan

$$R_{\text{north}} := \frac{30 \text{ kip} \cdot 28 \text{ ft}}{40 \text{ ft}}$$

$$R_{\text{north}} = 21 \cdot \text{kip}$$

$$R_{\text{south}} := \frac{30 \text{ kip} \cdot 12 \text{ ft}}{40 \text{ ft}}$$

$$R_{\text{south}} = 9 \cdot \text{kip}$$

$$M_{\text{midspan}} := R_{\text{north}} \cdot 20 \text{ ft} - 30 \text{ kip} \cdot 8 \text{ ft}$$

$$M_{\text{midspan}} = 180 \text{ kip}\cdot\text{ft}$$

Interior Girder

Lever Rule

$$LDF_{\text{Middle}} := \frac{0.5 \cdot (5 \text{ ft}) + 0.5 \cdot (5 \text{ ft})}{8 \text{ ft}}$$

$$LDF_{\text{Middle}} = 0.625$$

$$M_{\text{midgirder}} := LDF_{\text{Middle}} \cdot M_{\text{midspan}}$$

$$M_{\text{midgirder}} = 112.5 \text{ kip}\cdot\text{ft}$$

Exterior Girder

Lever Rule

$$LDF_{\text{Ext}} := \frac{0.5 \cdot (3 \text{ ft})}{8 \text{ ft}}$$

$$LDF_{\text{Ext}} = 0.188$$

$$M_{\text{extgirder}} := LDF_{\text{Ext}} \cdot M_{\text{midspan}}$$

$$M_{\text{extgirder}} = 33.75 \text{ kip}\cdot\text{ft}$$

$$LDF_{\text{Middle}} + 2 \cdot LDF_{\text{Ext}} = 1 \quad \text{check}$$

58 Kip Static Load

Moment at midspan

$$R_{\text{north2}} := \frac{58 \text{ kip} \cdot 28 \text{ ft}}{40 \text{ ft}}$$

$$R_{\text{north2}} = 40.6 \text{ kip}$$

$$R_{\text{south2}} := \frac{58 \text{ kip} \cdot 12 \text{ ft}}{40 \text{ ft}}$$

$$R_{\text{south2}} = 17.4 \text{ kip}$$

$$M_{\text{midspan2}} := R_{\text{north2}} \cdot 20 \text{ ft} - 58 \text{ kip} \cdot 8 \text{ ft}$$

$$M_{\text{midspan2}} = 348 \text{ kip}\cdot\text{ft}$$

Interior Girder

Lever Rule

$$LDF_{\text{Middle2}} := \frac{0.5 \cdot (5 \text{ ft}) + 0.5 \cdot (5 \text{ ft})}{8 \text{ ft}}$$

$$LDF_{\text{Middle2}} = 0.625$$

$$M_{\text{midgirder2}} := LDF_{\text{Middle2}} \cdot M_{\text{midspan2}}$$

$$M_{\text{midgirder2}} = 217.5 \text{ kip}\cdot\text{ft}$$

Exterior Girder

Lever Rule

$$LDF_{Ext2} := \frac{0.5(3ft)}{8ft}$$

$$LDF_{Ext2} = 0.188$$

$$M_{extgirder2} := LDF_{Ext2} M_{midspan2}$$

$$M_{extgirder2} = 65.25 \text{ kip}\cdot\text{ft}$$

$$LDF_{Middle2} + 2 \cdot LDF_{Ext2} = 1 \quad \text{check}$$

Experimental Transverse Splice Test Moments

Test 1

West Girder

$$\sigma_{t1west} := 0.15 \frac{\text{kip}}{\text{in}^2}$$

$$M_{t1west} := \sigma_{t1west} \cdot S_2$$

$$M_{t1west} = 7.157 \text{ kip}\cdot\text{ft}$$

Middle Girder

$$\sigma_{t1mid} := 1.06 \frac{\text{kip}}{\text{in}^2}$$

$$M_{t1mid} := \sigma_{t1mid} \cdot S$$

$$M_{t1mid} = 51.407 \text{ kip}\cdot\text{ft}$$

East Girder

$$\sigma_{t1east} := 1.217 \frac{\text{kip}}{\text{in}^2}$$

$$M_{t1east} := \sigma_{t1east} \cdot S_2$$

$$M_{t1east} = 58.064 \text{ kip}\cdot\text{ft}$$

Test 2

West Girder

$$\sigma_{t2west} := 1.24 \frac{\text{kip}}{\text{in}^2}$$

$$M_{t2west} := \sigma_{t2west} \cdot S_2$$

$$M_{t2west} = 59.161 \text{ kip}\cdot\text{ft}$$

Middle Girder

$$\sigma_{t2mid} := 1.05 \frac{\text{kip}}{\text{in}^2}$$

$$M_{t2mid} := \sigma_{t2mid} \cdot S$$

$$M_{t2mid} = 50.922 \text{ kip}\cdot\text{ft}$$

East Girder

$$\sigma_{t2east} := 0.14 \frac{\text{kip}}{\text{in}^2}$$

$$M_{t2east} := \sigma_{t2east} \cdot S_2$$

$$M_{t2east} = 6.68 \text{ kip}\cdot\text{ft}$$

Theoretical Transverse Splice Test Moments

Moment at midspan

$$R_{\text{north}3} := \frac{29.1\text{kip} \cdot [40\text{ft} - (8\text{ft} + 7\text{in})]}{40\text{ft}}$$

$$R_{\text{north}3} = 22.856\text{kip}$$

$$R_{\text{south}3} := \frac{29.1\text{kip} \cdot (8\text{ft} + 7\text{in})}{40\text{ft}}$$

$$R_{\text{south}3} = 6.244\text{kip}$$

$$M_{\text{midspan}3} := R_{\text{south}3} \cdot 20\text{ft}$$

$$M_{\text{midspan}3} = 124.888\text{kip} \cdot \text{ft}$$

Interior Girder

Lever Rule

$$LDF_{\text{Middle}3} := \frac{1 \cdot (4\text{ft})}{8\text{ft}}$$

$$LDF_{\text{Middle}3} = 0.5$$

$$M_{\text{midgirder}3} := LDF_{\text{Middle}3} \cdot M_{\text{midspan}3}$$

$$M_{\text{midgirder}3} = 62.444\text{kip} \cdot \text{ft}$$

Exterior Girder

Lever Rule

$$LDF_{\text{Ext}3} := \frac{1 \cdot (4\text{ft})}{8\text{ft}}$$

$$LDF_{\text{Ext}3} = 0.5$$

$$M_{\text{extgirder}3} := LDF_{\text{Ext}3} \cdot M_{\text{midspan}3}$$

$$M_{\text{extgirder}3} = 62.444\text{kip} \cdot \text{ft}$$

B.1.2 Maximum Stresses during Truck Roll Tests

The following tables include the maximum tensile and compression stresses found in strain gages located throughout the bridge deck during the truck roll tests. The maximum tensile and compression stresses are shown for each truck roll test position (i.e., transverse position). The longitudinal position of the truck when the maximum tensile and compression stresses were recorded is not shown. Stresses in the following tables are only shown for strain gages in critical locations and which were working properly during the truck roll tests.

Longitudinal Splice Rebar Stresses (ksi)												
Gage	Position 1		Position 2		Position 3		Position 4		Position 5		Position 6	
	T	C	T	C	T	C	T	C	T	C	T	C
94T	0.18	-0.20	0.51	-0.21	0.36	-0.20	0.24	-0.16	0.43	-0.18	NA	NA
95B	0.57	-0.22	1.75	-0.41	1.18	-0.36	0.72	-0.19	1.14	-0.03	NA	NA
107B	0.52	-0.21	1.11	-0.29	0.82	-0.28	0.62	-0.18	0.79	-0.11	0.60	-0.12
120T	0.66	-0.59	1.60	-0.54	1.36	-0.38	0.77	-0.26	1.37	-0.32	NA	NA
121B	0.87	-0.34	2.09	-0.51	1.63	-0.39	0.92	-0.18	1.45	-0.06	NA	NA

Longitudinal Splice Main Bar Gages (ksi)												
Gage	Position 1		Position 2		Position 3		Position 4		Position 5		Position 6	
	T	C	T	C	T	C	T	C	T	C	T	C
104	1.94	-0.01	1.62	-1.89	1.45	-0.02	0.61	-0.77	0.01	-2.18	NA	NA
105	0.08	-1.05	0.32	-0.49	0.03	-0.64	0.27	-0.27	0.52	-0.10	NA	NA
108	0.36	-0.21	0.92	-0.50	0.48	-0.38	0.11	-0.29	0.58	-0.26	NA	NA
109	0.59	-0.75	1.59	-2.39	1.34	-1.87	2.22	-0.01	0.44	-1.07	NA	NA

Continuous Main Bar Gages (ksi)												
Gage	Position 1		Position 2		Position 3		Position 4		Position 5		Position 6	
	T	C	T	C	T	C	T	C	T	C	T	C
3	0.45	-0.54	1.28	-0.54	0.71	-0.58	0.40	-0.48	0.63	-0.19	NA	NA
4	0.27	-0.39	0.43	-1.45	0.38	-0.69	0.27	-0.05	0.08	-0.65	NA	NA
13	0.02	-1.82	1.49	-1.11	0.03	-1.17	0.39	-0.53	1.07	-0.11	NA	NA
14	2.71	-0.05	1.67	-1.83	2.16	-0.03	0.75	-0.62	0.09	-1.99	NA	NA
15	0.50	-0.39	1.34	-0.61	1.02	-0.54	0.58	-0.52	0.75	-0.36	1.12	-0.16
16	0.42	-0.04	0.55	-0.88	0.55	-0.13	0.42	-0.19	0.31	-0.39	0.01	-0.86
17	0.63	-0.50	1.50	-1.08	1.22	-1.01	0.06	-1.27	0.22	-0.41	NA	NA
18	0.75	-0.89	1.92	-2.70	1.70	-1.92	2.25	-0.11	0.74	-1.27	NA	NA
29	0.40	-0.31	0.93	-0.42	0.62	-0.35	0.49	-0.27	0.63	-0.12	NA	NA
30	0.21	-0.23	0.43	-1.07	0.45	-0.47	0.25	-0.14	0.16	-0.50	NA	NA

Transverse Splice Rebar Stresses (ksi)												
Gage	Position 1		Position 2		Position 3		Position 4		Position 5		Position 6	
	T	C	T	C	T	C	T	C	T	C	T	C
39B	0.00	-1.14	0.54	-1.42	0.01	-0.75	0.01	-0.52	0.01	-0.42	0.01	-2.03
40T	0.00	-1.41	0.40	-1.60	0.00	-0.90	0.01	-0.65	0.01	-0.53	0.01	-2.25
E14T	0.03	-1.55	0.14	-1.43	0.07	-0.84	0.03	-0.62	0.07	-0.41	0.10	-2.13
51B	0.02	-0.60	0.58	-1.70	0.03	-1.36	0.02	-1.29	0.19	-1.85	0.04	-0.61
63B	0.04	-0.63	1.42	-1.18	0.26	-1.24	0.07	-1.20	0.15	-1.48	0.09	-0.51
64T	0.06	-0.42	0.77	-0.81	0.15	-0.91	0.15	-0.88	0.19	-1.02	0.12	-0.37
75B	0.04	-0.41	0.07	-0.80	0.26	-1.02	0.12	-0.89	0.13	-1.03	0.13	-0.35
76T	0.01	-0.48	0.06	-1.19	0.25	-1.58	0.01	-1.26	0.01	-1.47	0.02	-0.35
130T	0.01	-0.76	0.93	-0.96	0.01	-0.52	0.03	-0.33	0.05	-0.23	0.27	-0.87
131B	0.01	-0.78	1.05	-1.15	0.01	-0.60	0.03	-0.36	0.05	-0.25	0.38	-1.06
142T	0.13	-0.50	0.93	-1.36	0.05	-1.06	0.03	-1.04	0.71	-1.60	0.05	-0.36
143B	0.05	-0.44	1.08	-1.32	0.12	-0.99	0.03	-0.95	0.98	-1.53	0.05	-0.36
154T	0.04	-0.37	1.17	-1.06	0.45	-0.97	0.02	-0.89	0.34	-1.14	0.03	-0.29
155B	0.01	-0.34	0.79	-0.83	0.28	-0.80	0.02	-0.76	0.18	-0.93	0.03	-0.24
166T	0.01	-0.33	0.51	-1.00	1.22	-1.44	0.02	-1.09	0.01	-1.35	0.04	-0.22
167B	0.00	-0.31	0.34	-0.83	0.93	-1.16	0.03	-0.90	0.00	-1.06	0.03	-0.19

Transverse Splice Cross Bar Stresses (ksi)												
Gage	Position 1		Position 2		Position 3		Position 4		Position 5		Position 6	
	T	C	T	C	T	C	T	C	T	C	T	C
128	0.02	-0.97	2.56	-1.31	0.01	-0.59	0.04	-0.42	0.05	-0.33	0.73	-1.31
129	0.00	-0.73	0.00	-0.71	0.01	-0.49	0.01	-0.41	0.01	-0.31	0.03	-0.82
140	0.02	-0.39	4.83	-1.60	2.47	-1.02	0.52	-0.81	3.12	-1.57	0.07	-0.40
141	0.00	-1.03	0.04	-5.37	0.08	-4.30	0.08	-3.22	0.11	-4.80	0.03	-0.72
152	0.01	-0.45	4.57	-1.90	3.73	-1.50	0.64	-0.90	2.44	-1.67	0.07	-0.42
153	0.00	-1.11	0.02	-6.30	0.05	-6.42	0.08	-4.12	0.05	-5.92	0.01	-0.84
164	0.08	-0.37	3.69	-2.00	4.46	-2.14	0.65	-1.13	2.07	-1.77	0.08	-0.34
165	0.01	-0.94	0.07	-4.37	0.13	-5.48	0.12	-3.60	0.14	-4.56	0.02	-0.67

Transverse Splice Main Bar Stresses (ksi)												
Gage	Position 1		Position 2		Position 3		Position 4		Position 5		Position 6	
	T	C	T	C	T	C	T	C	T	C	T	C
132	2.15	-0.01	5.50	-0.01	1.12	-0.01	0.29	-0.37	0.14	-0.74	NA	NA
133	0.00	-0.30	0.06	-0.45	0.01	-0.17	0.03	-0.04	0.04	-0.01	NA	NA
144	0.35	-0.58	5.99	0.00	3.46	-0.06	2.38	-0.05	4.56	-0.08	NA	NA
145	0.31	-0.55	0.31	-4.51	0.15	-2.70	0.17	-1.68	0.06	-3.89	NA	NA
156	0.26	-0.45	4.53	0.00	4.78	-0.02	2.27	-0.08	2.55	-0.10	NA	NA
157	0.11	-0.05	0.01	-1.32	0.01	-1.69	0.01	-0.78	0.01	-1.12	NA	NA
168	0.20	-0.34	2.99	0.00	5.76	-0.01	2.16	-0.11	1.32	-0.11	NA	NA
169	0.11	-0.03	0.04	-0.57	0.05	-1.07	0.05	-0.44	0.11	-0.30	NA	NA

Girder Bottom Flange Stresses (ksi)												
Gage	Position 1		Position 2		Position 3		Position 4		Position 5		Position 6	
	T	C	T	C	T	C	T	C	T	C	T	C
85	4.78	0.00	2.23	0.00	1.27	0.00	0.55	0.00	0.10	0.00	5.99	0.00
88	3.99	0.00	4.80	0.00	4.60	0.00	4.07	0.00	3.39	0.00	3.34	0.00
91	0.43	0.00	2.14	0.00	3.31	0.00	4.63	0.00	6.04	0.00	0.01	0.00
176	3.07	0.00	1.17	0.00	0.60	0.00	0.26	0.00	0.07	0.00	4.04	0.00
179	2.44	0.00	3.19	0.00	3.02	0.00	2.58	0.00	1.97	0.00	1.84	0.00
182	0.22	0.00	1.12	0.00	1.92	0.00	2.89	0.00	3.88	0.00	0.02	0.00

B.1.3 Longitudinal Splice Test Static Load Stress Data

The following tables include the average stress in strain gages during the initial static tests during the longitudinal splice test. These stresses were collected when a total of 30 kips was applied by the actuator to the two load patches that were used during the longitudinal splice test. The locations of the strain gages and the load patches are shown in Appendix A. The strain gages shown in the following tables only include gages that were hooked up to the data logger and were working properly at the time of the static tests.

Longitudinal Splice Rebar	
Gage	Stress (ksi)
94T	0.37
95B	1.37
107B	1.10
120T	1.51
121B	1.68

Longitudinal Splice Main Bar	
Gage	Stress (ksi)
104	-1.31
105	-0.44
108	0.94
109	-1.40

Transverse Splice Rebar	
Gage	Stress (ksi)
130T	-0.56
131B	-0.60
142T	-0.83
143B	-0.85
154T	-0.65
155B	-0.52
166T	-0.60
167B	-0.57

Transverse Splice Cross Bar	
Gage	Stress (ksi)
128	-0.74
129	-0.41
140	-1.07
141	-0.74
152	-1.15
153	-0.80
164	-1.24
165	-0.59

Transverse Splice Main Bar	
Gage	Stress (ksi)
132	0.84
133	-0.14
156	0.95

Girder Bottom Flange	
Gage	Stress (ksi)
85	0.88
88	1.77
91	0.88
176	0.61
179	1.91
182	0.64

B.1.4 Transverse Splice Test #1 Static Load Stress Data

The following tables include the average stress in strain gages during the initial static tests during the transverse splice test #1. These stresses were collected when 29.1 kips was applied by the actuator to the load patch that was used during the transverse splice test #1. The locations of the strain gages and the load patches are shown in Appendix A. The strain gages shown in the following tables only include gages that were hooked up to the data logger and were working properly at the time of the static tests.

Longitudinal Splice Rebar	
Gage	Stress (ksi)
95B	0.04
120T	-0.25
121B	0.46

Longitudinal Splice Main Bar	
Gage	Stress (ksi)
109	0.96

Transverse Splice Rebar	
Gage	Stress (ksi)
142T	3.62
143B	3.54
154T	3.04
155B	2.08
166T	2.67
167B	2.68

Transverse Splice Cross Bar	
Gage	Stress (ksi)
140	7.07
141	-1.67
152	6.86
153	-3.02
164	6.53
165	-2.83

Transverse Splice Main Bar	
Gage	Stress (ksi)
144	9.94
145	-6.43
156	9.23
168	8.76
169	-1.17

Girder Bottom Flange	
Gage	Stress (ksi)
85	0.15
88	1.06
91	1.22
176	-0.09
179	1.78
182	1.79

B.1.5 Transverse Splice Test #2 Static Load Stress Data

The following tables include the average stress in strain gages during the initial static tests during the transverse splice test #2. These stresses were collected when 29.1 kips was applied by the actuator to the load patch that was used during the transverse splice test #2. The locations of the strain gages and the load patches are shown in Appendix A. The strain gages shown in the following tables only include gages that were hooked up to the data logger and were working properly at the time of the static tests.

Longitudinal Splice Rebar	
Gage	Stress (ksi)
95B	0.10
120T	0.96
121B	0.66

Longitudinal Splice Main Bar	
Gage	Stress (ksi)
104	1.07
105	-0.29

Transverse Splice Rebar	
Gage	Stress (ksi)
130T	3.42
131B	2.41
142T	-0.61
143B	-0.69
154T	-0.48
155B	-0.36

Transverse Splice Cross Bar	
Gage	Stress (ksi)
128	4.15
129	0.29
140	-0.55
141	-0.36
152	-0.58
153	-0.32

Transverse Splice Main Bar	
Gage	Stress (ksi)
132	9.65
133	-1.92
144	-1.46
145	1.19
156	-1.09

Girder Bottom Flange	
Gage	Stress (ksi)
85	1.25
88	1.05
91	0.14
176	1.80
179	1.76
182	-0.07

B.2 Subassembly Open Grid Deck Specimen #1 Experimentally Measured Stiffness

The stiffness of open grid deck specimen #1 was determined for the strong (D_x) and weak (D_y) axes, as well as in torsion (D_{xy}). Multiple runs of each test were done to ensure repeatability of the results as well as to determine averages.

B.2.1 Strong Direction Stiffness (D_x) Test

For the strong direction stiffness (D_x) tests, the load applied and corresponding displacement measurements were recorded at the locations shown in Appendix A. A line of these displacement measurements across the center of the deck (CH_36, CH_41 and CH_34) were used to determine the stiffness of the deck. CH_36 and CH_41 were displacements measured at the center of the support on each side of the deck and were used to account for any rigid body movement of the specimen. CH_34 was the displacement measured at the center of the deck under the location of the applied load. Although other measurements of displacement were recorded (e.g., at the edges of the supports and deck), these measurements confirmed the small rigid body movement across the width of the specimen.

The following plot shows the linear behavior of the specimen underneath the load (CH_34). However, the displacements measured at the supports (CH_34 and CH_41) are not linear and are much smaller as expected. It is noted that this plot is for test run #1 only. Since the other test runs provided very similar results, plots for the repeated test runs are not shown.

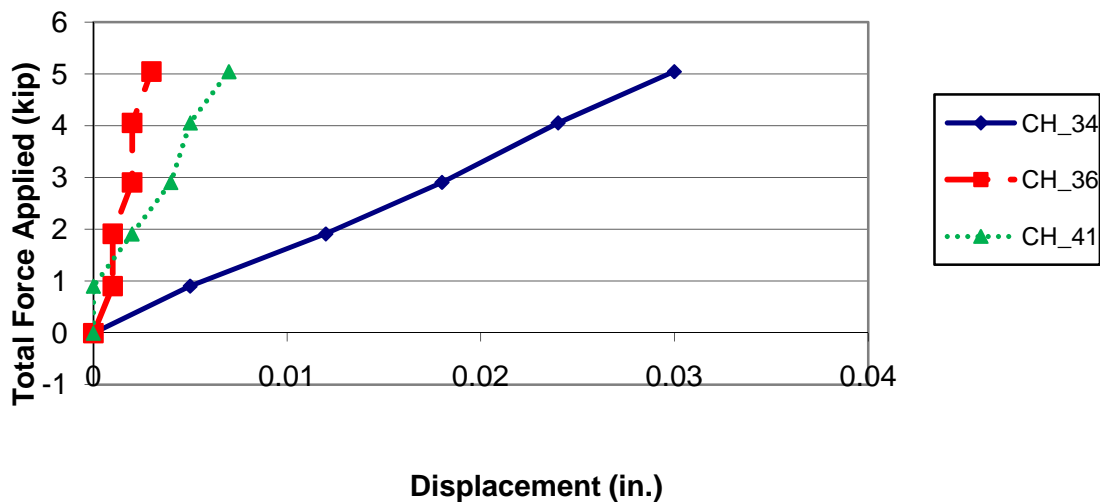


Figure B-1: Measured displacements in test run #1

Test Run #1. The span of the deck specimen tested was:

$$L = \left(6 \text{ ft.} * 12 \frac{\text{in.}}{\text{ft.}}\right) + 3 \text{ in.} = 75 \text{ in.}$$

The width of the deck, w, was also 75 in.

The maximum point load applied to the spreader beam was:

$$P = 5045.75 \text{ lbs.}$$

This load was spread over the width of the deck at midspan as a line load:

$$P' = \frac{P}{w}$$

$$P' = \frac{5045.75 \text{ lbs.}}{(75 \text{ in.} * 1000 \frac{\text{lbs.}}{\text{kip}})} = 0.0673 \frac{\text{kip}}{\text{in.}}$$

The displacements measured at the middle of each support for this load are shown in Table B-1.

Table B-1: Measured support displacements

Channel	Displacement (in.)
CH_36	0.003
CH_41	0.007
Average (Δ_s)	0.005

The displacement measured at the center of the deck underneath the load was:

$$\Delta_m = \text{CH}_{34} = 0.030 \text{ in.}$$

Therefore, the net vertical deflection at the centerline of the deck, Δ_{CL} , was computed as:

$$\Delta_{CL} = \Delta_m - \Delta_s$$

$$\Delta_{CL} = 0.03 \text{ in.} - 0.005 \text{ in.}$$

$$\Delta_{CL} = 0.025 \text{ in.}$$

Therefore, the stiffness of the deck in the strong direction (D_x) for this test run was computed as:

$$D_{x-open1-1} = \frac{P'L^3}{48 \Delta_{CL}} = \frac{\left(0.0673 \frac{\text{kip}}{\text{in.}}\right) (75 \text{ in.})^3}{(48)(0.025 \text{ in.})}$$

$$D_{x-open1-1} = 23,652 \frac{\text{kips-in.}^2}{\text{in.}}$$

Test Run #2. For the second run of this test, the span and width of the deck remain the same:

$$L = 75 \text{ in.}$$

$$w = 75 \text{ in.}$$

The maximum point load applied to the spreader beam was:

$$P = 5164.82 \text{ lbs.}$$

Therefore, this load spread over the width of the deck at midspan as a line load was computed as:

$$P' = \frac{P}{w}$$

$$P' = \frac{5164.82 \text{ lbs.}}{(75 \text{ in.} * 1000 \frac{\text{lbs.}}{\text{kip}})} = 0.0689 \frac{\text{kip}}{\text{in.}}$$

The displacements measured at the middle of each support for this load are shown in Table B-2.

Table B-2: Measured support displacements

Channel	Displacement (in.)
CH_36	0.003
CH_41	0.006
Average (Δ_s)	0.0045

The displacement measured at the center of the deck underneath the load was:

$$\Delta_m = CH_{34} = 0.031 \text{ in.}$$

Therefore, the net vertical deflection at the centerline of the deck, Δ_{CL} , was computed as:

$$\Delta_{CL} = \Delta_m - \Delta_s$$

$$\Delta_{CL} = 0.031 \text{ in.} - 0.0045 \text{ in.}$$

$$\Delta_{CL} = 0.0265 \text{ in.}$$

Therefore, the stiffness of the deck in the strong direction (D_x) for this test run was computed as:

$$D_{x-\text{open1-2}} = \frac{P'L^3}{48 \Delta_{CL}} = \frac{\left(0.0689 \frac{\text{kip}}{\text{in.}}\right) (75 \text{ in.})^3}{(48)(0.0265 \text{ in.})}$$

$$D_{x-\text{open1-2}} = 22,840 \frac{\text{kip} - \text{in.}^2}{\text{in.}}$$

Test Run #3. For the third run of this test, the span and width of the deck remain the same:

$$L = 75 \text{ in.}$$

$$w = 75 \text{ in.}$$

The maximum point load applied to the spreader beam was

$$P = 5067.53 \text{ lbs.}$$

Therefore, this load spread over the width of the deck at midspan as a line load was computed as:

$$P' = \frac{P}{w}$$

$$P' = \frac{5067.53 \text{ lbs.}}{(75 \text{ in.} * 1000 \frac{\text{lbs.}}{\text{kip}})} = 0.0676 \frac{\text{kip}}{\text{in.}}$$

The displacements measured at the middle of each support for this load are shown in Table B-3.

Table B-3: Measured support displacements

Channel	Displacement (in.)
CH_36	0.003
CH_41	0.006
Average (Δ_s)	0.0045

The displacement measured at the center of the deck underneath the load was:

$$\Delta m = CH_{34} = 0.030 \text{ in.}$$

Therefore, the net vertical deflection at the centerline of the deck, Δ_{CL} , was computed as:

$$\Delta_{CL} = \Delta m - \Delta s$$

$$\Delta_{CL} = 0.03 \text{ in.} - 0.0045 \text{ in.}$$

$$\Delta_{CL} = 0.0255 \text{ in.}$$

Therefore, the stiffness of the deck in the strong direction (D_x) for this test run was computed as:

$$D_{x-open1-3} = \frac{P'L^3}{48 \Delta_{CL}} = \frac{\left(0.0676 \frac{\text{kip}}{\text{in.}}\right) (75 \text{ in.})^3}{(48)(0.0255 \text{ in.})}$$

$$D_{x-open1-3} = 23,288 \frac{\text{kip} - \text{in.}^2}{\text{in.}}$$

Average Strong Direction Stiffness (D_x). The average measured strong direction stiffness (D_x) of subassembly open grid deck specimen #1 was:

$$\begin{aligned} D_{x-open1} &= \frac{D_{x-open1-1} + D_{x-open1-2} + D_{x-open1-3}}{3} = \frac{23,652 + 22,840 + 23,288}{3} \\ &= 23,260 \frac{\text{kip} - \text{in.}^2}{\text{in.}} \end{aligned}$$

B.2.2 Weak Direction Stiffness (D_y) Test

For the weak direction stiffness (D_y) tests, the load applied and corresponding displacement measurements were recorded at the locations shown in Appendix A. A line of these displacement measurements across the center of the deck (CH_35, CH_38 and CH_43) were used to determine the stiffness of the deck. CH_38 and CH_43 were displacements measured at the center of the support on each side of the deck and were used to account for any rigid body movement of the specimen. CH_35 was the displacement measured at the center of the deck under the location of the applied load. Although other measurements of displacement

were recorded (e.g., at the edges of the supports and deck), these measurements confirmed the small rigid body movement across the width of the specimen.

The following plot shows the linear behavior of the specimen underneath the load (CH_35). However, no displacement was measured at the supports (CH_38 and CH_43). It is noted that this plot is for test run #1 only. Since the other test runs provided very similar results, plots for the repeated test runs are not shown.

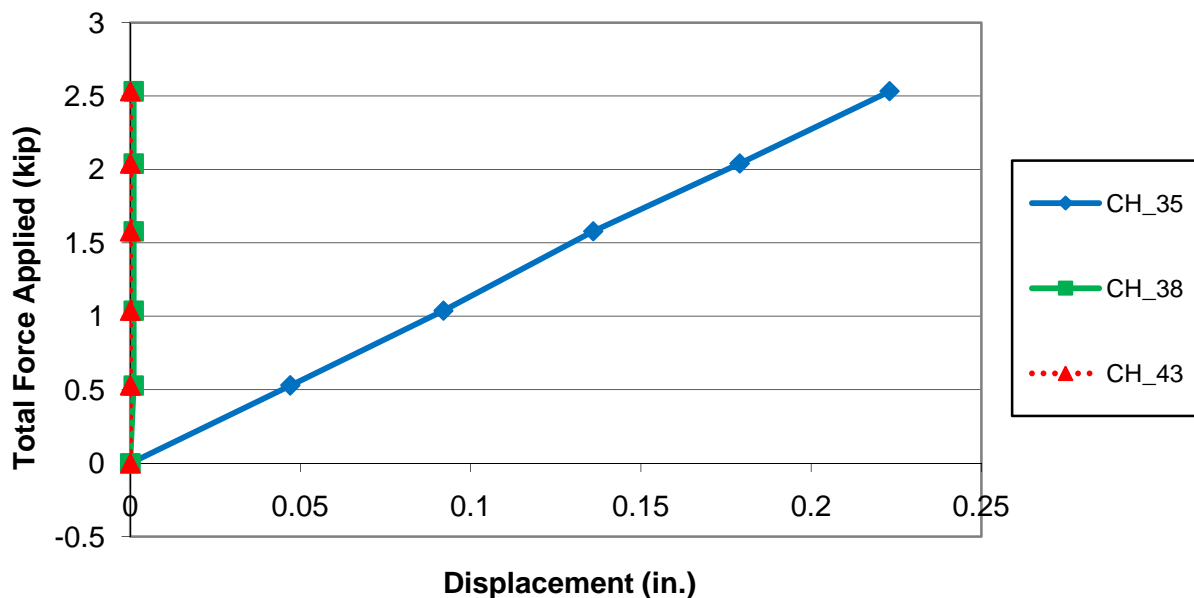


Figure B-2: Measured displacements in test run #1

Test Run #1. The span of the deck specimen tested was:

$$L = \left(6 \text{ ft.} * 12 \frac{\text{in.}}{\text{ft.}} \right) + 3 \text{ in.} = 75 \text{ in.}$$

The width of the deck, w , was also 75 in.

The maximum point load applied to the spreader beam was

$$P = 2503.33 \text{ lbs.}$$

This load was spread over the width of the deck at midspan as a line load:

$$P' = \frac{P}{w}$$

$$P' = \frac{2503.33 \text{ lbs.}}{(75 \text{ in.} * 1000 \frac{\text{lbs.}}{\text{in.}})} = 0.0334 \frac{\text{kip}}{\text{in.}}$$

The displacements measured at the middle of each support for this load are shown in Table B-4.

Table B-4: Measured support displacements

Channel	Displacement (in.)
CH_38	0
CH_43	0
Average (Δ_s)	0

The displacement measured at the center of the deck underneath the load was:

$$\Delta_m = CH_{35} = 0.218 \text{ in.}$$

Therefore, the net vertical deflection at the centerline of the deck, Δ_{CL} , was computed as:

$$\Delta_{CL} = \Delta_m - \Delta_s$$

$$\Delta_{CL} = 0.218 \text{ in.} - 0 \text{ in.}$$

$$\Delta_{CL} = 0.218 \text{ in.}$$

Therefore, the stiffness of the deck in the weak direction (D_y) for this test run was computed as:

$$D_{y-open1-1} = \frac{P' L^3}{48 \Delta_{CL}} = \frac{\left(0.0334 \frac{\text{kip}}{\text{in.}}\right) (75 \text{ in.})^3}{(48)(0.218 \text{ in.})}$$

$$D_{y-open1-1} = 1346 \frac{\text{kip} - \text{in.}^2}{\text{in.}}$$

Test Run #2. For the second run of this test, the span and width of the deck remain the same:

$$L = 75 \text{ in.}$$

$$w = 75 \text{ in.}$$

The maximum point load applied to the spreader beam was:

$$P = 2547.99 \text{ lbs.}$$

This load was spread over the width of the deck at midspan as a line load:

$$P' = \frac{P}{w}$$

$$P' = \frac{2547.99 \text{ lbs.}}{(75 \text{ in.} * 1000 \frac{\text{lbs.}}{\text{kip}})} = 0.0340 \frac{\text{kip}}{\text{in.}}$$

The displacements measured at the middle of each support for this load are shown in Table B-5.

Table B-5: Measured support displacements

Channel	Displacement (in.)
CH_38	0
CH_43	0
Average (Δ_s)	0

The displacement measured at the center of the deck underneath the load was:

$$\Delta_m = CH_{35} = 0.222 \text{ in.}$$

Therefore, the net vertical deflection at the centerline of the deck, Δ_{CL} , was computed as:

$$\Delta_{CL} = \Delta_m - \Delta_s$$

$$\Delta_{CL} = 0.222 \text{ in.} - 0 \text{ in.}$$

$$\Delta_{CL} = 0.222 \text{ in.}$$

Therefore, the stiffness of the deck in the weak direction (D_y) for this test run was computed as:

$$D_{y-open1-2} = \frac{P'L^3}{48 \Delta_{CL}} = \frac{\left(0.0340 \frac{\text{kip}}{\text{in.}}\right) (75 \text{ in.})^3}{(48)(0.222 \text{ in.})}$$

$$D_{y-open1-2} = 1345 \frac{\text{kip} - \text{in.}^2}{\text{in.}}$$

Test Run #3. For the third run of this test, the span and width of the deck remain the same:

$$L = 75 \text{ in.}$$

$$w = 75 \text{ in.}$$

The maximum point load applied to the spreader beam was:

$$P = 2534.12 \text{ lbs.}$$

This load was spread over the width of the deck at midspan as a line load:

$$P' = \frac{P}{w}$$

$$P' = \frac{2534.12 \text{ lbs.}}{(75 \text{ in.} * 1000 \frac{\text{lbs.}}{\text{kip}})} = 0.0338 \frac{\text{kip}}{\text{in.}}$$

The displacements measured at the middle of each support for this load are shown in Table B-6.

Table B-6: Measured support displacements

Channel	Displacement (in.)
CH_38	0.001
CH_43	0
Average (Δs)	0.0005

The displacement measured at the center of the deck underneath the load was:

$$\Delta_m = CH_{35} = 0.222 \text{ in.}$$

Therefore, the net vertical deflection at the centerline of the deck, Δ_{CL} , was computed as:

$$\Delta_{CL} = \Delta_m - \Delta_s$$

$$\Delta_{CL} = 0.222 \text{ in.} - 0.0005 \text{ in.}$$

$$\Delta_{CL} = 0.2215 \text{ in.}$$

Therefore, the stiffness of the deck in the weak direction (D_y) for this test run was computed as:

$$D_{y\text{-open1-3}} = \frac{P'L^3}{48 \Delta_{CL}} = \frac{\left(0.0338 \frac{\text{kip}}{\text{in.}}\right) (75 \text{ in.})^3}{(48)(0.2215 \text{ in.})}$$

$$D_{y\text{-open1-3}} = 1341 \frac{\text{kip} - \text{in.}^2}{\text{in.}}$$

Average Weak Direction Stiffness (D_y). The average measured weak direction stiffness (D_y) of subassembly open grid deck specimen #1 was:

$$D_{y\text{-open1}} = \frac{D_{y\text{-open1-1}} + D_{y\text{-open1-2}} + D_{y\text{-open1-3}}}{3} = \frac{1346 + 1345 + 1341}{3} = 1,344 \frac{\text{kip-in.}^2}{\text{in.}}$$

B.2.3 Torsional (D_{xy}) Stiffness Test

For the torsional stiffness (D_{xy}) tests, the load applied and corresponding displacement measurements were recorded at the locations shown in Appendix A. The displacement measured the free corner of the deck under the applied load (CH_38) was used to determine the torsion stiffness of the deck. Although other measurements of displacement were recorded, these measurements confirmed the no rigid body movement occurred at the supports.

The following plot shows the linear behavior of the specimen at the loaded free corner (CH_38). However, no displacement was measured at the supports. Therefore, they are not displayed in this plot. It is noted that this plot is for test run #1 of test rotation #1 only. Since the other test runs and rotations provided very similar results, plots for the repeated test runs and rotations are not shown.

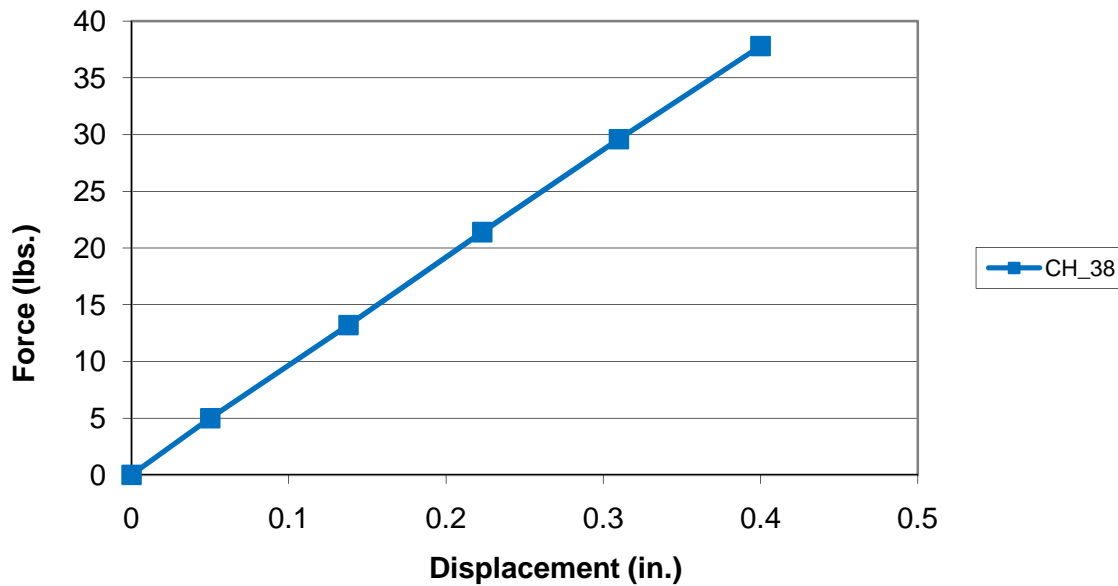


Figure B-3: Measured displacement at loaded free corner for test run #1 of test rotation #1

Test Rotation #1. The span of the deck specimen tested was:

$$L = \left(6 \text{ ft.} * 12 \frac{\text{in.}}{\text{ft.}} \right) + 3 \text{ in.} = 75 \text{ in.}$$

The maximum point load applied to the free corner of the deck was:

$$P = 37.8 \text{ lbs.} = 0.0378 \text{ kip}$$

For each test rotation, six test runs were completed to ensure repeatability of the data and to determine averages. The individual test run and average displacement measurements at the loaded free corner are shown in Table B-7.

Table B-7: Measured displacements at loaded free corner

Test Run #	CH_38 Displacement (in.)
1	0.400
2	0.392
3	0.392
4	0.397
5	0.391
6	0.391
Average (Δ_L)	0.3938

Therefore, the stiffness of the deck in torsion (D_{xy}) for this test rotation was computed as:

$$D_{xy-open1-1} = \frac{PL^2}{4 \Delta_L} = \frac{(0.0378 \text{ kip})(75 \text{ in.})^2}{(4)(0.3938 \text{ in.})}$$

$$D_{xy-open1-1} = 135 \frac{\text{kip} - \text{in.}^2}{\text{in.}}$$

Test Rotation #2. For the second test rotation, the deck was rotated 90° from rotation #1 and the procedure was repeated.

The span of the deck specimen and applied load remained the same.

$$L = 75 \text{ in.}$$

$$P = 37.8 \text{ lbs.} = 0.0378 \text{ kip}$$

For this test rotation, six test runs were completed to ensure repeatability of the data and to determine averages. The individual test run and average displacement measurements at the loaded free corner are shown in Table B-8.

Table B-8: Measured displacements at loaded free corner

Test Run #	CH_38 Displacement (in.)
1	0.429
2	0.425
3	0.425
4	0.425
5	0.422
6	0.423
Average (Δ_L)	0.4248

Therefore, the stiffness of the deck in torsion (D_{xy}) for this test rotation was computed as:

$$D_{xy-open1-2} = \frac{PL^2}{4 \Delta_L} = \frac{(0.0378 \text{ kip})(75 \text{ in.})^2}{(4)(0.4248 \text{ in.})}$$

$$D_{xy-open1-2} = 125 \frac{\text{kip} - \text{in.}^2}{\text{in.}}$$

Test Rotation #3. For the third test rotation, the deck was rotated 90° from rotation #2 and the procedure was repeated.

The span of the deck specimen and applied load remained the same.

$$L = 75 \text{ in.}$$

$$P = 37.8 \text{ lbs.} = 0.0378 \text{ kip}$$

For this test rotation, six test runs were completed to ensure repeatability of the data and to determine averages. The individual test run and average displacement measurements at the loaded free corner are shown in Table B-9.

Table B-9: Measured displacements at loaded free corner

Test Run #	CH_38 Displacement (in.)
1	0.387
2	0.384
3	0.385
4	0.386
5	0.385
6	0.385
Average (Δ_L)	0.3853

Therefore, the stiffness of the deck in torsion (D_{xy}) for this test rotation was computed as:

$$D_{xy-open1-3} = \frac{PL^2}{4 \Delta_L} = \frac{(0.0387 \text{ kip})(75 \text{ in.})^3}{(4)(0.3853 \text{ in.})}$$

$$D_{xy-open1-3} = 141 \frac{\text{kip} - \text{in.}^2}{\text{in.}}$$

Average Torsional Stiffness (D_{xy}). The average measured torsional stiffness (D_{xy}) of subassembly open grid deck specimen #1 was:

$$D_{xy-open1} = \frac{D_{xy-open1-1} + D_{xy-open1-2} + D_{xy-open1-3}}{3} = \frac{135 + 125 + 141}{3} = 134 \frac{\text{kip-in.}^2}{\text{in.}}$$

B.2.4 Measured Stiffness Properties of Subassembly Open Grid Deck Specimen #1

As previously computed, the average measured stiffness of the deck in the strong (D_x) and weak (D_y) directions as well as the torsion stiffness were:

$$D_{x-open1} = 23,260 \frac{\text{kip} - \text{in.}^2}{\text{in.}}$$

$$D_{y-open1} = 1,344 \frac{\text{kip} - \text{in.}^2}{\text{in.}}$$

$$D_{xy-open1} = 134 \frac{\text{kip} - \text{in.}^2}{\text{in.}}$$

Therefore, the orthotropic ratio of subassembly open grid deck specimen #1 was computed as:

$$D_{\text{open1}} = \frac{D_{x\text{-open1}}}{D_{y\text{-open1}}} = \frac{23,260}{1,344} = 17.3$$

Moreover, the torsion stiffness parameter for this specimen was computed as:

$$\alpha_{\text{open1}} = \frac{2D_{xy\text{-open1}}}{\sqrt{D_{x\text{-open1}}D_{y\text{-open1}}}} = \frac{2(134)}{\sqrt{(23,260)(1,344)}} = 0.05$$

B.3 Subassembly Open Grid Deck Specimen #1 Theoretical Stiffness

B.3.1 Strong Direction Stiffness (D_x)

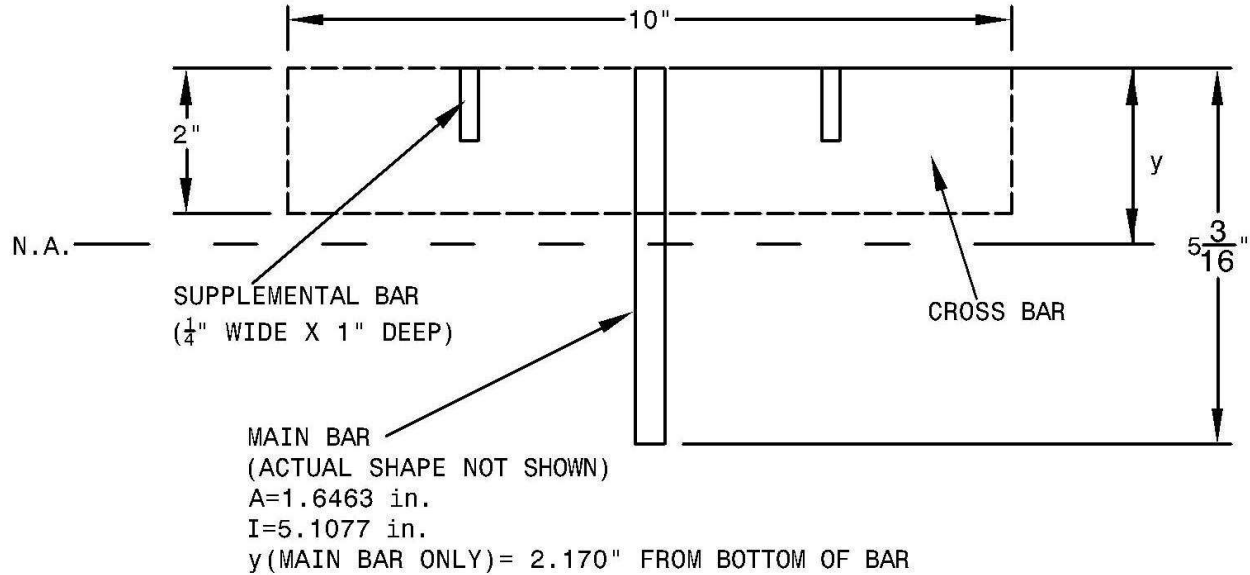


Figure B-4: Model of open grid deck specimen #1 strong direction (D_x)

To compute the theoretical stiffness of subassembly open grid deck specimen #1 in the strong direction (D_x), a standard 10 inch cross section was used as shown in Figure B-4.

The modulus of elasticity of steel (E_s) was taken as:

$$E_s=29000 \text{ ksi}$$

Computing the location of the neutral axis of the cross section:

$$y = \frac{2.179 * 1.6463 + 2 * 0.25 * (5.1875 - 0.5)}{1.6463 + 2 * 0.25}$$

$$y = 2.76 \text{ in. from the bottom of the main bar}$$

$$y = 2.42 \text{ in. from the top of the main bar}$$

When computing the moment of inertia, it was assumed that both the main and supplemental bars contributed to the stiffness of the specimen in this direction because welds were completed at every intersection of steel bars in the deck. Therefore, the moment of inertia was computed as:

$$I = \sum (I_0 + Ad^2)$$

$$I = (I_0 + Ad^2)_{\text{Main Bar}} + (I_0 + Ad^2)_{\text{Supplemental Bars}}$$

$$I = 5.1077 + 1.6463 * 0.581^2 + 2 * (0.02083 + 0.25 * 1.92^2)$$

$$I = 5.66 + 1.88$$

$$I = 7.54 \text{ in.}^4$$

Using the theoretical moment of inertia, the theoretical stiffness was computed as follows:

$$D_{x\text{-theoretical}} = \frac{EI}{W_{\text{cross-section}}} = \frac{29000 \frac{\text{kip}}{\text{in.}^2} * 7.54 \text{ in.}^4}{10 \text{ in.}} = 21,866 \frac{\text{kip} - \text{in.}^2}{\text{in.}}$$

As previously computed, the experimentally measured stiffness of subassembly open grid deck specimen #1 was:

$$D_{x\text{-measured}} = D_{x\text{-open1}} = 23,260 \frac{\text{kip} - \text{in.}^2}{\text{in.}}$$

Therefore, the ratio of the theoretical stiffness to the experimentally measured stiffness was:

$$\text{Ratio} = \frac{D_{x\text{-theoretical}}}{D_{x\text{-measured}}} = \frac{21,866}{23,260} = 0.94$$

Since the ratio showed that the stiffness of the theoretical model was within 15% of that experimentally measured, the model was considered adequate.

B.3.2 Weak Direction Stiffness (D_y)

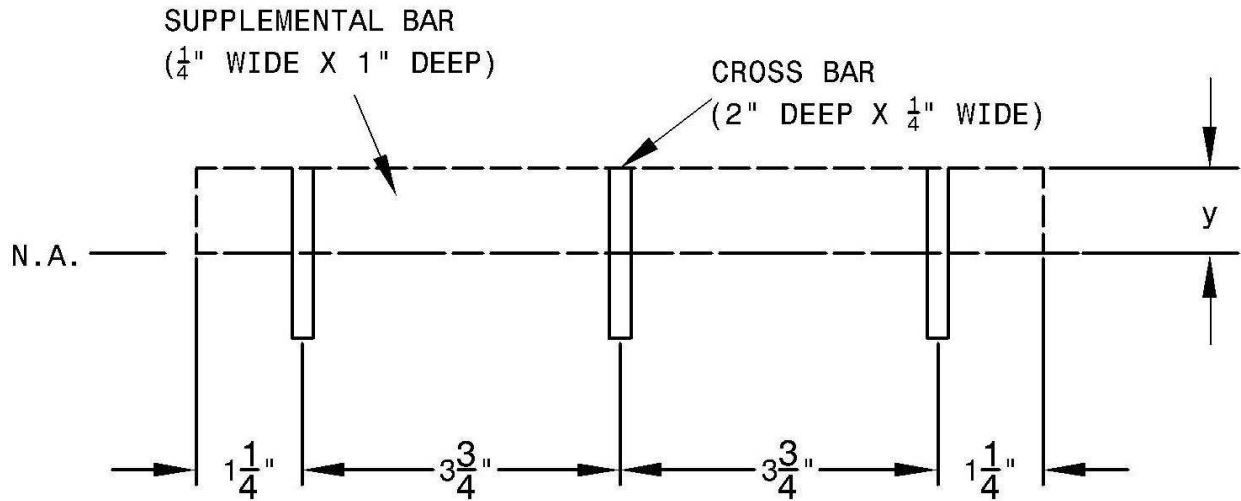


Figure B-5: Model of open grid deck specimen #1 weak direction (D_y)

To compute the theoretical stiffness of subassembly open grid deck specimen #1 in the weak direction (D_y), a standard 10 inch cross section was used as shown in Figure B-5.

The modulus of elasticity of steel (E_s) was taken as:

$$E_s = 29000 \text{ ksi}$$

Computing the moment of inertia for open grid deck specimen #1 was rather simple since only the cross bars would contribute to the stiffness in this direction. Therefore, the moment of inertia was computed as:

$$I = \sum (I_0)$$

$$I = 3 \left(\frac{0.25(2)^3}{12} \right)$$

$$I = 0.5 \text{ in.}^4$$

Using the theoretical moment of inertia, the theoretical stiffness was computed as follows:

$$D_{y\text{-theoretical}} = \frac{EI}{w_{\text{cross-section}}} = \frac{29000 \frac{\text{kip}}{\text{in.}^2} * 0.5 \text{ in.}^4}{10 \text{ in.}} = 1,450 \frac{\text{kip} - \text{in.}^2}{\text{in.}}$$

As previously computed, the experimentally measured stiffness of subassembly open grid deck specimen #1 was:

$$D_{y\text{-measured}} = D_{y\text{-open1}} = 1,344 \frac{\text{kip} - \text{in.}^2}{\text{in.}}$$

Therefore, the ratio of the theoretical stiffness to the experimentally measured stiffness was:

$$\text{Ratio} = \frac{D_{y\text{-theoretical}}}{D_{y\text{-measured}}} = \frac{1,450}{1,344} = 1.08$$

Since the ratio showed that the stiffness of the theoretical model was within 15% of that experimentally measured, the model was considered adequate.

B.4 Subassembly Open Grid Deck Specimen #2 Experimentally Measured Stiffness

The stiffness of open grid deck specimen #2 was determined for the strong (D_x) and weak (D_y) axes, as well as in torsion (D_{xy}). Multiple runs of each test were done to ensure repeatability of the results as well as to determine averages.

B.4.1 Strong Direction Stiffness (D_x) Tests

For the strong direction stiffness (D_x) tests, the load applied and corresponding displacement measurements were recorded at the locations shown in Appendix A. A line of these displacement measurements across the center of the deck (CH_40, CH_42 and CH_46) were used to determine the stiffness of the deck. CH_42 and CH_46 were displacements measured at the center of the support on each side of the deck and were used to account for any rigid body movement of the specimen. CH_40 was the displacement measured at the center of the deck under the location of the applied load. Although other measurements of displacement were recorded (e.g., at the edges of the supports and deck), these measurements confirmed the small rigid body movement across the width of the specimen.

The following plot shows the linear behavior of the specimen underneath the load (CH_40). However, the displacements measured at the supports (CH_42 and CH_46) are not linear and are much smaller as expected. It is noted that this plot is for test run #1 only. Since the other test runs provided very similar results, plots for the repeated test runs are not shown.

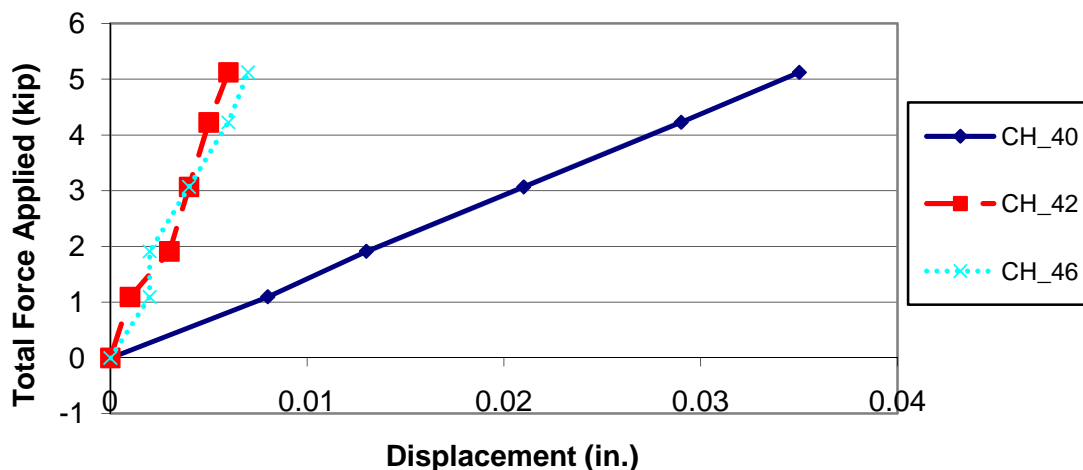


Figure B-6: Measured displacements for test run #1

Test Run #1. The span of the deck specimen tested was:

$$L = \left(5 \text{ ft.} * 12 \frac{\text{in.}}{\text{ft.}} \right) + 10 \text{ in.} = 70 \text{ in.}$$

The width of the deck was:

$$w = \left(6 \text{ ft.} * 12 \frac{\text{in.}}{\text{ft.}} \right) + 8 \text{ in.} = 80 \text{ in.}$$

The maximum point load applied to the spreader beam was

$$P = 5124.14 \text{ lbs.}$$

This load was spread over the width of the deck at midspan as a line load:

$$P' = \frac{P}{w}$$

$$P' = \frac{5124.14 \text{ lbs.}}{(80 \text{ in.} * 1000 \frac{\text{lbs.}}{\text{in.}})} = 0.0641 \frac{\text{kip}}{\text{in.}}$$

The displacements measured at the middle of each support for this load are shown in Table B-10.

Table B-10: Measured support displacements

Channel	Displacement (in.)
CH_42	0.006
CH_46	0.007
Average (Δ_s)	0.0065

The displacement measured at the center of the deck underneath the load was:

$$\Delta_m = \text{CH}_{40} = 0.035 \text{ in.}$$

Therefore, the net vertical deflection at the centerline of the deck, Δ_{CL} , was computed as:

$$\Delta_{CL} = \Delta_m - \Delta_s$$

$$\Delta_{CL} = 0.035 \text{ in.} - 0.0065 \text{ in.}$$

$$\Delta_{CL} = 0.0285 \text{ in.}$$

Therefore, the stiffness of the deck in the strong direction (D_x) for this test run was computed as:

$$D_{x-open2-1} = \frac{P'L^3}{48 \Delta_{CL}} = \frac{\left(0.0641 \frac{\text{kip}}{\text{in.}}\right) (70 \text{ in.})^3}{(48)(0.0285 \text{ in.})}$$

$$D_{x-open2-1} = 16,060 \frac{\text{kip} - \text{in.}^2}{\text{in.}}$$

Test Run #2. For the second run of this test, the span and width of the deck remain the same:

$$L = 70 \text{ in.}$$

$$w = 80 \text{ in.}$$

The maximum point load applied to the spreader beam was:

$$P = 4793.70 \text{ lbs.}$$

This load was spread over the width of the deck at midspan as a line load:

$$P' = \frac{P}{w}$$

$$P' = \frac{4793.7 \text{ lbs.}}{(80 \text{ in.} * 1000 \frac{\text{lbs.}}{\text{kip}})} = 0.0599 \frac{\text{kip}}{\text{in.}}$$

The displacements measured at the middle of each support for this load are shown in Table B-11.

Table B-11: Measured support displacement

Channel	Displacement (in.)
CH_42	0.005
CH_46	0.006
Average (Δ_s)	0.0055

The displacement measured at the center of the deck underneath the load was:

$$\Delta_m = CH_{40} = 0.033 \text{ in.}$$

Therefore, the net vertical deflection at the centerline of the deck, Δ_{CL} , was computed as:

$$\Delta_{CL} = \Delta_m - \Delta_s$$

$$\Delta_{CL} = 0.033 \text{ in.} - 0.0055 \text{ in.}$$

$$\Delta_{CL} = 0.0275 \text{ in.}$$

Therefore, the stiffness of the deck in the strong direction (D_x) for this test run was computed as:

$$D_{x-\text{open2-2}} = \frac{P'L^3}{48 \Delta_{CL}} = \frac{\left(0.0599 \frac{\text{kip}}{\text{in.}}\right) (70 \text{ in.})^3}{(48)(0.0275 \text{ in.})}$$

$$D_{x-\text{open2-2}} = 15,570 \frac{\text{kip} - \text{in.}^2}{\text{in.}}$$

Test Run #3. For the third run of this test, the span and width of the deck remain the same:

$$L = 70 \text{ in.}$$

$$w = 80 \text{ in.}$$

The maximum point load applied to the spreader beam was:

$$P = 4720.64 \text{ lbs.}$$

This load was spread over the width of the deck at midspan as a line load:

$$P' = \frac{P}{w}$$

$$P' = \frac{4720.64 \text{ lbs.}}{(80 \text{ in.} * 1000 \frac{\text{lbs.}}{\text{kip}})} = 0.0590 \frac{\text{kip}}{\text{in.}}$$

The displacements measured at the middle of each support for this load are shown in Table B-12.

Table B-12: Measured support displacement

Channel	Displacement (in.)
CH_42	0.006
CH_46	0.006
Average (Δ_s)	0.006

The displacement measured at the center of the deck underneath the load was:

$$\Delta m = CH_{40} = 0.032 \text{ in.}$$

Therefore, the net vertical deflection at the centerline of the deck, Δ_{CL} , was computed as:

$$\Delta_{CL} = \Delta m - \Delta s$$

$$\Delta_{CL} = 0.032 \text{ in.} - 0.006 \text{ in.}$$

$$\Delta_{CL} = 0.026 \text{ in.}$$

Therefore, the stiffness of the deck in the strong direction (D_x) for this test run was computed as:

$$D_{x\text{-open2-3}} = \frac{P'L^3}{48 \Delta_{CL}} = \frac{\left(0.0590 \frac{\text{kip}}{\text{in.}}\right) (70 \text{ in.})^3}{(48)(0.026 \text{ in.})}$$

$$D_{x\text{-open2-3}} = 16,218 \frac{\text{kip} - \text{in.}^2}{\text{in.}}$$

Average Strong Direction Stiffness (D_x). Therefore, the average measured strong direction stiffness (D_x) of subassembly open grid deck specimen #2 was:

$$\begin{aligned} D_{x\text{-open2}} &= \frac{D_{x\text{-open2-1}} + D_{x\text{-open2-2}} + D_{x\text{-open2-3}}}{3} = \frac{16,060 + 15,570 + 16,218}{3} \\ &= 15,949 \frac{\text{kip} - \text{in.}^2}{\text{in.}} \end{aligned}$$

B.4.2 Weak Direction Stiffness Tests (D_y)

For the weak direction stiffness (D_y) tests, the load applied and corresponding displacement measurements were recorded at the locations shown in Appendix A. A line of these displacement measurements across the center of the deck (CH_37, CH_40 and CH_46) were used to determine the stiffness of the deck. CH_37 and CH_46 were displacements measured at the center of the support on each side of the deck and were used to account for any rigid body movement of the specimen. However, these displacement measurements were taken during different test runs. Therefore, the average was used for locations with two measurements. For example, the force of the two test runs were averaged since they were very close in magnitude and would not skew the stiffness results. The displacement measured at the center of

the deck under the location of the applied load (CH_40) was also averaged since it recorded data for both test runs. Although other measurements of displacement were recorded (e.g., at the edges of the supports and deck), these measurements confirmed the small rigid body movement across the width of the specimen.

The following plot shows the linear behavior of the specimen underneath the load (CH_40). However, little displacement was measured at the supports (CH_37 and CH_46). It is noted that this plot is for test run #1/4 only. Since the other test runs provided very similar results, plots for the repeated test runs are not shown.

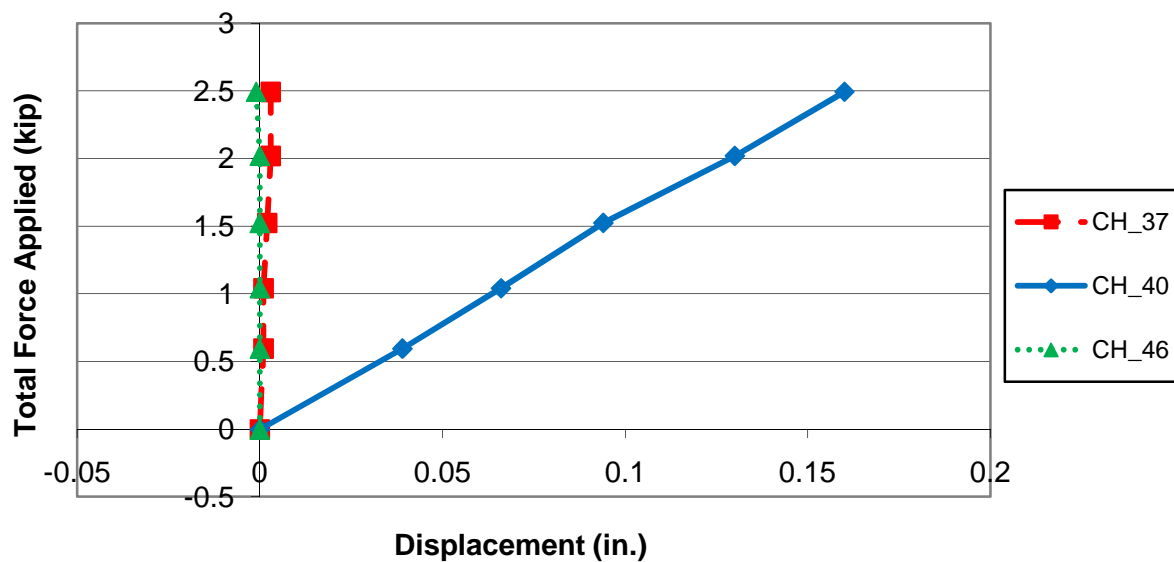


Figure B-7: Measured displacement for test run #1/4

Test Run #1/4. The span of the deck specimen tested was:

$$L = \left(5 \text{ ft.} * 12 \frac{\text{in.}}{\text{ft.}} \right) + 10 \text{ in.} = 70 \text{ in.}$$

The width of the deck was:

$$w = \left(6 \text{ ft.} * 12 \frac{\text{in.}}{\text{ft.}} \right) + 8 \text{ in.} = 80 \text{ in.}$$

The maximum point load applied to the spreader beam is shown in Table B-13.

Table B-13: Point loads recorded in test runs

Test Run #	Point Load (lbs.)
1	2503.95
4	2481.05
Average (P)	2492.5

This load was spread over the width of the deck at midspan as a line load:

$$P' = \frac{P}{w}$$

$$P' = \frac{2503.33 \text{ lbs.}}{(80 \text{ in.} * 1000 \frac{\text{lbs.}}{\text{kip}})} = 0.0312 \frac{\text{kip}}{\text{in.}}$$

The displacements measured at the middle of each support for this load are shown in Table B-14.

Table B-14: Measured support displacement

Channel	Displacement (in.)
CH_37	0.003
CH_46	-0.001
Average (Δs)	0.001

The displacement measured at the center of the deck underneath the load was recorded for each run. Therefore, it was averaged as shown in Table B-15.

Table B-15: Measured displacement at midspan

Test Run #	CH_40 Displacement (in.)
1	0.160
4	0.161
Average (Δm)	0.1605

Therefore, the net vertical deflection at the centerline of the deck, Δ_{CL} , was computed as:

$$\Delta_{CL} = \Delta_m - \Delta_s$$

$$\Delta_{CL} = 0.1605 \text{ in.} - 0.001 \text{ in.}$$

$$\Delta_{CL} = 0.1595 \text{ in.}$$

Therefore, the stiffness of the deck in the weak direction (D_y) for this test run was computed as:

$$D_{y-\text{open2-1/4}} = \frac{P'L^3}{48 \Delta_{CL}} = \frac{\left(0.0312 \frac{\text{kip}}{\text{in.}}\right) (70 \text{ in.})^3}{(48)(0.1595 \text{ in.})}$$

$$D_{y-\text{open2-1/4}} = 1396 \frac{\text{kip} - \text{in.}^2}{\text{in.}}$$

Test Run #2/5. For the second & fifth runs of this test, the span and width of the deck remain the same:

$$L = 70 \text{ in.}$$

$$w = 80 \text{ in.}$$

The maximum point load applied to the spreader beam is shown in Table B-16.

Table B-16: Point loads recorded in test runs

Test Run #	Point Load (lbs.)
2	2529.67
5	2524.67
Average (P)	2527.17

This load was spread over the width of the deck at midspan as a line load:

$$P' = \frac{P}{w}$$

$$P' = \frac{2527.17 \text{ lbs.}}{(80 \text{ in.} * 1000 \frac{\text{lbs.}}{\text{kip}})} = 0.0316 \frac{\text{kip}}{\text{in.}}$$

The displacements measured at the middle of each support for this load are shown in Table B-17.

Table B-17: Measured support displacement

Channel	Displacement (in.)
CH_37	0.003
CH_46	-0.001
Average (Δ_s)	0.001

The displacement measured at the center of the deck underneath the load was recorded for each run. Therefore, it was averaged as shown in Table B-18.

Table B-18: Measured displacement at midspan

Test Run #	CH_40 Displacement (in.)
2	0.160
5	0.160
Average (Δ_m)	0.160

Therefore, the net vertical deflection at the centerline of the deck, Δ_{CL} , was computed as:

$$\Delta_{CL} = \Delta_m - \Delta_s$$

$$\Delta_{CL} = 0.160 \text{ in.} - 0.001 \text{ in.}$$

$$\Delta_{CL} = 0.159 \text{ in.}$$

Therefore, the stiffness of the deck in the weak direction (D_y) for this test run was computed as:

$$D_{y-\text{open2-2/5}} = \frac{P'L^3}{48 \Delta_{CL}} = \frac{\left(0.0316 \frac{\text{kip}}{\text{in.}}\right) (70 \text{ in.})^3}{(48)(0.159 \text{ in.})}$$

$$D_{y-\text{open2-2/5}} = 1420 \frac{\text{kip} - \text{in.}^2}{\text{in.}}$$

Test Run #3/6. For the third & sixth runs of this test, the span and width of the deck remain the same:

$$L = 70 \text{ in.}$$

$$w = 80 \text{ in.}$$

The maximum point load applied to the spreader beam is shown in Table B-19.

Table B-19: Point loads recorded in test runs

Test Run #	Point Load (lbs.)
3	2503.43
6	2539.45
Average (P)	2521.44

This load was spread over the width of the deck at midspan as a line load:

$$P' = \frac{P}{w}$$

$$P' = \frac{2521.44 \text{ lbs.}}{\left(80 \text{ in.} * 1000 \frac{\text{lbs.}}{\text{kip}}\right)} = 0.0315 \frac{\text{kip}}{\text{in.}}$$

The displacements measured at the middle of each support for this load are shown in Table B-20.

Table B-20: Measured support displacement

Channel	Displacement (in.)
CH_37	0.003
CH_46	-0.001
Average (Δs)	0.001

The displacement measured at the center of the deck underneath the load was recorded for each run. Therefore, it was averaged as shown in Table B-21.

Table B-21: Measured displacement at midspan

Test Run #	CH_40 Displacement (in.)
3	0.158
6	0.159
Average (Δm)	0.1585

Therefore, the net vertical deflection at the centerline of the deck, Δ_{CL} , was computed as:

$$\Delta_{CL} = \Delta_m - \Delta_s$$

$$\Delta_{CL} = 0.1585 \text{ in.} - 0.001 \text{ in.}$$

$$\Delta_{CL} = 0.1575 \text{ in.}$$

Therefore, the stiffness of the deck in the weak direction (D_y) for this test run was computed as:

$$D_{y\text{-open2-3/6}} = \frac{P'L^3}{48 \Delta_{CL}} = \frac{\left(0.0315 \frac{\text{kip}}{\text{in.}}\right) (70 \text{ in.})^3}{(48)(0.1575 \text{ in.})}$$

$$D_{y\text{-open2-3/6}} = 1430 \frac{\text{kip-in.}^2}{\text{in.}}$$

Average Weak Direction Stiffness (D_y). The average measured weak direction stiffness (D_y) of subassembly open grid deck specimen #2 was:

$$\begin{aligned} D_{y\text{-open2}} &= \frac{D_{y\text{-open2-1/4}} + D_{y\text{-open2-2/5}} + D_{y\text{-open2-3/6}}}{3} = \frac{1,396 + 1,420 + 1,430}{3} \\ &= 1,415 \frac{\text{kip-in.}^2}{\text{in.}} \end{aligned}$$

B.4.3 Torsional Stiffness (D_{xy}) Test

For the torsional stiffness (D_{xy}) tests, the load applied and corresponding displacement measurements were recorded at the locations shown in Appendix A. The displacement measured the free corner of the deck under the applied load (CH_41) was used to determine the torsion stiffness of the deck. Measurements at the point supports (CH_34, CH_36, and CH_42) were also recorded throughout testing. These measurements confirmed that very little rigid body movement occurred at the supports. It is noted that only one test rotation was completed for this specimen.

The following plot shows the linear behavior of the specimen at the loaded free corner (CH_41). However, essentially no displacement was measured at the supports (CH_34, CH_36, and CH_42). Therefore, only the displacement at the loaded free corner was plotted. It is noted that this plot is for test run #1 of test rotation #1 only. Since the other test runs and rotations provided very similar results, plots for the repeated test runs and rotations are not shown.

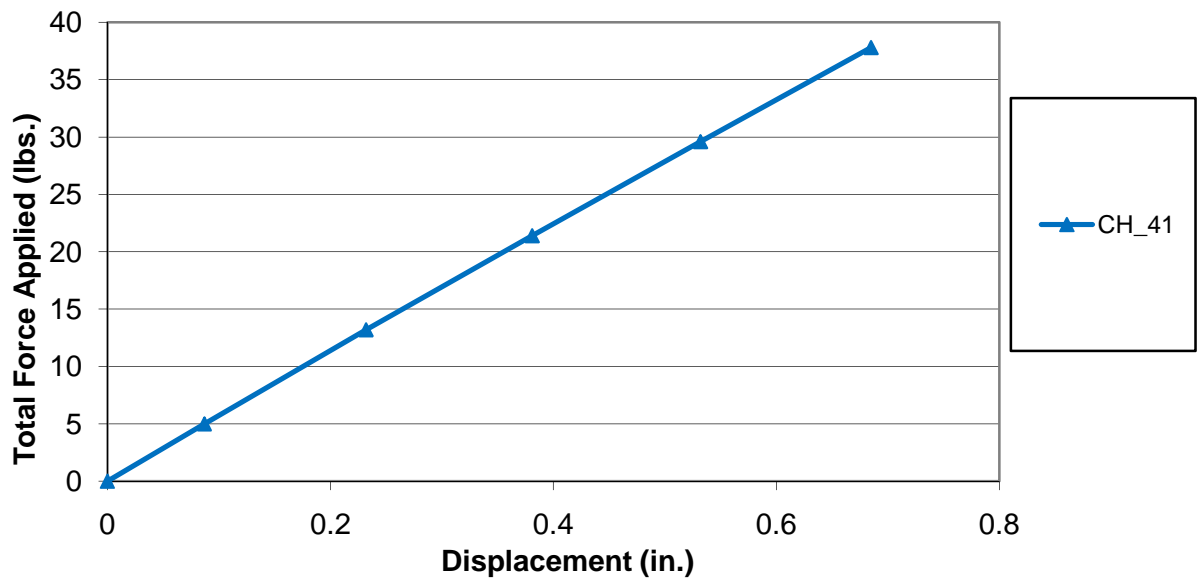


Figure B-8: Measured displacement at loaded free corner for test run #1 of test rotation #1

Test Rotation #1. The span of the deck specimen tested was:

$$L = \left(5 \text{ ft.} * 12 \frac{\text{in.}}{\text{ft.}} \right) + 10 \text{ in.} = 70 \text{ in.}$$

The maximum point load applied to the free corner of the deck was:

$$P = 37.8 \text{ lbs.} = 0.0378 \text{ kip}$$

For this test rotation, six test runs were completed to ensure repeatability of the data and to determine averages. Each individual test run and average displacement measurements at the loaded free corner are shown in Table B-22.

Table B-22: Measured displacement at loaded free corner

Test Run #	CH_38 Displacement (in.)
1	0.685
2	0.679
3	0.682
4	0.685
5	0.684
6	0.686
Average (Δ_{LF})	0.6835

The displacements at the point supports are shown in Table B-23.

Table B-23: Measured displacements at supports

Test Run #	CH_34 Displacement (in.)	CH_36 Displacement (in.)	CH_42 Displacement (in.)
1	-0.001	-0.002	0
2	-0.001	-0.002	0
3	-0.001	-0.002	0
4	-0.001	-0.002	0
5	-0.001	-0.002	0
6	-0.001	-0.002	0
Average	-0.001	-0.002	0

Although CH_36 shows some displacement, it was noted that this is not quite at the support location since access was denied by the point supports above and below the specimen at this point. Therefore, it was reasonable to assume that the displacement at this fully restrained support location was zero.

Hence, the average rigid body movement was computed as:

$$\Delta_{LS} = \frac{-0.001 \text{ in.}}{3} = -0.0003 \text{ in.}$$

Therefore, the net vertical displacement at the free corner of the specimen was computed as:

$$\Delta_L = \Delta_{LF} - \Delta_{LS}$$

$$\Delta_L = 0.6835 \text{ in.} - (-0.003 \text{ in.})$$

$$\Delta_L = 0.6838 \text{ in.}$$

Therefore, the stiffness of the deck in torsion (D_{xy}) for this test rotation was computed as:

$$D_{xy-\text{open2}} = \frac{PL^2}{4 \Delta_L} = \frac{(0.0378 \text{ kip})(70 \text{ in.})^2}{(4)(0.6838 \text{ in.})}$$

$$D_{xy-\text{open2}} = 68 \frac{\text{kip} - \text{in.}^2}{\text{in.}}$$

Average Torsional Stiffness (D_{xy}). Since only one rotation was tested for subassembly open grid deck specimen #2, the average measured torsion stiffness was that which was previously computed.

B.4.4 Measured Stiffness Properties of Subassembly Open Grid Deck Specimen #2

As previously computed, the average measured stiffness of the deck in the strong (D_x) and weak (D_y) directions as well as the torsion stiffness were:

$$D_{x-\text{open2}} = 15,949 \frac{\text{kip} - \text{in.}^2}{\text{in.}}$$

$$D_{y-\text{open2}} = 1,415 \frac{\text{kip} - \text{in.}^2}{\text{in.}}$$

$$D_{xy-\text{open2}} = 68 \frac{\text{kip} - \text{in.}^2}{\text{in.}}$$

Therefore, the orthotropic ratio of subassembly open grid deck specimen #1 was computed as:

$$D_{\text{open2}} = \frac{D_{x-\text{open2}}}{D_{y-\text{open2}}} = \frac{15,949}{1,415} = 11.3$$

Moreover, the torsion stiffness parameter for this specimen was computed as:

$$\alpha_{\text{open2}} = \frac{2D_{xy-\text{open2}}}{\sqrt{D_{x-\text{open2}}D_{y-\text{open2}}}} = \frac{2(68)}{\sqrt{(15,949)(1,415)}} = 0.03$$

B.5 Subassembly Open Grid Deck Specimen #2 Theoretical Stiffness

B.5.1 Strong Direction Stiffness (D_x)

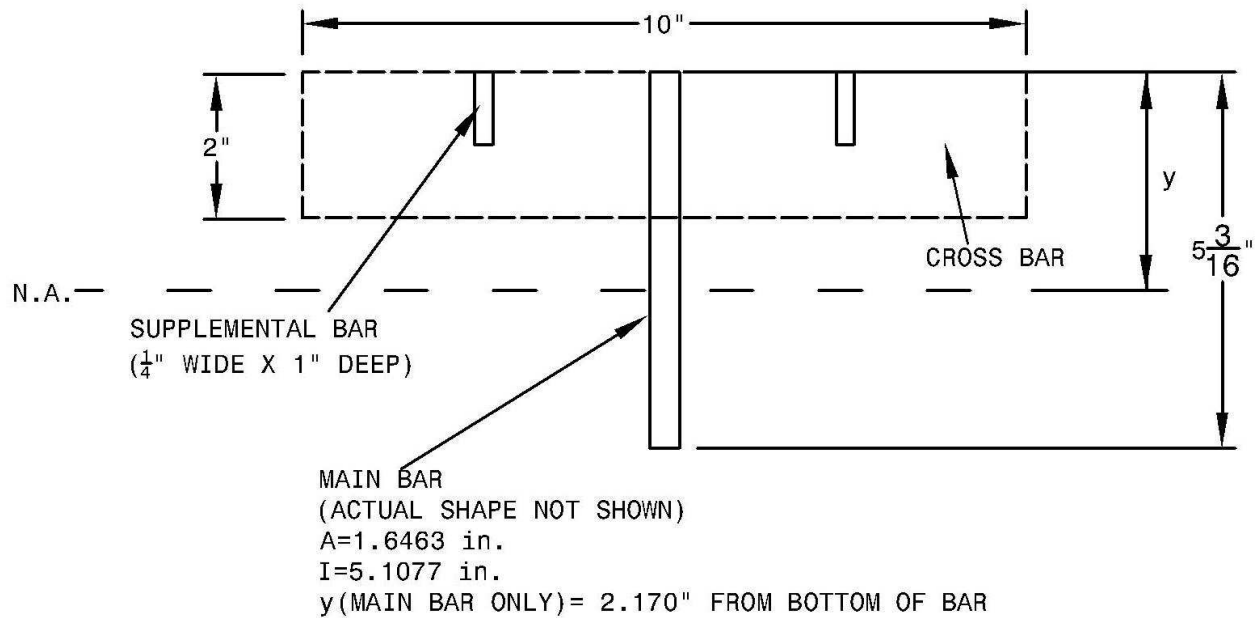


Figure B-9: Model of open grid deck specimen #2 strong direction (D_x)

To compute the theoretical stiffness of subassembly open grid deck specimen #1 in the strong direction (D_x), a standard 10 inch cross section was used as shown in Figure B-9

This specimen was originally modeled in the same manner as open grid deck specimen #1. Therefore, the original theoretical stiffness was:

$$D_{x\text{-original-theoretical}} = \frac{EI}{w_{\text{cross-section}}} = \frac{29000 \frac{\text{kip}}{\text{in}^2} * 7.54 \text{ in}^4}{10 \text{ in.}} = 21,866 \frac{\text{kip} - \text{in}^2}{\text{in.}}$$

However, the experimentally measured stiffness was measured as:

$$D_{x\text{-measured}} = 15,950 \frac{\text{kip} - \text{in}^2}{\text{in.}}$$

This produced a ratio of:

$$\text{Ratio} = \frac{D_{x\text{-original-theoretical}}}{D_{x\text{-measured}}} = \frac{21,866}{15,950} = 1.37$$

Since the ratio showed that the stiffness of the theoretical model was not within 15% of that experimentally measured, the model was considered inadequate. Therefore, the behavior of the deck was further investigated to ensure that a more accurate model was created.

New Model. It was found that only the main bars contributed to the stiffness of open grid deck #2 because not all bar intersections were welded within the deck. Therefore, the deck was remodeled in the strong direction using only the main bars.

Over a typical 10 inch cross-section, the geometric properties were as follows:

$$y = 2.179 \text{ in. from the bottom of the main bar}$$

$$I_o = 5.1077 \text{ in.}^4$$

Using the theoretical moment of inertia, the theoretical stiffness was computed as follows:

$$D_{x\text{-theoretical}} = \frac{EI}{w_{\text{cross-section}}} = \frac{29000 \frac{\text{kip}}{\text{in.}^2} * 5.1077 \text{ in.}^4}{10 \text{ in.}} = 14,812 \frac{\text{kip} - \text{in.}^2}{\text{in.}}$$

As previously discussed, the experimentally measured stiffness of subassembly open grid deck specimen #2 was:

$$D_{x\text{-measured}} = 15,950 \frac{\text{kip} - \text{in.}^2}{\text{in.}}$$

Therefore, the ratio of the theoretical stiffness to the experimentally measured stiffness was:

$$\text{Ratio} = \frac{D_{x\text{-theoretical}}}{D_{x\text{-measured}}} = \frac{14,812}{15,950} = 0.93$$

Since the ratio showed that the stiffness of the theoretical model was within 15% of that experimentally measured, this model was considered adequate.

B.5.2 Weak Direction Stiffness (D_y)

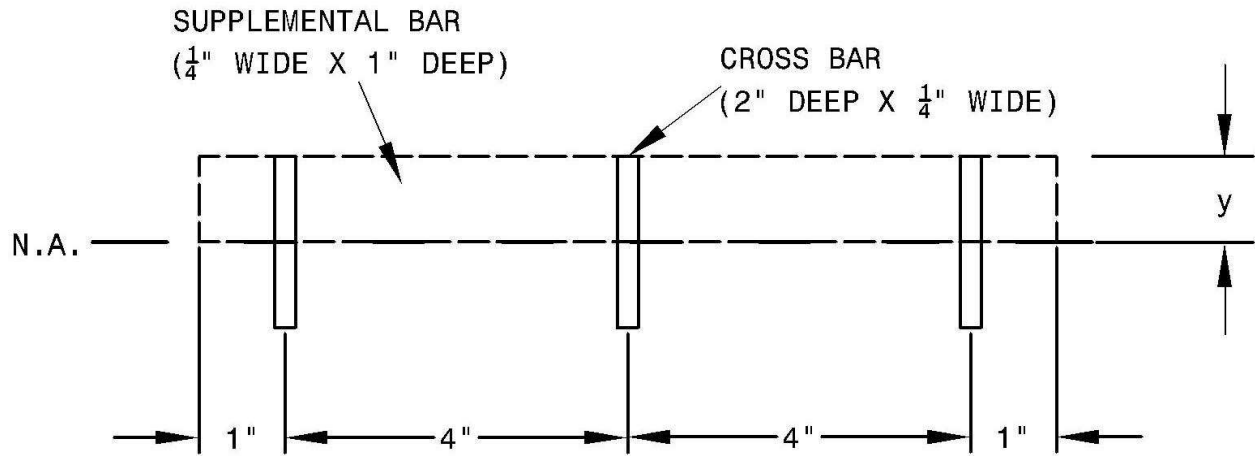


Figure B-10: Model of open grid deck specimen #2 weak direction (D_y)

The theoretical stiffness of subassembly open grid deck specimen #2 (Figure B-10) in the weak direction (D_y) was computed in the same manner as that of open grid deck specimen #1. Since the configuration of steel was very similar in this direction for both specimens, the theoretical stiffness was the same. Therefore:

$$D_{y\text{-theoretical}} = \frac{EI}{w_{\text{cross-section}}} = \frac{29000 \frac{\text{kip}}{\text{in.}^2} * 0.5 \text{ in}^4}{10 \text{ in.}} = 1,450 \frac{\text{kip} - \text{in.}^2}{\text{in.}}$$

As previously computed, the experimentally measured stiffness of subassembly open grid deck specimen #2 was:

$$D_{y\text{-measured}} = 1,415 \frac{\text{kip} - \text{in.}^2}{\text{in.}}$$

Therefore, the ratio of the theoretical stiffness to the experimentally measured stiffness was:

$$\text{Ratio} = \frac{D_{y\text{-theoretical}}}{D_{y\text{-measured}}} = \frac{1,450}{1,415} = 1.02$$

Since the ratio showed that the stiffness of the theoretical model was within 15% of that experimentally measured, the model was considered adequate.

B.6 Subassembly Partially Filled Grid Deck Specimen Experimentally Measured Stiffness

The stiffness of partially filled grid deck specimen was determined for the strong (D_x) and weak (D_y) axes, as well as in torsion (D_{xy}). Multiple runs of each test were done to ensure repeatability of the results as well as to determine averages.

B.6.1 Strong Direction Stiffness (D_x) Test

For the strong direction stiffness (D_x) tests, the load applied and corresponding displacement measurements were recorded at the locations shown in Appendix A. A line of these displacement measurements across the center of the deck (CH_40, CH_42 and CH_46) were used to determine the stiffness of the deck. CH_42 and CH_46 were displacements measured at the center of the support on each side of the deck and were used to account for any rigid body movement of the specimen. CH_40 was the displacement measured at the center of the deck under the location of the applied load. Although other measurements of displacement were recorded (e.g., at the edges of the supports and deck), these measurements confirmed the small rigid body movement across the width of the specimen.

The following plot shows the linear behavior of the specimen underneath the load (CH_40). However, the displacements measured at the supports (CH_42 and CH_46) are not linear and are much smaller as expected. It is noted that this plot is for test run #1 only. Since the other test runs provided very similar results, plots for the repeated test runs are not shown.

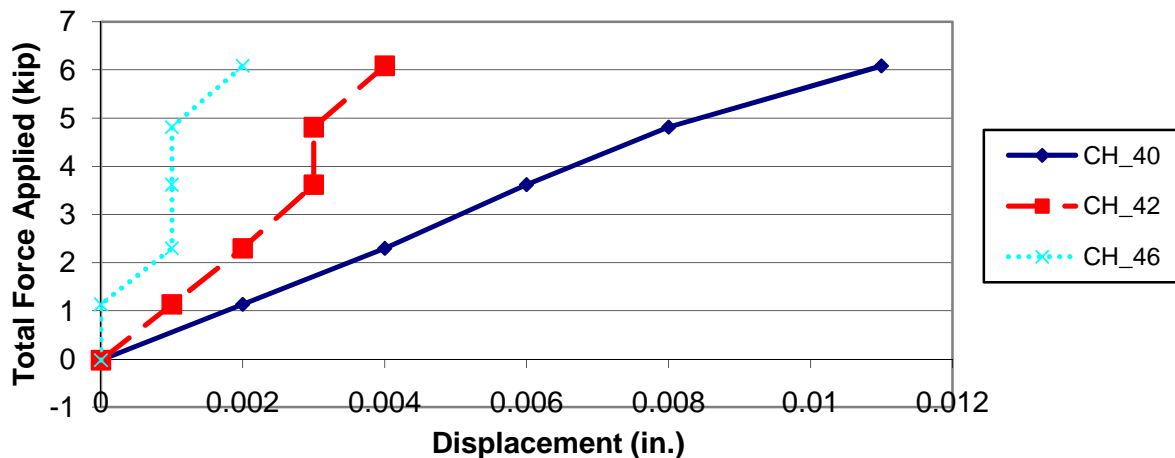


Figure B-11: Measured displacement for test run #1

Test Run #1. The span of the deck specimen tested was:

$$L = \left(5 \text{ ft.} * 12 \frac{\text{in.}}{\text{ft.}} \right) + 10 \text{ in.} = 70 \text{ in.}$$

The width of the deck was:

$$w = \left(6 \text{ ft.} * 12 \frac{\text{in.}}{\text{ft.}} \right) + 8 \text{ in.} = 80 \text{ in.}$$

The maximum point load applied to the spreader beam was:

$$P = 6084.61 \text{ lbs.}$$

This load was spread over the width of the deck at midspan as a line load:

$$P' = \frac{P}{w}$$

$$P' = \frac{6084.61 \text{ lbs.}}{(80 \text{ in.} * 1000 \frac{\text{lbs.}}{\text{kip}})} = 0.0761 \frac{\text{kip}}{\text{in.}}$$

The displacements measured at the middle of each support for this load are shown in Table B-24.

Table B-24: Measured support displacement

Channel	Displacement(in.)
CH_42	0.004
CH_46	0.002
Average (Δ_s)	0.003

The displacement measured at the center of the deck underneath the load was:

$$\Delta_m = \text{CH}_{40} = 0.011 \text{ in.}$$

Therefore, the net vertical deflection at the centerline of the deck, Δ_{CL} , was computed as:

$$\Delta_{CL} = \Delta_m - \Delta_s$$

$$\Delta_{CL} = 0.011 \text{ in.} - 0.003 \text{ in.}$$

$$\Delta_{CL} = 0.008 \text{ in.}$$

Therefore, the stiffness of the deck in the strong direction (D_x) for this test run was computed as:

$$D_{x-pf-1} = \frac{P'L^3}{48 \Delta_{CL}} = \frac{\left(0.0761 \frac{\text{kip}}{\text{in.}}\right) (75 \text{ in.})^3}{(48)(0.008 \text{ in.})}$$

$$\mathbf{D = 67,937 \frac{kip - in.^2}{in.}}$$

Test Run #2. For the second run of this test, the span and width of the deck remain the same:

$$L = 70 \text{ in.}$$

$$w = 80 \text{ in.}$$

The maximum point load applied to the spreader beam was:

$$P = 5916.82 \text{ lbs.}$$

This load was spread over the width of the deck at midspan as a line load:

$$P' = \frac{P}{w}$$

$$P' = \frac{5916.82 \text{ lbs.}}{(80 \text{ in.} * 1000 \frac{\text{lbs.}}{\text{kip}})} = 0.0740 \frac{\text{kip}}{\text{in.}}$$

The displacements measured at the middle of each support for this load are shown in Table B-25.

Table B-25: Measured support displacement

Channel	Displacement (in.)
CH_42	0.004
CH_46	0.002
Average (Δ_s)	0.003

The displacement measured at the center of the deck underneath the load was:

$$\Delta_m = CH_{40} = 0.010 \text{ in.}$$

Therefore, the net vertical deflection at the centerline of the deck, Δ_{CL} , was computed as:

$$\Delta_{CL} = \Delta_m - \Delta_s$$

$$\Delta_{CL} = 0.010 \text{ in.} - 0.003 \text{ in.}$$

$$\Delta_{CL} = 0.007 \text{ in.}$$

Therefore, the stiffness of the deck in the strong direction (D_x) for this test run was computed as:

$$D_{x-pf-2} = \frac{P' L^3}{48 \Delta_{CL}} = \frac{\left(0.0740 \frac{\text{kip}}{\text{in.}}\right) (70 \text{ in.})^3}{(48)(0.007 \text{ in.})}$$

$$D_{x-pf-2} = 75,501 \frac{\text{kip} - \text{in.}^2}{\text{in.}}$$

Test Run #3. For the third run of this test, the span and width of the deck remain the same:

$$L = 70 \text{ in.}$$

$$w = 80 \text{ in.}$$

The maximum point load applied to the spreader beam was:

$$P = 6020.02 \text{ lbs.}$$

This load was spread over the width of the deck at midspan as a line load:

$$P' = \frac{P}{w}$$

$$P' = \frac{6020.02 \text{ lbs.}}{(80 \text{ in.} * 1000 \frac{\text{lbs.}}{\text{kip}})} = 0.0753 \frac{\text{kip}}{\text{in.}}$$

The displacements measured at the middle of each support for this load are shown in Table B-26.

Table B-26: Measured support displacement

Channel	Displacement (in.)
CH_42	0.004
CH_46	0.001
Average (Δ_s)	0.0025

The displacement measured at the center of the deck underneath the load was:

$$\Delta m = CH_{40} = 0.010 \text{ in.}$$

Therefore, the net vertical deflection at the centerline of the deck, Δ_{CL} , was computed as:

$$\Delta_{CL} = \Delta m - \Delta s$$

$$\Delta_{CL} = 0.010 \text{ in.} - 0.0025 \text{ in.}$$

$$\Delta_{CL} = 0.0075 \text{ in.}$$

Therefore, the stiffness of the deck in the strong direction (D_x) for this test run was computed as:

$$D_{x-pf-3} = \frac{P'L^3}{48 \Delta_{CL}} = \frac{(0.0753)(70)^3}{(48)(0.0075)}$$

$$D_{x-pf-3} = 71,697 \frac{\text{kip} - \text{in.}^2}{\text{in.}}$$

Average Strong Direction Stiffness (D_x). The average measured strong direction stiffness (D_x) of the subassembly partially filled grid deck specimen was:

$$D_{x-pf} = \frac{D_{x-pf-1} + D_{x-pf-2} + D_{x-pf-3}}{3} = \frac{67,937 + 75,501 + 71,697}{3} = 71,712 \frac{\text{kip} - \text{in.}^2}{\text{in.}}$$

B.6.2 Weak Direction Stiffness (D_y) Test

For the weak direction stiffness (D_y) tests, the load applied and corresponding displacement measurements were recorded at the locations shown in Appendix A. A line of these displacement measurements across the center of the deck (CH_37, CH_40 and CH_46) were used to determine the stiffness of the deck. CH_37 and CH_46 were displacements measured at the center of the support on each side of the deck and were used to account for any rigid body movement of the specimen. However, these displacement measurements were taken during different test runs. Therefore, the average was used for locations with two measurements. For example, the force of the two test runs were averaged since they were very close in magnitude and would not skew the stiffness results. The displacement measured at the center of the deck under the location of the applied load (CH_40) was also averaged since it recorded data for both test runs. Although other measurements of displacement were recorded (e.g., at the

edges of the supports and deck), these measurements confirmed the small rigid body movement across the width of the specimen.

The following plot shows the linear behavior of the specimen underneath the load (CH_40). However, little displacement was measured at the supports (CH_37 and CH_46). It is noted that this plot is for test run #1/4 only. Since the other test runs provided very similar results, plots for the repeated test runs are not shown.

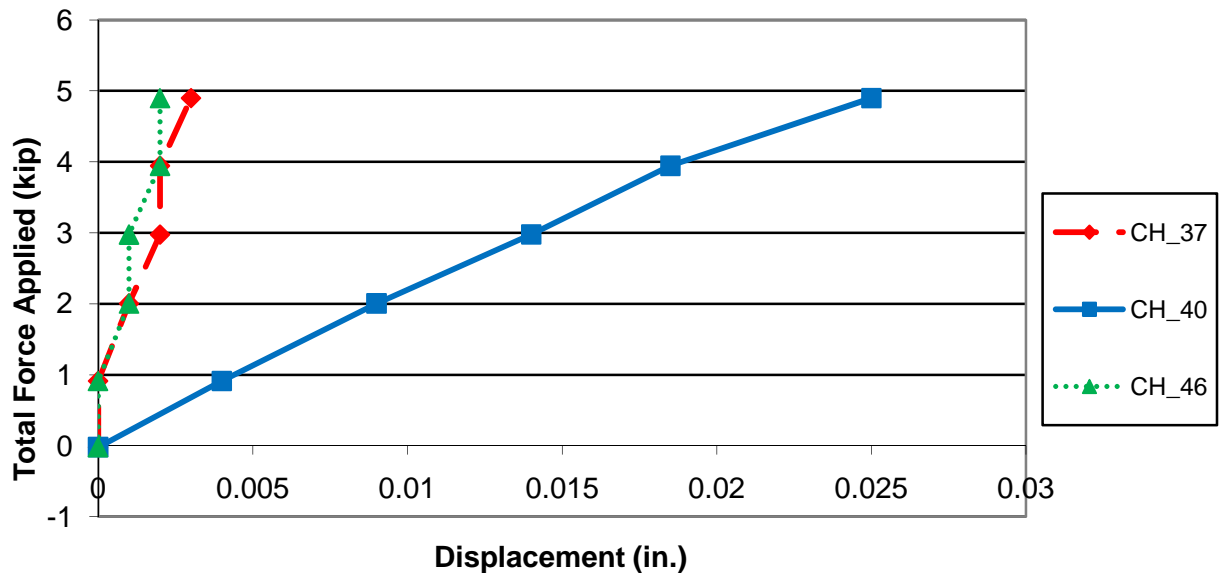


Figure B-12: Measured displacements for test run #1/4

Test Run #1/4. The span of the deck specimen tested was:

$$L = \left(5 \text{ ft.} * 12 \frac{\text{in.}}{\text{ft.}} \right) + 10 \text{ in.} = 70 \text{ in.}$$

The width of the deck was:

$$w = \left(6 \text{ ft.} * 12 \frac{\text{in.}}{\text{ft.}} \right) + 8 \text{ in.} = 80 \text{ in.}$$

The maximum point load applied to the spreader beam is shown in Table B-27.

Table B-27: Point loads recorded in test runs

Test Run #	Point Load (lbs.)
1	4867.52
4	4927.77
Average (P)	4897.645

This load was spread over the width of the deck at midspan as a line load:

$$P' = \frac{P}{w}$$

$$P' = \frac{4897.645 \text{ lbs.}}{(80 \text{ in} * 1000 \frac{\text{lbs.}}{\text{kip}})} = 0.0612 \frac{\text{kip}}{\text{in.}}$$

The displacements measured at the middle of each support for this load are shown in Table B-28.

Table B-28: Measured support displacement

Channel	Displacement (in.)
CH_37	0.003
CH_46	0.002
Average (Δ_s)	0.0025

The displacement measured at the center of the deck underneath the load was recorded for each run. Therefore, it was averaged as shown in Table B-29.

Table B-29: Measured displacement at midspan

Test Run #	CH_40 Displacement (in.)
1	0.026
4	0.024
Average (Δ_m)	0.025

Therefore, the net vertical deflection at the centerline of the deck, Δ_{CL} , was computed as:

$$\Delta_{CL} = \Delta_m - \Delta_s$$

$$\Delta_{CL} = 0.025 \text{ in.} - 0.0025 \text{ in.}$$

$$\Delta_{CL} = 0.0225 \text{ in.}$$

Therefore, the stiffness of the deck in the weak direction (D_y) for this test run was computed as:

$$D_{y-pf-1/4} = \frac{P'L^3}{48 \Delta_{CL}} = \frac{\left(0.0612 \frac{\text{kip}}{\text{in.}}\right) (70 \text{ in.})^3}{(48)(0.0225 \text{ in.})}$$

$$D_{y-pf-1/4} = 19,443 \frac{\text{kip} - \text{in.}^2}{\text{in.}}$$

Test Run #2/5. For the second & fifth runs of this test, the span and width of the deck remain the same:

$$L = 70 \text{ in.}$$

$$w = 80 \text{ in.}$$

The maximum point load applied to the spreader beam is shown in Table B-30.

Table B-30: Point loads recorded in test runs

Test Run #	Point Load (lbs.)
2	4923.46
5	4896.85
Average (P)	4910.155

This load was spread over the width of the deck at midspan as a line load:

$$P' = \frac{P}{w}$$

$$P' = \frac{4910.155 \text{ lbs.}}{(80 \text{ in.} * 1000 \frac{\text{lbs.}}{\text{kip}})} = 0.0614 \frac{\text{kip}}{\text{in.}}$$

The displacements measured at the middle of each support for this load are shown in Table B-31.

Table B-31: Measured support displacement

Channel	Displacement (in.)
CH_37	0.002
CH_46	0.002
Average (Δ_s)	0.002

The displacement measured at the center of the deck underneath the load was recorded for each run. Therefore, it was averaged as shown in Table B-32.

Table B-32: Measured displacement at midspan

Test Run #	CH_40 Displacement (in.)
2	0.024
5	0.023
Average (Δ_m)	0.0235

Therefore, the net vertical deflection at the centerline of the deck, Δ_{CL} , was computed as:

$$\Delta_{CL} = \Delta_m - \Delta_s$$

$$\Delta_{CL} = 0.0235 \text{ in.} - 0.002 \text{ in.}$$

$$\Delta_{CL} = 0.0215 \text{ in.}$$

Therefore, the stiffness of the deck in the weak direction (D_y) for this test run was computed as:

$$D_{y-pf-2/5} = \frac{P'L^3}{48 \Delta_{CL}} = \frac{\left(0.0612 \frac{\text{kip}}{\text{in.}}\right) (70 \text{ in.})^3}{(48)(0.0215 \text{ in.})}$$

$$D_{y-pf-2/5} = 20,400 \frac{\text{kip} - \text{in.}^2}{\text{in.}}$$

Test Run #3/6. For the second & fifth runs of this test, the span and width of the deck remain the same:

$$L = 70 \text{ in.}$$

$$w = 80 \text{ in.}$$

The maximum point load applied to the spreader beam is shown in Table B-33.

Table B-33: Point loads recorded in test runs

Test Run #	Point Load (lbs.)
3	4875.02
6	5046.75
Average (P)	4960.885

This load was spread over the width of the deck at midspan as a line load:

$$P' = \frac{P}{w}$$

$$P' = \frac{4960.855 \text{ lbs.}}{(80 \text{ in.} * 1000 \frac{\text{lbs.}}{\text{kip}})} = 0.0620 \frac{\text{kip}}{\text{in.}}$$

The displacements measured at the middle of each support for this load are shown in Table B-34.

Table B-34: Measured support displacement

Channel	Displacement (in.)
CH_37	0.002
CH_46	0.002
Average (Δ_s)	0.002

The displacement measured at the center of the deck underneath the load was recorded for each run. Therefore, it was averaged as shown in Table B-35.

Table B-35: Measured displacement at midspan

Test #	CH_40 Displacement (in.)
3	0.024
6	0.024
Average (Δ_m)	0.024

Therefore, the net vertical deflection at the centerline of the deck, Δ_{CL} , was computed as:

$$\Delta_{CL} = \Delta_m - \Delta_s$$

$$\Delta_{CL} = 0.024 \text{ in.} - 0.002 \text{ in.}$$

$$\Delta_{CL} = 0.022 \text{ in.}$$

Therefore, the stiffness of the deck in the weak direction (D_y) for this test run was computed as:

$$D_{y-pf-3/6} = \frac{P' L^3}{48 \Delta_{CL}} = \frac{\left(0.0620 \frac{\text{kip}}{\text{in.}}\right) (70 \text{ in.})^3}{(48)(0.022 \text{ in.})}$$

$$D_{y-pf-3/6} = 20,142 \frac{\text{kip} - \text{in.}^2}{\text{in.}}$$

Average Weak Direction Stiffness (D_y). The average measured weak direction stiffness (D_y) of the subassembly partially filled grid deck specimen was:

$$D_{y-pf} = \frac{D_{y-pf-1/4} + D_{y-pf-2/5} + D_{y-pf-3/6}}{3} = \frac{19,443 + 20,400 + 20,142}{3}$$

$$= 19,995 \frac{\text{kip} - \text{in.}^2}{\text{in.}}$$

B.6.3 Torsional Stiffness (D_{xy}) Test

For the torsion stiffness (D_{xy}) tests, the load applied and corresponding displacement measurements were recorded at the locations shown in Appendix A. The displacement measured the free corner of the deck under the applied load (CH_41) was used to determine the torsion stiffness of the deck. Although other measurements of displacement were recorded, these measurements confirmed the no rigid body movement occurred at the supports.

The following plot shows the linear behavior of the specimen at the loaded free corner (CH_41). However, no displacement was measured at the supports. Therefore, they are not displayed in this plot. It is noted that this plot is for test run #1 of test rotation #1 only. Since the other test runs and rotations provided very similar results, plots for the repeated test runs and rotations are not shown.

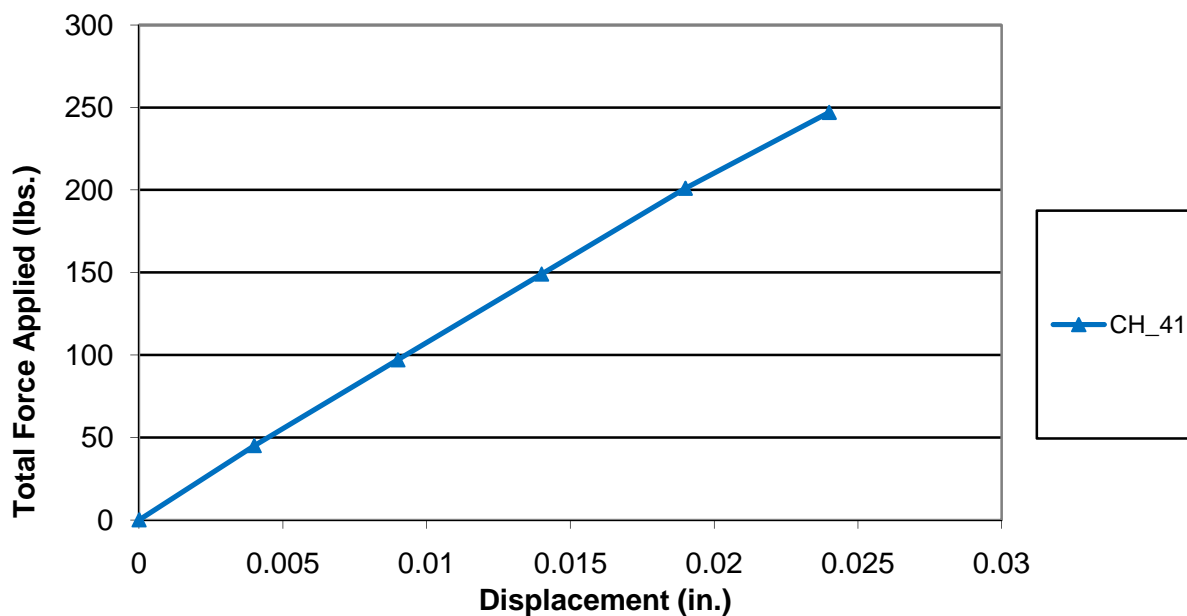


Figure B-13: Measured displacement at loaded free corner of test run #1 of test rotation #1

Test Rotation #1. The span of the deck specimen tested was:

$$L = (5 * 12) + 10 = 70 \text{ in.}$$

The maximum point load applied to the free corner of the deck was:

$$P = 247 \text{ lbs.} = 0.247 \text{ kip}$$

For this rotation, six test runs were completed to ensure repeatability of the data and to determine averages. The individual test run and average displacement measurements at the loaded free corner are shown in Table B-36.

Table B-36: Measured displacement at loaded free corner

Test Run #	CH_41 Displacement (in.)
1	0.024
2	0.023
3	0.023
4	0.024
5	0.023
6	0.023
Average (Δ_L)	0.0233

Therefore, the stiffness of the deck in torsion (D_{xy}) for this test rotation was computed as:

$$D_{xy-pf-1} = \frac{PL^2}{4 \Delta_L} = \frac{(0.247 \text{ kip})(70 \text{ in.})^2}{(4)(0.0233 \text{ in.})}$$

$$D_{xy-pf-1} = 12,968 \frac{\text{kip} - \text{in.}^2}{\text{in.}}$$

Test Rotation #2. For the second test rotation, the deck was rotated 90° from rotation #1 and the procedure was repeated.

The span of the deck specimen and applied load remained the same.

$$L = 78 \text{ in.}$$

$$P = 247 \text{ lbs.} = 0.247 \text{ kip}$$

For this test rotation, six test runs were completed to ensure repeatability of the data and to determine averages. The individual test run and average displacement measurements at the loaded free corner are shown in Table B-37.

Table B-37: Measured displacement at loaded free corner

Test Run #	CH_38 Displacement (in.)
1	0.023
2	0.022
3	0.023
4	0.024
5	0.023
6	0.023
Average (Δ_L)	0.023

Therefore, the stiffness of the deck in torsion (D_{xy}) for this test rotation was computed as:

$$D_{xy-pf-2} = \frac{PL^2}{4 \Delta_L} = \frac{(0.247 \text{ kip})(70 \text{ in.})^2}{(4)(0.023 \text{ in.})}$$

$$D_{xy-pf-2} = 13,155 \frac{\text{kip} - \text{in.}^2}{\text{in.}}$$

Test Rotation #3. For the third test rotation, the deck was rotated 90° from rotation #2 and the procedure was repeated.

The span of the deck specimen and applied load remained the same.

$$L = 70 \text{ in.}$$

$$P = 247 \text{ lbs.} = 0.247 \text{ kip}$$

For this test rotation, six test runs were completed to ensure repeatability of the data and to determine averages. The individual test run and average displacement measurements at the loaded free corner are shown in Table B-38.

Table B-38: Measured displacement at loaded free corner

Test Run #	CH_38 Displacement (in.)
1	0.023
2	0.022
3	0.023
4	0.024
5	0.022
6	0.021
Average (Δ_L)	0.0225

Therefore, the stiffness of the deck in torsion (D_{xy}) for this test rotation was computed as:

$$D_{xy-pf-3} = \frac{PL^2}{4 \Delta_L} = \frac{(0.247 \text{ kip})(70 \text{ in.})^3}{(4)(0.0225 \text{ in.})}$$

$$D_{xy-pf-3} = 13,448 \frac{\text{kip} - \text{in.}^2}{\text{in.}}$$

Average Torsional Stiffness (D_{xy}). The average measured torsional stiffness (D_{xy}) of the subassembly partially filled grid deck specimen was:

$$D_{xy-pf} = \frac{D_{xy-pf-1} + D_{xy-pf-2} + D_{xy-pf-3}}{3} = \frac{12,968 + 13,155 + 13,448}{3} = 13,190 \frac{\text{kip} - \text{in.}^2}{\text{in.}}$$

B.6.4 Measured Stiffness Properties of Subassembly Partially Filled Grid Deck Specimen

As previously computed, the average measured stiffness of the deck in the strong (D_x) and weak (D_y) directions as well as the torsion stiffness were:

$$D_{x-pf} = 71,712 \frac{\text{kip} - \text{in.}^2}{\text{in.}}$$

$$D_{y-pf} = 19,995 \frac{\text{kip} - \text{in.}^2}{\text{in.}}$$

$$D_{xy-pf} = 13,190 \frac{\text{kip} - \text{in.}^2}{\text{in.}}$$

Therefore, the orthotropic ratio of the subassembly partially filled grid deck specimen was computed as:

$$D_{pf} = \frac{D_{x-pf}}{D_{y-pf}} = \frac{71,712}{19,995} = 3.6$$

Moreover, the torsion stiffness parameter for this specimen was computed as:

$$\alpha_{pf} = \frac{2D_{xy-pf}}{\sqrt{D_{x-pf}D_{y-pf}}} = \frac{2(13,190)}{\sqrt{(71,712)(19,995)}} = 0.7$$

B.7 Subassembly Partially Filled Grid Deck Specimen Theoretical Stiffness

B.7.1 Strong Direction Stiffness (D_x)

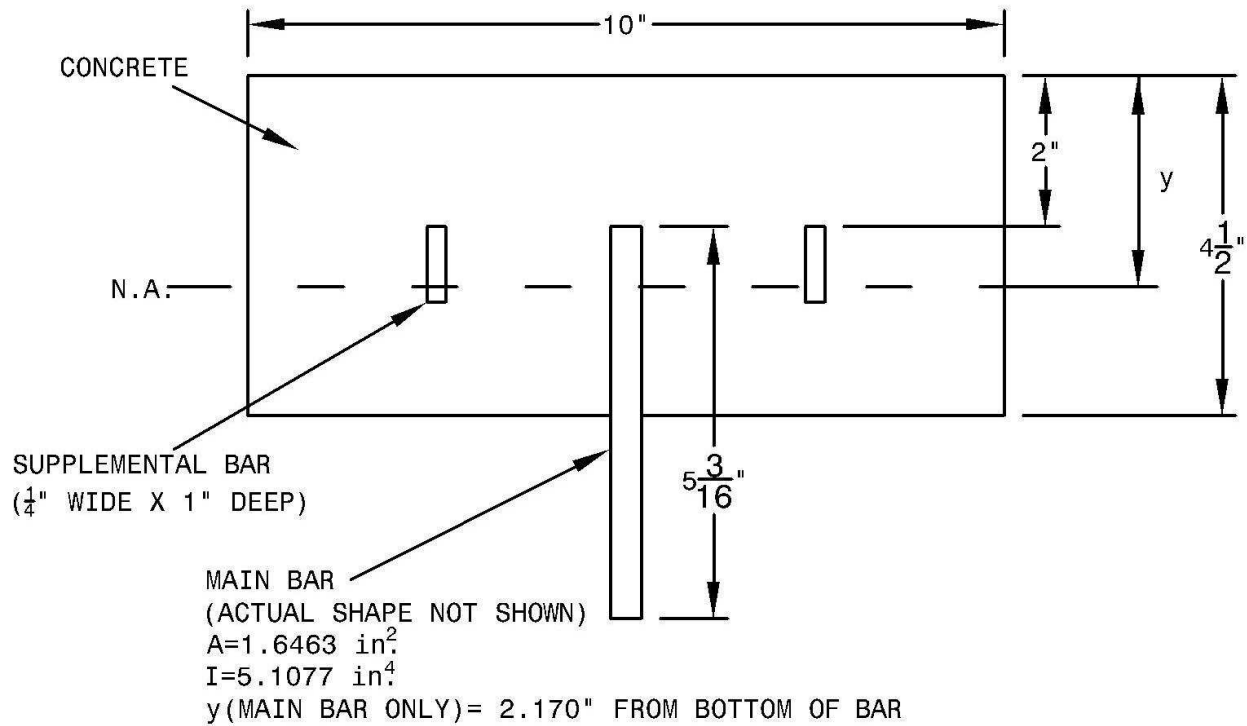


Figure B-14: Original model of partially filled grid deck specimen strong direction (D_x)

To compute the theoretical stiffness of the subassembly partially filled grid deck specimen in the strong direction (D_x), a standard 10 inch cross section was used as shown in Figure B-14. The transform section is used because the stiffness test was conducted at a very low load where the specimen remains pristine.

In the original computation of the theoretical stiffness of the subassembly partially filled grid deck specimen in the strong direction (D_x), the entire section contributed to the stiffness of the deck as shown in the following calculations.

Based on the concrete compressive strength tests performed at 28 days, the compressive strength of the concrete was taken as:

$$f'_c = 5500 \text{ psi}$$

This was greater than the minimum specified compressive strength of 4000 psi.

Based on the mill certifications provided by the fabricator, the yield strength of the steel in the deck was taken as:

$$F_y = 60 \text{ ksi}$$

This was also greater than the minimum specified yield strength required.

The modulus of elasticity of steel (E_s) was taken as:

$$E_s = 29000 \text{ ksi}$$

The modulus of concrete was computed as:

$$E_c = w^{1.5} \sqrt{f'_c}$$

$$E_c = 145^{1.5} \sqrt{5.5}$$

$$E_c = 4095 \text{ ksi}$$

Therefore, the modular ratio was:

$$n = \frac{E_s}{E_c} = \frac{29000}{4095} = 7.1$$

Computing the location of the neutral axis of the cross section:

$$y = \frac{2.170 * 1.6463 + (2 * 0.25) * (5.1875 - 0.5) + \left(\frac{10}{7.1} * 4.5\right) * \left(7.1875 - \frac{4.5}{2}\right)}{1.6463 + (2 * 0.25) + \left(\frac{10}{7.1} * 4.5\right)}$$

$$y = \frac{3.59 + 2.34 + 31.29}{1.6463 + 0.5 + 6.34}$$

$$y = 4.39" \text{ from bottom of the main bar}$$

$$y = 2.80" \text{ from top of concrete}$$

When computing the moment of inertia, it was assumed that all of the concrete contributed to the stiffness of the deck. Therefore, the moment of inertia of the cross-section was computed as:

$$I = \sum (I_0 + Ad^2)$$

$$I = (I_0 + Ad^2)_{\text{Main Bar}} + (I_0 + Ad^2)_{\text{Supplemental Bars}} + (I_0 + Ad^2)_{\text{Concrete}}$$

$$I = (5.1077 + 1.6463(2.211)^2) + [2 \left(\frac{0.25(1)^3}{12} + 2(0.25 * 1)(0.3)^2 \right) + \left[\frac{\frac{10}{7.1}(4.5)^3}{12} + \left(\frac{10}{7.1} * 4.5 \right) (0.55)^2 \right]]$$

$$I = [5.1077 + 8.05] + [0.02083 + 0.0135] + [10.70 + 1.92]$$

$$I = 25.82 \text{ in.}^4$$

Using the theoretical Moment of Inertia, the theoretical stiffness was computed as follows:

$$D_{x\text{-theoretical}} = \frac{EI}{w_{\text{cross-section}}} = \frac{29000 \frac{\text{kip}}{\text{in.}^2} * 25.82 \text{ in.}^4}{10 \text{ in.}} = 74,878 \frac{\text{kip} - \text{in.}^2}{\text{in.}}$$

As previously computed, the experimentally measured stiffness of the subassembly partially filled grid deck specimen was:

$$D_{x\text{-measured}} = 71,700 \frac{\text{kip} - \text{in.}^2}{\text{in.}}$$

Therefore, the ratio of the theoretical stiffness to the experimentally measured stiffness was:

$$\text{Ratio} = \frac{D_{x\text{-theoretical}}}{D_{x\text{-measured}}} = \frac{74,878}{71,700} = 1.04$$

Although this ratio showed that the stiffness of the theoretical model was within 15% of that experimentally measured, another model was developed and considered based on the behavior of this specimen in the weak axis direction (D_y).

New Model.

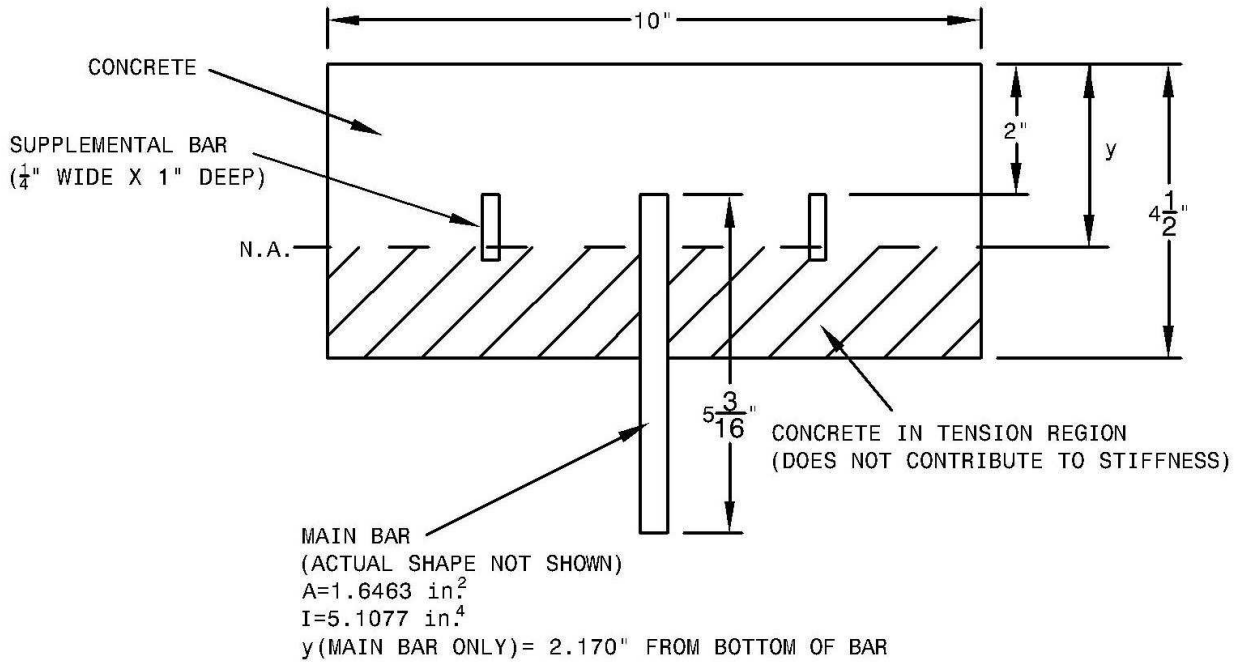


Figure B-15: New model of partially filled grid deck specimen strong direction (D_x)

It was found that the concrete below the neutral axis would not contribute to the stiffness of the deck since concrete is ineffective in tension. Therefore, the deck was remodeled such that the concrete below the axis did not contribute to the theoretical stiffness of the deck as shown in Figure B-15.

The following properties remained the same as originally measured or computed:

$$f'_c = 5500 \text{ psi}$$

$$F_y = 60 \text{ ksi}$$

$$E_s = 29000 \text{ ksi}$$

$$E_c = 4095 \text{ ksi}$$

$$n = \frac{E_s}{E_c} = \frac{29000}{4095} = 7.1$$

$$y = 4.39" \text{ from bottom of the main bar}$$

$$y = 2.80" \text{ from top of concrete}$$

As previously discussed, when computing the moment of inertia, it was assumed that the concrete below the neutral axis did not contribute to the stiffness of the deck because concrete cannot withstand tension. Therefore, the moment of inertia of the cross-section was computed as:

$$I = \sum (I_0 + Ad^2)$$

$$I = (I_0 + Ad^2)_{\text{Main Bar}} + (I_0 + Ad^2)_{\text{Supplemental Bars}} + (I_0 + Ad^2)_{\text{Concrete}}$$

$$I = (5.1077 + 1.6463(2.211)^2) + [2 \left(\frac{0.25(1)^3}{12} + (0.25 * 2 * 1)(0.3)^2 \right)] + \left[\frac{\frac{10}{7.1}(2.8)^3}{12} + \right.$$

$$\left. \left(\frac{10}{7.1} * 2.8 \right) \left(\frac{2.8}{2} \right)^2 \right]$$

$$I = [5.1077 + 8.05] + [0.04167 + 0.045] + [2.58 + 7.73]$$

$$I = 23.56 \text{ in.}^4$$

Using the theoretical moment of inertia, the theoretical stiffness was computed as follows:

$$D_{x\text{-theoretical}} = \frac{EI}{W_{\text{cross-section}}} = \frac{29000 \frac{\text{kip}}{\text{in.}^2} * 23.56 \text{ in.}^4}{10 \text{ in.}} = 68,324 \frac{\text{kip} - \text{in.}^2}{\text{in.}}$$

As previously computed, the experimentally measured stiffness of the subassembly partially filled grid deck specimen was:

$$D_{x\text{-measured}} = 71,700 \frac{\text{kip} - \text{in.}^2}{\text{in.}}$$

Therefore, the ratio of the theoretical stiffness to the experimentally measured stiffness was:

$$\text{Ratio} = \frac{D_{x\text{-theoretical}}}{D_{x\text{-measured}}} = \frac{68,324}{71,700} = 0.95$$

Since the ratio showed that the stiffness of the theoretical model was within 15% of that experimentally measured, the model was considered adequate. Moreover, based on the behavior of the deck from the weak direction stiffness (D_y) test, this model more accurately modeled the behavior of this deck than the original.

B.7.2 Weak Direction Stiffness (D_y)

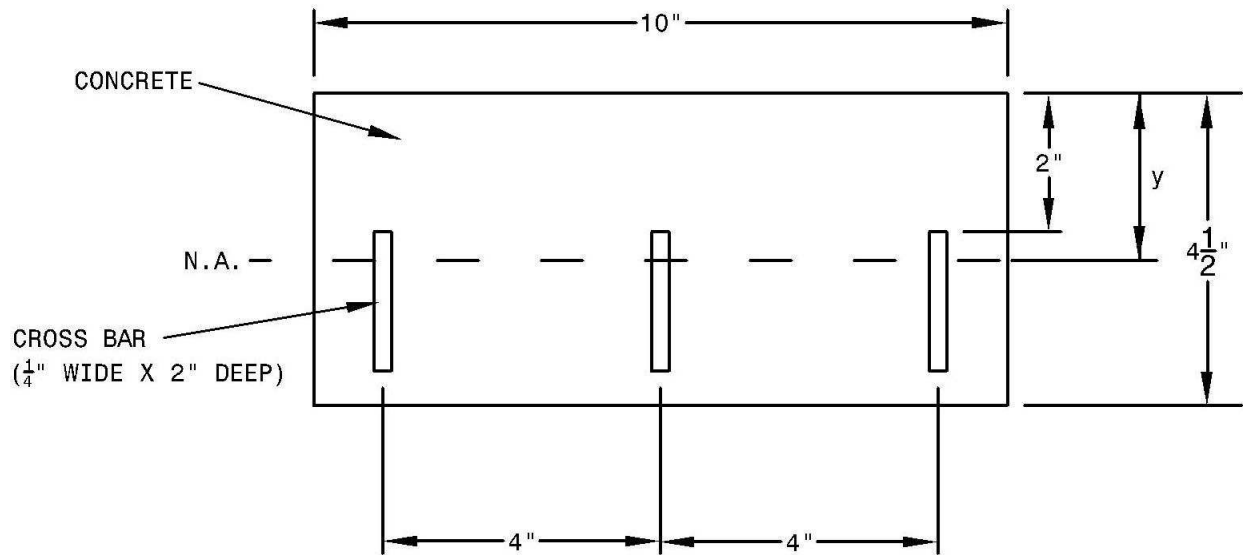


Figure B-16: Original model of partially filled grid deck specimen weak direction (D_y)

In the original computation of the theoretical stiffness of the subassembly partially filled grid deck specimen in the weak direction (D_y), the entire section contributed to the stiffness of the deck as shown in the following calculations (see Figure B-16).

Based on the concrete compressive strength tests performed at 28 days, the compressive strength of the concrete was taken as:

$$f'_c = 5500 \text{ psi}$$

This was greater than the minimum specified compressive strength of 4000 psi.

Based on the mill certifications provided by the fabricator, the yield strength of the steel in the deck was taken as:

$$F_y = 60 \text{ ksi}$$

This was also greater than the minimum specified yield strength required.

The modulus of elasticity of steel (E_s) was taken as:

$$E_s = 29000 \text{ ksi}$$

The modulus of concrete was computed as:

$$E_c = w^{1.5} \sqrt{f'_c}$$

$$E_c = 145^{1.5} \sqrt{5.5}$$

$$E_c = 4095 \text{ ksi}$$

Therefore, the modular ratio was:

$$n = \frac{E_s}{E_c} = \frac{29000}{4095} = 7.1$$

Computing the location of the neutral axis of the cross section:

$$y = \frac{3(2 * 0.25)(3) + \left(\frac{10}{7.1} * 4.5\right) * \left(\frac{4.5}{2}\right)}{3(2 * 0.25) + \left(\frac{10}{7.1} * 4.5\right)}$$

$$y = \frac{4.5 + 14.3}{1.5 + 6.3}$$

$$y = 2.41" \text{ from top of the concrete}$$

When computing the moment of inertia, it was originally assumed that all of the concrete in the cross section contributed to the stiffness of the deck. Therefore, the moment of inertia of the cross-section was computed as:

$$I = \sum (I_0 + Ad^2)$$

$$I = (I_0 + Ad^2)_{\text{Cross Bars}} + (I_0 + Ad^2)_{\text{Concrete}}$$

$$I = \left[\left(3 \frac{0.25(2)^3}{12} + 3(0.25 * 2)(3 - 2.41)^2 \right) + \left[\frac{\frac{10}{7.1}(4.5)^3}{12} + \left(\frac{10}{7.1} * 4.5 \right) \left(\frac{4.5}{2} - 2.41 \right)^2 \right] \right]$$

$$I = 0.5 + 0.52 + 10.70 + 0.16$$

$$I = 11.88 \text{ in.}^4$$

Using the theoretical moment of inertia, the theoretical stiffness was computed as follows:

$$D_{y\text{-theoretical}} = \frac{EI}{w_{\text{cross-section}}} = \frac{29000 \frac{\text{kip}}{\text{in.}^2} * 11.88 \text{ in.}^4}{10 \text{ in.}} = 34,452 \frac{\text{kip} - \text{in.}^2}{\text{in.}}$$

As previously computed, the experimentally measured stiffness of subassembly open grid deck specimen #1 was:

$$D_{y\text{-measured}} = 19,990 \frac{\text{kip} - \text{in.}^2}{\text{in.}}$$

Therefore, the ratio of the theoretical stiffness to the experimentally measured stiffness was:

$$\text{Ratio} = \frac{D_{x\text{-theoretical}}}{D_{x\text{-measured}}} = \frac{34,452}{19,990} = 1.72$$

Since the ratio showed that the stiffness of the theoretical model was not within 15% of that experimentally measured, the model was considered inadequate. Therefore, the behavior of the deck was further investigated to ensure that a more accurate model was created.

New Model.

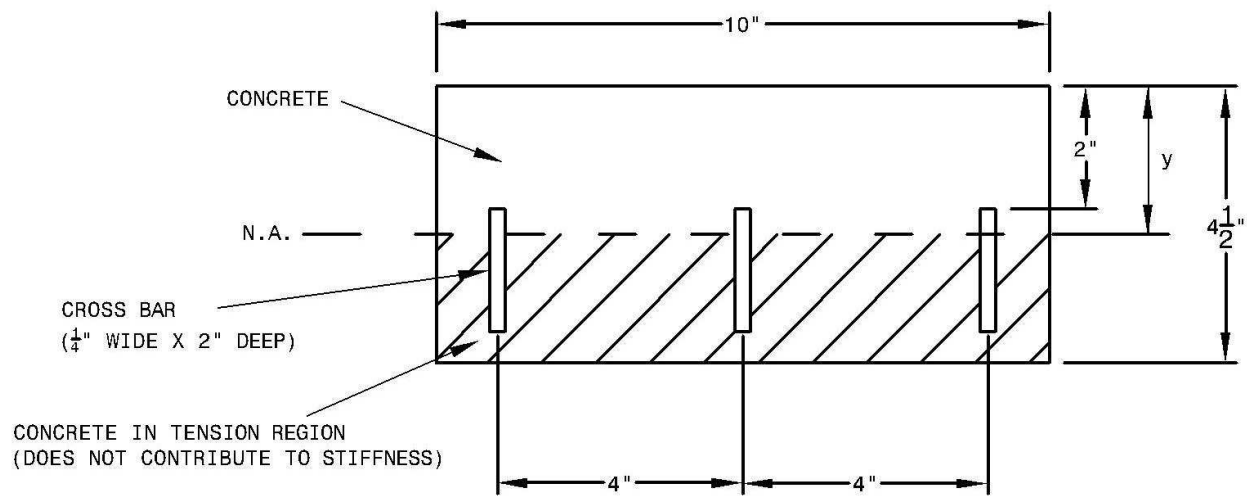


Figure B-17: New model of partially filled grid deck specimen weak direction (D_y)

It was found that the concrete below the neutral axis would not contribute to the stiffness of the deck since concrete is ineffective in tension. Therefore, the deck was remodeled such that the concrete below the axis did not contribute to the theoretical stiffness of the deck as shown in Figure B-17.

The following properties remained the same as originally measured or computed:

$$f'_c = 5500 \text{ psi}$$

$$F_y = 60 \text{ ksi}$$

$$E_s = 29000 \text{ ksi}$$

$$E_c = 4095 \text{ ksi}$$

$$n = 7.1$$

$$y = 2.41 \text{ " from top of the concrete}$$

As previously discussed, when computing the moment of inertia, it was assumed that the concrete below the neutral axis did not contribute to the stiffness of the deck because concrete is ineffective in tension. Therefore, the moment of inertia of the cross-section was computed as:

$$I = \sum (I_0 + Ad^2)$$

$$I = (I_0 + Ad^2)_{\text{Cross Bars}} + (I_0 + Ad^2)_{\text{Concrete}}$$

$$I = \left[\left(3 \frac{0.25(2)^3}{12} + 3(0.25 * 2)(3 - 2.41)^2 \right) + \left[\frac{\frac{10}{7.1}(2.41)^3}{12} + \left(\frac{10}{7.1} * 2.41 \right) \left(\frac{2.41}{2} \right)^2 \right] \right]$$

$$I = 0.5 + 0.52 + 1.64 + 4.93$$

$$I = 7.59 \text{ in.}^4$$

Using the theoretical moment of inertia, the theoretical stiffness was computed as follows:

$$D_{y\text{-theoretical}} = EI = 29000 \frac{\text{kip}}{\text{in.}^2} * 7.59 \text{ in.}^4 = 22,011 \frac{\text{kip} - \text{in.}^2}{\text{in.}}$$

As previously computed, the experimentally measured stiffness of subassembly open grid deck specimen #1 was:

$$D_{y\text{-measured}} = 19,990 \frac{\text{kip} - \text{in.}^2}{\text{in.}}$$

Therefore, the ratio of the theoretical stiffness to the experimentally measured stiffness was:

$$\text{Ratio} = \frac{D_{x\text{-theoretical}}}{D_{x\text{-measured}}} = \frac{22,011}{19,990} = 1.10$$

Since the ratio showed that the stiffness of the theoretical model was within 15% of that experimentally measured, the model was considered adequate.

B.8 Computing Loads to be Applied for Subassembly Strength Verification Tests

B.8.1 Subassembly Longitudinal Splice Strength Verification Test

Based on the results of the subassembly stiffness tests of the partially filled grid deck specimen, the properties of the deck to be used for the subassembly longitudinal splice were determined. Therefore, the properties of the subassembly longitudinal splice specimen were as follows:

Orthotropic Ratio, $D = 3.6$

Torsion Parameter, $\alpha = 0.7$

Span of Deck panel, $L = 6' = 72''$

Width of deck, $w = 3'8''$

Since these numbers are not explicitly shown in the Tables shown in Appendix F, linear interpolation was required to determine the load to be applied for a span of 72 inches. Table B-39 lists each of the parameters and the resulting loads based on the aforementioned tables. It is noted that all of these values correspond to a span (L) of 72 inches.

Table B-39: Prior to isolating variables of deck specimen

Load Number	Torsion parameter α	Orthotropic Ratio, $D=D_x/D_y$	Width, w (ft.)	Load to be applied, P (kips)
1	0.50	2.5	3	24.3
2	0.50	2.5	4	29.3
3	0.75	2.5	3	22.3
4	0.75	2.5	4	27.0
5	0.50	5	3	26.9
6	0.50	5	4	31.9
7	0.75	5	3	24.7
8	0.75	5	4	29.5

Linear interpolation was then used to find the load to be applied at a deck width 3'8" based on Table B-39. As shown in Table B-40, this eliminated the width variable, while the orthotropic ratio and torsion parameter remained.

Table B-40: After isolating width of deck specimen

Load Number	Torsion Parameter, α	Orthotropic Ratio, $D=D_x/D_y$	Width, w	Load to be Applied, P (kips)
9 (between 1 and 2)	0.50	2.5	3'8"	27.6
10 (between 3 and 4)	0.75	2.5	3'8"	25.4
11 (between 5 and 6)	0.50	5	3'8"	30.2
12 (between 7 and 8)	0.75	5	3'8"	27.9

Once again, linear interpolation was used to find the load to be applied at an orthotropic ratio of 3.6 based on Table B-40. As shown in Table B-41, this eliminated the orthotropic ratio and left only the torsion parameter remaining.

Table B-41: After isolating orthotropic ratio of deck specimen

Load Number	Torsion Parameter α	Orthotropic Ratio, $D=D_x/D_y$	Width, w	Load to be Applied P (kips)
13 (between 9 and 11)	0.50	3.6	3'8"	28.7
14 (between 10 and 12)	0.75	3.6	3'8"	26.5

One final interpolation was done based on Table B-41 to find the load to be applied for a torsion parameter of 0.7. Therefore, the load to be applied for a single span deck at midspan was 26.9 kips as shown in Table B-42.

Table B-42: Load applied for deck specimen

Deck Span, L (in.)	Deck Width, w	Orthotropic Ratio	Torsion Parameter, α	Load to be Applied, P (kips)
72	3'8"	3.6	0.7	26.9

Since this test had a two-span rather than a single-span bridge deck and the detail of concern (i.e., the longitudinal splice) was located in the negative moment region over the interior stringer, adjustments were made to the load.

For negative moment, a factor of 80% was applied to the computed load that would be applied at the midspan of a simple span deck. This would be the required load if the simple span deck was flipped upside down and tested in the same manner as for the positive moment.

$$P=0.8*26.9$$

$$P=21.5 \text{ kips}$$

Once the required load at the midspan of a simple span deck for negative moment was computed, the equivalent moment at midspan of the deck (i.e., the negative moment region when flipped upside down) could be computed.

$$R = \frac{P}{2} = \frac{21.5}{2} = 10.75 \text{ kips} \quad \text{Computation of the reactions for a simple span deck.}$$

Therefore,

$$M_{\text{negative}} = 10.75 * 3$$

$$M_{\text{negative}} = 32.25 \text{ kip-ft}$$

Now that the required moment in the negative moment region has been computed, the load to be applied at each patch can be computed based on a two-span deck with point loads applied at 2 feet off the centerline interior stringer on each side.

$$P_{\text{req}} = \frac{32.25}{1.111} = 29.03 \text{ kips} \quad \text{Load at each patch location.}$$

NOTE: 1.111 is the negative moment over the interior stringer based on applied unit loads at 2 feet off the centerline of the stringer on each side computed based on the 6th edition of the PCI handbook.

Therefore, the total load to be applied was:

$$P_{\text{total}} = 29.03 * 2$$

$$P_{\text{total}} = 58.06 \text{ kips}$$

Therefore, it was chosen to conservatively apply a load of:

$$\underline{P_{\text{total}} = 59 \text{ kips}}$$

B.8.2 Subassembly Transverse Splice Strength Verification Test

Based on the results of the subassembly stiffness tests of the partially filled grid deck specimen, the properties of the deck to be used for the subassembly transverse splice were determined. Therefore, the properties of the subassembly transverse splice specimen were as follows:

$$D = 3.6$$

$$\alpha = 0.7$$

$$L = 6' = 72''$$

$$w = 7'8''$$

Since these numbers are not explicitly shown in the Tables shown in Appendix F, linear interpolation was required to determine the load to be applied for a span of 72 inches. Table B-43 lists each of the parameters and the resulting loads based on the aforementioned tables. It is noted that all of these values correspond to a span (L) of 72 inches.

Table B-43: Prior to isolating variables of deck specimen

Load Number	Torsion Parameter, α	Orthotropic Ratio, $D = D_x/D_y$	Width, w (ft.)	Load to be Applied, P (kips)
1	0.50	2.5	7	38.7
2	0.50	2.5	8	40.4
3	0.75	2.5	7	36.2
4	0.75	2.5	8	38.0
5	0.50	5	7	40.2
6	0.50	5	8	41.9
7	0.75	5	7	37.8
8	0.75	5	8	39.3

Linear interpolation was then used to find the load to be applied at a deck width 7'8" based on Table B-43. As shown in Table B-44, this eliminated the width variable, while the orthotropic ratio and torsion parameter remained.

Table B-44: After isolating width of the deck specimen

Load Number	Torsion Parameter, α	Orthotropic Ratio, D	Width, w	Load to be Applied, P (kips)
9 (between 1 and 2)	0.5	2.5	7'8"	39.8
10 (between 3 and 4)	0.75	2.5	7'8"	37.4
11 (between 5 and 6)	0.5	5	7'8"	41.3
12 (between 7 and 8)	0.75	5	7'8"	38.8

Once again, linear interpolation was used to find the load to be applied at an orthotropic ratio of 3.6 based on Table B-44. As shown in Table B-45, this eliminated the orthotropic ratio and left only the torsion parameter remaining.

Table B-45: After isolating orthotropic ratio of deck specimen

Load Number	Torsion Parameter, α	Orthotropic Ratio, D	Width, w	Load to be Applied, P (kips)
13 (between 9 and 11)	0.5	3.6	7'8"	40.5
14 (between 10 and 12)	0.75	3.6	7'8"	38.0

One final interpolation was done based on Table B-45 to find the load to be applied for a torsion parameter of 0.7. Therefore, the load to be applied for a single span deck at midspan was 38.5 kips as shown in Table B-46.

Table B-46: Load applied for deck specimen

Deck Span, L (in.)	Deck Width, w	Orthotropic Ratio	Torsion Parameter, α	Load to be Applied, P (kips)
72	7'8"	3.6	0.7	38.5

Since this specimen was a single span bridge deck and the detail of concern (i.e., the transverse splice) was located in the positive moment region at midspan, the computed load could be used.

Therefore, it was chosen to conservatively apply a load of:

$$P_{\text{total}} = 40 \text{ kips}$$

B.9 Stresses Measured During Strength Verification Tests

B.9.1 Subassembly Longitudinal Splice Strength Verification Test

Flexible Stringers. Stresses at critical locations throughout the deck were monitored. For the strength verification test using flexible stringers, the stresses shown in Figure B-18 were measured at the reinforcing steel bars directly between the patch loads. CH_6 and CH_10 were on the top of the reinforcing steel bars at the centerline of the longitudinal splice. CH_7 and CH_11 were the corresponding strain gages on the bottom of the reinforcing steel. As can be seen from the stress data in this figure, the reinforcing steel was undergoing negative bending as expected. It can also be seen that there was some nonlinear behavior in the reinforcing steel at higher applied loads due to cracking of the concrete in this region.

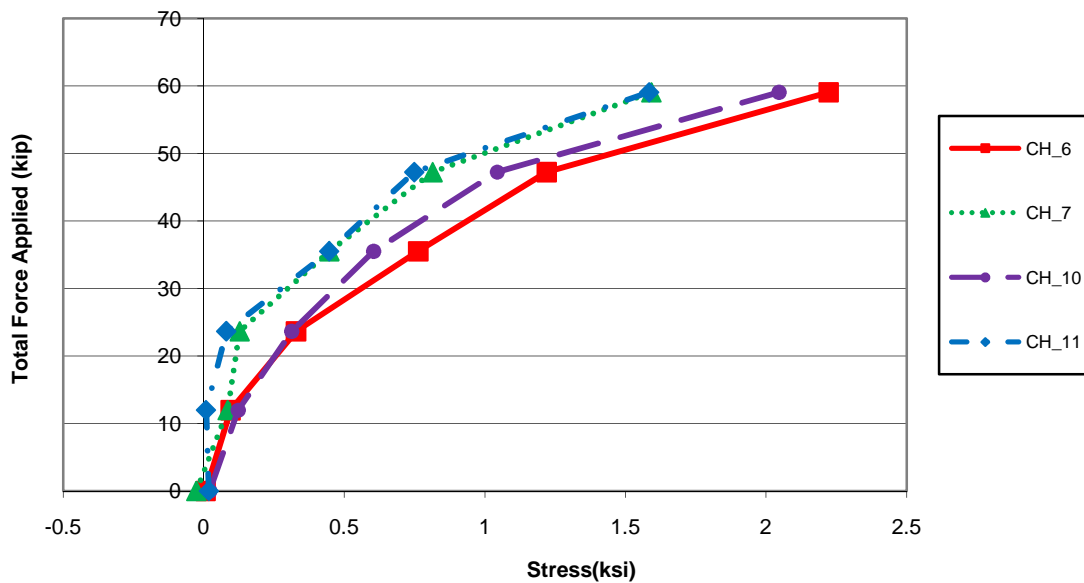


Figure B-18: Measured stresses at reinforcing steel bars directly between patch loads

Figure B-19 shows the stresses measured at midspan of the deck on the main bars in the positive transverse moment region (i.e., close to the patch loads). CH_17 and CH_27 were strain gages on the top of the main bars. CH_18 and CH_28 were the corresponding strain gages on the bottom of the main bars. It is noted that a negative stress represents a compressive stress in this figure. As shown in the figure, positive bending was experienced in this region as expected.

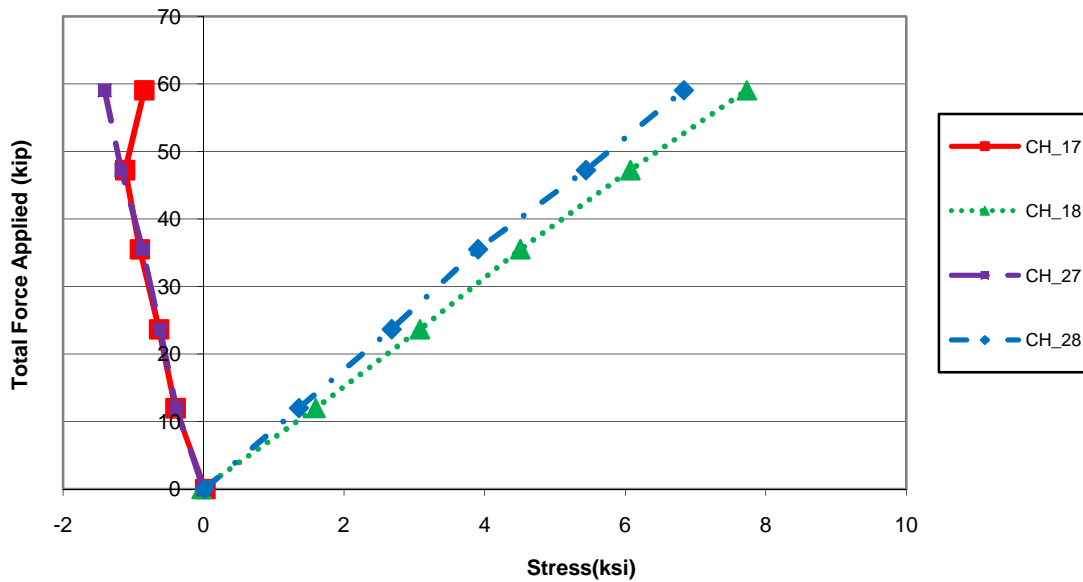


Figure B-19: Main bar stresses near patch loads

Rigid Stringers. The strength verification test was repeated with rigid stringers. The stresses, shown in Figure B-20, were measured at the same locations as for the strength verification test with flexible stringers. CH_6 and CH_10 were on the top of the reinforcing steel bars at the centerline of the longitudinal splice. CH_7 and CH_11 were the corresponding strain gages on the bottom of the reinforcing steel. It is noted that the stresses shown imply that the behavior was more linear than when flexible stringers were used. This is because the cracking of the concrete had already occurred prior to this test (i.e., using rigid stringers). Figure B-20 illustrates that the tensile stresses in the reinforcing steel were much greater than those measured when using flexible stringers.

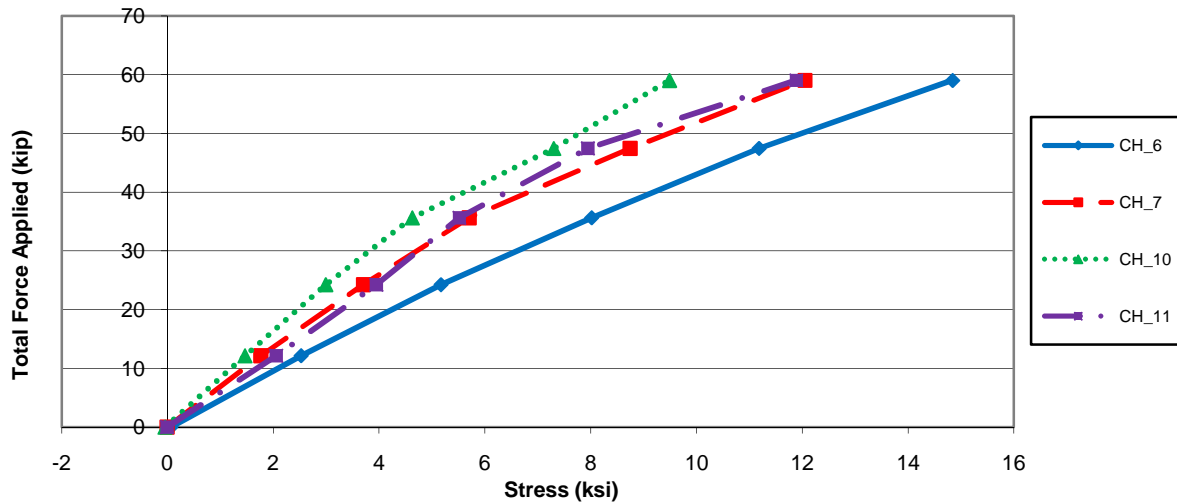


Figure B-20: Measured stresses at reinforcing steel directly between patch loads

Figure B-21 shows the stresses measured at midspan of the deck on the main bars in the positive transverse moment region (i.e., close to the patch loads) when using rigid stringers. Once again, CH_17 and CH_27 were strain gages on the top of the main bars. CH_18 and CH_28 were the corresponding strain gages on the bottom of the main bars. As can be seen in the figure, the positive bending in the main bars in this region was reduced from when flexible stringers were used.

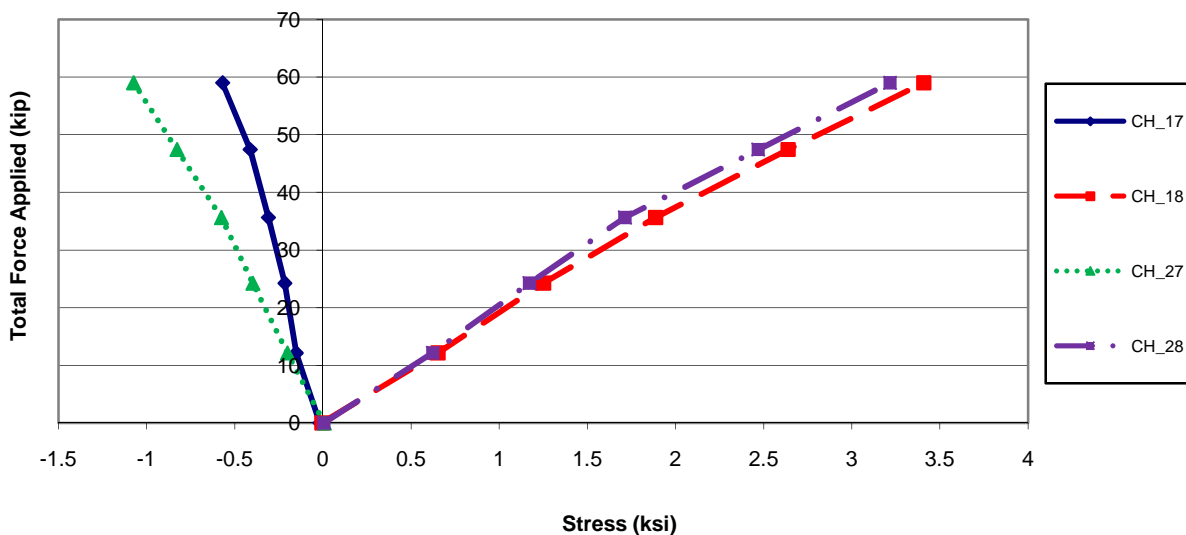


Figure B-21: Main bar stresses near patch loads

B.9.2 Subassembly Deck-to-Superstructure Connection Strength Test

Stresses were measured at critical locations of the deck-to-superstructure connection specimen for the strength test after the cyclic load test was terminated. The stresses on top of the bolt down plates on the interior stringer were measured near the weld toes and are shown in Figure B-22. It is evident that the stresses at the main bar to bolt down plate connection (i.e. welds) were relatively large. It is noted that the negative stress indicated compression. These connections were in compression because only a “pushing” load was applied to the deck for the strength. As can be seen from this figure, the behavior remained linear during this strength test.

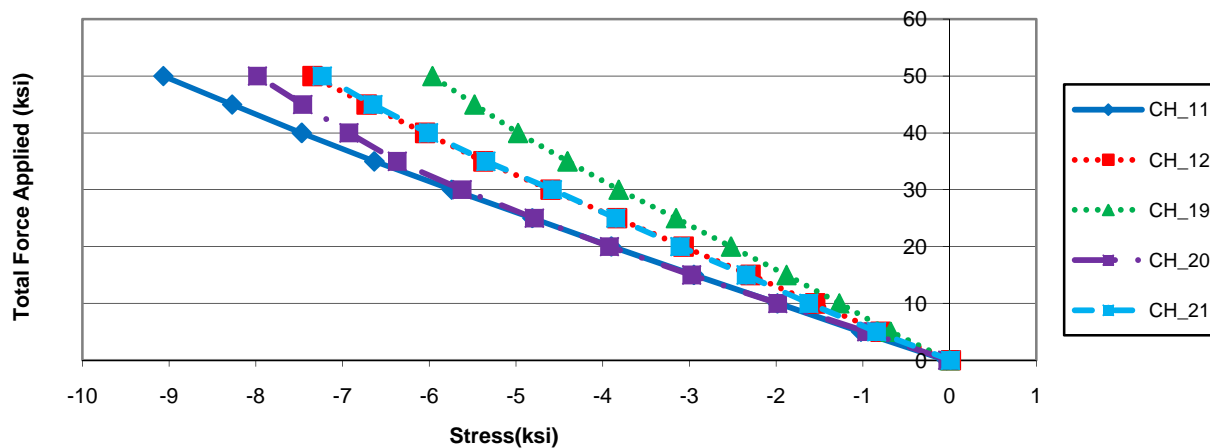


Figure B-22: Measured stresses on top of bolt down plate on interior stringer

B.9.3 Subassembly Transverse Splice Strength Verification Test

Stresses were measured at critical locations of the transverse splice deck specimen for the strength verification test and are shown in Figure B-23. CH_23 and CH_24 were strain gages located on the top and bottom, respectively, of a reinforcing steel bar under the patch load. CH_41 and CH_42 were strain gages located on the top and bottom, respectively, of another reinforcing steel bar approximately 8” away from the edge of the patch load (i.e., approximately halfway between the patch load and stringer). CH_43 and CH_44 were strain gages located on the top and bottom, respectively, of a reinforcing steel bar approximately 16” away from the edge of the patch load (i.e., close to the stringer). Figure B-23 shows that there positive bending

in the reinforcing steel at the centerline of the transverse splice. It is also evident that the behavior was linear. It is illustrated that the measured stress was greatest in the reinforcing steel under the patch load (i.e., CH_23 and CH_24) and decreased in the reinforcing steel as the distance from the load patch increased as expected. As can be seen from this figure, the behavior remained essentially linear during this strength verification test. It is noted that two more runs of this strength test were conducted. The results were very similar to the initial test completed. Therefore, only the results from the first test are shown in this appendix.

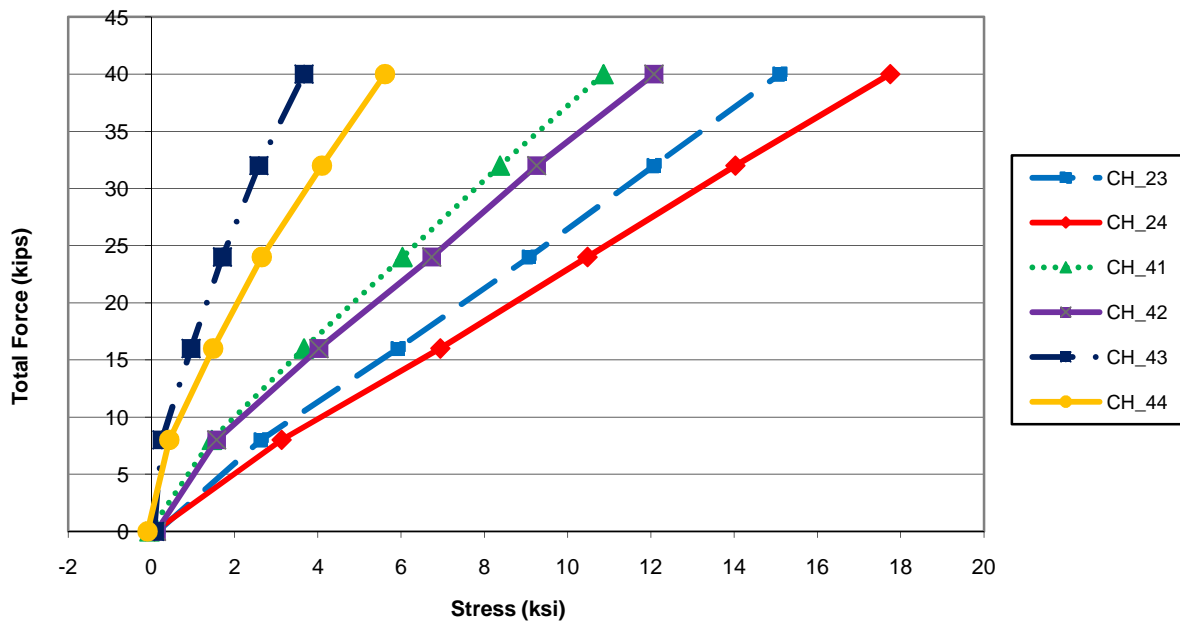


Figure B-23: Measured stress of reinforcing steel

APPENDIX C –
Results of Deck Specimen Coring

Concrete Cores LONGITUDINAL SPLICE TESTS. The damage caused by cracking of the concrete found on the bridge deck at the conclusion of the longitudinal splice test was further investigated by applying a low-viscosity epoxy with fluorescent dye to the cracks. Concrete cores were then removed from the bridge to evaluate the extent of cracking caused by the cyclic loading and the ability for the penetration of deicing salts to the deck steel. The locations where the concrete cores were removed are shown in Figure C-1.

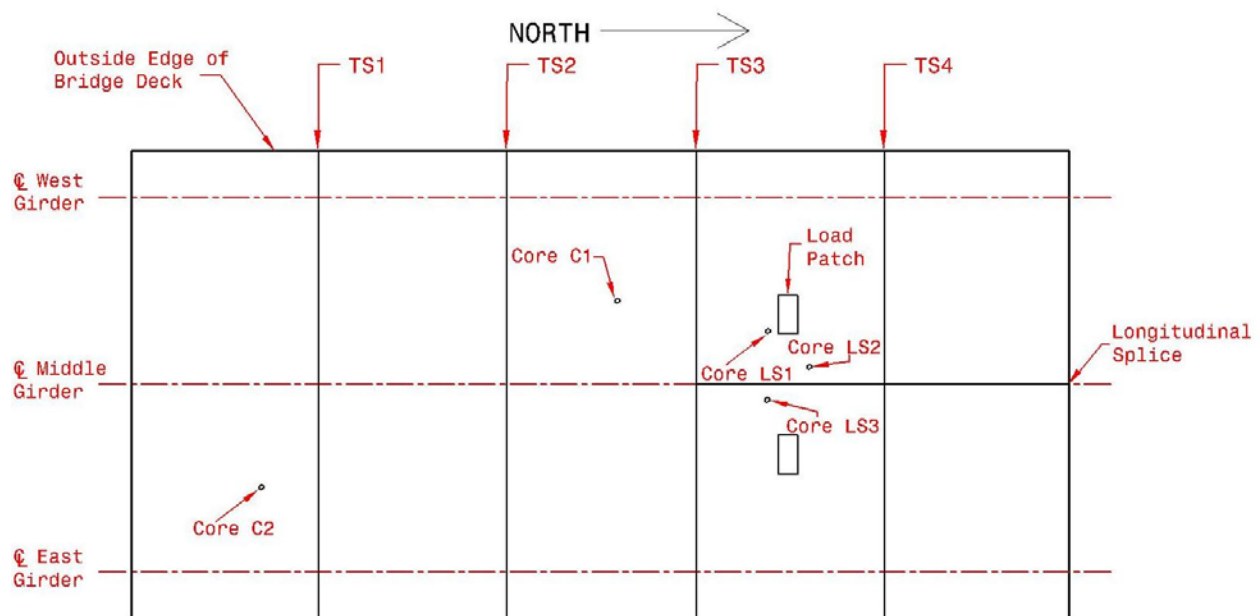


Figure C-1: Locations of longitudinal splice concrete cores

A total of five cores were removed from the deck. Two cores were taken from areas of the bridge deck away from the longitudinal splice cyclic test location. These cores were removed to evaluate the extent of significant cracks found throughout the bridge deck which were not expected to have grown due to the longitudinal splice test (i.e., these can be considered control specimens). These cores were labeled in Figure C-1 as Core C1 and Core C2.

Three cores were taken from the area affected by the longitudinal splice cyclic load test to evaluate the extent of cracking caused by the cyclic loading. One of the cores was taken from a location near the west load patch, which experienced significant positive transverse moments, and is labeled Core LS1 in Figure C-1. The other two cores (Cores LS2 and LS3 from Figure

C-1) were taken from locations near the middle girder, which was predominately loaded in negative transverse moment.

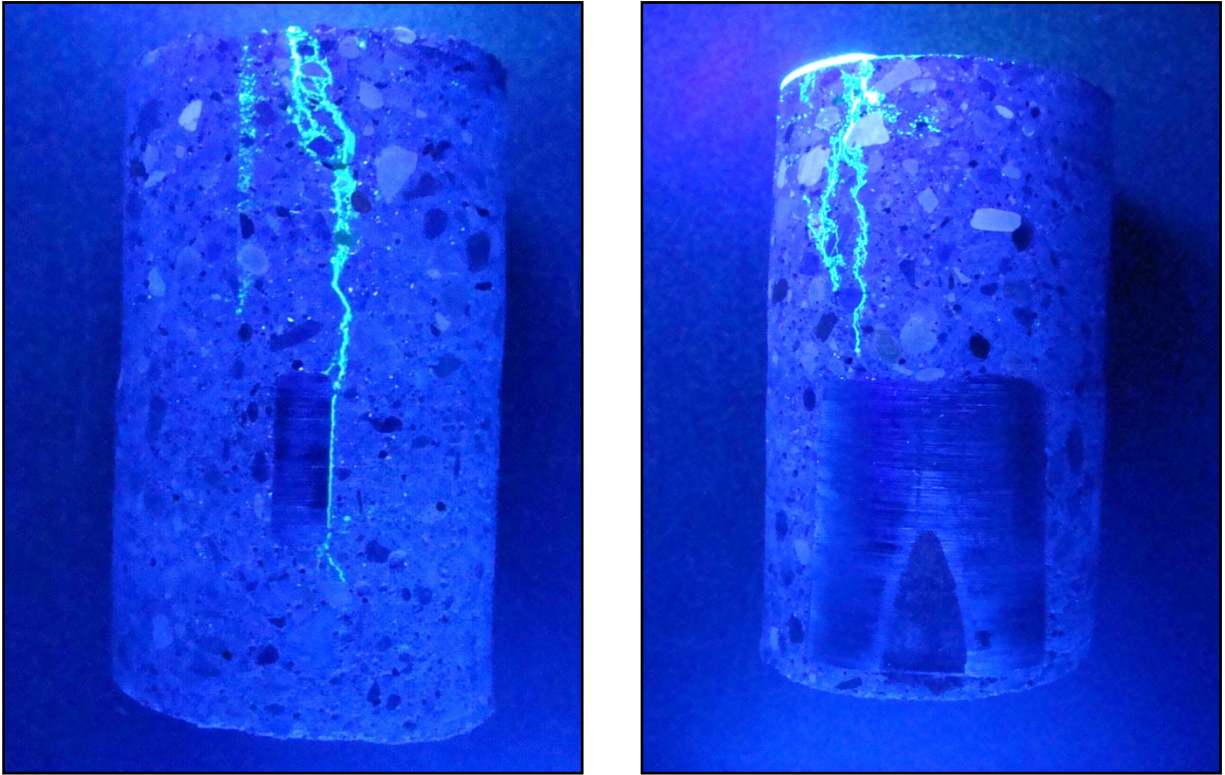


Figure C-2: Core C1 (left) west elevation; (right) east elevation

Figure C-2 illustrates a view of the west and east elevations of Core C1. This core was taken at the location of a large shrinkage crack, which is located away from the location of cyclic tests and other deck splice details. The crack in **Figure** C-2(left) extended through the deck to a steel supplemental bar. The epoxy then flowed along the bar and extended slightly beyond the bar. The crack shown in **Figure** C-2(right) extended through the core stopping just before reaching the top of a cross bar.

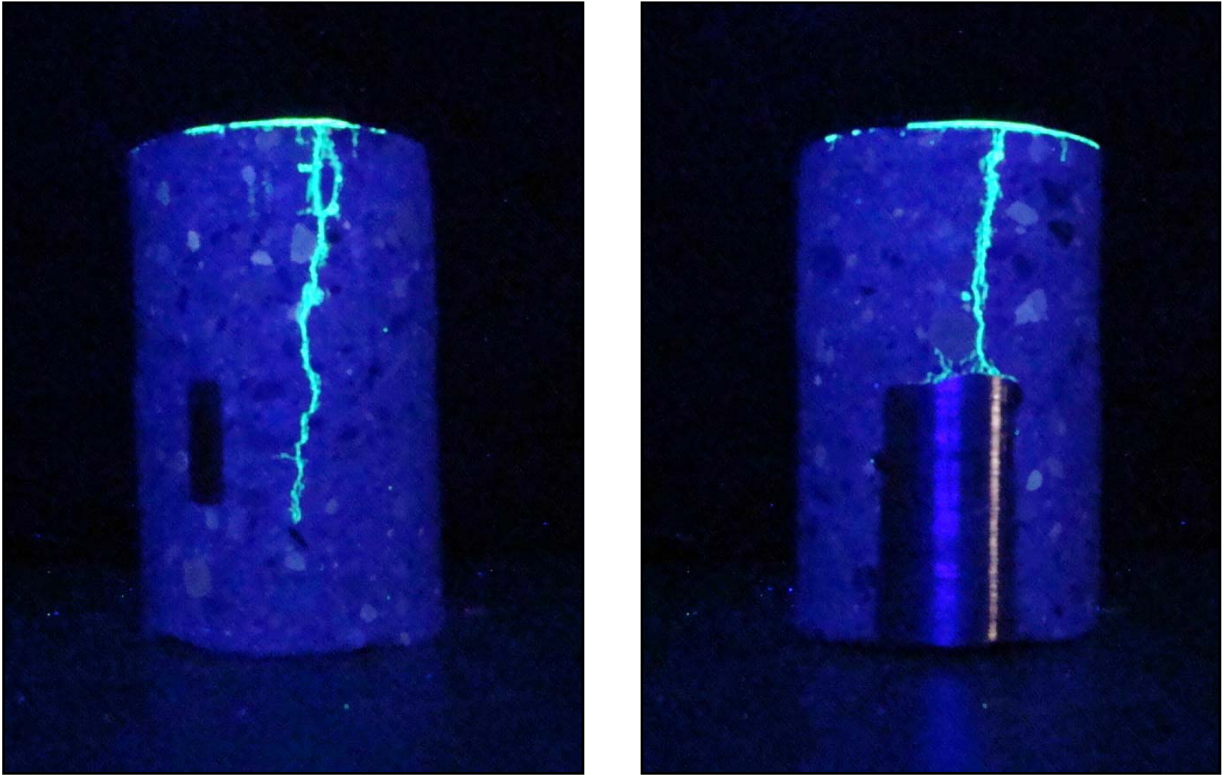


Figure C -3: Core C2 (left) west elevation; (right) east elevation

Figure C -3 illustrates a view of the west and east elevations of Core C2. This core was taken on another large shrinkage crack which was located away from the location of cyclic tests and other deck splice details. This location was similar to the location of Core C1. The crack in Figure C -3(left) extended through the deck to below a steel supplemental bar. This crack did not cross the supplemental bar at the location where the core was taken but it is likely that the crack would intercept the supplemental bars at another location along its length. The crack in Figure C -3(right) extended to a cross bar, which allowed the epoxy to flow along the cross bar for a small length.

The significant cracks found in Core C1 and Core C2 illustrate the extension of the cracking on the bridge deck away from the cyclic load beyond the concrete cover. These cracks seem to have been primarily caused by shrinkage of the deck.

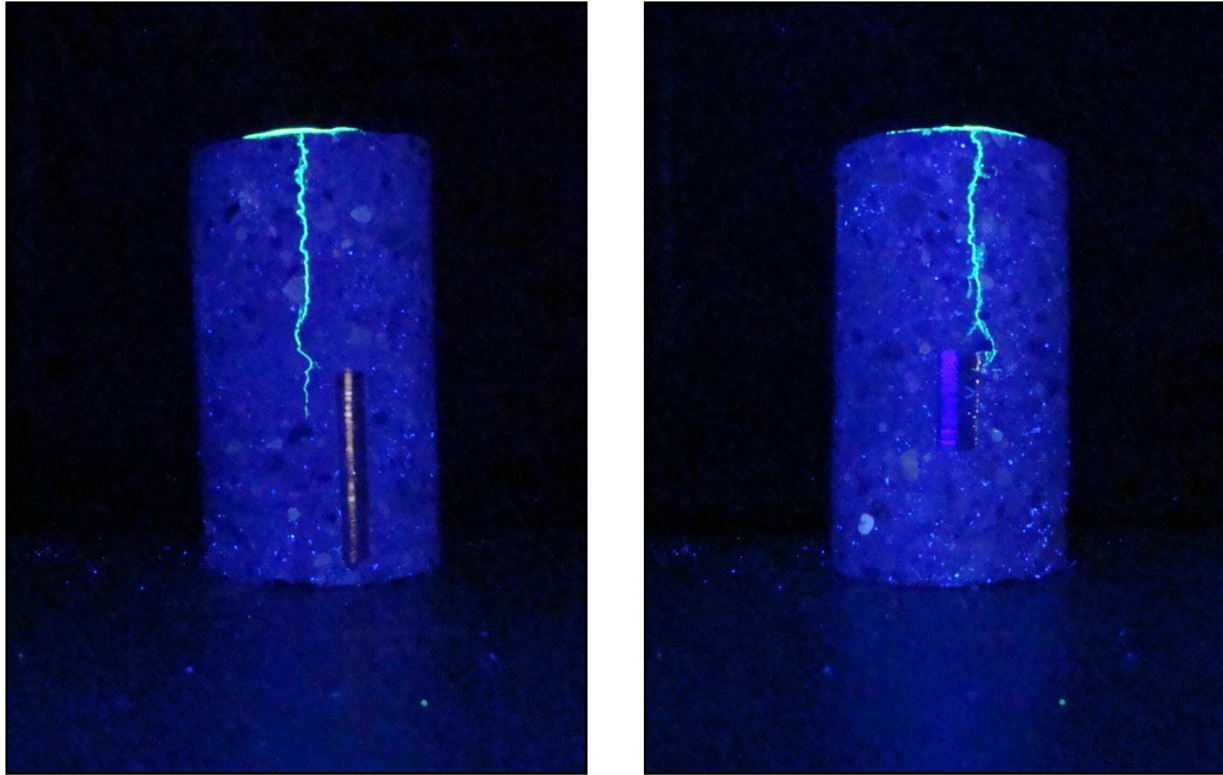


Figure C -4: Core LS1 (left) northeast elevation; (right) southwest elevation

Figure C -4 shows a view of the northeast and southwest elevations of Core LS1. This core was taken on a crack that was located near the west load patch in the longitudinal splice cyclic test. This position was chosen since it underwent the largest positive moment cycles during the longitudinal splice test. The crack in Figure C -4(left) extended through the deck to below the top of a cross bar. The crack did not cross the cross bar at the location where the core was taken, but it is likely that the crack would intercept the cross bar at another location along its length since the crack is not parallel to this bar. The crack in Figure C -4(right) extended to the top corner of a supplemental bar, but the epoxy did not flow along the side of the supplemental bar at the location where the core was taken.

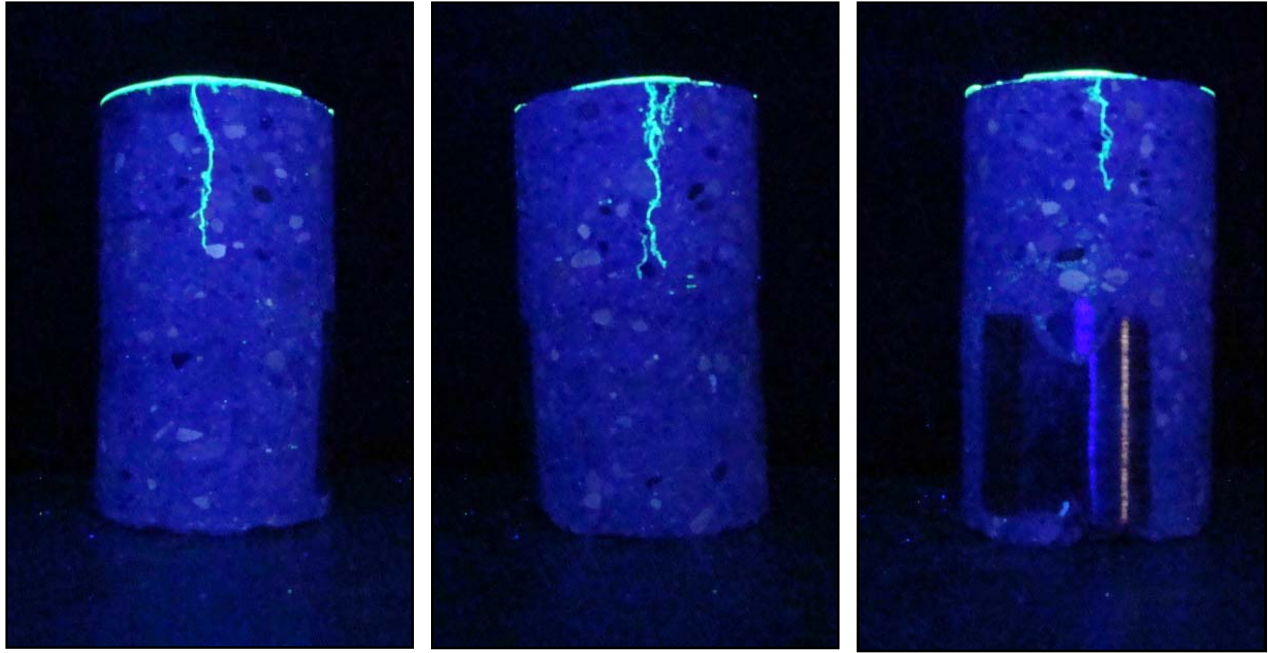


Figure C -5: Core LS2 (left) north elevation; (middle) south elevation; (right) west elevation

Figure C -5 shows views of the north, south, and west elevations of Core LS2. This core was taken on a crack located between the load patches during the longitudinal splice cyclic test. Since the middle girder was located directly below the splice, this core could not be taken through the centerline of the splice. Therefore, a core was taken next to the top flange of the middle girder. This position was chosen since it was very close to the splice and underwent negative moment cycles during testing. The cracks in **Figure C -5(left)** and **Figure C -5(middle)** extended into the deck for approximately one-third of the concrete depth. These cracks do not cross any deck steel at the location of the core. The crack in **Figure C -5(right)** joined with the other cracks in the middle of the core and is slightly smaller than the other cracks. This crack extended only slightly into the deck and did not reach the deck steel. It should be noted that the deck steel visible in **Figure C -5(right)** is a notched cross bar with a longitudinal splice reinforcing bar resting in this notch.

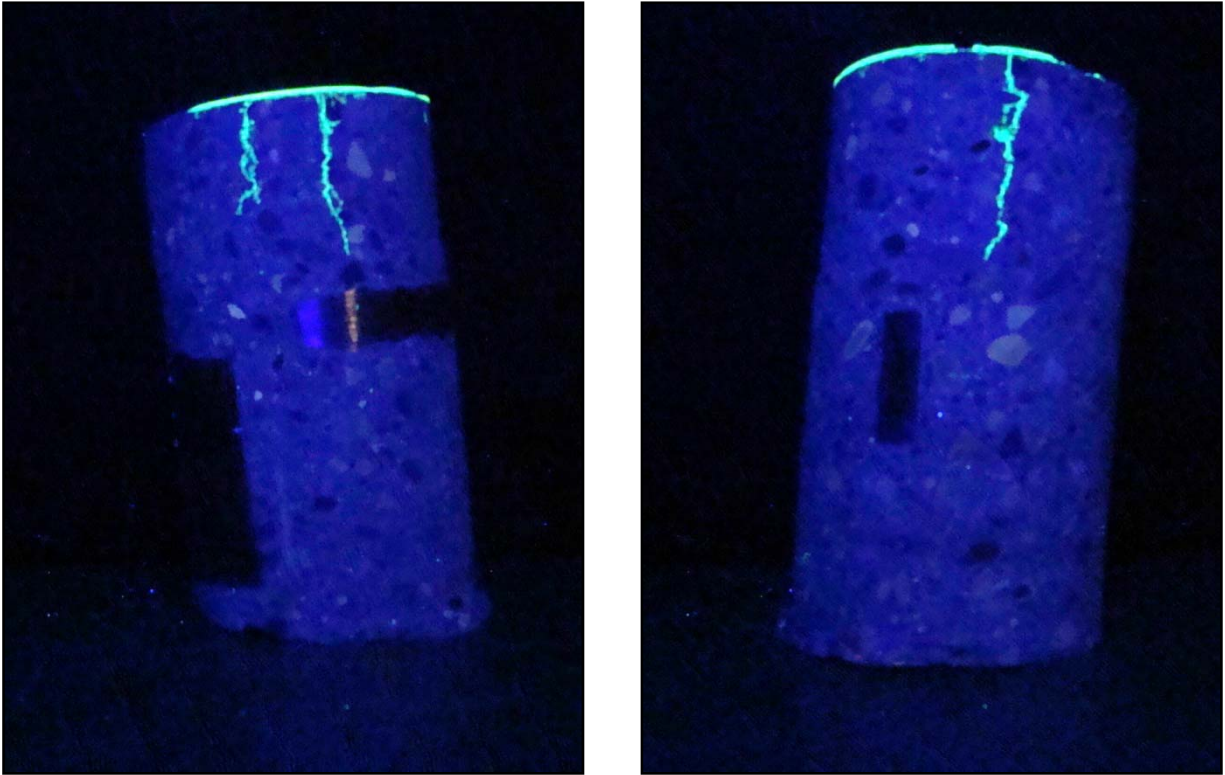


Figure C -6: Core LS3 (left) north-northeast elevation; (right) southwest elevation

Figure C -6 illustrates views of the north-northeast and southwest elevations of Core LS3. This core was taken on a crack located between the load patches during the longitudinal splice cyclic test. This core was taken near the top flange on the opposite side of the middle girder to Core LS2. This position was chosen since it underwent negative moment cycles during testing and was close to the centerline of the longitudinal splice. The cracks in **Figure C -6(left)** extended into the deck for approximately one-third of the concrete thickness. These cracks do not cross any deck steel at the location of the core although one of the cracks nearly extended to the longitudinal splice reinforcing steel. The crack in **Figure C -6(right)** also extended approximately one-third of the deck thickness. The crack did not reach the supplemental bar at the location of the core, but could cross this bar at another location along its length.

The cores taken near the longitudinal splice show that the cracking that occurred near the longitudinal splice during testing allowed the low-viscosity epoxy to penetrate into the deck. Although the epoxy in Cores LS1-LS3 (located in the longitudinal splice testing location) did not come into direct contact with the deck steel, it permeated through most, if not all, of the concrete

cover in some of the cores. Thus, deicing salts may be able to reach the deck steel in another location along the length of the cracks.

It should be noted that in Cores C1 and C2, which were located on wide cracks in areas away from the longitudinal splice test, the epoxy was able to reach the deck steel. Although the cracks near the longitudinal splice test may have experienced slight growth during the cyclic testing, it seems that these cracks did not grow significantly larger than other large cracks found throughout the bridge deck.

Concrete Cores – TRANSVERSE SPLICE TESTS. As previously discussed in Section 2.6.4, concrete cores were removed from the bridge at the conclusion of the transverse splice cyclic tests to evaluate the extent of cracking caused by the cyclic loading. The locations where the concrete cores were removed are illustrated in **Figure C -7**. The transverse splice area between exterior main bars of the connecting panels is cross-hatched in this **Figure**.

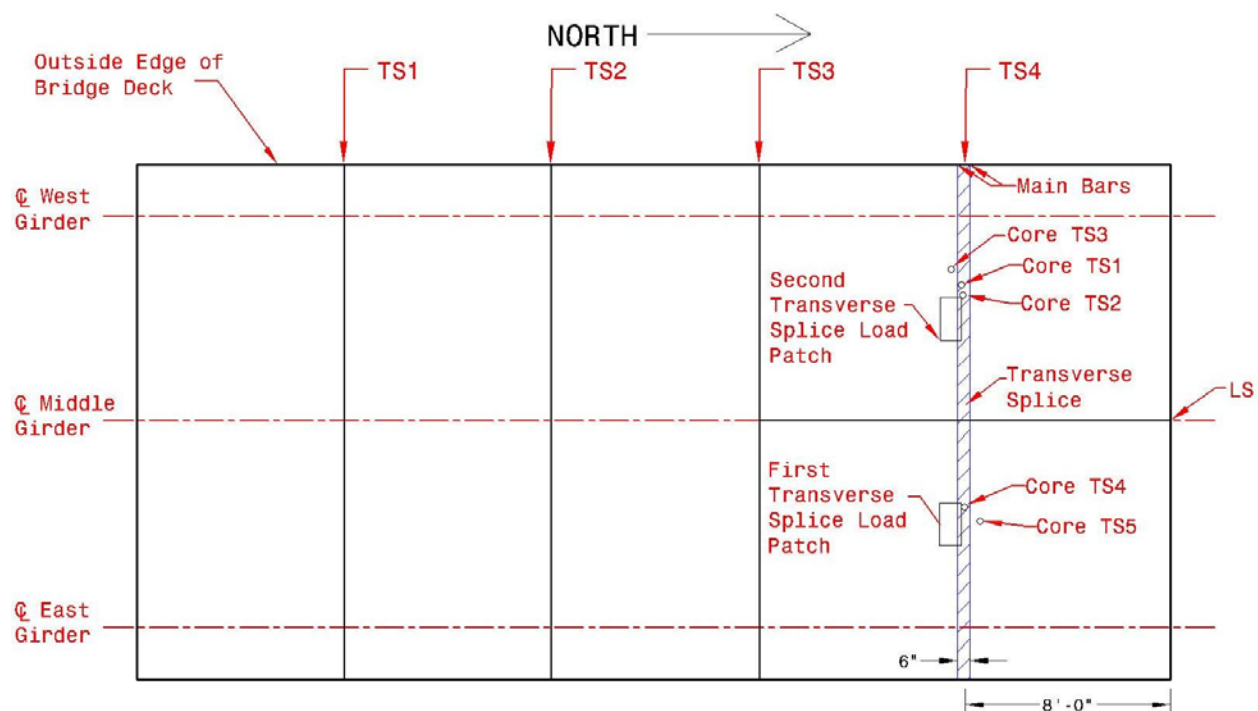


Figure C -7: Locations of transverse splice concrete cores

A total of five cores were removed from the deck near the transverse splice test location. Three cores, labeled Core TS1 – TS3, were removed near the load patch for transverse splice test #2. These cores will be discussed along with the other findings for that test in the next section.

Two cores, labeled Core TS4 and TS5, were removed near the load patch in transverse splice test #1. Core TS4 was located at the transverse splice on a crack running across the splice. Core TS5 was located on the same crack 9" to the northeast of Core TS4, placing this core outside of the transverse splice area.

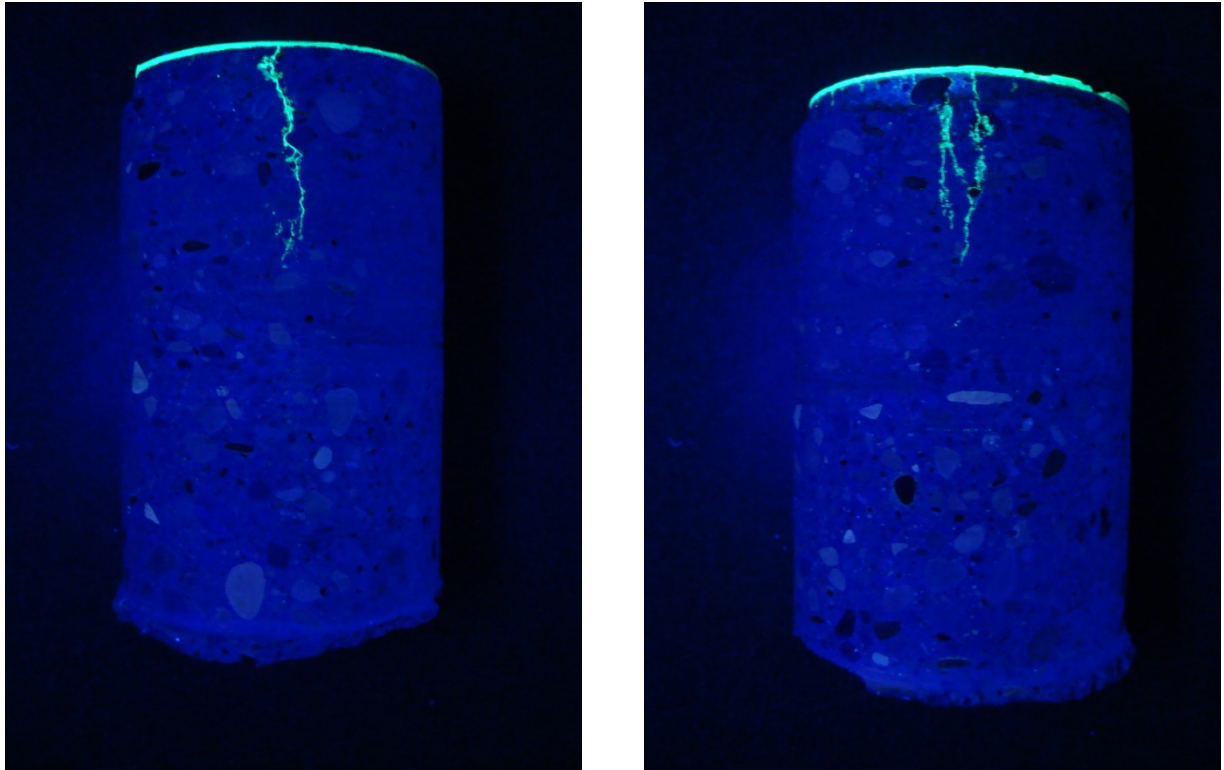


Figure C -8: Core TS4 (left) northeast elevation; (right) south elevation

Figure C -8 illustrates a view of the northeast and south elevations of Core TS4 located at the transverse splice near the cyclic test load patch. These cracks only extended to approximately one-third the depth of the concrete at the splice location. The crack in this core extended along the north-south direction, thus running perpendicular to the splice. This crack continued across the transverse splice and into the panels on either side.

It should be noted that, unlike many of the other cores taken on the bridge deck, no deck steel was cored through in this location. This is due to the fact that the only continuous steel within the transverse splice is the #3 reinforcing steel spaced at 8 inches center to center spacing, and there are no supplemental bars in the transverse splice region.

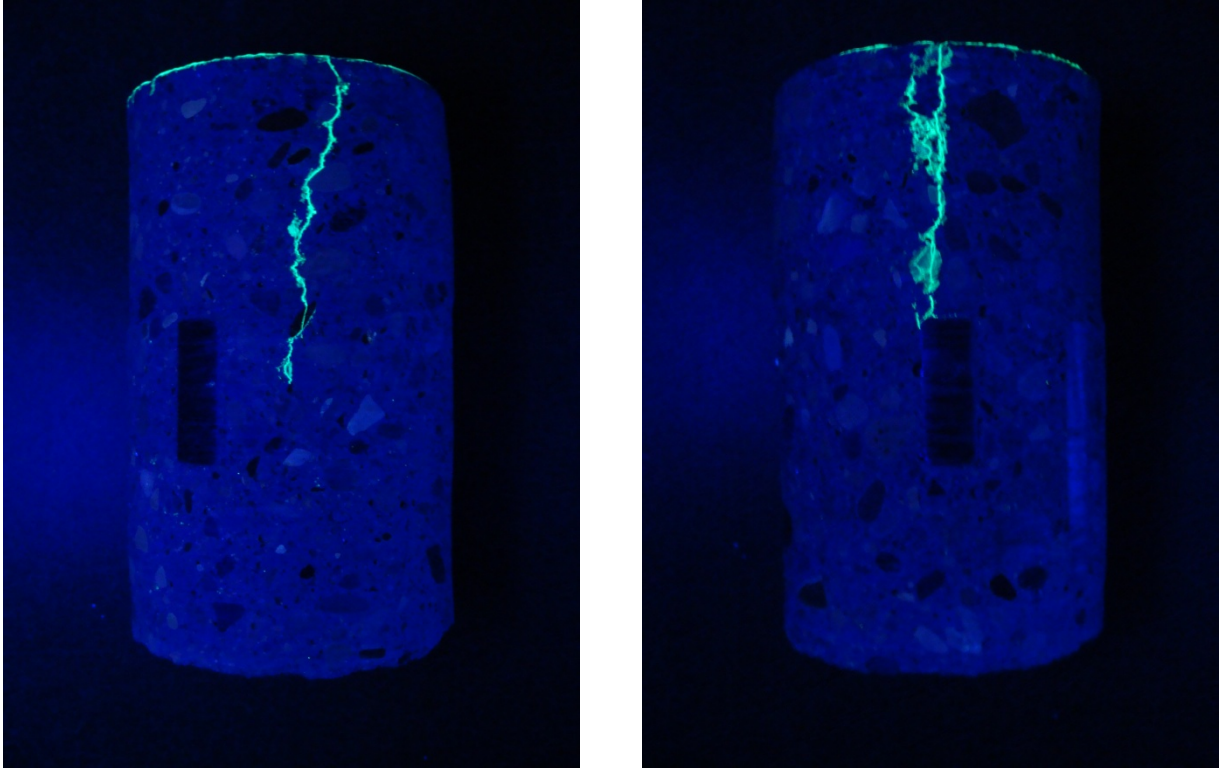


Figure C -9: Core TS5 (left) east-northeast elevation; (right) southwest elevation

Figure C -9 illustrates a view of the east-northeast and the southwest elevations of Core TS5. This core was located on the same crack as Core TS4, but outside of the transverse splice. The crack in this core is larger than the same crack in Core TS4 located at the transverse splice. The crack in Figure C -9(left) extended through almost half of the core and reached below the top of the supplemental bar. This crack reached the top of the same supplemental bar in Figure C -9(right).

Concrete Cores TRANSVERSE SPLICE TEST #2. Three concrete cores were removed from the deck near the load patch after termination of transverse splice test #2. Cores TS1 and TS2 were located along this crack within the transverse splice while Core TS3 was removed southwest of these cores, away from the transverse splice. The location of these cores is shown in Figure C -7.

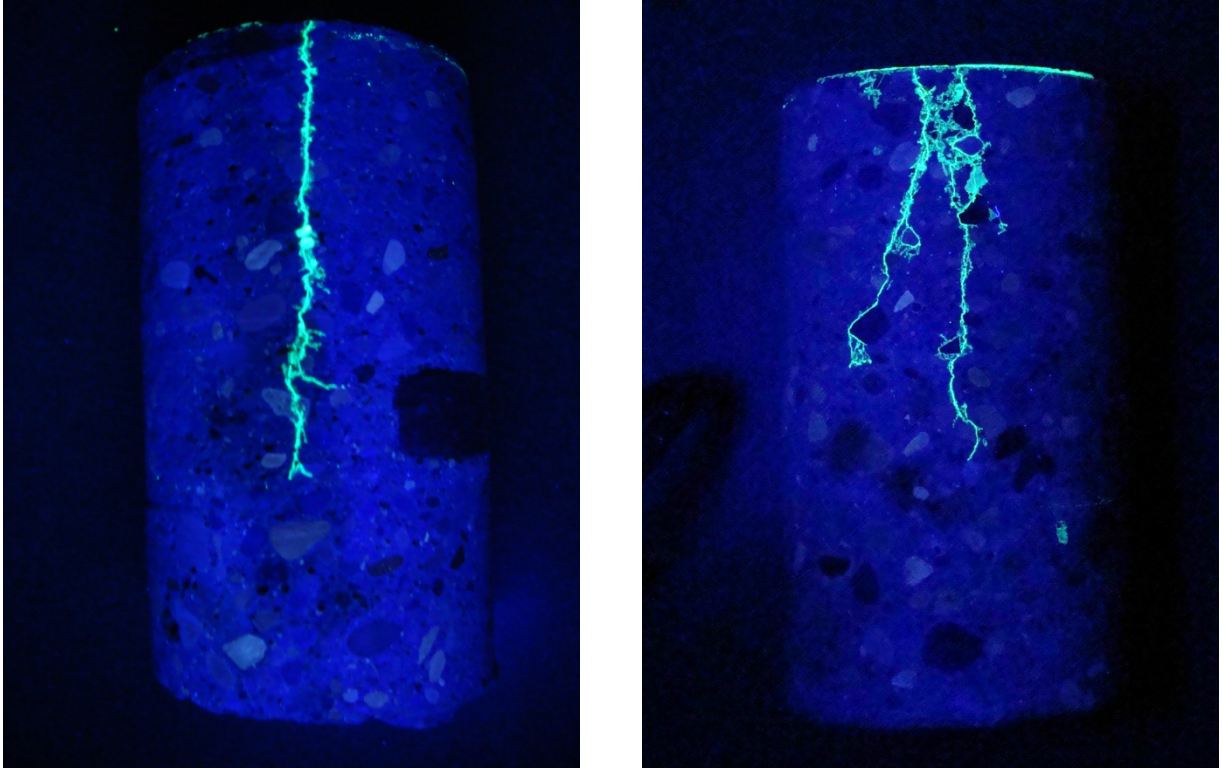


Figure C -10: Core TS1 (left) west elevation; (right) east elevation

Figure C -10 illustrates a view of the west and east elevations of Core TS1. This core was taken through the transverse splice over a large crack near the load patch in transverse splice test #2. The view of the west elevation of this core, **Figure C -10(left)**, illustrates that a crack extended approximately three-quarters through the core. This crack extended below the top of the main bar, but it did not cross the main bar at the location of the core. The view of the east elevation of the core, **Figure C -10(right)**, shows that a large branching crack extends over half of the thickness of the core. The fluorescent epoxy, which was applied to the surface, penetrated into many voids in the aggregate in the top of the core as shown in this **Figure**.

After visual inspection of the crack shown in **Figure C -10(right)**, evidence was found that seemed to show the crack extending completely through the core. Therefore, additional techniques were employed to further investigate this crack.

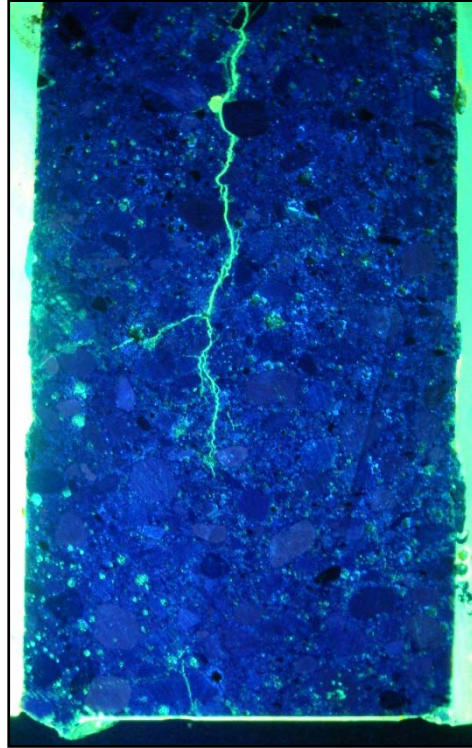


Figure C -11: Core TS1 after additional epoxy application

The core was placed into a container of fluorescent epoxy which would seep into any remaining portions of the crack that did not already contain hardened epoxy. The core was then cut in half perpendicular to the crack which allowed the crack length to be examined. **Figure C -11** shows the core after it was cut in half where the crack was found to not fully extend through the deck. Thus, although there were small cracks at the top and bottom of the deck at this location, they were not full depth.

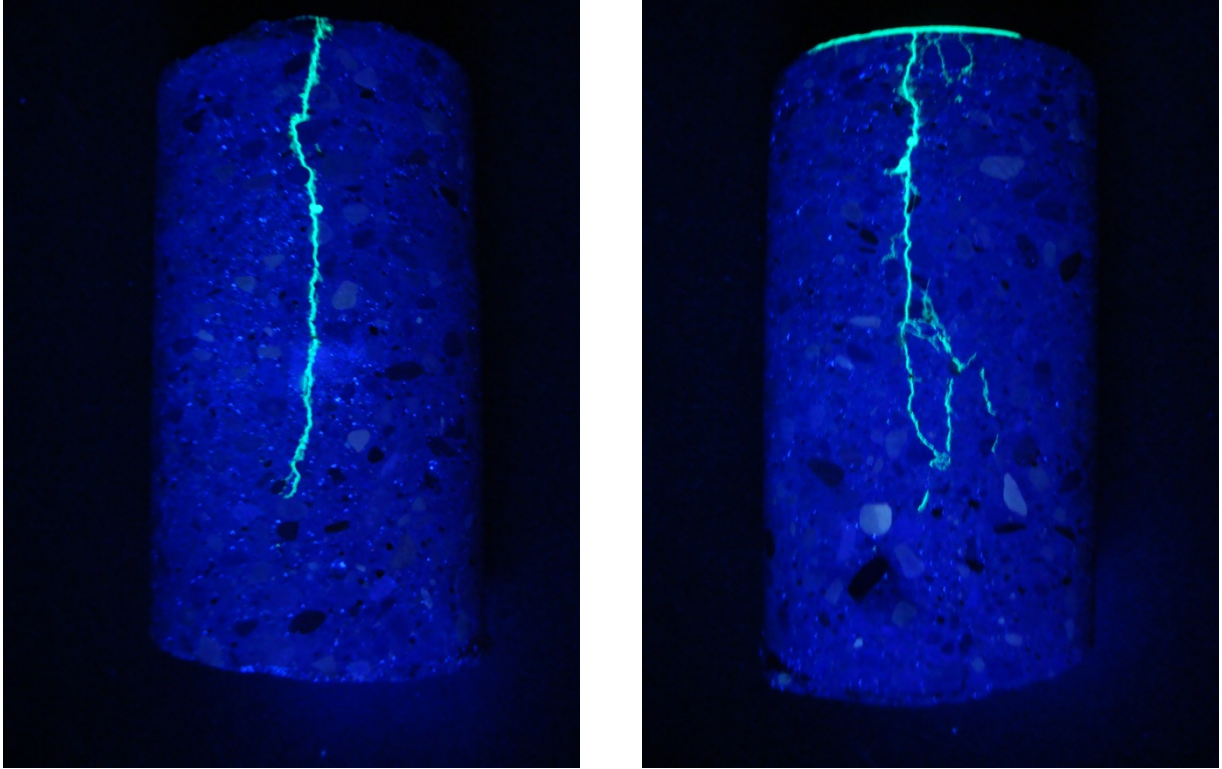


Figure C -12: Core TS2 (left) west elevation; (right) east elevation

Figure C -12 illustrates a view of the west and east elevation of Core TS2. This core was taken near Core TS1 in the transverse splice along the crack on the surface. **Figure C -12(left)** illustrates an extensive crack located on the west elevation of the core. The epoxy was able to penetrate most of the way through the deck at this location. **Figure C -12(right)** shows that the crack also penetrated much of the way through the core on its east elevation. The epoxy was able to branch off and extend across a wide portion of the core at this location.

Although there were small cracks on the bottom of the core in the same vertical plane as the cracks in the core highlighted by the fluorescent epoxy, it does not seem like these cracks were linked together. Thus, although the diagonal cracks on the top and bottom of the transverse splice, were located at the same location, they may not extend all the way through the transverse splice.

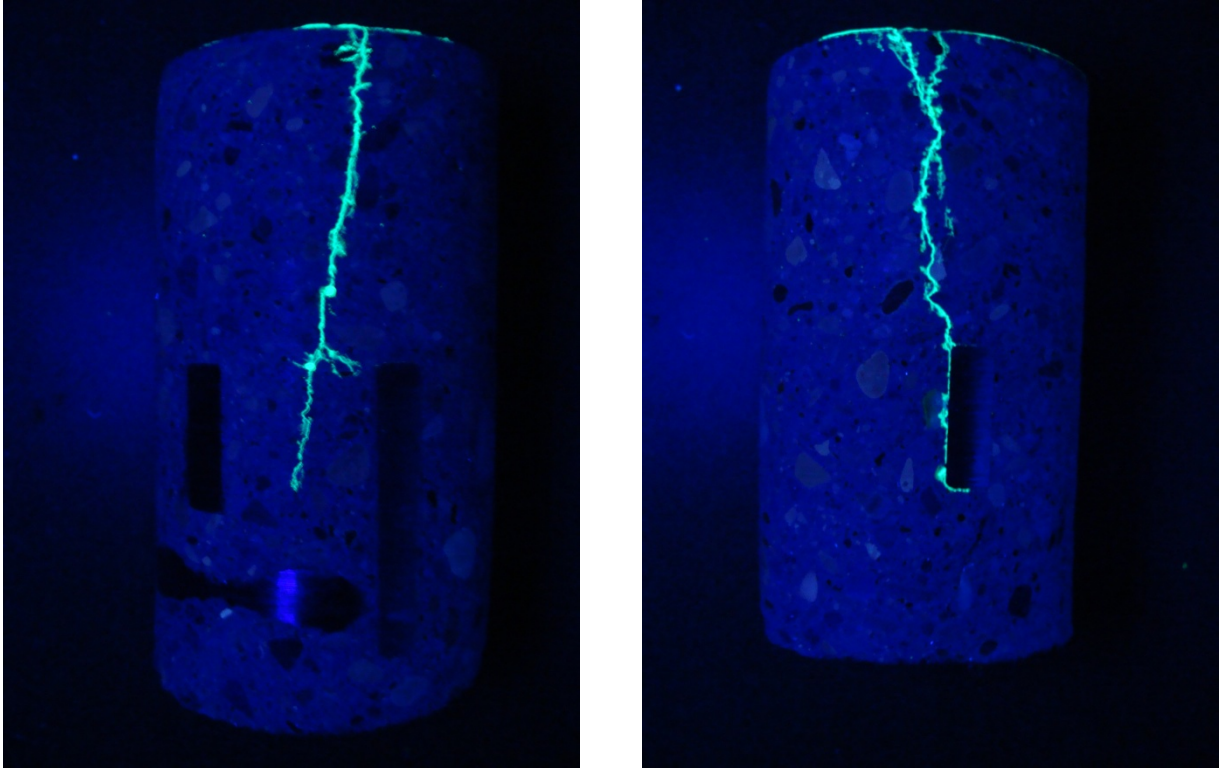


Figure C -13: Core TS3 (left) northeast elevation; (right) west elevation

Figure C -13 illustrates a view of the northeast and west elevation of Core TS3. This core was located along the same crack as cores TS1 and TS2, but was located outside of the transverse splice. **Figure C -13(left)** illustrates a view of the northeast elevation of the core where the crack extended through the concrete well below the top of the deck steel. This crack almost reached to the bottom of the supplemental bar and branched towards the top of the cross bar. It should be noted that the reinforcing steel, which crosses the transverse splice, can be seen in this core near the bottom of the deck. **Figure C -13(right)** illustrates a view of the west side of the core where the crack extended to the supplemental bar. Once the epoxy reached the supplemental bar, it flowed along the bar stopping at the bottom of the bar. Thus, at this location, deicing salts would be able to penetrate the concrete cover and reach this bar, which could cause long-term durability issues for the deck.

Even though this core was taken away from the transverse splice tested, the crack extended through the concrete of the deck to a similar depth as when it crossed through the transverse splice. Therefore, it seems that the cracking found in the transverse splice was also extended outside of the splice region.

3.1.1 Concrete Cores – SUBASSEMBLY TESTS

As previously discussed concrete cores were removed from the subassembly longitudinal splice specimen after the conclusion of the cyclic tests to evaluate the extent of cracking caused by the cyclic loading. The following cores were removed from specimen:

- SLS1 – near the load patch in positive transverse moment region;
- SLS2 – in transverse negative moment region near the edge of the deck specimen; and
- SLS3 – between the load patches in the transverse negative moment region.

Figure C -14 shows the west and east elevations of Core SLS1. These elevations are very similar, as expected. The fluorescent epoxy illustrates that the crack did not extend very deep into the concrete and did not reach the cross bar. Therefore, it is not expected that deicing salts would be able to penetrate the steel of the grid deck at this location along the crack for the number of cycles applied during this test.

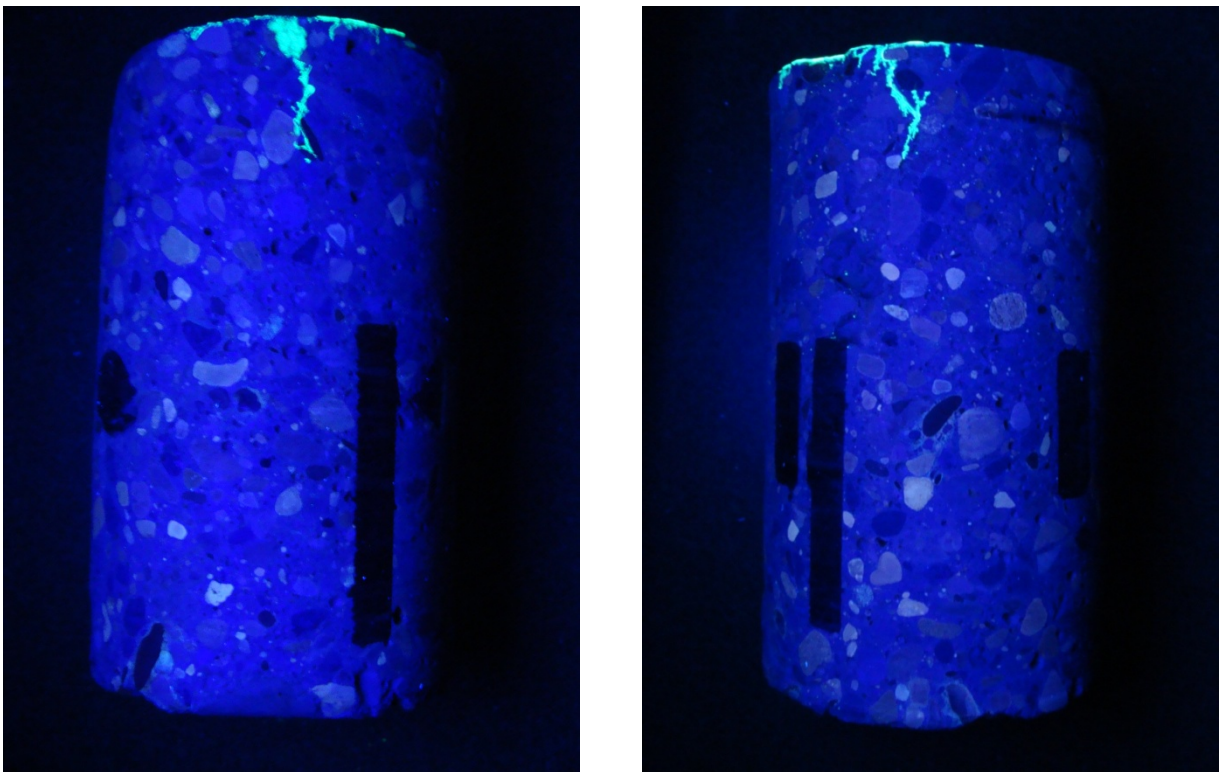


Figure C -14: Core SLS1 (left) west elevation; (right) east elevation

Figure C -15 shows the west and east elevations of Core SLS2. These elevations are also very similar. The fluorescent epoxy illustrates that the cracking near the edge of the deck did not extend very deep into the concrete and did not reach the cross bar. Therefore, it is not expected that deicing salts would be able to penetrate to the steel of the grid deck at this location to any significant extent for the number of cycles applied.

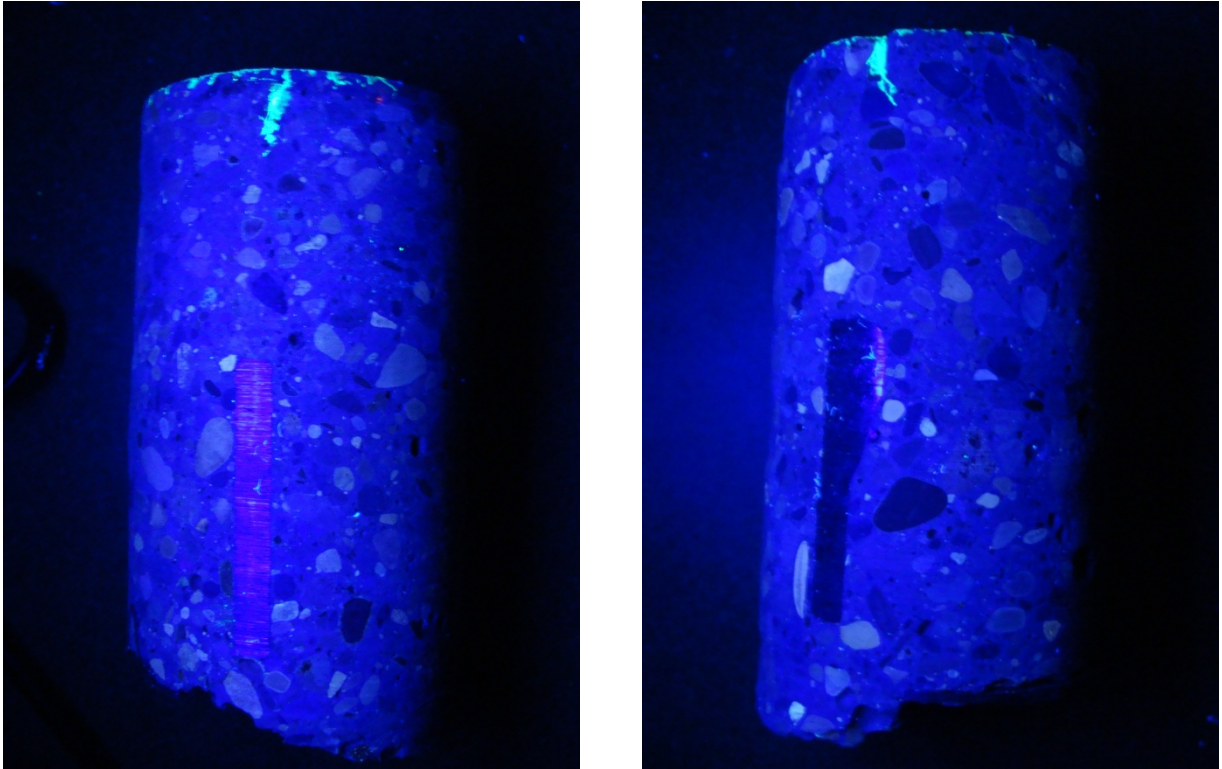


Figure C -15: Core SLS2 (left) west elevation; (right) east elevation

Figure C -16 shows the west and east elevations of Core SLS3. These elevations are also very similar. The fluorescent epoxy illustrates, again, that the cracking deck did not extend very deep into the concrete and did not reach to the cross bar. Therefore, it is not expected that deicing salts would be able to penetrate to the steel of the grid deck at this location for the number of cycles applied. It is noted that the cores shown in **Figure C -16** are deeper than the other cores because they were extracted from the deck at the centerline of the splice, where the concrete was the full-depth of the deck.

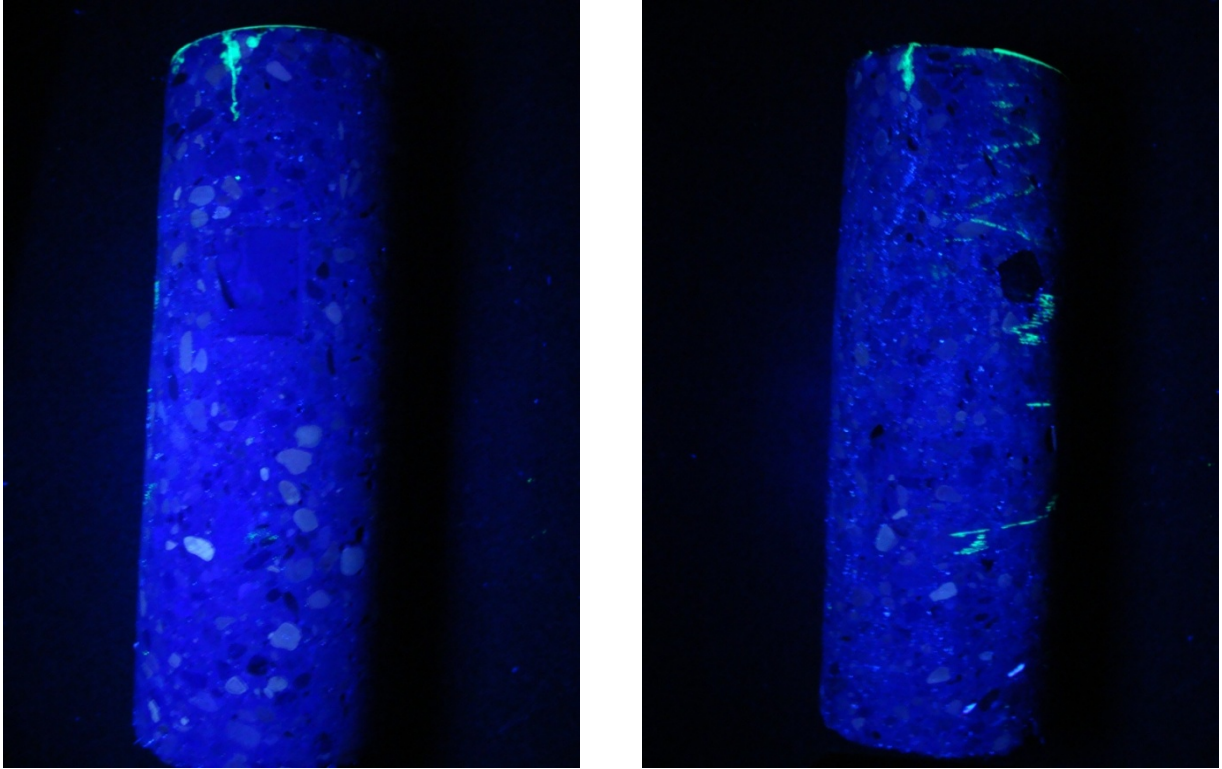


Figure C -16: Core SLS3 (left) west elevation; (right) east elevation

3.1.2 Comparison to Large-Scale Specimen

After completing the tests of the subassembly longitudinal splice, the displacements, stresses, and concrete cores taken from the subassembly longitudinal splice specimen were compared to those of the large-scale specimen. As discussed in Section 2.8, this was done to ensure the subassembly tests reasonably represented the large-scale bridge deck tested. The following sections discuss the comparison between results of these subassembly and large-scale longitudinal splice tests.

3.1.3 Concrete Cores – SUBASSEMBLY TESTS #2

As previously discussed, concrete cores were removed from the subassembly transverse splice specimen after the conclusion of the cyclic tests to evaluate the extent of cracking caused by the cyclic loading. The following cores were removed from specimen:

- STS1 – near the load patch at the centerline of the splice; and
- STS2 – slightly away from the transverse splice.

Figure C -17 shows the northwest and southeast elevations of Core STS1. These elevations are very similar, as expected. The fluorescent epoxy illustrates that the crack extended deep into the concrete. This crack was initiated when the deck was tightened down to superstructure by pretensioning the bolts (i.e., installing the deck-to-superstructure connection). As shown in **Figure** C -17(left), the crack extended to the depth of the supplemental bar. **Figure** C -17(right) shows that the crack extended to the depth of the crossbar. Therefore, deicing salts could potentially penetrate to the steel of the grid deck at this location.

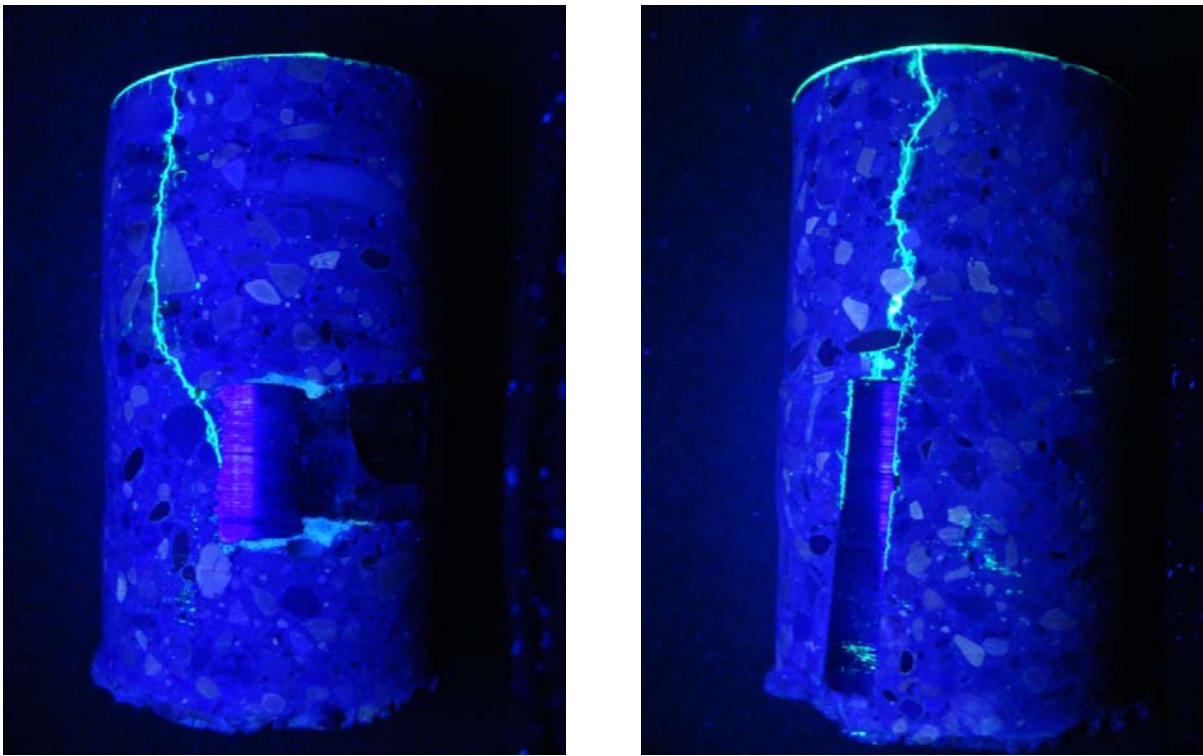


Figure C -17: Core STS1 (left) northwest elevation; (right) southeast elevation

Figure C -18 shows the northwest and southeast elevations of Core STS2. These elevations are also very similar. **Figure** C -18(right) shows that the crack extended to the depth of the cross bar, but did not reach the cross bar at this location. However, **Figure** C -18(left) shows that the crack did reach the cross bar at that location. Therefore, deicing salts could penetrate to the steel of the grid deck at the location of this core. Since cores STS1 and STS2 were taken on the same crack, the fluorescent epoxy illustrates that the cracking away from the transverse splice was very similar to the cracking at the centerline of the transverse splice.

Therefore, it is evident that the cyclic loading did not cause much additional damage after the damage found during an initial visual inspection.

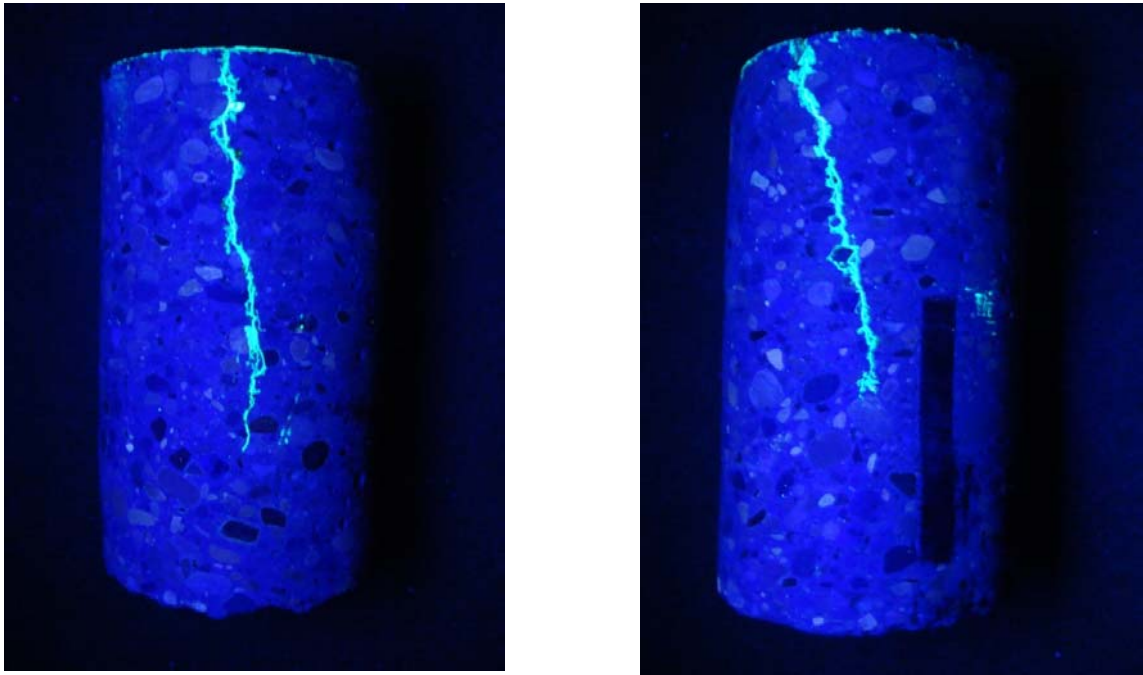


Figure C -18: Core STS2 (left) northwest elevation (right) southeast elevation

Concrete Cores. The concrete cores extracted from the subassembly and large-scale specimens exhibited similar damage from the cyclic loading tests. The findings of the comparison of the cores of the subassembly and large-scale transverse splice specimens are shown as follows:

- The cyclic loading did not cause significant damage in addition to the initial damage (i.e., shrinkage of concrete in the large-scale specimen or initial cracking in subassembly specimen).
- Damage observed at the transverse splice was similar to that slightly away from the transverse splice. This indicated that the damage caused by the cyclic loading to the transverse splice was not significant.

Unlike the subassembly longitudinal splice specimen, a large initial crack was created in the subassembly transverse splice specimen by installing the deck-to-superstructure connection after curing. This, coincidentally, resulted in similar crack depths between the subassembly and large-scale transverse splice specimens.